B 1
T392

Contents

1. Thermodynamic Methods for the Study of Interfacial Regions in Electrochemical Systems

Roger Parsons

1. Introduction 1
2. Thermodynamics of a Single Bulk Phase Containing Charged Particles. . 4
3. Thermodynamics of an Interphase Containing Charged Particles . . . 7
   - 3.1. The Basic Equation 7
   - 3.2. Other Forms of the Basic Equation 12
   - 3.3. The Gibbs Adsorption Equation 14
   - 3.4. Application of the Gibbs Adsorption Equation 16
   - 3.5. Temperature Dependence and Enthalpies and Energies of Adsorption 17
4. Solid Phases 19
5. Specific Examples 22
   - 5.1. Pure Metal in Contact with a Solution of a Single Salt in a Nondissociating Solvent. 22
   - 5.2. Pure Metal in Contact with a Solution of Two Salts in a Solvent . . 28
   - 5.3. Pure Metal in Contact with a Solution of an Electrolyte and a Nonelectrolyte in a Solvent 32
   - 5.4. Binary Alloy in Contact with a Solution of a Single Electrolyte . . 33
   - 5.5. Binary Alloy in Contact with a Solution of Two Electrolytes . . . 35
   - 5.6. Semiconducting Phase in Contact with an Electrolyte 36
   - 5.7. Nonionic, Nonconducting Phase in Contact with an Electrolyte . . 36
   - 5.8. Pure Ionic Solid in Contact with an Electrolyte Containing One of its Constituent Ions: $1A + KA + S|MX$ 36
   - 5.9. Ionic Crystal Containing Two Species in Solid Solution in Contact with an Electrolyte Containing One of the Constituent Ions: $MA + KA + S|MX + NX$ 37

5.10. Ion-Exchange Membrane in Contact with a Binary Electrolyte: MA + KA + S|MX + KX . . . 38
5.11. Three-Phase Electrode, in which a Gaseous Component is in Equilibrium with a Component in Solution . . . 38
5.12. Electrode with a Surface Species in Equilibrium with, but not Present in, a Bulk Phase . . . 41
6. Partial Dissociation and Partial Charge Transfer . . . 42
References . . . 43

2. The Electrode Potential

Sergio Trasatti

1. Introduction . . . 45
2. Components of the Electrode Potential . . . 47
2.1. Bulk Structure of Metals . . . 47
2.2. The Surface of Metals . . . 50
2.3. The Surface of Liquid Polar Phases . . . 55
2.4. Metal–Metal Contact . . . 56
3. Origin of the Electrode Potential . . . 60
3.1. Electrons in Liquid Polar Phases . . . 60
3.2. Metal–Polar-Liquid Contact . . . 62
3.3. Electron Work Function of Metals in Polar Liquids . . . 65
4. Meaning of Measured Potentials . . . 69
4.1. Measurement of Potentials . . . 69
4.2. Relative Electrode Potential . . . 70
4.3. Single Electrode Potential . . . 71
4.4. Absolute Electrode Potential . . . 72
4.5. Meaning of Potential in Terms of Electrode Reaction . . . 77
References . . . 78

3. The Double Layer in the Absence of Specific Adsorption

R. Reeves

1. Introduction . . . 83
2. Experiment Techniques and Some Useful Relationships and Definitions . . . 84
3. Introduction to the Use of Models to Describe the Double Layer . . . 100
4. Diffuse Layer Theory and Its Validity . . . 105
4.1. Fundamental Theory . . . 105
4.2. Applications of the Simple Theory . . . 110
5. Some Proofs, Limitations, and Possible Extensions of Diffuse Layer Theory 114
6. Models of the Inner Layer in the Absence of Specific Ionic Adsorption . . . 124
References . . . 132

4. Specific Adsorption of Ions

M. A. Habib and J. O'M. Bockris

1. Introduction . . . 135
2. Definition . . . 136

2.1. Introduction . . . 136
2.2. Definition in Terms of Gibbs Surface Excess . . . 137
2.3. Superequivalent Adsorption . . . 138
2.4. Contact Adsorption . . . 138
3. History of Specific Adsorption . . . 139
4. Phenomenology of Specific Adsorption . . . 141
5. Determinations of Specific Adsorption . . . 144
5.1. Quasithermodynamic Methods . . . 144
5.2. Discussion of the Electrocapillary Thermodynamics . . . 152
5.3. Direct Methods . . . 154
5.4. Method Based on Measurement of Surface Tension at Solid Metals . 160
6. Comparison of Different Methods for the Measurement of Specific Adsorption . . . 162
6.1. A Comparison of the Electrocapillary and Capacitance Integration Methods to Obtain Surface Tension . . . 162
6.2. Comparison of Results Obtained by Electrocapillary, Ellipsometry, and Radiotracer Methods . . . 172
7. The Validity of Diffuse Layer Theory . . . 175
8. Effect of the Neglect of Γ_{H_2O} . . . 179
9. Partial Charge Transfer in Specific Adsorption . . . 180
9.1. Introduction . . . 180
9.2. The Work of Lorenz and Co-Workers . . . 181
9.3. Discussion on Lorenz's Determination of Partial Charge . . . 182
9.4. The Work of Vetter and Schultze . . . 183
9.5. Summary . . . 186
10. Forces Involved in Specific Adsorption . . . 186
11. The Isotherms for Ionic Adsorption . . . 189
11.1. General . . . 189
11.2. The Single-Imaging Isotherm . . . 191
11.3. Multiple-Imaging Isotherm . . . 201
11.4. Conclusion . . . 202
12. Specific Adsorption and Solvation . . . 203
12.1. General . . . 203
12.2. Conclusion . . . 205
13. Simultaneous Specific Adsorption of Anions and Cations . . . 205
13.1. Introduction . . . 205
13.2. The Method of Delahay and Co-Workers . . . 206
13.3. The Method of Hurwitz and of Parsons and Co-Workers . . . 209
13.4. Discussion . . . 211
References . . . 213

5. Potentials of Zero Charge

A. N. Frumkin, O. A. Petrii, and B. B. Damaskin

1. Introduction . . . 221
2. The Notion of the Electrode Charge . . . 222
3. Methods of Determination of the Potentials of Zero Charge . . . 227
3.1. Direct Determination of the Value or Sign of the Surface Charge . . . 227

3.2. Development of Electrodes with Zero Charge 229
3.3. Electrocapillary Methods 231
3.4. Adsorption Methods. 235
3.5. Methods Based on the Dependence of the Properties of the Diffuse Part of the Double Layer on the Surface Charge 239
4. Influence of Metal Nature, Solution Composition, and pH on the Potentials of Zero Charge 246
5. Potentials of Zero Charge and the Adsorption of Organic Compounds on Electrodes. 259
6. Potentials of Zero Charge and the Nature of the Medium 267
6.1. Metal/Vacuum Interface 267
6.2. Metal/Nonaqueous Solution Interface. 274
6.3. Metal/Electrolyte Melt Interface 277
6.4. Metal/Solid Electrolyte Interface 282
7. Potentials of Zero Charge and Electrochemical Kinetics 282
8. Conclusions 285
References 285

6. Electric Double Layer on Semiconductor Electrodes
Yu. V. Pleskov

1. Introduction 291
2. The Theory of Double Layer on Semiconductor Electrodes 293
2.1. Charge and Potential Distribution 293
2.2. Surface Conductivity 298
2.3. Differential Capacity 301
2.4. Surface States. 302
3. The Semiconductor–Electrolyte Interface at Quasiequilibrium 306
3.1. Relaxation Characteristics of Space Charge and Surface States . . . 306
3.2. Photopotential 309
4. Distinctive Features of the Experimental Study of Semiconductor Electrodes 311
4.1. Basic Methods 311
4.2. Some Details of Experimental Techniques 312
5. Structure of the Double Layer on Semiconductor Electrodes. 312
5.1. Space Charge 312
5.2. The Helmholtz Layer 319
5.3. Fast Surface States 323
6. Conclusions 325
References 327

7. Insulator/Electrolyte Interface
L. I. Boguslavsky

1. Introduction 329
2. Concerning Differences between Insulating and Metal Electrodes . . . 330

3. Thermodynamic Approach to the Insulator/Electrolyte Interface . . . 332
4. Determination of the Potential due to Adsorbed Iodine at the Anthracene Electrode . . . 335
5. Electrochemical Injection and the Exchange Currents Occurring on the Insulating Electrodes . . . 339
6. Photoelectrochemical Processes on the Insulating Electrodes . . . 345
7. Reactions of Excitons at the Insulator/Electrolyte Interface . . . 347
8. Photosensitized Reactions with Participation of Excited Molecules in the Electrolyte . . . 349
9. Conclusion . . . 351
References . . . 351

8. The Adsorption of Organic Molecules

B. B. Damaskin and V. E. Kazarinov

1. Introduction . . . 353
2. Reversible Adsorption of Organic Substances . . . 354
2.1. Qualitative Relationships of Reversible Adsorption of Organic Substances on Ideally Polarizable Electrodes . . . 354
2.2. Thermodynamics of Surface Phenomena in the Case of Adsorption of Organic Substances on an Ideally Polarizable Electrode . . . 360
2.3. Phenomenological Description with the Use of Macromodels of the Reversible Adsorption of Organic Substances on Electrodes . . . 369
2.4. The Molecular Theory of Adsorption of Organic Compounds on Electrodes . . . 378
3. Irreversible Adsorption of Organic Substances . . . 381
3.1. General Regularities of the Adsorption of Organic Substances on Catalytically Active Electrodes . . . 381
3.2. Adsorption of Methanol on Platinum . . . 385
3.3. Adsorption on Platinum of Other Organic Compounds . . . 388
References . . . 391

9. The Double Layer in Colloidal Systems

Robert John Hunter

1. Charge and Potential Distribution at Interfaces . . . 397
1.1. Potential Distribution in the Double Layer . . . 397
1.2. Simultaneous Charge and Potential Measurements on the Double Layer . . . 401
2. Electrokinetic Phenomena . . . 404
2.1. The Electrokinetic (ζ) Potential . . . 404
2.2. Electro-osmosis . . . 405
2.3. Streaming Potential . . . 409
2.4. Electrophoresis . . . 412
2.5. Position of the Plane of Shear . . . 416
2.6. Electroviscous Effects . . . 417

3. The Double Layer in Colloid Stability 420
3.1. Coagulation Behavior of Electrostatically Stabilized Sols 420
3.2. Total Potential Energy of Interaction between Particles 422
3.3. The Potential Energy of Repulsion 423
3.4. The Potential Energy of Attraction 428
3.5. Experimental Tests of the DLVO Theory 430
4. Concluding Remarks 433
References 434

Annotated Author Index 439
Subject Index 445

1

Thermodynamic Methods for the Study of Interfacial Regions in Electrochemical Systems

ROGER PARSONS

1. Introduction

Thermodynamics is concerned with the relations between the observable properties of macroscopic pieces of matter. It is essentially an empirical science based on accumulated experience of the behavior of real systems. Its great utility is due to the fact that it enables information derived from experiment to be presented in a form which may be more readily understandable than the experimental results themselves. This transformation of information may be done without a detailed knowledge of the structure of the system being studied. Conversely, if no information about structure is contained in the original experimental data, no such information can be obtained by the operation of thermodynamic transformations on these data.

This chapter is concerned with the deduction of information about the composition of interfacial regions from a property such as the interfacial tension in a liquid system together with a knowledge of the equilibrium properties of the adjoining bulk phases. This particular transformation of information may be claimed as the most remarkable of the applications of classical thermodynamics. The technique by which this may be carried out was developed

ROGER PARSONS • Laboratoire d'Electrochimie Interfaciale du C.N.R.S., 92190 Meudon, France.

first by Gibbs[1] in 1878 in his comprehensive paper "On the Equilibrium of Heterogeneous Substances." He used the device of representing the real system (which consists of two bulk phases with an *interphase* between them) by an equivalent system in which the properties of the adjoining phases remain constant up to a mathematical plane, the *interface*, separating them. All differences of properties between the real system and this model system were then ascribed to the interface. This approach is often considered to be too abstract and certainly runs into difficulties when the interphase is curved or not at equilibrium.[2] Nevertheless, for a plane interphase, at equilibrium, the deductions from the Gibbs model are identical with those made from a model using an interfacial region of finite thickness,[3,4] and there is good reason to believe that they are completely correct. Gibbs' method was devised with great ingenuity at a time when little was known about the real thickness of interfacial regions and it is independent of this knowledge. However, the finite interphase method is probably easier to understand, as well as being capable of wider application; consequently this approach will be used in the present chapter.

The use of a model having an interphase of finite thickness also has advantages in the discussion of systems containing charged particles because of the long-range character of electrostatic forces. The region of inhomogeneity in such systems thus tends to be of greater extent than in the absence of particles carrying a net electric charge. It is possible for these inhomogeneous regions to become macroscopic, if the phases are poor conductors or if macroscopic pieces of matter carry finite charge. Under the latter condition the forces between pieces of charged matter become very large indeed, as illustrated dramatically by Feynman.[5] It is unusual to carry out electrochemical experiments using pieces of matter which bear a net charge, partly because large energies are required to create these charges. Consequently, it will be assumed here that there is no *macroscopic* separation of charge, although of course there is often free movement of charge within a phase as well as across an interphase.

Although Gibbs provided the basic foundation for the thermodynamic interpretation of interfacial phenomena, the application of his principles to charged interfaces has been the subject of much discussion in particular situations. In fact, the equation summarizing the most important characteristic of an electrochemical interphase was derived by Lippmann[6] even before Gibbs' work was published [Eq. (3.72)]. His derivation assumed that no charge transfer across the interface occurs; this situation has come to be known as an *ideal polarized* or *blocked* interface. The distinction between the ideal polarized interface and other types of interface, across which charge transfer can occur, has led to some controversy as to whether there is a difference in kind, or merely a difference in degree. In fact, the different points of view lead to the same practical results; an illustration of the lack of dependence of thermodynamics on the model adopted. Frumkin[7] seems to have been the first to show clearly that the ideal polarized interface is a limiting case of the interface with charge transfer. Later, Grahame[8] showed, in an illustrative and quantitative way, the reasons for the

existence of this limiting case, although in his thermodynamic analysis[9] he followed to a large extent the work of Koenig,[10] who assumed the existence of a physical barrier to charge transfer.

The reasons for the absence of finite charge transfer may be illustrated by considering, as an example, mercury in contact with aqueous KCl. The possible reactions which would transfer charge across the interphase are

$$Hg \rightleftarrows \tfrac{1}{2}Hg_2^{2+} + e \tag{1.1}$$

$$K(Hg) \rightleftarrows K^+ + e \tag{1.2}$$

$$Cl^- \rightleftarrows \tfrac{1}{2}Cl_2 + e \tag{1.3}$$

$$\tfrac{1}{2}H_2 + OH^- \rightleftarrows H_2O + e \tag{1.4}$$

each reaction being written in the standard way with the electron on the right-hand side. From the Nernst equation and the known standard electrode potentials, it is possible to calculate the concentration of the minority component in each couple at any given electrode potential. This has been done in Table 1 for two potentials, −0.2 and 0.8 V, with respect to the hydrogen electrode potential; the activities of Hg, KCl, and H_2O were assumed to be unity for each reaction. From these results it is then possible to find the charge required to change the concentration of the minority species from its equilibrium value at −0.2 V to the equilibrium value at −0.8 V if an assumption is made about the volume of the bulk phases. Here it is assumed that the volume of each bulk phase is 10^{-4} m^3 (100 cm^3). This charge is tabulated in the last column of Table 1. It is immediately evident that for the first three species the charge is extremely small and probably undetectable in a normal experiment. Reactions (1.1), (1.2), and (1.3) are fast reactions and this estimate is reliable. In contrast, reaction (1.4) is a very slow reaction at this interface and it will not come to equilibrium in the normal time scale. At −0.8 V the current due to this reaction would be about 0.04 A m^{-2}. This is sufficiently small for its effect on the interfacial properties to be neglected. This example illustrates the thermodynamic [reactions (1.1), (1.2), (1.3)] and kinetic [reaction (1.4)] reasons for the absence of significant charge transfer. It confirms the view that the ideal polarized interface is a limiting case,

Table 1

Equilibrium Concentration of Species at the Interface Hg|KCl + H_2O *at Two Different Potentials at* 25°C *and the Charge Required to Form These Quantities in a Volume of* 10^{-4} m^3

Concentration of minority species	E^H/V		
	−0.2 V	−0.8 V	Q/C
$[Hg_2^{2+}]$/mol m^{-3}	3.6×10^{-45}	1.9×10^{-63}	6.9×10^{-44}
[K(Hg)]/mol m^{-3}	5×10^{-24}	7×10^{-14}	6.7×10^{-13}
P_{Cl_2}/atm	1.8×10^{-64}	9.5×10^{-85}	1.5×10^{-61}
P_{H_2}/atm	5.8×10^{6}	1.11×10^{27}	9.6×10^{29}

not one for which some special mechanism must be invoked. In spite of this, it is not incorrect to carry out the thermodynamic analysis as if there were a "barrier" at the interface which permits no charge to cross.

It is important to note that the concept of the ideal polarized interface includes the case where a local transfer of charge can take place. For example, on a platinum electrode at potentials up to about 300 mV positive of the equilibrium hydrogen potential, hydrogen ions from the solution adsorb, reacting with electrons from the metal to form essentially neutral hydrogen atoms. This reaction which may be represented as

$$H_{ads.} \rightleftarrows H^+ + e \tag{1.5}$$

is fast on platinum and so may be assumed to be in equilibrium except on very short time scales. Although (1.5) is a charge transfer reaction, it does not result in the net transfer of charge from one bulk phase to the other, as do reactions (1.4)–(1.4). From the point of view of the externally observable parameters which are used in a thermodynamic analysis, there is no distinction between the adsorption of H^+ in the ionic form or in the atomic form, because the difference lies in the location of the charge within the interphase. This limiting case of charge transfer can in fact be identified by other methods and it was clearly recognized by Frumkin and his colleagues in their study of the platinum electrode in the 1930s.[11] However, the concept of a partial charge transfer and the way in which it enters the thermodynamic relations was enunciated by Lorenz and his coworkers from 1961.[12]

In this chapter the derivation of the thermodynamic relations will be made using the minimum of assumptions about the physical nature of the system. Specific assumptions may then be introduced in order to apply this more general treatment to specific physical situations, where other evidence indicates the nature of the interphase. Thus the general treatment of Sections 2 and 3 is followed by a series of more specific examples in Section 4 which illustrate the application of the thermodynamic method.

2. Thermodynamics of a Single Bulk Phase Containing Charged Particles

At first sight the simplest expression for the energy U of the bulk region of a single phase which may undergo thermal, mechanical, and matter exchange with its surroundings is

$$dU = T\,dS - p\,dV + \sum_i \bar{\mu}_i\,dm_i \tag{2.1}$$

where T is the temperature, S the entropy, p the pressure, V the volume, m_i the amount of species i in the phase, $\bar{\mu}_i$ is the electrochemical potential of species i if it carries a charge and the chemical potential if it carries no charge. The summation in Eq. (2.1) includes all independent components in the phase; that is, all

species whose concentration may be varied independently. It is usual to include ionic species or electrons separately in this summation and then to impose additionally the electroneutrality condition

$$\sum_i z_i m_i = 0 \tag{2.2}$$

since, as discussed above, only electrically neutral systems occur under normal conditions. The imposition of (2.2) allows any range of composition of positively and negatively charged particles provided that there is not an excess of charge of one sign.

However, the incorporation of Eq. (2.2) into Eq. (2.1) in a general way is cumbersome starting from the concept of ions as independent components, particularly when partial dissociation of some species exists in the sytem. Much of this difficulty can be avoided by adopting a more operational approach in terms of the amounts of species actually added to the phase when it is prepared. These are always uncharged species, metals in an alloy or "salts" in an electrolyte (the term "salt" here includes any neutral combination of ions such as an acid or a base as well as a conventional salt). Consequently, (2.1) may be replaced by

$$dU = T\,dS - p\,dV + \sum_j \sum_k \mu_{j,k}\,dm_{j,k} \tag{2.3}$$

where $\mu_{j,k}$ is the chemical potential of an uncharged species present in an amount $m_{j,k}$. The sum is then over all components of the phase as defined in conventional thermodynamics, which is one less than the sum in Eq. (2.1). It is evident that this reduction in the number of components is a result of the fact that (2.3) includes the electroneutrality condition; in other words, (2.3) is a solution for (2.1) and (2.2). The species indicated by the subscript j, k may be a species which does not dissociate into ions or one which dissociates into two or more kinds of ions. Strictly speaking, therefore, a varying number of subscripts would be required to indicate these possibilities. The use of two subscripts covers the commonest case of two kinds of ions. Nondissociating species will be indicated by putting $k = 0$. It will be assumed that there are J types of cations, K types of neutral species and $J_0 - J$ types of nondissociating species. Thus the summation covers the range $1 < j < J_0$, $0 < k < K$ although not every combination of cation and anion is necessarily present; some of the $m_{j,k}$ may be zero.

If the species denoted by the subscript j, k dissociates into species carrying z_j, z_k unit charges, this species may be regarded as being composed of $\nu_{j,k}$ positively charged particles and $\nu_{k,j}$ negatively charged particles. In metallic phases $\nu_{j,k} = 1$ and $\nu_{k,j} = z_j$, the number of electrons assumed to be produced by each metal atom (this number is arbitrary and may be taken as 1 or the conventional valency of the metal without affecting the thermodynamic argument). However, in electrolytes the relation between the charge number and the number of ions in the salt is not quite so simple, although it must always satisfy the

$$z_j \nu_{k,j} = -z_k \nu_{j,k} \tag{2.4}$$

A given ion may be present in more than one salt so that the relation between the m_i in Eq. (2.1) and the $m_{j,k}$ in Eq. (2.3) has the form

$$m_i = \sum_{k=1}^{k=K} \nu_{j,k} m_{j,k} \tag{2.5}$$

for the cations, or

$$m_i = \sum_{j=1}^{j=J} \nu_{k,j} m_{j,k} \tag{2.6}$$

and

$$m_i = m_{j,0} \tag{2.7}$$

for the nondissociating species. There are consequently $J_0 + K$ chemical species present in the phase, which as a result of the electroneutrality condition correspond to $J_0 + K - 1$ components.

It is convenient to define thermodynamic functions other than the energy. For a bulk phase, these are the enthalpy, H, the Helmholtz energy, A, and the Gibbs energy, G. These are defined by

$$H = U + pV \tag{2.8}$$

$$A = U - TS \tag{2.9}$$

$$G = H - TS \tag{2.10}$$

and it then follows from Eq. (2.3) that

$$dH = T\,dS + V\,dp + \sum_{j=1}^{j=J_0} \sum_{k=0}^{k=K} \mu_{j,k}\,dm_{j,k} \tag{2.11}$$

$$dA = -S\,dT - p\,dV + \sum_{j=1}^{j=J_0} \sum_{k=0}^{k=K} \mu_{j,k}\,dm_{j,k} \tag{2.12}$$

$$dG = -S\,dT + V\,dp + \sum_{j=1}^{j=J_0} \sum_{k=0}^{k=K} \mu_{j,k}\,dm_{j,k} \tag{2.13}$$

It is frequently convenient to express the equilibrium condition for a bulk phase in terms of the variation of the intensive variables. Since Eq. (2.3) is a complete differential, the standard technique of integrating with respect to the extensive variables to yield

$$U = TS - pV + \sum_{j=1}^{j=J_0} \sum_{k=0}^{k=K} \mu_{j,k} m_{j,k} \tag{2.14}$$

then differentiating

$$dU = T\,dS + S\,dT - p\,dV - V\,dp + \sum_{j=1}^{j=J_0} \sum_{k=0}^{k=K} (\mu_{j,k}\,dm_{j,k} + m_{j,k}\,d\mu_{j,k}) \tag{2.15}$$

and finally, comparing (2.15) with (2.3) yields

$$S\,dT - V\,dp + \sum_{j=1}^{j=J_0} \sum_{k=0}^{k=K} m_{j,k}\,d\mu_{j,k} = 0 \tag{2.16}$$

This is the Gibbs–Duhem equation for this bulk phase.

3. Thermodynamics of an Interphase Containing Charged Particles

3.1. The Basic Equation

An interphase may be treated in a similar way to a bulk phase except that its dimension in one direction is very small, being perhaps a few molecular diameters, and the properties vary marked with position in this direction. Provided that the radius of curvature is large, the interphase may be regarded as plane and its energy then differs from that of a bulk phase by a term expressing the contribution of changes of energy due to a change of the area of contact, A_s, of the two phases. For a liquid/liquid interface, this energy contribution is $\gamma\,dA_s$, where γ is the interfacial tension ("edge" effects are eliminated by considering a section of an interface in a larger system). Thus the energy is written as

$$dU^\sigma = T\,dS^\sigma - p\,dV^\sigma + \gamma\,dA_s + \sum_{j=1}^{j=J_0} \sum_{k=0}^{k=K} \mu_{j,k}\,dm_{j,k}^\sigma \tag{3.1}$$

where the superscript σ indicates interfacial properties; since the intensive variables, T, p, and the $\mu_{j,k}$ are uniform through a system at equilibrium, no subscript is necessary for them.

The amounts of matter in the interphase, $m_{j,k}^\sigma$, differ from those in a bulk phase in that they are usually far from uniformly distributed in the direction perpendicular to the interface. In an equilibrium system the density of each substance is uniform in the directions parallel to the interface. The nonuniformity perpendicular to the interface does not prevent a discussion of this problem in terms of equations like (3.1), but it may require special discussion when some of the species present in one of the adjoining phases are not present in the other. The way in which this may occur for charged species has been discussed in Section 1 for the ideal polarized electrode. This situation may affect the number of independent variables in the system of two phases with the intervening interphase. It is therefore necessary to discuss the variance of such a system.

In a system of two phases α and β which contain, respectively, a and b components, it follows from (2.16) that there are $a + b + 4$ independent intensive variables when the phases are separate. However, the existence of two equations like (2.16) means that the variance of the two separate phases is $a + b + 2$. When the two phases are brought into contact and allowed to equilibrate this system as a whole is subject to a number of equilibrium conditions. If no component is common to both phases the additional conditions are

thermal equilibrium, hydrostatic equilibrium, and electrostatic equilibrium. The first and second conditions are expressed by the equality of temperature and pressure of the two phases and the (plane) interphase. The third condition means that there is a single electroneutrality condition for the system as a whole in place of the two electroneutrality conditions for the two phases separately. Thus in fact only one degree of freedom is eliminated and $a + b + 3$ intensive variables remain. With the two Gibbs–Duhem equations for the separate phases this means that the variance is $a + b + 1$.

Charge transfer between the two phases may occur in two ways, either by oxidation–reduction reactions, like $Fe^{2+} \rightleftarrows Fe^{3+} + e$, between components which are present in only one phase, or by the transfer of a charged component from one phase to the other, like Fe^{2+} (m) $\rightleftarrows$ Fe^{2+} (s). If there are q types of charge transfer reaction of the first kind, then there are q equilibrium conditions and the variance is reduced to $a + b + 1 - q$. The second kind of charge transfer requires the presence of components common to both phases. If there are c such components then there are $a' + c = a$ components in phase α and $b' + c = b$ components in phase β. In the two phases separately there are then $a' + b' + 2c + 4$ intensive variables which on contact are reduced by 3 according to the thermal, hydrostatic, electrostatic, and Gibbs–Duhem conditions described above, but also by c conditions because of the identity of the c component in the two phases. The variance thus becomes $a' + b' + c + 1$, and in general for both kinds of charge transfer equilibrium and for the absence of charge transfer equilibrium the variance is $C + 1 - q$, where C is the total number of components in the two-phase system as a whole, the components being defined as neutral species in the way described in the previous section. If ionic components (described by m_i) are chosen the total number will be $C' = C + 2$ and the variance is then $C' - 1 - q$. The summation in Eq. (3.1) will then consist of $C - 1 - q$ (or $C' - 3 - q$) independent terms whereas it is written with C terms.

In the simplest example of a nonpolarizable interface there is one method of charge transfer and $q = 0$ or 1, the dependent terms are then eliminated by using the Gibbs–Duhem equation for the two bulk phases. If $q > 1$ there are relations between chemical potentials of species within each phase due to the oxidation–reduction equilibrium. The presence of such multiple equilibria does not bring any new features to the interfacial problem and it will not be discussed further here.

When charge transfer across the interphase occurs by only one species of reaction, it is convenient to separate the sum in Eq. (3.1) into two parts corresponding to the two phases adjoining the interphase. Many such systems are composed of an electronic conductor α and an ionic conductor β; for such a system (3.1) may be written

$$dU^\sigma = T\,dS^\sigma - p\,dV^\sigma + \gamma\,dA_s + \sum_{j=1}^{j=J^\alpha} \mu_{j,e}{}^\alpha\,dm_{j,e} + \sum_{j=1}^{j=J_0{}^\beta} \sum_{k=0}^{k=K} \mu_{j,k}{}^\beta\,dm_{j,k} \tag{3.2}$$

since electrons are the only negatively charged species which need to be considered in phase α and no uncharged component j, k is common to both phases.

This equation may be used in this form; if this is done the potential difference E across the interface (measured with respect to an electrode reversible with respect to an ionic species in phase β) is a dependent variable, controlled by the charge transfer equilibrium across the interface. On the other hand, it is also useful to introduce this charge transfer equilibrium explicitly and to replace one of the chemical potentials with the electrical potential. In order to do this, it is necessary also to specify the ion in phase β to which the reference electrode is reversible. It will be assumed here that this is the ion N, which for convenience is taken to be an anion, while the equilibrium reaction in the interphase under study involves the cation M. The assumption that M and N have charges of different sign is not necessary; they may both be cations or both anions. However, if M and N are identical, it follows immediately that E is zero or constant and no useful information can be obtained by using this quantity.

If the interfacial reaction consists of the transfer of the ion M^{z+} between the phases, the equilibrium condition is

$$\tilde{\mu}_{M^{z+}}{}^{\alpha} = \tilde{\mu}_{M^{z+}}{}^{\beta} \tag{3.3}$$

which may also be written

$$\mu_M{}^{\alpha} - z_M\tilde{\mu}_e{}^{\alpha} = \mu_{M,N}{}^{\beta} - (z_M/z_N)\tilde{\mu}_N{}^{\beta} \tag{3.4}$$

whence

$$z_M(\tilde{\mu}_N{}^{\beta}/z_N - \tilde{\mu}_e{}^{\alpha}) = \mu_{M,N}{}^{\beta} - \mu_M{}^{\alpha} \tag{3.5}$$

The quantity in brackets on the left-hand side of (3.5) will be defined as $F\varepsilon$, where F is Faraday's constant. ε is a quantity directly related to the potential difference E between the terminals of the cell by the relation

$$\varepsilon = E + K \tag{3.6}$$

where K is a sum of chemical potentials of the components of the reference electrode and is independent of the composition of the phases α and β. Thus

$$z_M F\varepsilon = \mu_{M,N}{}^{\beta} - \mu_M{}^{\alpha} \tag{3.7}$$

The terms in the species M, N and M may then be extracted from (3.2),

$$\mu_M{}^{\alpha}\, dm_M{}^{\sigma} + u_{M,N}{}^{\beta}\, dm_{M,N}{}^{\sigma} \tag{3.8}$$

and in view of (3.7) may be rewritten in the form

$$-z_M F\varepsilon\, dm_M{}^{\sigma} + \mu_{M,N}{}^{\beta}\, d(m_M{}^{\sigma} + m_{M,N}{}^{\sigma}) \tag{3.9}$$

The second term may be regarded as expressing the change in energy consequent on a change of the total amount of M^{z+} in the interphase, which can be denoted by $m_{\Sigma M}{}^{\sigma}$,

$$-z_M F\varepsilon\, dm_M{}^{\sigma} + \mu_{M,N}{}^{\beta}\, dm_{\Sigma M}{}^{\sigma} \tag{3.10}$$

Note that in writing (3.4) it has been implicitly assumed that M, N is the only species containing M in phase β. (This assumption can be dropped at the expense of some further algebra.) The total amount of M in the interphase is a well-defined quantity independent of the state of the charge transfer reaction, or the distribution of charge in the interphase. However, $m_M{}^\sigma$ is not so well defined because the amount of M (as metal atoms) does depend on the state of the charge transfer reaction. If it is *assumed* that the charge distribution in the interphase can be expressed in terms of an excess or deficiency of electrons on the side of the interphase adjoining phase α and a deficiency or excess of N ions on the side adjoining phase β, this may be related to $m_N{}^\sigma$. Since all other components are considered to be present always in electrically neutral groups j, k, then $z_M m_M{}^\sigma$ may be taken to represent the excess of electrons on the phase α side of the interphase. This contributes a charge Q^α given by

$$Q^\alpha = -z_M F m_M{}^\sigma \tag{3.11}$$

This is necessarily equal and opposite to the charge on the phase β side of the interphase represented by the N ions:

$$Q^\beta = -Q^\alpha = z_N F m_N{}^\sigma \tag{3.12}$$

It must be noted first that this definition of charge has a formal character and second that it depends on the nature of the ion N to which the reference electrode is reversible, because this affects the division of the total amount of M^{z+} in the interphase into a part on the α side of the interphase and a part on the β side.

The full equation (3.2) may now be written in the form

$$dU^\sigma = T\,dS^\sigma - p\,dV^\sigma + \gamma\,dA_s \sum_{j=1}^{j=J^\alpha-1} \mu_{j,e}{}^\alpha\, dm_{j,e}{}^\sigma + \sum_{j=J^\alpha+1}^{j=J_0-1} \sum_{k=0}^{k=K-1} \mu_{j,k}{}^\beta\, dm_{j,k}{}^\alpha + \varepsilon\,dQ^\alpha + \mu_{M,N}\, dm_{\sum M}{}^\sigma \tag{3.13}$$

A similar modification can be made if the interfacial reaction is an oxidation–reduction reaction, represented by

$$M^{z+} \rightleftarrows M^{(z+1)+} + e \tag{3.14}$$

The equilibrium condition is

$$\tilde{\mu}_{M^{z+}}{}^\beta = \tilde{\mu}^\beta_{M^{(z+1)}} + \tilde{\mu}_e{}^\alpha \tag{3.15}$$

which may be written

$$\mu^\beta_{M^{z+},N} + \tilde{\mu}_e{}^\alpha = \mu^\beta_{M^{(z+1)+},N} - \tilde{\mu}_N{}^\beta/z_N \tag{3.16}$$

where N is again the ion (assumed to be an anion) in equilibrium with the reference electrode. Thus

$$F\varepsilon = (-\tilde{\mu}_N{}^\beta/z_N - \tilde{\mu}_e{}^\alpha) = \mu^\beta_{M^{z+},N} - \mu^\beta_{M^{(z+1)+},N} \tag{3.17}$$

The terms extracted from (3.2) are now

$$\tilde{\mu}^\beta_{M^{z+},N}\, dm^\sigma_{M^{z+},N} + \tilde{\mu}^\beta_{M^{(z+1)+},N}\, dm^\sigma_{M^{(z+1)+},N} \tag{3.18}$$

which with (3.17) may be written

$$-F\varepsilon\, dm^{\alpha}_{M^{(z+1)+},N} + \mu^{\beta}_{M^{z+},N}\, dm^{\sigma}_{\Sigma M} \tag{3.19}$$

where it is assumed that the ion M exists in the interphase only in the two forms taking part in the oxidation–reduction reaction (3.14). Thus again in (3.19) the second term represents the effect on the energy of variation in the total amount of M in the interphase. The first term may be regarded as expressing the effect of excess of unit positive charges on the phase β side of the interphase or

$$Q^{\beta} = Fm^{\sigma}_{M^{(z+1)+},N} \tag{3.20}$$

so that when (3.19) is put back into Eq. (3.2) a form equivalent to (3.13) is obtained:

$$dU^{\sigma} = T\,dS^{\sigma} - p\,dV^{\sigma} + \gamma\,dA_s + \sum_{j=1}^{j=j^{\alpha}} \mu_{j,e^-}{}^{\alpha}\, dm_{j,e^-}{}^{\sigma} + \sum_{j=J^{\alpha}+1}^{j=J_0-2} \sum_{k=0}^{k=K-1} \mu_{j,k}{}^{\beta}\, dm_{j,k}{}^{\sigma} + \varepsilon\, dQ^{\alpha} + \mu_{M^{(z+1)+},N}\, dm_{\Sigma M}{}^{\sigma} \tag{3.21}$$

the difference being that, here, two terms are lost from the sum for phase β and none from the sum for phase α instead of one from each.

The ideal polarized interface is a special case of the two types of non-polarizable discussed above. If it is assumed that in (3.13), $m_M{}^{\alpha} \to 0$, the possibility of charge transfer vanishes. This causes modifications in the last two terms of (3.13). At first sight it would appear from (3.11) that Q^{α} also vanishes; however, it must be noted that this quantity actually represents the excess of electrons on the phase α side of the interphase. This in fact does not vanish as $m_M{}^{\alpha} \to 0$, but becomes more precisely interpretable as a physical charge because there is no longer any ambiguity about the location of the M^{z+} ions, since they may all be attributed to the phase β side of the interphase. At the same time the last term of (3.13) expresses simply the effect of a change of the amount of MN on the phase side of the interphase.

Similar changes occur in (3.21) if the corresponding assumption is made, namely, that the concentration $m^{\alpha}_{M^{(z+1)+}N} \to 0$. Again the possibility of charge transfer vanishes and again the interpretation of the last two terms is modified. Q^{β} remains finite and becomes clearly related to a physical charge on the β phase side of the interphase because it represents the excess of unit positive charges. At the same time $m_{\Sigma M}{}^{\sigma}$ reduces to $m_{M,N}{}^{\sigma}$. Consequently, both (3.13) and (3.21) lead to the basic result

$$dU^{\sigma} = T\,dS^{\sigma} - p\,dV^{\sigma} + \gamma\,dA_s + \varepsilon\,dQ^{\alpha} + \sum_{j=1}^{j=J_0-1} \sum_{k=0}^{k=K-1} \mu_{j,k}\, dm_{j,k}{}^{\sigma} \tag{3.22}$$

in which the concentration terms for both phases are regrouped together and the sum covers all but one of the neutral components of the two bulk phases. If one of the terms of this sum is given the interpretation of the last term of (3.13) or that of the last term of (3.21), then it is possible to use the form (3.22)

to represent the behavior of all these types of interphase. Nevertheless, the differences in the interpretation of Q^α for the polarizable and nonpolarizable interphases must be borne in mind.

The above discussion of the fundamental equation for the energy appears to be the simplest way of establishing this equation in terms of the composition of the system. However, it does involve a rather obscure definition of the charges Q^α and Q^β although the examples given below may help in understanding this. For an ideal polarized electrode it is simpler in practice and equally accurate to define these charges in terms of the ionic components making up the interface:

$$Q^\alpha = F \sum_{i=1}^{i=I^\alpha} z_i m_i^\sigma \tag{3.23}$$

$$Q^\beta = F \sum_{i=I^\alpha+1}^{i=I^\beta} z_i m_i^\sigma \tag{3.24}$$

where the components $1, \ldots, I^\alpha$ are present in phase α and those $I^\alpha + 1, \ldots, I^\beta$ are present in phase β. This definition emphasizes that the charges $z_i F$ on these species are *assumed*. Usually, they are taken as the charges on the same ions in the bulk of the phase. However, if an ion is chemisorbed at the interphase the charge distribution around it may be perturbed so that its actual charge may no longer correspond to $z_i F$. Consequently, it must be recognized that (3.23) and (3.24) may have a somewhat formal character as an electrical quantity. Nevertheless they have a precise interpretation in terms of a particular type of sum of interfacial concentrations. This aspect is perhaps more clearly emphasized in the definitions (3.11), (3.12), and (3.20).

3.2. Other Forms of the Basic Equation

As in the case of a bulk phase, it is possible to derive other characteristic equations from (3.22) using definitions such as (2.8), (2.9), (2.10) for the interfacial enthalpy, Helmholtz energy, and Gibbs energy. In these equations the composition term remains unchanged so that it is convenient to define

$$\sum = \sum_{j=I_0}^{j=I_0-1} \sum_{k=0}^{k=K-1} \mu_{j,k}\, dm_{j,k}^\sigma \tag{3.25}$$

in order to simplify the writing of these equations. It follows directly from (3.22) in combination with the differential forms of (2.8), (2.9), and (2.10), respectively that

$$dH^\sigma = T\,dS^\sigma + V^\sigma\,dp + \gamma\,dA_s + \varepsilon\,dQ^\alpha + \sum \tag{3.26}$$

$$dA^\sigma = -S^\sigma\,dT - p\,dV^\sigma + \gamma\,dA_s + \varepsilon\,dQ^\alpha + \sum \tag{3.27}$$

$$dG^\sigma = -S^\sigma\,dT + V^\sigma\,dp + \gamma\,dA_s + \varepsilon\,dQ^\alpha + \sum \tag{3.28}$$

It was noted by Everett[13] that the presence of the term $\gamma\, dA_s$ in these equations can lead to the definition of four new thermodynamic potentials:

$$\mathfrak{U} = U^\sigma - \gamma A_s \tag{3.29}$$

$$\mathfrak{H} = H^\sigma - \gamma A_s \tag{3.30}$$

$$\mathfrak{A} = A^\sigma - \gamma A_s \tag{3.31}$$

$$\mathfrak{G} = G^\sigma - \gamma A_s \tag{3.32}$$

These definitions lead to four new characteristic equations:

$$\mathrm{d}\mathfrak{U} = T\, dS^\sigma - p\, dV^\sigma - A_s\, d\gamma + \varepsilon\, dQ^\alpha + \sum \tag{3.33}$$

$$\mathrm{d}\mathfrak{H} = T\, dS^\sigma + V^\sigma\, dp - A_s\, d\gamma + \varepsilon\, dQ^\alpha + \sum \tag{3.34}$$

$$\mathrm{d}A = -S^\sigma\, dT - p\, dV^\sigma - A_s\, d\gamma + \varepsilon\, dQ^\alpha + \sum \tag{3.35}$$

$$\mathrm{d}\mathfrak{G} = -S^\sigma\, dT + V^\sigma\, dp - A_s\, d\gamma + \varepsilon\, dQ^\alpha + \sum \tag{3.36}$$

For an ordinary interphase there are consequently eight characteristic equations.

It was then pointed out[14] that the presence of the term $\varepsilon\, dQ^\alpha$ in the characteristic equations for an interphase containing ionic species leads to the definition of eight new thermodynamic potentials:

$$U_e = U^\sigma - \varepsilon Q^\alpha \tag{3.37}$$

$$H_e = H^\sigma - \varepsilon Q^\alpha \tag{3.38}$$

$$A_e = A^\alpha - \varepsilon Q^\alpha \tag{3.39}$$

$$G_e = G^\sigma - \varepsilon Q^\alpha \tag{3.40}$$

$$\mathfrak{U}_e = \mathfrak{U} - \varepsilon Q^\alpha \tag{3.41}$$

$$\mathfrak{H}_e = \mathfrak{H} - \varepsilon Q^\alpha \tag{3.42}$$

$$\mathfrak{A}_e = \mathfrak{A} - \varepsilon Q^\alpha \tag{3.43}$$

$$\mathfrak{G}_e = \mathfrak{G} - \varepsilon Q^\alpha \tag{3.44}$$

These definitions lead to eight new characteristic equations, making a total of 16 for an interphase containing charged species:

$$dU_e = T\, dS^\sigma - p\, dV^\sigma + \gamma\, dA_s - Q^\alpha\, d\varepsilon + \sum \tag{3.45}$$

$$dH_e = T\, dS^\sigma + V^\sigma\, dp + \gamma\, dA_s - Q^\alpha\, d\varepsilon + \sum \tag{3.46}$$

$$dA_e = -S^\sigma\, dT - p\, dV^\sigma + \gamma\, dA_s - Q^\alpha\, d\varepsilon + \sum \tag{3.47}$$

$$dG_e = -S^\sigma\, dT + V^\sigma\, dp + \gamma\, dA_s - Q^\alpha\, d\varepsilon + \sum \tag{3.48}$$

$$d\mathfrak{U}_e = T\, dS^\sigma - p\, dV^\sigma - A_s\, d\gamma - Q^\alpha\, d\varepsilon + \sum \tag{3.49}$$

$$dH_e = T\, dS^\sigma + V^\sigma\, dp - A_s\, d\gamma - Q^\alpha\, d\varepsilon + \sum \tag{3.50}$$

$$d\mathfrak{A}_e = -S^\sigma\, dT - p\, dV^\sigma - A_s\, d\gamma - Q^\alpha\, d\varepsilon + \sum \tag{3.51}$$

$$d\mathfrak{G}_e = -S^\sigma\, dT + V^\sigma\, dp - A_s\, d\gamma - Q^\alpha\, d\varepsilon + \sum \tag{3.52}$$

It should be noted that, for a nonpolarizable interphase, there is a choice of treatment, since, depending on the choice of variables, the εQ^α term may or may not appear. The choice depends essentially on whether a comparison with an uncharged interphase or with an ideal polarized interphase is more desirable. In this chapter the latter comparison is emphasized.

3.3. The Gibbs Adsorption Equation

By analogy with the derivation of the Gibbs–Duhem equation for a bulk phase from any one of the four characteristic equations, the interfacial Gibbs–Duhem equation can be derived from any one of the 16 characteristic equations for the charged interphase. As in the derivation of (2.16) the simplest route is from (3.22) where the variables are all extensive properties. This equation can be integrated [at (2.14)], differentiated [cf. (2.15)], and the result compared with (3.22) to obtain

$$S^\sigma\,dT - V^\sigma\,dp + A_s\,d\gamma + Q^\sigma\,d\varepsilon + \sum_{j=1}^{j=J_0-1}\sum_{k=0}^{k=K-1} m_{j,k}{}^\sigma\,d\mu_{j,k} = 0 \qquad (3.53)$$

Since the summation has one term less than the total number of components C in the system, this equation has $C + 2$ degrees of freedom. The system as a whole has only C degrees of freedom so that two of the variables in (3.53) are in fact dependent. They may be eliminated by using the Gibbs–Duhem equations for the two bulk phases. In view of the separation of components between the two phases, it is convenient to return to the separation of the sum in (3.53) into two parts as before; it thus becomes

$$\sum_{j=1}^{j=J^\alpha} m_{j,e}{}^\sigma\,d\mu_{j,e}{}^\alpha + \sum_{j=J^\alpha\neq 1}^{j=J_0-1}\sum_{k=0}^{k=K-1} m_{j,k}{}^\sigma\,d\mu_{j,k}{}^\beta \qquad (3.54)$$

The Gibbs–Duhem equations for the two bulk phases are

$$S^\alpha\,dT - V^\alpha\,dp + \sum_{j=1}^{j=J^\alpha} m_{j,e}{}^\alpha\,d\mu_{j,e}{}^\alpha = 0 \qquad (3.55)$$

$$S^\beta\,dT - V^\beta\,dp + \sum_{j=J^\alpha+1}^{j=J_0-1}\sum_{k=0}^{k=K} m_{j,k}{}^\beta\,d\mu_{j,k}{}^\beta = 0 \qquad (3.56)$$

These may be solved for one chemical potential which is then eliminated from (3.53) [with (3.54)]:

$$d\mu_{1,e} = -(S^\alpha/m_{1,e}{}^\alpha)\,dT + (V^\alpha/m_{1,e}{}^\alpha)\,dp - \sum_{j=2}^{j=J^\alpha} (m_{j,e}{}^\alpha/m_{1,e}{}^\alpha)\,d\mu_{j,e}{}^\alpha \qquad (3.57)$$

$$d\mu_0 = -(S^\beta/m_0{}^\beta)\,dT + (V^\beta/m_0{}^\beta)\,dp - \sum_{j=J^\alpha+2}^{j=J_0-1}\sum_{k=0}^{k=K} (m_{j,k}{}^\beta/m_0)\,d\mu_{j,k}{}^\beta \qquad (3.58)$$

where the single subscript 0 is used to denote the nondissociating substance $J^\alpha + 1$, 0. At the same time it is convenient to divide (3.53) by the area A_s so that the extensive quantities are replaced by quantities relative to unit area of interphase. The result is

$$S\,dT - v\,dp + d\gamma + q\,d\varepsilon + \sum_{j=2}^{j=J^\alpha} \Gamma_{j,e}^{(1)}\,d\mu_{j,e} + \sum_{j=J^\alpha+2}^{j=J_0-1} \sum_{k=0}^{k=K-1} \Gamma_{j,k}\,d\mu_{j,k}^{(0)} = 0 \tag{3.59}$$

where

$$S = A_s^{-1}[S^\sigma - (m_{1,e}^\sigma/m_{1,e}^\alpha)S^\alpha - (m_0^\sigma/m_0^\beta)S^\beta] \tag{3.60}$$

$$v = A_s^{-1}[V^\sigma - (m_{1,e}^\sigma/m_{1,e}^\alpha)V^\alpha - (m_0^\sigma/m_0^\beta)V^\beta] \tag{3.61}$$

$$q = Q^\alpha/A_s \tag{3.62}$$

$$\Gamma_{j,e}^{(1)} = A_s^{-1}[m_{j,e}^\sigma - (m_{1,e}^\sigma/m_{1,e}^\alpha)m_{j,e}^\alpha] \tag{3.63a}$$

$$\Gamma_{j,k}^{(0)} = A_s^{-1}[m_{j,k}^\sigma - (m_0^\sigma/m_0^\beta)m_{j,k}^\beta] \tag{3.63b}$$

are described as superficial excess quantities with respect to the reference components 1, e and 0. The excess quantities defined in (3.60)–(3.63) have the useful property that they are independent of the location of the boundaries dividing the interphase from the bulk phases, provided that these boundaries are placed outside the inhomogeneous interfacial region. This can be demonstrated in the following way. Suppose the original distance between the two boundaries enclosing the interphase is τ. If the boundary between α and σ is moved towards α by a distance $\Delta\tau$ the new thickness is $\tau + \Delta\tau$. The new entropy $S^{\sigma'}$ is larger than the original entropy of the interphase by the increased volume multiplied by the entropy per unit volume in the newly enclosed region. Since the latter is, by definition, homogeneous phase α, the new excess entropy may be written

$$S^{\sigma'} = S^\sigma + A_s\,\Delta\tau(S^\alpha/V^\alpha) \tag{3.64}$$

Similarly, the new amount of reference component 1, e in the interphase is

$$m_{1,e}^{\sigma'} = m_{1,e}^\sigma + A_s\,\Delta\tau(m_{1,e}^\alpha/V^\alpha) \tag{3.65}$$

The first two terms in the bracket in (3.60) then become

$$\begin{aligned} S^{\sigma'} - (m_{1,e}^{\sigma'}/m_{1,e}^\alpha)S^\alpha &= S^\sigma + A_s\Delta\tau(S^\alpha/V^\alpha) \\ &\quad - [m_{1,e}^\sigma + A_s\Delta\tau(m_{1,e}^\alpha/V^\alpha)](S^\alpha/m_{1,e}^\alpha) \\ &= S^\sigma - (m_{1,e}^\sigma/m_{1,e}^\alpha)S^\alpha \end{aligned} \tag{3.66}$$

That is, the magnitude of these two terms is invariant with such displacements of the boundary. A similar argument for the displacement of the boundary between σ and β shows that the sum of the first and third terms in (3.60) is invariant with displacement of this boundary. It is equally easy to show that v, and the interfacial excesses Γ, are equally independent of the positions of the

boundaries of the interphase and the adjoining phases. The same is true of q because it is defined as an excess quantity, being a measure of the local departure from electroneutrality in the interphase.

The coefficients of (3.59) are the only interfacial quantities which may be obtained from experiment, in contrast to S^σ, V, $m_{j,k}{}^\sigma$, etc., which depend on the placing of the boundary surfaces and have consequently an arbitrary magnitude.

When there is a component common to the two phases, it is possible to use this component as the sole reference component. The form of the excess quantities is then slightly different and more like that which is frequently used for nonelectrochemical systems (see Defay *et al.*,[2] for example). The form used here is based on the assumption that no component is common to phases α and β.

3.4. Application of the Gibbs Adsorption Equation

Equation (3.59) shows that the following quantities may be obtained from the experimental measurement of the interfacial tension γ:

$$s = -(\partial\gamma/\partial T)_{p,\varepsilon,\mu} \tag{3.67}$$

$$v = +(\partial\gamma/\partial p)_{T,\varepsilon,\mu} \tag{3.68}$$

$$q = -(\partial\gamma/\partial\varepsilon)_{T,p,\mu} \tag{3.69}$$

$$\Gamma_{j,e}{}^{(1)} = -(\partial\gamma/\partial\mu_{j,e}{}^\alpha)_{T,p,\varepsilon,\mu'} \tag{3.70}$$

$$\Gamma_{j,k}{}^{(0)} = -(\partial\gamma/\partial\mu_{j,k}{}^\beta)_{T,p,\varepsilon,\mu'} \tag{3.71}$$

where the subscript μ indicates that the chemical potentials of all the components of the system are kept constant, while the subscript μ' indicates that all but the chemical potential indicated in the differential coefficient are kept constant. When the temperature and pressure are constant, the constant K in Eq. (3.6) remains constant, so that $d\varepsilon = dE$. These are the conditions for (3.69), which may thus be written

$$q = -(\partial\gamma/\partial E)_{T,p,\mu} \tag{3.72}$$

This equation is known as the Lippmann equation as it was first derived by Lippmann[6] in 1875. For an ideal polarized electrode the quantity obtained in (3.72) has a unique value for a given set of conditions; the symbol q is then replaced by σ, which may often be interpreted as a physical charge. However, when the electrode is nonpolarizable, the value of q obtained depends on the choice of the set of chemical potentials as independent variables.[15]

It is often convenient to obtain quantities like those of (3.67), (3.68), (3.70), and (3.71) at constant charge q rather than at constant ε (or E). These may be obtained directly by defining a quantity[16]

$$\xi = \gamma + q\varepsilon \tag{3.73}$$

Since

$$d\xi = d\gamma + q\,de + \varepsilon\,dq$$

it follows immediately that (3.59) may be replaced by

$$s\,dT - v\,dp + d\xi - \varepsilon\,dq + \sum_{j=2}^{j=J^{\alpha}} \Gamma_{j,e}^{(1)}\,d\mu_{j,e} + \sum_{j=J^{\alpha}+2}^{j=J_0-1} \sum_{k=0}^{k=K-1} \Gamma_{j,k}^{(\sigma)}\,d\mu_{j,k} = 0 \tag{3.74}$$

from which

$$s = -(\partial\xi/\partial T)_{p,q,\mu} \tag{3.75}$$

$$v = +(\partial\xi/\partial p)_{T,q,\mu} \tag{3.76}$$

$$\Gamma_{j,e}^{(1)} = -(\partial\xi/\partial\mu_{j,e}^{\alpha})_{T,p,q,\mu'} \tag{3.77}$$

$$\Gamma_{j,k}^{(0)} = -(\partial\xi/\partial\mu_{j,k}^{\beta})_{T,p,q,\mu'} \tag{3.78}$$

It should be emphasized that this transformation provides no additional information, it merely may provide it in a more convenient form.

In addition, there are many useful relationships which may be derived by using the usual cross-differentiation rules for a complete differential and applying them to the Gibbs adsorption equation (3.59); for example,

$$-(\partial s/\partial\Gamma_{j,k})_{T,p,\varepsilon,\mu'} = (\partial\mu_{j,k}/\partial T)_{p,\varepsilon,\Gamma_{j,k},\mu'} \tag{3.79}$$

$$(\partial v/\partial\Gamma_{j,k})_{T,p,\varepsilon,\mu'} = (\partial\mu_{j,k}/\partial p)_{T,\varepsilon,\Gamma_{j,k},\mu'} \tag{3.80}$$

$$-(\partial q/\partial\Gamma_{j,k})_{T,p,\varepsilon,\mu'} = (\partial\mu_{j,k}/\partial\varepsilon)_{T,p,\Gamma_{j,k},\mu'} \tag{3.81}$$

$$-(\partial\Gamma_{j,k}/\partial\Gamma_{j,e})_{T,p,\varepsilon,\mu'} = (\partial\mu_{j,e}/\partial\mu_{j,k})_{T,p,\varepsilon,\Gamma_{j,e},\mu''} \tag{3.82}$$

$$(\partial q/\partial\mu_{j,k})_{T,p,\varepsilon,\mu'} = (\partial\Gamma_{j,k}/\partial\varepsilon)_{T,p,\mu} \tag{3.83}$$

$$(\partial q/\partial\Gamma_{j,k})_{T,p,\mu} = -(\partial\mu_{j,k}/\partial\varepsilon)_{T,p,q,\mu'} \tag{3.84}$$

$$(\partial q/\mu_{j,k})_{T,p,\Gamma_{j,k},\mu'} = (\partial\Gamma_{j,k}/\partial\varepsilon)_{T,p,q,\mu'} \tag{3.85}$$

where μ' again indicates that all the chemical potentials but one are held constant and μ'' indicates that the chemical potentials of all but two of the components are held constant.

3.5. Temperature Dependence and Enthalpies and Energies of Adsorption

While the excess entropy of the interphase may be obtained directly from (3.60) or (3.75), other properties may also be obtained from the temperature dependence using the definitions (2.8), (3.29), (3.30), (3.37), (3.38), (3.41), (3.42).

However, it must first be noted that the term $\sum$ defined in (3.25) must be modified to take account of the reduction of the number of variables as a result of the equilibrium of the interphase with the two adjoining phases. The most convenient form for $\sum$ which is compatible with (3.59) is

$$\sum = A_s \sum_{j=2}^{j=J^\alpha} \mu_{j,e}\, d\Gamma_{j,e}^{(1)} + \sum_{j=J^\alpha+2}^{j=J_0-1} \sum_{k=0}^{k=K-1} \mu_{j,k}\, d\Gamma_{j,k}^{(0)} \tag{3.86}$$

Then, from (3.22), it follows directly that

$$\left(\frac{\partial U}{\partial \Gamma_{j,k}}\right)_{T,V,A_s,q,\Gamma'} = T\left(\frac{\partial S^\sigma}{\partial \Gamma_{j,k}}\right)_{T,V,A_s,q,\Gamma'} + A_s\mu_{j,k} \tag{3.87}$$

and there is also a cross-differential relation

$$\left(\frac{\partial S^\sigma}{\partial \Gamma_{j,k}}\right)_{T,V,A_s,q,\Gamma'} = -A_s\left(\frac{\partial \mu_{j,k}}{\partial T}\right)_{V,A_s,q,\Gamma} \tag{3.88}$$

so that (3.87) may be written

$$\frac{1}{A_s}\left(\frac{\partial U}{\partial \Gamma_{j,k}}\right)_{T,V,A_s,q,\Gamma'} = -T\left(\frac{\partial \mu_{j,k}}{\partial T}\right)_{V,A_s,q,\Gamma} + \mu_{j,k}$$

$$= -T^2\left[\frac{\partial(\mu_{j,k}/T)}{\partial T}\right]_{V,A_s,q,\Gamma} \tag{3.89}$$

where the subscript Γ indicates that the surface excesses of all independent components are to be kept constant. The subscript Γ' indicates that the surface excesses of all independent components but one are to be kept constant.

The term on the left-hand side of (3.89) may be defined as the interfacial partial molar energy per unit area for the component j, k:

$$\bar{u}_{j,k} = A_s^{-1}(\partial U/\partial \Gamma_{j,k})_{T,V,A_s,q,\Gamma'} \tag{3.90}$$

The partial molar energy of this component in the bulk solution in its standard state is

$$U_{j,k}^\circ = -T^2[\partial(\mu_{j,k}^\circ/T)/\partial T]_V \tag{3.91}$$

If this is subtracted from (3.89) with the definition (3.90) a Clausius–Clapeyron equation is obtained

$$\bar{u}_{j,k} - U_{j,k}^\circ = -T^2[\partial[(\mu_{j,k} - \mu_{j,k}^\circ)/T]/\partial T]_{V,A_s,q,\Gamma} \tag{3.92}$$

There is an equation of this type for each independent component in the system, which, in principle, may be used to obtain the partial molar energy of adsorption of each component.

Similar arguments lead to similar sets of equations for each type of energy or enthalpy of adsorption:

$$\bar{h}_{j,k} - H^{\circ}_{j,k} = -T^2\left[\frac{\bar{\partial}(\mu_{j,k} - \mu^{\circ}_{j,k})/T}{\partial T}\right]_{p,A_s,q,\Gamma} \tag{3.93}$$

$$\bar{u}_{j,k} - U^{\circ}_{j,k} = -T^2\left[\frac{\bar{\partial}(\mu_{j,k} - \mu^{\circ}_{j,k})/T}{\partial T}\right]_{V,\gamma,q,\Gamma} \tag{3.94}$$

$$\bar{b}_{j,k} - H^{\circ}_{j,k} = -T^2\left[\frac{\bar{\partial}(\mu_{j,k} - \mu^{\circ}_{j,k})/T}{\partial T}\right]_{p,\gamma,q,\Gamma} \tag{3.95}$$

$$\bar{u}_{e,j,k} - U^{\circ}_{j,k} = -T^2\left[\frac{\bar{\partial}(\mu_{j,k} - \mu^{\circ}_{j,k})/T}{\partial T}\right]_{V,A_s,\varepsilon,\Gamma} \tag{3.96}$$

$$\bar{h}_{e,j,k} - H^{\circ}_{j,k} = -T^2\left[\frac{\bar{\partial}(\mu_{j,k} - \mu^{\circ}_{j,k})/T}{\partial T}\right]_{p,A_s,\varepsilon,\Gamma} \tag{3.97}$$

$$\bar{u}_{e,j,k} - U^{\circ}_{j,k} = -T^2\left[\frac{\bar{\partial}(\mu_{j,k} - \mu^{\circ}_{j,k})/T}{\partial T}\right]_{V,\gamma,\varepsilon,\Gamma} \tag{3.98}$$

$$\bar{h}_{e,j,k} - H^{\circ}_{j,k} = -T^2\left[\frac{\bar{\partial}(\mu_{j,k} - \mu^{\circ}_{j,k})/T}{\partial T}\right]_{p,\gamma,\varepsilon,\Gamma} \tag{3.99}$$

It should be noted that all of the eight types of "heats of adsorption" defined in (3.92)–(3.99) are measured at constant composition of the interphase, so that they are all isosteric heats of adsorption.

4. Solid Phases[40]

The general thermodynamics of electrified interfaces developed in Section 3 is based on the assumption that the interfacial tension is a well-defined and measurable quantity. It is possible to derive information about the interphase from other measurable quantities such as the charge or the capacity, but this does not avoid the problem that a well-defined quantity must appear in the basic equations, where γ appears in the equations of Section 3. This problem becomes important when one, or both, of the phases adjoining the interphase is a solid. Surface tensions of solids are difficult to measure and have been measured only under special circumstances, for example, at temperatures just below the melting point. These measurements are not particularly accurate and at present are not useful for the application of the Gibbs equation.

The problem of the equivalent for a solid phase of the liquid interfacial tension arises because of the very low mobility of atoms or molecules in a solid phase. It is therefore difficult to ensure that the formation of a new phase is an equilibrium process. Even if a state of partial equilibrium may be acceptable, there may be different ways of achieving this and different "equilibrium" states

may be achieved using these different routes in the same system. The surface tension of a liquid exists because the stress, which is isotropic in the bulk of the liquid, becomes anisotropic at the surface. The same is probably true in a solid, but the stress in the bulk of a solid is not necessarily isotropic. Also the quantity analogous to the surface tension of a liquid may itself not be isotropic.

To overcome this type of problem attempts have been made[17] to use quantities which must be isotropic such as the surface free energy. However, this depends on the choice of reference component (i.e., the position of the Gibbs dividing surface) and so its value is somewhat arbitrary. A closer approach to a measurable quantity is the free energy of formation of the interface, which might be measured in terms of the external work done by the system in the formation of the interface by an isothermal reversible process in which no "volume work" is done. Such conditions are difficult to achieve in practice. In effect, this method is equivalent, in the case of liquids, to defining the surface tension by the equation

$$\gamma = (\partial A_e/\partial A_s)_{T,V^\sigma,\varepsilon,\mu} \tag{4.1}$$

which follows from (3.47). The state of the liquid–liquid interphase is completely defined by the variables appearing in this equation, but this is no longer true when the system contains a solid whose state of internal strain varies from point to point. The use of (4.1) for such a system requires a knowledge of which variables must be maintained constant during the differentiation, and in general such knowledge is not available.

Defay *et al.*[17] point out that these problems can be avoided by defining the interfacial tension using a relation which contains only integral quantities. In the present system this definition takes the form

$$\gamma = (A_e/A_s) - \sum_{j=2}^{j=J} \Gamma_{j,e}{}^{(1)}\mu_{j,e} - \sum_{j=J^\alpha+2}^{j=J_0-1} \sum_{k=0}^{k=K-1} \Gamma_{j,k}{}^{(0)}\mu_{j,k} \tag{4.2}$$

in which A_e is defined with respect to the same reference components as the surface excesses $\Gamma_{j,e}$ and $\Gamma_{j,k}$. The advantage of this formula, in that the chemical potentials in the solid phase may be replaced by their values in a fluid phase in equilibrium with the solid, is of practical use only in rather simple systems like that of a crystal in equilibrium with its saturated solution. It would be difficult to apply to many electrochemical systems. Nevertheless, the definition is perhaps useful in a formal sense.

The quantity defined in (4.2) is perhaps better not called by the terms "surface" or "interfacial tension," and several other terms have been proposed. The situation has been summarized by Linford,[18] who suggests the term "specific surface work" and the symbol γ_π for this quantity, which may be thought of as the work of forming unit area of new surface by cleavage under ideal conditions. He suggests that the work required to form unit area of new surface by stretching under equilibrium conditions should be called the "surface

stress" $\mathbf{g}_{ij}$. This is, in general, an anistropic quantity and is therefore represented by a tensor. It is related to γ_π by

$$\mathbf{g}_{ij} = \delta_{ij}\gamma_\pi + (\partial\gamma_\pi/\partial\varepsilon_{ij})_{\text{all other strains}} \tag{4.3}$$

where $\delta_{ij} = 0$ if $i \neq j$, $\delta_{ij} = 1$ if $i = j$, and ε_{ij} is the natural strain (i.e., increase is length per unit length. $\mathbf{g}_{ij}$ may be defined as numerically equal to the force acting in the jth direction per unit length of exposed edge, the edge being normal to the ith direction, that must be applied to a terminating surface to keep it in equilibrium, the ith and jth directions lying in the plane of the surface. For an *isotropic* surface the shear stresses, i.e., the values of $\mathbf{g}_{ij}$ for which $i \neq j$, become zero and the $\mathbf{g}_{ij}$ may be replaced by the mean surface stress g, where

$$g = \tfrac{1}{2}(\mathbf{g}_{ii} + \mathbf{g}_{jj}) \tag{4.4}$$

and the strain ε_{ij} may be replaced by the mean strain dA_s/A_s, so that (4.3) becomes

$$g = \gamma_\pi + A_s\, d\gamma_\pi/dA_s \tag{4.5}$$

For liquids the second term on the right-hand side of (4.5) is zero and $g = \gamma_\pi = \gamma$ the interfacial tension.

Couchman and Davidson[19] have recently suggested that $d\gamma$ in the Gibbs equation for a liquid should, for a solid, be replaced by $(\gamma_\pi - \mathbf{g}_{ij})d\varepsilon_e + d\gamma_\pi$, where ε_e is the elastic surface strain. They suggest that, even with unrealistically large values of $\gamma_\pi - \mathbf{g}_{ij}$ and the electrostriction coefficient (which gives the effect of field on ε_e) the first of these terms contributes negligibly in comparison with $d\gamma_\pi$. Since the field arises from a change in composition of the interphase, it seems reasonable to extend this argument to the effect of composition changes on ε_e. If this is valid then it is probable that the specific surface work γ_π may be taken as the appropriate variable, replacing the surface or interfacial tension in solid systems. This is consistent with (4.2) if that equation is taken as defining γ_π. Provided that such a variable exists, it is possible to use differential forms of the Gibbs equation to obtain thermodynamic information about solid electrodes, in just the same way as for liquid electrodes. This is the procedure which has been used by the majority of electrochemists studying solid electrodes.

There is, however, one method developed by Gokhstein[20] in which the surface stress is measured directly with the aid of a piezoelectric element. This is done by using an alternating excitation either under potentiostatic or galvanostatic control. The quantity measured is the derivative of surface stress with respect to potential or charge, respectively. Gokhstein has called these quantities the "estance," a term derived from "elasticity" by analogy with "impedance," etc. It is therefore possible to measure the E estance $(\partial g/\partial E)_\sigma$ and the σ estance $(\partial g/\partial\sigma)_E$, these two quantities being directly related via the differential capacity of the electrode. It is evident that the σ estance has the dimensions of electrical potential and for that reason experimental curves of σ estance vs. E are particularly convenient. However, the σ estance must not be confused with the potential E;

it has a totally different significance. In a similar way the E estance has the dimensions of charge, but in fact is related to the charge on the electrode by

$$(\partial g/\partial E)_\sigma = -(\sigma + \partial\sigma/\partial\theta) \tag{4.6}$$

where θ is the relative extension of the extension of the surface $\Delta A_s/A_s$. Equation (4.6) is not a form of the Lippmann equation because it involves g not γ_s.

The above description is for an isotropic surface. If the surface is anisotropic, the estance, like the surface stress, is a tensor and, for example, in place of (4.6)

$$(\partial \mathbf{g}_{ij}/\partial E)_\sigma = -(\delta_{ij}\sigma + \partial\sigma/\partial\theta_{ij}) \tag{4.7}$$

must be written.

This brief mention is an inadequate account of the large development of this approach by Gokhstein,[20] which is certainly the most detailed study of the mechanical properties of electrodes yet made. It should be noted here, in the hope of avoiding confusion, that what has been called here the surface stress g is called by Gokhstein the surface tension γ. What has been called here the specific surface work γ_s, he calls σ.

5. Specific Examples

5.1. Pure Metal in Contact with a Solution of a Single Salt in a Nondissociating Solvent

5.1.1. Ideal Polarized Interface KA + S|M

The Gibbs equation reduces to the form

$$-d\gamma = S\,dT - v\,dp + \sigma\,d\varepsilon_\pm + \Gamma_{KA}\,d\mu_{KA} \tag{5.1}$$

The subscript to ε indicates the ion which is used to define the charge on the solution side of the interphase [cf. Eq. (3.20)], the "+" indicating the cation K and the "−" indicating the anion A. It is convenient to use a reference electrode which is reversible to this ion in the solution; the potential of M with respect to this electrode is then denoted E_+ or E_-.

At constant temperature and pressure the charge and surface excess of KA are obtained from the relations

$$\sigma = -(\partial\gamma/\partial E)_{T,p,\mu_{KA}} \tag{5.2}$$

$$\Gamma_{KA} = -(\partial\gamma/\partial\mu_{KA})_{T,p,E_\pm} \tag{5.3}$$

because at constant temperature, pressure, and composition, $d\varepsilon_\pm$ becomes equal to $dE_\pm$, the change of the potential of the electrode M measured with respect to any reference electrode, while at constant temperature and pressure $d\varepsilon_\pm$ becomes equal to $dE_\pm$. The change in the chemical potential μ_{KA} may be expressed in terms of the mean ionic activity $a_\pm$:

$$d\mu_{KA} = \nu RT\,d\ln a_\pm \tag{5.4}$$

at constant temperature and pressure, where ν is the total number of ions produced by the dissociation of one "molecule" of the salt, i.e., $\nu = 2$ for NaCl, $\nu = 3$ for $BaCl_2$, $\nu = 4$ for $La(NO_3)_3$, etc. Hence

$$\Gamma_{KA} = -(1/\nu RT)(\partial\gamma/\partial \ln a_\pm)_{T,p,E_\pm} \tag{5.5}$$

The interpretation of this quantity depends on the choice of the ion used to define the charge, as indicated by the sign of the subscript to E. Thus, if this ion is the cation, the solution side of the interphase is regarded as being composed of the cation K^+ and the salt KA. It follows that the surface excess of the anion is equal to that of the salt multiplied by the number of anions ν_- produced by the dissociation of one "molecule" of salt, i.e., $\nu_- = 1$ for NaCl, $\nu_- = 2$ for $BaCl_2$, $\nu_- = 3$ for $La(NO_3)_3$, etc. Consequently (5.5) may also be written with this choice of reference electrode

$$\Gamma_A = -(\nu_-/\nu RT)(\partial\gamma/\partial \ln a_\pm)_{T,p,E_+} \tag{5.6}$$

It may also be convenient to express this surface excess in terms of its equivalent charge. It is usually *assumed* that the charge of z_- unit charges carried by the ion solution is retained by the ion in the interphase; then

$$\sigma_- = z_- F\Gamma_A = (z_-\nu_- F/\nu RT)(\partial\gamma/\partial \ln a_\pm)_{T,p,E_+} \tag{5.7}$$

The surface excess of the cation is the sum of that regarded as making up the charge $-\sigma$ on the solution side of the interphase and that regarded as forming the surface excess of the salt KA. If the cation is also assumed to retain the charge of z_+ unit charges which it has in solution, this surface excess is then given by

$$\Gamma_K = -\sigma/z_+F + \Gamma_{KA} \tag{5.8}$$

or

$$\sigma_+ = z_+F\Gamma_K = -(\sigma + \sigma_-) \tag{5.9}$$

which is, in fact, a form of the condition of electroneutrality for the interphase. In this way the surface excesses of both ions may be found.

Exactly equivalent information is obtained if a reference electrode is used which is reversible to the anion in the solution. The interphase is then assumed to be composed of cation + salt. (5.7) is replaced by

$$\sigma_+ = z_+F\Gamma_K = (z_+\nu_+ F/\nu RT)(\partial\gamma/\partial \ln a_\pm)_{T,p,E_-} \tag{5.10}$$

and (5.9) may be used to find σ_-.

The classical method for these determinations is the measurement of electrocapillary curves, that is, the interfacial tension as a function of potential E at a given temperature, pressure, and composition. These curves are roughly parabolic and the maximum corresponds to $\sigma = 0$, i.e., the potential of zero charge (p.z.c.). From a family of such curves measured at different concentrations, interpolation at constant values of E_+ or E_- yields data which may be used to estimate σ_- or σ_+. Alternatively, the function $\xi_\pm$ [Eq. (3.73)], which at constant temperature and pressure becomes

$$\xi_\pm = \gamma + \sigma E_\pm \tag{5.11}$$

for an ideal polarized electrode, may be calculated and the interpolation done at constant values of σ. Hence

$$\Gamma_{\pm} = -(\partial \xi_{\mp}/\partial \mu_{KA})_{T,p,\sigma} \tag{5.12}$$

Besides using measurements of the interfacial tension as a function of E and composition, it is possible to use direct measurements of the charge σ. The ionic surface excess may then be obtained from the cross-differential relationship [cf. (3.83)]

$$(\partial \sigma/\partial \mu_{KA})_{T,p,E_{\pm}} = (\partial \Gamma_{KA}/\partial E_{\pm})_{T,p,\mu_{KA}} \tag{5.13}$$

whence

$$\Gamma_{KA}(E_{\pm}) = \Gamma_{KA}(E_{\pm}^{*}) + \int_{E_{\pm}^{*}}^{E_{\pm}} (\partial \sigma/\partial \mu_{KA})_{T,p,E_{\pm}}\, dE_{\pm} \tag{5.14}$$

In order to carry out this evaluation it is of course necessary to know the integration constant, that is, the value of Γ_{KA} at some particular value of the potential $E_{\pm}^{*}$. This may be found with the aid of a model of the double layer, such as the Gouy–Chapman theory (see Chapter 2) under conditions where there is no specific adsorption.

More often the differential capacity of the interface is measured. This is the capacity defined by

$$C = (\partial \sigma/\partial E)_{T,p,\mu_{KA}} \tag{5.15}$$

which by combination with (5.2) leads to

$$C = -(\partial^2 \gamma/\partial E^2)_{T,p,\mu_{KA}} \tag{5.16}$$

from which it can be seen that the differential capacity is the curvature of the electrocapillary curve. From measurements of C, it is possible to obtain σ and γ by integration:

$$\sigma = \int_{E_{\sigma_m=0}}^{E} C\, dE \tag{5.17}$$

and

$$\gamma = \gamma_{\sigma_m=0} - \int_{E_{\sigma_m=0}}^{E} \sigma\, dE \tag{5.18}$$

or

$$\gamma = \gamma_{\sigma_m=0} - \int_{E_{\sigma_m=0}}^{E} \int C\, dE^2 \tag{5.19}$$

The two integration constants are the potential of zero charge ($E_{\sigma_m=0}$) and the interfacial tension at this potential ($\gamma_{\sigma_m=0}$), although a more general relation in

terms of a potential E^*, at which known values of σ^* and γ^* are available, may also be used:

$$\sigma = \sigma^* + \int_{E^*}^{E} C\, dE \tag{5.20}$$

$$\gamma = \gamma^* - \int_{E^*}^{E} \sigma\, dE$$

or

$$\gamma = \gamma^* - \int_{E^*}^{E} \int C\, dE^2 \tag{5.21}$$

It is a useful check on the behavior of the system, especially to verify that equilibrium has been reached, to make measurements of two properties such as C and γ, and to confirm that they satisfy these relations.

The values of γ from (5.19) or (5.21) can then be used in (5.3) to obtain the surface excess. However, the order of integration and differentiation has no effect on the final result so that the derivative $(\partial C/\partial \mu_{KA})_{T,p,E\pm}$ may be determined first and then twice integrated. Grahame[21] defined the first integral of this quantity as a partial capacitance $C_\pm$:

$$C_+(E) = C_+(E^*) - (z_+\nu_+F)\int_{E^*}^{E} (\partial C/\partial \mu_{KA})_{T,p,E_-}\, dE \tag{5.22}$$

Subscripts are not necessary for the potentials in the integration because this is done at constant composition. Similarly,

$$C_-(E) = C_-(E^*) - (z_-\nu_-F)\int_{E^*}^{E} (\partial C/\partial \mu_{KA})_{T,p,E_+}\, dE \tag{5.23}$$

With these definitions and (5.13), it follows that

$$\sigma_+(E) = \sigma_+(E^*) - \int_{E^*}^{E} C_+\, dE \tag{5.24}$$

$$\sigma_-(E) = \sigma_-(E^*) - \int_{E^*}^{E} C_-\, dE \tag{5.25}$$

and

$$C_+ - C_- = C \tag{5.26}$$

Again the integration constants must be obtained from measurements other than those of capacity, or from a model of the double layer. Values of $C_+(E_{\sigma_m=0})$ or $C_-(E_{\sigma_m=0})$ may be found from measurements of $E_{\sigma_m=0}$ as a function of solution composition because it follows from (5.13) that

$$C_+ = -(z_+\nu_+F)^{-1}(\partial\sigma/\partial\mu_{KA})_{T,p,E_-} \tag{5.27}$$

Also from the properties of a complete differential like (5.1),

$$-(\partial\sigma/\partial\mu_{KA})_{T,p,E_-} = (\partial\sigma/\partial E_-)_{T,p,\mu_{KA}}(\partial E_-/\partial\mu_{KA})_{T,p,\sigma}$$
$$= C(\partial E_-/\partial\mu_{KA})_{T,p,\sigma} \tag{5.28}$$

Thus

$$C_+(E_{\sigma_m=0}) = -(z_+\nu_+F)C\ \partial E_-/\partial\mu_{KA}$$
$$= \frac{z_+\nu_+F}{\nu RT}C\left(\frac{\partial E_-}{\partial \ln \alpha_\pm}\right)_{T,p,\sigma_m=0} \tag{5.29}$$

which is the special case of the general relation valid for any value of σ.

Variations with pressure and temperature yield the surface excesses of entropy and volume, formally according to

$$s = -(\partial\gamma/\partial T)_{p,\varepsilon_\pm,\mu_{KA}} \tag{5.30}$$

$$v = -(\partial\gamma/\partial p)_{T,\varepsilon_\pm,\mu_{KA}} \tag{5.31}$$

but these derivatives are more difficult to evaluate in practice because of the requirements that $\varepsilon_\pm$ and μ_{KA} must be constant. This requires some care. The method which has been preferred[22,23] is that of using the cross-differential relationships

$$(\partial s/\partial\sigma)_{T,p,\mu_{KA}} = -(\partial\varepsilon_\pm/\partial T)_{p,\sigma,\mu_{KA}} \tag{5.32}$$

$$(\partial v/\partial\sigma)_{T,p,\mu_{KA}} = -(\partial\varepsilon_\pm/\partial p)_{T,\sigma,\mu_{KA}} \tag{5.33}$$

The temperature and pressure derivatives of $\varepsilon_\pm$ may be evaluated for given reference electrodes in the following way. If ε_+ is relative to a simple cation reversible electrode, that is, the cell may be written

$$\mathrm{Cu'|K|KA + S|M|Cu''} \tag{5.34}$$

where Cu′ and Cu″ represent the leads to the electrodes. By analogy with Eq. (3.5),

$$\varepsilon_+ = -\tilde{\mu}_K^{\beta}/z_K - \tilde{\mu}_e^{\alpha} \tag{5.35}$$

and with the equilibrium conditions at the interface in cell (5.34),

$$\tilde{\mu}_e^{\alpha} = \tilde{\mu}_e^{\mathrm{Cu''}} \tag{5.36}$$

$$\tilde{\mu}_K^{\beta} = \tilde{\mu}_K^{\mathrm{K}} = \mu_K^{\mathrm{K}} - z_K\tilde{\mu}_e^{\mathrm{K}} = \mu_K^{\mathrm{K}} - z_K\mu_e^{\mathrm{Cu'}} \tag{5.37}$$

it follows that

$$\varepsilon_+ = -\mu_K^{\mathrm{K}}/z_K + \tilde{\mu}_e^{\mathrm{Cu'}} - \tilde{\mu}_e^{\mathrm{Cu''}} \tag{5.38}$$

The measured cell potential is

$$E_+ = \phi^{\mathrm{Cu''}} - \phi^{\mathrm{Cu'}} = -(\tilde{\mu}_e^{\mathrm{Cu''}} - \tilde{\mu}_e^{\mathrm{Cu'}})/F \tag{5.39}$$

so that

$$\varepsilon_+ = E_+ - \mu_K^K/z_K F \tag{5.40}$$

In a similar way, when an anion reversible electrode is used, such as an electrode of the second kind with an insoluble silver salt $Ag_{z_A}A$ for example, the cell becomes

$$Cu'|Ag|Ag_{z_A}A|KA|M|Cu'' \tag{5.41}$$

and

$$\varepsilon_- = \tilde{\mu}_A^\beta/z_A - \tilde{\mu}_e^\alpha \tag{5.42}$$

By a similar use of equilibrium conditions this becomes

$$\varepsilon_- = E_- + \mu_{AgA}^{AgA}/z_A F - \mu_{Ag}^{Ag}/F \tag{5.43}$$

The required temperature and pressure coefficients are then

$$\begin{aligned}(\partial\varepsilon_+/\partial T)_{p,\sigma,\mu_{KA}} &= (\partial E_+/\partial T)_{p,\sigma,\mu_{KA}} - [(\partial\mu_K^K/z_K)/\partial T]_p \\ &= (\partial E_+/\partial T)_{p,\sigma,\mu_{KA}} + S_K/z_K\end{aligned} \tag{5.44}$$

where S_K is the molar entropy of the electrode material K.

Similarly,

$$(\partial\varepsilon_-/\partial T)_{p,\sigma,\mu_{KA}} = (\partial E_-/\partial T)_{p,\sigma,\mu_{KA}} - S_{AgA}/z_A + S_{Ag} \tag{5.45}$$

$$(\partial\varepsilon_+/\partial p)_{T,\sigma,\mu_{KA}} = (\partial E_+/\partial T)_{T,\sigma,\mu_{KA}} - V_K/z_K \tag{5.46}$$

$$(\partial\varepsilon_-/\partial p)_{T,\sigma,\mu_{KA}} = (\partial E_-/\partial p)_{T,\sigma,\mu_{KA}} + V_{AgA}/z_A - V_{Ag} \tag{5.47}$$

where V_i is the molar volume of a pure substance i which is a constituent of the reference electrode.

The temperature and pressure coefficients of E_+ or E_- under the appropriate restrictions can be found from the charge–potential curve (either measured directly or obtained by integrating capacity measurements) as a function of chemical potential and temperature or pressure. The identity

$$\begin{aligned}\left(\frac{\partial E_\pm}{\partial T}\right)_{p,\sigma,\mu_{KA}} &= \left(\frac{\partial E_\pm}{\partial T}\right)_{p,\sigma,c} - \left(\frac{\partial E_\pm}{\partial \mu_{KA}}\right)_{T,p,\sigma}\left(\frac{\partial \mu_{KA}}{\partial T}\right)_{p,c} \\ &= \left(\frac{\partial E_\pm}{\partial T}\right) + \left(\frac{\partial E_\pm}{\partial \mu_{KA}}\right)_{T,p,\sigma}\bar{S}_{KA}\end{aligned} \tag{5.48}$$

where $\bar{S}_{KA}$ is the partial molar entropy of the salt KA at the concentration of the solution, or similarly,

$$\left(\frac{\partial E_\pm}{\partial p}\right)_{T,\sigma,\mu_{KA}} = \left(\frac{\partial E_\pm}{\partial p}\right)_{T,\sigma,c} - \left(\frac{\partial E_\pm}{\partial \mu_{KA}}\right)_{T,p,\sigma}\bar{V}_{KA} \tag{5.49}$$

where $\bar{V}_{KA}$ is the partial molar volume of the salt KA at the concentration of the solution, may be used to evaluate the required coefficients from the experimentally determinable coefficients.

The final step is the integration of (5.32) or (5.33):

$$s(\sigma) = s(\sigma^*) - \int_{\sigma^*}^{\sigma} (\partial e_{\pm}/\partial T)_{p,\sigma,\mu_{KA}}\, d\sigma \tag{5.50}$$

$$v(\sigma) = v(\sigma^*) + \int_{\sigma^*}^{\sigma} (\partial e_{\pm}/\partial p)_{T,\sigma,\mu_{KA}}\, d\sigma \tag{5.51}$$

For each integration an integration constant is required. This must be obtained from interfacial tension measurements or from a model. $s(\sigma_m = 0)$ and $v(\sigma_m = 0)$ have been obtained by measurement of the temperature and pressure coefficients of $\gamma_{\sigma_m=0}$ according to (5.30) and (5.31).[22,24]

5.1.2. *Ideal Nonpolarizable Interphase: MA + S|M*

The Gibbs equation takes the form

$$-d\gamma = s\,dT - v\,dp + \Gamma_{MA}\,d\mu_{MA} \tag{5.52}$$

which is closely analogous to the form for a pure phase in equilibrium with a nonionic binary solution. The surface excess of the salt may be determined from

$$\Gamma_{MA} = -(\partial\gamma/\partial\mu_{MA})_{T,p} = -(\nu RT)^{-1}(\partial\gamma/\partial \ln a_{\pm})_{T,p} \tag{5.53}$$

This information may also be obtained by using a reference electrode which is reversible to the anion A. The emf of this cell E_A, which is an ordinary chemical cell without transport, is a measure of the activity of the salt in the solution, and as follows from the elementary theory of such cells,

$$(\partial E_A/\partial \ln a_{\pm})_{T,p} = \nu RT/z_+\nu_+F \tag{5.54}$$

so that (5.53) becomes

$$\Gamma_{MA} = -(z_+\nu_+F)^{-1}(\partial\gamma/\partial E)_{T,p} \tag{5.55}$$

No information about the surface composition can be obtained from (5.55) which cannot also be obtained from (5.53). In particular, there is no way in which the separate contributions of M and A to the interphase can be found from equilibrium measurements with the aid of thermodynamics. It may be assumed that $\nu_+\Gamma_{M^+} = \nu_-\Gamma_{A^+} = \Gamma_{MA}$, but this ignores any contribution from the metal phase to Γ_{M^+} for example.

The excess entropy and volume of the interphase may be obtained from the temperature and pressure derivatives of the interfacial tension, respectively.

5.2. *Pure Metal in Contact with a Solution of Two Salts in a Solvent*

5.2.1. *Ideal Polarized Interphase: KA + JA + S|M*

The Gibbs equation becomes

$$d\gamma = s\,dT - v\,dp + \sigma\,ds_- + \Gamma_{KA}\,d\mu_{KA} + \Gamma_{JA}\,d\mu_{JA} \tag{5.56}$$

Here the solution charge has been considered to be represented by the common anion A. This is the most convenient choice, although, of course, the same information can be derived if either of the cations is chosen. Similarly, the present discussion may readily be transposed to the cases of two salts with a common cation.

At constant temperature and pressure, the surface excesses of the two salts may be obtained directly from

$$\Gamma_{KA} = -(\partial\gamma/\partial\mu_{KA})_{T,p,E_-,\mu_{JA}} \tag{5.57}$$

$$\Gamma_{JA} = -(\partial\gamma/\partial\mu_{JA})_{T,p,E_-,\mu_{KA}} \tag{5.58}$$

However, it may not be convenient to prepare sets of solutions in which (i) μ_{KA} varies while μ_{JA} is constant and (ii) μ_{JA} varies while μ_{KA} is constant. One of these series may be obtained simply by saturating the solution with one salt, but it is not possible to obtain the two series in this way with the solution common to both series as a midpoint in both. To avoid this difficulty it is possible[25] to obtain the two surface excesses from measurements on two other series of solutions which will be called series a and series b. In these series the concentrations of the two salts are varied in an arbitrary but systematic way such that the chemical potentials of the salts vary with respect to one another at rates

$$r_a = \partial\mu_{KA}/\partial\mu_{JA} \tag{5.59}$$

in series a and

$$r_b = \partial\mu_{JA}/\partial\mu_{KA} \tag{5.60}$$

in series b such that

$$r_a \neq r_b^{-1} \tag{5.61}$$

It is not necessary that r_a and r_b be constant through the series but only that these quantities be known for the solutions common to the two series.

Then, in series a, it is possible to measure a quantity

$$\Gamma_a = -(\partial\gamma/\partial\mu_{JA})_{T,p,E_-,a} = \Gamma_{JA} + r_a\Gamma_{KA} \tag{5.62}$$

while, in series b it is possible to measure

$$\Gamma_b = -(\partial\gamma/\partial\mu_{KA})_{T,p,E_-,b} = \Gamma_{KA} + r_b\Gamma_{JA} \tag{5.63}$$

The surface excesses of the two salts may then be obtained by solving these two equations:

$$\Gamma_{JA} = (\Gamma_a - r_a\Gamma_b)/(1 - r_ar_b) \tag{5.64}$$

$$\Gamma_{KA} = (\Gamma_b - r_b\Gamma_a)/(1 - r_ar_b) \tag{5.65}$$

Particularly useful special cases of these general relations occur[26–28] when series a consists of a series of mixtures of two salts of the same valence type at constant

ionic strength, while series b consists of mixtures at constant mole ratio. In series a the salt concentrations are related to the ionic strength I by

$$m_{JA} = x(I/\alpha) \tag{5.66}$$

$$m_{KA} = (1-x)(I/\alpha) \tag{5.67}$$

where

$$\alpha = z_+^2\nu_+ + z_-^2\nu_- \tag{5.68}$$

Hence

$$r_a = \partial \ln [(1-x)\gamma_\pm^\nu(KA)]/\partial \ln [x\gamma_\pm^\nu(JA)] \tag{5.69}$$

If (5.62) is now multiplied by $\partial\mu_{JA}/\partial \ln x$, it becomes with the substitution of (5.69)

$$-[\partial\gamma/\partial \ln x]_{T,p,E,I} = \Gamma_{JA}[\partial\mu_{JA}/\partial \ln x]_{T,p,I} + \Gamma_{KA}\{\partial \ln [(1-x)\gamma_\pm^\nu(KA)]/\partial \ln x\}_{T,p,I} \tag{5.70}$$

or

$$-[\partial\gamma/\partial \ln x]_{T,p,E,I} = \Gamma_{JA} - [x/(1-x)]\Gamma_{KA} + \sum \nu\Gamma_i[\partial \ln \gamma_\pm(i)/\partial \ln x]_{T,p,I} \tag{5.71}$$

where the sum is over the two salts KA and JA. The last term in this equation is often quite small because activity coefficients in binary mixtures of constant ionic strength do not vary much. It may be noted also that the introduction of the well-established Gouy–Chapman model of the diffuse layer, together with the assumption that the ion K is present only in the diffuse layer, leads to the result that the second term on the right-hand side of (5.71) gives the amount of the ion J in the diffuse layer. Hence with these approximations (5.71) gives directly the amount of J which is specifically adsorbed.

For series b Eq. (5.63) may be multiplied by $\partial\mu_{KA}/\partial \ln I$ to obtain

$$-(\partial\gamma/\partial \ln I)_{T,p,E_-,x} = \Gamma_{KA}(\partial\mu_{KA}/\partial \ln I)_{T,p,x} + \Gamma_{JA}(\partial\mu_{JA}/\partial \ln I)_{T,p,x} \tag{5.72}$$

Since

$$(\partial\mu_i/\partial \ln I)_{T,p,x} = 1 + \nu[\partial \ln \nu_\pm(i)/\partial \ln I]_{T,p,x} \tag{5.73}$$

(5.72) becomes

$$-(\partial\gamma/\partial \ln I)_{T,p,E_-,x} = \Gamma_{KA} + \Gamma_{JA} + \sum \nu\Gamma_i[\partial \ln \gamma_\pm(i)/\partial \ln I]_{T,p,x} \tag{5.74}$$

It is evident that Γ_{KA} and Γ_{JA} may be obtained from (5.71) and (5.74) from the two slopes measured at the same composition, that is, where the series a and series b experiments cross.

A further simplification may be obtained in the special case of a very dilute solution of one salt, JA, in an excess of the other, KA, i.e., $x \ll 1$ in (5.66) and (5.67). (5.71) then reduces to

$$-(\partial\gamma/\partial \ln x)_{T,p,E_-} = \Gamma_{JA} \tag{5.75}$$

This technique can give results for only one of the two salts under a given set of circumstances.

It may be noted here that the solution of two salts in a nondissociating solvent is also the case to be considered in a precise analysis of a solution of a single salt in a dissociating solvent, one of the "salts" being the acid or base related to the anion or cation of the other salt. For example, a solution of NaCl in H_2O should be regarded as a solution of NaCl + NaOH or of NaCl + HCl in H_2O. It is then possible to determine the surface excess of both components and, together with the charge σ, using the technique described above, to determine the surface excesses of the three ionic components. (Note that H^+ and OH^- are not independent components because H_2O is chosen as a component—the reference component.) The effect of solvent dissociation may be neglected (and often is) if the concentration of ions derived from the solvent is small compared with that of the other ions (the region of neutral pH) and the adsorption of these ions is weak (they are not specifically adsorbed).

The techniques described here for two salts may be generalized for solutions with more than two salts. However, unless approximations like that leading to (5.75) are made, a considerable amount of information about the nonideal behavior of the solution must be available to extract the information about the surface excesses.

5.2.2. *Ideal Nonpolarizable Interphase: KA + MA + S|M*

The Gibbs equation takes the form

$$-d\gamma = s\,dT - v\,dp + \Gamma_{MA}\,d\mu_{MA} + \Gamma_{KA}\,d\mu_{KA} \tag{5.76}$$

At constant temperature and pressure the surface excesses of the two salts may be found from

$$\Gamma_{MA} = (\partial\gamma/\partial\mu_{MA})_{T,p,\mu_{KA}} = -(\nu_{MA}RT)^{-1}[\partial\gamma/\partial \ln a_{\pm}(MA)]_{T,p,\mu_{KA}} \tag{5.77}$$

$$\Gamma_{KA} = -(\partial\gamma/\partial\mu_{KA})_{T,p,\mu_{MA}} = -(\nu_{KA}RT)^{-1}[\partial\gamma/\partial \ln a_{\pm}(KA)]_{T,p,\mu_{MA}} \tag{5.78}$$

Special types of variations of composition may be used to evaluate these surface excesses, in a manner exactly analogous to that described in the previous section. However, here there is no third equation for the charge, so that in the general case, only the surface excesses of the two salts can be found, not those of their constituent ions, although it is reasonable to suppose that $\Gamma_{K^+} = \nu_+\Gamma_{KA}$ and $\Gamma_{A^-} = \nu_-(KA)\Gamma_{KA} + \nu_-(MA)\Gamma_{MA}$.

The potential of the electrode may be introduced in two alternative ways, in place of one or other of the salt chemical potentials. If the reference electrode is chosen to be reversible with respect to the anion, the result is essentially similar to that of Eqs. (5.54) and (5.55):

$$\Gamma_{MA} = -[z_+(M)\nu_+(MA)F]^{-1}(\partial\gamma/\partial E_A)_{T,p,\mu_{KA}} \tag{5.79}$$

and if Q_A is defined as

$$Q_A = z_+(M)\nu_+(MA)F\Gamma_{MA} \tag{5.80}$$

it is evident that (5.79) has the form of the Lippmann equation.

Alternatively, if the reference electrode is chosen to be reversible with respect to the cation K,

$$(\partial E_K/\partial \mu_{KA})_{T,p,\mu_{MA}} = [z_+(K)\nu_+(KA)F]^{-1} \tag{5.81}$$

and from (5.78)

$$\Gamma_{KA} = [z_+(K)\nu_+(KA)F]^{-1}(\partial\gamma/\partial E_K)_{T,p,\mu_{KA}} \tag{5.82}$$

If Q_K is defined as

$$Q_K = -z_+(K)\nu_+(KA)F\Gamma_{KA} \tag{5.83}$$

(5.82) also has the form of a Lippmann equation. It is evident that, in general, $Q_A \neq Q_K$ and it may be considered that this type of system has two "electrocapillary curves" depending on the conditions chosen for the measurement. Each of these will have a different potential of zero charge where $Q_A = 0$ or $Q_K = 0$, respectively.

If the concentration of MA is small compared with that of KA, it is reasonable to suppose that the concentration of M^+ in the diffuse layer is small and that the M^+ in the interphase is present entirely in the inner layer and at the surface of the metal. Q_A may then be thought of as the physical charge on the metal. With the choice of E_A in place of μ_{MA} as independent variable, (5.78) becomes

$$\Gamma_{KA} = [\nu(KA)RT]^{-1}[\partial\gamma/\partial \ln a_\pm(KA)]_{T,p,E_A} \tag{5.84}$$

which is identical with (5.5) expressed for an electrode reversible to the anion. The identification of the physical charge becomes exact for the limiting case when the concentration of MA approaches zero. Thus this example illustrates that the ideal polarized electrode is a limiting case of the nonpolarizable electrode, as well as showing that the interpretation of Q_A when [MA] is small is consistent with that for the ideal polarized electrode.

5.3. Pure Metal in Contact with a Solution of an Electrolyte and a Nonelectrolyte in a Solvent

5.3.1. Ideal Polarized Electrode: KA + O + S|M

The Gibbs equation takes the form

$$-d\gamma = s\,dT - v\,dp + \sigma\,d\varepsilon_\pm + \Gamma_{KA}\,d\mu_{KA} + \Gamma_O\,d\mu_O \tag{5.85}$$

and the calculation of the surface excesses follows closely that described in Sections 5.1.1 and 5.2.1. The main difference in the practical application of this equation arises from the way in which the chemical potentials of KA and O may

be obtained. Measurements of these quantities are rather rarely available for solutions of interest, although in recent years measurement of activities has become simpler with the use of ion-selective electrodes and gas chromatography.[29,30] The great majority of published measurements which have used (5.85) to obtain Γ_O at constant temperature and pressure have been made with the assumption that the uncharged species O behaves according to the laws of ideal dilute solutions and that μ_{KA} is constant if the concentration of KA is constant. At the same time, a constant reference electrode, like a calomel electrode, is used with the assumption that the liquid junction is unaffected by the presence of the uncharged species. These assumptions are correct in the limit of very low concentration of O, but the range in which they are valid within experimental accuracy is usually unknown. It will certainly depend on the nature of O, of KA, and of the solvent. Estimates of the importance of these approximations have been made for a number of systems.[31,32] One type of system in which great care must be exercised in making approximations is that where O is in fact a second solvent and the whole range of compositions between KA + S and KA + O can be studied. Here, it is essential to use an electrode reversible to one of the ions in the solution and to determine the activity coefficients of the components. The salt activity may be maintained constant by saturating the solution at all solvent compositions and if the solubility is low, the electrolyte may have little effect on the activity coefficients of O and S.

As in the case of the interphases of binary nonelectrolyte mixtures, it is possible only to determine the surface excess of O with respect to the reference component S, using equilibrium thermodynamics. O and S may be interchanged but this leads to no new information. A model may be used to estimate the individual surface concentrations.

5.3.2. *Ideal Nonpolarizable Electrode: MA + O + S|M*

The problems here are essentially the same as those described in Section 5.3.1 combined with those of Section 5.1.2. No additional comment is necessary.

5.4. Binary Alloy in Contact with a Solution of a Single Electrolyte

5.4.1. *Ideal Polarized Electrode: KA + S|M + N*

The Gibbs equation takes the form

$$-d\gamma = s\,dT - v\,dp + \sigma\,d\varepsilon_{\pm} + \Gamma_{KA}\,d\mu_{KA} + \Gamma_N\,d\mu_N \tag{5.86}$$

from which the surface excess of the alloy component N is readily obtained:

$$\Gamma_N = -(\partial\gamma/\partial\mu_N)_{T,p,E,\mu_{KA}} \tag{5.87}$$

The derivative here may be measured at constant composition of the solution and constant potential with respect to any reference electrode. The other

quantities are obtainable in the way described above in Section 5.1.1, with the additional condition that μ_N is constant.

As in the case of the binary solvent mixture, it is evident here that only the excess of N with respect to M can be obtained using equilibrium thermodynamics; the individual surface concentrations may, however, be obtained with the aid of a model.

5.4.2. *Ideal Nonpolarizable Electrode: MA + S|M + N*

The Gibbs equation takes the form

$$-d\gamma = s\,dT - v\,dp + \Gamma_{MA}\,d\mu_{MA} + \Gamma_M\,d\mu_M \tag{5.88}$$

if N is chosen as the reference component in the alloy. The two surface excesses may be found from

$$\Gamma_{MA} = -(\partial\gamma/\partial\mu_{MA})_{T,p,\mu_M} \tag{5.89}$$

$$\Gamma_M = -(\partial\gamma/\partial\mu_M)_{T,p,\mu_{MA}} \tag{5.90}$$

and these two equations may be replaced alternatively by derivatives with respect to a cell potential, using reference electrodes reversible to one or other of the ions in the solution. If the reference electrode is reversible to the anion A, the result is essentially that described in Section 5.1.2:

$$\Gamma_{MA} = -(z_+\nu_+F)^{-1}(\partial\gamma/\partial E_A)_{T,p,\mu_M} \tag{5.91}$$

with the addition of the condition that μ_M is constant.

If the reference electrode is reversible to the cation M, the variation of the cell potential with μ_M at constant μ_{MA} is given by

$$(\partial E_M/\partial\mu_M)_{T,p,\mu_{MA}} = -1/z_+F \tag{5.92}$$

and (5.90) becomes

$$\Gamma_M = (z_+F)^{-1}(\partial\gamma/\partial E_M)_{T,p,\mu_{MA}} \tag{5.93}$$

Hence, in this system, as in that described in Section 5.2.2, two alternative Lippmann equations may be obtained, each giving a different value of the total charge, defined as

$$Q_A = z_+F\Gamma_{MA} \tag{5.94}$$

or as

$$Q_M = -z_+F\Gamma_M \tag{5.95}$$

This multiplicity in the definition of the charge again arises from the fact that the location of the M^+ ions in the interface cannot be defined when there is free interchange of this ion between the two phases.

In the limit of very low concentration of M in the alloy it would appear at first sight that Γ_M should also become very small. However, $z_+\Gamma_M = \Gamma_e$, the

surface excess of electrons, which remains finite, and under these conditions represents the physical charge on the metal side of the interphase. Consequently this system approaches that of Section 5.1.1 as the concentration of M approaches zero (MA is equivalent to KA and N to M) and (5.93) becomes the unique Lippmann equation which gives the physical charge on the metal.

5.5. Binary Alloy in Contact with a Solution of Two Electrolytes

5.5.1. Ideal Polarized Electrode: KA + JA + S|M + N

This system may be analyzed by a combination of the analysis described in Section 5.2.1 with that of Section 5.4.1; no new features are introduced. Three surface excesses and the charge are directly obtainable.

5.5.2. Ideal Nonpolarizable Electrode: KA + MA + S|M + N

It is evident, by extending the treatment described in Section 5.4.2, that three surface excesses may be obtained:

$$\Gamma_{KA} = -(\partial\gamma/\partial\mu_{KA})_{T,p,\mu_{MA},\mu_M} \tag{5.96}$$

$$\Gamma_{MA} = -(\partial\gamma/\partial\mu_{MA})_{T,p,\mu_{KA},\mu_M} \tag{5.97}$$

$$\Gamma_M = -(\partial\gamma/\partial\mu_M)_{T,p,\mu_{KA},\mu_{MA}} \tag{5.98}$$

Each of these equations may in turn be expressed in the form of a Lippmann equation. If the electrode is reversible to the cation K, (5.81) is valid and (5.96) becomes

$$\Gamma_{KA} = [z_+(K)\nu_+(KA)F]^{-1}(\partial\gamma/\partial E_K)_{T,p,\mu_{MA},\mu_M} \tag{5.99}$$

If the electrode is reversible to the anion A, (5.54) is valid and (5.97) becomes

$$\Gamma_{MA} = -[z_+(M)\nu_+(MA)F]^{-1}(\partial\gamma/\partial E_A)_{T,p,\mu_{KA},\mu_M} \tag{5.100}$$

Finally, if the electrode is reversible to the ion M, (5.92) is valid and (5.98) becomes

$$\Gamma_M = (z_+F)^{-1}(\partial\gamma/\partial E_M)_{T,p,\mu_{MA},\mu_{KA}} \tag{5.101}$$

Thus in this system there is the possibility of three alternative Lippmann equations with the corresponding definitions of the total charge. The corresponding ideal polarized electrode may be obtained in two ways: the concentration of MA is decreased, so Eq. (5.100) then becomes the unique Lippmann equation, and the system becomes that described in Section 5.4.1. Alternatively, the concentration of M in the alloy is decreased; then Eq. (5.101) becomes the unique Lippmann equation, and the system becomes that described in Section 5.2.1.

5.6. Semiconducting Phase in Contact with an Electrolyte

From the thermodynamic point of view, there is no difference between a semiconductor and a metal, so that the analysis in the above sections may be applied directly to this type of system.

5.7. Nonionic, Nonconducting Phase in Contact with an Electrolyte

When the phase in contact with the electrolyte cannot support a charge, the situation is essentially that at an ideal polarized electrode with the charge maintained at zero. The analysis then follows directly from that described above for the components of the electrolyte as well as for the excess entropy and volume.

In some cases, however, it may be useful to attribute a charge to the nonconducting phase. For example, at the air–water or oil–water interphase, it is possible to spread an insoluble ionic surface-active agent. Although, the solubility of this compound in the two bulk phases may be so small that the techniques described here are not applicable (i.e., the use of bulk properties to deduce surface properties), the charge due to this compound is readily obtained from the amount to the system and the area of the interphase. It is then convenient to discuss the system as if this charge resided on the nonconducting phase, while all the other compounds are present on the electrolyte side of the interphase.

The interfacial tension in such a system can usually be measured, but the application of the Gibbs equation presents some difficulty because there is usually no way of measuring the chemical potential of a salt of the surface-active ion.

5.8. Pure Ionic Solid in Contact with an Electrolyte Containing One of its Constituent Ions: MA + KA + S|MX

The Gibbs equation takes the same form as that in Section 5.2.2, Eq. (5.76), and the surface excesses of MA and KA may be obtained from (5.77) and (5.78). These may be replaced by derivatives with respect to electrical potentials by considering the cells composed of (i) an electrode reversible to the cation M^{z+} combined with an electrode reversible to the anion A^{z-} and (ii) of an electrode reversible to the cation K^{z+} combined with an electrode reversible to the anion A^{z-}. Case (i) yields (5.79), or with (5.80),

$$Q_A = -(\partial\gamma/\partial E_A)_{T,p,\mu_{KA}} \tag{5.102}$$

while case (ii) yields

$$Q_K = -(\partial\gamma/\partial E_K)_{T,p,\mu_{MA}} \tag{5.103}$$

if E_K is the potential of the cation electrode with respect to that of the anion electrode [this choice of cell direction is the reason for the different sign in (5.103) compared with (5.82)], Q_K being defined by (5.83).

If the concentration of MA is small compared with that of KA, it is possible to assume, as in Section 5.2.2, that the concentration of M^+ in the diffuse layer is small in comparison with that of K^+; the M^{z+} in the interphase can then be assumed to be present entirely in the inner layer and in the crystal surface. Q_A may then be thought of as the physical charge on the crystal. As in Section 5.2.2 the surface excess of KA may then be calculated from (5.84).

This is the type of assumption usually used for ionic crystals such as AgI, which are most frequently studied in the colloidal form by a titration technique.[33] A typical system is $KNO_3 + AgNO_3 + H_2O|AgI$ in which the concentration of $AgNO_3$ is always much less than that of KNO_3. Of course, γ cannot be measured and the surface excess of KNO_3 is found using a cross-differential relation analogous to (5.13). The charge $\sigma = Q_A$ is determined directly by the difference between the amount of $AgNO_3$ added to the solution and the amount which remains after equilibration with a sol of AgI. This difference gives the difference in total charge of the colloidal system before and after this addition of $AgNO_3$. The shape of the total charge curve as a function of the potential E_A is thus found. Its position on the charge axis is fixed by a determination of the point of zero charge (for example, by studying the electrophoresis, if it can be assumed that there is no specific adsorption of the salt $KA = KNO_3$). The charge on unit area of interphase depends on a knowledge of the surface area of the colloid. The most reliable way to determine this is with the aid of diffuse layer theory.

5.9. Ionic Crystal Containing Two Species in Solid Solution in Contact with an Electrolyte Containing One of the Constituent Ions: MA + KA + S|MX + NX

By analogy with the alloy system of Section 5.4.2, the Gibbs equation takes the form

$$-d\gamma = s\,dT - v\,dp + \Gamma_{KA}\,d\mu_{KA} + \Gamma_{MA}\,d\mu_{MA} + \Gamma_{MX}\,d\mu_{MX} \qquad (5.104)$$

if NX is chosen as the reference component in the crystal phase. Thus at constant temperature and pressure, three surface excesses may be determined:

$$\Gamma_{MA} = -(\partial\gamma/\partial\mu_{MA})_{T,p,\mu_{KA},\mu_{MX}} \qquad (5.105)$$

$$\Gamma_{KA} = -(\partial\gamma/\partial\mu_{KA})_{T,p,\mu_{MA},\mu_{MX}} \qquad (5.106)$$

$$\Gamma_{MX} = -(\partial\gamma/\partial\mu_{MX})_{T,p,\mu_{MA},\mu_{KA}} \qquad (5.107)$$

As before, each of these equations may be replaced in turn by a Lippmann equation by considering, respectively, cells with electrodes reversible to (i) M^{z+} and A^{z-}, (ii) A^{z-} and K^{z+}, (iii) X^{z-} and M^{z+}. When the concentration of MA in solution is small compared with that of KA, the first of these is the most useful and it gives what may be assumed to be the physical charge on the crystal as described in the previous section. An alternative definition of the physical

charge is possible if (iii) is used with a small concentration of MX in the crystal. In the latter the interface becomes ideal nonpolarized in the limit and may be discussed as described either under Section 5.6 or Section 5.7, depending on the conductivity.

5.10. Ion-Exchange Membrane in Contact with a Binary Electrolyte: MA + KA + S|MX + KX

In comparison with the previous example, this has one degree of freedom fewer because there is an additional condition of equilibrium (the equilibrium of K^{z+} across the interphase). Hence the Gibbs equation takes the form

$$-d\gamma = s\,dT - v\,dp + \Gamma_{KA}\,d\mu_{KA} + \Gamma_{MA}\,d\mu_{MA} \qquad (5.108)$$

which is formally identical to that in Section 5.2.2, Eq. (5.76), or that of Section 5.8. As before two quantities Γ_{KA} and Γ_{MA} may be determined from experiments at constant temperature and pressure, or the equivalent charges Q_A and Q_K may be expressed in terms of the two alternative Lippmann equations. In contrast to the systems in Sections 5.2.2 and 5.8, it is not possible, in general, to find the physical charge by considering a system with a low concentration of MA in comparison with that of KA. This is because lowering the concentration of MA causes also a lowering of the equilibrium concentration of MX in the membrane and the limiting case reduces to a system with a single degree of freedom at constant temperature and pressure. This limit is equivalent to the system in Section 5.1.2 and only Γ_{KA} can be determined. It is possible that, in particular cases where the membrane absorbs M^{z+} with a high degree of preference over K^{z+}, a physical charge may be obtained with a good approximation by the route described in Section 5.2.2 or in Section 5.8.

5.11. Three-Phase Electrode, in which a Gaseous Component is in Equilibrium with a Component in Solution

Because of its importance, a particular example will be taken here: a platinum electrode at which hydrogen gas is in equilibrium with hydrogen ions in the solution: HA + KA + S|H_2|Pt. The Gibbs equation may be written in the form

$$-d\gamma = s\,dT - v\,dp + \Gamma_{HA}\,d\mu_{HA} + \Gamma_{KA}\,d\mu_{KA} + \Gamma_{H}\,d\mu_{H} \qquad (5.109)$$

if it is recognized that

$$d\mu_{H} = \tfrac{1}{2}\,d\mu_{H_2} \qquad (5.110)$$

and H is chosen as a component rather than H_2 because the form H is likely to predominate in the interphase. Note that, in this electrode, H_2 is strictly a solution component whose concentration is determined by the pressure in the gas phase above the solution and that the interphase is, of course, still one

between the electrolyte and the metal. However, because of the very low concentration of H_2 in the solution, it is still possible to treat the electrolyte as if it were simply a solution of two electrolytes in a solvent.

The surface excesses of the three components at constant temperature and pressure are obtainable from

$$\Gamma_{HA} = -(\partial\gamma/\partial\mu_{HA})_{T,p,\mu_{KA},\mu_H} \tag{5.111}$$

$$\Gamma_{KA} = -(\partial\gamma/\partial\mu_{KA})_{T,p,\mu_{HA},\mu_H} \tag{5.112}$$

$$\Gamma_H = -(\partial\gamma/\partial\mu_M)_{T,p,\mu_{KA},\mu_{HA}} \tag{5.113}$$

or from the related Lippmann equations

$$Q_A = \nu_+(HA)F\Gamma_{HA} = -(\partial\gamma/\partial E_A)_{T,p,\mu_{KA},\mu_H} \tag{5.114}$$

$$Q_K = -z_+(K)\nu_+(KA)F\Gamma_{KA} = -(\partial\gamma/\partial E_K)_{T,p,\mu_{HA},\mu_H} \tag{5.115}$$

$$Q_H = -F\Gamma_H = -(\partial\gamma/\partial E_H)_{T,p,\mu_{KA},\mu_{HA}} \tag{5.116}$$

where the potentials E_A, E_K, and E_H are, respectively, with reference to electrodes reversible to the anion A^{z-}, the cation K^{z+}, and the hydrogen ion.

Frumkin[34–36] and his colleagues developed a detailed analysis of the behavior of the electrodes of the platinum metals based essentially on equations such as (5.114) and (5.116). Q_H, which can be considered the charge equivalent to the surface excess of hydrogen atoms, was termed "the total charge of the first kind" and Q_A, the charge equivalent to the surface excess of hydrogen ion, was termed "the total charge of the second kind." Neither of these is equal to the physical charge on the double layer in the general case, but further discussion is possible with the aid of nonthermodynamic assumptions.

Because of the equilibrium between $H^+ + e$ and H at the interphase, it is not possible to find from equilibrium thermodynamics how much of the surface excess of hydrogen ions $\nu_+(H)\Gamma_{HA}$ is actually present as ions. The same is true of the surface excess of hydrogen atoms. Frumkin defined the terms A_{H^+} and A_H to represent the quantities of H^+ and H actually present in the interphase. These quantities are not, in general, equal to the Gibbs surface excess of these species, nor are they in general accessible from thermodynamics like the Gibbs surface excesses, although it must always be true that

$$\nu_+(HA)\Gamma_{HA} + \Gamma_H = A_{H^+} + A_H \tag{5.117}$$

$$= (Q_A - Q_H)/F \tag{5.118}$$

In terms of these quantities, the actual charge on the interphase may be introduced in the following way: with the choice of components used here, the interphase is regarded as being composed of H, Pt, HA, KA, H_2O or, if the acid is taken to be completely ionized, H, Pt, H^+, K^{z+}, A^{z-}, H_2O with the condition that the net charge due to H^+, K^{z+}, and A^{z-} be zero. However, if some of the $H^+(\Gamma_{H^+} - A_{H^+})$ has actually crossed to the metal and become H this contributes

an equivalent positive charge σ per unit area to the metal and this may be regarded as the actual charge on the metal, or,

$$\sigma = F(\Gamma_{H^+} - A_{H^+}) \tag{5.119}$$

$$= F[\nu_+(HA)\Gamma_{HA} - A_{H^+}] \tag{5.120}$$

Alternatively, if some of the H adsorbed on the metal surface ($\Gamma_H - A_H$) has actually crossed to the solution side to become H^+, this contributes an equivalent negative charge to the electrode:

$$-\sigma = F(\Gamma_H - A_H) \tag{5.121}$$

It is evident that (5.120) and (5.121) satisfy (5.117). It must be emphasized here that it is assumed that the ions K^{z+} and A^{z-} do not transfer any charge to the metal; this condition is achieved with most certainty, if these ions are not specifically adsorbed, i.e., they are present only in the diffuse part of the double layer.

In the usual type of charging curve experiment, in which a low-density current is passed into the electrode (or in a slow-speed linear-sweep voltammogram) the equilibrium between H_2 and the H on the surface of the metal is not maintained, although μ_{HA} and μ_{KA} are kept constant. Hence the experimental charge corresponds to Q_H, and a capacity

$$C_H = (\partial Q_H/\partial E_H)_{T,p,\mu_{HA},\mu_{KA}} \tag{5.122}$$

can be found from these measurements.

The other charges Q_A and Q_K are much more difficult to obtain experimentally because of the difficulty of maintaining μ_H constant while allowing μ_{KA} and μ_{HA} to vary (this may be done only when equilibrium between H_2 and H is maintained). On the other hand, it may be possible to study the effect of change of solution composition under conditions where Γ_H remains constant, by using an electrode at open circuit (Frumkin called this an "isoelectric" change). If the last term in (5.109) is substituted by $Q_H\,dE_H$, the cross-differential relationship [cf. (3.81)]

$$(\partial E_H/\partial \mu_{HA})_{T,p,\mu_{KA},Q_H} = -(\partial \Gamma_{HA}/\partial Q_H)_{T,p,\mu_{KA},\mu_{HA}} \tag{5.123}$$

can be obtained. (5.123) may also be written

$$(\partial E_H/\partial \mu_{KA})_{T,p,\mu_{KA},Q_H} = -(\partial \Gamma_{HA}/\partial E_H)_{T,p,\mu_{KA},\mu_{HA}}/C_H \tag{5.124}$$

using the definition of C_H in (5.122). If it is now assumed in the presence of an excess of salt KA ([KA] $\gg$ [HA]) and in the absence of specific adsorption of H^+ that $A_{H^+} = 0$, i.e., there is in fact no H^+ in the interphase; then it follows from (5.120) that

$$(\partial \Gamma_{HA}/\partial E_H)_{T,p,\mu_{KA},\mu_{HA}} = [\nu_+(HA)F]^{-1}(\partial \sigma/\partial E)_{T,p,\mu_{KA},\mu_{HA}}$$

$$= [\nu_+(HA)F]^{-1}C \tag{5.125}$$

where C is the double-layer capacity analogous to that defined at an ideal polarized electrode. This quantity may thus be obtained from (5.124) in the form

$$C = -C_H[\nu_+(HA)F](\partial E_H/\partial \mu_{HA})_{T,p,\mu_{KA},Q_H} \tag{5.126}$$

using experimental results for the capacity C_H together with those for the isoelectric potential shift with variation of the activity of HA.

5.12. Electrode with a Surface Species in Equilibrium with, but not Present in, a Bulk Phase

This type of system has in fact been discussed in the previous section, because once the platinum–metal–hydrogen system is no longer in equilibrium with molecular hydrogen, the chemical potential of the atomic hydrogen adsorbed at the electrode can no longer be controlled directly by the experimenter, although of course it is controlled indirectly in terms of the concentration of HA and the electrode potential. The same type of situation exists in the region of oxygen adsorption on platinum metals, where it is practically impossible to equilibrate the adsorbed oxygen species with gaseous molecular oxygen. However, there is evidence that, over a limited range of conditions, the adsorbed oxygen species are in equilibrium with the electrolyte phase according to such reactions as

$$H_2O \rightleftarrows OH_{ads.} + H^+ + e \tag{5.127}$$

$$H_2O \rightleftarrows O_{ads.} + 2H^+ + 2e \tag{5.128}$$

Provided that such equilibria are set up, it is possible to treat this situation thermodynamically in a way precisely analogous to that described in the previous section.

Similar situations arise when the interphase is between an amphoteric oxide and an electrolyte, or between a nonconducting phase and an electrolyte where an insoluble film is spread which can undergo acid–base reactions. These equilibria may be represented

$$M - OH + H^+_{solv.} \rightleftarrows MOH_2^+ \tag{5.129}$$

$$M - OH \rightleftarrows MO^- + H^+_{solv.} \tag{5.130}$$

where M − OH may be regarded as the amphoteric oxide or a molecule in the insoluble film. It would then be possible to write the Gibbs equation in the form of (5.109), where the term $\Gamma_H\, d\mu_H$ represents now the variation of the H adsorbed according to (5.129) and (5.130). However, when the nonelectrolyte phase is nonconducting, there is no independent way of varying μ_H, as could be done by varying the potential of a metal electrode. Hence μ_H is always linked to μ_{HA} by the equilibrium condition representing (5.129) and (5.130) and only the sum of Γ_{HA} and Γ_H can be determined. Again this means that it is not possible thermodynamically to divide the surface excess of hydrogen into a part due to ions

present in the ionic part of the double layer and a part due to hydrogen bonded to the oxide or the surfactant.

An assumption that is frequently made is that analogous to the one described above in Section 5.8. Provided that [HA] is small in comparison with [KA] and that KA is not specifically adsorbed, the concentration of H^+ in the solution side of the interphase may be neglected and all the adsorbed H^+ may be regarded as forming the charge on the nonelectrolyte phase. With these assumptions, the Gibbs equation may be written as

$$-d\gamma = s\,dT - v\,dp + \sigma\,dE_H + \Gamma_{KA}\,d\mu_{KA} \tag{5.131}$$

where E_H is defined, at constant temperature and pressure, by

$$dE_H = [\nu RT/\nu_+(HA)F]\,d\ln a_{HA} \tag{5.132}$$

The hydrogen ion (or any other ion playing a similar role in an analogous situation) is often described as the "potential-determining" ion, and (5.132) is described as the "Nernst equation" of the interfacial equilibrium. The latter description may be misleading; what (5.132) really represents is the measurement of an activity in the bulk electrolyte in terms of the emf of an equilibrium cell, which has in fact nothing to do with the interphase being studied.

The charge σ in (5.131) may be determined by the titration method described in (5.8) and the surface excess of KA from the dependence of the charge potential curves on μ_{KA} using a cross-differential relation analogous to (5.13).

6. Partial Dissociation and Partial Charge Transfer

The thermodynamic relations described above are valid irrespective of the state of dissociation of the electrolytes present in the system. The chemical potential of a weak acid HA, for example, will of course depend on its degree of dissociation, but provided that the correct value of μ_{HA} is known, this value may be used in the calculation of the surface excess of HA without knowledge of the degree of dissociation. The resulting surface excess Γ_{HA}, correspondingly, gives no information about the degree of dissociation of this species in the interphase. Inferences may be drawn from other information: for example, if it is found that HA is strongly adsorbed from solutions in which HA is known to be present predominantly as the undissociated molecule, while it is not adsorbed from solutions in which it is known to be fully ionized; then it is reasonable to suppose that HA is present in the interphase as the undissociated molecule.

Another type of argument which is less reliable concerns the shift of potential caused by the adsorption of HA at constant charge on the electrode. If HA is known to be essentially nonpolar, this shift might be expected to be small when the undissociated molecule adsorbs, while it could be large if HA adsorbed in the form of ions. This argument is less certain because the adsorption

of a nonpolar molecule may cause substantial modification of double-layer structure leading to a marked potential shift, whereas the ions could adsorb with displacement of other ions of the same type leading to a very small potential shift. Depending on the circumstances, it may or may not be possible to draw a clear distinction using this type of argument.

A similar problem arises with the possibility that adsorbed ions or molecules may bond to the interface with the partial transfer of charge to the other phase. The thermodynamic treatment of adsorption is independent of the occurrence of such charge transfer so long as it deals with the surface excess quantities Γ. However, when these quantities are related to charges by multiplying by factors such as z_+F, it must be recognized that some care is required in the interpretation of this charge. It may be regarded in a purely formal way as a charge equivalent to the surface excess, but if it is interpreted as a physical charge, this involves the assumption that there is no change in charge on the ion when it adsorbs. Other evidence is required to validate this assumption. This was clearly recognized by Lorenz.[12]

This problem has been discussed in terms of the quantity

$$l = (\partial \mu_{ij}/F\,\partial E)_{\Gamma_{ij}} \tag{6.1}$$

to which Vetter and Schultze[37] have given the term "electrosorption valency" which was chosen to indicate its relation with a charge transfer process. The name is an unfortunate one because the quantity, which is a well-defined thermodynamic quantity, may represent a number of effects, only one of which is partial charge transfer. The alternative ("formal charge transfer coefficient") proposed by Frumkin[38] is only slightly better. Barker stated clearly[39] that l is the average number of electrons (i.e., unit charges) supplied to the electrode when one molecule of species ij is absorbed at constant potential. The physical contributions to l were summarized by Vetter and Schulze[37] and include, besides partial charge transfer, dipole orientation of adsorbed species and the replaced solvent as well as movement of free charges within the interphase. Analysis of this important problem is beyond the scope of formal thermodynamics, although this can indicate the various experimental routes for the determination of l [see (3.81), for example].

References

1. J. W. Gibbs, *Trans. Conn. Acad.* 3, 108, 343 (1878).
2. R. Defay, I. Prigogine, A. Bellemans, and D. H. Everett, *Surface Tension and Adsorption*, Longmans, London (1966).
3. J. E. Verschaffelt, *Bull. Cl. Sci. Acad. R. Belg.* 22, 373 390, 402 (1936).
4. E. A. Guggenheim, *Trans. Faraday Soc.* 36, 397 (1940).
5. R. P. Feynman, R. B. Leighton, and M. Sands, *Lectures on Physics*, Vol. II, Addison-Wesley, Reading, Massachusetts (1965).
6. G. Lippmann, *Ann. Chim. Phys. 5* 5, 494 (1875).

7. A. N. Frumkin, *Philos. Mag.* **40**, 363 (1920).
8. D. C. Grahame, *Chem. Rev.* **41**, 441 (1947).
9. D. C. Grahame and R. B. Whitney, *J. Am. Chem. Soc.* **64**, 1548 (1942).
10. F. O. Koenig, *J. Phys. Chem.* **38**, 339 (1934).
11. B. V. Ershler and A. N. Frumkin, *Trans. Faraday Soc.* **35**, 1 (1939).
12. W. Lorenz and G. Salie, *Z. Phys. Chem.* **218**, 259 (1961); W. Lorenz, *Z. Phys. Chem.* **219**, 421 (1962).
13. D. H. Everett, *Trans. Farday Soc.* **46**, 453 (1950).
14. R. Parsons, *Can. J. Chem.* **37**, 308 (1959).
15. A. N. Frumkin, O. A. Petrii, and B. B. Damaskin, *J. Electroanal. Chem.* **27**, 81 (1970).
16. R. Parsons, *Trans. Faraday Soc.* **51**, 1518 (1955).
17. R. Defay, I. Prigogine, A. Bellemans, and D. H. Everett, *Surface Tension and Adsorption*, Longmans, London (1966), Chap. 17.
18. R. G. Linford, *Chem. Soc. Rev.* **1**, 445 (1972); *J. Electroanal. Chem.* **43**, 155 (1973).
19. P. R. Couchman and C. R. Davidson, *J. Electroanal. Chem.* **85**, 407 (1977).
20. A. Ya Gokhstein, *Poverknostnoe Natyazhenie Tverdykh Tel i Adsorbtsiya*, Izd. Nauka, Moskva (1976).
21. D. C. Grahame and B. A. Soderberg, *J. Chem. Phys.* **22**, 440 (1954).
22. G. J. Hills and R. Payne, *Trans. Faraday Soc.* **61**, 326 (1965).
23. J. A. Harrison, J. E. B. Randles, and D. J. Schiffrin, *J. Electroanal. Chem.* **48**, 359 (1973).
24. G. J. Hills and S. Hsieh, *J. Electroanal. Chem.* **58**, 289 (1975).
25. R. Parsons and S. Trasatti, *Trans. Faraday Soc.* **65**, 3314 (1969).
26. H. D. Hurwitz, *J. Electroanal. Chem.* **10**, 35 (1965).
27. E. Dutkiewicz and R. Parsons, *J. Electroanal. Chem.* **11**, 100 (1966).
28. S. Lakshmannan and S. K. Rangarajan, *J. Electroanal. Chem.* **27**, 127 (1970).
29. D. M. Mohilner, L. M. Bowman, S. J. Freeland, and H. Nakodomari, *J. Electrochem. Soc.* **120**, 1658 (1973).
30. D. M. Mohilner and H. Nakodomari, *J. Phys. Chem.* **77**, 1594 (1973).
31. A. de Battisti and S. Trasatti, *J. Electroanal. Chem.* **54**, 1 (1974).
32. B. A. Abd-el-Nabey, A. de Battisti, and S. Trasatti, *J. Electroanal. Chem.* **56**, 101 (1974).
33. J. Lyklema, *Trans. Faraday Soc.* **59**, 418 (1963).
34. A. N. Frumkin and A. Shlygin, *Acta Physicochim. URSS* **5**, 819 (1936).
35. A. N. Frumkin, *Adv. Electrochem. Electrochem. Eng.* **3**, 287 (1963).
36. A. N. Frumkin and O. A. Petrii, *Electrochim. Acta.* **20**, 347 (1975).
37. K. J. Vetter and J. W. Schultze, *Ber. Bunsenges. Phys. Chem.* **76**, 920, 927 (1972); *J. Electroanal. Chem.* **44**, 63 (1973); **53**, 67 (1974).
38. A. N. Frumkin, B. B. Damaskin, and O. A. Petrii, *J. Electroanal. Chem.* **53**, 57 (1974).
39. G. C. Barker, *Pure Appl. Chem.* **15**, 239 (1966).
40. The reader should also consult D. M. Mohilner and T. R. Beck, *J. Phys. Chem.* **83**, 1160 (1979), which appeared after this chapter was completed.

2

The Electrode Potential

SERGIO TRASATTI

1. Introduction

"Electrode potential" is certainly the most used term in electrochemistry, and is very likely to be one of the most popular in the entire field of chemistry. Sound knowledge of the physical and chemical phenomena involved in the establishment of electrode potentials does not correspond, however, to the very wide use of the term. None would be surprised by a 0.059-V change in potential of a hydrogen electrode as the activity of H^+ in solution is changed by a power of ten, but it would certainly be surprising if everyone knowing this were actually able to give a physical description of *what* is occurring at the electrode as the concentration of H^+ is changed and *why* the electrode potential changes. Further, when the term "electrode potential" is used, it generally refers to the potential as experimentally measured with respect to a given reference electrode. Conceptually, however, no reference electrode must necessarily be involved for an "electrode potential" to be defined. It follows that the physical meaning behind the same term "electrode potential" is quite different in the two cases. This is certainly not as well recognized as the term itself is.

Reasons for this situation are probably to be sought in the existence of two different approaches to electrochemistry: a traditional (thermodynamic) one[1] and a modern (physical) one.[2] The two approaches certainly do not lead to

SERGIO TRASATTI • Laboratory of Electrochemistry, University of Milan, 20133 Milan, Italy.

different results. Nevertheless, the way the various quantities are presented is different, and especially the concepts which are focused upon are different. Traditional electrochemistry derives from the concept of equality between chemical and electrical energies in electrode reactions. Thus the cell potential difference, E, is presented as determined by the free-energy change for the chemical reaction taking place there. The electrode potential then ensues from an arbitrary breaking up of E into two terms each assigned to one of the two electrodes on the basis of some standards of potential constituted by the reference electrodes. Eventually, the potential of an electrode results conceptually to be strictly bound up to the partial electrochemical reaction taking place there. This approach emphasizes chemical and energetic aspects of the problem, but the physical picture is certainly obscured.

The impact on electrochemistry occurs in various fields precisely through the thermodynamic approach which, thanks to its energetic implications, is very often all that is needed to be known for certain applications. A consequence of this has been that the physical aspect of electrochemistry (the interdisciplinary one) has for long been concealed and has emerged with difficulty. The modern approach moves from the physical description of the region of contact between a metal and a solution to arrive eventually at the electrochemical cell. Energetic aspects are less evident in this case and this is the reason why in many practical situations such an approach to electrochemistry is not favored. It is, however, increasingly clear that the behavior of metals in catalysis, electrochemistry, surface science, etc., is governed by the same electronic and surface properties.[3] It follows that a description on a molecular basis of the interfacial region is able to give a general picture capable of breaking down the traditional barriers between the various branches of science.

The merits of the physical approach to electrochemistry with respect to the traditional one are now indisputable especially from the educational point of view.[2] A detailed consideration of the physical meaning of electrode potential is therefore felt to be necessary. The study of the mechanism of establishing an electrode potential dates back to the end of last century when Nernst[4] developed his theory. Nernst's approach has been used for almost a hundred years, so the description of the basis of electrode potentials in textbooks of electrochemistry still relies essentially on the early arguments. However, Nernst's equation predicts indefinite results as the concentration of ions decreases below analytically detectable levels. Such a situation is not understandable unless the basic principles governing the contact between a metal and a *pure* solvent are well established.

The aim of this chapter is to present a self-contained approach to the concept of electrode potential including the basic principles of electrochemistry. The present approach will rely as much as possible on physical models, and is thus closely bound to the physics of metals. The discussion will be limited to metallic phases and polar liquids (possible solvents), but an extension of these concepts

to other less general cases is immediate, provided the nature of the phases in contact is known. Quantitative data will be restricted to metal–water interfaces.

Previous discussions[5–18] regarding the electrode potential were especially focused on the meaning of the splitting of the measured cell potential difference into two electrode potentials in terms of electric potential drop at the single interfaces. Various solutions have been suggested which represent simple steps on the way to the true single electrode potential. The consideration of the role of solvated electrons in all of the aspects of an electrochemical cell[19–21] will be shown to be able to produce a definite unifying view of the electrochemical equilibrium.

2. Components of the Electrode Potential

2.1. Bulk Structure of Metals

A metal may be envisaged as a giant atom whose nucleus consists of the ion cores of the single atoms and whose valence electrons consist of the outlying electrons of the component atoms.[22] The lattice formed by the ion cores is immersed in a sea of valence electrons which can move freely within the crystal provided electroneutrality is preserved at any point.

The energy binding electrons to the interior of a metal M is the electrochemical potential,[23–26] $\tilde{\mu}_e^M$, which in the particular case of uncharged phase takes the name of real potential, α_e^M. It follows that

$$\tilde{\mu}_e^M = \alpha_e^M - e\psi^M \tag{2.1}$$

where ψ^M is the mean electrostatic potential just outside the metal (outer potential). ψ^M is simply a function of the free-charge density on the metal (σ^M) and vanishes as $\sigma \to 0$. Equation (2.1) implies that α_e^M is not affected by the presence of free charges on the phase.

The minimum work required to extract electrons from an uncharged metal is the work function,[22,27–29] Φ^M. It follows that

$$\Phi^M = -\alpha_e^M \tag{2.2}$$

where both quantities are measured in electron volts. The electron work function is a measurable quantity, and is a characteristic property of the phase.[27,29] The definition of electron work function implies that either a metal is not in equilibrium with vacuum, or, if in equilibrium, this is destroyed when electrons are experimentally extracted so that it is not operative.

Physically, the energy of electrons in metals is the sum of two contributions, a potential and a kinetic energy[22,28,30] (Figure 1). The former in turn consists of a bulk and a surface contribution.[31,32] The bulk contribution to the potential energy originates from the coulombic interaction of the negative charges of

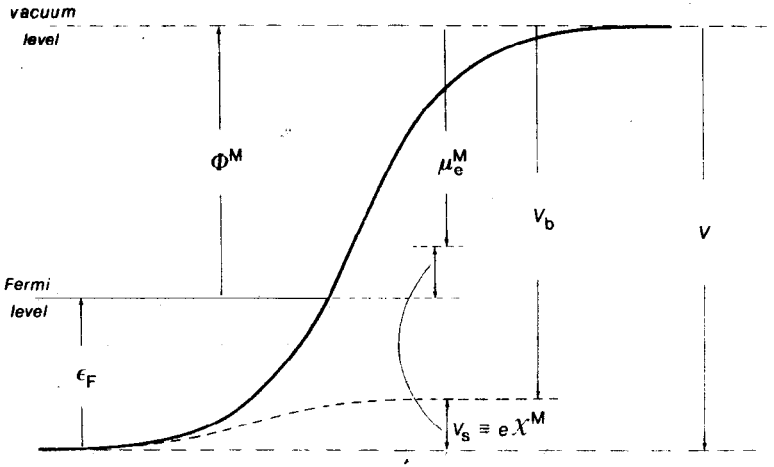


Figure 1. Potential energy profile at the metal–vacuum boundary. Bulk and surface contributions to V are separately shown.

electrons with the positive charges of the ion cores. Although the phase is electrically neutral, each electron statistically has at its disposal a given space from which all other electrons are excluded. The positive charge, the electron "sees" in that space, is responsible for the bulk potential energy.[33] The image charge is accounted for by this energy,[30] which physicists call the exchange and correlation part of the potential energy,[28,31,32] the surface contribution, discussed later, being called the electrostatic part.

The other form of energy is the kinetic energy.[22] All electrons in a metal are on the average attracted to the same extent by the lattice of positive charges but they actually interact with each other and, by the Pauli principle, only two electrons with opposite spins can be in exactly the same conditions. For this reason, electrons are actually placed on levels of increasing kinetic energy filled up to accommodate all of them. The highest level filled with electrons at 0 K is known as the *Fermi level*. If the kinetic energy of electrons is denoted by ε, the kinetic energy of electrons in the Fermi level will be denoted by ε_F. Fermi level is the term often used by physicists[22] to denote ε_F, which should be termed preferably *kinetic Fermi energy*. It is calculable according to the simple Sommerfeld model by the following equation[22,27]:

$$\varepsilon_F = (h^2/8\pi^2 m^*)[3\pi^2 D(e)]^{2/3} \tag{2.3}$$

where m^* is the effective mass of electrons and $D(e)$ is the electron density.

The potential energy is a negative, stabilizing energy; the kinetic energy is a positive, destabilizing energy. The latter operates practically as a repulsion. It follows that

$$\Phi^M = -(\varepsilon_F + V) = -(\varepsilon_F + V_b + V_s) \tag{2.4}$$

where V_b and V_s are the bulk and the surface contribution to V, respectively. In Eq. (2.4) the work function is defined on the basis of electrons at the Fermi level. Such electrons possess the highest kinetic energy and are those most unstable in the metal. As a consequence, they are the first to leave the metal in exchanges with the environment. Moreover, the Fermi level is the first to accept electrons injected into the metal from the exterior.

Electrons at rest in a vacuum at infinity are usually assumed as the reference state. There, due to the absence of interactions with other phases or particles, and the disappearance of kinetic energy it may be assumed that $V = 0$ and $\varepsilon = 0$. Due to entropic effects, the actual free energy of electrons at infinity may differ somewhat from zero,[34] but this aspect will be neglected here. A property of electrons at the Fermi level is that they possess the same energy throughout the crystal. If this were not the case, electrons would travel between points at different energy until the latter is again made uniform.

According to the accepted definition of electrochemical potential in the field of chemistry,[35] the electron work function is given by[23]

$$\Phi^M = -\mu_e{}^M + e\chi^M \tag{2.5}$$

where $\mu_e{}^M$ is the chemical potential of electrons in phase M and χ^M is the surface potential of the phase related to the presence of dipole layers.[25,26] Some confusion may arise because some physicists call (ε_F)[22,27,30,36] the chemical potential and others use ($\varepsilon_F + V_b$),[31,33,37,38] according to Eq. (2.4). Since, according to Eq. (2.5), the chemical potential is the energy binding electrons to the interior of an ideal metal with no surface effects, it follows that (Figure 1)

$$\mu_e{}^M \equiv \varepsilon_F + V_b \tag{2.6}$$

and

$$\chi^M \equiv V_s/e \tag{2.7}$$

$\mu_e{}^M$ is not amenable to direct experimental measurement and can only be calculated on the basis of models.[23] This task is well inside the field of theoretical physics. $\mu_e{}^M$ is evaluable with satisfactory approximation only for *sp* metals. The calculation is unsatisfactory for *d* metals. In addition, even within the group of *sp* metals calculations by different authors are satisfactorily consistent only for alkali metals. Values of $\mu_e{}^M$ available in the literature[27,28,30,31,37,39–41] have been simply averaged and are reported in Table 1. Values of ε_F and V are also reported for some metals.[22]

Charging a metal phase corresponds to changing V. The *whole* energy band is shifted downwards by the presence of a positive charge on M because more work must be done to extract electrons from the Fermi level. The opposite occurs with a negative charge. A charge does not affect the value of ε_F, and for simplicity also χ^M is assumed to be unperturbed. This is tantamount to simply shifting the electron density curve towards either the interior or the exterior of the metal phase depending on the sign of charge.

Table 1

Experimental Work Function (Φ) and Calculated Values of Chemical Potential of Electrons (μ_e), Surface Potential of Metals (χ), Kinetic Fermi Energy (ε), and Potential Energy (V) for Polycrystalline Metals

Metal	Φ^M (eV)	$-\mu_e^M$ (eV)	χ^M (V)	χ^M (V)[b]	ε_F (eV)[c]	$-V$ (eV)[d]
Li	3.10	1.80 ± 0.3	1.45 ± 0.2	1.3 ± 0.3	4.72	7.8
Na	2.70	2.06 ± 0.1	0.75 ± 0.1	0.6 ± 0.1	3.23	5.9
K	2.30	2.10 ± 0.1	0.30 ± 0.05	0.2 ± 0.1	2.12	4.4
Rb	2.20	2.09 ± 0.1	0.26 ± 0.05	0.1 ± 0.1	1.85	4.0
Cs	1.90	1.97 ± 0.2	0.10 ± 0.1	−0.1 ± 0.2	1.58	3.5
Mg	3.65	1.7[a]	1.9	—	7.13	10.8
Ca	2.70	1.5[a]	1.2	—	4.68	7.4
Sr	2.75	1.8[a]	1.0	—	3.95	6.7
Ba	2.35	1.5[a]	0.9	—	3.65	6.0
Zn	4.30	1.7 ± 0.4	2.2	2.3 ± 0.3 2.15[e]	9.39	13.7
Cd	4.12	2.2 ± 0.3	1.7	1.9 ± 0.3 1.53[e]	7.46	11.6
Al	4.20	0.8[a]	3.4	—	11.63	15.8
In	4.08	2.08 ± 0.3	1.5	1.4 ± 0.3	8.60	12.7

[a] Reference 42, from ($\Phi^M - e\chi^M$).
[b] From Eq. (2.4).
[c] From Eq. (2.3).
[d] From Eq. (2.4).
[e] Reference 95.

2.2. The Surface of Metals

Electrons in the bulk of metals experience a symmetric field of forces originating from the ion cores. It follows that μ_e^M is an isotropic quantity. If a metal could be cut without perturbing its original structure, electron and ion densities at the newly created surface would be found to be equal to those in the bulk with mutual compensation of charge. Under these circumstances a work equal and opposite to the chemical potential would be necessary to extract electrons from the Fermi level.

Actually, when a new surface is created on a metallic phase, electrons at the boundary with vacuum experience unbalanced forces. Ion cores too experience unbalanced forces, but the resulting effect is much less striking because they are bound up closely to their lattice sites. Some relaxation of the crystal structure is indeed possible[39,42,43] with a consequent change in the lattice parameters, but for the sake of simplification and clarity the density of positive charges may be considered as uniform up to the ideal surface. This is the model known as "jellium" in physics.[32,44] Only one parameter differentiates one metal from another, i.e., the electron density which is expressed in terms of the radius of the sphere containing one electron. Unbalanced forces are responsible for the onset of the surface tension.[45]

The density of negative charges can hardly be constant up to the ideal surface since electrons can freely move about. Electrons are "attracted" by a vacuum because expansion of the electron gas towards the exterior of the metal

results in a decreasing kinetic energy. A parallel increase in potential energy is unavoidable since electrons will travel to regions of lower coulombic interaction with the ion cores. The final position of electrons originates from a compromise between the above factors corresponding to constancy in energy at the Fermi level across the surface region. Although the electron density exhibits in calculations some (Friedel) oscillations increasing with decreasing electron density,[23,42,44] to a first approximation it may be pictured as smoothly decreasing to zero from the bulk of the metal to vacuum across the surface (Figure 2a).

It is difficult to give a definite value for the effective distance of electron escape into vacuum. As an order of magnitude, the length electrons spill over the edge of the ion cores may be set at about 0.1–0.2 nm.[46] The final situation is a stable separation of charges giving rise to a dipolar layer to which an electric potential drop is associated. This is termed the surface potential of the metal,[23,26] and is denoted[35] by χ^M. From a conceptual point of view, the presence of a dipolar layer may be envisaged on the energy diagram as a curvature of the bottom of the band in correspondence is the surface region.[46] The bottom is bent upwards for a positive χ^M, corresponding to a dipole layer with the positive end inwards[23] (Figure 1).

The mechanism by which electrons tend to protrude from the metal is known as the effect of "spreading," and it is expedient to denote by $\chi_{sp}{}^M$ the

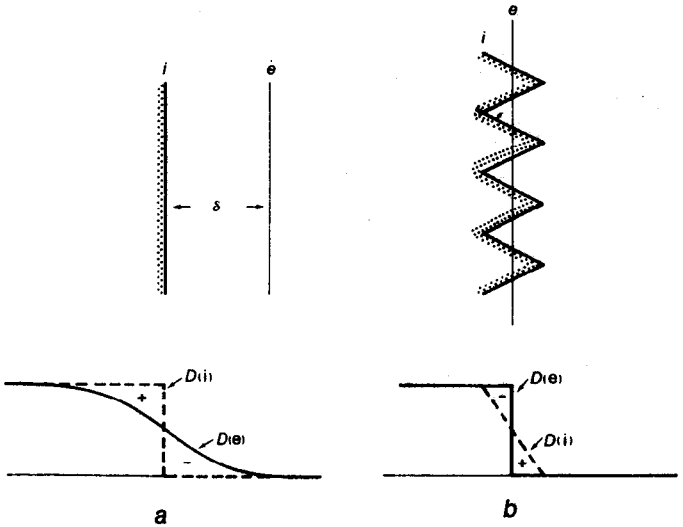


Figure 2. Mechanisms of surface potential onset. (a) "Spreading" effect; (b) "smoothing" effect. D(i) and D(e) are the ionic and electronic densities, respectively. i is the ion core surface profile; e is the limit of electron escape from the metal.

surface potential associated with the dipole arising from such a process.[28] χ^M as derived from the uniform-positive-background model (jellium) can be calculated by following a route[27,31,42] independent of that used for $\mu_e{}^M$. It may also be derived from the experimental Φ^M by subtracting the calculated value of $\mu_e{}^M$. Both directly calculated values[30,31,42,44] and values as derived from Eq. (2.5) are summarized in Table 1. Although the jellium model[31,44] gives upper values for χ^M, these agree with values derived from experimental Φ for low-melting metals because the actual surfaces of these metals approach the "jellium" surface best (see Sec. 2.2.2.). It is interesting that χ^M is positive for all metals (with the possible exception of Cs), which indicates that for jellium the prevailing distribution of the surface dipole is with the negative end toward the exterior of the phase. Note that the ratio of χ^M to Φ^M increases from monovalent to many-electron metals in the sense that for the latter the surface contribution is a large part of the measured work function.[43]

2.2.1. *Crystal Orientation*

The mechanism by which the actual value of χ^M is in fact a function of the surface topography of atoms is known as the effect of "smoothing."[28,47] The effect of the actual ion cores corresponds to a perturbation of the jellium surface[31] and is related to the surface roughness at an atomic scale.[47] Whereas the spreading effect derives from a flow of charges perpendicular to the surface, the smoothing effect originates from a lateral flow of electrons from high to low ionic density regions. Qualitatively, such an effect may be depicted in a conceptually similar way to that followed for $\chi_{sp}{}^M$. In this case, the electronic density is constant up to the ideal surface where it drops to zero abruptly (Figure 2b). The density of the positive charges may be pictured as linearly decreasing across the surface region from the bulk value to zero. Thus the smoothing effect contributes negatively to the value of χ^M.

The actual situation of the dipolar layer at the surface of a metal may be represented by superposing the two above partial effects, i.e.,

$$\chi^M = \chi_{sp}{}^M + \chi_{sm}{}^M \tag{2.8}$$

The magnitude of the surface roughness may be expressed through the rate of change of the ionic density. The positive value of χ^M is thus expected to decrease from smooth to atomically stepped surfaces.

The roughness referred to here may be best defined in crystallographic terms. Different values of Φ^M are experimentally measured for the same metal depending on crystal orientation.[27,29] Among the most common crystal systems, in the fcc (face-centered cubic) system the atom density increases in the sequence (110) < (100) < (111) for the three main faces. In the bcc (body-centered cubic) system the sequence is (111) < (100) < (110), and in the hexagonal system (1010) < (0001). The work function is expected to increase in the same sequence, which is in fact observed.[29,48]

2.2.2. Polycrystalline Surfaces

Polycrystalline surfaces deserve particular attention. Especially in electrochemistry, the use of single-crystal faces as electrodes, while highly desirable, is at present rather limited due to stringent precautions and difficulties involved in the preparation, control, and maintenance, which can be more easily overcome in the case of metals in a vacuum.[49,50] Most electrochemical information (and in gas-phase adsorption too[51]) is therefore available for surfaces without any definite or preferential orientation. A major problem is faced when defining such surfaces in terms of a work function.[52]

Polycrystalline surfaces are by definition the result of mixing of all possible orientations in a crystal. However, low-index faces are energetically the most probable ones. If patchy surfaces are considered, each patch with true work function Φ_i^M occupying the fractional area θ_i, the average work function of the surface is defined by[29]

$$\Phi^M = \sum_i \theta_i \Phi_i^M \tag{2.9}$$

The mean value of the atomic density for the three main faces of solids crystallizing in the fcc and bcc systems is located between those for the two main faces at lower atomic density. This rough prediction is not far from reality.[52]

Studies have shown that the work function of a metal film deposited at the temperature of liquid nitrogen (77 K) increases as the film is sintered at higher temperatures.[53,54] Some experimental data are reported in Figure 3. The increase in work function is not related to the temperature coefficient of the work function, which is of the order of $\pm 10^{-4}$ eV K^{-1}, so that its effect is within the experimental uncertainty of Φ^M.[28,29] The rise is related to packing of atoms resulting in increasing atomic density in the film. If polycrystalline surfaces

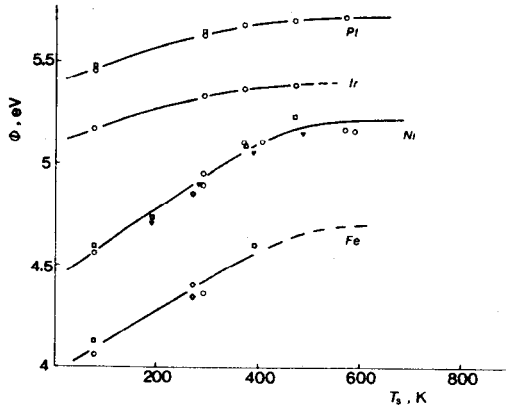


Figure 3. Electron work function as a function of sintering temperature T_s for evaporated metal films. ○, References 118 and 119; □, Reference 53; ▽, Reference 126; ◇, Reference 127.

Table 2

Electron Work Function for Evaporated Metal Films Sintered at Room Temperature, Φ^M(eV)

Metal	Value		Metal	Value	
Ag	4.33[a]	4.29[b]	Pt	5.62[a]	5.63[b]
Au	5.28	—	Rh	4.98	—
Cu	4.52	4.58	Ru	4.71	—
Fe	4.36	4.30	Cr	—	4.27
Ir	5.33	—	Co	—	4.70
Ni	4.90	4.72	Mn	—	3.90
Pd	5.12	5.05			

[a] Values in this column are from References 118 and 119.
[b] Values in this column are estimated[62] from data in Reference 53.

are assumed to be those of deposited films annealed around the room temperature, experimental measurements show that the work function for the same metal increases in the sequence (110) < poly < (100) for the fcc system and (111) < poly < (100) for the bcc. Table 2 summarizes some data of Φ^M for polycrystalline surfaces. Table 3 reports data of smoothing effect referred to the polycrystalline surface for some of the metals. Note that the rule to derive Φ^M for polycrystalline surfaces holds particularly well with high-melting metals. For low-melting metals close-packed surfaces are increasingly favored at room temperature as the melting point decreases so that the work function of the polycrystalline surface approaches that for the most densely populated surface. Hg is an exception. Being liquid at room temperature, it does not present the problem of the definition of its surface state, and its work function may be sharply defined under any circumstances. The most probable value is 4.5 $\pm$ 0.02 eV.[52]

For some metals, especially Ir, Au, and Pt, the polycrystalline Φ^M derived as above does not fit to the electrochemical behavior.[55] Reasons for this are perhaps to be sought in the fact that in a vacuum these metals undergo the phenomenon of surface reconstruction, consisting in a trend for atoms in the

Table 3

Smoothing Effect at Single-Crystal Faces of Metals Referred to the Polycrystalline Surface, $\Delta\chi^M$(V)

Metal	(111)	(100)	(110)	Ref.
Cu	0.39	0.04	−0.07	120
Mo	0.80	0.10	−0.15	121
Ni	0.42	0.09	−0.16	122
Ta	0.67	0.02	−0.13	123
W	0.70	0.08	−0.08	124

outermost layer to pack up as much as possible irrespective of crystal orientation.[56–58] When these metals are in contact with a solvent, some surface relaxation due to chemical interactions is possible. This explanation is, however, still tentative.

2.3. The Surface of Liquid Polar Phases

In the case of a liquid polar phase (solvent), which is of interest here, intermolecular forces are essentially isotropic in the bulk and no net orientation of molecular dipoles exists there. As the phase is cut abruptly and a new surface is created, particles on this surface are at different energy with respect to those in the bulk. The system reacts to this situation by trying to balance the difference in energy between molecules on the surface and those in the bulk. At equilibrium, the free-energy change associated with transfer of a particle from the bulk to the surface must be zero. Molecules on the surface are thus expected to seek out new molecular arrangements to allow them to achieve the same energy state as those in the bulk. The new state is reached at the expense of the formation of new bonds or by the adaptation of the old ones, both involving necessarily some modifications in molecular orientation that are sterically and physically possible. Such modifications are responsible for the onset of preferential orientations of molecules at the surface where on the average the normal component of the dipole moment is thus different from zero.[45,59] The potential drop across the surface region is known as the surface potential of the liquid phase and is denoted by χ^S.[23]

In the case of water, χ^{H_2O} has been discussed several times in the literature.[15,60–64] It is now widely accepted that it has a small positive value, which has recently been given[65] as

$$\chi^{H_2O} = 0.13 \pm 0.02 \text{ V} \tag{2.10}$$

by relying on a large number of indirect experimental observations. The positive value suggests that at the surface of the pure solvent the mean preferred orientation of H_2O molecules is with the oxygen atom towards the gas phase. Presence of electrolytes which may give rise to preferential penetration of anions or cations into the surface layer may lead to some variation in χ^{H_2O}.[61,64,66,67] The experimental temperature coefficient $d\chi^{H_2O}/dT$ has been found to be -40 mV K^{-1}.[63,68] The sign is consistent with a simple model of oriented dipoles disordered by an increase in T, and the value is also consistent with a linear decrease of χ^{H_2O} with T up to the critical temperature (647 K).[61]

The actual value of χ^{H_2O} is important to derive the chemical free energy of hydration of single ions from the measured real free energy of hydration[69] according to the equation[23,62]

$$\alpha_i^{\circ,H_2O} = \mu_i^{\circ,H_2O} + ze\chi^{H_2O} \tag{2.11}$$

where z is the charge of ion i including sign. Table 4 summarizes real and chemical free energy of hydration of some ions.

Table 4

Standard Chemical and Real Potentials of Ions in Water

Ion	$-\mu^{\circ,H_2O}$ (kcal mol^{-1})	$-\alpha^{\circ,H_2O}$ (kcal mol^{-1})[a]
H^+	263.1	260.1
Li^+	124.7	121.7
Na^+	100.8	97.8
K^+	83.2	80.2
Rb^+	78.1	75.1
Cs^+	70.4	67.4
Cu^+	138.8	135.8
Ag^+	117.1	114.1
Tl^+	84.6	81.6
Mg^{2+}	460.7	454.7
Ca^{2+}	386.0	380.0
Mn^{2+}	443.0	437.0
Cu^{2+}	502.4	496.4
Cd^{2+}	435.7	429.7
Zn^{2+}	489.8	483.8
Pb^{2+}	363.1	357.1
Ce^{3+}	853.3	844.3
Ga^{3+}	1113.8	1104.8
In^{3+}	982.0	973.0
Al^{3+}	1111.1	1102.1
Fe^{3+}	1043.3	1034.3
F^-	96.5	99.5
Cl^-	68.1	71.1
Br^-	62.3	65.3
I^-	54.6	57.6
S^{2-}	301.4	304.4
e^-	33.2	36.2
e^-(m)	23.8	26.7

[a] Value of α°,H_2O} from References 18, 69, and 125.

2.4. Metal–Metal Contact

Consideration of the bringing of two different metals into contact is useful in rationalizing and comprehending more easily some of the basic phenomena which occur in the establishment of an electrode potential.

Consider two metals with different work functions and electron densities. For the sake of simplification, let us assume that the two metals possess different ε_F but the same V. As the metal with the lower work function touches the other, electrons of the former on expanding toward the exterior of the phase now find energy levels available in the lattice of the latter. This will promote some transfer of electrons from one metal to the other, together with some redistribution of the electron density in the surface double layers.[70–73] The potential energies experienced by electrons in the phases are thus modified.

The movement of electrons from one metal to the other goes on until the

work required to extract electrons from both is the same. This means that the Fermi levels have been modified up to be equal in both of the metals. Accordingly, equality in electrochemical potential in the two phases is established[23,25]:

$$\tilde{\mu}_e{}^{M_1} = -\Phi^{M_1} - e\psi^{M_1} = \tilde{\mu}_e{}^{M_2} = -\Phi^{M_2} - e\psi^{M_2} \tag{2.12}$$

ψ^M measures the excess interaction felt by the electrons leaving the metal as a result of the presence of free charges. This means that at least some of the charges transferred from one metal to the other upon contact must be located at the free surfaces of the phases towards vacuum to modify the work function.

At equilibrium between the two metals in contact, it follows from Eq. (2.12) that the difference in additional work compensates the original difference in work function:

$$\Delta_{M_2}{}^{M_1}\Phi = e\Delta_{M_1}{}^{M_2}\psi \tag{2.13}$$

$\Delta_{M_1}{}^{M_2}\psi$ is the difference in electric potential between one point close to the surface of M_1 and one point close to the surface of M_2. Both points being in the same phase (vacuum), $\Delta_{M_1}{}^{M_2}\psi$ is an experimentally measurable quantity.[23] It is known as the contact potential difference (cpd),[29] or Volta potential difference.[23]

The movement of electrons to reach equilibrium between the phases is compositionally negligible.[25] This means that the bulk electron density in each of the phases remains unchanged, thus leaving $\mu_e{}^M$ unchanged as well. No change in the kinetic energy of electrons at the Fermi level has therefore occurred. Changes have occurred only in the position of the bottoms of the energy bands. Thus

$$e\Delta_{M_1}{}^{M_2}\psi = \Delta_{M_1}{}^{M_2}V_{\text{fin}} - \Delta_{M_1}{}^{M_2}V_{\text{in}} \tag{2.14}$$

An electron crossing the ideal plane of separation between the two phases sees the lattice of the ion cores change abruptly. Figure 4 shows that, under equilibrium conditions, the electron density changes smoothly from the bulk value of M_1 to the bulk value of M_2 (Friedel oscillations are neglected). It is, however, practically impossible to distinguish where the surface of M_1 ends and the surface of M_2 begins. However, the interphasial region certainly differs from either of the two bulk structures.

The separation at the interface between two metals of dipolar and free-charge contributions involves excessive and unnecessary speculations. Since the, final electron distribution is practically symmetric with respect to the two phases, it is expedient to assume that upon contact the two surface double layers vanish, or still better, that the redistribution of the electron density ultimately results in a separation of free charges between the two phases. Thus, across the interface, it is convenient to separate chemical from electrical effects. It follows from Eqs. (2.5) and (2.12):

$$-\mu_e{}^{M_1} + e(\Delta_{M_2}{}^{M_1}\phi) + \mu_e{}^{M_2} = 0 \tag{2.15}$$

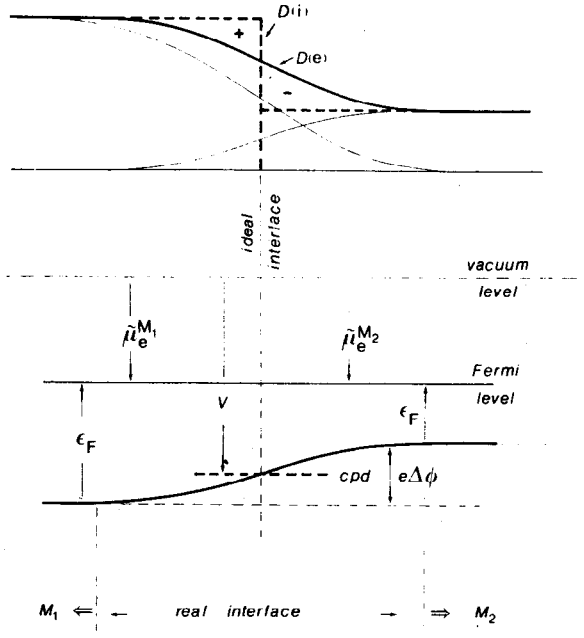


Figure 4. Electron density and potential energy profiles at a metal–metal interface. Electron density and potential energy (the same for both metals) before contact are also shown.

Rearrangement of Eq. (2.15) gives

$$\Delta_{M_1}{}^{M_2}\mu_e = e\Delta_{M_2}{}^{M_1}\phi \tag{2.16}$$

ϕ^M is the electric potential in a point inside phase M.[23] Equation (2.16) means that the magntidue of $\Delta\mu_e$ determines the magnitude of $\Delta\phi$. A dipolar and a free-charge contribution may be distinguished if electrons are transferred from M_1 to M_2 across the free surfaces and vacuum:

$$\Delta_{M_2}{}^{M_1}\phi = \Delta_{M_2}{}^{M_1}\chi + \Delta_{M_2}{}^{M_1}\psi \tag{2.17}$$

whereas such a distinction is impossible if they travel across the interface. If at a metal–metal contact dipolar contributions are regarded as nonexistent and included in the free-charge contribution, it is then possible to write

$$\Delta_{M_2}{}^{M_1}\phi = g_{M_2}{}^{M_1}(\text{ion}) \tag{2.18}$$

where it is intended[23,35] that g denote quantities relevant to interfaces rather than to free surfaces, and (ion) stands for free charges. It follows from Eqs. (2.17) and (2.18) that:

$$g_{M_2}{}^{M_1}(\text{ion}) \neq \Delta_{M_2}{}^{M_1}\psi \tag{2.19}$$

Equation (2.19) means that in principle the free-charge contribution at the free surface differs from that at the interface of the same phase with another phase. The two contributions could be equal only if the surface dipolar layers were not modified upon contact in the interphasial region. In particular, for the contact between two metals, the sign of the free charge on each of the metal as estimated from the relative values of Φ^M is that residing at the free surfaces of the phases. As Eq. (2.19) stresses, the values of Φ^M cannot predict the sign of the free charge on each metal at the interface, which on the contrary depends on the relative values of chemical potential of electrons. Since μ_e^M as a rule decreases as the electron density increases, and the opposite approximately occurs for Φ^M,[31] it follows that the sign of the charge at the interface is often opposite to that at the free surface.

Metal overlayers are a particular case of metal–metal contact.[74,75] Experiments show that the work function of a metal M changes from Φ^M to $\Phi^{M'}$ as M becomes progressively covered by a film of M'.[76] The thickness at which $\Phi^{M'}$ is measured depends on the nature of M'. With low-electron-density *sp* metals $\Phi^{M'}$ is already measured at the completion of the first monolayer. A few

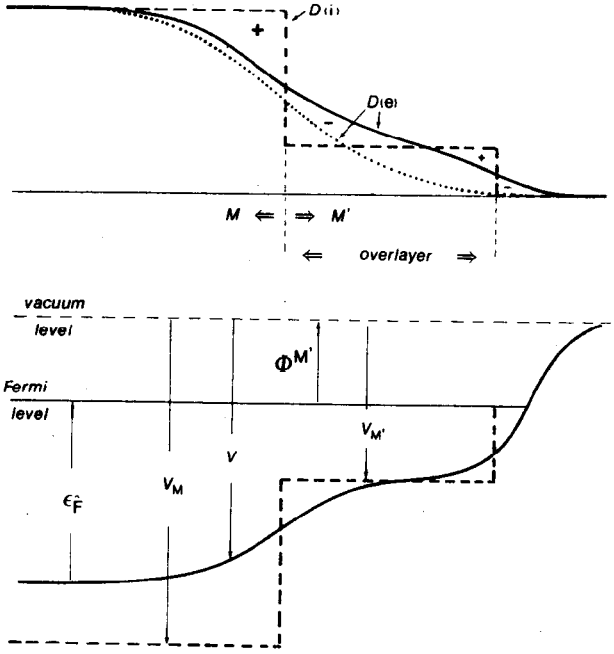


Figure 5. Electron density and potential energy profiles across a metal overlayer. The situation before interaction is also shown.

monolayers are, on the contrary, needed in the case of IB group and transition metals.[77] This phenomenon is relevant to electrochemistry in the case of underpotential deposition of metals.[78,79] At the interface between M and a metal overlayer M′ it is more difficult to assume that dipolar layers vanish. However, the basic arguments introduced for the metal–metal contact are in principle valid also in this case. The situation is depicted in Figure 5, as derived from the work of Lang.[74]

3. Origin of the Electrode Potential

3.1. Electrons in Liquid Polar Phases

Free electrons are not intrinsic components of liquid polar phases. In principle, they can, however, be held in the bulk of a solution.[80–83] Practically, free electrons are usually unstable in a solution since they are very reactive and tend to reduce the solvent. However, they may be quite stable in some solvents so that they can be considered as possible components of a solution.[84]

Different energy states are possible for electrons in a liquid polar phase depending on the achievement or less of equilibrium conditions.[85] The energy of electrons in an uncharged liquid polar phase at the bottom of the potential well is defined by the real potential[23]

$$\alpha_e{}^S = \mu_e{}^S - e\chi^S \tag{3.1}$$

$\mu_e{}^S$, the chemical potential, may be conceptually split into several contributions[85] (Figure 6):

$$\mu_e{}^S = \mu_{e(m)}{}^S + \Delta G_{in} - \Delta G_{or} \tag{3.2}$$

$\mu_{e(m)}{}^S$ is the chemical potential of delocalized electrons interacting with solvent molecules only through the electronic polarization. This state corresponds to the bottom of the conduction band and corresponds to electrons traveling so fast that solvent molecules have no time to reorient. ΔG_{or} is the energy change associated with the reorganization of solvent molecules under the stable influence of the electronic charge. This reorganization corresponds to orientation polarization with creation of a potential well. ΔG_{in} is the gain in energy associated with the interaction of electrons with polarized solvent molecules in the potential well.

$\mu_e{}^S$ corresponds to the bulk energy of solvated electrons in thermal equilibrium with the solvent. Electrons are thus localized in this state and formally correspond to donor levels in impurity semiconductors, although in solution such levels have some possibility of diffusing within the phase.[86] Differently from the case of electrons in a metal, the actual value of $\mu_e{}^S$ may depend on the electron population:

$$\mu_e{}^S = \mu_e{}^{\circ,S} + kT \ln a_e \tag{3.3}$$

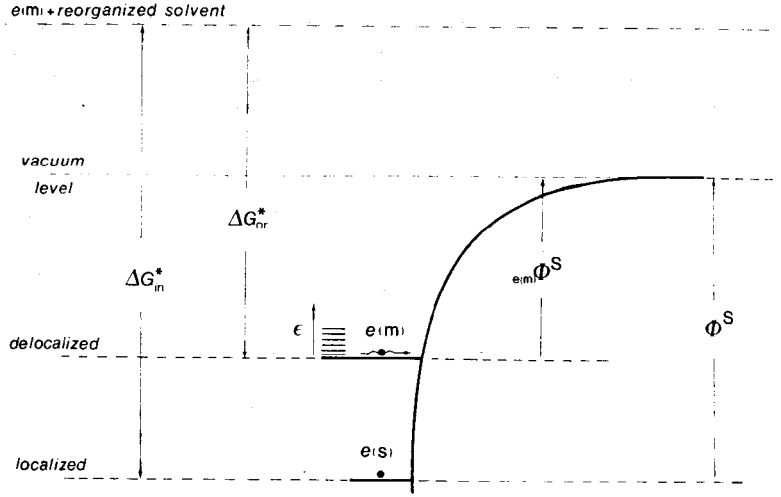


Figure 6. Energy diagram for electrons in polar liquids. ϵ is the kinetic energy of delocalized electrons.

according to a Boltzmann distribution determined by fluctuations in the solvent configurations.[87] According to Eq. (3.3), $\mu_e^{\circ,S}$ is referred to the condition of 1 electron per liter. It can be derived by a thermodynamic cycle applied to the reaction[88,89]

$$H(H_2O) \rightarrow H^+(H_2O) + e(H_2O) \tag{3.4}$$

which gives for α_e°,H_2O} the value of -1.57 eV.[88] Thus, according to Eq. (2.11), $\mu_e^{\circ,S}$ results in the value -1.44 eV.

If reference is made to the state of a single particle interacting with a large volume of solvent as calculated by a model, then $\mu_e^{\circ,S}$ must be corrected[85] for the concentration term $(-kT \ln [(2\pi\, mkT/h^2)^{3/2}(V/N)])$ and transformed into a concentration independent quantity. Thus it is possible to write

$$\Phi^S = -\mu_e^{*,S} + e\chi^S \tag{3.5}$$

which is the equilibrium electron work function of the solution, the exact analogue of the electron work function of metals. The value of $\alpha_e^{*,H_2O} = -\Phi^S$ is -1.47 eV.[85] Thus $\mu_e^{*,H_2O} = -1.34$ eV.

If the concentration term is operative in Eq. (3.3), it is better to use the term "real potential" rather than "work function" because no unique value would exist for α_e^S. From a conductivity point of view, when the concentration of solvated electrons increases transition from nonmetal to metal behavior is possible because localized levels can interact as the average distance among them decreases.[90] A hopping mechanism of conduction is possible at intermediate concentrations.

A nonequilibrium work function is in principle measured by the photoelectric method[85,91] since transition of electrons from the potential well to vacuum occurs according to the Frank–Condon principle. If the configuration of the solvent has not time to relax during the rapid process, the nonequilibrium work function is actually given by

$$_{\text{n.e.}}\Phi^{\text{S}} = -\mu_{e_m}{}^{*,\text{S}} - \Delta G_{\text{in}}{}^{*} + e\chi^{\text{S}} \tag{3.6}$$

However, another quantity is more relevant to the present discussion. This is the energy difference between an electron in a vacuum and a "dry" electron in solution (delocalized electron). In this case it is possible to define a further electron work function for *mobile* electrons[85] (Figure 6):

$$_{e_m}\Phi^{\text{S}} = -\mu_{e_m}{}^{*,\text{S}} + e\chi^{\text{S}} \tag{3.7}$$

Actually, $_{e_m}\Phi^{\text{S}}$ can have different values depending on the kinetic energy which mobile electrons possess by definition. However, this aspect will be neglected here and negligible kinetic energy will be assumed in the definition of $_{e_m}\Phi^{\text{S}}$. The way such a work function may be quantitatively measured will be shown later.

3.2. Metal–Polar-Liquid Contact

Consider an isolated system consisting of a metal M and a liquid polar phase S. Assume further that electrons are stable in S.

3.2.1. Thermodynamic Aspects

The contact between M and S cannot be treated as the contact between two metals since the liquid phase does not contain free electrons as an intrinsic component. This means that $\mu_e{}^{\text{S}}$ is not definable before the contact and the sole equation (2.16) is unable to define unambiguously the conditions for the electronic equilibrium between M and S. Upon contact, electrons enter the liquid phase since empty levels are available there, provided charges of opposite sign accompany them to preserve the electroneutrality of the solution in the bulk. It follows that the equilibrium conditions are related not only to the energetic situation of electrons alone or of ions alone in the two phases but to the simultaneous energetic situation of ions plus electrons in the two phases. The relevant equilibrium[88,92,93] is

$$\text{M}^+(\text{M}) + \text{e}(\text{M}) \rightleftarrows \text{M}^+(\text{S}) + \text{e}(\text{S}) \tag{3.8}$$

Equation (3.8) may be rewritten in the form

$$\text{M}(\text{M}) \rightleftarrows \text{M}(\text{S}) \tag{3.9}$$

Equation (3.9) indicates that on the whole a chemical equilibrium is established between metal atoms in the lattice of the solid and metal atoms in the liquid

phase. Equation (3.9) fixes unambiguously the chemical conditions that must be satisfied for a metal to reach equilibrium with a pure solvent.[80,81]

Equation (3.9) describes a situation quite similar to that of a sparingly soluble salt.[92] The solubility of such a salt is governed by a chemical equilibrium, but this does not rule out in fact the possibility that separate electrochemical equilibria are established for the single ionic species. Thus from Eq. (3.8) it follows that

$$\tilde{\mu}_{M^+}{}^{M} + \tilde{\mu}_{e}{}^{M} + \tilde{\mu}_{M^+}{}^{S} + \tilde{\mu}_{e}{}^{S} \tag{3.10}$$

and, simultaneously,

$$\tilde{\mu}_{M^+}{}^{M} = \tilde{\mu}_{M^+}{}^{S} \tag{3.11}$$

$$\tilde{\mu}_{e}{}^{M} = \tilde{\mu}_{e}{}^{S} \tag{3.12}$$

in that at equilibrium the exchange rate of differently charged particles across the interface must be separately balanced to avoid continuous accumulation of free charges. However, from Eq. (3.9),

$$\mu_{M}{}^{M} = \mu_{M}{}^{S} \tag{3.13}$$

Equation (3.13) indicates that the amount of M dissolved is actually independent of the electrical state of the interface. However, while respecting the equimolarity of oppositely charged species in the bulk of the solution, an electric potential drop must be present across the interface, causing the conditions expressed by Eqs. (3.11) and (3.12) to be simultaneously operative. From the above equations, it follows that

$$\Delta_{S}{}^{M}\phi = -\Delta_{S}{}^{M}\mu_{M^+}/e \tag{3.14}$$

$$\Delta_{S}{}^{M}\phi = \Delta_{S}{}^{M}\mu_{e}/e \tag{3.15}$$

Equations (3.14) and (3.15) present the electrochemical equilibria, usually separately introduced to derive the Nernst equation, as part of a chemical equilibrium. Thus the electrode can be treated as a sparingly soluble salt. The electric potential drop thus arisen at equilibrium between a metal and a pure solvent is a characteristic quantity of that interface and may be termed the *solubility equilibrium potential* by analogy with the solubility product.[88]

If M^+ ions are now added to the solution $\Delta_{S}{}^{M}\phi$ will change but the concentration of e will also change so that Eqs. (3.14) and (3.15) are again simultaneously valid. The same occurs if e is hypothetically added to the solution, which means that on a strict thermodynamic basis the concept of potential-determining ion is not unambiguous. $\Delta_{S}{}^{M}\phi$ becomes more positive if M^+ ions are added to the solution and more negative if electrons are hypothetically added. One potential in this range is the potential at which the charge on the metal vanishes (potential of zero charge). Such a potential is thus a quantity electrostatically well definable but thermodynamically not sharply recognizable.

3.2.2. Structural Aspects

When a metal comes into contact with a solvent, electrons can no longer expand freely towards vacuum but they encounter a different dielectric medium. They experience a different potential energy and in addition the region they expand into is already occupied by other electrons (electron clouds of solvent molecules). Factors giving rise to χ^M have thus changed and electrons subjected to different forces are expect to adopt a different distribution at the surface with a different associated surface potential. It is thus possible to write[13,15,23,55,94]

$$g^M(\text{dip}) = \chi^M + \delta\chi^M \tag{3.16}$$

Attempts at an estimation of $\delta\chi^M$ have been made for a few metals in water.[55,95] Analogous phenomena are to be expected on the solution side. Thus

$$g^S(\text{dip}) = \chi^S + \delta\chi^S \tag{3.17}$$

The M/S potential drop thermodynamically defined by Eqs. (3.14) and (3.15) may structurally be split into a free charge and a dipolar contribution[23] (Figure 7). The dipolar contribution consists of the difference between Eqs. (3.16) and (3.17), while the free-charge contribution includes the electronic polarization of solvent molecules, the orientation polarization being accounted for by $g^S(\text{dip})$. Thus, across the interface,

$$\Delta_S^M\phi = g_S^M(\text{dip}) + g(\text{ion}) \tag{3.18}$$

and across the free surfaces through vacuum

$$\Delta_S^M\phi = \Delta_S^M\chi + \Delta_S^M\psi \tag{3.19}$$

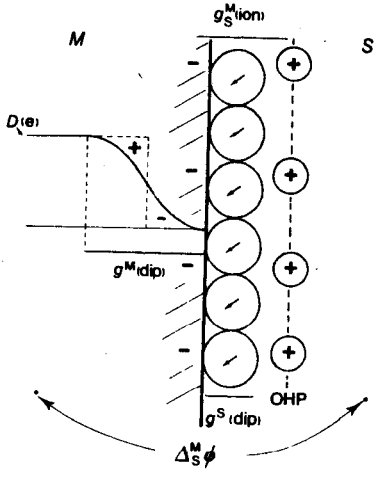


Figure 7. Components of the Galvani potential difference at a metal–solution interface (operative electrode potential).

where $\Delta_S^M\psi$ is the Volta potential difference and is a measurable quantity. It follows that

$$\Delta_S^M\chi + \Delta_S^M\psi = g_S^M(\text{dip}) + g(\text{ion}) \tag{3.20}$$

However, recalling Eqs. (3.16) and (3.17), as a rule,

$$\Delta_S^M\chi \neq g_S^M(\text{dip}) \tag{3.21}$$

from which

$$\Delta_S^M\psi \neq g(\text{ion}) \tag{3.22}$$

Equations (3.21) and (3.22) indicate that free-charge and dipolar contributions are usually different at the free surfaces and at the metal–solution interface.[9,94] In particular, when $\sigma^M = 0$, from Eq. (3.20)

$$\Delta_S^M\psi_{\sigma=0} = \Delta_S^M g(\text{dip}) - \Delta_S^M\chi \tag{3.23}$$

i.e, recalling Eqs. (3.16) and (3.17)[15]

$$\Delta_S^M\psi_{\sigma=0} = \delta\chi^M - \delta\chi^S \tag{3.24}$$

Equation (3.24) shows that when the M/S interface is uncharged (potential of zero charge), the free surfaces of the phases can be uncharged only either no change occurs in the surface potentials of the phases upon contact, or the change in χ^S compensates exactly for the change in χ^M. These are possible exceptions but not the rule.

3.3. Electron Work Function of Metals in Polar Liquids

A *general* definition of electron work function of metals may be "the minimum work to extract electrons from the Fermi level." Accordingly,

$$\Phi^{M/X} = -(\bar{\mu}_e^M - \bar{\mu}_e^X) \tag{3.25}$$

where χ is the environment in which the metal is immersed. The actual value of Φ^M thus depends on the final state of electrons in the environment around the metal. In particular, in solvent S

$$\Phi^{M/S} = -(\bar{\mu}_e^M - \bar{\mu}_e^S) \tag{3.26}$$

Whereas, by the nature of the M/V boundary, only one work function is definable, i.e., that corresponding to the state of the uncharged phase, charging of the M/S interface is a normal occurrence in electrochemistry. A continuous spectrum of electron energy jumps is thus conceptually definable at the M/S boundary. Although the term "work function" should strictly be applied only to the quantity defined in terms of uncharged metal, it is, however, a pratice in electrochemistry to call work function the electronic energy jump at the M/S contact,[96–99] taken with the reverse sign, under any circumstances. If this practice is accepted [and it is indeed implied in Eq. (3.18)] it is necessary to label

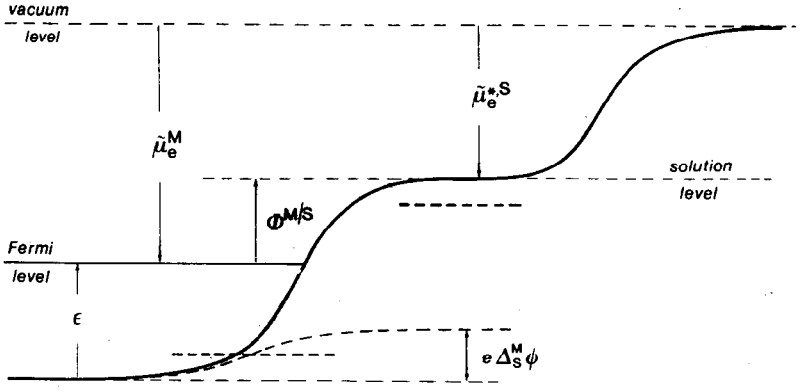


Figure 8. Potential energy profile across a metal–polar-liquid–vacuum system. Position of energy levels before contact and electrostatic part of the energy are also shown.

the work function for the uncharged metal because only this quantity is a characteristic property of the M/S system.

$\Phi^{M/S}$ may be related to structural parameters of the interface by recalling Eqs. (2.5), (3.16), and (3.17). Thus

$$\Phi^{M/S} = \Phi^{M} + e\delta\chi^{M} - eg^{S}(\text{dip}) + eg(\text{ion}) + \mu_e^{S} \tag{3.27}$$

The actual value of $\Phi^{M/S}$ depends on the final state of electrons in phase S, all other parameters being the same. Thus two limiting situations must be distinguished[100]: (i) the thermodynamic equilibrium is established across the interface (nonpolarizable interfaces), and (ii) the thermodynamic equilibrium is not established (polarizable interfaces). In the former case the situation must be treated as rigorous thermodynamics sees it, in the latter case the interface must be treated as physicists treat the metal–vacuum interface.

3.3.1. Nonpolarizable Interfaces

If the interface is treated in terms of thermodynamic equilibria,[19,21] then Eqs. (3.12) and (3.25) mean that the electron work function of metals in solution is zero under any circumstances, the condition of zero charge on the metal included.[20] This is tantamount to assuming that extraction of electrons from the metal always takes place under conditions of reversibility.

3.3.2. Polarizable Interfaces

Since in the absence of electronic equilibrium no electrons are expected to be present in solution, the final state of electrons in the liquid phase may be identified by $\mu_e^{*,S}$. Thus (Figure 8)

$$\Phi^{M/S} = \Phi^{M} + e\delta\chi^{M} + eg(\text{ion}) - eg^{S}(\text{dip}) + \mu_e^{*,S} \tag{3.28}$$

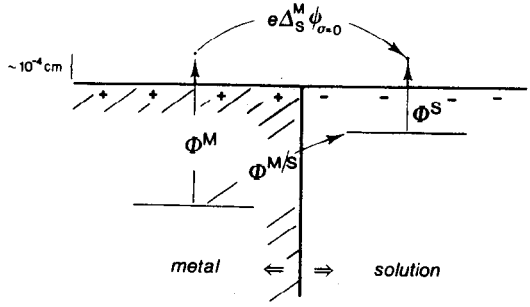


Figure 9. Sketch to show why the work function of a metal in solution is not simply the difference between the vacuum work function of the metal and that of the solution.

Equation (3.28) defines the equilibrium work function of metals in solution. Actually, the final state of electrons in the liquid phase may correspond to $\mu_{e_m}^{*,S}$, i.e., to delocalized electrons.[21,85,98,99] In such a case a nonequilibrium work function may also be defined:

$$_{e_m}\Phi^{M/S} = \Phi^M + e\delta\chi^M - eg^S(\text{dip}) + eg(\text{ion}) + \mu_{e_m}^{*,S} \tag{3.29}$$

By recalling Eqs. (3.5) and (3.20), it may be written[96,101]

$$\Phi^{M/S} = \Phi^M + e\Delta_S{}^M\psi - \Phi^S \tag{3.30}$$

which represents the relationship between the various kinds of electron work functions defined above. In the particular case of $\sigma^M = 0$, from Eq. (3.29)

$$\Phi_{\sigma=0}{}^{M/S} = \Phi^M + e\delta\chi^M - eg^S(\text{dip}) + \mu_e^{*,S} \tag{3.31}$$

It follows from Eq. (3.24) (Figure 9) that

$$\Phi_{\sigma=0}{}^{M/S} = \Phi^M + e\Delta_S{}^M\psi_{\sigma=0} - \Phi^S \tag{3.32}$$

Equations (3.30) and (3.32) are also valid for nonpolarizable interfaces but the symbol Φ^S should be replaced by $-\alpha_e{}^S$.

3.3.3. Actual Interfaces

It is possible that the occurrence of equilibrium across the interface, expected thermodynamically, is not realized in practice. If the theoretical concentration of electrons in solution for the electronic equilibrium is much lower than the amount of electrons extracted by a quantum of light by the photoelectric effect, the equilibrium is certainly not operative and the extraction cannot be considered to occur under reversible conditions. In such a case Eq. (3.32) rather than Eq. (3.12) applies. This means that the concept of polarizability of an interface must be applied separately to each of the components of the system. For instance, it is possible to calculate by a Born–Haber cycle applied to

Eq. (3.8) that the concentration of electrons in water thermodynamically expected in equilibrium with Ag at the solubility potential amounts to about 10^{-31} mol dm^{-3}.[88] This means that only about 1 electron in 10^7 dm^3 should be present in solution in equilibrium with the metal. If the solution is made 1 *M* in Ag^+ ions, then a concentration of electrons of only 10^{-62} mol dm^{-3} is expected at equilibrium. The interface can be regarded as nonpolarizable with respect to Ag^+ but polarizable with respect to electrons. This means that in such a case Eq. (3.12) does not hold, the electronic equilibrium is not established, and Eq. (3.28) is operative.

The same happens as the concentration of M^+ is decreased by diluting a solution of M^+ in contact with M. The concentration of M^+ can decrease by diluation only down to the solubility value. It could be further decreased only by introducing a hypothetical electronic salt, M'e. In such a case, the interface becomes progressively nonpolarizable with respect to electrons, but ultimately it becomes polarizable as regards M^+. This means that some deviation from the Nernst equation which is expressed by Eqs. (3.11) and (3.12) is to be expected at such low concentrations of the active species that the electrochemical equilibrium can no longer be operative in real times and volumes (Figure 10). The fact that practically the solubility of most metals in most solvents is so low as to be negligible at all does not rule out that *in principle* an electrode behaves as a sparingly soluble salt. Thus a smooth transition from nonpolarizable to polarizable interfaces may be expected.

When M^+ is added to a nonpolarizable M/S interface, the potential of M is shifted to more positive values. Part of this shift is associated with free charges crossing the interface and part with reorganization of the dipolar layers on the phases. It is generally assumed that g^M(dip) is charge independent in that all of

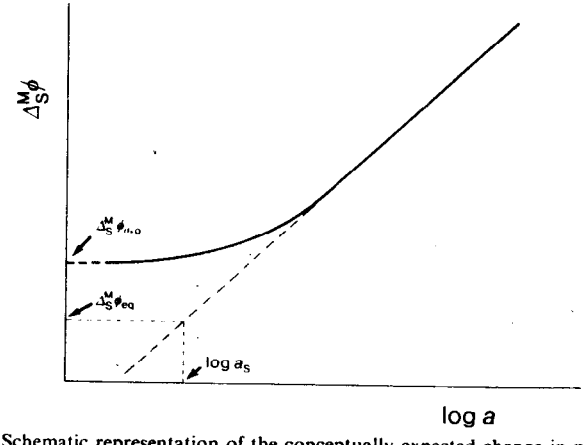


Figure 10. Schematic representation of the conceptually expected change in potential with changing activity of the potential-determining ion for a negligibly soluble metal.

the variation in electron distribution is accounted for in the value of σ. Thus it may be written[102]

$$\Delta_0{}^{\sigma}\Delta_S{}^{M}\phi_{\Delta} = g(\text{ion}) - \Delta_0{}^{\sigma}g^{S}(\text{dip}) \tag{3.33}$$

This equation holds for any kind of interface. The difference is that with polarizable interfaces the electrical state cannot be changed by changing the chemical composition of the solution so that the electrode must be polarized by means of an external voltage source. With nonpolarizable interfaces the electrical state cannot be changed without changing the chemical composition of the solution. The actual difference is thus in the origin of free charges but structurally the two kinds of interface are equal.

Electronically nonpolarizable interfaces are realized with alkali metals dissolving in some nonaqueous solvents such as NH_3 and hexamethylphosphoramide moderately concentrated solutions.[84] In such systems exchange of electrons between metal and solution is realized under practically reversible conditions.[93,103,104]

4. Meaning of Measured Potentials

4.1. Measurement of Potentials

Since movements of charged particles are involved in electrochemistry, the usual term "potential" implies the specification "electric." As a current flows along a metallic wire, we know that a potential drop must be operative between the ends of the wire. Accordingly, as charged particles cross the interface between a metal and a solution, this is naively associated with the existence of a difference in electric potential between the two phases. The usual way to think of the electrode potential is therefore as the electric potential drop between a point in the bulk of the metal and a point in the bulk of the solution, viz., $\Delta_S{}^{M}\phi$. However, the essential difference between $\Delta_S{}^{M}\phi$ and $\Delta\phi$ operating along a metal wire as current flows, is that in the latter case the composition of the phase is constant throughout, whereas with electrodes, electrons, or, more generally, charged particles travel between dissimilar phases. It follows that the relevance of $\Delta_S{}^{M}\phi$ to electrochemical processes is in principle quite different from the relevance of $\Delta\phi$ along a wire to the movements of electrons.

In principle, $\Delta_S{}^{M}\phi$ is not a measurable quantity.[23] This is because instruments for potential measurements work on the basis of the total energy of electrons in a phase and not only of the electrical energy. In order to measure $\Delta\phi$, the terminals of the instrument must be connected to suitable points in the phases to pick up the signal. The mobile parts of instruments unavoidably experience the difference in electrochemical energy of electrons entering from the opposite ends of the system under measurement. It is thus easy to show that instruments cannot measure the actual $\Delta\phi$ between dissimilar phases, although they can measure the difference in $\Delta\phi$ with respect to the equilibrium value defined by Eq. (2.16). However, $\Delta\phi$ within the same phase can be measured.[23]

Thus, since electrodes always involve a contact between dissimilar phases, $\Delta_S{}^M\phi$ cannot be measured. As soon as the terminals of the instrument were connected to a point *in* M and a point *in* S, an electrochemical cell would be constructed and the measured potential would in fact be a potential difference.

4.2. Relative Electrode Potential

Consider the cell

$$M'|Ref|S|M \tag{4.1}$$

where the metal of the electrode under measurement is for simplicity assumed to be the same as that constituting the measuring instrument. Usually, the measured cell potential difference, denoted by E, is arbitrarily split into two terms each assigned to one of the two electrodes:

$$E = E^M - E^{Ref} \tag{4.2}$$

It follows that E is given the meaning of potential of M relative to Ref. The hydrogen electrode with $p_{H_2} = 1$ and $a_{H^+} = 1$ is usually chosen as the reference standard and its potential arbitrarily assumed as zero.

The meaning of E° (H^+/H_2) in terms of $\Delta_S{}^M\phi$ has been discussed but no satisfactory conclusion has been reached.[15–17] This is because no direct relationship exists between E and $\Delta_S{}^M\phi$.[18,60] In fact, the electric potential drop between the ends of cell (4.1) is actually the sum of *three* and not of *two* electric potential drops[2,15–17,23,105] (Figure 11). This becomes evident if the cell potential difference is written as

$$E = \Delta_{M'}{}^M\phi = \Delta_S{}^M\phi + \Delta_{ref}{}^S\phi + \Delta_{M'}{}^{Ref}\phi \tag{4.3}$$

It has been proved that in terms of $\Delta\phi$ alone there is no unambiguous way of

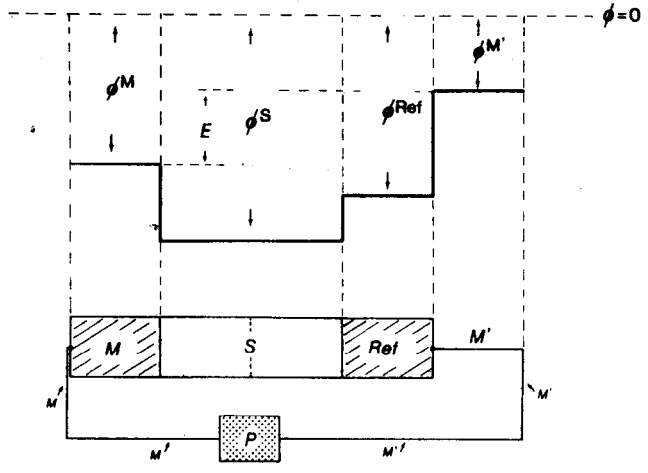


Figure 11. Electric potential profile across an electrochemical cell. P is a potentiometer.

splitting the right-hand side of Eq. (4.3) into two parts each assigned to one of the electrodes.[18,60] This means that for a single electrode

$$E^{M} \neq \Delta_{S}{}^{M}\phi \tag{4.4}$$

Thus at least two kinds of potentials should be distinguished. E^{M} as customarily measured may be referred to as the *thermodynamic electrode potential* because it is a result of the thermodynamic technique of measurement.[3,18] $\Delta_{S}{}^{M}\phi$, known as the Galvani potential difference, may be referred to as the *operative (physical) electrode potential* because it is the electric potential drop which actually operates at the interface.[3,18]

4.3. Single Electrode Potential

The only way the right-hand side of Eq. (4.3) can be split into two terms, each relevant to a single electrode, is to consider that at the Ref/M′ contact there exists electronic equilibrium. Then, recalling Eq. (2.16),

$$E = (\Delta_{S}{}^{M}\phi - \mu_{e}{}^{M}/e) - (\Delta_{S}{}^{Ref}\phi - \mu_{e}{}^{Ref}/e) \tag{4.5}$$

It follows that[13,15,18]

$$E^{M} = \Delta_{S}{}^{M}\phi - \mu_{e}{}^{M}/e \tag{4.6}$$

Since the right-hand side of Eq. (4.6) contains quantities relevant only to the M/S interface, the equation expresses a single electrode potential. Equation (4.6) shows that different electrodes at the same value of E^{M} as a rule possess different values of $\Delta_{S}{}^{M}\phi$. Conversely, different faces of the same metal, if kept at the same potential E, also exhibit the same value of $\Delta_{S}{}^{M}\phi$. However, since different χ^{M} characterize different faces of the same metal, the same value of $\Delta_{S}{}^{M}\phi$ is achieved by different free-charge and dipolar contributions.

Since E^{M} as actually measured is a relative quantity, it raises the question of what is the absolute value of a single electrode potential.[10-21,23,106-108] This problem actually has not a great practical relevance since in practice only relative potentials are measured, but conceptually this matter fills the apparent gap between physics and electrochemistry. $\Delta_{S}{}^{M}\phi$ is very often regarded as the absolute electrode potential,[15,105,109,110] but Eq. (4.6) proves that this is not the case. This would be the case only if E were the difference between two and not three $\Delta\phi$. The quantity defined by Eq. (4.6) was recognized as the absolute electrode potential,[18] but this was criticized[19,21] in that the same Eq. (4.5) is obtained if a constant term K is added to Eq. (4.6).[11,13] Thus Eq. (4.6) defines in fact still a "conditional" potential based on $K = 0$.[19] Therefore this potential has been termed the *reduced absolute electrode potential*.[20] It is the form of single potential mostly encountered in practice when the cell potential difference is written in terms of interfacial parameters. Thus

$$_{r}E^{M} = \Delta_{S}{}^{M}\phi - \mu_{e}{}^{M}/e \tag{4.7}$$

This potential can be easily related to thermodynamic parameters of the electrode reaction by applying a Born–Haber cycle.[13,15,18] Thus, for the hydrogen electrode

$$\Delta_S{}^M\phi - \mu_e{}^M/e = (\tfrac{1}{2}\Delta G_{diss}^{\circ,H_2} + \Delta G_{ion}{}^{\circ,H} + \mu_{H^+}{}^{\circ,S})/e = {}_rE^\circ(H^+/H_2) \qquad (4.8)$$

The reduced absolute potential for the standard hydrogen electrode can be computed readily by introducing the appropriate quantities into Eq. (4.8). The actual accuracy of ${}_rE^\circ(H^+/H_2)$ depends only on the value of χ^S which determines the value of $\mu_{H^+}{}^{\circ,S}$. In the case of aqueous solutions, ${}_rE^\circ(H^+/H_2)$ has been found to be 4.31 V.[18] Note that this potential has often been claimed to be the absolute potential of the hydrogen electrode. The various values calculated[13–15,111,112] differ from that derived here by the different accuracy in the estimation of $\mu_{H^+}^{\circ,H_2O}$ and for other minor corrections.[18]

For any other electrode, since

$$E(\text{nhe}) = {}_rE^M - {}_rE^\circ(H^+/H_2) \qquad (4.9)$$

it follows that:

$${}_rE^M = E(\text{nhe}) + {}_rE^\circ(H^+/H_2) \qquad (4.10)$$

4.4. Absolute Electrode Potential

The conditionality of ${}_rE^M$ results from the fact that it is derived from Eq. (4.5) where any constant common term necessarily disappears because it cancels out ultimately. Actually, the cell potential difference as written by Eq. (4.3) is already a partial view of things, because only electrical terms are considered in a cycle where electrons are transferred from M to Ref through the external circuit and taken back from Ref to M through the internal circuit. It is easy to show that in Eq. (4.3) $\mu_e{}^M$ has been actually dropped. In fact, the measuring instrument reacts to the difference in electrochemical energy of electrons at the two ends of the cell. Thus

$$E = -(\tilde{\mu}_e{}^M - \tilde{\mu}_e{}^{M'})/e = \Delta_{M'}{}^M\phi \qquad (4.11)$$

and the single contribute each electrode makes to E is best recognized by following the profile of μ_e across the cell. Since this pathway necessarily involves the state of electrons in solution, it is necessary to distinguish between electronically polarizable and nonpolarizable interfaces.

4.4.1. Electronically Nonpolarizable Interfaces

If the individuality of each of the two electrodes must be preserved, solutions in contact with the two metals must be separated in this case[21,100] and cell (4.1) must be replaced by the following cell without transport:

$$M'|\text{Ref}|S(\text{Ref})\|S(M)|M \qquad (4.12)$$

where S(M) indicates the solution in the compartment of the cell containing electrode M. The energetic situation, recalling Eqs. (2.15) and (3.12), is (Figure 12a)

$$E = -(\tilde{\mu}_e^{M} - \tilde{\mu}_e^{M'})/e = -(\tilde{\mu}_e^{M} - \tilde{\mu}_e^{Ref})/e = -(\tilde{\mu}_e^{S/M} - \tilde{\mu}_e^{S/Ref})/e \quad (4.13)$$

Thus the absolute contribution each single electrode makes to E is

$${}_{abs}E^{M}_{(np)} = -(\tilde{\mu}_e^{S/M}/e) \quad (4.14)$$

The absolute electrode potential may thus be defined in terms of the work to extract electrons from the free surface of the solution in electronic equilibrium with the metal.[21] Also, recalling Eq. (3.12):

$${}_{abs}E^{M}_{(np)} = -(\tilde{\mu}_e^{M}/e) \quad (4.15)$$

which defines the absolute electrode potential also in terms of the work to extract electrons from the free surface of the metal in electronic equilibrium with the solution.

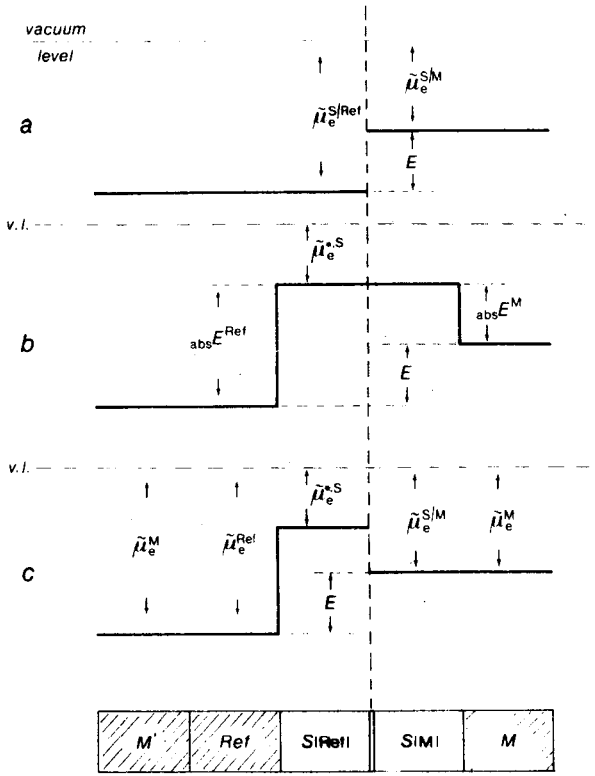


Figure 12. Profile of electrochemical potential of electrons across a cell. (a) Electronic equilibrium at both electrodes; (b) electronic equilibrium at neither electrode; (c) electronic equilibrium at one electrode only.

4.4.2. Electronically Polarizable Interfaces

In this case no separation between the two compartments of the cell is necessary. With reference to cell (4.1) it results (Figure 12b)

$$E = -(\tilde{\mu}_e^{M} - \tilde{\mu}_e^{Ref})/e = -(\tilde{\mu}_e^{M} - \tilde{\mu}_e^{*,S})/e + (\tilde{\mu}_e^{Ref} - \tilde{\mu}_e^{*,S})/e \quad (4.16)$$

Therefore the absolute contribution each single electrode makes to the cell potential difference is now

$${}_{abs}E_{(p)}^{M} = -(\tilde{\mu}_e^{M} - \tilde{\mu}_e^{*,S})/e \quad (4.17)$$

According to Eq. (3.33) this is precisely the electron work function of metal M in solvent S. Thus

$${}_{abs}E_{(p)}^{M} \equiv \Phi^{M/S}/e \quad (4.18)$$

where the final state chosen for electrons in solution corresponds to solvation.

Equation (4.18) is important in that it tells us that different electrodes kept at the same potential E^M possess electrons at the Fermi level with the same energy. As Figure 12a shows, this is the case also with nonpolarizable interfaces. With polarizable electrodes the electronic energy jump between metal and solvent is the same at the same potential irrespective of the nature of the metal.[96,101] This has been verified experimentally by photoelectric measurements.[97,113] Results have shown that for a given energy of light ($h\nu$), the photoelectric threshold, i.e., the potential at which electrodes start emitting electrons into the solution is the same for different metals. Equation (4.18) also explains why the electron work function of metals in a vacuum does not appear in equations of electrochemical kinetics.[96,101,114–116] This is because $\Phi^{M/S}$ and not Φ^{M} is operative at the M/S interface and $\Phi^{M/S}$ is the same for all electrodes at the same potential.[96,101]

4.4.3. Practical Situations

Two different absolute contributions of single electrodes to E are thus obtained. It is, however, easy to show that no confusion is possible in that both ${}_{abs}E_{(p)}^{M}$ and ${}_{abs}E_{(np)}^{M}$ *reduce* to ${}_{r}E^{M}$ in an electrochemical cell because either $\mu_e^{*,S}$, or ϕ^S are constants and cancel out ultimately. Thus, from Eqs. (3.18) and (4.9) it results, for instance for the potential of zero charge of metal M,

$$E_{\sigma=0}(\text{nhe}) = \Phi^{M}/e + \delta\chi^{M} - g^{S}(\text{dip}) - {}_{r}E^{\circ}(H^{+}/H_2) \quad (4.19)$$

This equation holds irrespective of the electronic polarizability or not of the interfaces. Equation (4.19) is widely used in electrochemistry, and relates directly the thermodynamic electrode potential to the electron work function at the metal–vacuum boundary.[15,55,94] By recalling Eqs. (3.17) and (3.24), Eq. (4.19) may be rewritten as

$${}_{r}E^{\circ}(H^{+}/H_2) = \Phi^{M}/e - E_{\sigma=0}^{M}(\text{nhe}) - \chi^{S} + \Delta_{S}^{M}\psi_{\sigma=0} \quad (4.20)$$

Equation (4.20) provides another route to the calculation of ${}_rE^\circ(H^+/H_2)$. Since Φ^M, $E_{\sigma=0}{}^M$ and the cpd are experimental quantities, ${}_rE^\circ(H^+/H_2)$ depends only on the estimation of χ^S so that its uncertainty in the case of aqueous solutions is not expected to be higher than ± 0.05 V.

If M is an electronically polarizable electrode, and a nonpolarizable interface is assumed for reference electrode, the result is (Figure 12c)

$$E = -(\tilde{\mu}_e{}^M - \tilde{\mu}_e{}^{*,S})/e - (\tilde{\mu}_e{}^{*,S} - \tilde{\mu}_e{}^{S/Ref})/e - (\tilde{\mu}_e{}^{S/Ref} - \tilde{\mu}_e{}^{Ref})/e \qquad (4.21)$$

which may be rewritten as

$$E = -(\tilde{\mu}_e{}^M - \tilde{\mu}_e{}^{*,S})/e + (\tilde{\mu}_e{}^{*,S} - \tilde{\mu}_e{}^{Ref})/e \qquad (4.22)$$

The outcome is that also in this case the absolute potential *appears* in the form of Eq. (4.17). It is concluded that in absolute terms the cell potential difference is to be regarded as the difference, expressed in electric potential units, of the work function in solution of the metals constituting the two electrodes.[3]

The actual value of ${}_{abs}E$ [subscript (p) will be understood henceforth] for the standard hydrogen electrode can be calculated from the equation

$${}_{abs}E^\circ(H^+/H_2) = {}_rE^\circ(H^+/H_2) + \mu_e^{*,H_2O} \qquad (4.23)$$

From the values given above it results that ${}_{abs}E^\circ(H^+/H_2) = 2.97(0)$ V. The physical meaning of this absolute potential is that 2.97 eV are required to transfer electrons from the Fermi level of the metal of a standard hydrogen electrode into the solvent. This work is conventionally taken as zero when potentials are measured in the (nhe) scale. For any other electrode it follows that

$${}_{abs}E^M = E^M(\text{nhe}) + {}_{abs}E^\circ(H^+/H_2) \qquad (4.24)$$

In particular, at the potential of zero charge

$${}_{abs}E_{\sigma=0}{}^M \equiv \Phi_{\sigma=0}^{M/S}/e = E_{\sigma=0}{}^M(\text{nhe}) + {}_{abs}E^\circ(H^+/H_2) \qquad (4.25)$$

Table 5 summarizes values of electron work function for some metals in water at the potential of zero charge. In particular, since $E_{\sigma=0}{}^{Hg}(\text{nhe}) = 0.19$ V,[49] it results that $\Phi_{\sigma=0}^{Hg/H_2O} = 2.78$ eV. Actually, experimental results indicate that the work function of Hg in H_2O is about 3.09 V.[117] This discrepancy is thought to be due to the fact that the reaction of electrons with the solvent is so rapid that the final state in solution actually corresponds to delocalized electrons.[21,98,99] Thus 3.09 V corresponds to the reactions

$$e(Hg) \rightarrow e_m(H_2O) \qquad (4.26)$$

It follows that $3.09 - 2.78 = 0.31$ eV measures the distance between localized and delocalized electron levels in water. Thus, $\alpha_{e_m}^{*,H_2O} = -1.16$ eV and $\mu_{e_m}^{*,H_2O} = -1.03$ eV. The value of the former quantity differs from previous estimates essentially because a different value has been used for the experimental work function of Hg in H_2O.[21,85,99]

Table 5

Equilibrium Work Function for Metals in Aqueous Solutions[a]

Metal	$\Phi_{\sigma=0}^{M/H_2O}$ (eV) [$\equiv {}_{abs}E_{\sigma=0}{}^{M}$ (V)]	Metal	$\Phi_{\sigma=0}^{M/H_2O}$ (eV) [$\equiv {}_{abs}E_{\sigma=0}{}^{M}$ (V)]
Ag	2.27	Nb	(2.18)
Al	(2.19)[b]	Ni	(2.67)
Au	3.15	Pb	2.41
Bi	2.57	Pd	2.97
Cd	2.25	Rh	2.95
Co	(2.52)	Sb	2.82
Cu	3.06	Sn	2.59
Fe	(2.62)	Ta	(2.12)
Ga	2.28	Ti	(1.92)
Hg	2.78	Tl	2.22
In	2.32	Zn	~2.35

[a] From Eq. (4.25) and $E_{\sigma=0}$ from References 49 and 55.
[b] Estimated (values in parentheses are less reliable).

Operative potentials, $\Delta_s{}^{M}\phi$, can be calculated from Eqs. (4.7) and (4.9):

$$\Delta_s{}^{M}\phi = E^{M}(\text{nhe}) + {}_{r}E^{\circ}(H^{+}/H_2) + \mu_e{}^{M}/e \qquad (4.27)$$

Table 6 summarizes some standard and zero charge operative potentials. As opposed to the absolute potential scale, once $\Delta_s{}^{M}\phi^{\circ}$ is calculated for the hydrogen electrode, it is not possible to convert ${}_{abs}E^{M}$ into $\Delta_s{}^{M}\phi$ for all other metals. Further, Eq. (4.2) shows that if different metals are used for the standard hydrogen electrode E^{M} is always the same but $\Delta_s{}^{M}\phi^{\circ}$ depends on the nature of the metal. $\Delta_s{}^{M}\phi_{\sigma=0}$ for Hg cannot be calculated because $\mu_e{}^{Hg}$ is unknown. How-

Table 6

Operative Standard and Zero Charge Potentials of Metals

Metal	$\Delta_s{}^{M}\phi^{\circ}$ (V)	$\Delta_s{}^{M}\phi_{\sigma=0}$ (V)	
Li	−0.54 ± 0.3	—	
Na	−0.46 ± 0.1	—	
K	−0.72 ± 0.1	—	
Rb	−0.71 ± 0.1	—	
Cs	−0.58 ± 0.2	—	
Zn	1.85 ± 0.4	2.0 ± 0.4	1.71[a]
Cd	1.71 ± 0.3	1.4 ± 0.3	1.02[a]
In	—	0.9 ± 0.3	
Mg	~0.2	—	
Al	~1.8	—	
Ca	~−0.1	—	
Sr	~−0.4	—	
Ba	~−0.1	—	

[a] From Reference 95.

ever, since χ^M becomes paramount as the number of valence electrons increases, $\Delta\phi_{\sigma=0}$ is very likely to be positive and of the order of 2–3 V.

4.5. Meaning of Potential in Terms of Electrode Reaction

In contrast to ${}_{abs}E^M$, which can in principle be measured experimentally, both $\Delta_S{}^M\phi$ and ${}_rE^M$ are not amenable of direct experimental measurement. If an electrode reversible to species in solution, for instance M/M^+, is taken into consideration, it is possible to demonstrate that the above various kinds of potential actually correspond to different ways of writing the interfacial reaction.[13,18,100] Thus, from Eq. (4.8)

$$\Delta_S{}^M\phi = (\Delta G_{ev}{}^{\circ,M} + \Delta G_{ion}{}^{\circ,M} + \mu_{M^+}{}^{\circ,S} + \mu_e{}^M)/e \tag{4.28}$$

It is easy to show that Eq. (4.28) results from the application of a Born–Haber cycle to the reaction

$$M(M) \rightarrow M^+(S) + e(M) \tag{4.29}$$

which is the customary way of writing electrode equilibria and which, according to arguments above, does indeed not correspond to the reaction defining E^M. It is easy to show that the difference between the various potentials physically corresponds to the storage in different phases of the electrons coming from the reaction. Thus Eq. (4.29) corresponds to the ionization of a metal atom in solvent S, while the produced electron is stored back in the metal. This corresponds to a partial view of the electrode equilibrium because only one component of the metal is assumed to cross the interface. Actually, this is a practical point of view which neglects the role of electrons.

According to Eq. (4.8), ${}_rE(M^+/M)$ derives from the application of a Born–Haber cycle to the reaction

$$M(M) \rightarrow M^+(S) + e(V) \tag{4.30}$$

where e(V) is an electron in a vacuum where $\mu_e{}^V = 0$. Equation (4.30) actually means that the state of the resulting electrons is not important when considering an electrochemical cell because the electronic parameters of the reactions in the two half-cells cancel out ultimately. ${}_rE^M$ is a "conditional" potential because it is the part of the absolute potential of an electrode which results under the condition of coupling the electrode with a reference electrode to build up a cell to measure the potential.[19] Equation (4.30) can thus be replaced in principle by a general equation:

$$M(M) \rightarrow M^+(S) + e(X) \tag{4.31}$$

where X is any other phase where electrons can be stored with the sole condition of being the same for both electrodes in the same cell. This is a direct consequence of the fact that building up a cell to measure E in fact realizes a system where the terminals are always of the same nature, i.e., the electrons coming from the reactions in the two half-cells are always stored in the same phase.

Finally, it is easy to show that ${}_{abs}E^{M}$ derives from the application of a Born–Haber cycle to the reaction

$$M(M) \rightarrow M^{+}(S) + e(S) \tag{4.32}$$

which is the same as Eq. (3.8). It is not an unexpected result that the actual absolute value of E^{M} should correspond to the electrode equilibrium as it actually takes place. This means that the correct way of looking at electrode equilibria is the chemical point of view relevant to sparingly soluble salts, even though most of the time the equilibrium is actually realized for only one species across the interface, or, alternatively, consideration of the interfacial equilibrium for a single species only is enough to characterize relative electrochemical parameters.

Acknowledgments

Financial support of this work by the National Research Council (C.N.R., Rome) is gratefully acknowledged. The author is grateful to his colleague, A. De Battisti, for stimulating discussion during the preparation of this chapter.

References

1. D. A. MacInnes, *The Principles of Electrochemistry*, Reinhold, New York, Dover Ed. (1961).
2. J. O'M. Bockris and A. K. N. Reddy, *Modern Electrochemistry*, Plenum Press, New York (1970).
3. S. Trasatti, in *Advances in Electrochemistry and Electrochemical Engineering*, H. Gerischer and C. W. Tobias, eds., Wiley, New York, (1977), p. 213.
4. W. Nernst, *Z. Phys. Chem.* **4**, 129 (1889).
5. P. Bowden and E. Rideal, *Proc. R. Soc. London Ser. A* **120**, 59 (1928).
6. A. Frumkin, *Sov. Phys.* **4**, 260 (1933).
7. A. Frumkin, *Ergeb. Exact. Naturwiss.* **7**, 235 (1928).
8. J. A. V. Butler, *Electrocapillarity*, Methuen, London (1938).
9. A. Frumkin, *J. Chem. Phys.* **7**, 552 (1939).
10. V. Pleskov, *Usp. Khim.* **16**, 254 (1947).
11. E. Kanevsky, *Zh. Fiz. Khim.* **22**, 1397 (1948); **24**, 1511 (1950); **25**, 854 (1951); **26**, 633 (1952); **27**, 296 (1953).
12. B. Ershler, *Usp. Khim.* **21**, 237 (1952).
13. B. Jakuszewski, *Bull. Soc. Sci. Lett. Lodz Cl. III* **8**, 1 (1957).
14. B. Jakuszewski, *J. Chem. Phys.* **31**, 846 (1959).
15. J. O'M. Bockris and S. D. Argade, *J. Chem. Phys.* **49**, 5133 (1968).
16. J. O'M. Bockris, *Energy Convers.* **10**, 41 (1970).
17. E. Gileadi and G. Stoner, *J. Electroanal. Chem.* **36**, 492 (1972).
18. S. Trasatti, *J. Electroanal. Chem.* **52**, 313 (1974).
19. A. Frumkin and B. Damaskin, *J. Electroanal. Chem.* **66**, 150 (1975).
20. S. Trasatti, *J. Electroanal. Chem.* **66**, 155 (1975).
21. A. N. Frumkin and B. Damaskin, *Dokl. Akad. Nauk SSSR* **221**, 395 (1975).
22. C. Kittel, *Elementary Solid State Physics*, Wiley, New York (1962).

23. R. Parsons, in *Modern Aspects of Electrochemistry*, J. O'M. Bockris, ed., Vol. 1, Butterworths, London (1954).
24. E. A. Guggenheim, *J. Phys. Chem.* **33**, 842 (1929).
25. E. A. Guggenheim, *Thermodynamics*, 5th Ed., North-Holland, Amsterdam (1967).
26. E. Lange and K. Mischenko, *Z. Phys. Chem.* **149**, 1 (1939).
27. G. A. Hass and R. E. Thomas, in *Measurements of Physical Properties*, Part I, E. Passaglia, ed., Interscience, New York (1972).
28. C. Herring and M. H. Nichols, *Rev. Mod. Phys.* **21**, 185 (1949).
29. J. C. Rivière, in *Solid State Surface Science*, M. Green, ed., Vol. 1, Marcel Dekker, New York (1969).
30. J. R. Smith, *Phys. Rev.* **181**, 522 (1969).
31. N. D. Lang and W. Kohn, *Phys. Rev. B* **3**, 1215 (1971).
32. J. A. Appelbaum and D. R. Hamann, *Rev. Mod. Phys.* **48**, 479 (1976).
33. R. A. Oriani and C. A. Johnson, in *Modern Aspects of Electrochemistry*, J. O'M. Bockris and B. E. Conway, eds., Vol. 5, Butterworths, London (1969).
34. J. Jortner and R. M. Noyes, *J. Phys. Chem.* **70**, 770 (1966).
35. Appendix III of the IUPAC Manual of Symbols and Terminology for Physicochemical Quantities and Units, *Pure Appl. Chem.* **37**, 499 (1974).
36. P. K. Rawlings and H. Reiss, *Surf. Sci.* **36**, 580 (1973).
37. V. Heine and C. H. Hodges, *J. Phys. C* **5**, 225 (1972).
38. M. M. Pant and M. P. Das, *J. Phys. F* **5**, 1301 (1975).
39. M. Hietschold, G. Paasch, and P. Ziesche, *Phys. Status Solidi B* **70**, 653 (1975).
40. A. O. E. Animalu and V. Heine, *Philos. Mag.* **12**, 1249 (1965).
41. T. Schneider, *Phys. Status Solidi* **32**, 323 (1965).
42. G. Paasch and M. Hietschold, *Phys. Status Solidi B* **67**, 743 (1975).
43. G. Paasch, H. Eschrig, and W. John, *Phys. Status Solidi B* **51**, 283 (1972).
44. N. D. Lang, *Solid State Commun.* **7**, 1047 (1969).
45. J. T. Davies and E. K. Rideal, *Interfacial Phenomena*, Academic Press, London (1961).
46. J. Horiuti and T. Toya, in *Solid State Surface Science*, M. Green, ed., Vol. 1, Marcel Dekker, New York (1969).
47. R. Smoluchowski, *Phys. Rev.* **60**, 661 (1941).
48. S. Trasatti, *J. Chim. Phys.* **72**, 561 (1975).
49. D. I. Leikis, K. V. Rybalka, E. S. Sevastyanov, and A. N. Frumkin, *J. Electroanal. Chem.* **46**, 161 (1973).
50. A. Hamelin and J. Lecoeur, *Surf. Sci.* **57**, 771 (1976).
51. S. Trasatti, *J. Chem. Soc. Faraday Trans. I* **68**, 229 (1972).
52. S. Trasatti, *Chim. Ind. Milan* **53**, 559 (1971).
53. R. Suhrmann and G. Wedler, *Z. Angew. Phys.* **14**, 70 (1962).
54. R. Bouwman and W. M. H. Sachtler, *Surf. Sci.* **24**, 350 (1971).
55. S. Trasatti, *J. Electroanal. Chem.* **33**, 351 (1971).
56. S. Trasatti, *J. Electroanal. Chem.* **54**, 19 (1974).
57. T. N. Rhodin, P. W. Palmberg, and E. W. Plummer, in *The Structure and Chemistry of Surfaces*, G. A. Somorjai, ed., Wiley, New York (1969), contribution 22.
58. D. M. Zehner, T. S. Noggle, and L. H. Jenkins, *Surf. Sci.* **41**, 601 (1974).
59. A. W. Adamson, *Physical Chemistry of Surfaces*, 2nd Ed., Interscience, New York (1967).
60. S. Trasatti, *J. Chem. Soc. Faraday Trans. I* **70**, 1752 (1974).
61. J. E. B. Randles, XVième Conseil International de Chimie, Solvay, June 1972.
62. B. Case and R. Parsons, *Trans. Faraday Soc.* **63**, 1224 (1967).
63. J. E. B. Randles and D. J. Schiffrin, *J. Electroanal. Chem.* **10**, 480 (1965).
64. A. N. Frumkin, Z. A. Iofa, and M. A. Gerovich, *Zh. Fiz. Khim.* **30**, 1455 (1956).
65. A. De Battisti and S. Trasatti, *Croat. Chem. Acta* **48**, 607 (1976).

66. J. E. B. Randles, in *Advances in Electrochemistry and Electrochemical Engineering*, P. Delahay and C. W. Tobias, eds., Vol. 3, Interscience, New York (1963).
67. R. I. Kaganovich and A. N. Frumkin, *Elektrokhimiya* **9**, 1265 (1965).
68. D. J. Schiffrin, *Trans. Faraday Soc.* **66**, 2464 (1970).
69. J. E. B. Randles, *Trans. Faraday Soc.* **52**, 1573 (1956).
70. J. Lowell, *J. Phys. D* **8**, 53 (1975).
71. A. J. Bennett and C. B. Duke, *Phys. Rev.* **160**, 541 (1967).
72. A. J. Bennett and C. B. Duke, *Phys. Rev.* **162**, 578 (1967).
73. H. F. Budd and J. Vannimenus, *Phys. Rev. B* **14**, 854 (1976).
74. N. D. Lang, *Solid State Commun.* **9**, 1015 (1971).
75. J. E. Inglesfield and E. Wikborg, *J. Phys. F* **5**, 1706 (1975).
76. R. L. Gerlach and T. N. Rhodin, *Surf. Sci.* **19**, 403 (1970).
77. A. Cetronio and J. P. Jones, *Surf. Sci.* **44**, 109 (1974).
78. D. M. Kolb, M. Przasnyski, and H. Gerischer, *J. Electroanal. Chem.* **54**, 25 (1974).
79. S. Trasatti, *Z. Phys. Chem. N.F.* **98**, 75 (1975).
80. D. C. Walker, *Quart. Rev.* **21**, 79 (1967).
81. B. E. Conway, in *Modern Aspects of Electrochemistry*, B. E. Conway and J. O'M. Bockris, eds., Vol. 7, Butterworths, London (1972).
82. G. A. Kenney and D. C. Walker, in *Electroanalytical Chemistry*, A. J. Bard, ed., Marcel Dekker, New York (1971).
83. E. J. Hart and M. Anbar, *The Hydrated Electron*, Wiley-Interscience, New York (1970)
84. L. I. Krishtalik and N. M. Alpatova, *Electrokhimiya* **12**, 163 (1976).
85. R. R. Dogonadze, L. I. Krishtalik, and Yu. V. Pleskov, *Elektrokhimiya* **10**, 507 (1974).
86. N. Gremmo and J. E. B. Randles, *J. Chem. Soc. Faraday Trans. I* **70**, 1480 (1974).
87. A. Henglein, *Ber. Bunsenges. Phys. Chem.* **78**, 1078 (1974).
88. A. De Battisti and S. Trasatti, *J. Electroanal. Chem.* **79**, 251 (1977).
89. Z. A. Rotenberg, *Elektrokhimiya* **8**, 1198 (1972).
90. K. G. Breitschwerdt and H. Radscheit, *Ber. Bunsenges. Phys. Chem.* **80**, 797 (1976).
91. P. Delahay, *J. Chem. Phys.* **55**, 4188 (1971).
92. S. Makishima, *J. Fac. Eng. Tokyo Imp. Univ.* **21**, 115 (1938); quoted in Reference 93.
93. H.A. Laitinen and C. J. Nyman, *J. Am. Chem. Soc.* **70**, 3002 (1948).
94. A. Frumkin, B. Damaskin, I. Bagotskaya, and N. Grigoryev, *Electrochim. Acta* **19**, 75 (1974).
95. J. O'M. Bockris and M. A. Habib, *J. Electroanal. Chem.* **68**, 367 (1976).
96. A. N. Frumkin, *J. Electroanal. Chem.* **9**, 173 (1965).
97. Z. A. Rotenberg, Yu. A. Prishchepa, and Yu. V. Pleskev, *J. Electroanal. Chem.* **56**, 345 (1974).
98. M. Heyrovsky, *Croat. Chem. Acta* **45**, 247 (1973).
99. D. J. Schiffrin, *J. Electroanal. Chem.* **63**, 283 (1975).
100. A. De Battisti and S. Trasatti, *J. Chim. Phys.* **74**, 60 (1977).
101. A. N. Frumkin, *Elektrokhimiya* **1**, 394 (1965).
102. S. Trasatti, *J. Electroanal. Chem.* **64**, 128 (1975).
103. N. M. Alpatova, S. E. Zabusova, and L. I. Krishtalik, *Elektrokhimiya* **12**, 625 (1976).
104. L. I. Krishtalik and N. M. Alpatova, *J. Electroanal. Chem.* **65**, 219 (1975).
105. K. J. Vetter, *Electrochemical Kinetics*, Academic Press, New York (1967).
106. W. M. Latimer, K. S. Pitzer, and C. M. Slansky, *J. Chem. Phys.* **7**, 108 (1939).
107. A. J. de Bethune, *J. Chem. Phys.* **29**, 616 (1958).
108. B. E. Conway and D. J. MacKinnon, *J. Phys. Chem.* **74**, 3663 (1970).
109. S. Glasstone, *An Introduction to Electrochemistry* Van Nostrand, Princeton (1942).
110. J. Koryta, J. Dvorak, and V. Bohackova, *Electrochemistry*, Methuen, London (1970).
111. E. Gapon, *Zh. Fiz. Khim.* **20**, 1025, 1209 (1946).
112. F. Lohmann, *Z. Naturforsch.* **22a**, 843 (1967).

113. Z. A. Rotenberg and Yu. V. Pleskov, *Elektrokhimiya* **4**, 826 (1968).
114. R. Parsons, *Surf. Sci.* **2**, 418 (1964).
115. P. Rüetschi and P. Delahay, *J. Chem. Phys.* **23**, 195, 1167 (1955).
116. J. O'M. Bockris and H. Wroblowa, *J. Electroanal. Chem.* 7, 428 (1964).
117. A. N. Frumkin, Symposium on Electrode Kinetics, Jablonna, May 1975.
118. B. E. Nieuwenhuys, R. Bowman, and W. M. H. Sachtler, *Thin Solid Films* **21**, 51 (1974).
119. R. Bowman, H. P. Van Keulen, and W. M. H. Sachtler, *Ber. Bunsenges. Phys. Chem.* **74**, 198 (1970).
120. P. O. Gartland, S. Berge, and B. J. Slagsvold, *Phys. Rev. Lett.* **28**, 738 (1972).
121. N. G. Imangulova and E. P. Sytaya, *Izv. Akad. Nauk. Uzb. SSR Ser. Fiz.-Mat. Nauk* **17**, 30 (1973).
122. A. Kashetov and N. Gorbatyi, *Fiz. Tverd. Tela* **10**, 2135 (1968).
123. R. Ya. Kamilova and E. P. Sytaya, *Dokl. Akad. Nauk Uzb. SSR* **27**, 20 (1970).
124. R. W. Strayer, W. Mackie, and L. W. Swanson, *Surf. Sci.* **34**, 225 (1973).
125. L. Benjamin and V. Gold, *Trans. Faraday Soc.* **50**, 797 (1954).
126. G. Wedler, C. Woelfing, and P. Wissmann, *Surf. Sci.* **24**, 302 (1971).
127. R. Suhrmann, J. M. Heras, L. Viscido de Heras, and G. Wedler, *Ber. Bunsenges. Phys. Chem.* **68**, 511 (1964); **72**, 854 (1968).

3

The Double Layer in the Absence of Specific Adsorption

R. REEVES

1. Introduction

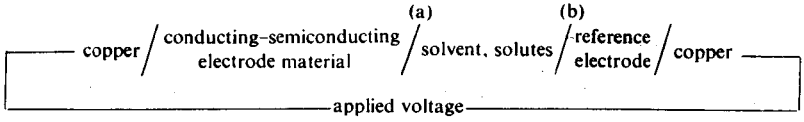
The discussion of adsorption in terms of classical thermodynamic models has been the subject of the first chapter of this volume. The term "model" is deliberately used since the development of the interrelationships pertaining to the electrochemical interface are of importance in the ensuing discussions of the detailed structure of the interface. The practicing electrochemist needs models to describe the entire region adjacent to the electrode as it is the detailed potential and concentration profiles that to a large extent control the rates of kinetic processes occurring at the electrode. This need for, at worst, an analytical description and, at best, a quantum mechanical description of the interfacial region has been one of the prime driving forces for studies of adsorption in the interface. In spite of the huge amount of effort exerted to date to attempt an understanding, deep comprehension of the detailed structure is still sadly lacking. Recent advances in the description of the bulk state of liquids have increased our insight into the complexity of the interactions required for an adequate description of a homogeneous phase.[1] Some limited success has been achieved in the description of complex associated systems like water, and even the problems of the introduction of ions into such systems are being attempted.[2] These recent studies are an attempt to overcome the restrictions of

R. REEVES • Laboratoire d'Electrochimie Interfaciale de C.N.R.S., 92190 Meudon, France.

classical models, such as those assumed in the Debye–Hückel calculations.[3] The problems are immediately magnified when the interface is introduced. The symmetry which can be used to simplify the bulk system is lost a further degree of uncertainty is introduced by the surface itself, a detailed description of which has proved to be very difficult even where the interface is gas phase. As will be seen, the influence of the surface can be a crucial parameter in the model of the region. The discussions in this chapter attempt to describe our current understanding of one limiting case that might be compared to the limiting law of Debye–Hückel. This is the case in which no specific adsorption occurs at the electrode. The succeeding two sections are presented as a practical definition of the terms in the preceding sentence, and the remainder of the chapter is a description of the various theories that can be used to understand the interface in this case, and their limitations.

2. Experimental Techniques and Some Useful Relationships and Definitions

The system under discussion in general comprises the following:



The battery provides a source/sink for electrons and the charge can flow either way around the system. The interface at (b) between reference electrode and the working solution must be stable and defined by the usual Nernst–Plank relationships. The experimental system being sought is one in which the interface at (a) does not pass current under steady state conditions. No electrolysis occurs at (a) and all the charge in the system derived from the voltage source is distributed across the interface (a). The majority of early work was carried out with water as the solvent. Recent studies have made extensive use of nonaqueous solvents. Useful solvents for these studies should allow dissociation of dissolved solutes and be resistant to oxidation or reduction. Amides, cyclic esters, and low-molecular weight alcohols fall naturally into this category.[4] The metal itself also is of great importance. The early studies were exclusively made using mercury but advances in metal technology now permit the use of high-purity noble metals and many types of oxide and semiconducting interfaces. Noble metal studies are frequently made using single crystals to allow complete definition of the solid surface.[5] The essential characteristic here is that there should be conductivity in the material up to the surface and that there should be a potential range in which the metal is not oxidized by the solute or solvent.

Metals displaying this type of behavior are said to have a range of *ideal polarizability*.

So far we have only referred obliquely to adsorption in the above system. In one sense, if a comparison is made with the gas phase, adsorption is always present in this system, i.e., the solvent, but this is specifically the reason why the two systems are different.

Thus in this system it is the *relative* strengths of the interactions between metal and solvent and metal and solute that is important in determining the characteristics of the system. The solvent concentration in reasonably dilute systems remains constant (e.g., water at 55.5 mol l^{-1} with a salt at 0.5 M). The presence of an interface in the system results in a redistribution of both solvent and solute. This is clearly shown in Chapter 1 of this volume. If the system of equations produced by thermodynamic argument is to be useful, a reference state must be chosen. Logically this must be the solvent as it is normally present in an overwhelming excess. This is the state of the system existant for all the studies pertaining to the weakly adsorbed state. If in other cases this condition cannot be met, alternative models have to be introduced at an early stage to aid analysis. Thermodynamic argument produces the relative surface excess, Γ_i, of species i and can be seen as the amount of that species present in the system between the surface and the bulk due to the influence of the surface on the system. It is the excess amount of species i in that region there in the presence of the interface over the amount that would have been there had the interface been absent. The solutes employed may be ionic or neutral, inorganic or organic. There is one proviso in these possiblities. Some dissociated ionic species must be present in the region (a)–(b), otherwise there is no possibility of charge redistribution in the solvent phase and the thermodynamic considerations do not apply.

The methods for the determination of the excess functions, Γ_i, derive naturally from the thermodynamic functions presented in Chapter 1. Basic among these is the Gibbs equation, which at constant temperature and pressure for an ionic system takes the form

$$-d\gamma = \sigma_m \, dE_\pm + \Gamma_\mp \, d\mu \tag{2.1}$$

where σ_m is the electrical charge on the electrode system, γ is the interfacial tension of the metal, $E_\pm$ is the potential of the working electrode measured with respect an electrode reversible to cation (E_+) or anion (E_-), $\Gamma_\mp$ are the cation (Γ_+) or anion (Γ) relative surface excesses, and z is the valence of the ionic species. This is the fundamental equation for an ideally polarized electrode in the system defined above. It is a complete differential and hence all the partial derivatives are valid:

$$\left(\frac{\partial\gamma}{\partial E_-}\right)_{T,P,\mu} = \left(\frac{\partial\gamma}{\partial E_+}\right)_{T,P,\mu} = -\sigma_m \qquad \text{(Lippmann equation)} \tag{2.2}$$

$$\left(\frac{\partial \gamma}{\partial \mu}\right)_{T,P,E_\pm} = -\Gamma_\mp \tag{2.3}$$

All the cross-differential relationships are also valid:

$$\left(\frac{\partial E_\pm}{\partial \mu}\right)_{\sigma_m} = -\left(\frac{\partial \Gamma_\mp}{\partial \sigma_m}\right)_\mu \tag{2.4a}$$

$$\left(\frac{\partial \sigma_m}{\partial \mu}\right)_{E_\pm} = \left(\frac{\partial \Gamma_\mp}{\partial E_\pm}\right)_\mu \tag{2.4b}$$

$$\left(\frac{\partial \sigma_m}{\partial \Gamma_\mp}\right)_{E_\pm} = -\left(\frac{\partial \mu}{\partial E_\pm}\right)_{\Gamma_\mp} \tag{2.4c}$$

$$\left(\frac{\partial E_\pm}{\partial \Gamma_\mp}\right)_{\sigma_m} = \left(\frac{\partial \mu}{\partial \sigma_m}\right)_{\Gamma_\mp} \tag{2.4d}$$

If Eq. (2.3) is further differentiated a series of very useful relationships results:

$$C = -\left(\frac{\partial \sigma_m}{\partial E_+}\right)_{T,P,\mu} = -\left(\frac{\partial \sigma_m}{\partial E_-}\right)_{T,P,\mu} = -\left(\frac{\partial \sigma_m}{\partial E_+}\right)_{T,P,\mu} = -\left(\frac{\partial^2 \gamma}{\partial E^2}\right)_{T,P,\mu} \tag{2.5}$$

The units of the ratio of charge to potential always have the units of capacity and this set of relationships constitutes the definition of a differential capacity.

Intuitively the surface excesses are associated with surface processes before considering the definition of adsorption in the system. In practice the measurement of $\Gamma_\mp$ and its variation with μ and $E_\pm$ are a good experimental basis for the definition of the adsorbed state. The methods we refer to are documented in the electrochemical literature and are only briefly described:[8] (1) radiotracer technique,[6] (2) measurement of γ,[7] (3) measurement of σ_m,[9] (4) measurement

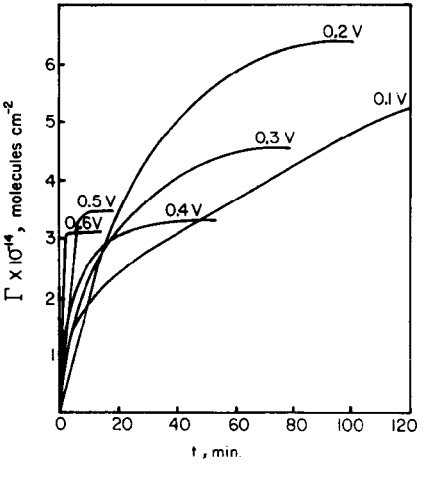


Figure 1. Adsorption of methanol from aqueous solution of platinum as a function of potential and time.[6]

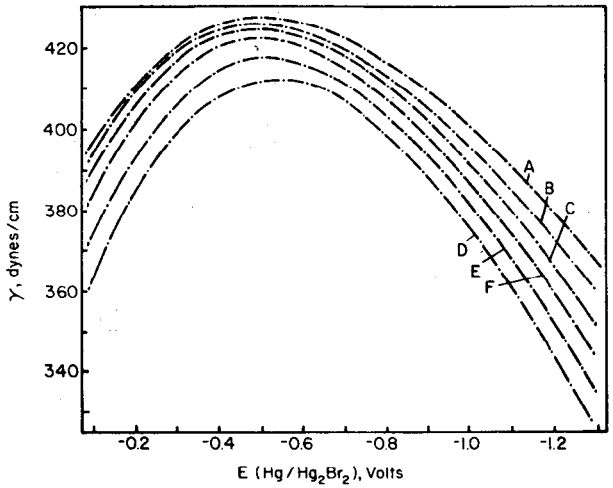


Figure 2. Electrocapillary curves for the mercury–aqueous KBr interface. Concentration of KBr solution (A) 0.01 F, (B) 0.03 F, (C) 0.1 F, (D) 0.3 F, (E) 1.0 F, (F) 3.0 F. E vs. Hg/Hg_2Br_2 electrode.[61]

of C.[10] In all cases, μ must be varied to obtain $\Gamma_{\mp}$ and $E_{\pm}$ is varied to obtain the dependence of $\Gamma_{\mp}$ on electrode charge. Each of these techniques is in principle applicable to any system but in practice they each have their own particular problems and correlations between the techniques are sometimes difficult to make. Method (1) is usually restricted to low-concentration systems and requires the use of thin-film electrodes attached to the end of the detector tube. It is therefore sensitive to impurities and requires extensive corrections to be made for the background count from the bulk of the electrolyte (Figure 1). Method (2) is useful for liquid metals, e.g., mercury, gallium, amalgams, and other low-melting-point metals and semimetals in simple solvent systems and has been used with metals such as lead in molten salt baths. Some typical electrocapillary curves are shown in Figure 2. There are many experimental problems involved in this technique if data of the highest accuracy are required and it is only recently that the relationships in Eq. (2.5) have been proved by double differentiation (see below). Method (3) has not been widely used for the study of adsorption in simple systems. It does find a very useful place in the measurement of interfacial parameters at very short times and for the detection of intermediates or absorbed species during the redox process at an electrode (cf. Figure 3).[73]

Method (4) is the most widely used technique as it tends to be sensitive to the small changes in surface properties. It has been used extensively for liquid metals and recently has been used in the characterization of solid–solution interfaces. Some typical examples of the results of these measurements are

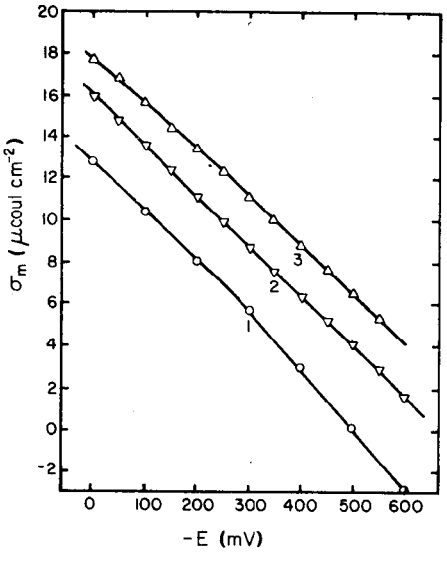


Figure 3. Charge–potential curves at constant values of adsorbed $Cr(OH_2)_3(NCS)_3$. (1) 1 *M* NaClO–0.01 M_2HClO_4, $T = 0$; (2) same electrolyte but $I = 1.25 \times 10^{-10}$ mol cm^{-2}; (3) same electrolyte but $T = 2.1 \times 10^{-10}$ mol cm^{-2}. The charges were obtained from coulostatic and potentiostatic steps from -100 mV.[73]

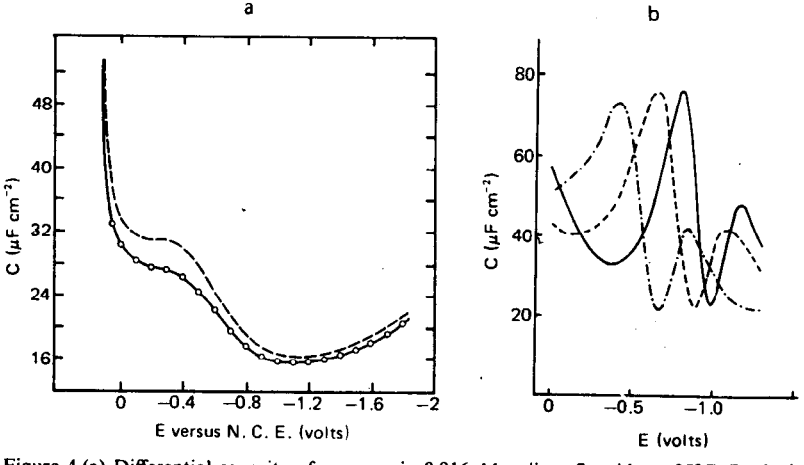


Figure 4.(a) Differential capacity of mercury in 0.916 *M* sodium fluoride at 25°C. Dashed line represents the differential capacity C_{M-2} of the compact double layer.[62] (b) Differential capacity curves for silver in aqueous solution of 0.01 *M* NaF. Measurements on single crystal faces using superimposed frequency of 20 Hz. Potential measured vs. S.C.E. (——) 110, (– – –) 100, (–·–) 111.[5]

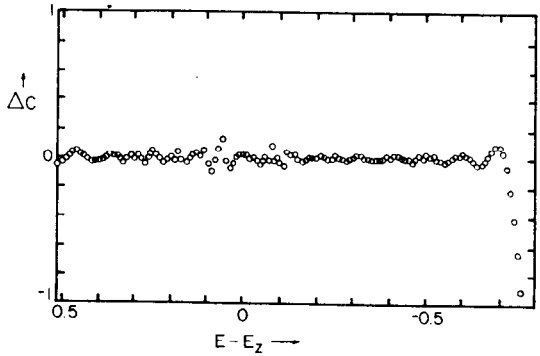


Figure 5. The difference between Grahame's original data and those reconstructed by double integration followed by double differentiation, as a function of "rational" potential $E_2 - E_z$, where E_z denotes the potential of zero charge. ΔC is in $\mu F\ cm^{-2}$, $E - E_z$ in V.[62,63] Conditions: 10^{-3} M $NaF/H_2O/Hg$.

shown in Figures 4a and 4b. Double integration of the C vs. E functions should yield the γ vs. E relationship according to Eq. (2.5). This is the most precise route for the definition of electrocapillary curves but the reverse is possible, i.e., derivation of capacity vs. potential functions from γ vs. E functions as shown in Figure 5. Up to this point in the discussion, no models other than those demanded for compatability by thermodynamics have been introduced. A number of models are used. The separation of chemical and electrochemical potentials requires the introduction of a model. Although intrinsically the measured excesses are independant of the position of the surface, in practice, when they are used, a model is implied in the way they are used.

Some Definitions Based on Experimental Observation

The discussion in this section has the following structure. The relative surface excesses discussed in the last section are presented and their characteristics analyzed. The basic models used to aid the interpretation of these results and which are explicitly described in the next section, are then applied to these data and the trends in the resultant functions analyzed. Further simplifying assumptions are then made and the various definitions of adsorption in the electrochemical system are proposed on the basis of the experimental evidence. Some of the problems involved in the testing of these definitions are outlined. The models, which are widely accepted for the description of the interface, then result as a natural consequence of these discussions.

The results that must be further analyzed are the thermodynamic surface excess functions derived using Eq. (2.1). The precise details of the manipulations required for their calculation will not be presented.[6,11] The details vary depending on the type of raw data available, but in all cases they require a precise

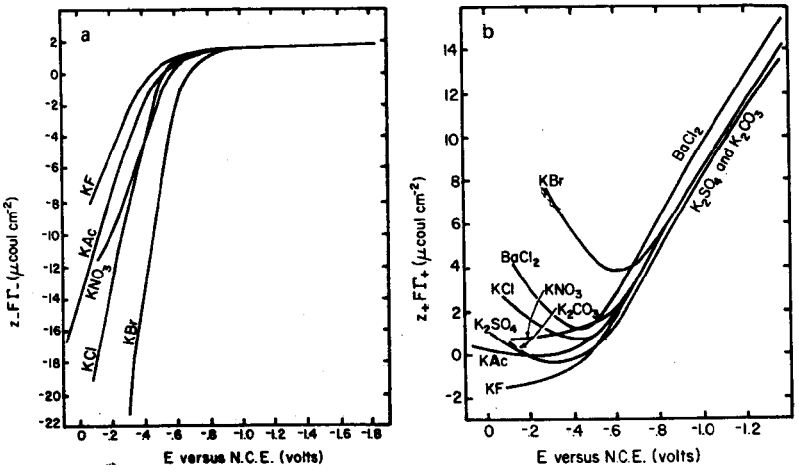


Figure 6. (a) Relative (to water) surface excesses of anions. (b) Relative (to water) surface excess of cations. All data for 0.1 *M* solutions of electrolytes at 25°C on mercury. Surface excess expressed as a charge.[64]

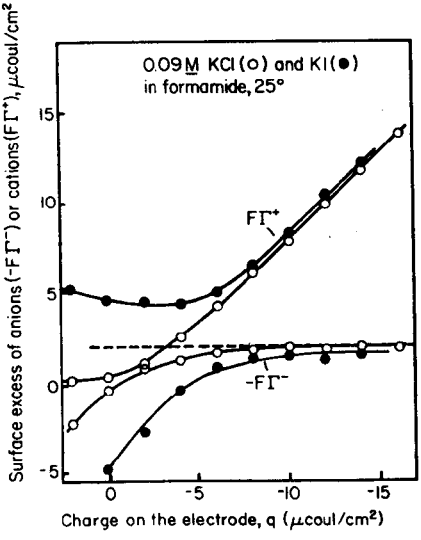

0.09 M KCl (o) and KI (●)
in formamide, 25°
Fτ+
-Fτ-
Surface excess of anions (-Fτ-) or cations (Fτ+), μcoul/cm2
Charge on the electrode, q (μcoul/cm2)

Figure 7. Ionic surface excesses for 0.09 *M* KCl and KI solutions in formamide at 25°C. Dashed line indicates diffuse layer limiting repulsion of anions for a 0.09 *M* solution.[65,4]

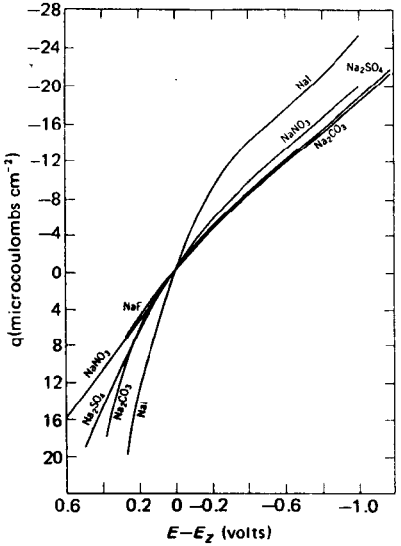


Figure 8. Charge on mercury in contact with various 1 *M* electrolytes at 25°C. Potentials referred to E_z for each electrolyte.

application of the given thermodynamic relations. Typical plots of $\Gamma_{\mp}$ are shown for a number of solutes in Figure 6a as a function of electrode potential for the mercury interface in aqueous solution. These display a number of marked characteristics. In Figure 6a the values of Γ_- converge at negative potentials and diverge markedly at less negative potentials, the deviation being a function of the anion present in the system. Similarly with Γ_+ in Figure 6b, on the negative potential branch a linear dependence on potential is displayed. There seems to be little dependence on the type of cation, for univalent species, although cation charge does appear to influence the plots. At less negative potentials the curves diverge rapidly, the divergence starting in the same potential region as the divergence already noted in Figure 6b. In this region the divergence of *cation* surface excesses is quantitatively comparable with the deviations noted for *anion* surface excesses. Similar characteristics are found for other metals and other solvents (cf. Figure 7).

There are certain theoretical consequence of this behavior. An absence of significant variation with cation or anion type means that the differential in Eq. (2.3) must be the same for all the systems. It also implies that the capacity C in all the systems, defined by Eq. (2.5), is invariant at a particular potential in this region (cf. Figure 8).

A second useful relationship can be readily derived from Eq. (2.2), the relationship between electrode charge and the applied potential. This is plotted for a series of salts in Figure 8, where the potential scales for the different systems have been aligned at zero electrode charge, $\sigma_m = 0$. The potential at this charge are usually referred to as E_{pzc}, the potential at the point of zero charge,

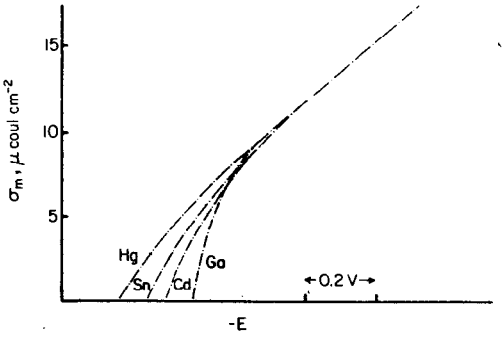


Figure 9. Charge vs. potential relationships for a number of metals shifted on the potential axis so that they form a common curve (at $\sigma_m \ll 0$).[41]

i.e., where $(\partial\gamma/\partial E)_{T,P,\mu} = 0$. At $\sigma_m \ll 0$ the lines have the same slopes, while at $\sigma_m \gtrsim 0$ considerable divergence in the slopes can be detected. It is useful to compare these plots with Figures 6 and 7. The coincidence of all the data for a particular valence system at $\sigma_m \ll 0$ suggests that a common description may be applied to the processes occurring in this region. The electrode charge in this region is negative and because of the overall electroneutrality of the system the excess charge on the solution side of the interface must be positive. As this excess charge will be composed of both anionic and cationic contributions, in general we may write

$$-\sigma_m = \sigma_s = zF\Gamma_- + zF\Gamma_+ \tag{2.6}$$

At $\sigma_m \ll 0$ there is a large excess of cations (Figures 6a and 6b) and it is proposed to identify this with zF_+. In the same region for anions their excess may be identified with zF_-. If a theory can now be found that depends on ionic valence and the simple bulk properties of electrolytes, and can describe the variation of these charges for cations and anions with electrode charge and bulk concentration, some further description of the system might be possible. Without such a theory no such progress is possible. The theory of the diffuse layer discussed in detail in the next section is such a theory and its results will be employed without further justification at this point.

For a z–z electrolyte, Eqs. (4.28) and (4.29) can be used to calculate the charge that would reside in the diffuse region of the double layer. If it is assumed that the experimental charges are also resident in the same region then comparison of the two values with the experimental values would give the possibility of a more extended theoretical treatment of the adsorption process. In practice, plots of σ_m vs. E, Γ_+ vs. E, and Γ_- vs. E give very good agreement with the predictions of the theory for the simple salts in the systems described above at $\sigma_m \ll 0$. If the description is adequate in this region, an attempt might be made to use it to describe the rest of the observed phenomena. If the tenets of the

diffuse layer theory are correct, the agreement found on a negatively charged electrode means that the charge in this region must reside only in the diffuse region. Electrostatically, cations might be expected to be attracted to and anions repelled from the negatively charged electrode, and the trends in Figures 6a and 6b confirm this trend. As σ_m becomes more positive, so the charge on the solution becomes more negative and anions might be expected to be attracted to the electrode and cations repelled. The surface excess due to anions does increase markedly, but after an initial decrease, in all cases except fluoride-containing salts, the cation excess also increases, in apparent contradiction to the diffuse layer model. This deviation of the system from the predicted behavior is the basis for all definitions of adsorption.

If cations were only present in the diffuse layer when they were positively attracted to the electrode, it is highly unlikely that under unfavorable electrostatic conditions they will approach the electrode surface any more closely at $\sigma_m > 0$, so the assumption is made that for cations whose surface excesses agree with diffuse layer predictions at $\sigma_m < 0$, they reside totally in the diffuse layer at $\sigma_m > 0$. In Eq. (2.6) above, σ_m and the cation diffuse layer charge, $zF\Gamma_{+,d}$, are known and the theory of the diffuse layer, Eqs. (4.28) and (4.29), can be used to calculate the balancing charge due to anions that will reside in the diffuse layer. This is precisely the amount of charge that must be present to satisfy the electroneutrality condition for the diffuse layer model for the given σ_m, i.e., the diffuse layer surface excess of anions $\Gamma_{-,d}$. The assumption has again been made that the diffuse layer cation and anion excesses are equivalent to the thermodynamically derived values, and under these conditions the following relation may be written:

$$\sigma_i = zF\Gamma_- - zF\Gamma_{-,d} \tag{2.7}$$

The first term is the thermodynamic term and the second the calculated term. The *difference* between these quantities is the specifically adsorbed charge σ_i. The charge σ_i is therefore the quantity of charge that cannot be accounted for by the diffuse layer model and is therefore assumed to lie outside the diffuse layer. In this case and in view of the considerations in the next section it is generally assumed to lie between the inner part of the diffuse layer and the electrode. Any species whose surface excesses are not totally described by the diffuse layer theory are therefore said to be *specifically adsorbed.* By analogy, if the surface excesses in the system are totally described by the diffuse layer theory, the system is said to be *nonspecifically adsorbed.* This thus implies that there is no excess of charge between the inner part of the diffuse layer and the electrode and all species whose surface excesses have been measured, residing totally in the diffuse region. (Note that the above calculations apply only to z–z electrolytes and that equivalent expressions exist for other systems.)

Having made these definitions and indicated the degree of involvement of modelistic ideas in the arguments, it is necessary to examine the methods available for the detection of the specifically adsorbed charge. It is also

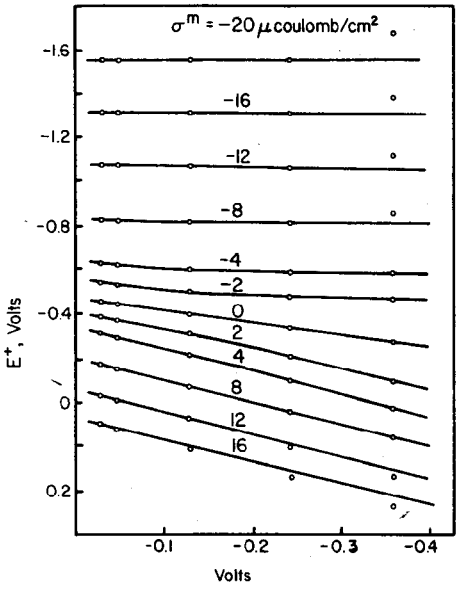


Figure 10. Essin and Markov plots for NaF solutions calculated from the data of Grahame.[69]

important to consider the reliability of these tests as for the purposes of electrode kinetic studies it is well known that even small values of σ^i can have a marked effect on kinetic processes. The Gouy–Chapman–Stern theory is the basis for all these tests and in every case it is a comparison of predicted parameters with experimental data. Gouy[7] was the first to observe that at E_{pzc} the value of the interfacial tension could increase or decrease with increased solute concentration, but at that time theoretical treatments were not available and specific adsorption could not be defined. He also observed that the value of E_{pzc} varied with the same variables. If the system is nonadsorbed and the equivalence of data is assumed, calculations using Eqs. (2.4a) and (5.2) yield equivalent quantities, i.e., $(\partial\Gamma_{\mp}/\partial\alpha_m)_{T,P,\mu}$. This is the Esin and Markov coefficient, and a typical plot for a nonadsorbed electrolyte is shown in Figure 10. As with all tests of the experiment against diffuse layer theory, the contribution of the diffuse layer is largest at $\sigma_m \sim 0$ (see discussion in the next section). The points are derived from experiment and the solid lines are the theoretical plots and, as can be seen in the figure, the agreement is good at all values of σ_m. This confirms that at $\sigma_m \sim 0$, there is no deviation from the charges calculated by diffuse layer theory, the system does not exhibit specific adsorption. Although there is apparently the same agreement at larger values of electrode charge, the lower contribution of the diffuse layer to the observed function significantly reduces the sensitivity of the test in these regions. At higher concentrations and at higher charges the deviations may be significant, but cumulative experimental

error reduces the significance of the points. This is a problem common to all attempts to detect very low degrees of specific adsorption. If adsorption is strong these plots are markedly different (cf. Figure 7).

A second method has already been presented above in order to derive the definition of adsorption (cf. Figures 6a and 6b). This method has an extra source of error as it requires the use of Eq. (2.6), a difference equation. If specific adsorption is very weak, $\Gamma_{-,d}$ is almost the same as Γ_-, and any errors in either or both of these values will be reflected in a large error in the difference. An additional and more general complication is brought out by these considerations. The number of manipulations of that data that must be carried out in order to produce the required variable may become a significant source of error. For example, in both the methods described above, data are interpolated at constant σ_m, requiring one integration of C vs. E with the correct integration constants or one differentiation of γ vs. E. These methods produce different types of errors. A systematic error in C would clearly give a large error in the integral, while small random deviations from the correct function in the second case could markedly alter the slope at a particular point, again yielding an incorrect σ_m vs. E function. Numerical differentiation is normally considered to be less precise and the second method is doubly insecure as it requires repeated differentiations. One way of testing the error in the system is to use an alternative method for the detection of specific adsorption. C can be measured precisely and if diffuse layer theory describes the system and no ions reside in the inner layer, the capacity of the inner layer might be expected to be independent of solute concentration. The capacity of the diffuse layer C_d can be calculated from Eq. (4.30) and the following series capacitor model applied:

$$1/C = 1/C_d + 1/C_i \tag{2.8}$$

where C_i is the concentration-independent value of inner-layer capacity. The relation between experimental electrode charge and potential must be calculated by integration to use the diffuse layer calculation, and the experimental capacity must be interpolated at the same charge values. In the absence of adsorption, at constant σ_m, a plot of $1/C$ vs. $1/C_d$ should be linear with a slope of unity. Typical plots are shown in Figure 11. The influence of systematic error in determining the capacity might be derived in the following manner. It is found experimentally that at $|\sigma_m| \gg 0$ the capacity errors increase. This is one of the more direct methods and can readily be applied.

Grahame and Soderberg also used a technique based on the use of the C vs. E data. They argued that if the capacity in the diffuse part of the double layer were defined, then the components of the capacity contributed by anions and cations were also defined, and related to the total measured capacity by

$$\left(\frac{\partial \sigma_m}{\partial E_-}\right)_\mu = -\left(\frac{\partial \sigma_+}{\partial E_-}\right)_\mu - \left(\frac{\partial \sigma_-}{\partial E_-}\right)_\mu \tag{2.9}$$

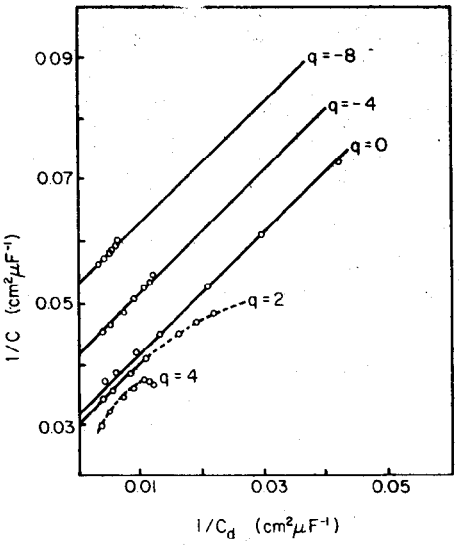


Figure 11. Plot of reciprocal capacity vs. reciprocal diffuse-layer capacity for a nonadsorbed electrolyte. Lines are drawn with unit slope. Aqueous KOH is at the mercury/solution interface.[66]

for an anion reversible indicator electrode. This is equivalent to

$$C = C_+ + C_- \tag{2.10}$$

C_+ and C_- are then, by the same arguments as were used above, defined as thermodynamic variables by

$$C_+ = -\left(\frac{\partial \sigma_+}{\partial E_-}\right)_\mu = -zF\left(\frac{\partial \Gamma_+}{\partial E_-}\right)_\mu \quad \text{and} \quad C_- = -\left(\frac{\partial \sigma_-}{\partial E_-}\right)_\mu = -zF\left(\frac{\partial \Gamma_-}{\partial E_-}\right)_\mu \tag{2.11}$$

Also we have that

$$\left(\frac{\partial \sigma_m}{\partial \mu}\right)_{E_-} = \left(\frac{\partial \Gamma_+}{\partial E_-}\right)_\mu \tag{2.12}$$

As differentials of functions tend to be more sensitive indicators of the characteristics of the function than the original function, the last relationship is again differentiated to yield

$$zF\left(\frac{\partial C_-}{\partial \mu}\right)_{E_-} = -\left(\frac{\partial C_+}{\partial E_-}\right)_\mu \tag{2.13}$$

If there is no specific adsorption

$$zF\Gamma_+ = \sigma_{+,d} = A\{\exp[-\sinh^{-1}(\sigma_m/2A)] - 1\} \tag{2.14}$$

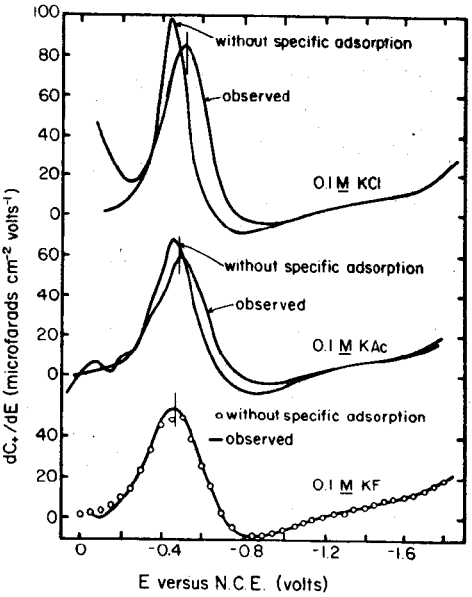


Figure 12. Observed and calculated values of dC_+/dE for three electrolytes in contact with mercury at 25°C. Calculated curves were computed from Eq. (2.15) on the assumption of no specific adsorption.[64]

using diffuse layer theory, it is a simple matter to obtain the differential coefficient in Eq. (2.13) by double differentiation,

$$\left(\frac{\partial C_{+,\mathrm{d}}}{\partial E_-}\right)_\mu = \frac{C}{2(\sigma_\mathrm{m}/2A + 1)]^{1/2}} \times \left(\left\{\left[\left(\frac{\sigma_\mathrm{m}}{2A}\right)^2 + 1\right]^{1/2} - \frac{\sigma_\mathrm{m}}{2A}\right\} \frac{1}{C}\left(\frac{\partial C}{\partial E_-}\right)_\mu - \frac{C}{2A[(\sigma_\mathrm{m}/2A)^2 + 1]}\right) \tag{2.15}$$

This equation is a theoretical relationship which shows how the differential coefficient $(\partial C_+/\partial E_-)_\mu$ would behave if the system were described by diffuse layer theory alone with a concentration-independent inner-layer capacity. The relationship is implemented by calculating the experimental value of the coefficient using Eq. (2.15) and comparing this curve with the theoretical curve. If the two curves coincide, the assumed nonadsorbed model would be an adequate description of the system within experimental error. Again the sensitivity of the technique depends on the differential contribution of the diffuse layer to the coefficients and as can be seen from Figure 12 the most sensitive region will be around -0.3 to -0.7 V for the systems shown in this figure at the mercury interface.

The agreement between theory and practice seems to be good at very negative potentials in all cases, but whereas for F^- systems this agreement extends

to less negative potentials, for the other systems there are deviations from the theoretical plots. This method depends crucially on the precision of the capacity measurements and the accuracy with which the potential is controlled as the concentration of solute is varied. The variation of capacity with chemical potential of the solute is not large in many cases and data of the highest accuracy are necessary for this type of interpolation. Some deviations even occur with F^- near the maximum in the function and at positive potentials. The latter may be associated with specific adsorption but near the maximum where the theory is most sensitive to testing, the origin of the deviations is unclear. This may be associated with the inadequacy of the model or be due to inadequate experimental data.

An alternative approach which utilizes diffuse layer theory in a less obvious way is a differential technique based on the different adsorption characteristic of two species. If the adsorption experiment is carried out at constant ionic strength with two salts whose adsorption characteristics differ, an apparent surface excess can be calculated according to the following relationship:

$$\left(\frac{1}{RT}\right)\left(\frac{\delta\gamma}{\partial \ln x}\right)_{E,T,P} = -\Gamma_{A,i} = \frac{\sigma_i}{zF} \tag{2.16}$$

(The reader is referred to the original literature for the derivation of this relationship.) In this equation x is the concentration of one of the anions in the mixture MB + MC, where M is a common nonspecifically adsorbed cation and B and C are anions. The specific adsorption of anions will only be considered to be possible in this system. The surface excess derived above is already corrected for the influence of the diffuse layer and is therefore an apparent specifically adsorbed excess charge, $\Gamma_{A,i}$. The relationship to the individual specifically adsorbed charges is as follows:

$$\Gamma_{A,i} = \Gamma_{B,i} - \frac{x_B}{m - x_B}\Gamma_{C,i} \tag{2.17}$$

where m is the total molarity of the system. It is evident from this relationship that if one of the ions is nonspecifically adsorbed, Γ_i for the ion will be zero. In this case the observed specifically adsorbed charge is the true specifically adsorbed charge. If, however, one of the components is weakly specifically adsorbed in the presence of a second more strongly specifically adsorbed ion, the second term in the equation becomes important and the observed adsorption measured by σ_i will be less than the true degree of specific adsorption. Some plots which apparently show this effect are shown in Figure 13. There are a number of problems with this apparently simple technique. It requires that some assumption be made about the charge dependence of the specific adsorption of one of the ions. It assumes the diffuse layer theory is equally applicable to the two ions and that at constant ionic strength all the mixtures behave in the same way. The two salts must have similar variations of activity coefficients with concentration, and ideally the ions should be the same size to eliminate the possible differences

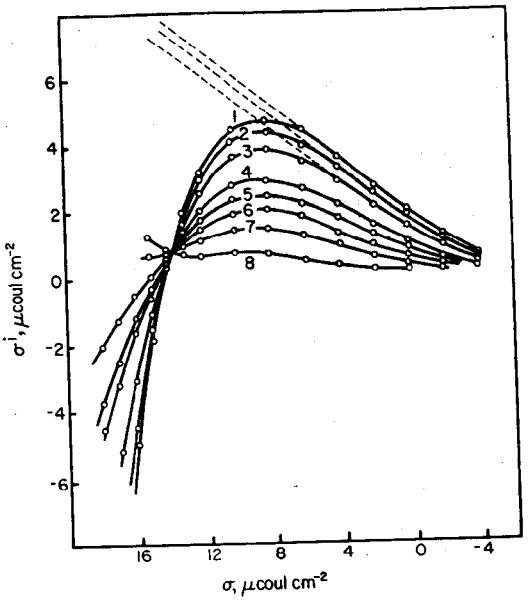


Figure 13. (——) Charge due to specifically adsorbed hexafluorophosphate ions (σ^1) as a function of charge on the metal (σ) and bulk concentration of KPF_6; (– – –) estimated "true" adsorbed charge due to hexafluorophosphate ions. x '(1) 0.3, (2), (3) 0.1, (4) 0.075, (5) 0.050, (6) 0.035, (7) 0.020, (8) 0.010.[97]

in the distance of approach to the electrode surface. In practice many of these conditions are mutually exclusive but the differential technique may be of help where all other techniques have failed.

These are the principal methods for the detection of specific adsorption currently in general use. There are other direct methods such as the radio tracer technique, which finds application in specialized situations, and there are a number of indirect techniques. The idea behind the indirect techniques is to find something that can detect the influence of specifically adsorbed charge in the inner region and reflect this change in the macroscopic parameters of the system. There are two approaches, one based on adsorption of organic molecules and a second based on electrode kinetic studies. The adsorption of organic molecules takes place in a similar manner to the adsorption processes outlined above. Ideal adsorption involves the replacement of the interfacial water molecules and some degree of solvent reorganization. If specifically adsorbed ions are present, the reorganization of the water structure will be different and there will be in addition interactions between ions and organic molecules in the adsorbed layer. In principle, these should be reflected in the adsorption properties of the system, and indeed differences are found when the same ion is studied

in different electrolytes, but the method suffers from the same problems as the last method outlined above in that some assumptions about the characteristics of the adsorption of the organic species in the absence of specific ion adsorption must be made. This either requires a model or an ideal system to be found for comparison. The alternative technique based on the influence of the specific adsorption on the kinetics of electrode processes has been widely used.[60] This is based on the principle that the driving potential for an electrochemical redox reaction is not the applied potential but the potential drop between the reaction site and the electrode. If the potential at the inner plane of the diffuse layer is assumed to be this site then the diffuse layer theory may be used to calculate the potential. The total potential drop in the cell can then be corrected for the potential drops from reference electrode to the reaction site and the potential dependence of the kinetic parameters investigated using this corrected potential as the driving potential for the redox process.

3. Introduction to the Use of Models to Describe the Double Layer

The tendency of a solution-soluble species to adsorb at the electrode solution interface is a function of a number of parameters in any system: (1) the strength of the interaction of the solvent with the electrode, (2) the strength of the solvation of the adsorbing species in the bulk, (3) the strength of the interaction of the electrode with the adsorbing species, and (4) the energy associated with the rearrangement of the solvent at the electrode when the species is adsorbed. There are a number of other terms that could be included but it is useful to consider the various systems available for study in the light of this set of divisions. From the earlier discussions it will be clear that if $\sigma_m \neq 0$ there are always the surface excess terms in the system to balance the electrode charge, a necessary consequence of thermodynamics. What we are concerned with now is the precise location of the species that comprise this surface excess, and their location is controlled by the above factors. If (1) and (2) are strong and the remainder are weak there will be little tendency for the species to locate itself close to the electrode. This would be typical of the conditions required to produce a nonadsorbing system as defined in the previous section. On the other hand if (1) were weak and (3) were strong then it is likely that the species could approach the electrode closely and would hence be specifically adsorbed.

Considering (1) in more detail leads to the natural division into the influence of the metal on the behavior of the solvent and the relationship between solvent type for a particular metal and the strength of adsorption. If the metal is considered, two types of correlations are possible, a general correlation of the surface parameters of the metal with the adsorbed solvent and the detailed influence of surface structure on the observed behavior of the system. In the former case there is a good correlation in general between the work function Φ,

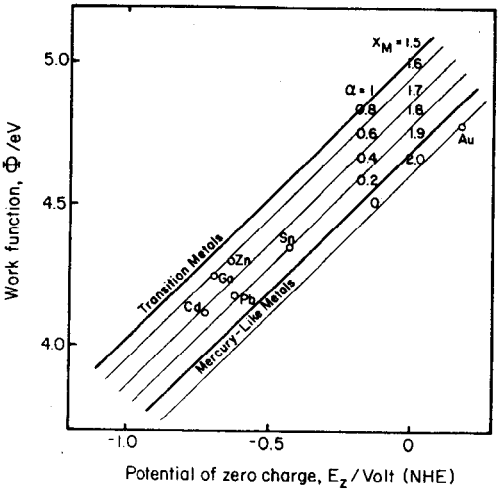


Figure 14. Plots of potential of zero charge against work function of metals. X_m is the Pauling electronegativity and α is the degree of orientation of water molecules at the interface.[13]

the electronegativity χ_m, and the point of zero charge for metals. A relationship of the form[12,13]

$$E_{pzc} = \Phi - 4.61 - 0.666(2.10 - \chi_m) \tag{3.1}$$

has been proposed. This applies to aqueous systems for a very wide range of metals. It is possible to deduce from this type of relationship the relative strengths of interactions of the metal with the solvent, in this case water, in terms of the relative degree of orientation of water against the metals. The order was found to be as follows for some common metals in the absence of an external field:

$$\text{Au, Cu} < \text{Hg, Ag, Sb, Bi} < \text{Pb} < \text{Cd} < \text{Ga}$$

a series similar to the Pauling electronegativity scale for the metals. Using the same relationship for a range of metals it is possible to show (cf. Figure 14) that the transition from a fully oriented layer of water on the surface to a very weakly interacting system involves a potential shift of ~ 0.4 V. If the potential of a dipole layer is now calculated using classical electrostatics,

$$g_{H_2O} = 4\pi\mu n/\varepsilon = 0.75 \text{ V} \tag{3.2}$$

where μ is the dipole moment of water, ε is the dielectric constant, and an area of 12.5 Å^2 has been assumed for the water molecule. In order to obtain agreement with the experimental data it is necessary to orient the molecule at the interface at an angle of 32° to the surface, which is not unreasonable if the hydrogen bond

angles are considered between the surface molecule and the molecules in a second layer. Information on orientation can also be derived from the temperature coefficient of the surface potentials at metals. For mercury this is negative, as it is at the air/solution interface, thus tending to confirm this conclusion. The detailed interaction parameters that should be considered are evident when capacity vs. potential data are recorded for the precisely defined faces of single crystals. Some examples of the specificity of these interactions may be seen in Figure 4b.

The solvent itself requires special consideration and examples of the differences found for different solvents with the same metallic interface are clearly seen in the earlier sections.[4,14] From the solution side, the adsorption of a species may be seen as a combination of all four points. If for the moment the process is simplified and reduced to the problem of creating a vacancy on the surface to receive two adsorbing species, two effects need to be described. The first is a formulation of the energy involved in the solvation of the interface and the second in a similar description of the forces controlling the desorption of solvent. A simple cycle might be imagined in which the free metal is first covered with the solvent and then a vacancy is created in the interfacial solvent structure to accept the adsorbing species. The work of adsorption of the solvent might be described by the Dupré equation

$$W_a = \gamma_{m/a} + \gamma_{s/a} + \gamma_{m/s} \tag{3.3}$$

where the γ's refer to interfacial tensions at the metal/air, solution/air, and metal/solution, respectively. The work of displacement involves the work of adhesion and a contribution from the difference between stabilization energies for the molecules between surface and bulk and can be similarly expressed through

$$W_d = \gamma_{m/s} - \gamma_{m/a} \tag{3.4}$$

A number of values of these coefficients for common systems is to be found in Table 1. According to the values of W_a, water adheres to mercury more firmly than many other organic solvents. From Eq. (3.4) and Table I the situation for adsorption of ions is seen to be more complex. Low interfacial tension generally means that the solvent is difficult to displace from the interface but does not necessarily imply strong interaction of the solvent with the metal. Water seems to be the easiest solvent to displace and it might be expected to show the strongest adsorption of solutes. The subdivision between the contributions of solvation energy and competitive solvent adsorption is difficult to make convincingly and the problem is emphasized in solvents such as dimethylsulfoxide, where very strong adsorption is found for anions, which are rather weakly solvated in the bulk, although the solvent itself seems to be strongly adsorbed. The balance is difficult to predict *a priori*, and before it can be made, better correlations between the differences in specific solvation behavior must be made for the different solvents employed.

Table 1

Work of Adhesion of Pure Liquids onto Mercury[4][a]

Solvent	Surface tension, erg/cm²	Interfacial tension, erg/cm²	Work of adhesion, erg/cm²
Water	72.0[b]	425.4[b]	130.6
Methanol	22.1[b]	392.5	113.6
Ethanol	22.8	386.9	119.9
n-Propanol	23.8	383.5	124.3
n-Butanol	24.6	382.7	125.9
t-Butanol	20.7	386.9	117.8
sec-Octanol	27.5	375.0	136.5
Formic acid	37.6	399.0	122.6
Acetic acid	27.8	392.0	119.8
n-Butyric acid	26.8	381.8	129.0
Glycol	47.7	381.4	150.3
Glycerol	63.4	384.8	162.6
Ethyl ether	17.0	379	122
Chloroform	27.1	369.6	141.5
Ethyl bromide	24.2	367.3	140.9
Ethyl iodide	(24)	346.8	161
Formamide	58.2	388.6[b]	153.6
Dimethylformamide	36[c]	376[f]	144
Acetonitrile	29.3	393[e]	120
Acetone	23.7	388.2	119.5
Dimethylsulfoxide	45[b]	370.6[b]	158.4
Sulfolane	53.3[c]	373.5[c]	163.8
4-Butyrolactone	43.8[d]	377.0[b]	150.8
Ammonia	26.0[e]	390	120
Aniline	42.9	357.2	169.7
Pyridine	38.0	363.4	158.6
Benzene	28.9	357[f]	155.9

[a] See Ref. 4 for details of data sources and methods of calculation.
[b] At 25°C.
[c] At 30°C.
[d] At 23°C.
[e] At 0°C.
[f] At 20°C.

Other parameters that might be expected to control the observed behavior are the different dielectric constants of the solvents and the different molecular sizes. Also the degrees of association that different solvents display in the bulk may be of importance. It is now clear that in the region adjacent to the electrode it is molecular size rather than the bulk dielectric constant that is the principal controlling factor in the capacity minimum (cf. Figure 15). This is a region in which there is no specific adsorption and the observed parameters reflect almost totally the influence of the solvent. For the amide series of solvents the correlations are shown in Table 2. Other properties of the observed capacity vs.

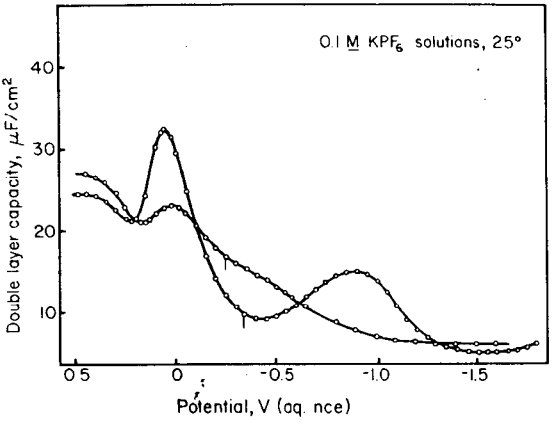


Figure 15. Differential capacity curves for 0.1 *M* KPF_6 solutions in dimethylacetamide and *N*-methylpropionamide at 25°C.[4]

potential function are associated with the degree of association displayed by the solvents, and these are discussed fully elsewhere.

It is apparent from the experimental observations that one approach to the problem of devising a model is to assume that the system can be subdivided into two parts consistent with the approaches used to interpret the thermodynamic variables. The above discussions show clearly that the solvent-metal interaction and the behavior of the solvent in the region close to the electrode are principal factors in determining the features of the system, and the subsequent sections discuss the region adjacent to the electrode surface and the diffuse region, which extends from the outer part of this inner region to the bulk

Table 2

Physical Properties and Double Layer Capacity in Amide Solvents at 25°C[4]

Solvent	C_{min},[a] μF/cm²	Molecular weight	Length of molecule,[c] Å	Dielectric constant
Formamide	12.5[b]	45	5.6	109.5
N-Methylformamide	8.5[b]	59	6.4	182.4
Dimethylformamide	6.8	73 } isomers	6.7	36.7
N-Methylacetamide	6.7	73 } isomers	6.8	178.9
Dimethylacetamide	6.0	87 } isomers	6.9	37.8
N-Methylpropionamide	5.6	87 } isomers	7.8	172.2

[a] C_{min} is measured at the minimum on the cathodic branch of the capacity-potential curve for 0.1 *M* KPF_6 solutions except where otherwise stated.
[b] For 0.1 *M* KCl.
[c] Estimated from Courtaulds molecular models.

of solution, as two distinct entities. The dangers intrinsic to such a separation are important and are the main imperfections in the whole theoretical treatment of this region, and comment pertaining to this problem form an important part of the discussion of these models.

4. Diffuse Layer Theory and Its Validity

4.1. Fundamental Theory

The introduction of modelistic ideas to aid in the description of the interfacial problem has already been clearly demonstrated in the earlier part of this chapter and in Chapter 1 of this volume. At this stage, some assumption must be made about the validity of parameters that can be calculated from the earlier analysis. If it is assumed that the values of relative surface excess, capacity, and charge as functions of potential are the source material, some attempts can be made to split up the various contributions in the system. The general concept behind the following subdivision is an attempt to describe the properties of part of the system using the concepts of statistics in continuous bulk phases while leaving the remainder for description by molecular models. The experimental data that are frequently used to justify this approach are presented later in this section but the overall approach is common to much of physical chemistry.

The model widely adopted in this context was first suggested by Gouy[7] and Chapman[15] independently. The electrode is considered to be planar and the distribution of ions adjacent to the charged surface is calculated using an approach similar to that used by Debye and Hückel. Thus in general terms the solvent and ions surrounding the electrode might be thought of as an effective ion atmosphere adjacent to an ion of variable charge. (This theory preceded the Debye–Hückel theory by more than a decade.[3]) The theory must be as consistent as possible with the thermodynamic approach, and the treatment assumes equilibrium conditions,

$$\mu_{\text{bulk}} = \mu_{\text{diffuse}} \tag{4.1}$$

for all the species in the system. The solvent is considered to be an isotropic medium and there can therefore be no discontinuities in the system. All potentials are average smeared quantities, and equipotential planes in the system are precisely defined irrespective of the size or location of the subsystem being considered. One immediate consequence of this initial model is that only one coordinate need be considered, the axis normal to the electrode surface, x. All charge and potential distributions can therefore be expressed in terms of this one coordinate.

The overall aim of the derivation is to use the classical Boltzmann distribution function to relate the energy differences in the chosen system to the parameters we require to define, e.g., charge or potential distribution. To achieve

this, the classical concept of potential is used to define two potential differences (work done to move a point test charge from place to place in the system). These are the potential in the bulk of the phase ϕ_s ($0 \ll x < \infty$) and the potential at a site at a distance x from the surface ϕ_x ($0 < x \ll \infty$). These two potentials are defined with respect to the same reference point, which, however, does not require further definition. We can now write the work which must be done to move ions from one potential site to the other, $z_iF(\phi(x) - \phi_s)$ for 1 mol of species i carrying a charge z.

The distribution function is introduced at this point and this yields directly the concentration of species i at the chosen coordinate x,

$$c_i(x) = c_i(s) \exp\left[-\frac{z_iF}{RT}(\phi(x) - \phi_s)\right]$$

$$= c_i(s) \exp(-f\phi) \tag{4.2}$$

where $c_i(s)$ is the concentration of species i in the bulk of the phase, $f = z_iF/RT$, $\phi = \phi(x) - \phi_s$, R is the universal gas constant, and T is the absolute temperature of the system.

It is now necessary to convert this formulation into a practical solution for a real system in which there is electroneutrality of totally dissociated salts. As there is to be a comparison between results of this type of calculation and thermodynamic excess functions, the calculations are better expressed in the form of charge.

The charge due to species i in a unit volume element at a distance x from the electrode is given by

$$\sigma(x) = z_iFc_i(x) \tag{4.3}$$

If this function is summed over all charged species in the volume element, the sum must be the charge density in the chosen volume element at x, i.e.,

$$\sigma(x) = \sum_i z_iFc_i(x) \tag{4.4}$$

The second important variable with which we require a relationship is the potential. This is necessary to link the charge definition to the concentration function defined by Eq. (4.2). The classical Poisson equation relates potential gradient to the charge density per unit volume of an isotropic medium. As our model is one dimensional it can now be written in the following simple form:

$$\frac{d}{dx}\left\{\varepsilon\frac{d\phi}{dx}\right\} = -\sigma(x) \tag{4.5}$$

The constant ε in this relationship is the permittivity of the dielectric and is related to the dielectric coefficient (dielectric constant) K_D through the relationship

$$\varepsilon = \varepsilon_0 K_D \tag{4.6}$$

where $\varepsilon_0 = 8.849 \times 10^{-12}$ F M^{-1}, the permittivity of free space. A further assumption can be made at this point to simplify the solution of Eq. (4.5). The permittivity is assumed to be constant throughout the region of variation of x, i.e., $d\varepsilon/dx = 0$. This apparently simple assumption is one of the weak points of the theory and is further discussed in a later section.

The Poisson equation can now be written in the following form:

$$\frac{d^2\phi}{dx^2} = -\sigma(x)/\varepsilon \tag{4.7}$$

a straightforward second-order differential equation. This yields after substitution for $\sigma(x)$,

$$\frac{d^2\phi}{dx^2} = -\frac{F}{\varepsilon}\sum_i z_i c_i(s) \exp(-f\phi) \tag{4.8}$$

This is the basic relationship derived by Gouy and Chapman. The first integration can be elegantly performed using the following transformation

$$\frac{d}{dx}\left(\frac{d\phi}{dx}\right)^2 = 2\frac{d\phi}{dx}\frac{d^2\phi}{dx^2} \tag{4.9}$$

This yields directly the following result:

$$\left(\frac{d\phi}{dx}\right)^2 = \frac{2RT}{\varepsilon}\sum_i c_i(s) \exp(-f\phi) + K \tag{4.10}$$

where K is the integration constant. To evaluate this constant the definition of ϕ_s is used (the inner potential of the solution phase). As long as the phase is homogeneous and the limiting condition

$$\phi_s = \operatorname*{Lt}_{x\to\infty} \phi(x) \tag{4.11}$$

applies, the limiting value of the field as $x \to \infty$ is

$$\operatorname*{Lt}_{x\to\infty} \frac{d\phi}{dx} = 0 \tag{4.12}$$

If this condition is applied to Eq. (4.10), the electric field strength at any point x in the diffuse region is given by

$$-\mathscr{E}(x) = \frac{d\phi}{dx} = \pm\left(\frac{2RT}{\varepsilon}\right)^{1/2}\left(\sum c_i(s)\{\exp[-(f+1)]\}\right)^{1/2} \tag{4.13}$$

The taking of square roots always produces an ambiguity of sign. This is readily resolved by the following arguments. The interphase must be electrically neutral (solution plus metallic phase). On the metallic side, the electrons' density can be varied but because there is no discharge mechanism the charge remains at all times contained in the metal and can therefore be identified by σ_m, a charge associated solely with the metal. Because of the electroneutrality of the interphase, an equal and opposite charge must reside on the solution side of the

interface, $\sigma_s = -\sigma_m$. The calculation of the distribution of σ_s is possible with this theory as is shown below. The direction of migration of cations will be from regions of higher to lower potential, i.e., in the direction of the field, while anions will migrate in the opposite direction. The sign of the right-hand side of Eq. (4.13) is chosen to maintain these conditions. If charge is chosen as the variable of interest, the argument runs as follows: if the electrode is positively charged, an excess of anionic charge will be necessary in the solution to balance the metallic charge. If the electrode is negatively charged, the field $d\phi/dx$ must be positive so that the cations will be attracted towards the electrode and anions will be repelled.

In setting up the model, the zero of the coordinate system was chosen to be the metallic surface so the original Gouy and Chapman relationship for the field applies from the surface to the bulk of solution.

In order to test these relationships a functional relationship with the observed experimental variables is more useful. As capacity of the double layer is readily measured as a function of charge on the metal or electrode potential, this suggests that a further relationship between field and charge at the surface is necessary before a suitable analytic expression for capacity can be derived.

The charge on the surface is related to the field through Gauss' theorem

$$\sigma_m = -\varepsilon\left(\frac{d\phi}{dx}\right)_{x=0} \tag{4.14}$$

so that by combination with Eq. (4.13) the following is obtained:

$$\sigma_m = \pm(2RT\varepsilon)^{1/2}\left(\sum_i c_i(s)\exp\{[-f\phi(0)] - 1\}\right)^{1/2} \tag{4.15}$$

where $\phi(0)$ is now defined as $\phi(x = 0) - \phi(s)$ the potential difference between the surface and the bulk of solution.

The capacity is derived from this expression by using the relationship

$$C = \frac{\partial\sigma_m}{\partial\phi} \tag{4.16}$$

This yields, in the case of a z–z electrolyte,

$$C_d = \frac{2z^2F^2\varepsilon c(s)}{RT}\cosh\frac{zF\phi(0)}{2RT} \tag{4.17}$$

This predicts that the capacity of the diffuse region is a symmetrical cosh function of the potential in the system if we identify $\phi(x = 0)$ with the measured potential in the experimental system. The asymmetry in the measured experimental curves is immediately evident from Figure 4. This led Gouy to suggest that the integration limits were probably wrong but it was left to Stern to put forward modifications with a reasonable molecular grounding.[16] He suggested that the finite size of ions might be of importance when the value of x was of the same order of magnitude as the ion size.

The model proposed by Stern[16] abandons the limit $x = 0$, the metallic

surface, as the inner limit of the diffuse layer. He proposed an equipotential plane at $x = x_2$ at an unspecified distance from the electrode surface. This was not identified with particular molecular properties in the system but allows for a region with different non-diffuse-like properties to exist in series with the diffuse layer proper. This plane is now commonly called the "outer Helmholtz plane" (OHP). The principal characteristic of this plane is that it is the plane of closest approach of ions to the electrode surface. On a realistic molecular basis, this presents certain problems. As the OHP must be a function of solvation characteristics and ion size, such a model implies a symmetrical set of interactions with and across the inner layer to the electrode. Both Stern[16] and Grahame[20] noted these defects but the detailed consequence of this assumption have only been indirectly evaluated quite recently and there is no general agreement as to the real influence of this assumption.

The expression for the capacity can now be rederived using

$$\sigma_m = -\varepsilon\left(\frac{\partial\phi}{\partial x}\right)_{x=x_2} \tag{4.18}$$

which then yields

$$\sigma_m = \pm(2RT\varepsilon)^{1/2}\left(\sum c_i(s)\{\exp[(-f\phi_2) - 1]\}\right)^{1/2} \tag{4.19}$$

where ϕ_2 is the potential at the OHP defined by $\phi_2 = \phi(x_2) - \phi(s)$. Formally, Gauss' theorem applies to an isotropic charge free region and it is difficult to reconcile the molecular characteristics of such a region with these criteria. Such an interpretation does help give a physical picture to the system and allows the inner layer to be interpreted as a condenser with parallel plates in series with the diffuse layer contribution.

It is possible to redefine a nonspecifically adsorbed system at this point. This would be an experimental system in which no ionic species are found in the inner nondiffuse region. A second consequence of this interpretation pertains to the displacement D of the inner region. This must be constant, i.e.,

$$D = \varepsilon E \tag{4.20}$$

or the product of the permittivity and the field is a constant. Individually, the field and the permittivity can vary and the problems this gives when molecular models for the inner region are constructed will be discussed in a later section.

As the electrode charge is now given in terms of ϕ_2 in Eq. (4.19) [cf. Eq. (4.15)], an alternative approach is necessary to test the Stern modifications. In the first place Eq. (4.19) is expanded, yielding in the case of a z–z electrolyte,

$$\sigma_m = \pm[2RT\varepsilon c(s)]^{1/2}[\exp(f\phi_2) + \exp(-f\phi_2) - 2]^{1/2} \tag{4.21}$$

This is the basic Gouy–Chapman–Stern (GCS) relationship between σ_m and ϕ_2.†

† This can be transformed into the more usual relationship

$$\sigma_m = (8RT\varepsilon)^{1/2}[c(s)]^{1/2}\sinh\frac{zF\phi_2}{2RT}$$

by simple algebra.

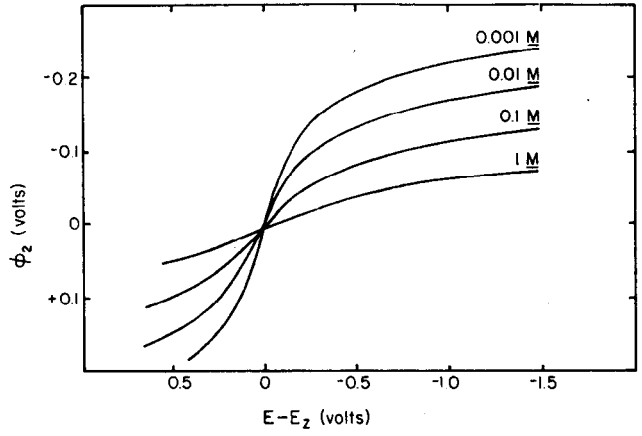


Figure 16. Variations of the potential ϕ_2 between the plane of closest approach and the bulk of the solution with $E - E_z$ for the mercury in sodium fluoride solutions at 25°C. Calculated from Grahame's data.[62,68,20]

The problem is now to relate this relationship to the experimental data. This may be in one of three basic forms: (i) capacity vs. potential, (ii) charge vs. potential, or (iii) interfacial tension vs. potential. The aim is to obtain data in the form σ_m vs. potential. This requires integration for (i) and differentiation for (iii) according to Eqs. (2.2)–(2.5).

The evaluation sequence is then as follows: (1) use the experimental values of σ_m to obtain ϕ_2; (2) find the experimental potential corresponding to the values of σ_m chosen; (3) plot ϕ_2 vs. E_m interpolated experimental potentials (cf. Figure 16). If the electrolyte is not z–z the same procedure can be applied using Eq. (4.19) instead of Eq. (4.21). This usually requires a numerical integration of the concentration–potential function. A number of explicit solutions are available for particular systems and the reader is referred to the original literature for details.

The theory is now not an attempt to describe the experimental variables *in toto* but because it only describes a part of the system, experimental verification is much more difficult. The next section is dedicated to applications of the basic theory, some of which may be interpreted as partial confirmation of the theory.

4.2. Applications of the Simple Theory

Diffuse layer theory can be used to calculate diffuse layer ionic concentrations and potential profiles, diffuse layer capacity, and the potential at the OHP. All these values except total potential profiles have been employed in the studies of a range of electrochemical systems.

If a nonspecifically adsorbing ionic system is chosen for study, the total excess concentration $\Gamma_{i,d}$ in the diffuse layer of species i is in general

$$\Gamma_{i,d} = c_i(s) \int_0^\infty \left\{ \exp\left[-\frac{z_i F\phi(x)}{RT} \right] - 1 \right\} dx \tag{4.22}$$

from Eq. (4.2). This is not the relative surface excess as defined by thermodynamic developments discussed in Chapter 1 of this volume. The link is made through the following relationships:

$$-\sigma_s = \sigma_m \tag{4.23}$$

If *all* the charge resides in the diffuse region, the total diffuse layer charge σ_d is defined by

$$-\sigma_m = \sigma_s = \sigma_d = \sum z_i F \Gamma_{i,d} \tag{4.24}$$

where the sum extends over *all* ionic species in the system. This derivation is then consistent with the invariance of σ_m with the placement of the Gibbs dividing surface in the system (see Chapter 1 of this volume).

For unsymmetrical electrolytes and mixtures, Eq. (4.22) is usually solved by numerical integration. However, for z–z electrolytes a convenient analytical expression is available:

$$\Gamma_{+,d} = -2c_i(s) \int_0^\infty \left\{ \sinh\left[\frac{zF\phi(x)}{2RT} \right] \right\} \exp\left[-\frac{zF\phi(x)}{2RT} \right] dx \tag{4.25}$$

where the negative sign is required to make Γ_i^d positive when $\phi(x)$ is negative. Rearranging Eq. (4.13) for the field strength for this case gives

$$dx = -\left(\frac{\varepsilon}{8RTc_i(s)} \right)^{1/2} \operatorname{csch}\left[\frac{zF\phi}{2RT} \right] d\phi \tag{4.26}$$

which with $\phi \to \phi_2$ as $x \to x_2$ and $\phi \to 0$ as $x \to \infty$ yields

$$\Gamma_{i,d} = \left[\frac{\varepsilon c_i(s)}{2RT} \right]^{1/2} \int_{\phi_2}^0 \exp\left(-\frac{zF\phi}{2RT} \right) d\phi \tag{4.27}$$

This on integration gives for the anion in the solution,

$$\Gamma_{-,d} = [2RT\varepsilon c_i(s)]^{1/2}(zF)^{-1}[\exp(zF\phi_2/2RT) - 1] \tag{4.28}$$

and for the cation,

$$\Gamma_{+,d} = [2RT\varepsilon c_i(s)]^{1/2}(zF)^{-1}[\exp(-zF\phi_2/2RT) - 1] \tag{4.29}$$

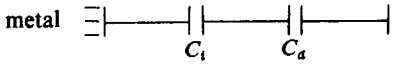
The values calculated here satisfy Eq. (4.24) and can be used to calculate the specially adsorbed charge densities in the inner region as shown in the next chapter.

Of greater interest at this point is the use of this theory to detect specific

adsorption. The first approach is via the capacity of the diffuse layer which is calculated by differentiating Eq. (4.21):

$$C_d = \left[\frac{2z^2F^2\varepsilon c_i(s)}{RT}\right]^{1/2} \cosh\frac{zF\phi_2}{2RT} \tag{4.30}$$

In light of the previous discussions, a series capacitor model can be proposed for the double layer,



where C_d is defined by Eq. (4.30) and C_i is the contribution from the inner layer. As these two capacitors are in series, the experimentally measured capacity C_E is related to these components in a nonadsorbed system through

$$\frac{\partial E}{\partial\sigma} = \frac{\partial(\phi_m - \phi_2)}{\partial\sigma} + \frac{\partial(\phi_2 - \phi_s)}{\partial\sigma} \quad \text{hence} \quad \frac{1}{C_E} = \frac{1}{C_i} + \frac{1}{C_d} \tag{4.31}$$

If C_i is not a function of concentration and is invariant at constant charge, a plot of $1/C_E$ vs. $1/C_d$ at constant charge will yield straight lines of unit slope (cf. Figure 11). Alternatively, the diffuse layer contribution is subtracted numerically from the total experimental capacity, and the residual capacity is examined for systematic concentration dependence.

There are a number of drawbacks to these tests for specific adsorption. If capacity vs. potential data are the available raw data, the procedure outlined in the previous section is necessary to calculate ϕ_2, and then the measured capacity is interpolated at the chosen charge values. The errors in this procedure are not large but as can be seen from Eq. (4.30) and Figure 17b, the largest influence of the diffuse layer capacity is found near $\sigma_m = 0$. The diffuse layer capacity values rapidly rise to large values on either side of this point and consequently give small contributions at large σ_m values. A second experimental problem is that there is frequently little spread of experimental capacity values in the experimentally accessible range. This places a heavy reliance on the precision of the experimental data. The technique, although used by numerous workers, is not very sensitive and alone is not a definitive test for the absence of specific adsorption. Further discussion of these and other problems relating to the applicability of diffuse layer theory is presented in a later section.

A number of other useful relationships may be derived from this theoretical development. The potential profile in the diffuse region may be derived by integrating Eq. (4.13) with the boundary conditions $\phi = \phi_2$ at $x = x_2$ to yield for a z-z electrolyte,

$$\phi(x') = \pm\frac{4RT}{zF}\left(\tanh\left|\frac{zF\phi_2}{4RT}\right|\right)\exp(-\kappa x') \tag{4.32}$$

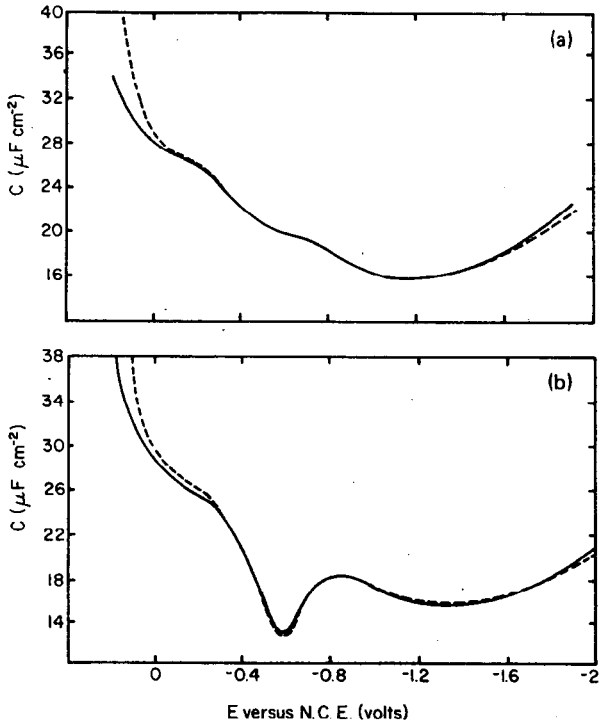


Figure 17. Experimental (solid curve) and calculated (dashed curve) differential capacities of mercury in (a) 0.1 M sodium fluoride at 25°C and (b) 0.01 M sodium fluoride at 25°C.[62]

where $x' = x - x_2$ and $\kappa = [2z^2F^2c(s)/\varepsilon RT]^{1/2}$ is the Debye length. This indicates an almost exponential decay of potential with increasing distance from the electrode. At low values of ϕ_2 this reduces to

$$\phi(x') = \phi_2 \exp(-\kappa x') \tag{4.33}$$

and allows the diffuse layer thickness to be defined in a way analogous to that employed in normal electrolyte theory, i.e., $\tau_{99.99} = \ln(10^{-4})/\kappa$ $\kappa = 3 \times 10^7 z[c(s)]^{1/2}$ cm^{-1} at 298 K with $c(s)$ in mol liter^{-1}. For 1–1 electrolytes at 0.1 M, a thickness ($\tau_{99.99}$) of 8.8×10^{-7} cm is found, while at 10^{-4} M this increases to 2.8×10^{-5} cm.

A further interesting calculation may be made of the field at the OHP. This is derived directly from Gauss' theorem Eqs. (4.13) and (4.14) for known values of electrode charge. For z–z electrolytes at 298 K in aqueous solution this becomes

$$\left(\frac{d\phi}{dx}\right)_{\phi=\phi_2} = -1.44 \times 10^5 \sigma \text{ V cm}^{-1}$$

where σ is in $\mu C\ cm^{-2}$. This clearly shows that the field at electrode charges within the experimental range are in excess of $10^6\ V\ cm^{-1}$.

5. Some Proofs, Limitations, and Possible Extensions of Diffuse Layer Theory

As already indicated it is not easy to prove or disprove conclusively the theory so far presented. One of the earliest detailed attempts was by Grahame,[17] who used data derived from aqueous fluoride systems with the arguments pertaining to Eq. (4.31), i.e., looking for a concentration-independent residual inner-layer capacity. In our present state of knowledge, no system exhibits this idealized behavior over its entire ideally polarizable range. Grahame found that for fluoride there was a considerable range of potentials over which the model fitted within reasonable error (cf. Figure 17). This of course makes the assumption that fluoride ions in the inner region will change the inner-layer capacity, if we are considering the exercise as one for the detection of specific adsorption of ions, but if the argument is reversed and this is used as a test of applicability of the diffuse layer theory, then there are a number of problems. The contribution of the diffuse layer is largest in solutions at very low ionic concentration where the ionic adsorption would be weakest, but even here the range of potentials over which the diffuse layer influence is strong is still small. In the regions of general interest, high electrolyte concentrations and well away from the zero charge potential, the diffuse layer influence on the capacity potential function is minimal, and therefore in regions where it might be expected to find deviations, this type of test is totally insensitive. Any direct testing is hampered by the possibility of cumulative error in the charge calculations required for the calculations and the resultant problems of deciding on the significance of small differences in large values. However, the observations by Grahame of a region of concentration-independent inner-layer capacity in the region near the point of zero charge suggest the theory may not be totally incorrect and may be reasonable near the point of zero charge.

If the capacity–potential relationship is not a sensitive approach, there are a number of alternatives which must be considered. One of the fundamental relationships derived from thermodynamics is the Esin and Markov relationship

$$\left(\frac{\partial E_{\pm}}{\partial \mu}\right)_{\sigma_m} = -\left(\frac{\partial \Gamma_{\mp}}{\partial \sigma_m}\right)_{\mu} \tag{2.4a}$$

This equation relates the shift in thermodynamic potential to the thermodynamic relative surface excess. If the model predicted by the application of diffuse layer theory is valid, the following argument may be applied: for a z–z

electrolyte Eq. (2.4a) may be rewritten as

$$\frac{\partial E_{\pm}}{\partial \ln a^2_{\pm}} = \pm \frac{1}{zF} \left(\frac{\partial \sigma_{\mp}}{\partial \sigma_m}\right)_{a_{\pm}}$$

and in the absence of specific adsorption

$$\sigma_{\mp} = \sigma_{\mp,d}$$

where $\sigma_{\mp,d}$ is now the diffuse layer charge. Relationships (5.1a) and (5.1b) can then be used to calculate the differentials,

$$\sigma_{-,d} = -A[\exp(zf\phi_2/2) - 1] \tag{5.1a}$$

and

$$\sigma_m = 2A \sinh(zf\phi_2/2) \tag{5.1b}$$

where $A = [2RT\varepsilon c(s)]^{1/2}$.

Substituting for ϕ_2 in Eqs. (5.1a) and (5.1b) and differentiating with respect to σ_m yields after rearrangement

$$\left(\frac{\partial E^+}{\partial \ln a_{\pm}{}^2}\right)_{T,p,\sigma_m} = -\frac{RT}{2zF}\left\{1 + \frac{\sigma_m/2A}{[1 + (\sigma_m/2A)^2]^{1/2}}\right\} \tag{5.2}$$

This was tested by Parsons on Grahame's data for NaF solutions at a mercury electrode. The results are clearly shown in Figure 10. The limiting slopes are as follows:

$$\left(\frac{\partial \sigma_-}{\partial \sigma_m}\right)_{a_{\pm}} \to 0 \quad \text{as} \quad \sigma_m \to -\infty$$

$$\left(\frac{\partial \sigma_-}{\partial \sigma_m}\right)_{a_{\pm}} \to -1 \quad \text{as} \quad \sigma_m \to \infty$$

$$\left(\frac{\partial \sigma_-}{\partial \sigma_m}\right)_{a_{\pm}} = 0 \quad \text{as} \quad \sigma_m = 0$$

These limiting slopes are in agreement with the theoretical predictions for a nonadsorbing system and at least near the zero charge potential are a valid test of the theory. As in the case of capacity data, the contribution of the diffuse layer is small at large $|\sigma_m|$, and hence again the test is not sensitive far from $\sigma_m = 0$. The same arguments apply when considering this as a sensitive test for the presence or absence of specific adsorption. In general all the direct tests of the theory suffer from the same limitations.

A totally different approach to testing the theory was proposed by Joshi, Parsons, and Trasatti.[18] The principle of this technique is as follows. The adsorption of ions into the diffuse region is dependent on the charge of the ion. The above theory can be extended to calculate the ionic composition of the diffuse region for mixtures of ions of different charges. If the experimental conditions are carefully defined, the surface excesses can be derived independently

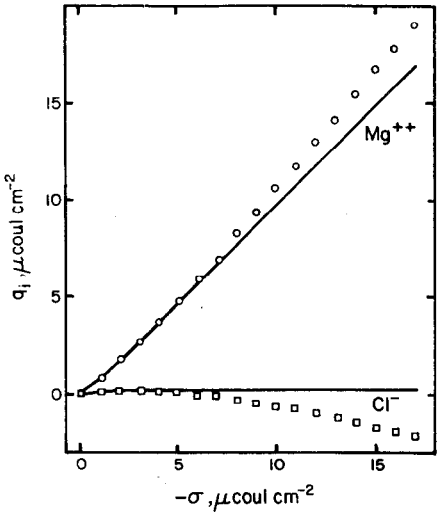


Figure 18. Experimental (O and □) and calculated (——) surface concentration of Mg^{2+} and Cl^- in 5 m*M* $MgCl_2$.[18]

by two different routes, from electrocapillary data and from capacitance data. As the latter would normally use diffuse layer theory and the former would not, a viable test of the diffuse layer might be found if (1) the ions do not enter the layer; and (2) the data errors can be minimized.

The systems chosen for study were aqueous mixtures of HCl + $BaCl_2$ and aqueous mixtures of KCl + $MgCl_2$. For a complete study of such a system it is evident that the total concentration should be varied over the widest possible range (m) and the concentration ratios of the two components should be varied over the complete range (n). This means that ($m \times n$) experiments are necessary, and approach not really feasible at the time of this study. These workers chose one point for calibration in their study. A second essential point in this study is that the proper bulk activity coefficients were employed. The excess values calculated from theory and experiment are compared in Figure 18. The experimental values are in all cases and at all charges significantly higher than the theoretical values irrespective of ion type or charge. All deviations are of the same order of magnitude and it can be concluded that the ion size–charge parameter does not seem to be at variance with diffuse layer theory. The GCS theory could therefore be said to be at least as good as the best experimental data for calculating diffuse layer charge densities. It can be argued that any errors in potential distribution might also show up in this type of test but the sensitivity of the test to this type of function has not been clearly delineated. The only direct test of potential distribution derives from the use of ϕ_2 in the Frumkin correction to the kinetic parameters of electrode reactions, e.g.,[8,19]

$$i = i_0 \exp(\alpha n - z)f\phi_2 \tag{5.3}$$

This is obviously a test that depends on a number of subsidiary models, e.g., the model for electron transfer, the identification of reaction site with the plane at ϕ_2, etc.[20] Early studies by Frumkin, assuming a "constant" rate constant for a redox process, indicated that the reduction site could be between 3 and 10 Å from the surface. The modern tests have revolved around studies of polyvalent systems, in particular Eu^{2+}/Eu^{3+}, which is reduced near $\sigma_m = 0$.[21,72] Studies in thiocyanate–perchlorate mixtures have been made by Anson and Sluyters. Extreme care is necessary to define the ionic species in solution since small errors in the concentration of polyvalent species at low concentrations give relatively large rate constant corrections. Both workers found a significant lack of dependence of rate on ϕ_2 potential but as observed before these tests are applied near to $\sigma_m = 0$, where the theory is most likely to be correct. A second consequence of this type of study concerns the use of a plane of closest approach. Fawcett suggested that the plane of closest approach was not the same for all ions and, using kinetic methods, in this case the heats of activation for oxyanion reduction in the presence of different cations, probed the inner region.[22] The observed heats of reaction increase with the atomic number of the cation, i.e., with decreased cation solvated radius and decreased inner-layer thickness for the series Na^+, K^+, Cs^+, respectively. Although these reactions are more complex and require consideration of the inner-layer properties in the presence of specific adsorption, these results, which support the idea of a variable inner-layer thickness, imply that the diffuse layer model may not be very precise near the OHP. More so than in the previous cases, a large number of models are required before the final conclusions can be drawn, and the influence of these requires very careful evaluation before definitive conclusions regarding the applicability of the diffuse layer can be drawn.

Theoretical advances in the theory of the diffuse region have not been impeded by the lack of satisfactory experimental evidence and there exists in the literature a considerable body of theoretical developments which are, to a very large extent, unproven in the experimental domain. It is possible to divide these approaches into two types, one type which takes the basic GCS theory and then attempts to correct for the possible sources of error without changing the general formulation of the theory, and a second type which attempts to redefine the system from fundamental, usually statistical mechanical considerations. There are parallels to be drawn between the GCS theory and the later Debye–Hückel theory. A list of these might include (1) inapplicability of the Boltzmann postulate, (2) the inclusion of a position dependent dielectric constant, (3) the electrostriction of ionic atmospheres, (4) the polarizability of ions and real ion–ion interactions, (5) the problem of the location of the OHP, (6) the formation of ion pairs and field dissociation effects, (7) the use of local activity coefficients. Some of these factors are obviously strongly linked, e.g., (1)–(4) and (6)–(7). The problems presented by some of these factors will now be briefly discussed.

The Boltzmann postulate normally implies that the system can be considered

as a system of point charges. In fact it can easily be shown that if large but still experimentally accessible values of OHP potential are used in the Boltzmann equation, impossibly high ionic concentrations result. Two types of correction have been tried, one using the formulations of local thermodynamics, while the second introduces some form of space restriction factor into the Boltzmann equation.

A correction of this type was suggested by Bickerman[23]:

$$n_i = \frac{n_* \exp(\omega_1/kT)(1 - n_1 - n_2 v_2)}{1 - 2n_* v} \tag{5.4}$$

where the subscripts are for the two ions (1, 2), with volumes v_1 and v_2 in the diffuse layer and with a mean volume in the bulk v. The same technique has also been used by other authors. As in the description of the local thermodynamic approach which follows this description, the problem is the choice of the solvation model for the ion. Haydon and Taylor used a hard sphere model for the ionic volume and derived the following expression[24]:

$$\sigma_m = \left(\frac{DkT}{2\pi}\right)\left(\frac{1}{\phi_i}\ln\left\{\phi_i k_1\left[\exp\left(\frac{-2e\phi_2}{kT}\right) - 1\right] + 1\right\} + \frac{1}{\phi_j}\ln\left\{\phi_i k_1\left[\exp\left(\frac{2e\phi_2}{kT}\right) - 1\right] + 1\right\}\right) \tag{5.5}$$

where ϕ_i and ϕ_j are the space restriction factors for the ions and

$$k_1 = \frac{n_{i(j)0}}{1 - \sum \phi_i n_{i0}} \tag{5.6}$$

This expresses in a closed form the influence of ionic radius on such a system and it can be readily shown that if an ion, $z/z = 1$, for example, sodium ion, is considered, with the rigid model of this type, a radius of 4 Å could be employed. This, when inserted in the above, yields an increase in ϕ_2 over the ϕ_2 predicted by the GCS theory of 41% in 0.1 M bulk electrolyte concentration at 26.8 μC cm^{-2}.

The Poisson equation contains a term for the dielectric constant of the medium. A bulk value for this is not reasonable in the inner region of the diffuse layer where the simple theory predicts fields $\sim 10^6$ V cm^{-1}. There have been numerous suggestions for empirical correction. Malsch, at rather low field strengths, found experimental data to fit an expression of the type[25]

$$\varepsilon = \varepsilon_0 + \alpha E^2 \tag{5.7}$$

which was extended empirically to higher fields by Grahame[17]:

$$\varepsilon = \frac{\varepsilon_0 - \varepsilon_\alpha}{[1 + (b/m)E^2]^m} + \varepsilon_\alpha \tag{5.8}$$

where b and m are empirical constants. This was then substituted into the GCS theory and empirically fitted to the experimental data. He was able to fit Eq. (5.8) for $m < 2$ by comparison with the expected capacitor model for a non-adsorbed system, a slightly dubious procedure in view of the number of assumptions involved. This test was, however, sensitive to the value of m, unlike the calculation of ϕ_2, which was rather insensitive. Allowance for dielectric saturation increased ϕ_2 by only 7% for a 0.1 M z–z electrolyte at $m = 1$ and $\sigma_m = 26\ \mu C\ cm^{-2}$. These findings, it must be emphasized, refer only to the water in the system; ions are ignored in these dielectric considerations. As ionic concentrations are high near the OHP, it might be expected that the influence of these might be overriding. The dependence of dielectric constant of electrolyte solutions on concentration ($\leqslant 2$ M) is given by Hasted[26]:

$$\varepsilon = \varepsilon_0 + \delta_+ c_+ + \delta_- c_- \tag{5.9}$$

where $c_{+/-}$ is the ion concentration and δ_+ and δ_- are the contributions from the two ions. A norm $\delta_+ = \delta_-$ was assumed for Na^+Cl^- and consistent values for the other ions calculated. (This was also used by Hurwitz *et al.* in their local thermodynamic derivation.[27]) From this it is obvious that, for conditions where the additional terms are significant at large c_i differences, the dielectric constant can be expected to differ significantly. This is a totally unsatisfactory approach as a linear separation of ion and field effects is not physically realistic. A solution to this impasse was suggested by Sparnaay, who combined the Malsch correction with the Hasted effect to yield for low field strengths,

$$\varepsilon = \varepsilon_0 + \alpha E^2 + \delta_+ c_+ + \delta_- c_- \tag{5.10}$$

This solution is, however, untried as is the alternative possibility of replacing the Malsch expression by Grahame's extended expression in this combined relationship:

$$\varepsilon = \varepsilon_0 + \frac{\varepsilon_0 - \varepsilon_\alpha}{[1 + (b/m)E^2]^m} + \delta_+ c_+ + \delta_- c_- \tag{5.11}$$

When an ion is transferred from a field-free region to a region where there exists a field, at least two work terms are involved, the simple potential work term and a second term arising from the ion itself, which is of finite size and has a labile charge sheath, the polarization term. At least two approaches have been tried. If the Boltzmann equation is written in the form

$$n_i = n_0 \exp\left[-\frac{1}{kT}(zF\psi + \beta_+ + \cdots)\right] \tag{5.12}$$

some further modelistic definition is required. If the ion is a spherical cavity of radius a with a dielectric constant ε_i, Bolt writes[29]

$$\beta_+ = -\frac{a^3}{6}\frac{3\varepsilon_0(\varepsilon_i - \varepsilon_0)E^2}{2\varepsilon_0 + \varepsilon_i} \tag{5.13}$$

On the other hand, Sparnaay and Hurwitz use (as is shown later in this section[27,28]),

$$\beta_{\pm} = -\frac{E^2}{8\pi}\left(\frac{\partial \varepsilon}{\partial c_i}\right)_{T,\ V,c_i,E} \tag{5.14}$$

where the differential is derived from the empirical relationship,

$$\beta_{\pm} = -\frac{E^2}{8\pi}\delta_{\pm} \tag{5.15}$$

This is more applicable to the low (ϕ_2, σ_m) region due to the limiting validity of the Hasted relationship, Eq. (5.9).

A third work term may also be important in the Boltzmann expression, i.e., the fact that a site in the diffuse layer has to be created when the ion is brought up from the bulk of solution, a self-atmosphere effect. Loeb[30] and Williams[31] showed that at a conducting surface, a change of about 5% could be expected in ϕ_2 if a term of this type were included in the Boltzmann energy term.

A combination of these types of corrections has been attempted by a number of workers. Brodowsky and Strehlow[32] combined ionic volume and dielectric saturation corrections and showed that at $\sigma_m > 16\ \mu C\ cm^{-2}$, ϕ_2 could be $> 30\%$ larger than predicted by GCS models. A poor model for ionic volumes was used and this could lead to serious errors in the model employed at high diffuse layer ionic concentrations.

Sparnaay[28] included ionic volume, dielectric effects and polarization corrections and it seems that the analysis may hold when $\phi_2 < 100$ mV and at concentrations $< 10^{-2}\ M$. The corrections are very sensitive to the value chosen for the radius of the counterion. Taking into account the uncertainty in choosing a reasonable hard sphere radius for the ion, the estimated differences with GCS were of the order of 2%–3%. The polarization and self-atmosphere terms to some extent seem to cancel out the ionic volume and dielectric effects and as will be seen below, this type of compensation of effects is a feature of these types of corrections to GCS theory. Bolt[29] considered simultaneously a Boltzmann correction, dielectric saturation, ion polarization, and the self-atmosphere effect but omitted the influence of ions on the dielectric constant. The dielectric constant was corrected using the Grahame equation with $m = 1$. He found that the dielectric and polarization corrections cancel each other out as do the self-atmosphere and ionic volume effects, at least at low concentrations. This agrees with the idea that GCS is reasonably precise at low concentrations. At concentrations $\geqslant 10^{-2}\ M$, $\phi_2 \sim 100$ mV, ionic volume effects dominate and a correction to ϕ_2 of $> 3\%$ could be applicable. Eventually at higher concentrations again the dielectric and ionic volume corrections would be expected to dominate. It is conceivable that under experimentally accessible conditions corrections of the order of $+30\%$–40% might have to be applied to ϕ_2.

Two further attempts to correct and modify the original theory are now presented briefly, the first by Levine *et al.*, which to some extent bridges the gap

between the local thermodynamic formulation which follows and the preceding discussion.[33] Levine noted that no one has combined all the corrections in one theory and considers that the basic list of factors was wanting; he particularly pointed to two further factors: (8) the effect of the self-atmosphere of the ions and of the related screened image forces acting on an ion in the region of the diffuse layer adjacent to the OHP,[35] and (9) the effect of the compressibility of the medium of the diffuse layer. The introduction of (8) is crucial to the derivation presented by Levine. It arises because of the problem of creating a hole in the layer for the incoming ion and because this ion can "see" the electrode electrically. The classical way of handling this type of electrode ion interaction is via an imaging force. Unfortunately the system is inhomogeneous in a direction normal to the electrode, and a solution to the problem of calculating this potential was found by Buff and Stillinger, who used cluster theory.[35] If the new corrections are ignored the treatment is compatible with the previous discussion and more particularly with that of Sparnaay. After a long and complex theoretical development, Levine concluded that the new term (8) was a major contributor to the energy term in the Boltzmann equation and is at normal concentrations of electrolytes the overriding term. The calculations presented pertain to a system with a dielectric material in place of the electrode and yielded a new potential ~ -5 times the volume effect, which became the dominant factor in the earlier corrections. With a metallic wall this might be expected to be even larger. The picture now becomes more confusing because the nature of an image force has to be clearly defined at the metal–electrolyte interface. This type of force only occurs because there is a difference in the dielectric constant on the metallic side of the OHP. In principle, a dielectric discontinuity does not exist in a real system and, as Buff *et al.*[34] have clearly shown, the value of the image force depends crucially on the form chosen to model the change in dielectric constant between one part of the system and the other. This would be expected to act in such a way as to reduce the magnitude of the cavity potential included by Levine.

Prigogine *et al.* have developed expressions for the electrochemical potential at any point in an ionic system with an electric field imposed.[36] Hurwitz and Sanfeld used this formulation,[27]

$$\bar{\mu}_\gamma = \mathrm{b}_{\gamma 0}(T, P = 0, C_1 \cdots C_c) \frac{E^2}{8\pi} \left(\frac{\partial \varepsilon}{\partial C_\gamma}\right)_{T(C)} + z_\gamma F \psi \qquad (5.16)$$

where $\mu_{\gamma 0}$ is the chemical potential at T, C_γ, $\bar{E} = 0$, $P = 0$, C_γ is the concentration expressed as number of moles per cm^3, E is the modulus of the electric field $\bar{E}$, ψ the macroscopic electric potential, $\bar{E} = -\mathrm{grad}\psi$, and $\bar{P}$ is the polarization per unit volume, $\bar{P} = k\bar{E}$. As can be readily seen this relation builds into the development a dependence on system variables lacking in the GCS approach. The reader is referred to the original paper for details of the calculations. However, the argument proceeds by introducing successively a description of the pressure in the diffuse region, dielectric constant variations and their relationships to

ionic volumes as a function of ionic concentration, as well as the derivatives with respect to field, yielding a distribution function of the type

$$\frac{C_s}{C_s'} = \frac{f_{s0}'}{f_{s0}} \exp\left\{\frac{V_{s0}^*}{RT}\left[-\frac{\varepsilon E^2}{8\pi} - \frac{1}{8\pi}\int_{0,c}^{E^2}\left[\sum_\gamma c_\gamma\left(\frac{\partial \varepsilon}{\partial C_\gamma}\right)_{T,E(C)} - \frac{1}{V_{s0}^*}\left(\frac{\partial \varepsilon}{\partial C_s}\right)_{T,E(C)} + \frac{1}{2}E\left(\frac{\partial \varepsilon}{\partial E}\right)_{T,c}\right] dE^2\right] - \frac{z_s F\psi}{RT}\right\} \quad (5.17)$$

where the superscript(′) refers to the standard state and V_{s0}^* is the solute specific molar volume in the standard state. This relationship is consistent with the GCS approach if the point charge model and its various attributes are reintroduced. Having found a new distribution function, the authors apply it along with the Poisson equation to calculate the usual diffuse layer parameters. The approach chosen by these authors was to compare by ratio with the predictions of the GCS theory suitable parameters, e.g., for electrode charge the following expression, in the authors' original terminology, results:

$$\left(\frac{\sigma_m}{\sigma_m^{GCS}}\right)^2 = 1 - \frac{\int_0^{y_\delta} 2(\varepsilon_{10} - \varepsilon)\sinh y\, dy + \int_0^{y_\delta} \varepsilon(e^{-y}\Delta_+ - e^{y}\Delta_-)\, dy}{\int_0^{y_\delta} 2\varepsilon_{10}\sinh y\, dy} \quad (5.18)$$

where Δ_- and Δ_+ are complicated functions of field, solvent molar volume, field, and dielectric constant. Solution of this problem then requires a successive approximation technique and the selection of feasible values for the parameters. The results show that the deviations at OHP potentials of 70 mV increase rapidly from up to 2% at 10^{-5} mol cm^{-3} to up to nearly 20% at 10^{-4} mol cm^{-3} for a simple electrolyte. The percentage deviations in the capacity data derived in this way are even larger and could approach a 50% error in the worst case. How far these errors might be realistic in a real system is open to some doubt as experimental evidence for deviations of this magnitude in solutions at these concentrations and at charges of $\sim +6$–$8\ \mu$C cm^{-2} has not been forthcoming.

In principle, this approach combines, as does Levine's, all the available correction terms in one theory, but Levine[33] maintains that effect (8) is not properly accounted for. These developments have done little to clarify the situation for the experimentalist requiring to know at what level of confidence to apply diffuse layer theory, and to date there is a significant paucity of experimental observations to support the predicted deviations from GCS.

The second type of approach to the problem of describing the diffuse region finds its origin in statistical mechanics. One of the early attempts in this direction was by Stillinger and Kirkwood,[37] who applied the methods of Kirkwood and Poirier[38] to a hard sphere ionic system. At low concentration of electrolytes the results agreed with the linearized Poisson–Boltzmann theory, but when $1/\kappa$ is of the same order of magnitude as the ionic diameters the theory predicts a series of layers of charge of alternating sign ($\sim 0.5\ M$) extending into the solution. The concentration of onset of this phenomena depends on the type of ion chosen

for the model. The advances in this paper have made possible a number of other developments in the statistical mechanical theory of the diffuse layer.

Buff and Stillinger[35] have extended the general cluster theory of inhomogeneous fluids to the determination of ion and mean potential distributions in the interfacial region. This enables them to confirm some of the assumptions of the local thermodynamic method in the dilute solution limit. In accounting for ion size effects, local thermodynamic approaches are shown to be in error, although no direct comparison with experiment was included in the discussion nor was the magnitude of expected deviations from GCS theory.

A slightly different approach has been adopted by the Russian school. Krylov and Levich[39] deduced the conditions under which the methods proposed by Kirkwood *et al.*[37] for finding approximate correlation functions for the distribution of ions in the bulk solution and in the diffuse region including short-range ion–ion interactions, were valid. This then allows the linearized Boltzmann equation to be bypassed by functions valid to an ionic concentration 10^2–10^3 larger. It allowed these workers to estimate diffuse layer characteristics from a statistical model up to 0.1–0.5 *M* at the metal–solution interface. Their principal conclusion was that at very low concentrations the linearized Boltzmann equation is satisfactory, but at higher concentrations the potential in the diffuse part of the double layer falls off much more rapidly than the GCS theory would predict with increasing distance from the electrode. Unfortunately no calculation of the OHP potential–charge relationship has been made using this theory, neither has an estimate of the percentage deviation from GCS theory been made for ϕ_2. Krylov[57] has made estimates of the probable error in the diffuse layer capacity when calculated from this theory, and this is compared with the GCS values in Table 3. The increased rate of drop of potential from the OHP increases markedly the diffuse layer capacity even at $\sigma_m = 0$. Elkin *et al.*[58] ascribe an additional potential drop in the double layer, found during the application of nonlinear ac techniques to the study of the double layer, to the errors introduced

Table 3

Estimates of Probable Error in the Diffuse Layer Capacity Calculated from GSC Theory, Compared with GSC Values[57]

Concentration, *M* ($\times 10^{-3}$)	C_d, theor./C_{GCS}
4.4	1.00
0.10	1.07
0.35	1.32
0.44	1.45
0.47	1.51
0.50	1.58
0.60	1.82

by the application of classical GCS theory and state that the phenomenon can be explained if the statistical approach outlined above, extended to asymmetrical electrolytes[59], is adopted. (Their studies were of aqueous Na_2SO_4 at the Hg–aqueous-solution interface.)

Similar considerations, also using a modified Bogoliubov equation, have been presented by Martynov.[40] Although able to predict the charge-layered diffuse region observed in molten salt systems, the correlations with capacity data prove to be poor at concentrations $> 10^{-2}$ *M* for aqueous NaF media, but as the author points out, the capacity vs. potential function is not the best type of function for comparisons with theoretical predictions of this type.

6. Models of the Inner Layer in the Absence of Specific Ionic Adsorption

As this chapter is concerned with the ideal nonadsorbed state, it is natural that the preceding sections have dealt with the part of the interfacial region susceptible to a reasonably direct experimental–theoretical correlation. If the preceding models are correct, the residual inner-layer region has a set of well-defined characteristics that beg explanation. Many attempts have been made to build satisfactory models of this region since the early qualitative attempts of Mackor. Experimental evidence indicates that the inner-region thickness is of the same order as the dimensions of the solvent. This section of course presumes that the separation procedures described in the previous section are precise, i.e., Eq. (2.8) holds for the system.

Any molecular model for this region must explain at least the following phenomena:

(1) The overall shape of the experimental capacity–charge–potential results;
(2) the variation of these functions with external variables, e.g., temperature (enthalpy and entropy functions), salt concentration, and salt types and solvent variation; and
(3) the influence of metal type on the curves in (1) and (2).

Most workers have directed their attention at the system F^-/Hg to the exclusion of (3). Typical of the type of function to be derived is the variation of differential capacity with potential and temperature shown in Figure 19. In view of the thickness of the region, most approaches attempt a description of these phenomena by using a monolayer solvent model which is placed inside the plates of an imaginary condenser, one side comprising the metallic interface, the other side, in practice the diffuse layer, also being treated as if it were a psuedo-metallic plate.

To clarify the approach to this modeling, the discussion suggested by Trasatti is helpful.[41] The metal/solution potential drop is usually split into two contributions:

$$\Delta\phi = g(\text{ion}) + g(\text{dip}) \tag{6.1}$$

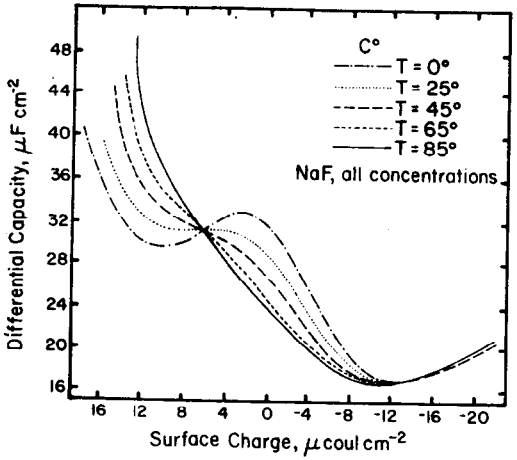


Figure 19. Calculated values of C°, the differential capacity of the inner part of the electrical double layer, between mercury and aqueous solutions of sodium fluoride at several temperatures. Calculations made from data obtained with 0.8 N solutions.[68]

where g(ion) is associated with the presence of free charges on the metal and in the diffuse region and g(dip) with the dipole layers that comprise the interphase. If the dipole layer in the metal is charge invariant ($\varepsilon_{\text{metal}} = \infty$) and the polarization components of the solvent are linearly separable[42], this relationship can be used to relate potential to charge:

$$\frac{\partial \Delta\phi}{\partial \sigma} = \frac{\partial g(\text{ion})}{\partial \sigma} - \frac{\partial g(\text{dip})}{\partial \sigma} \quad \text{or} \quad \frac{1}{C} = \frac{1}{C_1} + \frac{1}{C_{\text{GCS}}} = \frac{1}{C_{\text{ion}}} - \frac{1}{C_{\text{dip}}} + \frac{1}{C_{\text{GCS}}} \tag{6.2}$$

If the molecular polarizability of the solvent can be regarded as a constant isotropic property, C_{ion} becomes an integral capacity K_{ion} and the inner-layer capacity C_1 is described by

$$\frac{1}{C_1} = \frac{1}{K_{\text{ion}}} - \frac{1}{C_{\text{dip}}} \tag{6.3}$$

This type of separation imposes certain restrictions on the expected behavior of components in the system but does not require a solvent model for the interface. This base equation is used by all workers and there are then two possible routes for modeling the inner layer. In the one case the values of C_{dip} as a function of σ_m can be constructed using a molecular model. This usually requires the fitting of the experimental data to a theoretical function, the parameters hopefully having some theoretical significance. The alternative approach is to start with the experimental observables and to use simple assumptions and correlations to derive the same type of parameters without the need for a complex model *a priori*.

The central observation leading to dipolar modeling was the observation that the electrode charge at which the net orientation of water is zero occurs at a small negative σ_m. This was derived from three types of observation, the maximum in the adsorption of small organic molecules,[43] the temperature dependence (entropy) of the interphase,[44] and the temperature dependence of the point of zero charge.[45] The obvious difference between this observation and the maximum in the capacity–potential function, Figure 4, is clear and the literature is ripe with heated discussion of this point. The first treatment of inner-layer water was by Macdonald,[40] but the basis for recent modeling can be traced to Watts-Tobin,[47] who proposed that the water dipoles in the monolayer could adopt one of two positions giving a dipole contribution normal to the surface equal and opposite in sign $\pm p$. If the numbers of nolecules in these positions in $N_{\pm}$, then

$$g_{dip} = -\frac{(N_+ - N_-)}{\varepsilon} p = \left(P \frac{N_T}{\varepsilon}\right) R \tag{6.4}$$

where $N_T = N_+ + N_-$ and $R = (N_+ - N_-)/N_T$.

The dipole term was then added to the g_{ion} term, Eq. (5.19), to yield the total integral capacity of the inner region K_1:

$$K_1 = K_{ion}\left(1 - \frac{g_{dip}}{\Delta\phi}\right) \tag{6.5}$$

$$= \frac{\varepsilon - \varepsilon g_{dip}/\Delta\phi}{x_2}$$

There is evidently an additional term in the permittivity due to the contribution of dipoles. If ε and x_2, the inner-layer thickness, are independent of charge, the inner-layer capacity is found by differentiation:

$$C_1 = K_{ion}\left(1 - \frac{\partial g_{dip}}{\partial \Delta\phi}\right) \tag{6.6}$$

The contribution due to orientation was calculated assuming a different image interaction in the two dipole positions. A uniform field $\Delta\phi/x_2$ was assumed across the inner region, and the ratio of dipole orientations is then given by

$$N_+/N_- = \exp\left[-(U_0 - 2p\,\Delta\phi/x_2)/kT\right] \tag{6.7}$$

where U_0 is the interaction energy between neighboring dipoles. Choosing to define potentials relating to $N_+ = N_-$ at $\Delta\phi_0 = x_2 U_0/2p$, i.e., $\Delta\phi' = \Delta\phi - \Delta\phi_0$ allows Eq. (6.7) to be rewritten as

$$N_+/N_- = \exp\left(2p\,\Delta\phi'/x_2 kT\right) \tag{6.8}$$

This allows R in Eq. (6.4) to be replaced by $-\tanh(p\,\Delta\phi/x_2 kT)$, and hence the required derivative $dg_{dip}/d\,\Delta\phi$ becomes

$$-\left(\frac{p^2 N_T}{\varepsilon x_2 kT}\right) = -\lambda \tag{6.9}$$

The dipole contribution is maximal at $\Delta\phi_0$ and, by virtue of the sech^2 function, decreases to K_{ion} in a symmetrical fashion about $\Delta\phi_0$. The source of asymmetry in the experimental curves is not apparent from this formulation and led to the suggestion that it was caused by specific ionic adsorption.[48] While this is true in many systems, the evidence at 298 K in aqueous fluorides is not consistent with this suggestion.

Bockris, Devanathan, and Muller (BDM) proposed an alternative model of the inner layer to include dipole–dipole interaction U_c and wrote the inner-layer field using Gauss' equation.[48] Thus in the BDM model,

$$\frac{1}{C_{D_2}} = \frac{1}{C_{ion}} - \frac{1}{C_{dip}}$$

In the Watts-Tobin model,

$$C_{D_2} \propto C_{dip}$$

Thus Eq. (6.8) becomes

$$N_+/N_- = \exp\left[(2p\sigma'/\varepsilon + 2U_cR)/kT\right] \tag{6.10}$$

and Eq. (6.4) becomes

$$R = -\tanh\left[(p\sigma'/\varepsilon + U_cR)/kT\right] \tag{6.11}$$

Inserting these in the previous derivation leads to the following result for the inner-layer capacity in the absence of specific adsorption:

$$(C_i)^{-1} = K_{ion}^{-1}\{1 - \lambda[(1 - R^2)^{-1} + U_c/kT]^{-1}\} \tag{6.12}$$

A comparison between Watts-Tobin and BDM has been made by Parsons.[49] When U_c, the lateral interaction term, is zero, Eq. (6.12) reduces to

$$\frac{K_{ion}}{C_i} = 1 - \lambda(1 - R^2) \tag{6.13}$$

which may be compared with that derived from Eqs. (6.6) and (6.8)

$$C_i/K_{ion} = 1 + \lambda(1 - R^2) \tag{6.14}$$

The two results are identical when λ is $\ll 1$. There are other basic differences. In Eq. (6.13), R is a function of σ, while in Eq. (6.14) it is a function of $\Delta\phi$. Watts-Tobin used the whole potential drop to calculate the field with which the dipole interacts and, according to Damaskin, this automatically allows for the field due to other dipoles. As this was shown to be equivalent to pairwise interaction in hexagonally close-packed dipole layer, i.e., the same function assumed for U_c, the latter term must be nonzero in the BDM model. Cooper and Harrison[50] objected to the negative sign before the dipole term in Eq. (6.13), pointing out that this could lead to the possiblity of negative capacities being predicted, i.e., the maximum value of the second term, kT/U_c, has a maximum permissible value, < 1. This condition is only satisfied when U_c is large.

The above models are concerned with a dipole representation identical in the two orientations. Recent developments have relaxed this restriction, and at the expense of mathematical complexity and increased difficulty in matching theory to the experimental results, have tried to introduce more realistic representations for the first layer of water. Levine, Bell, and Smith[51] improved the method of accounting for dipole–dipole interactions by developing a statistical mechanical model for the dielectric properties of the layer of orientable solvent dipoles. For a two-position model, the field experienced by a dipole in the mololayer was shown to be

$$E = 4\pi\sigma_m + [c_e(p_s R - 4\pi\alpha_s\sigma_m)/A\, d^3] = 4\pi\sigma_m + X \tag{6.15}$$

where c_e is the effective coordination number of a dipole, α_s the polarizability of a dipole, d the hard sphere solvent diameter, and $A = 1 + \alpha_s c_e/d^3$. p is the molecule's permanent dipole moment. This led to an expression for the capacity of the form

$$\frac{1}{C_1} = 4\pi d + \frac{4\pi N_T d^3}{c_e}\frac{\partial X}{\partial\sigma} \tag{6.16}$$

This approach was used by Levine *et al.* in a system where the two dipole contributions were not the same. In this way the required asymmetry was introduced and although there was a correlation between theory and experiment near the peak of the capacity–potential function, the values proved too small at $|\sigma_m| > 0$. Attempts to fit this model to nonaqueous media in the nonadsorbed state have been equally unsuccessful.

The next major advance was made by Damaskin and Frumkin,[52] who, for the first time, pointed out that the metal type was important in certain parts of the capacity–potential function and should be included in the model. They also pointed out the lack of large shift in potential when neutral species were adsorbed and suggested that this meant that the organic molecules were not replacing an oriented dipole layer but clusters of molecules with a total dipole moment smaller than the sum of the individual dipole moments. They also included in their model a term that allowed for the chemisorption of water, via the oxygen lone pair, at $\sigma_m \gg 0$. Using this model they were able to fit the differences in behavior of cadmium and mercury interfaces (cf. Figure 20). This model was then refined by Parsons, who defined N_T as follows[53]:

$$N_T = N_s^{\uparrow} + N_s^{\downarrow} + N_c^{\uparrow} + N_c^{\downarrow} \tag{6.17}$$

where N_c is the number of molecules in clusters with an overall orientation $\uparrow$ or $\downarrow$ and N_s is the same for the free molecules. The number of species in each configuration can then be derived using classical Boltzmann statistics. From this an expression was derived

$$g_{dip} = \frac{4\pi p_s}{\varepsilon}(N_s^{\uparrow} - N_s^{\downarrow}) + \frac{4\pi p_c}{\varepsilon}(N_c^{\uparrow} - N_c^{\downarrow}) \tag{6.18}$$

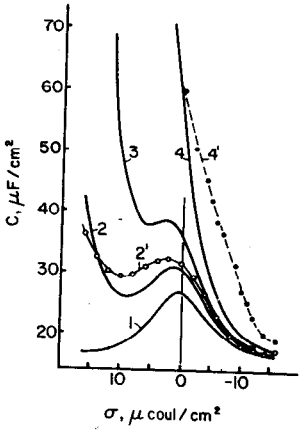


Figure 20. Fitting of experimental data for (2′) mercury in NaF and (4′) cadmium in KF at 0°C[70] to the Damaskin and Frumkin inner layer water theory.[52] Unprimed numbers refer to theoretical curves for different values of the fitting parameters.

for the potential drop across the dipole layer. The capacity is then obtained by differentiation and combination with K_{ion}. The parameters requiring definition in this approach were the dielectric constant, solvent molecule diameter, dipole moment of a molecule in the cluster, p_c, and the residual energies of the solvent against the surface in both positions. A good fit was obtained for this approach to Grahame's data at 273 K. The essential features are described, the maxima and the two minima, and it is possible to associate particular molecular behavior with the observed experimental phenomena. For example, the hump is associated with the reorientation of clusters while the destruction of the clusters accounts for the anodic and cathodic rises in capacity.

Bockris and Habib[74] have suggested an equilibrium between water monomers and dimers on the electrode, a concept arising from entropy measurements at the gas–metal interface. The model is consistent with the position of the entropy maximum for water in the double layer, and with the absence of a capacitance hump depending on water. Other models give a maximum entropy on the anodic side, but this is not consistent with the position at which the entropy maximum is observed.

A more rigorous treatment of the problem has been proposed by Fawcett.[54] The treatment of the clusters was improved by introducing Flory–Huggins statistics, and this yielded the following expression for the inner-layer capacity:

$$\frac{1}{C_i} = 4\pi d + 4\pi\left[p_s\left(\frac{\partial N_s^{\uparrow}}{\partial \sigma_m} - \frac{\partial N_s^{\downarrow}}{\partial \sigma_m}\right) + p_c n\left(\frac{\partial N_c^{\uparrow}/n}{\partial \sigma_m} - \frac{\partial N_c^{\downarrow}/n}{\partial \sigma_m}\right) - 4\pi g_s - g_s\left(N_s + q\frac{N_c}{n}\right)\frac{X}{\sigma_m} - g_s\left(N_s + q\frac{N_c}{n}\right)\frac{X}{\sigma_m}\right] \tag{6.19}$$

where the number of clusters per unit area is N_c/n and c is the true coordination number for a given molecule. The number of first neighbor sites around a cluster

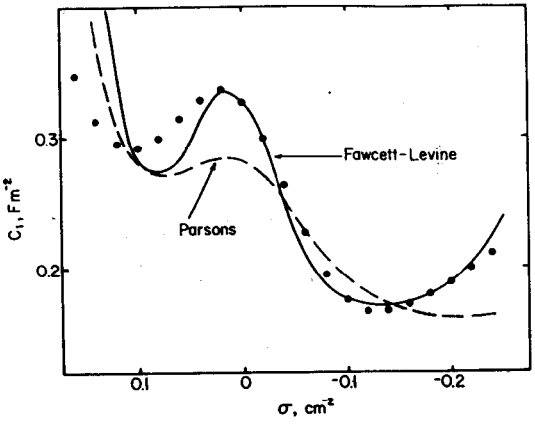


Figure 21. Comparison of Fawcett–Levine and Parsons expression.

is given by $qc = n(c - n + 1)$. A comparison of this expression with that of Parsons is shown in Figure 21. This approach reduces the number of parameters from 5 to 4 for the fitting and seems to give an improved agreement with the experimental data. In addition the residual energies for the solvent, which were unreasonably large, in the Parsons model $U_0^{\uparrow} = 20.9$ kJ mol^{-1} and $U_0^{\downarrow} = 10.5$ kJ mol^{-1}, are reduced to physically more reasonable values, $U_0^{\uparrow} = 6.9$ kJ mol^{-1} and $U_0^{\downarrow} = 0.9$ kJ mol^{-1}.

Fawcett also noted that the usual practice of fitting aqueous experimental data provides extra modeling problems as the solvent association has to be included. As a consequence he proposed a model in which three solvent positions were counted, the up/down dipole orientations and the position where the dipole is parallel to the electrode surface. If up/down molecules predominate, the system reduces to a two-position model with one hump, but if the parallel dipoles predominate a capacity minimum results. Such a type of model has been applied to the interface mercury–ethylene carbonate in the absence of specific adsorption and as can be seen from Figure 22 the fit is very satisfactory and gives an inner-layer thickness of the length of the molecule along the dipole vector. The polarizability term in both this and the previous treatment is rather large but the author suggests that this is due to the neglect of hyperpolarizability terms at high fields.

In general, molecular rotation might be important but preliminary calculations using a model including this were not promising.[55] The inclusion of more than one molecular layer in the calculation of the dipole potential might be attempted for small molecule solvents but this would lead to difficulties with the current statistical methods for calculating the dielectric properties. In addition Conway has pointed out that the specific influence of counterions at the outer Helmholtz plane is totally ignored in current treatments and the extension of

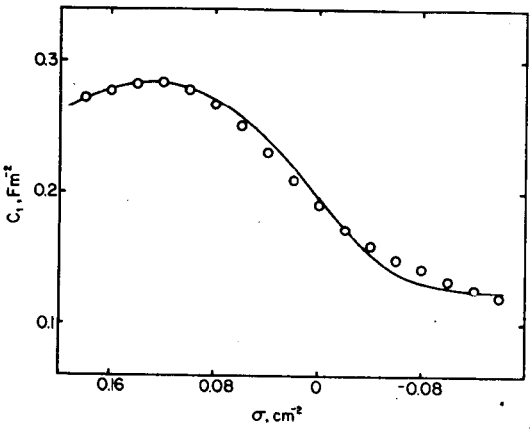


Figure 22. Variation of capacity of the inner layer in the presence of ethylene carbonate.

theories in this direction might help answer questions about the position of the OHP, of great importance to the study of electrode kinetics.[56] One final model must be mentioned again before leaving this type of approach—the early study of Macdonald and Barlow.[46] Ignored to a large extent by current theorists, this model provided a reasonable fit to the cathodic branch of the capacity–potential function using such parameters as compressibility of the solvent and dielectric saturation of the inner-layer dielectric. Possibly the time is ripe for the inclusion of some of these ideas in modern theories.

As mentioned at the outset, there is an alternative approach to molecular modeling and this has been adopted by Trasatti.[41] It has been shown that C_i at $\sigma_m = 0$ is strictly related to the extent of water orientation on the metal. C_i was shown to increase as the water dipole potential $g_{dip}^{H_2O}$ increases. It is found that the charge–potential relationship, corrected for the effects of surface roughness, is superimposable (cf. Figure 9). The construction of this curve has required potential shifts of the various systems along the potential axis, but the common slope at $\sigma_m \ll 0$ implies that K_{ion} has a constant value independent of metal type at these charges, $\sim 17\ \mu F\ cm^{-2}$. This capacity contribution may be considered to arise as a result of the distortional polarization of water molecules. The curved portion can be assumed to be determined by C_{dip}, which then depends on the type of metallic substrate.

A correlation between the enthalpy of formation of metal oxides, the surface potential of the oriented water layer, and $1/C_i$ at $\sigma_m = 0$ was used to obtain a value for C_{dip} when the maximum randomness is found in the surface layer, i.e., the surface potential of the layer in zero. Correlations with data on oxides are to be regarded with some suspicion as the typical oxide bond is strongly ionic, very different from the metallic interface situation. At $\sigma_m = 0$ a

value of $C_1 \sim 23\ \mu F\ cm^{-2}$ was found under these conditions. This assumes the value of surface potential suggested by Trasatti, 70 mV at $\sigma_m = 0$. The value for K_1 and C_1 are, in this case different, although C_1 has the same value as that found by extrapolating the enthalpy data to zero. This latter extrapolation could be taken to imply a system in which the solvent showed no specific interactions with the metal. Whether it is a real effect or the data from the enthalpy extrapolation should be very different from the surface potential extrapolation, if the correct enthalpy were used, remains to be seen.

Some generalities may be drawn from the preceding discussions.

(1) The phenomenon of nonspecific adsorption exists for a small number of systems over restricted potential ranges.

(2) The basic Gouy–Chapman–Stern theory is adequate at low ionic concentrations but may become progressively more imprecise as the concentration increases to the 0.1–1.0 *M* level.

(3) The collection of corrections to the GCS theory to be found in the literature are most unhelpful to the practicing electrochemist and almost all the effects predicted have not been discovered experimentally.

(4) The description of the inner layer in the absence of specific adsorption seems at first sight rather better. If the diffuse layer theory is seriously in error then these models will require drastic modification. Future theories of the inner layer will require a much improved description of the precise ionic distribution in the few solution layers adjacent to the OHP in the diffuse region. As Conway[56] has pointed out this could be of vital importance in associated solvent systems.

References

1. F. Franks, *Water*, Plenum Press, New York (1973), Vols. 1, 2, 3; A. Rahman and F. H. Stillinger, *J. Chem. Phys.* **55**, 3336 (1971); S. Toxvaerd and E. Praestgaard, *J. Chem. Phys.* **67**, 5291 (1977); F. H. Stillinger and H. L. Lemberg, *J. Chem. Phys.* **62**, 1340 (1975).
2. H. L. Friedman, *J. Electrochem. Soc.* **124**, 421C (1977); L. Parozzo, G. Corongui, C. Petrongolo, and E. Clementi, *J. Chem. Phys.* **68**, 787 (1978).
3. R. A. Robinson and R. H. Stokes, *Electrolyte Solutions*, Butterworths, London (1965).
4. R. Payne, in *Advances in Electrochemistry and Electrochemical Engineering*, P. Delahay and C. W. Tobias, eds., Interscience, New York (1970), Vol. 7, p. 1.
5. G. Valette and A. Hamelin, *J. Electroanal. Chem.* **45**, 301 (1973); T. Vitanov and A. Popov, *Dokl. Akad. Nauk. SSSR* **226**, 42 (1976).
6. B. B. Damaskin, O. A. Petrii, and W. W. Batrakov, *Adsorption of Organic Compounds at Electrodes*, Plenum Press, London (1971); J. Sobkowski and A. Wieckowski, *J. Electroanal. Chem.* **34**, 186 (1972).
7. G. Gouy, *J. Phys.* **9**(4), 457 (1910); *C. R. Acad. Sci.* **149**, 654 (1910); *Ann. Chim. Phys.* **29**, 159 (1903).
8. P. Delahay, *Double Layer and Electrode Kinetics*, Interscience, New York (1966).
9. G. Lauer, R. Abel, and F. C. Anson, *Anal. Chem.* **39**, 765 (1967).
10. D. C. Grahame, *J. Am. Chem. Soc.* **76**, 4819 (1954); *Chem. Rev.* **41**, 441 (1947).

11. D. M. Mohilner, in *Electroanalytical Chemistry*, A. J. Bard, ed., Marcel Dekker, New York (1966), Vol. 1, p. 241.
12. A. N. Frumkin and A. Gorodetskaya, *Z. Phys. Chem.* **136**, 215 (1928); A. N. Frumkin, *Svensk. Kem. Tidskr.* **77**, 300 (1965).
13. S. Trasatti, *J. Electroanal. Chem.* **33**, 351 (1971); *J. Electroanal. Chem.* **28**, 257 (1970).
14. R. M. Reeves, in *Modern Aspects of Electrochemistry*, B. E. Conway and J. O'M. Bockris, eds., Plenum, New York (1974), Vol. 9, p. 239.
15. D. L. Chapman, *Philos. Mag.* **25**, 475 (1913).
16. O. Stern, *Z. Electrochem.* **30**, 508 (1924).
17. D. C. Grahame, *J. Chem. Phys.* **18**, 903 (1950).
18. K. M. Joshi and R. Parsons, *Electrochim Acta* **4**, 129 (1961); R. Parsons and S. Trasatti, *Trans. Farday Soc.* **65**, 3314 (1969).
19. A. N. Frumkin, *Z. Phys. Chem.* **164A**, 121 (1933).
20. A. N. Frumkin, *Z. Electrochem.* **59**, 807 (1955); also in *Advances in Electrochemistry and Electrochemical Engineering*, P. Delahay, ed., Interscience, New York (1961), Vol. 1, p. 65; (1963), Vol. 3, p. 287; R. Parsons, in *Advances in Electrochemistry and Electrochemical Engineering*, P. Delahay, ed., Interscience, New York (1967), Vol. 1, p. 1.
21. C. W. de Kreuk, J. H. Sluyters, and M. Sluyters-Rehbach, *J. Electroanal. Chem.* **33**, 267 (1971).
22. W. R. Fawcett, *J. Electroanal. Chem.* **22**, 19 (1969); B. G. Chauhan, W. R. Fawcett, and T. A. McCarrick, *J. Electroanal. Chem.* **58**, 275 (1975).
23. J. J. Bickerman, *Philos. Mag.* **33**, 384 (1942).
24. D. A. Haydon and F. H. Taylor, *Philos. Trans.* **A253**, 255 (1960).
25. J. Malsch, *Phys. Z.* **29**, 770 (1928).
26. J. B. Hasted, D. M. Ritson, and C. H. Collie, *J. Chem. Phys.* **16**, 1 (1948).
27. H. D. Hurwitz, A. Sanfeld, and A. Steinchen-Sanfeld, *Electrochim. Acta* **9**, 929 (1964).
28. M. J. Sparnaay, *Rec. Trav. Chim.* **77**, 872 (1958).
29. G. H. Bolt, *J. Colloid Sci.* **10**, 206 (1955).
30. A. L. Loeb, *J. Colloid Sci.* **6**, 75 (1951).
31. W. E. Williams, *Proc. Phys. Soc.* **66**, 372 (1953).
32. H. Brodowsky and H. Strehlow, *Z. Electrochem.* **63**, 262 (1959).
33. G. M. Bell and S. Levine, *Chemical Physics of Ionic Solutions*, B. E. Conway and R. G. Barradas, eds. Wiley and Sons, New York (1966), p. 409.
34. F. P. Buff and N. S. Goel, *J. Chem. Phys.* **51**, 4983, 5363 (1969); **56**, 4245 (1972).
35. F. P. Buff and F. H. Stillinger, *J. Chem. Phys.* **39**, 1911 (1963).
36. I. Prigogine, P. Mazur, and R. Defay, *J. Chim. Phys.* **50**, 146 (1953).
37. F. H. Stillinger and J. G. Kirkwood, *J. Chem. Phys.* **33**, 1282 (1960).
38. J. G. Kirkwood and J. C. Poirier, *J. Phys. Chem.* **58**, 591 (1954).
39. V. S. Krylov and V. G. Levich, *Russ. J. Phys. Chem.* **37**, 50 (1963); 1224 (1963) (English translation).
40. G. A. Martynov, *Usp. Kolloid Khim.*, 86 (1973).
41. S. Trasatti, *J. Electroanal. Chem.* **91**, 293 (1978).
42. S. Trasatti, *J. Electroanal. Chem.* **64**, 173 (1975).
43. E. Blomgren, J. O'M. Bockris, and C. Jesch, *J. Phys. Chem.* **65**, 2000 (1961).
44. G. J. Hills and R. Payne, *Trans. Faraday Soc.* **61**, 325 (1965); J. A. Harrison, J. E. B. Randles, and D. J. Schiffrin, *J. Electroanal. Chem.* **48**, 359 (1973); N. H. Coung, C. V. D'Alkaine, A. Jenard, and H. D. Hurwitz, *J. Electroanal. Chem.* **51**, 377 (1974); D. Schuhmann, P. Vanel, and C. Bertrand, *J. Chim. Phys. (Paris)*, 643 (1977).
45. J. E. B. Randles and K. S. Whiteley, *Trans. Faraday Soc.* **52**, 1509 (1956).
46. J. R. Macdonald and C. A. Barlow, *J. Chem. Phys.* **36**, 3062 (1962); J. R. Macdonald, *J. Chem. Phys.* **22**, 1857 (1954).

47. R. J. Watts-Tobin, *Philos. Mag.* **6**, 133 (1961).
48. J. O'M. Bockris, M. A. V. Devanathan, and K. Muller, *Proc. R. Soc. London Ser. A* **274**, 55 (1963); J. O'M. Bockris, E. Gileadi, and K. Muller, *Electrochim Acta* **12**, 1301 (1967).
49. R. Parsons, *Transactions S.A.E.S.T.* **13**, 239 (1978).
50. I. L. Cooper and J. A. Harrison, *J. Electroanal. Chem.* **66**, 85 (1975).
51. S. Levine, G. M. Bell, and A. L. Smith, *J. Phys. Chem.* **73**, 3634 (1969).
52. B. B. Damaskin and A. N. Frumkin, *Electrochim Acta* **19**, 173 (1974).
53. R. Parsons, *J. Electroanal. Chem.* **59**, 229 (1975).
54. W. R. Fawcett, *J. Phys. Chem.* **82**, 1385 (1978).
55. K. B. Oldham and R. Parsons, *Elektrokhimiya* **13**, 866 (1977).
56. B. E. Conway, *Adv. Colloid Interface Sci.* **8**, 91 (1977).
57. V. S. Krylov, *Electrochim Acta* **9**, 1247 (1964).
58. V. V. Elkin, V. N. Alekseev, E. A. Solomantin, V. Ya. Mishuk, D. I. Leikis, and L. L. Knots, *J. Electroanal. Chem.* **65**, 11 (1975).
59. V. S. Krylov and V. A. Kir'yanov, *Electrokhimiya* **7**, 276 (1971).
60. R. de Levie and M. Nemes, *J. Electroanal. Chem.* **58**, 123 (1975).
61. M. A. V. Devanathan and P. Peries, *Trans. Faraday Soc.* **50**, 1236 (1954).
62. D. C. Grahame, *J. Am. Chem. Soc.* **76**, 4819 (1954).
63. R. de Levie, S. Sarangapani, P. Czekaj and G. Benke *Anal. Chem.* **50**, 110 (1978).
64. D. C. Grahame and B. A. Soderberg, *J. Chem. Phys.* **22**, 449 (1954).
65. R. Payne, *J. Chem. Phys.* **42**, 3371 (1965).
66. R. Payne, *J. Electroanal. Chem.* **7**, 343 (1964).
67. G. J. Hills and R. M. Reeves, *J. Electroanal. Chem.* **31**, 269 (1971).
68. D. C. Grahame, *J. Am. Chem. Soc.* **79**, 2093 (1957).
69. R. Parsons, *Proceedings of the 2nd International Congress on Surface Activity, Vol. 3*, Butterworths, London (1957), p. 38.
70. V. Panin, K. Rybalka, and D. Leikis, *Elektrokhimiya* **9**, 1062 (1973).
71. W. R. Fawcett and M. D. Mackey, *J. Chem. Soc. Faraday Trans. 1* **69**, 634 (1973).
72. R. S. Rodgers and F. C. Anson, *J. Electroanal. Chem.* **42**, 381 (1973).
73. M. J. Weaver and F. C. Anson, *J. Electroanal. Chem.* **58**, 95 (1975).
74. J. O'M. Bockris and H. A. Habib, *Electrochem Acta* **22**, (1977) 41–46.

4

Specific Adsorption of Ions

M. A. HABIB and J. O'M. BOCKRIS

1. Introduction

The adsorption of ions constitutes the underlying phenomenology of the double layer and contributes to the most experiment-consistent molecular model of the interface. The rate of electrochemical reactions is influenced by the double-layer structure, i.e., by the presence of adsorbed ions on the electrode. The potential distribution in the inner layer is determined partially by contributions from the ions present and thus the double-layer capacitance is a function of ionic adsorption. The nature of the forces which cause the adsorption of ions is not only determined by the nature of the ions, but also by the nature of the metal and other interfacial species including the solvent dipoles and the properties of the ionic hydration sheath.

A primary tool in studies of adsorption in chemistry has been the isotherm. In the electrochemical situation, the isotherm also plays a fundamental role in elucidating the phenomena of adsorption at interfaces. However, in electrochemistry, the corresponding experimental quality is the Gibbsian idea of specific surface excess, Γ_i. This concept is not to be confused simplistically with adsorption. Its unambiguous determination is important in elucidating models of increasing sophistication with which progress in the double layer is associated.

M. A. HABIB • School of Physical Sciences, The Flinders University of South Australia, Bedford Park, South Australia 5042. **J. O'M. BOCKRIS** • Department of Chemistry, Texas A & M University, College Station, Texas 77843.

However, it is difficult to evaluate Γ_i with a given degree of certainty. The elucidation is associated with a number of assumptions which must be tested. Their acceptibility changes with time.

These matters are brought out, here, along with interpretive aspects of double-layer phenomena which are dependent upon specific adsorption, e.g., that of the capacitance hump.

2. Definition

2.1. Introduction

Although the concept of specific adsorption is subject to exact discussion, its definition is not a straightforward one.

From the qualitative point of view, the definition is easy. The specific adsorption at the interface between an electronic and ionic conductor is the adsorption which is in excess or deficit of the amount which would be expected to be present at the interface from simple coulombic considerations. Thus, if there is an excess charge of σ_m on the metal, the coulombic adsorption is $-\sigma_m/nF$ mol per unit area. When the adsorption exceeds $-\sigma_m$ or less than it, then the excess or deficit is called specific adsorption.

Historically, discussion of the definition of specific adsorption arose at first in a vague way by noting the asymmetric shape of the electrocapillary curves (Figure 1). This was noted particularly by Gouy[1] when he made measurements at the mercury–solution interface. The surface tension changes differently on the anodic side to that on the cathodic side, in a manner characteristic of the anion in solution. As it is evidently anions which will tend to be adsorbed in preference to cations when the metal surface bears an excess positive charge, (positive branch), the concept arose that adsorption on the positive side included a part extra to the coulombic, and this part is called specific. This concept arose from the fact that because a decrease in surface tension is known to indicate adsorption, as this decrease in surface tension changes with each anion, for the same coulombic charge, it must imply that there is something else in the adsorption over and above the coulombic consideration.

Thus arose the idea of a specific adsorption not associated in a one-to-one manner with excess electric charges on the metal and in the solution.

After the exact definition given above and the qualitative historical origin now stated, we may look at some other approaches to a definition of specific adsorption.

One has to grapple with three matters:

(a) The adsorption is specific and a special characteristic of an ion and not characteristic only of the charge on the metal.

(b) The adsorption is only that part of the total adsorption which differs from the adsorption which is expected on coulombic grounds.

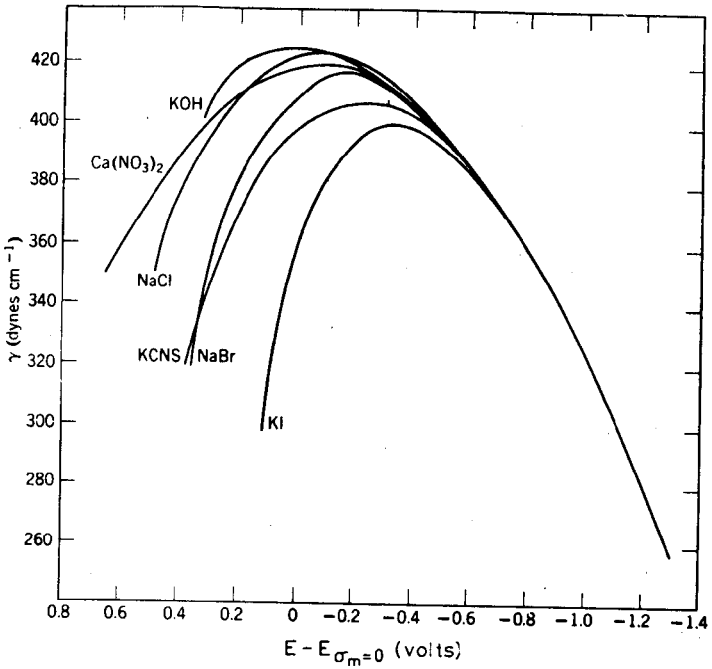


Figure 1. Interfacial tension of mercury in contact with aqueous solutions of different electrolytes. $T = 18°C$. Potentials referred to $E_{\sigma_m=0}$ are the potentials of zero charge for mercury in contact with NaF solution.[2]

(c) The quantity we measure is the Gibbs surface excess and this is a special kind of adsorption, not simply the number of ions adsorbed on the electrode.

2.2. Definition in Terms of Gibbs Surface Excess

A practical definition of specific adsorption may be given in three parts: At the potential of zero charge, it is said that there is specific adsorption if the measured surface excess of any ionic species is positive. At potentials more positive than the point of zero charge ($\sigma_m > 0$), one says there is specific adsorption if the surface excess of any cation is positive. At potentials more negative than the point of zero charge ($\sigma_m < 0$), if the surface excess of any anion is greater than zero, then specific adsorption is said to have occurred.

Another operational definition may be stated in terms of diffuse layer theory. According to this definition there is specific adsorption, if the experimental data cannot be explained by the diffuse layer theory. Although this

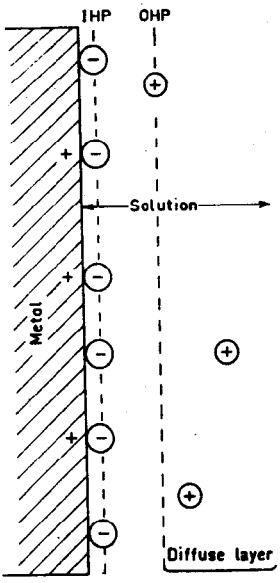


Figure 2. Pictorial representation of superequivalent adsorption.

definition is less satisfying in view of the defects in the diffuse layer theory, it is widely used in practice.

Other definitions of specific adsorption, which have been developed by Frumkin[3] and by Bockris *et al.*[4] are not operational, but descriptive or phenomenological or modelistic, as discussed below.

2.3. Superequivalent Adsorption[3]

The concept of superequivalent adsorption may be seen in the diagram (Figure 2). Let us suppose that the surface excess charge on the metal is σ_m. Then there will be a charge in the first layer in the solution which will be, neglecting the sign, numerically greater (for anion adsorption) than the excess charge on the metal. Overall electroneutrality must be maintained and the excess charge is made up by a charge in the solution.

It is clear that the charge in the inner Helmholtz plane (IHP) is more than equivalent to the coulombic charges on the metal, i.e., it is superequivalent.

2.4. Contact Adsorption

In the school of Bockris and co-workers,[4] the word "contact adsorption" is used to stress the physical nature of the model used for the double layer when specific adsorption is present. According to this view, specific adsorption occurs when ions are sufficiently large so that there are no longer any primary solvation sheaths present.

Thus, on approach of an ion to the electrode, the absence of a primary solvation sheath means that the ion can contact the metal directly ("contact adsorption"), penetrate into the inner layer and become attached to the metal, having its electrical center at the IHP.

Specific adsorption, superequivalent adsorption, and contact adsorption are all the same, but the term "contact adsorption" has the attraction of describing the situation modelistically.

3. History of Specific Adsorption

In considering the history of specific adsorption, it is important first to realize the position towards the end of the 19th century, when the structural concepts of the double layer were Helmholtzian. In the Helmholtz view,[5] the double layer was a simple structure indicated by its name. A layer of charges existed on the electrode, and a layer of charges of the same number existed in solution in a simple 1:1 way. A similar view was given by Quincke[6] in 1861, though he did not use the term "double layer."

The early work which led to the concept that a part of the adsorption would be "specific" was done by M. Gouy,[1]† and was based upon the very large number of electrocapillary curves which he recorded. In these, it was always seen that on the negative side of the pzc where the cations would be the adsorbing entity, the surface tension was lowered by roughly the same amount at the same potential on the electrode, independently of what cation was involved. However, on the positive side of the pzc where anions would tend to be the adsorbing entities, there was a difference in the behavior of surface tension, for different ions. Because the difference in the lowering of the surface tension was thought of as due to adsorption, this is referred to as specific.

The first treatment of specific adsorption in terms of a model was that of Stern.[7] There are two significant ideas in the Stern model. Firstly, Stern took explicit account of the fact that, owing to the finite size, the ions of the diffuse layer cannot approach the electrode surface closer than a certain minimum distance, x_2, differing in this view from the point charge treatment of G. Gouy.[8] Secondly, Stern[7] recognized that some ions might be held to the electrode in a rigid monolayer through the operation of close-range forces, and thus Stern implied the necessity of considering different distances of closest approach for cations and anions.

It is not entirely clear whether the Stern concepts implied that the outer Hemholtz plane charge should be divided into two parts, a part corresponding to a layer of charge at the beginning of the outer Helmholtz plane, for those ions

† It is noteworthy that M. Gouy,[1] to whom reference is made so greatly in double-layer work for his experimental contributions, is not the Gouy (G. Gouy[8]) who wrote the well-known paper on the diffuse double layer.

from the solution which are not specifically adsorbed but which are in contact with the electrode through their hydration sheaths; or whether in fact the Stern concepts saw the diffuse layer as having no particular *layer* of charge at the outer Helmholtz plane. The latter is the present view.

Grahame[2] developed Stern's model in an important way by bringing out the idea that the specifically adsorbed ions are *closer* to the electrode surface than the plane of closest approach of nonspecifically adsorbed ions of the diffuse layer (Stern had merely distinguished two layers). Grahame[2] denoted the distance of closest approach of the specifically adsorbed layer of ions by x_1 and he called the plane of closest approach of the electrical centers of these ions the inner Helmholtz plane (IHP). The plane of closest approach of the nonspecifically adsorbed ions, located at a distance $x_2 > x_1$ from the electrode surface, was called the outer Helmholtz plane (OHP). Thus the OHP forms the boundary between the inner and the diffuse layer. When the specific adsorption of ions occurs, it takes place inside the inner layer.

The first evaluation of amounts adsorbed from experimental data using the Stern model and the Gouy[8]–Chapman[9] theory of the diffuse layer is due to Grahame.[2] In this he took the experimental surface excess of the ions and subtracted from this the diffuse layer charge calculated from diffuse layer theory and thus obtained the amount of specifically adsorbed charge. This procedure, of course, involves the assumption of nonspecific adsorption of cation. The method is discussed in the next section.

Until the 1950s, all measurements of adsorption were oriented towards some variant of the electrocapillary thermodynamics, albeit that the measurement might be capacitance ones (as were nearly all of Grahame's[2]).

However, from the mid 1950s, other measurements began to be made. Radiotracer methods for the measurement of adsorption were first carried out by Balashova[10] in 1955 and continued in a series of later works.[11–14] The radiotracer method for the measurement of adsorption at the solid electrode was first reported in a paper by Blomgren and Bockris[15] in 1960. The Blomgren and Bockris[15] work was oriented towards the adsorption of organic compounds and did not deal with the adsorption of anions and cations.

The measurement of the concentration changes of the silver ions in a silver nitrate solution was used for the investigation of their adsorption long before in 1922 by Euler[16] and for the determination of the charge on a silver surface under steady state conditions by Proskurnin and Frumkin[17] in 1933. The adsorption of organic compounds on nickel, copper, and silver was studied on the basis of the concentration changes determined by means of spectrophotometry by Conway and Barradas[18,19] in 1958 and 1963, respectively.

Two main dates in the history of specific adsorption are concerned with (a) the first quantitative theory of forces in specific adsorption, due to Anderson and Bockris[20] in 1964, and (b) the first method of measuring the surface tension of solids at the solid–solution interface, due to Fredlein, Damjanovic, and Bockris[21] in 1971.

A new technique for the measure of adsorption, the ellipsometric method, was pioneered by Chiu and Genshaw.[22,23] This method began to be used from the late 1960s to measure specific adsorption.[24,25]

The various methods, their applicability and results, are discussed in detail in the next section.

4. Phenomenology of Specific Adsorption

Dependence on Charge Density. The amount of specifically adsorbed ions increases with increase of electrode charge of opposite sign to the ion (Figure 3). Negative ions may adsorb at negative electrode charges, but with decrease of negative charge on the electrode, the amount of the anions adsorbed increases.

Ion Size Effect. In general, the greater the size of the ion, the more is its specific adsorption (Figure 4).

Type of the Ions. Anions have a much greater tendency to be adsorbed specifically, in comparison to cations. Large cations like tetra-alkylammonium ions,[27,28] $Cs,^{+}$[29,30] and Tl^{+}[31], are found to adsorb specifically.

Hydration. Ions with strong primary hydration sheaths undergo little

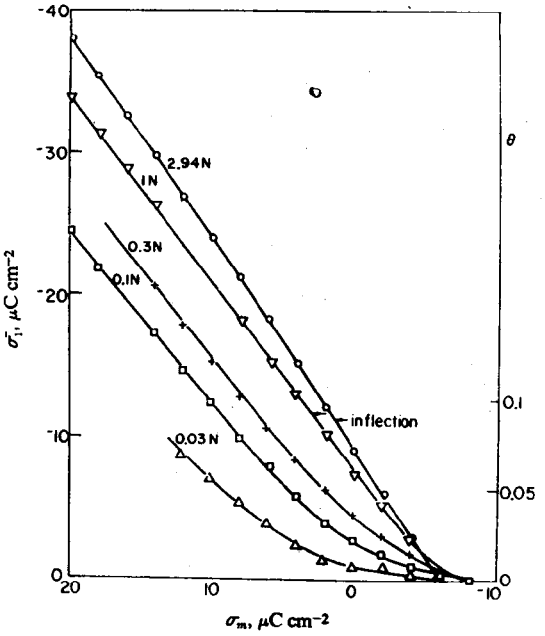


Figure 3. Specific adsorption of Cl^- ions as a function of electrode charge.[4]

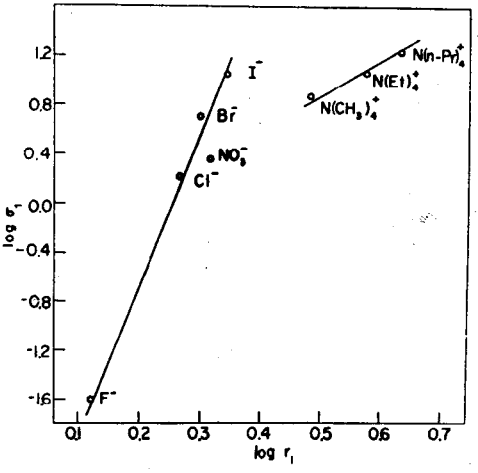


Figure 4. Specific adsorbability, σ_1, plotted against the ionic radius, r_i, for some anions and cations (logarithmic scale) at the potential of zero charge.[20]

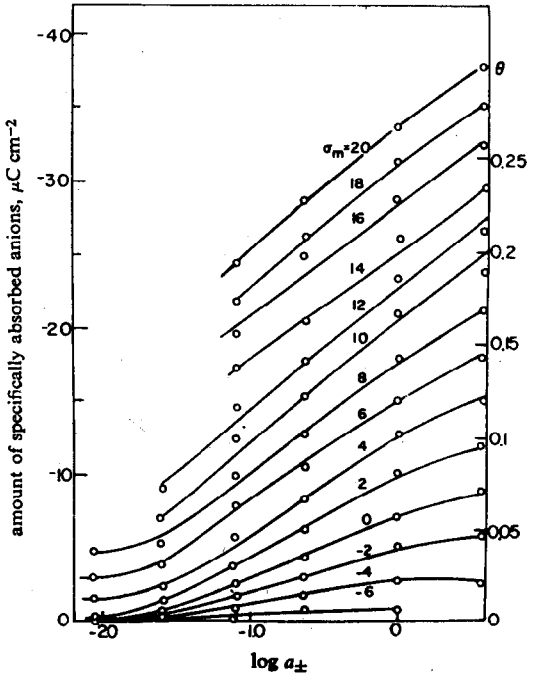


Figure 5. Logarithmic isotherms: HCl solutions.[4]

Table 1

Ion–Solvent Interaction Energy, ΔH_{ion-w} for Various Anions[20] *(in kcal mol^{-1})(1 cal = 4.18 J)*

F^-	Cl^-	Br^-	I^-
−20.6	−13.6	−12.2	−10.7

specific adsorption. Specific adsorption depends upon the nature of the solvent, increasing with decrease of ion–water interaction. For example, for halide ions, the ion–solvent interaction decreases in the sequence $F^- > Cl^- > Br^- > I^-$ (Table 1). Consequently, at any fixed potential, the specific adsorption decreases in the sequence $I^- > Br^- > Cl^- > F^-$.

Effect of Concentration Change. Specific adsorption increases with increase of concentration of the electrolyte at a constant charge or potential (Figure 5). To describe the way that surface concentration changes with increase of bulk concentration, several adsorption isotherms are applied. These isotherms differ from each other in ways by which the particle–surface interactions and particle–particle interactions are accounted for. Detailed discussion on isotherms is given in Section 11.

Effect of Temperature. Experimental works investigating the temperature effect on specific adsorption are scanty. However, available experimental data[32] suggest that specific adsorption of ions decreases with increase of temperature (Figure 6).

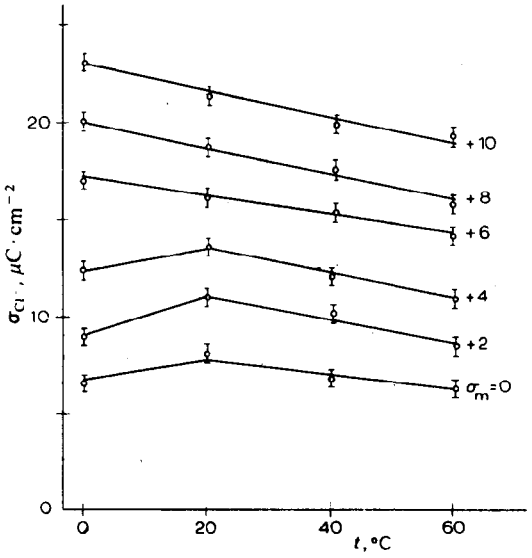


Figure 6. Temperature dependence of specific adsorption.[32]

5. Determinations of Specific Adsorption

5.1. Quasithermodynamic Methods

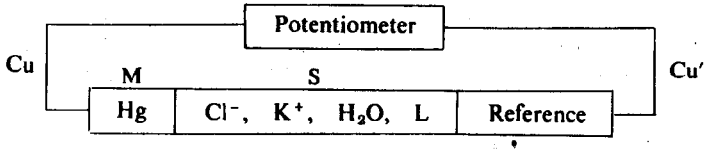
5.1.1. Electrocapillary Method

5.1.1.1. Introduction

Application of the Gibbs adsorption theorem to the phenomena of electrocapillary curves leads to the evaluation of the specific adsorption of ions on electrode surfaces. The methods of evaluation are not purely thermodynamic because, to derive the amount of specifically adsorbed charges, one needs to use a nonthermodynamic evaluation of the diffuse layer charge along with some nonthermodynamic assumptions concerning the adsorbability of cations as discussed below. These methods are thus termed "quasithermodynamic."

5.1.1.2. Derivation of Electrocapillary Equations

Let us consider the following cell with an ideally polarizable electrode Hg, and an aqueous solution KCl and undissociated organic compound, L.



The method of applying thermodynamics to an ideally polarizable interface is based on the Gibbs adsorption equation. The ideally polarized electrode is characterized by the existence of an electrostatic rather than an electrochemical equilibrium between the two phases. This equilibrium is analogous to that in a charged parallel plate condenser. This condition is realized in practice, either when no transfer of charged particles between the two phases is possible or, when such transfer, though thermodynamically possible, occurs extremely slowly as a result of a high energy of activation.

The interphase (σ) between the metallic phase M and the solution phase S is regarded as a region of finite thickness which extends into the phase M and S until the composition of its boundaries is equal to that in the bulk of the adjoining phase.

The Gibbs adsorption equation for the interphase, σ, is[33]

$$d\gamma = \tau\, dP - S^{\sigma}\, dT - \sum_i \Gamma_i\, d\bar{\mu}_i \tag{5.1}$$

where γ is the interfacial tension, τ is the thickness of the interphase, S^{σ} is the entropy per unit area of the interphase, Γ_i is the surface excess of the component i in the interphase, and P and T are pressure and temperature, respectively.

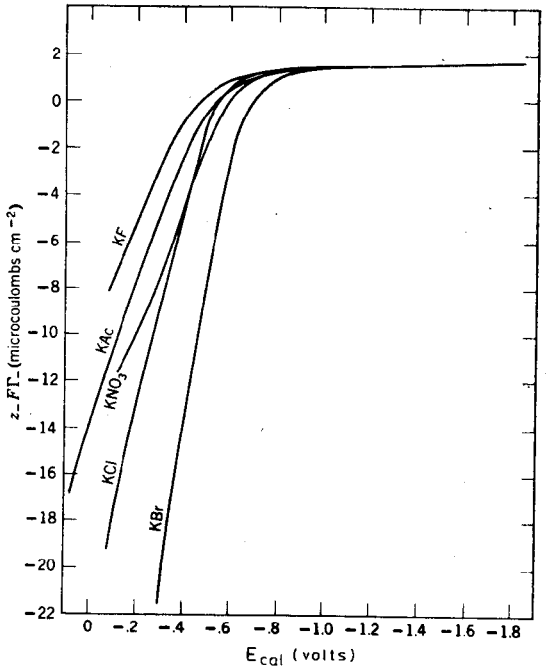


Figure 7. Surface excesses (relative to water) of various anions at the mercury–solution (0.1 N) interphase as a function of potential.[38]

For the present example in Figure 7, Eq. (5.1) becomes, at constant pressure and temperature,

$$-d\gamma = \Gamma_{Hg_2^{2+}}\, d\bar{\mu}^{M}_{Hg_2^{2+}} + \Gamma_e\, d\bar{\mu}_e{}^{M} + \Gamma_K + d\bar{\mu}_{K^+}{}^{S} + \Gamma_{Cl} - d\bar{\mu}_{Cl^-}{}^{S} + \Gamma_L + \Gamma_w\, d\mu_w{}^{S} \tag{5.2}$$

The measured potential difference is defined by the equation

$$E_\pm = \phi^{Cu} - \phi^{Cu'} = (\bar{\mu}_e{}^{Cu'} - \bar{\mu}_e{}^{Cu})/F \tag{5.3}$$

where ϕ^{Cu} and $\phi^{Cu'}$ are the inner potentials of the indicated metal used to connect each electrode to the potentiometer, respectively. E_+ and/or E_- is the potential of the ideally polarized electrode with respect to the reference electrode. (E_+ or E_- is used depending on whether the reference electrode is reversible to cation or anion of the solution, respectively.)

The condition for equilibrium between the components in phase M is

$$\mu_{Hg}{}^{M} = \bar{\mu}^{M}_{Hg_2^{2+}} + 2\bar{\mu}_e{}^{M} \tag{5.4}$$

For contact equilibrium of electrons between the copper wire Cu and phase M,

$$\bar{\mu}_e{}^{M} = \bar{\mu}_e{}^{Cu} \tag{5.5}$$

Now, the total charge per cm^{-2} of the interphase due to components of phase M is defined by†

$$\sigma_m = (2\Gamma_{Hg_2^{2+}} - \Gamma_e)e \tag{5.6}$$

Similarly, in the phase S, the condition for equilibrium is

$$\mu_{KCl}^{S} = \bar{\mu}_{K^+}^{S} + \bar{\mu}_{Cl^-}^{S} \tag{5.7}$$

and the charge per cm^2 of the interphase due to the components of phase S is defined by

$$\sigma_s = (\Gamma_{K^+} - \Gamma_{Cl^-})e \tag{5.8}$$

Utilization of (5.3)–(5.8) in (5.2) gives rise to

$$-d\gamma = \sigma_m\, dE + \Gamma_{Hg_2^{2+}}\, d\mu_{Hg}^{M} + \Gamma_{Cl^-}\, d\mu_{KCl}^{S} + \Gamma_L\, d\mu_L^{S} + \Gamma_w\, d\mu_w^{S} \tag{5.9}$$

Now, the Gibbs–Duhem equation for the metallic phase at constant temperature and pressure is given by

$$x_{Hg}^{M}\, d\mu_{Hg}^{M} = 0 \tag{5.10}$$

and for the solution phase

$$x_{KCl}^{S}\, d\mu_{KCl}^{S} + x_w^{S}\, d\mu_w^{S} + x_L^{S}\, d\mu_L^{S} = 0 \tag{5.11}$$

where x represents the mole fractions of the indicated components.

Substituting for $d\mu_w$ from Eq. (5.11) into (5.9) one may obtain

$$-d\gamma = \sigma_m\, dE_+ + \left(\Gamma_{Cl^-} - \Gamma_w \frac{x_{KCl}^{w}}{x_w}\right) d\mu_{KCl}^{S} + \left(\Gamma_L - \frac{x_L}{x_w}\Gamma_w\right) d\mu_L \tag{5.12}$$

in which the reference electrode is reversible to the cation. If the anion is reversible to the reference electrode, then in the above equation (5.12), Γ_{Cl^-} should be replaced by Γ_{K^+}.

† The modelistic concepts which underlie the presence of a Gibbsian surface excess of mercurous ions should be noted. The symbol $\Gamma_{Hg_2^{2+}}$ corresponds to an overly simple presentation of the fact that metals can be crudely regarded as mixtures of ions and electrons. Thus, as in the present proof, we are concentrating the electrons in the metal, and whether they are more or less than the number of ions present, it is important to realize that the number of metal ions varies in concentration as we approach the surface from the bulk. Thus, regarding the concentration of mercurous ions as a function of distance along the X coordinate orthogonal to the metal surface but inside the metal, it would be likely that this concentration would rise as the surface grew more negative and fall as the surface grew more positive. Thus a somewhat charge dependent $\Gamma_{Hg_2^{2+}}$ is a reasonable concept. Note that it seems unlikely that one should bring into account any simplistic "neutralization process" between the electrons and these mercurous ions. When we speak about a surface excess charge which is negative, it means that the net of the positive mercurous surface excess and electron surface excess amounts to a deficit of electrons compared with that number of electrons which would be present in the sample of metal when the surface charge is zero. It is unlikely that any "neutralization" of the mercurous ions to atoms occurs.

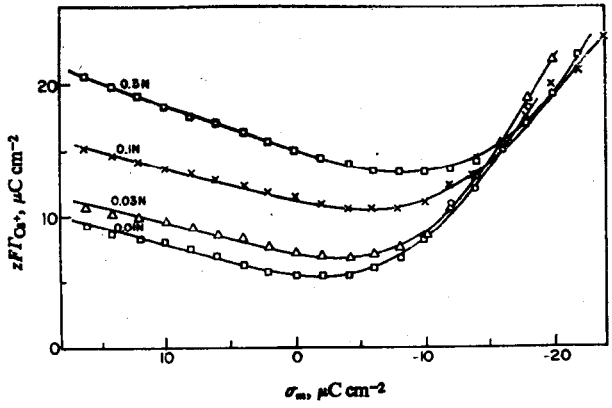


Figure 8. Surface excess of Cs^+ ions at the mercury–CsI solution interphase as a function of charge density on the metal.[4]

In terms of relative surface excesses, Eq. (5.12) may be written as

$$-d\gamma = \sigma_m\, dE_+ + \Gamma_{Cl^-,w}\, d\mu_{KCl} + \Gamma_{L,w}\, d\mu_L \tag{5.13}$$

Instead of introducing *relative* surface excesses, Grahame and Whitney[34] selected $\Gamma_{H_2O} = 0$. Nothing is gained by this arbitrary procedure for it must be realized that only relative surface excesses can be obtained from thermodynamic argument. (See discussion in Section 5.2.)

Thus, for a system of a Hg electrode in contact with an aqueous solution of z–z electrode,

$$-\left(\frac{d\gamma}{d\mu}\right)_{E_\pm} = \Gamma_{\pm,w} \tag{5.14}$$

where $\Gamma_{\pm,w}$ is the relative surface excesses for the cations (Γ_+) or anions (Γ_-). Equation (5.14) holds for constant pressure, temperature, and composition of the electrode. $E_\pm$ is the potential with respect to a reference electrode which is reversible either to the cation (E_+) or the anion (E_-). For a salt $B_{\nu_+}A_{\nu_-}$, Eq. (5.15) may be written as

$$-\nu_\pm\left(\frac{\partial\gamma}{d\mu}\right)_{E_\mp} = \Gamma_\pm \tag{5.15}$$

where μ is the chemical potential of the salt.

Since

$$\mu = \mu_0 + \nu_\pm RT \ln a_\pm \tag{5.16}$$

Eq. (5.16) may also be represented by

$$\Gamma_\pm = -\frac{1}{\nu_\pm RT}\left(\frac{d\gamma}{d\ln a_\pm}\right)_{E_\pm} \tag{5.17}$$

At a constant composition, Eq. (5.13) gives

$$\left(\frac{d\gamma}{dE_+}\right)_\mu = \sigma_m \tag{5.18}$$

the charge on the metal, i.e., the Lippmann equation.[35]

Thus from the slope of the electrocapillary curves the charge density on the metal may be determined and surface excesses may be obtained from the electrocapillary curves and Eqs. (5.15) or (5.17), (Figures 7 and 8).

5.1.1.3. Evaluation of Specific Adsorption

To obtain *specifically* adsorbed charge from the measured relative surface excesses, one needs to assume a nonthermodynamic procedure. The charges on the metal must be equal to the charges in the solution represented by the charges of cations and anions in the double layer, i.e.,

$$-\sigma_m = \sigma^+_{soln} + \sigma^-_{soln} \tag{5.19}$$

or

$$-\sigma_m = zF\Gamma_+ + zF\Gamma_- \tag{5.20}$$

where Γ's represent the total adsorption,

$$\Gamma = \int_0^\infty (c_x - c_\infty)\, dx \tag{5.21}$$

due to both simple electrostatic and specifically absorbed ions.

Let us consider the case of a monovalent ion, where $z = 1$, and thus

$$F\Gamma_\pm = \sigma_1{}^\pm + \sigma_{2-b}{}^\pm \tag{5.22}$$

where $\sigma_1{}^\pm$ is the specifically adsorbed charges and $\sigma_{2-b}{}^\pm$ is the diffuse layer charges. Now, an assumption originated from Grahame[2,34] is made that the cations are not specifically adsorbed at all so that

$$\sigma_1{}^+ = 0 \tag{5.23}$$

and

$$F\Gamma^+ = \sigma_{2-b}{}^+ \tag{5.24}$$

This means that all the charges due to the adsorption of cations are in the diffuse region of the double layer. From diffuse layer theory

$$\sigma_{2-b}{}^+ = \left(\frac{\epsilon kTn_i}{2\pi}\right)^{1/2}\left[\exp - \left(\frac{ze\phi_{2-b}}{2kT}\right) - 1\right] \tag{5.25}$$

where n_i is the concentration of the ions in the bulk of the solution and ϕ_{2-b} is the fall of potential in the diffuse layer.

Introducing (5.25) in (5.22) and from the experimentally derived $\Gamma_\pm$ [Eqs. (5.15) or (5.17)], the specifically adsorbed charge $\sigma_1{}^-$ can thus be obtained. A plot of $\sigma_1{}^-$ vs. σ_m is shown in Figure 3.

Alternatively, one can obtain the charge and interfacial tension from measurements of differential capacity curves and by the application of the following definitive equations:

$$\sigma_m = \int_{E_{\sigma_m=0}}^{E} C\,dE \tag{5.26}$$

and

$$\iint_{E_{\sigma_m=0}}^{E} C\,dE^2 = \gamma_{\sigma_m=0} - \gamma \tag{5.27}$$

For the integrations (5.26) and (5.27) to be performed, it requires independent measurement of $E_{\sigma_m=0}$ and $\gamma_{\sigma_m=0}$. The surface tension of a liquid metal, e.g., Hg, may be measured but substantial problems are usually encountered in measuring γ for solid metals as discussed in Section 5.4. By performing these integrations, one can obtain the electrocapillary curves from which the procedure described in the last section may be followed to obtain surface excesses and consequently the specifically adsorbed charges.

5.1.2. Parson's Method

The basic electrocapillary equation [Eqs. (5.12) or (5.13)] may also be represented in terms of σ_m as an independent variable, instead of $E_\pm$, by using Parson's[37] auxiliary function $\xi_\pm$ defined by

$$\xi_\pm = \gamma + \sigma_m E_\pm \tag{5.28}$$

If one takes the first derivative of (5.28) and substitutes in the electrocapillary Eq. (5.13) one gets

$$d\xi_\pm = E_\pm\,d\sigma_m - \Gamma_\pm\,d\mu \tag{5.29}$$

for a simple system of Hg-aqueous-solution interface. Graphical differentiation of Eq. (5.29) with respect to μ, the chemical potential of the salt, gives the surface excess values at constant electrode charge, i.e.,

$$\left(\frac{d\xi_\pm}{d\mu}\right)_{\sigma_m} = \frac{\partial(\gamma + \sigma_m{}^+ E_\pm)}{d\mu} = -\Gamma_\pm \tag{5.30}$$

Thus, obtaining $\Gamma_\pm$ from (5.30) one may evaluate $\sigma_1{}^-$ as a function of electrode charge from equations (5.22)–(5.25).

5.1.3. Grahame's Capacitance Method

Grahame and Soderberg[38] used the following method to evaluate the excess charges in the double layer.

Differentiation of Eq. (5.15) with respect to E_- gives, e.g.,

$$\Gamma_+\left(\frac{\partial^2\gamma}{\partial\mu\,\partial E_-}\right)_{E_+} = -\left(\frac{\partial\Gamma_+}{\partial E_-}\right)_\mu \tag{5.31}$$

where ν_+ is the number of cations formed by the dissociation of one molecule of the electrolyte. The quantity at the right-hand side of Eq. (5.31) is proportional to C_+, the component of capacitance attributable to the approach or departure of cations from the interface when the overall potential is changed slightly and may be represented by

$$z_+ F(\partial\Gamma_+/\partial E_-)_\mu = -C_+ \tag{5.32}$$

From (5.31), (5.32), and (5.18),

$$z_+\nu_+ F(\partial\sigma_m/\partial\mu)_{E_-} = -C_+ \tag{5.33}$$

Similarly,

$$z_-\nu_- F(\partial\sigma_m/\partial\mu)_{E_+} = -C_- \tag{5.34}$$

Since the charge on the solution side is $-\sigma_m$, $C_\pm$ is preceded by a minus sign in Eqs. (5.32)–(5.34).

From Eq. (5.33), on differentiation,

$$z_+\nu_+ F(\partial^2\sigma_m/\partial\mu\,\partial E_-) = -\partial C_+/\partial E \tag{5.35}$$

Since the double-layer capacity due to total charges is given by

$$C = \left(\frac{\partial\sigma_m}{\partial E}\right)_\mu \tag{5.36}$$

one gets from (5.35) and (5.36),

$$z_+\nu_+ F(\partial C/\partial\mu)_{E_-} = -\partial C_+/\partial E \tag{5.37}$$

Similarly, one may obtain

$$z_-\nu_- F(\partial C/\partial\mu)_{E_+} = -\partial C_-/\partial E \tag{5.38}$$

The left-hand side of the equations (5.37) and (5.38) can be evaluated experimentally, thus enabling the calculation of dC_+/dE, C_+, Γ_+, and the corresponding quantities for anions. Thus

$$C_+ = \int (dC_+/dE)\,dE + K \tag{5.39}$$

and

$$z_+ F\Gamma_+ = -\int C_+\,dE + K' \tag{5.40}$$

Supposing $(\partial C/\partial\mu)_{E_-}$ is known from experiment, the complication is in the determination of the constants of integrations K and K'. Grahame and Soderberg[38] suggested the evaluation of these constants from a study of the rate of change of the potential of zero charge with chemical potential. From Eq. (5.33)

$$z_+\nu_+ F(\partial\sigma_m/\partial E_-)(\partial E_-/\partial\mu)_{\sigma_m=0} = (C_+)_{\sigma_m=0} \tag{5.41}$$

or from Eq. (5.36),

$$z_+ \nu_+ F C_{\sigma_m = 0} (\partial E_- / \partial \mu)_{\sigma_m = 0} = (C_+)_{\sigma_m = 0} \tag{5.42}$$

at the pzc and as the equation shows, a measurement of $\partial E^- / \partial \mu$ at the potential of zero charge provides means for the calculation of $(C_+)_{\sigma_m = 0}$ and hence, in effect, of the constant K in Eq. (5.39).

For evaluation of K', the equation needed is

$$\left(\frac{\partial \gamma}{\partial \mu}\right)_{\sigma_m = 0} = -(\Gamma_{\text{salt}})_{\sigma_m = 0} = -\frac{(\Gamma_+)_{\sigma_m = 0}}{\nu_+}$$

$$= -\frac{(\Gamma_-)_{\sigma_m = 0}}{\nu_-} \tag{5.43}$$

The evaluation of $(\Gamma_{\text{salt}})_{\sigma_m = 0}$ through Eq. (5.43) *which needs surface tension measurements as in the earlier methods*, provides a value of K' because it provides a value of Γ_+ at one potential.

An alternative method of evaluating K and K' has been suggested by Grahame and Soderberg[38] by using the diffuse layer theory. Grahame[39] derived

$$\sigma_{+,d} = A[v + (1 + v^2)^{1/2} - 1] \tag{5.44}$$

where $\sigma_{+,d}$ is the positive charge in the diffuse layer and v is $-\sigma_{+,d}/2A$, where

$$A = \left(\frac{\varepsilon k T n_i}{2\pi}\right)^{1/2} \tag{5.45}$$

Here ε is the dielectric constant, k is Boltzmann's constant, and n_i is the number of ions of one kind per cm^3.

Now the diffuse double-layer capacitance due to cations is given by

$$C_{+,\text{diff}} = \frac{C_{\text{diff}}}{2}\left[1 + \frac{v}{(1 + v^2)^{1/2}}\right] \tag{5.46}$$

and

$$\frac{dC_{+,\text{diff}}}{dE} = \frac{C_{\text{diff}}}{2(1 + v^2)^{1/2}}\left\{[(1 + v^2)^{1/2} + v]\frac{dC_{\text{diff}}}{C_{\text{diff}}\, dE} - \frac{C_{\text{diff}}}{2A(1 + v^2)}\right\} \tag{5.47}$$

In these equations, C_{diff} is the differential capacity given by $d\sigma_d/dE$, where σ_d is the total charge of the diffuse double layer only and E is the whole potential difference across the interface (not the potential across the diffuse layer); $C_{+,\text{diff}}$ is $d\sigma_+/dE$, and is that part of the measured capacity attributable to cations in the diffuse layer alone.

The features of these equations are that they provide means for the calculation of $C_{+,\text{diff}}$ and $dC_{+,\text{diff}}/dE$ from a single differential capacity curve at a

single concentration, under conditions in the system chosen so that there is negligible specific adsorption. The procedure is as follows: the observed differential capacity curve is numerically integrated once with respect to potential to give σ_m, the surface charge density. When specific adsorption is absent, this is identical with σ_d. Hence, one can find $t(=\sigma_d/2A)$ as a function of E. In the absence of specific adsorption, and at sufficiently dilute concentration, C_{diff} is identical with the total double-layer capacity, C. This makes it possible to evaluate σ_d, $C_{+,diff}$, and $dC_{+,diff}/dE$ from Eqs. (5.44)–(5.47) and experimental data from a single capacity curve. $C_{+,diff}$ is wanted for the evaluation of K [Eq. (5.39)], $\sigma_{+,d}$ is wanted for the evaluation of K', and $dC_{+,diff}/dE$ is wanted for comparison with dC_+/dE obtained from an experimental evaluation of $(\partial C/\partial\mu)_{E,-}$ with Eq. (5.37).

At sufficiently negative potentials, the anion adsorption may be assumed to be zero and for solutions of these small cations which may also be assumed not to adsorb specifically at that potential, it is possible to find the values of $C_{+,diff}$ from differential capacity data. A reliable value of $C_{+,diff}$ gives in effect a value of K in Eq. (5.39). Similarly, a value of $\sigma_{+,d}$ at sufficiently cathodic potentials gives a value of K'.

Grahame preferred the evaluation of K and K' from the latter method, i.e., from diffuse layer theory. Since the anions are assumed to be completely repelled from the interface at sufficiently cathodic potentials, the capacity C_1 can be calculated from the diffuse layer theory. Thus, by experimentally measuring $(\partial C/\partial\mu)_{E,-}$, Γ_+ values are evaluated by integration. Similar procedure may be followed to obtain Γ_-.

After determining the relative surface excess Γ_-, one may then derive the specifically adsorbed charge σ_1^- from Eqs. (5.22)–(5.25).

The advantage of the alternative method of Grahame and Soderberg[38] is that one does not have to measure surface tension to find the integration constant. However, one relies to a greater extent than in the other methods on diffuse layer theory. This is acceptable enough because the extra use of the diffuse layer theory here is in reference to dilute solutions, where the diffuse layer theory is relatively free from objections (see Section 7).

5.2. Discussion of the Electrocapillary Thermodynamics

The first equations which were written in this field were those of Gibbs,[40] but the applicability of the Gibbs adsorption theorem to the polarizable electrode–solution interphase remained somewhat enigmatic because of the lack of clarity within the double-layer field of the idea of a polarizable electrode, namely, the one across which the passage of charge is very difficult, and in limiting cases, does not occur. Thus it is difficult to accept the applicability of thermodynamic relations across an interphase which is not at chemical equilibrium.

One of the earlier attempts to solve this difficulty was due to Warburg,[41]

Gibbs,[42] and Frumkin,[43] who gave the concentration polarization theory in which they took the attitude that the potential of the electrode was fixed according to the Nernst equation with respect to the reversibility of mercurous ions. This approach is proved to be incorrect by several methods[44]; in particular, by a direct observation of the change of concentration of electrolyte produced near an electrode surface by flowing a current across it, it was found[45] that even for quite small polarizations the observed concentration change is very much less than that predicted by the theory of concentration polarization.[41-43]

Koenig[46] derived a general equation of electrocapillary, based on the Gibbs theorem, by assuming the existence of a barrier at the electrode surface impermeable to charged particles. Grahame and Whitney[34] showed that the equations developed by Koenig[46] are not peculiar to the type of system he postulated, but may be derived for a polarized electrode at equilibrium with respect to the distribution of its charged components. They[34] argued that the properties of an interface are affected chiefly by the composition of the phases in the immediate neighborhood of the interface and since the polarizable interface readily reaches a steady state only slightly different from an equilibrium state, the observable properties should be those of a system at equilibrium. Parsons and Devanathan[47] essentially accepted the view of Grahame and Whitney[34] concerning the equilibrium state of a polarizable interface. Thus the equilibrium referred to here,[47] that at the polarizable interphase, is termed "an electrostatic equilibrium."

The difficulty of accepting the validity of this approach is that it is the overall cell (Figure 7) which is treated thermodynamically, and it is this which is supposed to be, therefore, in equilibrium. However, it is embarrassing to find that the vital part of the several interfaces which make up the cell, namely, the polarizable mercury–solution interface, is one which is not at equilibrium in any normal sense and hence the actual cell system as a whole does not appear to be in equilibrium.

A positive way out of this difficulty is to regard the mercury–solution interface as being subject to the normal conditions demanded within electrochemical equilibria. This does not pose an immediate contradiction in predicting a Nernstian behavior with respect to the activity of chloride ions in solution, because the unknown (presumably infinitesimally small) activity of the chloride ion in the mercury would vary with the activity of chloride in solution. However, such concepts appear to be far from any reality which could be experimentally determined. The difficulty that we are reviewing here does not imply some total wrongness of electrocapillary thermodynamics, as is indeed verified by the fact that there is a degree of testing of the electrocapillary thermodynamic results by entirely independent methods such as the radiotracer method[10-15], and also, to some extent, the relatively new ellipsometric results.[22-25] However, it does appear that the electrocapillary thermodynamics retains a degree of formality and abstraction which is perhaps still not sufficiently closely connected to hard and clear quantities.

5.3. Direct Methods

5.3.1. Method Based on Change in Adsorbate Concentration in Solution

Measurement of the change in bulk concentration of the adsorbate before and after the adsorbing surface has been placed in the solution provides the value of the amount of adsorbed species on the surface. This requires a very small volume of the solution and low concentration of the solute (10^{-4}–10^{-7} M). The true area of the adsorbent should be as large as possible, with respect to the solution in which the changed concentration is to be observed. Substances with large areas such as various charcoals[48] or fine-mesh wire gauze electrodes Cu, Ni, and Au[18] have been used and the change in concentration in the solution in contact with such electrode is determined, e.g., spectrophotometrically.[18] The change in concentration may also be studied by the radiotracer method, as discussed in Section 5.3.2.

The amount of adsorbed material can also be found by measuring the weight[49,50] of the adsorbent before and after a process of adsorption. This method is possible if the area of the adsorbent is large enough so that the change in weight can be detected.

Both the methods involve large errors due to the calculation of the adsorbed amount as a numerically small difference of two relatively large numbers, and due to experimental errors connected with removal of a film of adhering solution from the adsorbent.

5.3.2. Radioactive-Tracer Method

Methods of radioactive tracers may also be used to measure specific adsorption of ions, particularly, on solid metals, by determining the increase in the count rate of the labeled adsorbate upon contact with the adsorbent. There are three ways in which the radio tracers are used to investigate specific adsorption.

5.3.2.1. Method Based on the Change in Adsorbate Concentration in Solution

In this method, the radioactivity (pulse/min) I_0, of some solution of a fixed volume, V, containing labeled adsorbate is first measured. Then a metal sample of surface area, A_0, is placed in the solution and kept there under given conditions, whereupon the radioactivity I of the same solution is determined and the surface excess of the ions is obtained from[51,52]

$$\Gamma_i = \frac{(I_0 - I_1)cV}{A_0 I_0} \tag{5.48}$$

The quantity $(I_0 - I)/I_0$ characterizes the relative change in the adsorbate concentration.

Surface excesses, obtained this way, may be utilized to obtain specific adsorption with the help of diffuse layer theory, as described in the last section.

This method was used for the investigation of the adsorption of SO_4^- ions[10] and Br^- on platinized platinum[53] as well as I^- on lead[54] and on iron.[55]

5.3.2.2. *Radiotracer Measurement of a Sample Removed from Solution*

The metal sample on which adsorption is to be measured, is placed in a solution containing labeled adsorbate under given conditions and then removed from it to measure radioactivity. When the metal has been removed from the solution, it contains adsorbate in the adsorbed state and in the wetting layer of the solution. Due to the presence of adsorbate in the wetting layer, this measurement becomes uncertain, even though the wetting layer is sometimes removed by washing it off with liquids.[52] When the sample is washed in a solution of same composition as that used for adsorption but without labeled adsorbate, at a constant potential, an uncertainty is introduced in the measured amount of adsorption due to the possibility of an exchange between the adsorbed particles and those of the washing solution. In spite of the difficulties, mentioned above, this method has been used to measure the adsorption of SO_4^{2-} on iron[56,57] and to investigate the potential dependence of ionic adsorption on Pt[58,59] as well as on semiconductors.[60–62]

All these methods of measuring adsorption by radioactive tracer method by removing the sample from solution, have a common drawback which is the interruption of the adsorption process.

5.3.2.3. *Radiotracer Measurement of a Metal Immersed in Solution*

In this method, first employed by F. Joliot Curie[64] to study the electrodeposition of radioelements, an increased radioactivity at the metal–electrolyte interface due to the adsorption of labeled substance is detected without removing the metal sample from solution, i.e., without interrupting the adsorption process. A cell had the metal sample forming one of its sides and the radiation counter was located in close proximity to the metal.

The principle of this method was used by Blomgren and Bockris,[15] and by Schwabe and co-workers,[65,66] in measurements of organic and inorganic materials on platinum; by Kafalos and Gatos,[70] and by Green and co-workers[67–69] for the measurement of organic adsorption on electrodes. The radioacitivity of the adsorbed substance is obtained from the difference between the measured value of the radioactivity of the metal with the adsorbed layer and that of the solution measured independently.

Blomgren and Bockris[15] used a method similar to one suggested independently and in principle by Aniansson.[71] A mica foil is used to make the window of a gas proportional counter and a thin layer of a metal is deposited on

the external side of this mica foil. The counter is mounted above the surface of the solution containing the labeled adsorbate so that the metal film and the surface of the film are parallel to one another. The count rate is determined as a function of distance by decreasing the distance between the metal film and solution. When the solution comes into contact with the metal film, the count rate increases by an amount corresponding to the formation of the adsorbed layer.

The absolute values of the amount adsorbed are obtained from the general expression of the count rate, I_s, from the solution[67]

$$I_s = 3.7 \times 10^{10} \alpha c A \bar{K} \int_0^\infty \exp(-\mu_f x)\, dx \tag{5.49}$$

and the count rate for the adsorbed material,

$$I_a = 3.7 \times 10^{10} \Gamma_m \alpha \theta A \bar{K} R \tag{5.50}$$

where α is the specific radioactivity and c, A, $\bar{K}$, μ_f, and x are the concentration of the adsorbate, area of the adsorbent, counting efficiency of the apparatus, radiation adsorption coefficient of the solution, and the distance measured normal from the electrode surface into the solution, respectively. Γ_m, θ, and R are the maximum amount adsorbed, which corresponds to a monolayer, fractional coverage of the adsorbed material, and the roughness factor of the surface, respectively. From Eqs. (5.49) and (5.50),

$$I_a = I_s \Gamma_m \theta R \mu_f c^{-1} \tag{5.51}$$

Thus, with a known value of Γ_m, R, and μ_f, one may obtain I_a corresponding to a monolayer coverage and θ may be found corresponding to any I_a.

The method devised by Blomgren and Bockris[15] has been used in a series of later works by Bockris' school[80,81] and by Gileadi.[82]†

Kafalos and Gatos[70] suggested a technique in which a thin layer of solution is allowed to flow near the metal surface and isotopes with hard β and γ radiation may be used for measuring adsorption. This technique was used to study adsorption of I^- on germanium[72] and platinum[73] as well as of phosphate ions on zirconium.[74]

Kazarinov[75,76] suggested another technique in which the electrode is made in the form of a thick disk and after the labeled adsorbate has been adsorbed on the surface, the electrode is lowered to the bottom of the cell for measuring radioactivity by means of a counter placed near the bottom. The bottom of the cell is usually made from thin glass, mica, polyethylene, or some other material. This method has been also applied recently by Kazarinov *et al.*[77] and Wieckowski *et al.*,[78] mainly for the measurement of organic adsorption, but this method may be employed for measuring ionic adsorption

† Swinkels, Green, and Bockris[63] devised another version of the present method in which a band-shaped electrode is rotated over pulleys through the solution and emerges with the solution layer intact to pass under a counter.

cases.[75,79] The determination of the absolute values of the amounts of adsorbed ions is performed in the same way as in the techniques described earlier.

Some of the results on the amount of specifically adsorbed ions measured by radiotracer methods are discussed and compared with those obtained by the electrocapillary method, in Section 6.

5.3.3. Ellipsometric Method

Ellipsometry,[22–25,83,93,94] an experimental technique involving the analysis of the phase change (Δ) and the change in amplitude ratio ($\tan\psi$) of polarized light reflected from a surface, which has often been used in the study of very thin films, has also been applied first by Chiu and Genshaw[22] to the determination of the adsorption from solution of ions at an electrode surface.

When plane-polarized light is reflected from a film-covered metal surface, the two components of the light, perpendicular and parallel to the plane of incidence, are reflected with different amplitude reductions and phases. The ratio of the complex reflection coefficients of the parallel ($R_\parallel$) and perpendicular ($R_\perp$) components of light defines the relative amplitude reduction $\tan\psi$ and the relative phase retardation Δ as

$$\tan\psi\, e^{i\Delta} = \frac{R_\parallel}{R_\perp} \tag{5.52}$$

ψ and Δ are the experimentally measured quantities.

This ratio is related to the refractive index, n_1, of the electrolyte solution, the complex refractive indices of the adsorbed layer (which may be less than, or more than, a monolayer), and the substrate metal, respectively, $\hat{n}_2$ and $\hat{n}_3$, the thickness of the film, τ, wavelength λ, and angle of incidence, ϕ.

$$\tan\psi\, e^{i\Delta} = f(n_1, \hat{n}_2, \hat{n}_3, \lambda, \tau, \phi) \tag{5.53}$$

The functional form of f can be found, e.g., in McCrakin and Colson[84] or Heavens.[85] In the case of a dielectric film (of which refractive index is real) covering the metal surface (as in the case of ionic adsorption), by computing ψ and Δ from Eqs. (5.52) and (5.53) using a different set of film parameters, n_2 and τ, it is possible to correlate n_2 and τ with the experimentally observed ψ and Δ.

In order to analyze the experimental data, a model must be made of the layer of the adsorbed ions. Chiu and Genshaw[22,23] assumed that a layer of ions and water molecule of a thickness equal to the length of the ion is always present at the surface. The refractive index of this layer is assumed to be a linear combination of the refractive index of the ion and water,

$$n_{\text{film}} = n_{H_2O}(1 - \theta) + n_{\text{ion}}\theta \tag{5.54}$$

where $n_{H_2O} = 1.33$ and θ is the surface coverage of the ions.

The refractive index is calculated from the Lorentz–Lorenz equation[86]

$$R = V_m \frac{n^2 - 1}{n^2 + 2} \tag{5.55}$$

where R is the molar refractivity, V_m is the molar volume, and n is the refractive index.

The Δ and ψ values were calculated for different refractive indices of the film by using the exact ellipsometric equation, and from the experimental values of the change in Δ, the θ values are directly obtained.

The experimental θ was compared with Kovac's[87] result in Figure 19 for the thiocyanate ion on mercury, as shown in the next section. Agreement is good within experimental error (up to 20%). Satisfactory agreement is also obtained[22] when the θ values obtained by ellipsometry for bromide ion were compared with those obtained by electrocapillary measurement made by Lawrance *et al.*[88] (Figure 20). Adsorption of halides and SO_4^{2-} was also measured by Chui and Genshaw ellipsometrically.[23] Paik, Genshaw, and Bockris[25] argued that instead of the linear combination of refractive indices, a more realistic model would be one based on the assumption of the additivity of molecular polarizabilities. Meyer *et al.*[89 92] used

$$\frac{n^2 - 1}{n^2 + 2} = \frac{4}{3}\frac{\pi\alpha}{V} \tag{5.56}$$

or

$$n^2 - 1 = \frac{4\pi\alpha}{V} \tag{5.57}$$

for the case of adsorption from a gaseous phase. Here, α is the polarizability of the adsorbate molecule and V is the average volume taken by each molecule in the layer.

The assumption of additivity of molecular polarizability for mixtures led Paik, Genshaw, and Bockris[25] to the relation

$$\frac{n_2^2 - 1}{n_2^2 + 2} = N_i R_i + N_w R_w \tag{5.58}$$

where N_i and N_w are the average number of moles of ions and solvent, respectively, in a unit volume of the adsorbed layer whose thickness τ, is determined by the molecular (or ionic) dimension,.

If the fraction of surface covered by ions is denoted by θ,

$$N_i = \theta N_i' \quad \text{and} \quad N_w = (1 - \theta)N_w' \tag{5.59}$$

where N_i' and N_w' are the N_i and N_w values for $\theta = 1$ and $\theta = 0$, respectively. If S_i is the covered area of the electrode per ion, N_0 is the Avogadro number,

V_w is the molar volume of water, and τ_i is the thickness of the adsorbed layer, one has

$$N_i' = \frac{1}{S_i \tau_i N_0} \text{ (mol cm}^{-3}\text{)} \tag{5.60}$$

$$N_w' = \frac{1}{V_w} \text{ (mol cm}^{-3}\text{)} \tag{5.61}$$

Then,

$$\frac{\theta R_i}{W_i \tau_i N_0} + (1 - \theta)\frac{R_w}{V_w} = \frac{n_2^2 - 1}{n_2^2 + 2} \tag{5.62}$$

Now,

$$\theta = \sigma_a / \sigma_{a,max} \tag{5.63}$$

where σ_a is the adsorbed charge and $\sigma_{a,max}$ is the value of σ_a at full coverage, which can be equated to e/S_i, e being the electronic charge, and S_i is the area occupied by one ion. Equations (5.62) and (5.63) enable one to obtain σ_a.

In deriving Eq. (5.62) a model is used in which all the adsorbed ions are assumed to be in a layer of thickness τ_i, which is the layer in which the specific adsorption occurs, but any surface excess of ions, regardless of its degree of separation from the metal, will contribute to the overall effect on the reflected light. A suitable optical model for the entire double layer would be an inhomogeneous film in which the index of refraction varies in the direction perpendicular to the direction of the film. McCrakin *et al.*[84,93] showed that for such an inhomogeneous film the ellipsometer readings are directly related to the integral $\int \Delta n \, d\tau$, where Δn is the difference between the refractive index of a layer of thickness $d\tau$ and the refractive index of the surrounding medium. Since Δn is proportional to the excess concentration of the adsorbed ions, Δc, the above integral is proportionalto the integral $\int \Delta c \, d\tau$, which is the total amount of surface excess per unit area of the surface. Therefore, σ_a calculated from the ellipsometer readings as outlined in the above equations (5.52), (5.53), and (5.62), is approximately the total amount of the adsorbed anions. Thus

$$\sigma_a = \sigma_1 + \sigma_d$$

where σ_1 is the specifically adsorbed charge and σ_d is the amount of that in the diffuse layer. Some of the results obtained by Paik, Genshaw, and Bockris[25] are shown in Figure 9.

An advantage of the method is that it easily gives total adsorption for solids. A disadvantage lies in the practicality of making calculations of σ_d. Thus no analog of the procedure with the electrocapillary thermodynamics is possible, i.e., there is no way to obtain the potential across the diffuse layer (unambiguously). However, in concentrated solutions (> 1 M, say), the value is generally a

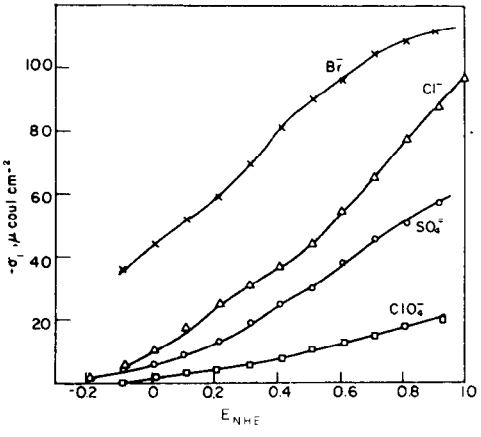


Figure 9. Specific adsorption of anions from 10^{-2} *M* solutions on gold electrode.[25]

few millivolts, and, e.g., the error arising from an uncertainty of ± 3 mV is only a few tenths of a microcoulomb.

The principal limitations of ellipsometric method is that it can only be applied to ions which have refractive indices significantly different from that of the solution. The theory of ellipsometry is based upon the reflection from an ideally smooth surface of a substrate and hence when the surface attains a roughness, as is often inevitable in a practical method of surface preparation and by deterioration of the surface during experiments, the conclusions deduced from the optical measurements are expected to include error due to the non-ideality of the surface topography. Theories of roughness effect on optical properties have been discussed by Bockris *et al.*[127,128] Sato and Kudo[129] made an empirical correction in the measurement on passive film by subtracting the difference between the optical parameters obtained from the initial surface and the surface that was reduced after the passivation experiment.

5.4. Method Based on Measurement of Surface Tension at Solid Metals

The electrocapillary thermodynamics has been extensively applied to liquid-metal–electrolyte interfaces, but the corresponding studies on solid-metal–electrolyte interface are lacking mainly because to measure the surface tension of a solid is difficult and thus capacitance measurement has got the advantage of being applicable for the determination of specific adsorption at the solid–solution interface, though the problem of the determination of integration constants still remains.

However, measurements of surface tension of solid metals have been attempted by Frumkin *et al.*[121,122] by a method based on contact angle measurement. The measurement of the contact angle, θ', between a gas bubble and the

metal surface immersed in an electrolyte gives the change of interfacial tensions $\gamma_{\text{solid-gas}}$, $\gamma_{\text{solid-liquid}}$, and $\gamma_{\text{liquid-gas}}$ through Eq. (6.1). Frumkin *et al.* earlier suggested that it is only the $\gamma_{\text{solid-liquid}}$ which is potential dependent. However, later Tverdovskii and Frumkin[122] found that θ' remained constant with the potential when measurements were made in ethanolic solution. This type of behavior was explained on the assumption that not only $\gamma_{\text{solid-liquid}}$ is a function of potential, but also $\gamma_{\text{solid-gas}}$ varies in the same way with potential, due to the presence of a film of moisture, thus giving rise to a constant value of θ'. This method has been applied for solid metals such as Cu, Ni, Ag.[121] However, this method was not as accurate as the electrocapillary one; the results were not reproducible.

Beck[123] devised a ribbon extension method to measure differential surface tension. While the differential surface tension can be related only to the differential surface excess,

$$\frac{1}{2RT}\left(\frac{\partial\,\Delta\gamma}{\partial \ln a_{\pm}}\right)_{E_+,T,P} = \Delta\Gamma_- \tag{5.64}$$

useful information may still be obtained by careful selection of reference states.

Fredlein, Damjanovic, and Bockris[21] developed a technique for determining the change of surface tension as a function of potential at solid–solution interfaces. A change of potential produces a change of interfacial tension, $\Delta\gamma$, and the electrode bends. The radius of curvature, R, for small bending is given by[124]

$$R = LI/M \tag{5.65}$$

where

$$I = \delta^3 d/12 \tag{5.66}$$

and L is the Young's modulus, d is the width of the electrode, δ its thickness, and M is the bending moment given by

$$M = \delta\,\Delta\gamma\,d/2 \tag{5.67}$$

Consequently, the angular deflection, ϕ, at the end of an electrode of length l is

$$\phi = \Delta\gamma 6l/L\,\delta^2 \tag{5.68}$$

Measurement of the angular deflection gives the value of the differential surface tension (Figure 10).

In Figure 10 the differential surface tension is plotted from an arbitrary zero. This technique does not yet give pzc values to better than ± 0.1 V. However, it seems to offer a significant advance towards the goal of measuring differential surface tension at the solid–solution interfaces, and with the application of electrocapillary thermodynamics one might perhaps obtain information on individual ion adsorption.†

† The validity of this argument no doubt depends upon the degree of reversibility of the measurement conditions. It would be of interest to study a comparison of the bending electrode method with that of Gokstein, discussed in Chapter 1.

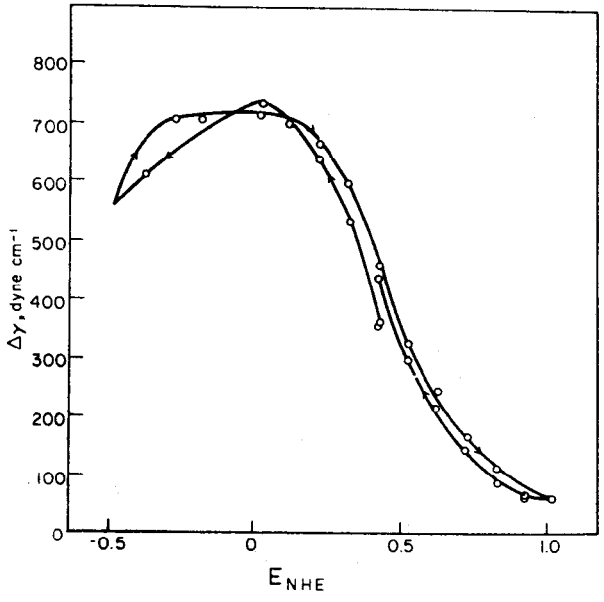


Figure 10. Change of interfacial tension ($\Delta\gamma$) with potential for a gold electrode in 0.100 *M* KCl solution.[21]

6. Comparison of Different Methods for the Measurement of Specific Adsorption

6.1. A Comparison of the Electrocapillary and Capacitance Integration Methods to Obtain Surface Tension

6.1.1. Introduction

Until the mid-1960s the capacitance approach, whereby double integration of the capacitance curve gives rise to the surface tension, and the electrocapillary approach, where the surface tension is measured directly, were regarded as having the same degree of validity, although the capacitance method needed an integration constant, γ_{max}, which implies that at least one measurement of surface tension is required to use the capacitance approach.

However, during the last decade a number of doubts have been thrown upon each method, and in this section the situations pertaining to this topic are presented.

Earlier work was published by Grahame and Parsons,[95] who compared the results of electrocapillary and capacitance measurements as a function of concentrations (Figure 11), but they restricted the comparison to the potential of zero charge. They concluded that the discrepancies will arise in concentrated

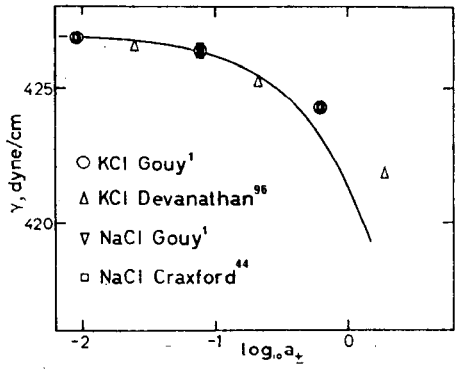


Figure 11. Interfacial tension, γ, as a function of log $a_{\pm}$ from direct measurements and by integration (curve).[95]

solutions, the surface excesses obtained from differential capacity measurements (with the use of diffuse layer theory) being too large owing to a shift in reference plane from the Gibbs surface where the surface excess of water is zero, to the outer Helmholtz plane (OHP). Frumkin, Ivanova, and Damaskin[97] supported in essence this view and concluded that Grahame's method becomes inapplicable in concentrated solutions, because the plane where Γ_{H_2O} is zero is charge dependent. Devanathan and Canagaratna[98] attributed the discrepancies between capacitance and electrocapillary methods to the insufficient accuracy of the capacitance-concentration dependence. Frumkin *et al.*[99,100] and Devanathan

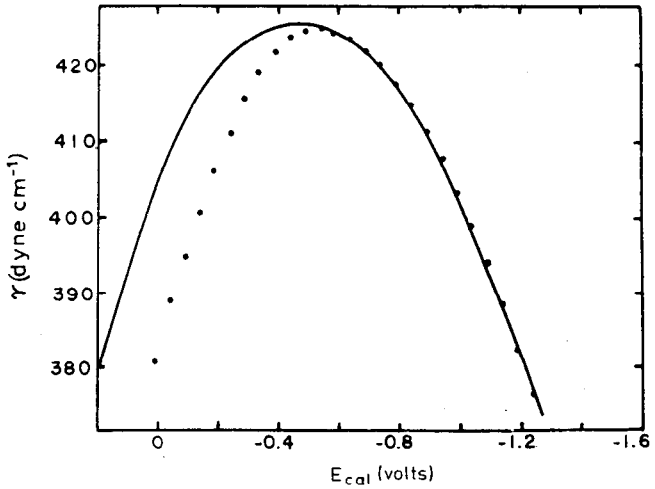


Figure 12. Comparison of electrocapillary curve obtained by integration of the capacity (solid line) with direct electrocapillary measurements (data points) for 0.01 *M* NaF[88] (1 dyne = 10^{-5} *N*).

and Peries[96] did not observe any significant discrepancy in their comparison between the results of the two approaches.

The two methods were tested in the same laboratory by Parsons and Zobel,[101] who studied Na_2HPO_4 solutions (cf. also Parry and Parsons[102]) and found that values of interfacial tensions measured directly are lower than those obtained from capacity data at positive potentials (anodic branch). The discrepancy was attributed by these workers to the existence of a finite contact angle. Lawrance, Parsons, and Payne[88] observed a similar discrepancy (Figure 12) in 0.01 *M* NaF solutions and also attributed this to the occurrence of a finite contact angle.

6.1.2. *Work of Bockris, Müller, Wroblowa, and Kovac*[103]

By far the most comprehensive study made of the comparison between the results obtained from the electrocapillary and by integration of capacitance curves was that of Bockris, Müller, Wroblowa, and Kovac[103] (BMWK). The measurements consisted of a comparison of the results for KCl systems at 2.94 *N*, 1.0 *N*, 0.3 *N*, 0.1 *N*, 0.03 *N*, and 0.01 *N*.

The capacitance was measured at the dropping mercury electrode with a transformer ratio arm bridge, Wayne–Kerr B221, using a sine-wave signal. The interfacial tension, γ, of the mercury solution was measured with a capillary electrometer. The mercury was in a capillary of internal radius 0.01 mm, the meniscus being observed with a microscopic magnification of 25 × through an optically flat window in the cell. It was brought to rest at 0.1 mm from the tip by means of nitrogen pressure control and the heights were read with 0.01 mm accuracy. Sticking of the mercury to the capillary as well as in the limbs of the manometer was avoided by connecting to the open side of the manometer a rubber ball with which the mercury was made to vibrate around its equilibrium position before coming to rest. A few drops of mercury were always expelled from the capillary before a new value of γ was measured.

It must be stressed that the BMWK work was carried out in the same laboratory, by the same workers, who interchanged method and equipment from time to time and with the same solution preparation.

The principal result of the BMWK measurements, and the more important of the two kinds of result, was that for nearly all ranges of measurement, the degree of agreement with respect to the surface tension measured directly and obtained through integration of the capacitance, was *excellent*, namely, ± 0.2 erg cm^{-2} except at extremely cathodic and anodic potentials, whereupon it was 0.8 erg cm^{-2}. Where the concentration of the electrolytes overlapped, these data agreed within these limits with the data of Devanathan.[101]

However, in 0.03 *N* and 0.01 *N* solutions of HCl, a discrepancy arose so long as the data were plotted against potential. The discrepancy is shown in Figure 13. As seen on the anodic side, it maximizes at about 1.8 dynes, but on the cathodic side it goes up to 4 dynes.

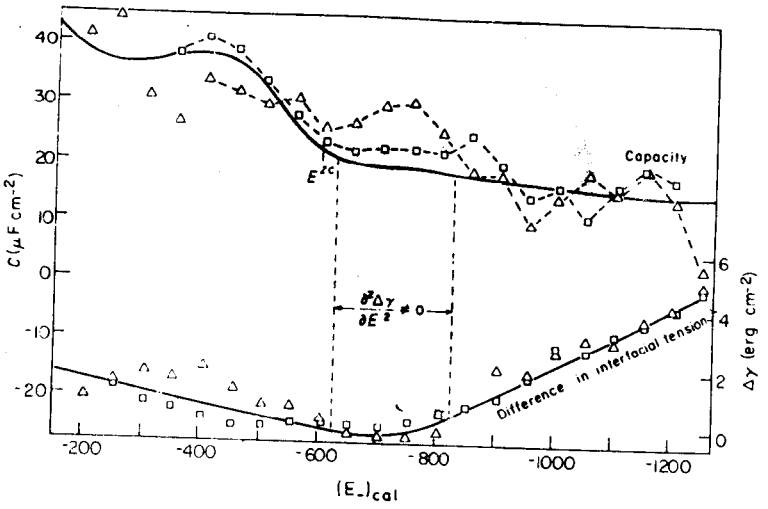


Figure 13. Discrepancies in the system Hg/0.03 *N* HCl aq. Upper part: (——), capacity measured by BMWK[103]; – – –, capacity calculated from interfacial tension. Lower part: difference between interfacial tension values obtained by double integration from capacity data and those measured directly. □, BMWK[103]; △, Devanathan.[104]

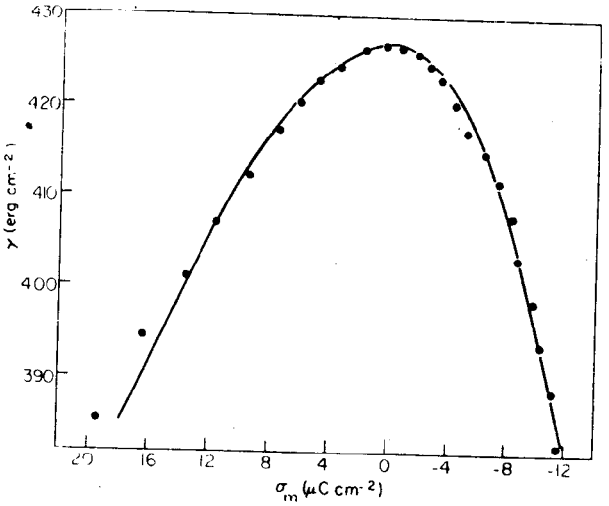


Figure 14. Interfacial tension of the system Hg/0.01 *N* HCl as a function of the charge density. ——, Calculated from capacity data by double integration; ●, measured (Devanathan[104]).

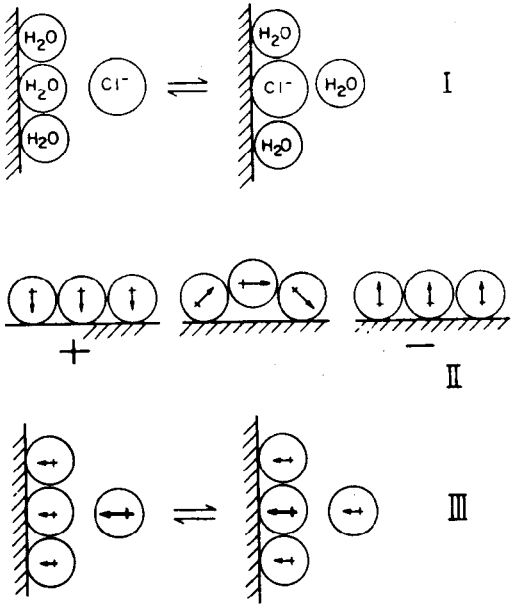


Figure 15. Mechanisms for ac effects.

A very significant matter, however, concerns what happens when the results are replotted as a function of charge, and in Figure 14 the interfacial tension of the system 0.01 *N* HCl is given both from electrocapillary measurements as also be double integration of capacitance. It is clear that *now there is no discrepancy.*

Bockris *et al.*[103] put forward the following three ac mechanisms (Figure 15) for the discrepancies occurring at low concentration:

(a) Ions change their positions from the diffuse layer to the compact layer: mechanism I.
(b) Dipoles reorient and unsaturate: mechanism II.
(c) Oriented dipoles are replaced by adsorbing ions: mechanism III.

According to mechanism I, an additional capacity would be introduced (not contained in $-\partial^2\gamma/\partial E^2$) under conditions when $\partial^2\sigma_1/\partial\sigma_m{}^2 \neq 0$ (σ_1 denotes ions in contact with the electrode or specifically adsorbed). This condition is satisfied in the region where contact adsorption begins. There, $\partial^2\sigma_1/\partial\sigma_m{}^2 < 0$; in other regions $\partial^2\sigma_1/\partial\sigma_m{}^2 \simeq 0$ and the ac field would not be expected to have any effect on capacitance. These predictions are found to be consistent with the phenomena in 0.03- and 0.01 *N* HCl.[103]

No effect is expected to be observed, however, in concentrated solutions

since then the potential differences across the compact and diffuse layer are no longer comparable, as in dilute solutions. But this is necessary if effects of a redistribution are to be observed besides the net changes in surface excess occurring in the dc case as well as the ac case.

The analogy to Faradaic rectification has been suggested for this mechanism. The presence of ac signal leads to the recording of a lower capacity; upon integration, the effect is the same as that of a shift in the (dc) potential of zero charge, and indeed a shift is different for different parts of σ_m–E and γ–E relationship.

Mechanism II is of a different nature but is related to the diffuseness of the double layer. When the double layer is most diffuse, and σ_m and σ_1 are very small, the contribution of the surface potential of solution g_s (dipole) to the potential drop will be relatively great. The water dipoles have a preferential orientation with their negative ends to the metal surface.[105,256-260] Under the conditions of the ac field, there is a net effect such that reorientation is larger and the ionic character is smaller (and hence the measured capacity is smaller) than the corresponding changes under dc conditions. The effect will be largest under two conditions: diffuseness of the double layer and in the vicinity of the turning point of water, i.e., at a potential where the water molecules have maximum entropy.[105] This mechanism does not seem to be applicable to the present results.

According to mechanism III, oriented water dipoles are replaced by adsorbing ions or by other dipoles. Consequently, there will be an effect upon the measured capacity proportional to $\partial^2\sigma_1/\partial\sigma_m^2$ (ions) or $\partial^2\Gamma/\partial\sigma_m^2$ (dipoles), and also proportional to the net orientation of water. The latter increases at extremes of polarization. In agreement with this, the discrepancies are greater at the more negative and more positive branches.

The discrepancies in surface tension obtained by the two methods disappear when surface tensions obtained by each method are potted against electrode charge, σ_m (Figure 14). The use of σ_m as the electric variable is equivalent to maintaining a constant electric field in the double layer during measurement. Thus, in considering potential as the variable, we take into account not only the effect of the σ_m upon the electrode potential, but also the contributions of the water dipoles. When the ac measuring field is upon the electrode, there is the variation in the capacitance already indicated. However, if one plots against the charge on the surface, this charge is not affected by the variation in dipole position, or other aspects of the causes of the deviations.

Looking back to the three causes given above for the discrepancies between ac and dc mechanisms, we see all the processes will be affected by change of potential due to the change in orientation (and hence of potential) of dipoles on the surface, so that if potential is used as a variable, small extra components of capacitance at low concentrations may be introduced.

Thus, for example, the change of the ionic positions from the diffuse layer to the compact layer does not affect the total charge on the electrode, but it does affect the potential.

Correspondingly, when oriented dipoles are replaced by adsorbing ions there is an effect on the potential at the surface but not on the total charge.

Thus any effective comparison should be made by plotting γ against electrode charge.

Mechanism I is not expected to cause any effect at higher concentration since the PD across the diffuse layer, ϕ_{2-b}, and that across the compact layer are no longer comparable, as in dilute solutions.

6.1.3. Work of Payne[106]

Payne criticized the work of BMWK,[103] on the basis that he disagreed with the values of the potential of zero charge published by BMWK.[103] His criticism was indirect in the sense that he compared the value for LiCl, RbCl, and CsCl, published by Wroblowa, Kovac, and Bockris,[4] with the values obtained by Grahame and Parsons[95] for KCl. The discrepancies implied are in a concentration range outside that in which the discrepancy between the capacitance and the surface tension measurements in highly comparable systems was reported by BMWK.[103] Bockris *et al.*[107] showed that the errors possible with the setup used in their comparison are about ten times less than the implied discrepancies discussed by Payne. Deviations between surface tension values obtained from integrated capacitance and those of direct measurements are systematic (Figure 16). Were the origin of such discrepancies the sticking of the meniscus, as suggested by Payne, they would be sporadic. There is no sticking

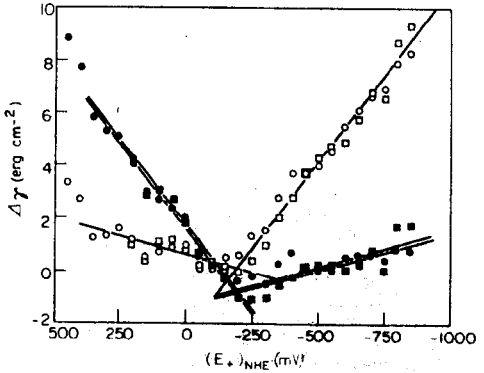


Figure 16. Effect of the choice of the potential of zero charge upon discrepancies in the system Hg/0.01 *N* HCl. ○, □, $E^{+}_{\sigma_m=0} = -133$ mV ($E^{-}_{\sigma_m=0} = -642$ mV); ●, ■, $E^{+}_{\sigma_m=0} = 83$ mV ($E_{\sigma_m=0} = -592$ mV). Circles, Devanathan's values[104]; squares, values of Bockris *et al.*[103] as compared to values calculated by integration of the measured differential capacities, using either of $E_{\sigma_m=0}$ given. The difference in slopes between the times on the anodic and cathodic side is equivalent in either case to 1.6 μC cm^{-2} or a discrepancy of $\Delta C = -10$ μF cm^{-2} over a region of 160 mV near $E_{\sigma_m=0}$.

even in the more dilute solutions of HCl and KCl. The degree of error in the potential of zero charge likely does not account for the deviations observed in the work of BMWK.

6.1.4. The Work of Lawrance, Parsons, and Payne[88]

Lawrance *et al.*[88] measured the capacity of the double layer at a mercury electrode in contact with aqueous KBr solutions and derived the surface tension. These data, together with those of other halides, are compared with surface tension values obtained by electrocapillary measurements of Devanathan and Peries,[96] Grahame,[108] Grahame and Parsons.[95] Under most conditions, they found no discrepancy, in agreement with BMWK.[103] However, they observed discrepancy for 0.01 *M* NaF solution (Figure 12), on the anodic side. Lawrance *et al.*[88] inferred that a discrepancy in dilute NaF solution is possibly due to occurrence of a finite contact angle. The results obtained by Lawrance *et al.*, using the drop time method, were not reproducible, and the existence of contact angle as a possible source of discrepancy of two methods to obtain γ, as inferred from the work of Lawrance *et al.*,[88] is ambiguous.

6.1.5. Work of Schiffrin[109]

Schiffrin[109] measured the surface tension of Hg as a function of potential by using a maximum bubble pressure method, which is independent of contact angle. For 0.01 *N* KF and 0.1 *N* KF solution, he[109] obtained agreement between the doubly integrated capacitance results and those measured directly. However, for 0.1 *N* and 0.01 *N* KCl solution, Schiffrin[109] showed agreement when the doubly integrated capacitance curves of Grahame[110] are compared with γ obtained by maximum bubble pressure method. On the other hand, when the electrocapillary results from the work of BMWK are compared with the doubly integrated cpacitance values, a discrepancy of about 2 dynes cm^{-1} is observed on the *anodic* branch but there is no discrepancy on the cathodic branch. BMWK, however, obtained a larger discrepancy on the *cathodic* side, between the γ values obtained from the two different approaches. Therefore, the comparison of Schiffrin, using BMWK[103] results, is not consistent with the original work of BMWK.[103] To get an effective comparison, it is desirable to have the capacitance results from direct surface tension measurements compared with those calculated from capacitance, and done under the same condition in the same laboratory by the same people. But this has only been done by BMWK.

6.1.6. Work of Lawrance and Mohilner[111]

Lawrance and Mohilner[111] used the capacitance data from Grahame[112] to derive the surface tension of Hg and compared this with the values measured directly by maximum bubble pressure method for NaF and NaCl solutions and

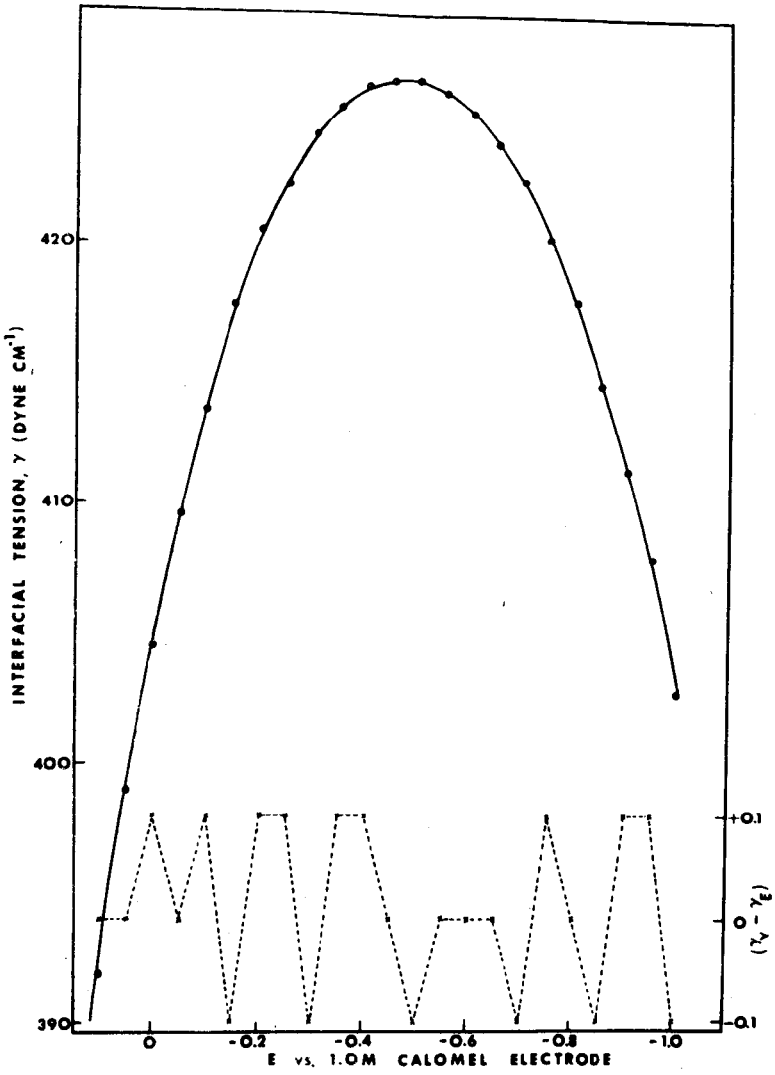


Figure 17. Electrocapillary curve[111] for 0.01 *M* aq. NaF at 25°C. Solid curve is doubly integrated differential capacitance. Points are determined by the maximum bubble pressure method both visually and by electronic birth detection. Lower points connected by dotted lines indicate difference ($\gamma_V - \gamma_E$) between visual and electronic detection. Scale for these differences is on lower right of figure.

found good agreement (Figure 17). Lawrance *et al.*[111] superimposed a 10 KHz ac potential on the dc potential of the working electrode and found no effect, and inferred that the ac mechanism suggested by BMWK[103] is not the cause of the discrepancy. However, their ac was in the top range of the frequencies of that generally used, nearly 10 kHz, whereas the measurements of BMWK[103] were in the region of 1.5 kHz, so a relevant comparison was not made.

6.1.7. *Work of Trasatti*[113]

Lastly, Trasatti[113] discussed the discrepancy between the doubly integrated capacitance data and those measured by the electrocapillary method, in terms of adhesion between glass and mercury due to double-layer interaction, and supported the view that contact angle variation is responsible for the discrepancy. Trasatti[113] mainly discussed the situation with NaF and showed that larger discrepancy is observable in fluoride but much smaller with chloride (Figure 18). It is of course well known that NaF attacks glass[114] so that the constant stress in Trasatti's[113] work upon what great effects are observed is hardly germane to the much lesser effects observed with Cl^- ions.

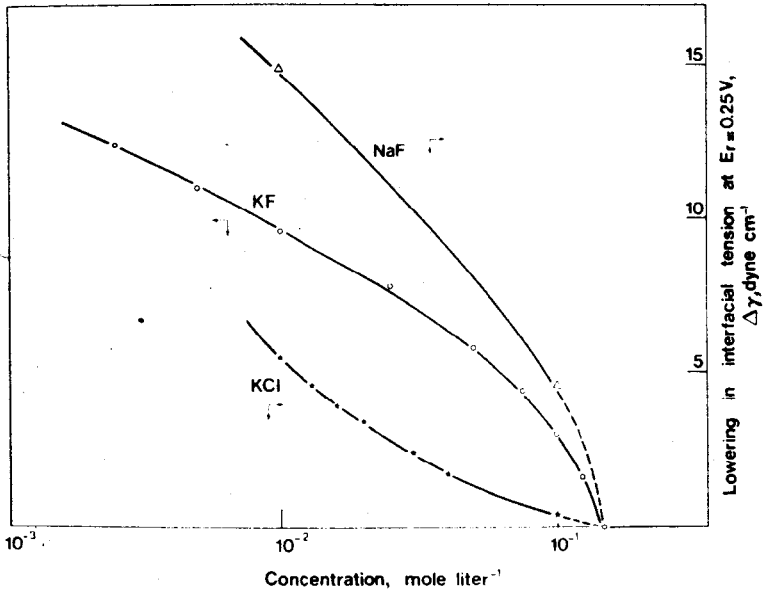


Figure 18. $\Delta\gamma$, the difference at the rational potential of 0.25 V between the interfacial tension measured with capillary electrometer and that obtained by double integration of corresponding capacity curves, plotted as a function of electrolyte concentration.[113]

6.1.8. Conclusion

Thus, concerning the discrepancy between the surface tension values obtained from doubly integrated capacitance curves and those measured by electrocapillary methods, there are two views:

(a) The view of BMWK[103] that there is a small intrinsic difference between ac measurements and electrocapillary measurements. The effect would occur only at low concentrations: the major result is that there is agreement between the two methods above 0.03 M.

(b) The alternative explanation is to hypothesize a contact angle greater than zero, but then only in dilute solutions.

To verify the view on contact angle, what is needed, then, is a study of contact angle at the mercury–solution interface. There are several methods[115,116] for the measurement of contact angle. However, in the electrocapillary situation, the measurement of contact angle is made by Bockris and Cahan,[117] who found that for the Pt-solution interface, the finite contact angle is between 1° and 3°.

According to Young[118] and Dupré,[119]

$$\cos\theta = \frac{\gamma_{\text{solid-gas}} - \gamma_{\text{solid-liquid}}}{\gamma_{\text{liquid-gas}}} \qquad (6.1)$$

If the discrepancy between the doubly integrated capacitance results and those obtained by electrocapillary method is, say, 4 dynes cm^{-1}; then from Eq. (6.1), $1-\cos\theta = \Delta\gamma/\gamma_{\text{Hg-gas}} = 4/484$, where 484 is the surface tension of the Hg–vapor interface,[120] and this gives $\theta = 8°$, which is a very large value. If $\Delta\gamma = 10$ dyne cm^{-1}, as reported in some cases,[101] then $\theta = 12°$, which is not expected for Hg. Therefore, to establish the view on contact angle as a major factor for the discrepancy, one should precisely measure the contact angle to see if it corresponds to the high value as required to explain the discrepancy. Moreover, the discrepancy disappears at higher concentrations, and if finite contact angle is the cause then one would have to explain why the contact angle is reduced to zero at higher concentrations.

The crucial experiment is a plot of the $\Delta\gamma$ against charge: clearly there would be no effect on the discrepancy were this due to contact angle changes. However, a significant effect is observed. Studies in the same solutions, in the same laboratory, with the same apparatus and degree of purification seem necessary. In the mean time, it is advisable to use methods which are independent of contact angle and to plot the results of any surface tension differences between ac and direct methods against σ_m. It is interesting to observe that results obtained in concentrations above 0.03 *M* are not in doubt.

6.2. Comparison of Results Obtained by Electrocapillary, Ellipsometry, and Radiotracer Methods

The surface coverages of ions on mercury measured by ellipsometry (Chiu and Genshaw[22]) and by the electrocapillary method (Kovac[87] and Lawrance

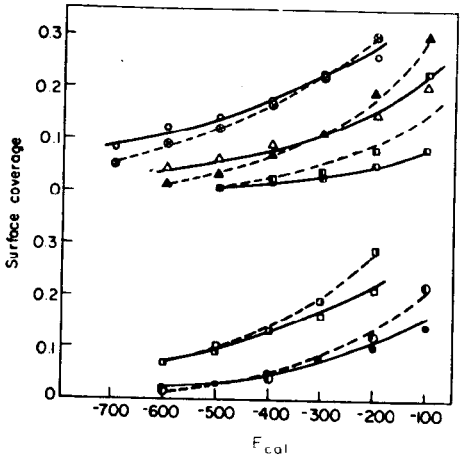


Figure 19. Comparison of surface coverage obtained by ellipsometry[22] and electrocapillary[87] methods for sodium thiocyanate solutions: – – –, ellipsometry; ——, electrocapillary; ○, ⊗, 1 *M*; ◐, ●, 0.03 *M*; □, ◨, 0.3 *M*; □, ◧, 0.01 *M*; △, ▲, 0.1 *M*.

et al.[88]) are compared in Figures 19 and 20. The values originally given by Kovac[87] and Lawrance *et al.*[88] are expressed in $\mu C\,cm^{-2}$, and have been converted to the ionic coverage, θ, by assuming that the ions are packed into a square array and the maximum number of ions for a monolayer is equal to $1/4r_i^2$, where r_i is the radius of the ion. The agreements between the results of ellipsometry and electrocapillary (Figures 19 and 20) and are within the experimental error.

Chiu and Genshaw[23] compared θ values obtained by ellipsometry and radiotracer data[125] on platinum. The ellipsometric method did not register adsorbed sulfate until the concentration was increased to 0.1 *M*. The θ values obtained for higher concentration are in agreement with the radiotracer result.

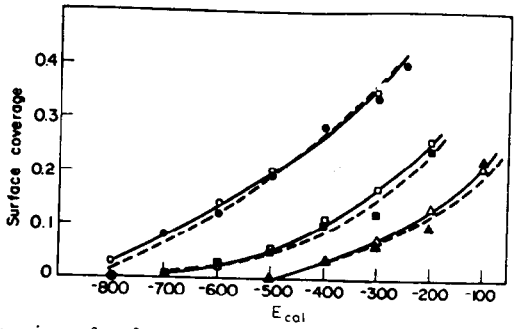


Figure 20. Comparison of surface coverage obtained by ellipsometry and electrocapillary methods for KBr solution: – – –, ellipsometry[22]; ——, electrocapillary[88]; ○, ●, 1 *M*; □, ■, 0.1 *M*; △, ▲, 0.01 *M*.

Table 2

Comparison of Radiotracer and Ellipsometric Adsorption of Br^- (10^{-3} M)

Potential E_{NHE}	Radiotracer[125]	Ellipsometry[23]
0.177	0	—
0.377	0.106	0
0.518	0.138	0.01
0.577	0.143	0.03
0.777	0.170	0.075
0.977	0.184	0.175

$\theta = 4.6 \times 10^8 \Gamma$ (= fraction of surface covered)

Comparison of radiotracer and ellipsometric adsorption of 10^{-3} M Br^- was also made by Chiu and Genshaw,[23] as shown in Table 2.

Comparison of three techniques is made for adsorption on platinum in Table 3 for Cl^- ion.

The comparison is rather poor, as it involves the roughness factor in the radiotracer measurements,[125] and the monolayer coverage of hydrogen in converting the one result to the other. The ellipsometry data agree roughly with the radiotracer results at higher coverages. Chiu and Genshaw[23] put forward two probable explanations of the discrepancies between these two methods.

(a) The radiotracer method involves making correction for the adhering solution and the potential of the electrode is not controlled during removal from solution.

(b) The ellipsometric method is subject to the problem of determining the zero point of adsorption, as discussed below.

The results obtained for iodide adsorption are compared with the radiotracer data in Table 4.

The radiotracer method gives higher values than the single-reflection ellipsometry. Chiu and Genshaw[23] applied a zero correction of 0.09 in θ for

Table 3

Comparison of Chloride Adsorption on Platinum by Various Techniques[23]

Potential E_{NHE}	Coverage		
	Radiotracer[125]	Potential sweep[126]	Ellipsometric[23]
0.177	0.000	—	—
0.377	0.018	0.27	0.00
0.577	0.070	0.35	0.01
0.777	0.101	0.50	0.05
0.977	0.120	—	0.11

Table 4

Comparison of Radiotracer and Ellipsometric Adsorption of I^- (10^{-3} M) on Platinum

Potential E_{NHE}	Radiotracer[125]	Ellipsometry[23]	Ellipsometry[23] with correction
0.023	0.069	—	0.09
0.177	0.092	0.05	0.14
0.377	0.144	0.07	0.16
0.518	0.230	0.11	0.20
0.577	0.258	0.13	0.22
0.677	0.310	0.14	0.23

10^{-3} *M* NaI obtained by making measurements at constant potential with varying concentration, and thus obtained the values in the last column of Table 4. To avoid the interference of hydrogen, ellipsometric data were taken at a potential from the pzc which resulted in a higher zero correction. They suggested that one way to correct the ellipsometry error of the zero determination is the determination of the change in Δ at a constant potential in the presence and absence of adsorbing species.

7. The Validity of Diffuse Layer Theory

The calculation of specifically adsorbed ionic concentrations in the double layer (Section 5) is made with the aid of diffuse layer theory. By the nature of specific adsorption, the concentration to which we are referring in such discussions is always a high one, e.g., more than 0.1 *M*.

This raises the question as to whether the simple diffuse layer theory, as originally derived by Gouy[8] and Chapman,[9] is applicable in the concentration ranges in which it is applied. The diffuse layer theory of these workers[8,9] is the origin of the more discussed theory of Debye and Hückel[130] for electrolyte solutions, and it is known that such a theory has fundamental difficulties in concentrations much above 0.001 *M*.

The Gouy–Chapman theory of the diffuse layer is based on a model of point charges in a structureless dielectric medium. Thus, among other aspects of the real situation which have not been taken into account by the theory of Gouy and Chapman is the fact that the dielectric constant to be used is certainly not that of the bulk dielectric.[131] Under most conditions at which specific adsorption is determined, there will be a difficulty with respect to ion pair formation, for the concentration of ion pairs as given by Bjerrum[132] and Fuoss[133] will be appreciable. Lastly, the question of ion imaging should be analyzed, for this has been neglected in the simple treatment of Gouy[8] and Chapman.[9]

However, there is a more important reason why we should be rather reserved about the applicability of the diffuse layer theory to high concentrations. There

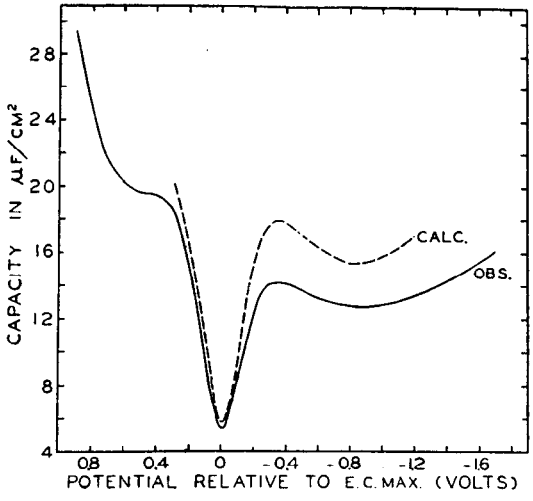


Figure 21. Calculated and observed differential capacity[2] of mercury in contact with 0.001 M NaF. $T = 25°C$.

is a limiting concentration, around 0.001 M[134] for 1–1 electrolytes, at which ionic atmosphere concepts (upon which diffuse layer theory is based) becomes inapplicable. The average distance, $r = (1000/2N_0c)^{1/3}$, between ions in a solution of concentration c becomes greater than κ^{-1}. Thus, above this limiting concentration, the model tells one that the diffuse layer contains no ions. Under these rather empty circumstances, it seems meaningless to use diffuse layer equations at concentrations above the limit at which "graininess" commences.

One obtains, thus, a negative impression of the application of ionic atmosphere formulas, above 0.001 M. Thus if one takes the expression for the activity coefficient obtained by the application of the zeroth approximation Debye–Hückel theory, it is not simply a weak approximation, but totally wrong at concentrations in the 1 M region. The danger exists, therefore, that a similar result would be obtained in the diffuse layer theory with very poor implications for the calculation hitherto made of specific adsorption.

Several authors have attempted to make an examination of the diffuse layer theory. The first test was carried out by D. C. Grahame in 1947 and published in his well-known review.[2] Grahame found that for sodium fluoride, in potential regions near the potential of zero charge, he could calculate the double-layer capacitance from the diffuse-layer theory. (Figure 21). His calculations were carried out up to 0.1 M concentrations.

This test is not an appropriate one because of the concentration at which it was carried out, which was ten times less than the concentration at which we

apply the diffuse layer theory in calculations connected with specific adsorption determinations.

Joshi and Parsons[135] and Parsons and Trasatti[136] carried out an examination of the dependence of σ_d on σ_m. For the charge due to ith ion in the diffuse layer, they used the equation[135,136]

$$\sigma_d = Gz_i \int_{u_2}^{i} \frac{n_i(U^{z_i} - 1)\, du}{u[\sum n_i (U^{z_i} - 1)]^{1/2}} \tag{7.1}$$

where $G = (kT\varepsilon/8\pi)^{1/2}$, $u = \exp(-e\phi/kT)$, ϕ is the potential at a distance x from the electrode, n_i is the concentration of the ion species i, and z_i is the valence of the ith ion species. The value of u_2 is the value of u at the distance of the OHP. Using Eq. (7.1), σ_d was calculated by numerical integration as a function of ϕ_2 for given compositions. The charge density σ_m on the electrode was calculated as a function of ϕ_2 making use of the equation[135,136]

$$\sigma_m = \pm 2G\left[\sum n_i(U_2^{z_i} - 1)\right]^{1/2} \tag{7.2}$$

With the assumptions made (mainly that there is no significant degree of specific adsorption at concentrations in the region of 0.02 M), the diffuse layer charges, for example, for Mg^{2+} and K^+ cations and Cl^- anions, were plotted against σ_m as shown in Figure 22. The experimental diffuse charges seem to be slightly greater than that predicted by the simple diffuse layer theory.

The anion is correspondingly positively adsorbed, whereas according to theory it should be repelled from the negatively charged electrode. The same effect of increasing positive adsorption of anions as the electrode charge becomes more negative has previously been reported[137] in dilute aqueous solutions of NaOH, KNO_3, and Na_2SO_4. Similar deviations from diffuse layer behavior in some nonaqueous solutions[138–140] and in concentrated aqueous solutions have been attributed to specific adsorption of cations. It has been suggested[140] that the anomaly arises from slow relaxation of the diffuse layer in dilute solutions which would lead to frequency dependence of the capacity. However, the capacitance is highly independent of frequency variation (Reference 141, p. 50).

However, the tests made by Parsons and Trasatti,[136] though giving fair agreement for Mg^{2+} and K^+, are not very convincing of the applicability of the diffuse layer equations because the concentration used is much lower than that at which the diffuse layer concepts are applied in specific adsorption determinations.

A different test is due to Grahame,[2] who calculated the limiting value of anion charge in the diffuse layer at highly negative potentials, when the anions are repelled into the double layer and compared with the measured limiting value of Γ_-. At concentrations such as 0.3 M, Grahame obtained excellent agreement for this limiting value. For 1 M NaF, the agreement was within 6% for the limiting value of Γ_-. However, Grahame's test is not demanding. In the limiting anion concentration at highly negative metal charges, the value of the

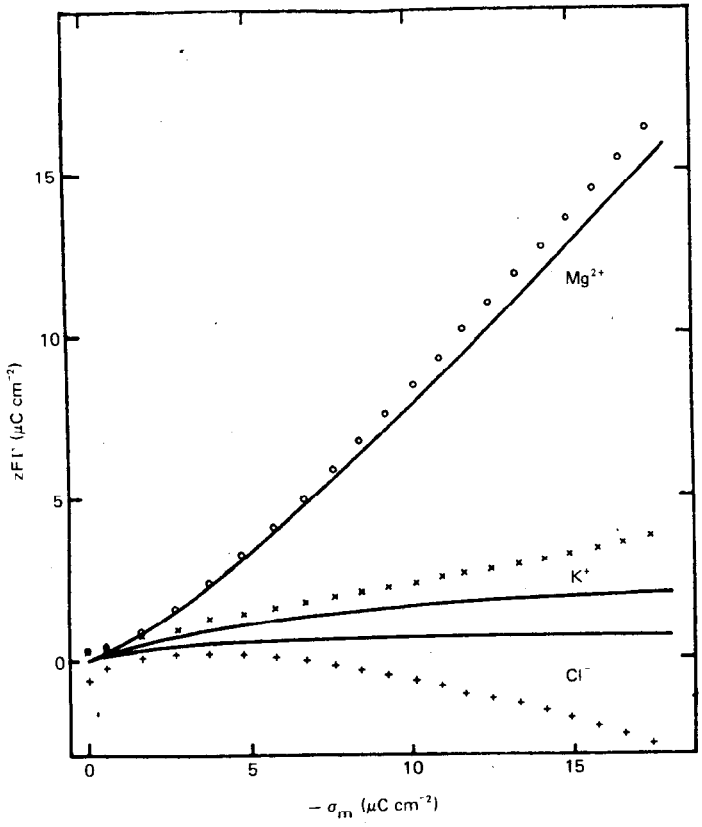


Figure 22. Surface excesses[136] of Mg^{2+}, K^+, and Cl^- ions at a mercury electrode in 0.0208 *M* KCl + 0.0555 *M* $MgCl_2$. Points are experimental. Lines calculated from diffuse layer theory assuming no specific adsorption of Cl^-.

exponential part of the equation giving diffuse layer charges becomes negligible, and the equation becomes insensitive to errors in it.

In summary, the situation with respect to the diffuse layer theory seems weak. Tests of its quantitative applicability have not been carried out under conditions at which the theory is applied for the calculations of specific adsorption. The diffuse layer theory should break down well below 1 *M*. The lack of good equations for the calculation of diffuse layer charges is one of the weakest in the field of the double layer, and it is conceivable that it introduces errors of several microcoulombs into the calculated α_d. The effect of this on the calculations of contact adsorption have not been significantly studied.

There is a lack of discussion of the validity of this theory in the literature:

some workers maintain that the theory works better than it ought to. Justification for this position is not clear.

Many attempts[142-151] have been made to improve the Gouy–Chapman theory†. However, corrections to the Gouy–Chapman theory seem to be small unless the potential ϕ_{2-b} at the plane separating the inner and outer layer (OHP) is greater than about 100 mV,[152] which occurs in practice only in dilute solutions where, also, the effect of these corrections is reduced.

The direction of work in the diffuse layer theory is clear: modern methods which have been recently applied to the treatment of electrolytes in high concentration and the application of McMillan–Mayer solution theory,[153] effective ionic potentials, and statistical mechanical methods, will probably give improvements, as described recently by H. Anderson.[154]

8. Effect of the Neglect of Γ_{H_2O}

Thermodynamic analysis of the double layer yields the relative ionic surface excesses, i.e., the surface excesses from the interfacial tension are evaluated by assuming $\Gamma_{H_2O} = 0$ in the equation [cf. Eqs. (5.12) and (5.13)]:

$$-\left(\frac{\partial \gamma}{d\mu}\right)_{E_+} = \Gamma_{i(H_2O)} = \Gamma_i - \Gamma_{H_2O}\frac{x_{salt}}{x_{H_2O}} \tag{8.1}$$

where Γ_i represents the absolute surface excess, $\Gamma_{i(H_2O)}$ is the relative surface excess, and x's are the mole fractions. The difference between the relative and the absolute values of the surface excesses may be approximately evaluated by an estimation of the value of Γ_{H_2O} (x_{salt}/x_{water}). Assuming a square array, the water concentration on the surface is $c_{H_2O,s} = 1/4r_w^2 = 1.31 \times 10^{15}$ molecules $cm^{-2} = 2.17 \times 10^{-9}$ mol cm^{-2} (with $r_w = 1.38$ Å). Concentration of bulk water per unit area is $c_{H_2O,b} = (N_0/V_m)^{2/3} = 1.72 \times 10^{-9}$ mol cm^{-2}, where N_0 is the Avogadro's number and V_m is the molar volume of water. Therefore,

$$\Gamma_{H_2O} = (c_{H_2O,s} - c_{H_2O,b}) = 4.5 \times 10^{-10} \text{ mol cm}^{-2} \tag{8.2}$$

This estimate approximates by assuming that the water structure is intact up to the electrode. With this approximation, it is the surface excess of water at the charge free surface in the absence of any other component in the system.

Let us now find the surface excess of water in, say, 3 *N* HCl, i.e., a high

† However, there seems to be misunderstanding concerning mathematical improvements of Gouy–Chapman theory. It is not correct to state that improvement has been made by taking into account the nonexpanded form, as is done in the double-layer theory. This is because of the principle of superposition, which demands that there is a linear relationship between the charge density and the potential. These comments are relevant to statements made by Mohilner,[155] to the effect that the success of the diffuse double-layer theory at high concentrations was due to the use of the nonexpanded form in the mathematical treatment.

value in the range of concentrations usually studied. The mole fraction of HCl is given by

$$x_{HCl} = \frac{0.001cM_1}{\rho - 0.001cM_2 + 0.01cM_1} \tag{8.3}$$

where c is the concentration in moles per liter, ρ is the density of the solution, and M_1 and M_2 are the molecular weights of the solvent and solute, respectively.[156] For 3 N HCl, $\rho = 1.049$,[87] and with $M_1 = 18$ and $M_2 = 36.5$, one gets from the above equation, $x_{HCl} = 0.055$. Now, concentration of bulk water in this 3 N solution of HCl is $c_{H_2O,b} = c_{HCl}\,(x_{H_2O}/x_{HCl}) = 51.4\ M = 1.62 \times 10^{-9}$ mol cm^{-2}. As mentioned before, the surface water concentration is 2.17×10^{-9} mol cm^{-2}. Therefore, the surface excess of water when the electrolyte concentration is 3 N is

$$\Gamma_{H_2O} = (2.17 - 1.62) \times 10^{-9} = 5.5 \times 10^{-10} \text{ mol cm}^{-2}$$

Thus, passing from pure water to 3 N HCl, Γ_{H_2O} changes from 4.5×10^{-10} mol cm^{-2} to 5.5×10^{-10} mol cm^{-2}. Now, $\Gamma_{H_2O}(x_{HCl}/x_{H_2O}) = 5.5(0.055/0.945) = 3.2 \times 10^{-11}$ mol cm^{-2}, which amounts to 3.1 μC cm^{-2}.

This is a higher value of the probable deviation introduced, since with dilution Γ_{H_2O} and x_{HCl}/x_{H_2O} decrease. Further, the error will decrease with increasing anodic charge since the specifically adsorbing ions will replace some water molecules from the surface.

9. Partial Charge Transfer in Specific Adsorption

9.1. Introduction

Until 1961, it was assumed that ions remained fully charged during the adsorption process, i.e., the binding between the metal and the adsorbed ions is purely electrostatic. With this model, it was possible for Anderson and Bockris[20] to predict the correct order of specific adsorption of halide ions, and to show that most of the cations would not be specifically adsorbed.

In recent times, Lorenz and co-workers[157-171] have suggested that a purely electrostatic bond between the ion and the metal is not a reality, and that, in specific adsorption, there is a degree of charge transfer tantamount to covalent bonding.†

This important suggestion raises the possibility that equations of the double layer, whereby the double layer charge is related to the amount adsorbed on the assumption that the charge on the adsorbed ion is the same as the charge it maintains whilst in solution, are not correct.

† Before the concept of partial charge of specifically adsorbed ions was introduced by Lorenz, Conway, and Bockris[172] had obtained evidence for the idea of partial charge for cations adsorbed onto metals. For example, on silver, in silver deposition, they calculated the partial charge of the anion adsorbed at the surface as about 0.5e.

9.2. The Work of Lorenz and Co-Workers[157-171]

Lorenz assumed the following adsorption process:

$$R^z = R_{ads}^{z(1-\lambda)} + \lambda ze \tag{9.1}$$

where R^z is the adsorbing species of charge ze, and λ is a dimensionless coefficient, denoted as the partial charge coefficient. Thus in the generally accepted model, $\lambda = 0$. If $\lambda = 1$, then this would imply an entirely covalent bond. Lorenz then introduced the following concept. He suggested[160] that there exists a charge σ_m, which is the charge which would have been on the metal in the case considered, were it not for the fact that partial charge transfer had occurred. He then assumes that the electrode is isolated from the external circuit and that the charge σ_m with which the thought experiment began can be changed by charge transfer from the adsorbing ion, to a charge σ_e, so that

$$\sigma_e = \sigma_m + \lambda zF\Gamma_i \tag{9.2}$$

Lorenz regards the charge σ_e as "the electron charge on the electrode." He assumes that the charge given by the slope of the electrocapillary curve is σ_m in Eq. (9.2) and that the real electron excess charge σ_e cannot be determined directly. However, it may be thought more reasonable to take the slope of the electrocapillary curve as the actual excess charge present on the electrode, i.e., σ_e by Lorenz' definition, and not the would-be charge, σ_m. Since this hypothetical charge σ_m cannot be determined by experiment directly, the determination of λ would have to be indirect.

Assuming that the partial charge coefficient, λ, does not depend on Γ, differentiation of Eq. (9.2) with respect to Γ, gives

$$\lambda = -\frac{1}{zF}\left(\frac{\partial\sigma_m}{\partial\Gamma}\right) + \frac{1}{zF}\left(\frac{\partial\sigma_e}{\partial\Gamma}\right) \tag{9.3}$$

Lorenz defined, further, the dimensionless quantity

$$I = -\left(\frac{\partial\sigma_m}{\partial\Gamma}\right)\frac{1}{zF} \tag{9.4}$$

and hence rewrote Eq. (9.3) as

$$\lambda = I + \frac{1}{zF}\left(\frac{\partial\sigma_e}{\partial\Gamma}\right) \tag{9.5}$$

When the frequency of the measurement of capacitance exceeds the reciprocal of the relaxation time of the charge transfer, if the charge transfer reaction is the only reason for the variation of adsorption with potential,† variation of

† There are, of course, reasons why the electrode coverage should vary with E, independently of the charge transfer hypothesis.

adsorption with potential would cease. Thus Lorenz proposed that the capacity C_∞, corresponding to $\omega \to \infty$, is

$$C_\infty = \left(\frac{\partial \sigma_e}{\partial E}\right)_\Gamma \tag{9.6}$$

Since $\sigma_e = \sigma_e(E, \Gamma)$, we have by virtue of the total differential

$$\frac{\partial C_\infty}{\partial \Gamma} = \frac{\partial}{\partial \Gamma}\left(\frac{\partial \sigma_e}{\partial E}\right)_\Gamma = \frac{\partial}{\partial E}\left(\frac{\partial \sigma_e}{\partial \Gamma}\right)_E \tag{9.7}$$

and hence,

$$\left(\frac{\partial \sigma_e}{\partial \Gamma}\right)_E = \int_{E_x}^{E} \frac{\partial C_\infty}{\partial \Gamma}\, dE \tag{9.8}$$

where E_x is the potential where $\partial \sigma_e / \partial \Gamma = 0$. Substitution of Eq. (9.8) in (9.5) gives

$$\lambda = I + \frac{1}{zF} \int_{E_x}^{E} \frac{\partial C_\infty}{\partial \Gamma}\, dE \tag{9.9}$$

Equation (9.9) is a basic relation in Lorenz' work and is used by him for the determination of the partial charge coefficient, λ. Lorenz obtains I experimentally by Eq. (9.4) (assuming that the Lippmann equation gives σ_m, and not σ_e) and with measured $(\partial C_\infty / \partial \Gamma)$, then obtains λ from Eq. (9.9). Since it is experimentally found[173] that $(\partial C_\infty / \partial \Gamma) \approx 0$ one may write from (9.9),

$$\lambda \approx I \tag{9.10}$$

Thus one only needs to determine I from Eq. (9.4) to obtain λ.† Lorenz[163] found that I for Br^- and I^- adsorption was independent of potential and was equal to 0.48 ± 0.06 and 0.34 ± 0.08, respectively.

9.3 Discussion on Lorenz's Determination of Partial Charge

(a) Equations (9.8) and (9.9) are applicable only if the value of E_x at which $(\partial \sigma_e / \partial \Gamma) \approx 0$ is known.

(b) Lorenz's result with $(\partial C_\infty / \partial \Gamma) \approx 0$ gives from Eq. (9.9), $\lambda \approx I$. However, this does not seem necessarily consistent with Eq. (9.7) because if $(\partial C_\infty / \partial \Gamma) \approx 0$, then

$$\frac{\partial \sigma_e}{\partial \Gamma} = \text{const} \tag{9.11}$$

† Essentially, regarding (9.4), it is clear that, at constant capacitance, the variation of electrode charge with specific adsorption would have, roughly, a slope of 1 if the charge per anion is $-1\,e$.

with respect to potential, but not equal to zero. From (9.5) then

$$\lambda = l + \text{const} \tag{9.12}$$

which may cause difficulty when compared with (9.10).

(c) The quantity $(\partial\sigma_m/\partial\Gamma)$ in Eq. (9.4) can easily be related to the distance ratio $(x_2 - x_1)/x_2$ as[173]

$$l = -\frac{1}{zF}\frac{\partial\sigma_m}{\partial\Gamma} = \frac{x_2 - x_1}{x_2} \tag{9.13}$$

where x_1 and x_2 are the distances of the IHP and OHP, respectively, from the metal surface. The distance ratio found for I^-[173] and Br^-[88] are potential dependent, while the values found by Lorenz[163] are potential independent.

All these matters are seen to be subject to the general criticism in which it has been assumed that there are two quantities σ_m and σ_e which describe the charge on the electrode. The concept σ_m (the charge which would be on the electrode if there were no charge transfer) has been assumed to be an experimentally determinable quantity and is given by electrocapillary thermodynamics and the Lippmann equation. On the other hand, it is then assumed that σ_e is "the electron excess charge" on the electrode. Thus the model appears to imply that there is a situation in which, momentarily, there is a charge σ_m on the electrode and that thereafter, with the electrode out of contact with an electronic circuit, charge travels across the double layer and thus alters the net charge upon the electrode. However, the instrumentation determines the charge, and the net charge (including any transfer from the charge particles of the adsorbed layer) seems to be what is determined by electrocapillary thermodynamics. The Lorenz concept of partial charge transfer has also been discussed by Vetter and Plieth[174,175] and Parsons[176] and Damaskin.[177]

Nevertheless, the idea of partial charge transfer during adsorption is of great interest. If values of λ can be known with confidence, then it will be possible to relate the specific surface excess to electrical charge measurements, as in the classical electrocapillary thermodynamics.

9.4. The Work of Vetter and Schultze[178–181]

Vetter and Schultze[178–181] considered the partial charge concept, but took a somewhat different viewpoint from that of Lorenz. They considered an adsorption equilibrium such as the following:

$$\nu M\text{–}OH_2 + S_{aq}^{z} \rightleftarrows M\text{–}S^{z+\lambda} + \lambda e^- + \nu H_2O_{(aq)} \tag{9.14}$$

where ν is the stoichiometric number, S^z is the adsorbing species, λ is the partial charge coefficient, M stands for the metallic atom, and $S^{z+\lambda}$ is the specifically adsorbed substance.

In discussing the equation, they introduced the concept of "electrosorption valency," which is defined by the relation

$$\gamma' = -\frac{1}{F}\left(\frac{\partial \sigma_m}{\partial \Gamma}\right)_{\Delta\phi} = \frac{1}{F}\left(\frac{\partial \mu_s}{\partial\, \Delta\phi}\right)_{\Gamma} \tag{9.15}$$

where μ_s is the chemical potential of the adsorbing species in solution and $\Delta\phi$ is the potential difference across the interface.

The term "electrosorption valency" was chosen because of the analogy between the value, γ', and the charge on the ion, z, which enters into Faraday's Law as well as the Nernst equation. Thus, for a metal deposition reaction, the Nernst equation may be represented by

$$E = E_0 + \frac{RT}{zF} \ln \frac{a_{s(\text{electrolyte})}}{a_{m(\text{metal})}} \tag{9.16}$$

which yields a derivative analogous to Eq. (9.15),

$$\left(\frac{\partial \mu_s}{\partial E}\right)_{a_m} = zF \tag{9.17}$$

Vetter and Schultze[178] derived an equation which relates the electrosorption valency, γ', with the potentials at different regions of the double layer, the double-layer capacitance, and the dipolar properties of the adsorbing species, namely,

$$\gamma' = zg - \lambda(1 - g) + \kappa_{ad} - \nu\kappa_w - \frac{1}{F}\int_0^{\Delta\phi}\left(\frac{\partial C_{DL}}{\partial \Gamma}\right)_{\Delta\phi} d\,\Delta\phi \tag{9.18}$$

where ν is the number of water molecules replaced by one ion and

$$C_{DL} = \left(\frac{\partial \sigma_m}{\partial\, \Delta\phi}\right)_{\Gamma} \tag{9.19}$$

and g is a geometric factor, which describes the position of the center of the adsorbed ion in the double layer in terms of potential and is defined by

$$g = \frac{\phi_{ad} - \phi_s}{\phi_m - \phi_s} \tag{9.20}$$

where ϕ_{ad}, ϕ_m, and ϕ_s are the potentials in the IHP, metal surface, and solution, respectively. The coefficients κ_{ad} and κ_w take into account that part of the electrical energy which is due to the adsorption of oriented dipoles with a dipole moment μ_i and are given by the equation

$$\kappa_i = \pm\mu_i/el_i \tag{9.21}$$

where μ_i/e is the dipole length and

$$l_i = (\phi_m - \phi_s)/(d\phi/dx) \tag{9.22}$$

is a length of the order of magnitude of the thickness of the compact double layer. Thus what κ_i means physically is the ratio of the dipole moment of the adsorbed molecule to the dipole moment of the compact layer. The coefficient, λ, is defined by the difference between the actual charge of adsorbate per ion, $z_{ad}e$, and the ionic charge, ze:

$$\lambda = z - z_{ad} \tag{9.23}$$

λ varies in the range between 0 and z. In the case of an ionic electrosorption system, however, κ_{ad} is zero and $\nu\kappa_w$ is small compared with the charge terms.[182] Thus, Eq. (9.18) may be approximated to

$$\gamma' = zg - \lambda(1 - g) - \frac{1}{F}\int_0^{\Delta\phi}\left(\frac{\partial C_{DL}}{\partial \Gamma}\right)_{\Delta\phi} d\,\Delta\phi \tag{9.24}$$

Vetter and Schultze determined γ' experimentally as follows: Measurement of the capacity or surface tension yields σ_m and Γ_{ads} as a function of potential and the slope of σ_m–Γ curve gives the value of γ' (results are given below).

Another method of obtaining γ' is to utilize the method of Grahame and Parsons[88,173,183] to evaluate the ratio of integral capacitances K_{M-OHP} and $K_{IHP-OHP}$ given by

$$\frac{K_{M-OHP}}{K_{IHP-OHP}} = -\frac{1}{F}\frac{(\partial\sigma_m/\partial\,\Delta\phi)_\Gamma}{(\partial\Gamma/\partial\,\Delta\phi)_{\sigma_m}} = +\frac{1}{F}\left(\frac{\partial\sigma_m}{\partial\Gamma}\right)_{\Delta\phi} = -\gamma' \tag{9.25}$$

This ratio has been interpreted as $(x_2 - x_1)/x_2$ by Parsons *et al.*[88]

The coefficient l, given by Eq. (9.4) and determined by Lorenz and Kruger,[161] can be correlated to γ', since $l = (1/F)(\partial\sigma_m/\partial\Gamma)_{\Delta\phi} = -\gamma'$.

The value of electrosorption valency obtained experimentally may be substituted in (9.24), and from measured $(\partial C_{DL}/\partial\Gamma)_{\Delta\phi}$ one can estimate λ from (9.24), so long as a reasonable estimate of g can be made from modelistic considerations.

If one takes a measured value of γ' when $\Delta\phi = 0$, then Eq. (9.24) may be written as

$$\gamma'_N = zg - \lambda(1 - g) \tag{9.26}$$

and the need for knowing C_{DL} is eliminated. For Cl^-, $\gamma'_N \approx -0.16$ from Eq. (9.18) and hence from (9.26), a range of g and λ may be obtained[179]:

$$0 \leqslant g \leqslant 0.16 \quad \text{and} \quad 0 \leqslant \lambda \leqslant 0.16 \tag{9.27}$$

For the halide ions, the γ'_N values increase in the sequence

$$|\gamma'_{N,Cl^-}| < |\gamma'_{N,Br^-}| < \gamma'_{N,I^-} \tag{9.28}$$

and Schultze and Vetter[179] explained the differences $\gamma'_{N,Br^-} - \gamma'_{N,Cl^-}$ and $\gamma'_{N,I^-} - \gamma'_{N,Cl^-}$ by a partial charge transfer from the ion to the metal. They found

$$\left.\begin{aligned}\gamma'_{N,Br^-} - \gamma'_{N,Cl^-} &= -0.17\\ \text{and}\qquad \gamma'_{N,I^-} - \gamma'_{N,Cl^-} &= -0.24\end{aligned}\right\} \tag{9.29}$$

Hence, *assuming* $\lambda_{Cl^-} = 0$ and g = const for all ions, they[179] obtained from Eqs. (9.26) and (9.29)

$$\lambda_{Br^-} \geqslant \frac{0.17}{1-g} = -\frac{\gamma'_{N,Br^-} - \gamma'_{N,Cl^-}}{1-g} \tag{9.30}$$

and

$$\lambda_{I^-} \geqslant \frac{0.24}{1-g} = -\frac{\gamma'_{N,I^-} - \gamma'_{N,Cl^-}}{1-g} \tag{9.31}$$

The conclusion involves the assumption that g is the same for all ions.

9.5. Summary

The original suggestion of Lorenz *et al.* that the specific adsorption is associated with partial charge transfer contains some unclarities and internal difficulties.

Vetter and Schultze's development based on the interpretation of electrosorption valency, however, does seem to give indications of the reality of partial charge transfer, albeit involving geometrical and modelistic estimates of g, which involve fairly significant approximations.

On the whole, partial charge transfer seems to be supported. However, there is another viewpoint which seems to be negative to that developed here. This is an approach taken by Bockris, Devanathan, and Müller[26] which compared the adsorbability of halide ions at mercury with covalent bond energies and concluded that the covalent bond formation does not contribute to the adsorption. Anderson and Bockris[20] and later Bode[184] came to the same conclusion. Anderson, Anderson, and Eyring[185] compared the adsorbability of various ions with the standard free energy of the reaction $M_{(g)} + \frac{1}{2}X_{2(g)} \rightarrow MX_{(g)}$. They[185] found no correlation and concluded that the covalent bonds are negligible in adsorption of anions. Bonding of, e.g., Cl^- to a metal is difficult to modelize in terms of MO concepts. Thus, with the concept of partial charge transfer, we are at an uncertain frontier of a developing field.

10. Forces Involved in Specific Adsorption

The nature of the forces involved in specific adsorption is regarded differently by different authors. Grahame[2] did consider specifically adsorbed anions to be "covalently" bonded to the metal, the strength of the bond increasing with positive charge on the metal. This was allowed for formally as an electrical dependence of the specific adsorption potential in the Stern theory.[7] However, the idea of a covalent bonding of variable strength, without a clear formulation of the orbitals involved to a closed, e.g., Cl^- shell seems inconsistent. Various attempts have been made, therefore, to calculate adsorption energy from electrostatic models neglecting covalent bonding.

Using a modified form of Stern's adsorption isotherm and taking into account the effects of discreteness of the adsorbed charge, Levine and coworkers[186–188] calculated the electrical dependence of Stern's specific adsorption potential. The applicability of this procedure is discussed in detail in the next section. Anderson and Bockris[20] were able to calculate the entire free energy of adsorption from purely electrostatic considerations. The procedure used by Anderson and Bockris[20] was followed up by Bode.[184] Specific interactions, e.g., image forces, dispersion interactions, field ion interaction (field due to electrode charge), lateral repulsions, and their explicit forms are discussed in the next section where an isotherm is developed with inclusion of all these forces. For the free energy of specific adsorption, Anderson and Bockris[20] and Bode[184] used the sum of the changes in ethalpy and entropy resulting from differences in ion–metal, ion–water, and water–metal interactions for the ions as it is removed from the bulk solution and brought near the electrode. The contributions for the enthalpy can be summarized as follows:

ΔH_1 is due to loss of interaction energy for n desorbing water molecules with the surroundings, which includes losses due to breakage of hydrogen bonds with the second layer and lateral interaction between these n water molecules and their adsorbed neighbors and with the metal surface.

ΔH_2 is the gain of interaction of n desorbed water molecules with the bulk.

ΔH_3 is the change in enthalpy due to metal–ion interaction (image, dispersion, and repulsion).

ΔH_4 is the difference of interaction of the ion with n_1 primary water molecules in the bulk solution and with n_1' at the electrode, i.e., $(n_1' - n_1)\Delta H_{\text{ion-w}}$.

ΔH_5 is the loss of interaction energy of ion with water beyond nearest neighbors.

ΔH_6 corresponds to the change in hydrogen bonding for all water molecules associated with the ion when going from the bulk to the surface.

ΔH_7 is the change in interaction energy of the ion due to reorientation of adsorbed neighboring water molecules caused by ion–water interaction. In the Anderson and Bockris treatment, this is taken as one-half of the water metal interaction.

Entropy changes accompanying specific adsorption were regarded as follows:

ΔS_1 is the gain in entropy due to the desorption of n water molecules from the electrode surface into the solution. ΔS_2 is the difference in entropy due to changes in the degrees of freedom for the ion upon adsorption. ΔS_3 is the change in entropy due to change in the number of water molecules primary to the ion when the ion is adsorbed onto the surface from solution. ΔS_4 is the change due to gain in hydrogen bonding by nonprimary water molecules which surrounded the ion in solution and that due to the loss in hydrogen bonding by the neighboring water molecules on the electrode.

Two modifications to the calculation of Anderson and Bockris[20] were

Table 5

Free Energies of Adsorption[184]

Metal/ ion	ΔG° (kcal/mol)	Metal/ ion	ΔG° (kcal/mol)
Hg/Br	−11.9	Ag/F	− 2.4
Hg/Cl	−10.3	Ag/OH	− 3.4
Hg/F	2.6	Au/Br	−14.0
Hg/OH	2.6	Au/Cl	−11.7
Ag/Br	−17.3	Au/F	− 2.7
Ag/Cl	−15.0	Au/OH	− 3.7

made by Bode.[184] One is involved in the determination of the equilibrium separation distance r_e. Instead of using only the ion–metal interactions to determine r_e, all contributions to ΔG° were included. The second modification involves the water–metal interaction. Anderson and Bockris[20] assumed that the separation distance of the water molecule from the electrode is the same as its radius and that the molecules which reoriented in the presence of an adjacent adsorbed ion lost one-half of their water–metal interaction. In Bode's[184] treatment, the orientation of primary waters of hydration is constrained by both the metal surface and the ion. The calculated free energies of specific adsorption for various ions are listed in Table 5.[184]

For adsorption of the halides on silver, gold, and mercury the calculated ΔG° show the experimentally observed[20,189] order $Br^- > Cl^- > F^-$. It is found experimentally that OH^- is adsorbed more than Cl^- on Au, less than Cl^- on Ag, and OH^- is not adsorbed at all on Hg.[184] This repositioning of OH^- in order of adsorbability, depending on the electrode, is not evident in the calculations. The calculated ΔG° for OH^- is only slightly more negative than that for F^- and both are more positive than the ΔG° for Cl^-. Bode[184] inferred that Cl^- and Br^- would be specifically adsorbed in the IHP, while F^- and OH^- would be adsorbed in the OHP.

These results show the correct trend in the adsorbability of the ions. However, there are no experimental results with which these may be compared other than the value for I^- adsorption on Hg, which is -8.5 kcal mol^{-1}.[190] Since I^- is adsorbed more than other halide ions, the calculated results must be too negative. Bode[184] mentioned that this error may be due to the rudimentary calculation of dispersion interaction. Another error may be in the image energy because the lines of force passing from the ion through neighboring water molecules were assumed not to experience a change in dielectric. The effect of this approximation might have increased the metal–water interaction. This is offset by neglecting such secondary effects as metal-induced dipoles in the ion interacting with the metal. The repulsive energy is approximate. However, an error in the values of the repulsive constants for an ion interacting with a given electrode will appear to the same degree within the series of ions for that electrode

and it should not alter the ordering of relative magnitudes for ΔG° for the ions adsorbing on that electrode. The ordering in magnitudes of the calculated ΔG° for a given electrode should correspond with experimentally observed trends in adsorption for those ions on that electrode. The uncertainties in this type of calculation for the water–metal and the ion–water interactions are discussed by Andersen and Bockris.[20] They affect the magnitudes of the free energies of adsorption, but will not alter the relative order of adsorbabilities.

Recently Trasatti[191] discussed the change in specific adsorption of I^- ions on the series of metals Au, Hg, Bi, Pb, Cd, and Ga. From the data of specifically adsorbed charge and potential of zero charge, he[191] inferred that the work connected with the water desorption as an ion becomes adsorbed is the main factor in determining the change in adsorbability along the series of metals. The adsorbability of ions increases as the desorption energy of water increases or adsorbability of water decreases on the series of metals mentioned above.

11. The Isotherms for Ionic Adsorption

11.1. General

In a nonelectrochemical system, the isotherm is a function of concentration alone. However, at an electrode, one must also take into account the additional electrical variable which determines the state of the system. Thus, an electrochemical adsorption isotherm must show how adsorption varies with both bulk activity and the electrode charge σ_m or the potential E.

When there is equilibrium between a species in the adsorbed state and in the bulk of the solution at an electrode, the corresponding electrochemical potentials are equal. Thus

$$\bar{\mu}^\circ_{i,\text{ads}} + RT \ln f(\theta) = \bar{\mu}^\circ_{i,\text{soln}} + RT \ln a_i \tag{11.1}$$

where $\bar{\mu}^\circ_{i,\text{ads}}$ and $\bar{\mu}^\circ_{i,\text{soln}}$ are the standard electrochemical potentials of the ion in the adsorbed state and in solution, respectively, $f(\theta)$ is a function of surface concentration expressed in terms of surface coverage θ of the adsorbed ion, and a_i is the activity of the adsorbing ion in solution.

The above equation (11.1) can be written as

$$f(\theta) = a_i e^{-\Delta\bar{G}^\circ/RT} = \beta_{(\sigma_m)} a_i \tag{11.2}$$

where $\Delta^{\bar{G}^\circ} = \bar{\mu}^\circ_{i,\text{ads}} - \bar{\mu}^\circ_{i,\text{soln}}$ is the standard electrochemical free energy of adsorption and may be a function of charge or potential, a_i is the activity of the adsorbing ion in solution, and

$$\beta_{(\sigma_m)} = e^{-\Delta\bar{G}^\circ/RT} \tag{11.3}$$

To formulate particular adsorption isotherms, the particle–particle and particle–metal interactions have to be considered. Adsorption isotherms are

Table 6

Adsorption Isotherms[a]

Name	Isotherms
Henry[194]	$\beta a_i = RT\theta$
Langmuir[195]	$\beta a_i = \dfrac{\theta}{1-\theta}$
Volmer[196]	$\beta a_i = \dfrac{RT\Gamma_i}{1-b\Gamma_i} \exp \dfrac{b\Gamma_i}{1-b\Gamma_i}$
van der Waals[197]	$\beta a_i = \dfrac{RT}{1-b\Gamma_i} \exp\left[\dfrac{b\Gamma_i}{1-b\Gamma_i}\right] \exp(-2a\theta)$
Virial[192]	$\beta a = \Gamma_i \exp(-2a\theta)$
Frumkin[198]	$\beta a_i = \dfrac{\theta}{1-\theta} \exp(-2a\theta)$
Modified H.F.L.[199] (Helfand, Frisch, and Lebowitz, modified by Parsons)	$\beta a_i = \dfrac{\theta}{1-\theta} \dfrac{b}{0.907} \exp\left[\dfrac{1+\theta(1-\theta)}{(1-\theta)^2}\right] \exp(-2a\theta)$
Blomgren and Bockris[200]	$\beta a_i = \dfrac{\theta}{1-\theta} \exp(a_1\theta^{1/2} - a_2\theta^3)$
BDM[26] (Bockris, Devanathan, and Müller)	$\beta_{(\sigma_m)} = \dfrac{\theta}{1-\theta} \exp a_1'\theta^{3/2}$
LBC[186] (Levine, Bell, and Calvert)	$\beta_{(\sigma_m)} = \dfrac{\theta}{(1-p\theta)^p} \exp(a_2'\theta)$
BH[201] (Bockris and Habib)	$\beta_{(\sigma_m)} = \dfrac{\theta}{pe^{p-1}(1-\theta)^p} \exp\left\{a_3\theta^{1/2} \sum_{n=1}^{\infty}\left[1-\left(1+\dfrac{h'\theta}{n^2}\right)^{-1/2}\right] + a_4\theta^3 \sum_{n=1}^{\infty}\dfrac{1}{n^5}\left[1+\left(1+\dfrac{h'\theta}{n^2}\right)^3\right]\right\}$

[a] a_i = activity of the ions; a = interaction parameter determinable from experiment in isotherms 1-7; b = van der Waals constant; a_1, a_2, a_1', a_2', a_3, and a_4 in isotherms 8-11 have definite forms depending on molecular properties of the ions; $p = r_i^2/r_w^2$; $h' = \pi/4$; and θ is the fraction of the surface covered by ions.

derived at a constant electrical state through the use of two-dimensional equations of state analogous to the various equations of state for three-dimensional gases. A two-dimensional equation of state, applicable for interfacial adsorption, relates a two-dimensional pressure, the area, the temperature, and the number of moles. Parsons,[192] following the work of Everett,[193] has examined the forms of several possible equations of state for the adsorbed film and has given the form of the corresponding isotherms. Several more forms of isotherms are listed by Damaskin *et al.*[261] The more commonly used isotherms, including more recently developed ones, are included in Table 6.

Interaction parameters used in most isotherms (isotherms 1–7) are qualitative, empirical, and mostly derived to obtain a fit to the experimental data. Blomgren and Bockris[200] made the first attempt to give an expression for the interaction parameters based on molecular or ionic properties, independent of adjustable parameters. Blomgren and Bockris[200] started with the Langmuir isotherm and corrected the standard free energy of adsorption, in the case of ion adsorption, for coulombic interaction and dispersive forces. The interaction parameters a_1 and a_2 in the BB[200] isotherm is given by

$$a_1 = \frac{N_0 e^2}{\varepsilon S_1^{1/2}} \quad \text{and} \quad a_2 = \frac{3}{4\pi^3} \frac{N_0 h\nu}{\varepsilon_{opt}} \tag{11.4}$$

where ε is the static dielectric constant of water in the adsorbed layer, ε_{opt} is the optical dielectric constant, ν is the characteristic frequency of the electronic oscillator in the adsorbate ion, and S_1 is the area occupied by one ion. The BB isotherm lacked wide acceptance because of the lack of inclusion of imaging contribution to the free energy of adsorption.

11.2. The Single-Imaging Isotherm

Bockris, Devanathan, and Müller[26] developed more quantitative expression for ΔG° than that of Blomgren and Bockris.[200] They considered lateral repulsion, field dipole interaction, and interaction of the ions with their images in the metal (single imaging). The expression for lateral interaction was expanded binomially up to only three terms in the BDM approximation, which, however, was shown to be inadequate at higher coverage.[202] Bockris and Habib[201] (BH) developed the initial BDM isotherm by assuming no approximation in the summation of lateral interaction energy; dispersion interaction is included and the Flory–Huggins[210] statistics are used to encounter the effect of the relative size of the ions and water molecules. The BH isotherm[201] also used the single-imaging approximation, i.e., the ions are assumed to have their images in the metal only. A single-imaging approximation is based on the fact that imaging of the adsorbed ions in the solution across the smoothly varying dielectric medium is negligible as shown by the following procedure.

11.2.1. Multiple-Image Interaction Energy across a Smoothly Varying Dielectric Medium

The double-layer field strength decreases with distance from the electrode surface towards the solution and, consequently, the dielectric constant of solution gradually increases from its lower saturated value as the distance from the electrode increases[203] and attains its bulk value of 78.54[204] for aqueous solution at a distance where the influence of the double-layer field has become negligible. A dielectric constant distance relation in the interfacial region has been constructed by Bockris and Habib,[201] as shown in Figure 23. This smooth dielectric profile may be considered to be a combination of an infinitely large number of dielectric slabs. The energy of interaction of a single charge with its

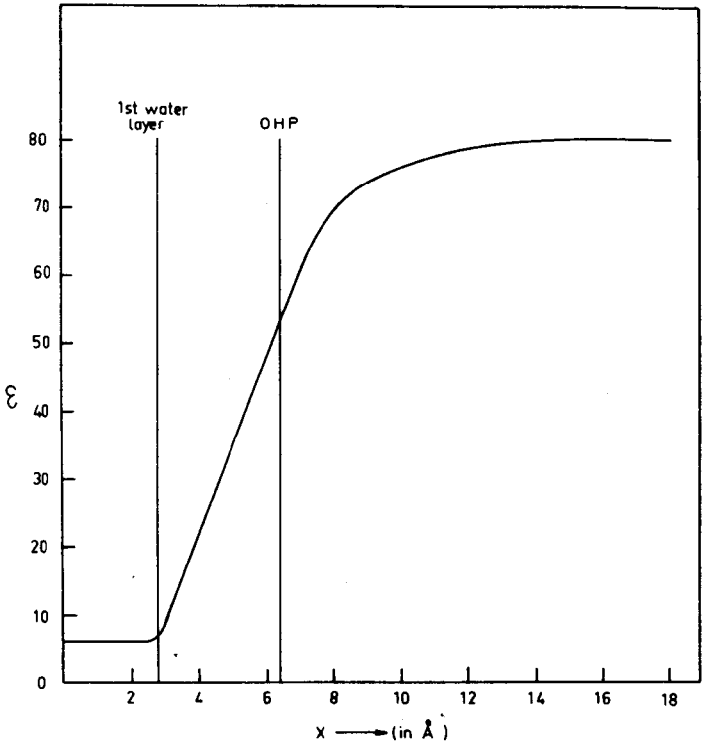


Figure 23. Variation of dielectric constant of solution with distance from the electrode surface.[201]

multiple images across a number of dielectric media may be obtaiend by the method of Fourier–Bessel integral.[205–207] Bockris and Habib[201] found the interaction energies across the first few dielectric slabs, respectively, and generalized these expressions to represent the interaction energy across an infinite number of such slabs on the solution side.

11.2.1.1. Energy across Two Dielectric Media

The interaction energy of a charge situated in the IHP with its images in the metal and in the solution [with a dielectric discontinuity at the OHP] (Figure 24) can be shown to be given by[205]

$$E_{21} = \frac{e^2}{\varepsilon_1}\left\{\int_0^\infty J_0(k\rho)\, e^{-k|x|}\, dk + \int_0^\infty a_{21}(k) J_0(k\rho)\, e^{kx}\, dk + \int_0^\infty b_{21}(k) J_0(k\rho)\, e^{-kx}\, dk\right\} \tag{11.5}$$

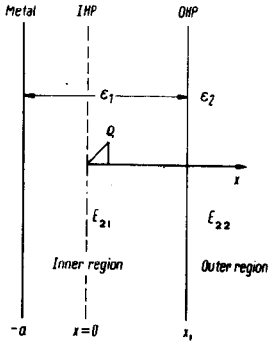


Figure 24. Relative positions of the planes of dielectric discontinuity at the metal ($x = -a$) and the OHP ($x = x_1$).

where $J_0(k)$ is the Bessel function of the first kind of zero order. In the outer region (Figure 24)

$$E_{22} = \frac{e^2}{\varepsilon_1}\int_0^\infty a_{2-\infty}(k)J_0(k\rho)\, e^{-kx}\, dk \tag{11.6}$$

Using the boundary conditions, the potential (E_{21}/e) is zero at $x = -a$ and continuous at $x = x_1$, and

$$\varepsilon_1 \frac{\partial(E_{21}/e)}{\partial x}\bigg|_{x=x_1} = \varepsilon_2 \frac{\partial(E_{22}/e)}{\partial x}\bigg|_{x=x_2}$$

The functions $a_{21}(k)$ and $b_{21}(k)$ may be evaluated,[208] and substituting for $a_{21}(k)$ and $b_{21}(k)$ in Eq. (11.5) and evaluating at $x = 0$ and $\rho = 0$, one gets

$$E_{21} = \frac{e^2}{\varepsilon_1}\left[\int_0^\infty -e^{-2ka}\, dk - \int_0^\infty \frac{\beta_1\, e^{-2kx_1}(1 - e^{-2ka})^2}{1 - \beta_1\, e^{-2k(x_1+a)}}\, dk\right] \tag{11.7}$$

Equation (11.7) represents the interaction energy of an adsorbed ion both with respect to its interaction with its images in the metal and also with those in solution.

11.2.1.2. Energy across Three Dielectric Media

This corresponds to a situation when the solution is considered to be a combination of three dielectric media with dielectric constants, ε_1, ε_2 and ε_3, respectively; and the energies in the three regions are, then, given by

$$E_{31} = \frac{e^2}{\varepsilon_1}\left[\int_0^\infty J_0(k\rho)\, e^{-k|x|}\, dk + \int_0^\infty a_{31}(k)J_0(k\rho)\, e^{+kx}\, dk + \int_0^\infty b_{31}(k)J_0(k\rho)\, e^{-kx}\, dk\right] \tag{11.8}$$

$$E_{32} = \frac{e^2}{\varepsilon_1}\left[\int_0^\infty a_{32}(k)J_0(k\rho)\, e^{-kx}\, dk + \int_0^\infty b_{32}(k)J_0(k\rho)e^{kx}\, dk\right] \tag{11.9}$$

and

$$E_{33} = \frac{e^2}{\varepsilon_1}\int_0^\infty a_{33}(k)J_0(k\rho)\, e^{-kx}\, dk \tag{11.10}$$

respectively.

Using the respective boundary conditions, and the thickness of the first, second, and third regions being $x_1 + a$, d, and infinity, respectively, one gets

$$E_{31} = \frac{e^2}{\varepsilon_1}\left[\int_0^\infty - e^{-2ka}\, dk - \int_0^\infty \frac{e^{-2kx_1}(1 - e^{-2ka})^2}{(1 + \beta_1\beta_2 e^{-2kd})/(\beta_1 + \beta_2 e^{-2kd}) - e^{-2k(x_1+a)}}\, dk\right] \tag{11.11}$$

where $\beta_2 = (\varepsilon_3 - \varepsilon_2)/(\varepsilon_3 + \varepsilon_2)$ and a is the distance of the charge in region I from the metal and x_1 is that from the dielectric boundary between the regions I and II.

11.2.1.3. Energy across Four Dielectric Plates

When the solution side is made up of four dielectric regions I, II, III, and IV with thickness $x_1 + a$, d, d, and infinity (the last one), respectively, dielectric constants ε_1, ε_2, ε_3, and ε_4, respectively, then the interaction energy of charge situated in region I, with its multiple images in solution across three other dielectric media and with those in the metal, is obtained by the similar method mentioned above and this is

$$E_{41} = \frac{e^2}{\varepsilon_1}\left\{\int_0^\infty - e^{-2ka}\, dk - \int_0^\infty \frac{e^{-2kx_1}(1 - e^{-2ka})^2}{\mathrm{B} - e^{-2k(x_1+a)}}\, dk\right\} \tag{11.12}$$

where

$$\mathrm{B} = \left[\frac{1 + (\beta_1\beta_2 + \beta_2\beta_3)\, e^{-2kd} + \beta_1\beta_3 e^{-4kd}}{\beta_1 + (\beta_2 + \beta_1\beta_2\beta_3)\, e^{-2kd} + \beta_3 e^{-4kd}}\right]$$

and

$$\beta_3 = (\varepsilon_4 - \varepsilon_3)/(\varepsilon_4 + \varepsilon_3)$$

11.2.1.4. Energy across Five Dielectric Plates

When the region having varying dielectric constant is considered to be a combination of five dielectric media I, II, III, IV, and V with thickness of the first and last region being $x_1 + a$ and infinity and the intermediate regions with thickness d each, then following the procedure described above, the multiple-image interaction energy of a charge situated in region I is given by

$$E_{51} = \frac{e^2}{\varepsilon_1}\left\{\int_0^\infty - e^{-2ka}\, dk - \int_0^\infty \frac{e^{-2kx_1}(1 - e^{-2ka})^2}{\mathrm{C} - e^{-2k(x+a)}}\, dk\right\} \tag{11.13}$$

where

$$C = \frac{1 + (\beta_1\beta_2 + \beta_2\beta_3 + \beta_3\beta_4)\, e^{-2kd} + (\beta_1\beta_3 + \beta_2\beta_4 + \beta_1\beta_2\beta_3\beta_4)\, e^{-4kd} + \beta_1\beta_4\, e^{-6kd}}{\beta_1 + (\beta_2 + \beta_1\beta_2\beta_3 + \beta_1\beta_2\beta_3\beta_4)\, e^{-2kd} + (\beta_3 + \beta_1\beta_2\beta_4 + \beta_2\beta_3\beta_4)\, e^{-4kd} + \beta_4\, e^{-6kd}}$$

11.2.1.5. Energy across Smoothly Varying Dielectric Medium

By analogy to Eqs. (11.7), (11.11), (11.12), and (11.13), the total interaction energy of a charge situated on the IHP with its multiple images in the metal and in the solution across the real varying dielectric medium may be represented by†

$$E_T = \frac{e^2}{\varepsilon_1}\left[\int_0^\infty - e^{-2ka}\, dk - \int_0^\infty \frac{e^{-2kx_1}(1 - e^{-2ka})^2 \sum_{n=0}^{\infty} \beta_{n+1} e^{-2nkd}}{1 + \beta_1 \sum_{n=1}^{\infty} \beta_{n+1} e^{-2nkd} - e^{-2k(x_1+a)} \sum_{n=0}^{\infty} \beta_{n+1} e^{-2nkd}}\, dk\right] \quad (11.14)$$

where $\beta_n = (\varepsilon_{n+1} - \varepsilon_n)/(\varepsilon_{n+1} + \varepsilon_n)$, where n is an integer and $\varepsilon_{n+1} > \varepsilon_n$, $\varepsilon_{n+1} - \varepsilon_n \geqslant \varepsilon_{n+2} - \varepsilon_{n+1}$ so that $\beta_n > \beta_{n+1}$. The function $\beta_n(x)$ is calculated from Figure 23, and the above integral is solved numerically[201] on a DEC 10 computer. For $x_1 = 2$ Å and $a = 2$ Å it was found that $E_T = -(e^2/\varepsilon_1)$ ($0.253\ 102 \times 10^8$ cm^{-1}). Now, the energy of interaction of an adsorbed charge on the IHP's with its single image in the metal is (for $a = 2$ Å), $E_s = -(e^2/2\varepsilon_1 a) = -e^2(0.25 \times 10_1\ cm^{-1})/\varepsilon_1$.

Therefore, when the solution side is considered to be a smoothly varying dielectric medium, the multiple-image interaction energy is $[(E_T - E_s)/E_s] \times 100 \simeq 1\%$ more than the single-image interaction energy.

If the dielectric boundary at a distance $x_1 = 2$ Å is assumed to be sharp, then the total energy (including the multiple imaging) which is represented by the equation (11.7), is $E_{21} = -(e^2/\varepsilon_1)$ ($0.3450 \times 10^8\ cm^{-1}$) $= 1.38E_s$. If the dielectric boundary were sharp, therefore, it would be important to use multiple imaging but the situation in the solution is that there is no sharp dielectric boundary, and hence an approach based on such a model will be a less good approximation than one based on a more realistic, diffuse boundary. The correctness of this assertion is tested below by a comparison of the abilities of discrete and diffuse approaches to replicate experiments.

11.2.2. Deduction of the Isotherm

The fraction of the surface covered by the ions adsorbed from solution may be represented by the following equation[209] derived on the basis of Flory–Huggins statistics[210]:

$$\frac{\theta}{e^{p-1}(1 - \theta)^p} = \frac{X_{1,\text{soln}}}{(X_{w,\text{soln}})^p}\, e^{-\Delta G^\circ/RT} \quad (11.15)$$

† Since $1 \gg \beta_n > \beta_{n+1}$, in generalization of the expression (11.14) the conditions, $1 \gg \beta_n\beta_{n+1} \gg \beta_{n+1}\beta_{n+2}$, have been used.

where p is the ratio of the area covered by an ion and that by a water molecule, θ is the fraction of the surface covered by the ions, $X_{i,soln}$ and $X_{w,soln}$ are the mole fractions of ions and water, respectively, in solution, and ΔG° is the standard free-energy change upon adsorption.

The standard free-energy change ΔG° is contributed by (i) a coverage-independent chemical free energy ΔG_c° and (ii) lateral interaction energy U_{lat} of an adsorbed ion with the surrounding ions.

If one considers a reference ion surrounded by a hexagonal array of ions, effectively in concentric rings of radii $1r$, $2r$, ..., nr, the energy due to interaction of the reference ion with the ions on the nth ring and their single images in the metal only is[211]

$$U_{lat} = \frac{6e^2}{\varepsilon r}\left\{1 - \left[1 + \left(\frac{2r_i}{nr}\right)^2\right]^{-1/2}\right\} \qquad (11.16)$$

where r_i is the ionic radius and r is the distance between the two successive rings, given by

$$r = \left(\frac{4}{n_a\pi}\right)^{1/2} = \left(\frac{4e}{\pi Q_{max}\theta}\right)^{1/2} = \frac{4r_i}{\pi^{1/2}\theta^{1/2}} \qquad (11.17)$$

in which n_a is the number of specifically adsorbed ion per unit area and $Q_{max} = e/4r_i^2$ is the maximum amount of contact adsorbed charge per unit area.

Substitution of (11.17) in (11.16) gives for the total lateral coulombic interaction of all ions with the central ion:

$$U_{lat} = \frac{3}{2}\frac{\pi^{1/2}e^2\theta^{1/2}}{\varepsilon r_i}\sum_{n=1}^{\infty}\left[1 - \left(1 + \frac{\pi\theta}{4n^2}\right)^{-1/2}\right] \qquad (11.18)$$

11.2.2.1. The Dispersion Interaction Energy

The dispersion interaction energy between two like ions at a distance r apart may be given by[212–214]

$$U_{disp} = -\frac{3}{4}\frac{h\nu\alpha^2 s^{1/2}}{\varepsilon_{opt} r^6} \qquad (11.19)$$

where ν is the frequency occurring in dispersive coupling between the ions, α is their polarizability, s is the number of electrons in the outer shell of the ions, and ε_{opt} is the optical dielectric constant of the medium between the interacting ions. Following the similar geometric arrangement of ions as assumed in the case of coulombic interaction, the total dispersive interaction energy of a central ion with all other adsorbed ions and their images is

$$U_{disp} = -\frac{18}{4^7}\frac{h\nu\alpha^2\pi^3\theta^3 s^{1/2}}{\varepsilon_{opt} r_i^6}\sum_{n=1}^{\infty}\frac{1}{n^5}\left[1 + \left(1 + \frac{\pi\theta}{4n^2}\right)^{-3}\right] \qquad (11.20)$$

11.2.2.2. Electrostatic Interaction of the Ion with the Electrode Charge in the Process of Adsorption

The electrostatic interaction of the ion with the electrode charge in the process of adsorption is given by

$$U_{2-1} = -\frac{4\pi\sigma_m e(x_2 - x_1)}{\varepsilon_1} \tag{11.21}$$

where σ_m is the electrode charge, x_2 and x_1 are the distances of the outer Helmholtz plane (OHP) and the inner Helmholtz plane (IHP), respectively, from the electrode surface, and ε_1 is the mean dielectric constant of the medium between the OHP and the IHP. Since the major part of U_{2-1} is done in the region where the dielectric constant attains its saturated lower value, a value of 6 to ε_1 is used in the calculations.

With $\Delta G^\circ = \Delta G_c^\circ + U_{2-1} + U_{lat} + U_{disp}$, Eq. (11.15) may be written as

$$\ln \frac{\theta}{pe^{p-1}(1-\theta)^p} = \ln N - \frac{\Delta G_c^\circ}{RT} + B_1\sigma_m - B_2\theta^{1/2}\sum_{n=1}^{\infty}\left[1 - \left(1 + \frac{\pi\theta}{4n^2}\right)^{-1/2}\right] + B_3\theta^3\sum_{n=1}^{\infty}\frac{1}{n^5}\left[1 + \left(1 + \frac{\pi\theta}{4n^2}\right)^{-3}\right] \tag{11.22}$$

where

$$B_1 = \frac{4\pi e(x_2 - x_1)}{N_0\varepsilon_1 kT}, \qquad B_2 = \frac{3}{2}\frac{e^2\pi^{1/2}}{\varepsilon_1 r_1 N_0 kT}, \qquad B_3 = \frac{18}{4^7}\frac{h\nu\alpha^2\pi^3 s^{1/2}}{\varepsilon_{opt}N_0 kTr_1^6} \tag{11.23}$$

and

$$N = \frac{X_{1,soln}}{(X_{w,soln})^p} = \frac{c_1(pc_1 + c_w)^{p-1}}{c_w{}^p} \tag{11.24}$$

where c_1 and c_w are the concentrations of ions and water, respectively, in solution.

11.2.3. Prediction of Inflection Points on θ–σ_m Curve

An inflection is observed on a θ–σ_m curve.[4,215] The single-imaging isotherm[20] [Eq. (11.22)] is shown by the inflection points. The slope of the θ–σ_m curve given by Eq. (11.22) is given by

$$\frac{d\theta}{d\sigma_m} = B_1\left\{\frac{[1 + \theta(p-1)]}{\theta(1-\theta)} + \frac{B_2}{2\theta^{1/2}}\sum_{n=1}^{\infty}\left[1 - \left(1 + \frac{\pi\theta}{4n^2}\right)^{-3/2}\right] - 3B_3\theta^2\sum_{n=1}^{\infty}\left|\frac{1}{n^5}\left[1 + \left(1 + \frac{\pi\theta}{4n^2}\right)^{-4}\right]\right\}^{-1} \tag{11.25}$$

An inflection on the θ–σ_m plot will occur when $d^2\theta/d\sigma_m{}^2 = 0$, i.e., when

$$\frac{2\theta - 1 + \theta^2(p-1)}{\theta^2(1-\theta)^2} + \frac{B_2}{4\theta^{3/2}}\sum_{n=1}^{\infty}\left|\frac{1 + \pi\theta/n^2}{(1 + \pi\theta/4n^2)^{5/2}} - 1\right| - 6B_3\theta\sum_{n=1}^{\infty}\frac{1}{n^5}\left|1 + \frac{(1 - \pi\theta/4n^2)}{(1 + \pi\theta/4n^2)^5}\right| = 0 \tag{11.26}$$

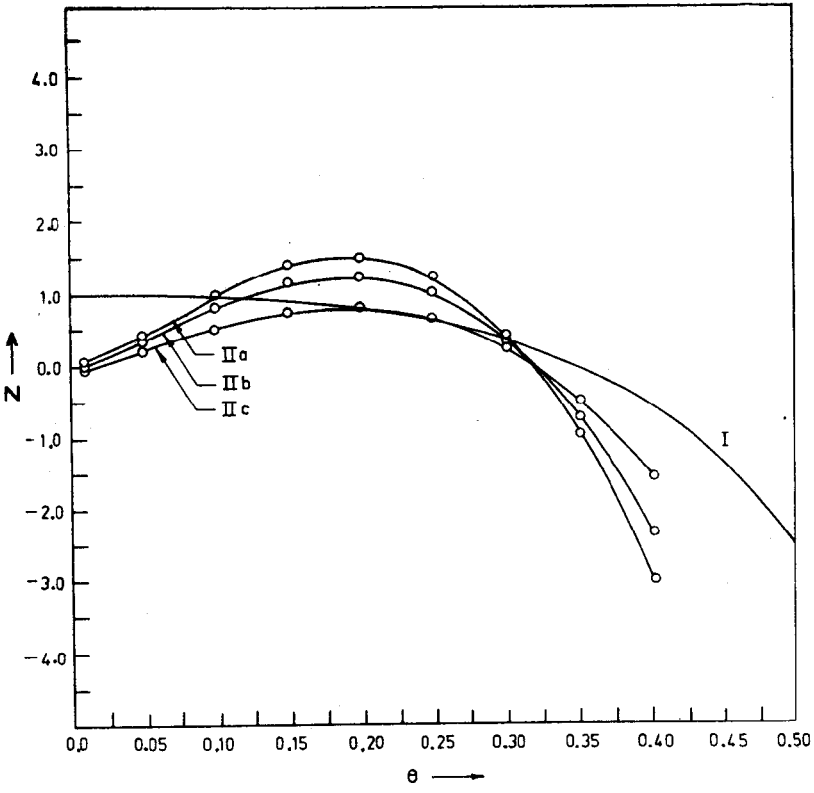


Figure 25. Plots of $Z_2(\theta)$ at temperatures 25°C (IIa), 100°C (IIb), 300°C (IIc), and $Z_1(\theta)$ (I) against θ.[201]

The roots of Eq. (11.26) may be found by plotting the functions

$$Z_1(\theta) = \frac{1 - 2\theta - \theta^2(p-1)}{(1-\theta)^2} \tag{11.27}$$

and

$$Z_2(\theta) = \frac{B_2\theta^{1/2}}{4} \sum_{n=1}^{\infty} \frac{1 + \pi\theta/n^2}{(1 + \pi\theta/4n^2)^{5/2}} - 1 - 6B_3\theta^3 \sum_{n=1}^{\infty} \frac{1}{n^5}\left[1 + \frac{1 - \pi\theta/4n^2}{(1 + \pi\theta/4n^2)^5}\right] \tag{11.28}$$

against θ.

In Figure 25 $Z_1(\theta)$ and $Z_2(\theta)$ are plotted against θ for NO_3^- ion. The

Table 7

The Values of the Parameters Used in Eqs. (11.27) *and* (11.28) *and Prediction of the Capacitance Hump*[201]

Ions	Radii (Å)[a]	$\nu \times 10^{-15}$ (sec)	s	p	Concentration (M)	θ_{hump} (expt)	θ_1	$\left(-\frac{d^2y}{d\theta^2}\right)_{\theta=\theta_1}$
				Monatomic ions				
Cl^-	1.81	1.167	8	1.72	0.3	0.01	0.070	−3622.9822
Br^-	1.96	1.035	8	2.00	0.1	0.10	0.075	−2874.5565
I^-	2.19	0.877	8	2.52	0.1	0.12	0.082	−2157.0264
				Polyatomic ions				
ClO_3^-	2.43	0.750	15	3.10	0.1	0.07	0.100	− 936.5961
BrO_3	2.43	0.750	15	3.10	0.1	0.12	0.100	− 936.5961
ClO_4^-	2.54	0.702	17	3.39	0.1	0.10	0.095	−1279.9057
NO_3^-	2.61	0.674	13	3.58	0.3	0.11	0.100	−1030.0512
SCN^-	1.6	1.404	9	1.34	1.0	0.07	0.065	−4466.4510

[a] The radii of halides are assumed as their crystallographic radii. The effective radii of ClO_3^-, BrO_3^-, ClO_4^-, and SCN^- are taken from the Reference 87 and that of NO_3^- is noted from Reference 216.

functions $Z_1(\theta)$ and $Z_2(\theta)$ intersect at two points, i.e., the Eq. (11.26) has two roots θ_1 and θ_2 and thus two inflection points on the θ–σ_m curve.

Similar inflection points are obtained for other anions. The radii and other calculated parameters are given in Table 7. The values of θ_1 and θ_2 for the anions are shown in Table 7 and 8, respectively.

Table 8

Positions of the Capacitance Minimum[201][a]

Ions	σ_m at C_{min} (expt) in ($\mu C\ cm^2$)	σ_1 at C_{min} (expt) in ($\mu C\ cm^2$)	θ_2 (expt)	θ_2 (calc)	$\left(-\frac{d^2y}{d\theta^2}\right)_{\theta=\theta_2}$
		Monatomic ions			
Cl^-	10.0	12.4	0.100	0.310	292.2027
Br^-	7.0	14.0	0.135	0.320	251.2408
I^-	3.0	16.0	0.192	0.335	200.7443
		Polyatomic ions			
ClO_3^-	13.0	8.0	0.110	0.270	222.8464
BrO_3^-	11.6	9.5	0.145	0.270	222.8464
ClO_4^-	11.5	15.0	0.240	0.275	211.1774
NO_3^-	11.1	15.0	0.256	0.305	175.6135
SCN^-	20.0	31.0	0.198	0.285	386.0631

[a] The experimental values are for solution of 0.1 N concentration. θ_{min} increases with increase of ionic radii with the exception of SCN^-. Probably the linear SCN^- ion does not adsorb normal to the surface but adsorbs flat to the surface so that the effective radii is higher than 1.6 Å.

11.2.4. Significance of the First Inflection Point, θ_1

The reciprocal of the double-layer capacitance may be represented by

$$\frac{1}{C} = \frac{1}{K_{\text{M-OHP}}} + \left(\frac{1}{K_{\text{M-OHP}}} - \frac{1}{K_{\text{M-IHP}}}\right)\frac{d\sigma_1}{d\sigma_m} + \sigma_m \frac{d}{d\sigma_m}\left(\frac{1}{K_{\text{M-IHP}}}\right) \quad (11.29)$$

where the K's are the integral capacities of the region indicated by the subscripts.

It has been shown numerically that the variations of the first and third terms in Eq. (11.29) are negligible compared with that of the second term.[218] Therefore the maxima and minima of C are caused only by the term $d|\sigma_1|/d\sigma_m$, i.e., $d\theta/d\sigma_m$ given by the condition $(d^2\theta/d\sigma_m^2) = 0$. The two roots, θ_1 and θ_2 obtained from Eq. (11.28), thus correspond to the maxima and minima on the capacitance-charge curve.

To determine which of the two roots correspond to maxima and minima, the Eq. (11.25) is differentiated twice to evaluate

$$\frac{d^3\theta}{d\sigma_m^3} = \frac{3y}{B_1}\left(\frac{d^2\theta}{d\sigma_m^2}\right)^2 - \frac{B_1^3}{y^4}\frac{d^2y}{d\theta^2} \quad (11.30)$$

where

$$y = \frac{1 + \theta(p-1)}{\theta(1-\theta)} + \frac{B_2}{2\theta^{1/2}}\sum_{n=1}^{\infty}\left[1 - \left(1 + \frac{\pi\theta}{4n^2}\right)^{-3/2}\right]$$

$$- 3B_3\theta^2\sum_{n=1}^{\infty}\frac{1}{n^5}\left[1 + \left(1 + \frac{\pi\theta}{4n^2}\right)^{-4}\right] \quad (11.31)$$

At the inflection point $d^2\theta/d\sigma_m^2 = 0$, therefore, the sign of the values of the term $-(B_1^3/y^4)(d^2y/d\theta^2)$ determines the maximum and minimum. Since B_1^3/y^4 is always positive, the maximum or minimum on the capacitance charge curve is determined by the sign of $-d^2y/d\theta^2$ for θ_1 and θ_2.

From Eq. (11.31),

$$-\frac{d^2y}{d\theta^2} = \frac{6\theta - 6\theta^2 - 2\theta^3(p-1) - 2}{\theta^3(1-\theta)^3}$$

$$- \frac{3}{8}\frac{B_2}{\theta^{5.2}}\sum_{n=1}^{\infty}\left[1 - \frac{(\pi\theta/n^2)(1 + \pi\theta/2n^2) + 1}{(1 + \pi\theta/4n^2)^{7/2}}\right]$$

$$+ 6B_3\sum_{n=1}^{\infty}\frac{1}{n^5}\left\{1 + \frac{1}{(1 + \pi\theta/4n^2)^6}\left[1 - \frac{3}{2}\frac{\pi\theta}{n^2} + \frac{3\pi^2\theta^2}{(4n^2)^2}\right]\right\} \quad (11.32)$$

In Table 7, the values of $-d^2y/d\theta^2$ obtained from Eq. (11.32) with θ_1 are shown. These are negative for all the investigated anions. Hence, the root θ_1

signifies the maximum (or hump) on the capacitance–charge curve. Good agreement is found (Table 7) by comparing the experimentally obtained coverages at which the capacitance hump occurs, with the values of θ_1 obtained from Eq. (11.27).

11.2.5. Significance of the Second Inflection Point, θ_2

The values of $-d^2y/d\theta^2$ obtained from Eq. (11.32) with the values of θ_2, are found to be positive for all the ions tested (Table 8). Therefore θ_2 signifies a minimum on the C–σ_m curve. The values of θ_2 are compared with the experimentally observed coverages at which the capacitance minimum occurs. θ_2 is higher than $C_{min,expt}$; however, with increase of ionic radii, $C_{min,expt}$ and θ_2 both increase. The discrepancy might have arisen from the rudimentary calculation of the ion–ion dispersive energy.

11.2.6. Prediction of Disappearance of Capacitance Hump and Minimum with Rise of Temperature

The capacitance hump and, consequently, the capacitance minimum disappear with rise of temperature.[217] Theoretically obtained values of θ_1 and θ_2 are shown at different temperatures for NO_3^- ion in Figure 25. In agreement with experiment,[217] as the temperature increases, the two roots θ_1 and θ_2, i.e., hump and minimum, come closer to each other and disappear.

11.3. Multiple-Imaging Isotherm

If there is a sharp dielectric discontinuity in the solution side of the interface, i.e., at the OHP, then the specifically adsorbed ions are expected to have imaging in solution and also in the metal, giving rise to the phenomena of multiple imaging. Multiple imaging has been considered by Levine, Bell, and Calvert[186] and Macdonald and Barlow.[219,220]

The isotherm given by Levine, Bell, and Calvert[186] with multiple-imaging assumption may be represented by

$$\ln \frac{\theta}{(1 - p\theta)^p} = -\frac{\Delta G_c^\circ}{RT} + \ln \frac{a_\pm}{a_0} + A'\sigma_m - C'\theta + \frac{e\psi_{diff}}{kT} \qquad (11.33)$$

where $A' = 4\pi e\gamma/\epsilon kT$, $\gamma = x_2 - r_i$, where x_2 is the distance between the electrode and OHP, $C' = 4\pi\gamma e\sigma_{max}(1 - r_i/x_2)/\epsilon kT$, ψ_{diff} is the mean potential at the OHP, and ΔG_c° has the significance as in Eq. (11.22).

The isotherm (11.33) may be written as

$$\ln \frac{\theta}{(1 - 2\theta)^2} = \text{const} + \ln a_\pm + A'\sigma_m - C'\theta \qquad (11.34)$$

where $p = 2$ as suggested by Levine,[221] and ψ_{diff} has been neglected since it is negligible in a fairly concentrated solution.

11.3.1. Inflection on the θ–σ_m Curve

At the inflection point, from (11.34)†

$$\frac{d^2\theta}{d\sigma_m{}^2} = \frac{-A'^2(4\theta^2 + 4\theta - 1)}{[1/\theta + 4/(1 - 2\theta) + C']^3\theta^2(1 - 2\theta)^2} = 0 \tag{11.35}$$

From (11.35), an inflection can occur only when

$$4\theta^2 + 4\theta - 1 = 0 \tag{11.36}$$

i.e., $\theta_1 = 0.207$ or $\theta_2 = -1.207$. A negative value of θ has no physical significance. Thus Eq. (11.36) has only one inflection point at $\theta = 0.207$ and this inflection is independent of the type of the anions, which contradicts experiment.[4]

11.3.2. Prediction of the Hump and the Minimum on the C–σ_m Curve

Whether θ_1 corresponds to a maximum or minimum on the C–σ_m curve may be determined from the value of $d^3\theta/d\sigma_m{}^3$ obtained from (11.34), i.e.,

$$\frac{d^3\theta}{d\sigma_m{}^3} = \frac{3y'}{A'}\left(\frac{d^2\theta}{d\sigma_m{}^2}\right)^2 - \frac{A'^3}{y'^4}\frac{d^2y'}{d\theta^2} \tag{11.37}$$

where

$$y' = \frac{1}{\theta} + \frac{4}{1 - 2\theta} + C' \tag{11.38}$$

For either maximum or minimum, $d^2\theta/d\sigma_m{}^2 = 0$ and hence the sign of the quantity $-(A'^3/y'^4)(d^2y'/d\theta^2)$ determines whether θ_1 represents a maximum or minimum. A'^3/y'^4 being always positive, the maxima or minima is determined by the sign of $-d^2y'/d\theta^2$. From (11.38)

$$-\frac{d^2y'}{d\theta^2} = -\left(\frac{2}{\theta^3} + \frac{32}{(1 - 2\theta)^3}\right) \tag{11.39}$$

For $\theta_1 = 0.207$, $-d^2y'/d\theta^2 = -384.5077$; hence θ_1 signifies a maximum on the C–σ_m curve. Moreover, θ_1 being independent of the nature of the anion, the capacitance maximum predicted by Eq. (11.34) is the same for all anions and thus contradicts experiment.[4] In comparison to $\theta_{hump,expt}$, the value of θ_1 is also too high (Table 7). No capacitance minimum is predicted. Disappearance of capacitance hump and minimum with rise of temperature cannot be rationalized from (11.34).

11.4. Conclusion

It may therefore be concluded that the isotherm deduced on the basis of multiple imaging across a sharp dielectric boundary is able to rationalize the

† These properties of the equations of Levine *et al.* were first pointed out by R. K. Sen.[218]

properties of the double-layer capacitance–charge curve less well than that based on the diffuse dielectric boundary, which corresponds more nearly to the real situation.

Recently, Levine and co-workers[187,188] have attempted to overcome the difficulties arising from their original model and the sharp boundary. They have assumed an arbitrary variation of dielectric constant as a function of distance from the electrode but used fixed values of dielectric constants (termed mean values) ε_1 and ε_2 over certain arbitrary distances, implying dielectric discontinuity at an arbitrary point in the inner region and at OHP. In such a case, the multiple-image energy is still significant.[201] Thus if there are two sharp boundaries, it is still important to use multiple imaging, as it is for one sharp boundary. However, *in the real situation, the existence of sharp dielectric boundary is unknown*, and the appropriate analysis for the imaging contribution to the double-layer properties should be done using a diffuse dielectric situation (continuous variation) and, in that case, the multiple-imaging contribution constitutes of only a 1% addition to the single-imaging energy.[201] The recent approach of Levine *et al.*,[187,188] therefore, still greatly overestimates the imaging energy. More discussion on Levine's approach is given in Reeves' review.[222]

12. Specific Adsorption and Solvation

12.1. General

In the early ideas of the nature of specific adsorption forces the stress was upon adsorption in a covalent sense.[2] However, the fact that ions adsorb primarily as a function of ionic radius, adsorbing more as the radius increased (cf. Figure 4), suggested that this was not a concept which lay well with the facts and this stresses that the radius-dominant forces in specific adsorption and indicate the effectiveness of dispersion interactions.

In the cases of the larger ions, no permanent "solvation sheath" comes between the ion and the electrode. It is relevant to mention the concept of primary solvation as apart from secondary solvation. Thus[223–225] there are, qualitatively, two concepts of the immediate environment of the ion. One concept refers to the coordination number of the ion, and this is a geometric and a space-filling concept: the ion will be surrounded by a certain number of water molecules independent of their orientation. The coordination number must increase, with the size of the ion. However, there is another concept in which the ionic environment depends largely upon the orientation of the water molecules in the first layer near the ion. If these are oriented to maximize the ion dipole force, and *if the radius of the ion is small enough*, the water molecules will tend to move with the ion during its translation through the solution, so that there is a mobile solvation sheath which the ion drags along with it. When the ions are sufficiently large, an effective solvation sheath does not exist, although there will

Table 9

Solvation Numbers[223] of Various Ions

Li^+	Na^+	K^+	Rb^+	Cs^+	F^-	Cl^-	Br^-	I^-
4.5	4.5	3.8	3.0	2.5	4.0	2.2	1.8	1.5

still be a "coordination number" of water molecules which do not stay with the ion during its movement.

Typical solvation numbers refer to the primary solvation sheath, which is that which moves with the ion during its migration from solution to the electrode. In Table 9, solvation numbers determined by Bockris and Saluja[223] are listed for some ions.

Similar trends in the decrease of solvation numbers for cations and anions are also observed by several other workers[225,226] (see the recent comparison made by Bockris and Saluja[227] of solvation number of ions determined by several workers). The greater is the radius the less is the solvation number. The less is the solvation number, the greater is the specific adsorption, i.e., specific adsorption decreases in the order[4,20,26] $I^- > Br^- > Cl^- > F^-$.

Thus, according to the solvation oriented structural theory of specific adsorption, although the actual bonding and the interplay between hydration heats, dispersion forces, etc., is important in determining specific adsorption, the primary determining factor is the hydration number (rather than coordination number). Thus as an ion migrates toward the electrode, it will or will not come into close contact with the electrode (the ion contacts the electrode surface), depending upon whether there is a primary hydration sheath or not. Ions with a primary hydration sheath will tend not specifically to adsorb, because they will be maintained out of contact with the electrode by the primary hydration sheath, and thus the distance between the center of the ion core and the center of the atom of the surface will be greater than that for an ion with a larger radius, such as Cl^- or I^-. The smaller ion with its larger hydration sheath will, therefore, not be specifically adsorbed because its distance-dominant forces, such as dispersion forces (r^{-6} dependent), will be small.

The solvation approach has been criticized by Barclay,[114,228] who goes back to the idea of covalent bond. Barclay argues that S^{2-} is a strongly hydrated ion; neverhteless, it is adsorbed more than any other anion. Barclay's views, involving only one ion, may be an exception of the solvation concept which correctly predicts the trend of specific adsorption of most of the other ions studied.

Vijh[229] attempted to reconcile the two views. He suggests that both the solvation effect and covalent bonding factors can be taken into account if a Born–Haber cycle is applied to the specific adsorption process regarded as a formation reaction of a surface compound:

$$X^-(S) + M \rightarrow MX + e \qquad (12.1)$$

where $X^-(S)$ is the halide ion in solution and M is the bulk compound in that the formation of a surface compound gives rise to *demetallization* of the surface. The enthalpy change in reaction (12.1) is represented on the basis of a Born–Haber cycle[230] by

$$-\Delta H^\circ_{ads} = -\Delta H_f + \tfrac{1}{2}\Delta H_{diss} + A_{x^-} + \Delta H_{hydr} + \Phi \qquad (12.2)$$

where ΔH_f is the heat of formation per anion of the surface compound MX formed, ΔH_{diss} is the heat of dissociation of a halide molecule in the gas phase to create the halide atom X, A_{x^-} is the electron affinity of the X atom, ΔH_{hydr} is heat of hydration of the halide ion X^-, and Φ is the work function of the metal. Apart from any detailed criticism of quantities involved in Eq. (12.2), this gives a reasonable trend for the adsorbability of the ions to increase with increasing calculated energy from Eq. (12.2). Complete demetallization of the surface is a debated idea[231,232] and, therefore, the model involved in this approach of Vijh[229] must be regarded as under discussion.

12.2. Conclusion

Thus, the concept of a primary solvation sheath as an important aspect of specific adsorption seems valid, i.e., the ions *tend* to be specifically adsorbed if they are bereft of their primary hydration sheath. The adsorption is determined by several quantities, solvation probably being the most important, and perhaps sometimes covalent bonding is important. There remains the difficulty in accepting a covalent view of the lack of apparently available orbitals in simple halide ions.

13. Simultaneous Specific Adsorption of Anions and Cations

13.1. Introduction

Larger cations, e.g., tetraalkylammonium ions,[27,28,233] Ti^+,[3,31,235–240] Cs^+,[29,30,234,241,242,244–247] and some aromatic cations,[200,243,244] undergo specific adsorption. The nonspecific adsorbability of cations, as assumed by Grahame[2] in the evaluation of the amount of anion specific adsorption, is thus not valid for systems with salts involving the aforesaid cations. The cation-specific adsorption is evaluated in the same way as the anion-specific adsorption with the assumption that only one ionic species undergoes specific adsorption. Thus, for the cationic adsorption case, the usual choice has been the fluoride salts of the adsorbing cations with the assumption of no specific adsorption of F^- ion. Thus the surface excess Γ_+ of cations is obtained by the electrocapillary or capacitance measurements and the specifically adsorbed charge $\sigma_1{}^+$ due to cations is calculated by subtracting from $F\Gamma_+$, the charge σ_{diff} obtained from the diffuse layer theory (cf. Section 4).

Methods which assume specific adsorption of only one ionic species are not applicable to systems in which both cations and anions undergo simultaneous specific adsorption. Delahay and co-workers[237] were the first to attempt, in the particular case of $TlNO_3$, to separate cation- and anion-specific absorption when both species undergo simultaneous specific adsorption (see below).

13.2. The Method of Delahay and Co-Workers[237]

Delahay and co-workers[237] followed a nonthermodynamic approach based on a simple electrostatic relationship and the diffuse layer theory and evaluated the specific adsorption of Tl^+ and NO_3^- ions from $TlNO_3$ electrolyte. In this case, there are two IHP's, one due to Tl^+ and the other due to NO_3^- at distances x_1^+ and x_1^- from the electrode surface, respectively (Figure 26).

For the potential difference across the different regions of the interphase, they wrote[237]

$$\phi_m - \phi_1^+ = (4\pi/\varepsilon_0)\sigma_m x_1^+ \tag{13.1}$$

$$\phi_1^+ - \phi_1^- = (4\pi/\varepsilon_0)(\sigma_m + \sigma_1^+)(x_1^- - x_1^+) \tag{13.2}$$

and

$$\phi_1^- - \phi_{2-b} = -(4\pi/\varepsilon_0)\sigma_{2-b}(x_2 - x_1^-) \tag{13.3}$$

where the ϕ's represent the average potentials on the planes denoted by the subscripts, and the superscripts + and − correspond to that by Tl^+ and NO_3^-, respectively, and ε_0 is the dielectric constant in the compact layer. Now,[8,9]

$$\sigma_{2-b} = \sigma_{2-b}^+ + \sigma_{2-b}^- = -2(RT\varepsilon C/2\pi)^{1/2} \sinh(F\phi_{2-b}/2RT) \tag{13.4}$$

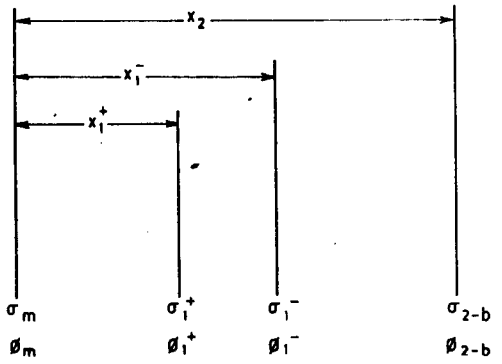


Figure 26. Model of the compact double layer with simultaneous adsorption of anions and cations.

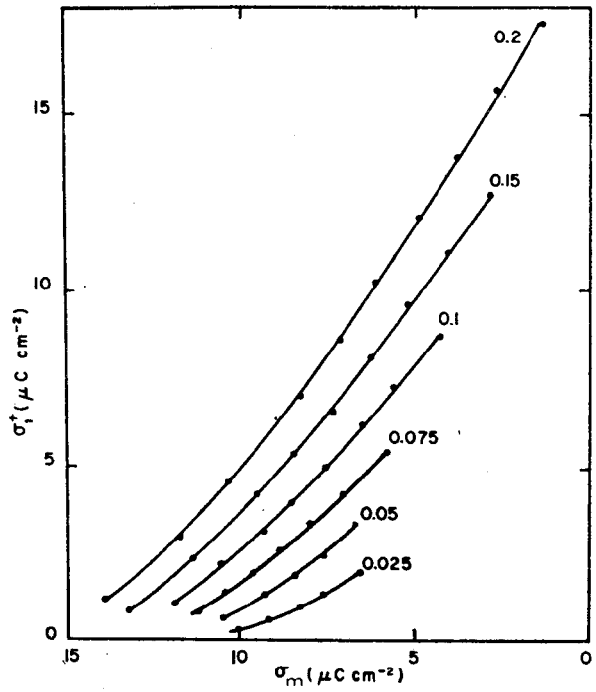


Figure 27. Amount of specifically adsorbed Tl^+ against charge density on the electrode for different $TlNO_3$ concentrations (M).[237]

The surface excesses obtained from electrocapillary or capacitance measurements may be equated to

$$F\Gamma_{Tl^+} = \sigma_1^+ + \sigma_{2-b}^+ \tag{13.5}$$

and

$$-F\Gamma_{NO_3^-} = \sigma_1^- + \sigma_{2-b}^- \tag{13.6}$$

where σ_{2-b}^+ and σ_{2-b}^- are the diffuse layer charges given by the diffuse layer theory[8,9] [cf. Eq. (5.25)].

For electroneutrality, one has

$$\sigma_m + \sigma_1^+ + \sigma_1^- + \sigma_{2-b} = 0 \tag{13.7}$$

The above equations (13.1)–(13.7) have been solved for the unknowns ϕ_1^+, ϕ_1^-, ϕ_{2-b}, σ_1^+, σ_1^-, and σ_{2-b} by iteration with the assumed values of x_1^+, x_1^-, and ε_0 ($x_1^+ = 2$ Å, $x_1^- = 3.15$ Å, $\varepsilon_0 = 6$). The amount of specifically obtained charge σ_1^+ due to Tl^+ and σ_1^- due to NO_3^- thus obtained are plotted in Figures 27 and 28, respectively.

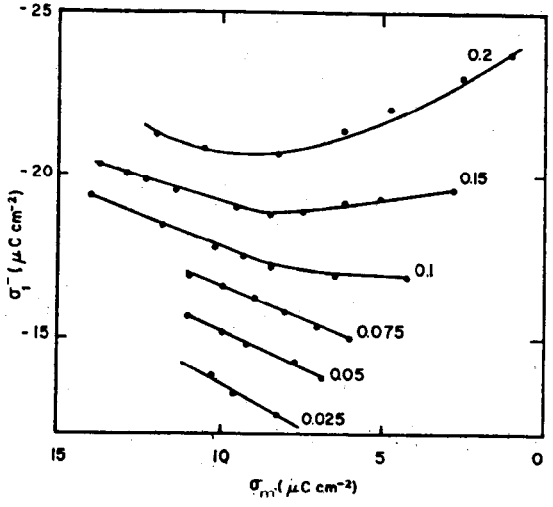


Figure 28. Amount of specifically adsorbed NO_3^- against electrode charge density for different $TlNO_3$ concentrations (M).[237]

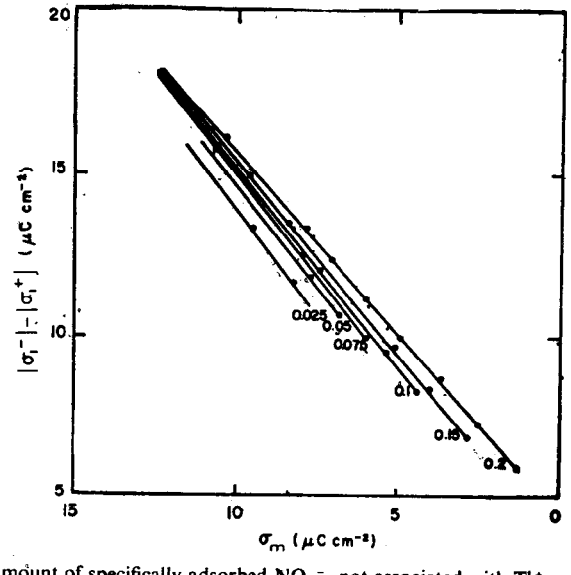


Figure 29. Amount of specifically adsorbed NO_3^-, not associated with Tl^+, against charge density on the electrode for different $TlNO_3$ concentrations (M).[237]

When values of σ_1^+ adsorbed from $TlNO_3$ are compared with those from TlF[236] it is found that the amount of Tl^+ adsorbed from both $TlNO_3$ and TlF is almost the same at lower concentrations ($c \leqslant 0.05\ M$), but values of σ_1^+ for $TlNO_3$ are higher than those for TlF at concentrations 0.075 M and higher (e.g., for a 2 M solution $\sigma_1^+ = 11.8\ C\ cm^{-2}$ for $TlNO_3$ and $\sigma_1^+ = 9.0\ C\ cm^{-2}$ for TlF at a constant electrode charge $\sigma_m = 5\ \mu C\ cm^{-2}$). Thus specific adsorption of Tl^+ is found to be enhanced by the specific adsorption of NO_3^-, and thus there is a probability of ion pair formation between the specifically adsorbed Tl^+ and NO_3^-.

Since $|\sigma_1^-| > |\sigma_1^+|$ at constant σ_m (Figures 27 and 28), one may divide σ_1^- into the amount Tl^+ associated with NO_3^- as ion pair and the remaining non-associated amount $|\sigma_1^-| - |\sigma_1^+|$ of the specifically adsorbed NO_3^- ion, as shown in Figure 29.

In the approach of Delahay *et al.*[237,238], the *a priori* choice of x_1^+, x_1^-, and ε_0 is only a first approximation, and the evaluated potentials are sensitive to these parameters. An alternative thermodynamic approach has been suggested by Hurwitz[245] and by Dutkiewicz and Parsons[246] and has been used later by Baron, Delahay, and Kelsh,[247] as discussed below.

13.3. The Method of Hurwitz[245] and of Parsons and Co-Workers[246]

Determination of simultaneous specific adsorption of anions and cations by this method involves measurements in a mixture of two salts, one containing the adsorbing cation and the other with adsorbing anion, and the measurement is made in two series as follows:

$$\text{(a)} \quad (1 - x)\text{M TlF} + x\text{M } TlNO_3 \tag{13.8}$$

$$\text{(b)} \quad (1 - x)\text{M } KNO_3 + x\text{M } TlNO_3 \tag{13.9}$$

where x is the mole fraction of $TlNO_3$.

For (a), the appropriate form of the Gibbs equation at constant temperature and pressure is

$$-d\gamma = \sigma_m\, dE_+ + \Gamma_{F^-}\, d\mu_{TlF} + \Gamma_{NO_3^-}\, d\mu_{TlNO_3} \tag{13.10}$$

If one assumes that the activity coefficients of both salts are constant, then

$$d\mu_{TlNO_3} = RT\, d \ln M_{TlNO_3} = RT\, d \ln x \tag{13.11}$$

where M_{TlNO_3} is the molal concentration of $TlNO_3$ and $x = M_{TlNO_3}/(M_{TlNO_3} + M_{TlF})$ and $M_{TlNO_3} + M_{TlF}$ is constant. Similarly,

$$d\mu_{TlF} = RT\, d \ln (1 - x) = -RT[x/(1 - x)]\, d \ln x \tag{13.12}$$

Substitution of Eqs. (13.11) and (13.12) in (13.10) gives

$$-d\gamma = \sigma_m\, dE_+ + RT\left(\Gamma_{NO_3^-} - \frac{x}{1 - x}\Gamma_{F^-}\right) d \ln x \tag{13.13}$$

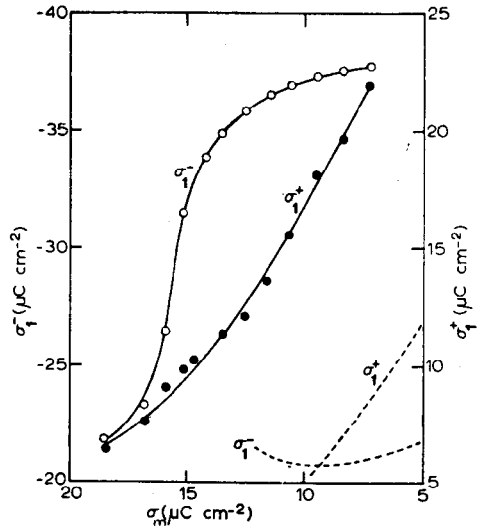


Figure 30. Simultaneous specific adsorption of Tl^+ (●) and NO_3^- (○) for 0.2 *M* $TlNO_3$ vs. electrode charge.[247] Dashed curve according to nonthermodynamic approach of Delahay *et al.*[237]

Since the concentration in the diffuse layer of ions of the same charge is directly proportional to their bulk concentration, and F^- ion is assumed to be present in the diffuse layer only, then it follows that

$$\frac{\Gamma^{2-b}_{NO_3^-}}{\Gamma_{F^-}} = \frac{x}{1-x} \tag{13.14}$$

where $\Gamma^{2-b}_{NO_3^-}$ is that part of the surface excess of NO_3^- ions which are present in the diffuse layer. Substituting Eq. (13.14) in Eq. (13.13) one gets

$$-d\gamma = \sigma_m\, dE_+ + (RT/F)\sigma_{(NO_3^-)}\, d\ln x \tag{13.15}$$

where $\sigma_{1\,(NO_3^-)}^- = F(\Gamma_{NO_3^-} - \Gamma^{2-b}_{NO_3^-})$ is the specifically adsorbed charge due to NO_3^- ions.

Similarly, for series (b),

$$-d\gamma = \sigma_m\, dE_- + \frac{RT}{F}\sigma_{1\,(Tl^+)}^+ d\ln x \tag{13.16}$$

The amount of specifically adsorbed charge may now be obtained from Eqs. (13.15) and (13.16) with measured values of interfacial surface tension at a constant potential. In Figure 30, the amounts of specifically adsorbed Tl^+ and NO_3^- ions obtained by this method by Baron, Delahay, and Kelsh[247] are shown and compared with those obtained earlier by the nonthermodynamic approach

of Delahay *et al.*[237] This method[245,246] has also been applied by Hills and Reeves[248] for their studies of Br^- adsorption from a mixture of KBr and KF salts.

13.4. Discussion

The nonthermodynamic approach of Delahay *et al.*[237] suffers from the disadvantages of the *a priori* choice of x_1^+, x_1^-, and ε_0, which may only be considered as a first approximation. This method also relies heavily on the diffuse layer theory and incorporates the shortcomings of this theory discussed earlier in Section 7.

The thermodynamic approach of Hurwitz[245] and Parsons *et al.*[246] has its advantage in that it avoids the use of Gouy–Chapmann theory and the specifically adsorbed charges are derived from the direct experimentally measured surface tension. Comparison of results in Figure 30 shows that the amount of specifically adsorbed charge of Tl^+ and NO_3^- obtained by the nonthermodynamic approach is substantially lower than those obtained by thermodynamic approach. Baron *et al.*[247] attributed these discrepancies to the unsatisfactory nature of the assumptions made in the nonthermodynamic method based on a simple electrostatic model for distribution of potentials in the compact double layer.

The thermodynamic approach has its disadvantage in assuming the same plane of losest approach for F^- and NO_3^- and the nonspecific adsorbability of F^- ion, which, however, is now found to undergo specific adsorption,[249–251] at least at electrode charges $\sigma_m \geq 6\ \mu C\ cm^{-2}$. Therefore evaluation of specific adsorption at charges greater than $\sigma_m = 6\ \mu C\ cm^{-2}$ by the thermodynamic method[245–247] is uncertain and must be corrected by taking into account the specific adsorption of F^- ion.

Development in this direction has been made by Lakshmanan and Rangarajan,[252] who have shown that information on simultaneous specific adsorption of two individual anions (or cations) may be obtained by making measurements of the two salts with common anions (or common cations) at constant mole ratio, but varying the total ionic strength $I = \frac{1}{2}\sum m_i z_i^2$ and through a knowledge of another differential coefficient such as $(\partial\gamma/\partial \ln I)_{E_+}$, or $(\partial\xi^+/\partial \ln I)_{\sigma_m,E}$, where xI is the mole fraction of one of the anions and $(1 - x)I$ is that of the other and $\xi = \gamma + \sigma_m E$. The procedure is as follows:

For a system of one metallic phase and a mixture of two 1:1 salt with a common cationic species, viz., j and two anionic species i_1 and i_2 and the neutral component of the solvent, say, H_2O only, then the electrocapillary equation for ideally polarized electrode, when the reference electrode (sometimes referred to as indicator electrode[155]) is reversible to the cation, may be written as

$$d\gamma = -\sigma_m\, dE_+ - \sum_{i=1,2} \Gamma_{i,H_2O}\, d\mu_i \qquad (13.17)$$

where Γ_{i,H_2O} denote the relative surface excesses of the anions and $[\mu_i]_{i=1,2}$ is the chemical potential of the two salts. Since the solution is now a mixture of two salts, the interfacial tension is a function of chemical potential of both the salts, i.e.,

$$\gamma = f(\mu_1, \mu_2) = f(\mu_1, I)$$

where I is the total molal ionic strength.

If the individual molality of salt 1 be $m_1 I$ then the molality of the salt 2 is $(1 - m_1)I$ so that the total molal ionic strength is I; then from Eq. (13.17),

$$\frac{1}{RT}\left(\frac{\partial \gamma}{\partial \ln m_1}\right)_{E_+,I} = -\left(\Gamma_1 - \frac{m_1}{1-m_1}\Gamma_2\right) - 2\sum_{i=1,2}\Gamma_i\left(\frac{\partial \ln \gamma_{i\pm}}{\partial \ln m_1}\right)_I \quad (13.18)$$

where the $\gamma_{i\pm}$'s are the mean activity coefficients of the salts 1 and 2 in the mixture, and m_1 is the mole ratio of the salt 1.

If the total ionic strength is varied, say $I = 1, 2, 3$, etc., then it is possible to write from Eq. (13.17) that

$$\frac{1}{2RT}\left(\frac{\partial \gamma}{\partial \ln I}\right)_{E_+,m_1} = -(\Gamma_1 + \Gamma_2) - \sum_{i=1,2}\Gamma_i\left(\frac{\partial \ln \gamma_{i\pm}}{\partial \ln I}\right)_{m_1} \quad (13.19)$$

By solving Eqs. (13.18) and (13.19), it is possible to get individual surface excesses of the anions. Having evaluated the total surface excesses of the two anions, the surface excess of cations may be obtained from

$$-\sigma_m = F(\Gamma_+ - \Gamma_-) \quad (13.20)$$

If all Γ_+ are assumed to be in the diffuse layer the total diffuse layer charge due to anions as well as their individual contributions $\Gamma_{1,d}$ and $\Gamma_{2,d}$ may be obtained with the help of diffuse layer theory. The specifically adsorbed charge due to individual anions σ_1^- and σ_2^- may then be obtained from

$$\sigma_i^- = F(\Gamma_i - \Gamma_{i,d}) \quad (13.21)$$

where $i = 1$ or 2.

Simultaneous solution of the equations (13.18) and (13.19) to obtain individual surface excesses Γ_1 and Γ_2 of the anions demands a knowledge of $(\partial \ln \gamma_{i\pm}/\partial \ln m_1)_I$ and $(\partial \ln \gamma_{i\pm}/\partial \ln I)_{m_1}$ requiring activity coefficient data in mixed-electrolyte systems. Such data have been reported in the literature[253] for some salts at various molal ratios of the salts in the mixture and at constant total molal ionic strengths. In the earlier analysis of results in mixed electrolytes, either the variation of activity coefficients of the salts with change in composition of the mixture was neglected or the activity coefficient was assumed to be unity. The former assumption is reasonable when the activity coefficients of the salts in the mixture are closely similar as for KI–KF mixtures.[246] This method of Lakshmanan and Rangarajan[252] has been applied recently by Baugh and Parsons[254] to study the adsorption of guanidium ion from solutions containing also sodium and chloride ions and also from solutions containing potassium and

chloride ion. The effect of the activity coefficient term in Eqs. (13.18) and (13.19) is estimated by assuming that the activity coefficient of guanidium chloride is the same as that of tetramethylammonium chloride[255] in its pure aqueous solution and also by assuming that the activity coefficients in the mixtures were equal to those in the single-salt solution at the same ionic strength. These are rough approximations and therefore, though the method of Lakshmanan and Rangarajan[252] is an advancement towards the understanding of simultaneous adsorption of more than one anion (or cation), further development is needed which takes into account the variation of activity coefficients of the salts in the mixture.

References

1. M. Gouy, *Ann. Chim. Phys* **29**(7), 145 (1903); **8**(8), 291 (1906); **9**, 75 (1906).
2. D. C. Grahame, *Chem. Rev.* **41**, 441 (1947).
3. A. N. Frumkin and A. S. Titievskaya, *Zh. Fiz. Khim.* **31**, 485 (1957).
4. H. Wroblowa, Z. Kovac, and J. O'M. Bockris, *Trans. Faraday Soc.* **61**, 1523 (1965).
5. H. L. F. von Helmholtz *Ann. Phys.* (*Leipzig*) **89**(2), 211 (1853); **7**(3), 337 (1879); *Wiss. Abhandl. Physik. Tech. Reichsanstalt I*, p. 925 (1879); *Monatsh. Preuss Akad. Sci.* (November 1881).
6. G. Quincke, *Ann. Phys.* (*Leipzig*) **113**(2), 513 (1861).
7. O. Stern, *Z. Elektrochem.* **30**, 508 (1924).
8. G. Gouy, *J. Phys.* **9**, 457 (1910).
9. D. L. Chapman, *Philos. Mag.* **25**(6), 475 (1913).
10. N. A. Balashova, *Dokl. Aka. Nauk SSSR* **103**, 639 (1955).
11. N. A. Balashova, *Z. Phys. Chem.* **207**, 340 (1962).
12. N. A. Balashova, *Electrochim. Acta* **7**, 559 (1962).
13. N. A. Balashova and N. Merkulova, *Soviet Electrochemistry*, Vol. 1, Consultants Bureau, New York (1961), p. 23.
14. V. E. Kazarinov and N. A. Balashova, *Dokl. Akad. Nauk SSSR* **157**, 1174 (1964).
15. E. A. Blomgren and J. O'M. Bockris, *Nature* **186**, 305 (1960).
16. H. V. Euler, *Z. Electrochem.* **28**, 446 (1922).
17. M. A. Proskurnin and A. N. Frumkin, *Z. Phys. Chem.* (*Leipzig*) **A155**, 29 (1933).
18. B. E. Conway and R. G. Barradas, and T. Zavidsky, *J. Phys. Chem.* **62**, 676 (1958).
19. R. G. Barradas and B. E. Conway, *J. Electroanal. Chem. Interfacial Electrochem.* **6**, 314 (1963).
20. T. N. Anderson and J. O'M. Bockris, *Electrochim. Acta* **9**, 347 (1964).
21. R. A. Fredlein, A. Damjanovic, and J. O'M. Bockris, *Surface Sci.* **25**, 261 (1971).
22. Y. Chiu and M. A. Genshaw, *J. Phys. Chem.* **72**, 4325 (1968).
23. Y. Chiu and M. A. Genshaw, *J. Phys. Chem.* **73**, 3571 (1969).
24. E. Passaglia, R. R. Stromberg, and J. Kruger, eds., *Ellipsometry in the Measurement of Surfaces and Thin Films, Symposium Proceedings, Washington, 1963, U.S. Department of Commerce*, National Bureau of Standards Miscellaneous Publications 256, U.S. Government Printing Office, Washington D.C. (1964).
25. Woon-kie Paik, M. A. Genshaw, and J. O'M. Bockris, *J. Phys. Chem.* **74**, 4266 (1970).
26. J. O'M. Bockris, M. A. V. Devanathan, and K. Müller, *Proc. R. Soc. London Ser., A* **274**, 55 (1963).
27. T. Yoshida, S. Nomoto, and N. Kimizuka, *Mem. Sch. Sci. Eng. Waseda Univ.* **31**, 81 (1967).

28. R. J. Meakins, M. G. Stevens, and R. J. Hunter, *J. Phys. Chem.* 73, 112 (1969).
29. R. Parsons and A. Stockton, *J. Electroanal. Chem.* 25 (1970), App. 10.
30. R. V. Ivanova, B. B. Damaskin, and I. Mazurek, *Elektrokhimiya* 6, 1041 (1970); B. B. Damaskin and R. V. Ivanova, *Divinoi Sloi Absorbt. Tuerd. Elektrodakh. Mater. Simp. 2nd*, 139 (1970).
31. N. S. Polianovskaya, A. N. Frumkin, and B. B. Damaskin, *Elektrokhimiya* 7, 578 (1971).
32. S. Minc and M. J. Jurkiewicz-Herbich, *J. Electroanal. Chem. Interfacial Electrochem.* 40, 229 (1972).
33. R. Parsons, in *Modern Aspects of Electrochemistry*, J. O'M. Bockris and B. E. Conway, eds., Vol. 1, Butterworths, London (1954) (Reprinted 1968).
34. D. C. Grahame and R. W. Whitney, *J. Am. Chem. Soc.* 64, 1548 (1942).
35. G. Lippmann, *Ann. Chim. Phys.* (5) 5, 494 (1875).
36. M. A. V. Devanathan and B. V. K. S. R. A. Tilak, *Chem. Rev.* 65, 635 (1965).
37. R. Parsons, *Trans. Faraday Soc.* 51, 1518 (1955).
38. D. C. Grahame and B. A. Soderberg, *J. Chem. Phys.* 22, 449 (1954).
39. D. C. Grahame, *J. Chem. Phys.* 21, 1054 (1953).
40. J. W. Gibbs, *Collected Works*, Vol. 1, Longmans, Green, New York (1928).
41. E. Warburg, *Ann. Phys. (Leipzig)* 41, 1 (1891).
42. J. W. Gibbs, *Collected Works*, Vol. 1, Longmans, Green, New York (1928) p. 336.
43. A. N. Frumkin, *Z. Phys. Chem.* 103, 55 (1923).
44. S. R. Craxford, *Trans. Faraday Soc.* 36, 85 (1940).
45. A. G. Samercev, *Z. Phys. Chem.* 168, 45 (1934).
46. F. O. Koenig, *J. Phys. Chem.* 38, 111, 339 (1934).
47. R. Parsons and M. A. V. Devanathan, *Trans. Faraday Soc.* 49, 404 (1953).
48. R. S. Hansen, Y. Fu, and F. E. Bartell, *J. Phys. Colloid Chem.* 53, 769 (1949).
49. N. Hackerman and A. H. Roebuck, *Ind. Eng. Chem.* 46, 1481 (1954).
50. E. L. Cook and N. Hackerman, *J. Phys. Chem.* 55, 541 (1951).
51. N. A. Balashova and V. E. Kazarinov, in *Electroanalytical Chemistry*, A. J. Bard, ed., Vol. 3, Marcel Dekker, New York (1969).
52. N. A. Balashova and N. S. Merkulova, in *New Methods of Physical and Chemical Researches, Proceedings of Institute of Physical Chemistry*, Vol. 6, Academy of Sciences, USSR, (1957).
53. V. E. Kazarinov and N. A. Balashova, *Dokl. Akad. Nauk SSSR* 139, 641 (1961).
54. L. A. Medvedeva and Ya. M. Kolotyrkin, *Zh. Fiz. Khim.* 31, 2668 (1957).
55. K. E. Heusler and G. H. Cartledge, *J. Electrochem. Soc.* 108, 732 (1961).
56. N. Hackerman and S. Spethans, *J. Phys. Chem.* 58, 904 (1954).
57. I. Bordeaux and N. Hackerman, *J. Phys. Chem.* 61, 1323 (1957).
58. K. Schwabe, K. Wagner, and Ch. Weissmantel, *Z. Phys. Chem.* (*Leipzig*) 206, 309 (1957).
59. V. E. Kazarinov and N. A. Balashova, *Dokl. Akad. Nauk SSSR* 134, 864 (1960).
60. S. P. Wolsky, P. M. Rodriguez, and W. Weining, *J. Electrochem. Soc.* 103, 606 (1956).
61. V. S. Sotnikov and A. S. Belanovsky, *Radiochemistry* 4, 725 (1962).
62. N. A. Balashova, V. V. Eletsky, and W. Weining, *J. Electrochem. Soc.* 103, 606 (1956).
63. M. Green, D. A. J. Swinkles, and J. O'M. Bockris, *Rev. Sci. Instrum.* 33, 18 (1962).
64. F. Joliot Curie, *J. Chem. Phys.* 27, 119 (1930).
65. K. Schwabe, *Chem. Tech.* (*Berlin*) 13, 275 (1961).
66. K. Schwabe, *Isotopentechnik* 1, 175 (1960–1961).
67. H. Wroblowa and M. Green, *Electrochim. Acta* 8, 679 (1963).
68. H. Dahms, M. Green, and J. Weber, *Nature* 188, 1310 (1962).
69. H. Dahms and M. Green, *J. Electrochem. Soc.* 110, 1075 (1963).
70. J. A. Kafalos and H. C. Gatos, *Rev. Sci. Instrum.* 29, 47 (1958).

71. J. A. Anninanson, *J. Phys. Chem.* **55**, 1286 (1951).
72. W. W. Harvey, W. I. la Fleuer, and H. G. Gatos, *J. Electrochem. Soc.* **109**, 155 (1962).
73. K. Schwabe and W. Schwenke, *Electrochim. Acta* **9**, 1003 (1964).
74. R. Dreyer and I. Dreyer, *Z. Phys. Chem.* (*Leipzig*) **220**, 283, 423 (1963).
75. V. E. Kazarinov, *Elektrokhimiya* **2**, 1170 (1966).
76. V. E. Kazarinov, *Elektrokhimiya* **8**, 393 (1972).
77. V. E. Kazarinov, G. Ya. Tysyschnaya, and V. N. Andreev, *J. Electroanal. Chem. Interfacial Electrochem.* **65**, 391 (1975).
78. A. Wieckowski and J. Sobkowski, *J. Electroanal. Chem. Interfacial Electrochem.* **73**, 317 (1976).
79. V. E. Kazarinov and G. N. Mansurov, *Elektrokhimiya* **2**, 1338 (1966).
80. E. Gileadi, B. T. Rubin, and J. O'M. Bockris, *J. Phys. Chem.* **69**, 335 (1965).
81. E. Gileadi, L. Duic, and J. O'M. Bockris, *Electrochim. Acta* **13**, 1915 (1968).
82. E. Gileadi, *J. Electroanal. Chem. Interfacial Electrochem.* **11**, 137 (1966).
83. W. Paik, in *M.T.P. International Review of Science* (*Physical Chemistry Series One*) J. O'M. Bockris, ed., Vol. 6, Butterworths, London (1972).
84. F. L. McCrakin and J. P. Colson, in *Ellipsometry in the Measurement of Surfaces and Thin Films, Symposium Proceedings, Washington, 1963, U.S. Department of Commerce*, E. Passaglia, R. R. Stromberg, and J. Kruger, eds., National Bureau of Standards, Miscellaneous Publications 256, U.S. Government Printing Office, Washington, D.C. (1964), p. 229.
85. O. S. Heavens, *Optical Properties of Thin Solid Films*, Butterworths, New York and London (1955), pp. 125, 126.
86. E. A. Moelwyn-Hughes, *Physical Chemistry*, Pergamon Press, New York (1958), p. 164.
87. Z. Kovac, Ph.D. thesis, University of Pennsylvania, Philadelphia, Pennsylvania, 1964.
88. J. Lawrance, R. Parsons, and R. Payne, *J. Electroanal. Chem. Interfacial Electrochem.* **16**, 193 (1968).
89. G. A. Bootsma and F. Meyer, *Surface Sci.* **14**, 52 (1969).
90. F. Meyer and G. A. Bootsma, *Surface Sci.* **16**, 221 (1969).
91. F. Meyer, E. E. Dekluizenaar, and G. A. Bootsma, *Surface Sci.* **27**, 88 (1971).
92. F. Meyer, *Surface Sci.* **27**, 107 (1971).
93. F. L. McCrakin, E. Passaglia, R. R. Stromberg, and H. L. Steinberg, *J. Res. Natl. Bur. Stand. Part A* **67**, 363 (1963).
94. K. H. Zaininger and A. G. Revesz, *R.C.A. Rev.* **25**, 85 (1964).
95. D. C. Grahame and R. Parsons, *J. Am. Chem. Soc.* **83**, 1291 (1961).
96. M. A. V. Devanathan and P. Peries, *Trans. Faraday Soc.* **50**, 1236 (1954).
97. A. N. Frumkin, R. V. Ivanova, and B. B. Damaskin, *Dokl. Akad. Nauk SSSR* **157**, 1202 (1964).
98. M. A. V. Devanathan and S. G. Canagaratna, *Electrochim. Acta* **8**, 77 (1963).
99. A. N. Frumkin, N. B. Grigorjev, and N. A. Bagotskaya, *Dokl. Akad. Nauk SSSR* **157**, 957 (1964).
100. A. N. Frumkin, N. S. Polyanovkaya, and N. B. Grigorjev, *Dokl. Akad. Nauk SSSR* **157**, 1455 (1964).
101. R. Parsons and F. G. R. Zobel, *J. Electroanal. Chem. Interfacial Electrochem.* **9**, 333 (1965).
102. J. M. Parry and R. Parsons, *Trans. Faraday Soc.* **59**, 241 (1963).
103. J. O'M. Bockris, K. Müller, H. Wroblowa, and Z. Kovac, *J. Electroanal. Chem. Interfacial Electrochem.* **10**, 416 (1965).
104. M. A. V. Devanathan, thesis, University of London, 1951.

105. J. O'M. Bockris and M. A. Habib, *J. Electroanal. Chem. Interfacial Electroehem.* **65**, 473 (1975).
106. R. Payne, *J. Electroanal. Chem. Interfacial Electrochem.* **15**, 95 (1967).
107. J. O'M. Bockris, K. Müller, H. Wroblowa, and Z. Kovac, *J. Electroanal. Chem. Interfacial Electrochem.* **15**, 101 (1967).
108. D. C. Grahame, *J. Am. Chem. Soc.* **76**, 4819 (1954).
109. D. J. Schiffrin, *J. Electroanal. Chem. Interfacial Electrochem.* **23**, 168 (1969).
110. D. C. Grahame, *J. Am. Chem. Soc.* **71**, 2975 (1949).
111. J. Lawrance and D. M. Mohilner, *J. Electrochem. Soc.* **1118**, 259 (1971).
112. D. C. Grahem, ONR Tech Report No. 14, February 18, 1954, Project NR 051–150.
113. S. Trasatti, *J. Electroanal. Chem. Interfacial Electrochem.* **31**, 17 (1971).
114. D. J. Barclay, *J. Electroanal. Chem. Interfacial Electrochem.* **28**, 443 (1970).
115. B. D. Cahan, Ph.D. thesis, University of Pennsylvania, 1968.
116. A. W. Adamson, *Physical Chemistry of Surfaces*, 2nd Ed. Interscience Publishers, New York (1967), p. 355.
117. J. O'M. Bockris and B. D. Cahan, *J. Chem. Phys.* **50**, 1307 (1969).
118. T. Young, *Miscellaneous Works*, G. Peacock, ed., Vol. I Murray, London (1855), p. 418.
119. A. Dupré, *Theorie Mecanique de la Chaleur*, Paris (1869), p. 368.
120. C. Kemball, *Proc. R. Soc. London Ser. A* **190**, 117 (1947).
121. A. N. Frumkin, A. W. Gorodetzkaya, B. Kabanov, and N. Nekrasov, *Zh. Fiz. Khim.* **1**, 225 (1932).
122. J. P. Tverdovskii and A. N. Frumkin, *Zh. Fiz. Khim.* **21**, 819 (1947).
123. T. R. Beck, *J. Phys. Chem.* **73**, 466 (1969).
124. J. O. Draffin and W. L. Collins, *Statics and Strength of Materials* (Ronald Press, New York, 1950).
125. N. A. Balashova and V. E. Kazarinov, *Elektrokhimiya* **1**, 512 (1965).
126. S. Gilman, *J. Phys. Chem.* **68**, 2098, 2112 (1964).
127. M. A. Genshaw, V. Brusic, H. Wroblowa, and J. O'M. Bockris, *Electrochim. Acta* **16**, 1859 (1971).
128. H. Wroblowa, V. Brusic, and J. O'M. Bockris, *J. Phys. Chem.* **75**, 2823 (1971).
129. N. Sato and K. Kudo, *Electrochim. Acta* **6**, 447 (1971).
130. P. Debye and E. Huckel, *Z. Phys. (Leipzig)* **24**, 185, 305 (1923).
131. B. E. Conway, J. O'M. Bockris, and I. A. Ammar, *Trans. Faraday Soc.* **47**, 756 (1951).
132. N. Bjerrum, *Kgl. Danske Vidensk. Selskab* **7**, No. 9 (1926).
133. R. M. Fuoss, *J. Am. Chem. Soc.* **55**, 2387 (1933); **57**, 1 (1935).
134. J. O'M. Bockris and A. K. N. Reddy (eds.), *Modern Electrochemistry*, Vol. 1, Plenum Rosetta Edition, Plenum Press, New York (1973).
135. K. M. Joshi and R. Parsons, *Electrochim. Acta* **4**, 129 (1961).
136. R. Parsons and S. Trasatti, *Trans. Faraday Soc.* **65**, 3314 (1969).
137. R. Payne, *J. Electrochem. Soc.* **113**, 999 (1966).
138. B. B. Damaskin, R. V. Ivanova, and A. A. Survila, *Elektrokhimiya* **1**, 767 (1965).
139. G. H. Nancollas, D. S. Reid, and C. A. Vincent, *J. Phys. Chem.* **70**, 3300 (1966).
140. B. B. Damaskin and R. V. Ivanova, *Zh. Fiz. Khim.* **38**, 176 (1964).
141. P. Delahay, *Double Layer and Electrode Kinetics*, Interscience, New York (1965).
142. D. C. Grahame, *J. Chem. Phys.* **18**, 903 (1950).
143. M. J. Sparnay, *Rec. Trav. Chim.* **77**, 872 (1958).
144. H. Brodowsky and H. Strehlow, *Z. Elektrochim.* **63**, 262 (1959).
145. A. Sanfeld, A. Steinchen-Sanfeld, H. Hurwitz, and R. Defay, *J. Chim. Phys. Phys.-Chim. Biol.* **59**, 139 (1962).
146. J. R. Macdonald, *J. Chem. Phys.* **22**, 1857 (1952).
147. V. Freise, *Z. Elektrochem.* **56**, 822 (1952).
148. F. H. Stillinger and J. G. Kirkwood, *J. Chem. Phys.* **33**, 1282 (1960).

149. V. G. Levich and V. S. Krylov, *Doklady Akad. Nauk SSSR* **141**, 1403 (1961).
150. V. S. Krylov and V. G. Levich, *Zh. Fiz. Khim.* **37**, 106, 2273 (1963).
151. Bikerman, *Philos. Mag.* **33**, 384 (1942).
152. R. Parsons, in *Advances in Electrochemistry and Electrochemical Engineering*, P. Delahay, ed., Vol. 1, Interscience Publishers, New York, (1961), Chap. 1.
153. W. G. McMillan and J. E. Mayer, *J. Chem. Phys.* **13**, 276 (1945).
154. H. C. Anderson, in *Modern Aspects of Electrochemistry*, B. E. Conway and J. O'M. Bockris, eds., Vol. 11, Plenum Press, New York (1975).
155. D. M. Mohilner, in *Electroanalytical Chemistry*, A. J. Bard, ed., Vol. 1, Marcel Dekker, New York (1966).
156. S. Glasstone, *Textbook of Physical Chemistry* (Van Nostrand, Princeton, 1946), p. 961.
157. W. Lorenz and G. Salie, *Z. Phys. Chem. (Leipzig)* **218**, 259 (1961).
158. W. Lorenz, *Z. Phys. Chem. (Leipzig)* **218**, 272 (1961).
159. W. Lorenz and G. Salie, *Z. Phys. Chem. Neue Folge* **29**, 390, 408 (1961).
160. W. Lorenz, *Z. Phys. Chem.* **219**, 421 (1962).
161. W. Lorenz and G. Kruger, *Z. Phys. Chem. (Leipzig)* **221**, 231 (1962).
162. G. Krüger, W. Lorenz, and P. Theml, *Z. Phys. Chem.* **222**, 81 (1963).
163. W. Lorenz, *Z. Phys. Chem.* **224**, 145 (1963).
164. W. Lorenz, *Z. Phys. Chem.* **227**, 419 (1964).
165. G. Salie and W. Lorenz, *Z. Elektrochem. N.F.* **68**, 197 (1964).
166. W. Lorenz and U. Gaunitz, *Collect Czech. Chem. Commun.* **31**, 1389 (1966).
167. W. Lorenz, *Z. Phys. Chem. (Leipzig)* **232**, 176 (1966).
168. W. Lorenz and G. Kruger, *Z. Phys. Chem. (Leipzig)* **236**, 253 (1967).
169. W. Lorenz, *Z. Phys. Chem. Neue Folge* **54**, 191 (1967).
170. W. Lorenz and G. Kruger, *Z. Phys. Chem. Neue Folge* **56**, 268 (1967).
171. W. Lorenz, *Z. Phys. Chem. (Leipzig)* **244**, 65 (1970).
172. B. E. Conway and J. O'M. Bockris, *Proc. R. Soc. London Ser. A* **248**, 394 (1958).
173. D. C. Grahame, *J. Am. Chem. Soc.* **80**, 4201 (1958).
174. K. J. Vetter and W. J. Plieth, *Z. Phys. Chem. Neue Folge* **61**, 282 (1968); **65**, 189 (1969); *Collect. Czech. Chem. Commun.* **36**, 816 (1971).
175. K. J. Vetter and J. W. Plieth, *Ber. Bunsenges. Phys. Chem.* **72**, 673 (1968); **73**, 79 (1969).
176. R. Parsons, *Advances in Electrochemistry and Electrochemical Engineering*, P. Delahay and C. W. Tobias, eds., Vol. 7, Interscience Publishers, New York (1970).
177. B. B. Damaskin, *Elektrokhimiya* **5**, 771 (1969).
178. K. J. Vetter and J. W. Schultze, *Ber. Bunsenges. Phys. Chem.* **76**, 920, 927 (1972).
179. J. W. Schultze and K. J. Vetter, *J. Electroanal. Chem. Interfacial Electrochem.* **44**, 63 (1973).
180. K. J. Vetter and J. W. Schultze, *J. Electroanal. Chem. Interfacial Electrochem.* **53**, 67 (1974).
181. J. W. Schultze and F. D. Koppitz, *Electrochimica Acta* **21**, 327, 337 (1976).
182. J. W. Schultze, Proceedings of the 2nd International Summer School on Quantum Mechanical Aspects of Electrochemistry, Ohrid, Yugoslavia, 1972.
183. D. C. Grahame and R. Parsons, *J. Am. Chem. Soc.* **83**, 1291 (1961).
184. D. D. Bode, Jr., *J. Phys. Chem.* **76**, 2915 (1972).
185. T. N. Anderson, J. L. Anderson, and H. Eyring, *J. Phys. Chem.* **73**, 3562 (1969).
186. S. Levine, G. M. Bell, and D. Calvert, *Can. J. Chem.* **40**, 518 (1962).
187. K. Robinson and S. Levine, *J. Electroanal. Chem. Interfacial Electrochem.* **47**, 395 (1973).
188. S. Levine and K. Robinson, *J. Electroanal. Chem. Interfacial Electrochem.* **54**, 237 (1974).
189. D. D. Bode, T. N. Anderson, and H. Eyring, *J. Phys Chem.* **71**, 792 (1967).

190. W. Anderson and R. Parsons, in *Proceddings of the 3rd International Congress on Surface Activity*, 1957, p. 45.
191. S. Trasatti, *J. Electroanal. Chem. Interfacial Electrochem.* **65**, 815 (1975).
192. R. Parsons, in *Soviet Electrochemistry (Proceedings of the 4th Conference on Electrochemistry, 1959, Moscow, USSR)*, Vol. 1, Consultants Bureau, New York (1961), pp. 18–22.
193. D. H. Everett, *Trans. Faraday Soc.* **46**, 453, 942 (1950).
194. D. C. Henry, *Philos Mag.* **44**, 689 (1920).
195. I. Langmuir, *J. Am. Chem. Soc.* **40**, 1361 (1918).
196. M. Volmer, *Z. Phys. Chem.* **115**, 253 (1925).
197. H. van der Waals, *Die Continuität des gasförmigen und flussigen Zustandes* Barth, Leipzig (1899–1900).
198. A. N. Frumkin, *Z. Phys. Chem.* **166**, 466 (1925).
199. E. Helfand, H. L. Frisch, and J. L. Lebowtiz, *J. Chem. Phys.* **34**, 1037 (1961); modified by R. Parsons, *J. Electroanal. Chem. Interfacial Electrochem.* **7**, 136 (1964).
200. E. Blomgren and J. O'M. Bockris, *J. Phys. Chem.* **63**, 1475 (1959).
201. J. O'M. Bockris and M. A. Habib, *Z. Phys. Chem. Neue Folge* **98**, 43 (1975); *J. Res. Inst. Catal. Hokkaido Univ.* **23**, 47 (1975).
202. S. Levine, private communication, 1973.
203. F. Booth, *J. Chem. Phys.* **19**, 391, 1327, 1615 (1951).
204. *Handbook of Chemistry and Physics*, 52nd Ed., R. C. Weast, ed., The Chemical Rubber Co., Cleveland, Ohio (1972).
205. W. R.Smythe, *Static and Dynamic Electricity*, 3rd Ed., McGraw-Hill, New York (1968).
206. S. Levine and K. Robinson, *J. Electroanal. Chem. Interfacial Electrochem.* **41**, 159 (1973).
207. F. P. Buff and F. H. Stillinger, *J. Chem. Phys.* **39**, 1911 (1963).
208. M. A. Habib, Ph.D. thesis, Flinders University of South Australia, 1975.
209. H. P. Dhar, B. E. Conway, and K. M. Joshi, *Electrochim. Acta* **18**, 789 (1973).
210. P. J. Flory, *J. Chem. Phys.* **10**, 51 (1942); M. L. Huggins, *Ann. N.Y. Acad. Sci.* **43**, 1 (1942).
211. J. O'M. Bockris and A. K. N. Reddy (eds.), *Modern Electrochemistry*, Vol. 2, Plenum Rosetta Edition, Plenum Press, New York (1973).
212. J. C. Slater and J. G. Kirkwood, *Phys. Rev.* **37**, 683 (1931).
213. R. A. Pierotti and G. D. Halsey, Jr., *J. Phys. Chem.* **63**, 680 (1959).
214. D. Eisenberg and W. Kauzman, *The Structure and Properties of Water*, Oxford University Press, New York (1969).
215. H. Wroblowa and K. Muller, *J. Phys. Chem.* **73**, 3528 (1969).
216. R. Payne, *J. Phys. Chem.* **69**, 4113 (1965).
217. D. C. Grahame, *J. Am. Chem. Soc.* **79**, 2093 (1957).
218. R. K-Sen, Ph.D. dissertation, University of Pennsylvania, 1972.
219. C. A. Barlow, Jr. and J. R. Macdonald, *J. Chem. Phys.* **40**, 1535 (1964).
220. J. R. Macdonald and C. A. Barlow, Jr., *J. Electrochem. Soc.* **113**, 978 (1966).
221. S. Levine, *J. Colloid Interface Sci.* **37**, 619 (1971).
222. R. M. Reeves, in *Modern Aspects of Electrochemistry*, B. E. Conway and J. O'M. Bockris, eds., Vol. 9, Plenum Press, New York (1974).
223. J. O'M. Bockris and P. P. S. Saluja, *J. Phys. Chem.* **76**, 2140 (1972).
224. J. O'M. Bockris and P. P. S. Saluja, *J. Electrochem. Soc.* **119**, 1060 (1972).
225. O. Ya Samoilov, *Structure of Electrolyte Solutions and Hydration of Ions*, English transl., Consultants Bureau, New York (1965); *Discuss. Faraday Soc.* **24**, 141 (1957).
226. B. Case, in *Reactions of Molecules at Electrodes*, N. Hush, ed., Wiley-Interscience, New York (1972).
227. J. O'M. Bockris and P. P. S. Saluja, *J. Phys. Chem.* **77**, 1598 (1973).

228. D. J. Barclay and J. Coja, *Croat. Chim. Acta* **43**, 221 (1971).
229. A. K. Vijh, *J. Phys. Chem.* **78**, 2240 (1974).
230. A. K. Vijh, *Electrochemistry of Metals and Semiconductors*, Marcel Dekker, New York (1973).
231. W. M. H. Sachtler and P. van der Plank, *Surface Sci.* **18**, 62 (1969).
232. Z. Bastl, *Surface Sci.* **22**, 465 (1970).
233. M. A. V. Devanathan and M. J. Fernando, *Trans. Faraday Soc.* **58**, 368 (1962).
234. A. N. Frumkin, B. B. Damaskin, and N. N. Fedorovich, *Dokld. Akad. Nauk SSSR* **115**, 751 (1957).
235. A. N. Frumkin and N. Polyanskaya, *Zh. Fiz. Khim.* **32**, 1958 (1958); P. Delahay, *Double Layer and Electrode Kinetics*, Interscience, New York (1965), pp. 57, 58.
236. P. Delahay and G. G. Susbielles, *J. Phys. Chem.* **70**, 647 (1966).
237. G. G. Susbielles, P. Delahay, and E. Solon, *J. Phys. Chem.* **70**, 2601 (1966).
238. P. Delahay, *J. Electrochem. Soc.* **118**, 967 (1966).
239. G. C. Barker, in *Transactions of the Symposium on Electrode Processes*, E. Yeager, ed., John Wiley and Sons, New York (1961), pp. 325–365.
240. M. Sluyters-Rahbach, B. Timmer, and J. H. Sluyters, *Rec. Trav. Chim.* **82**, 553 (1963).
241. A. N. Frumkin, *Z. Elektrochem.* **59**, 811 (1955).
242. L. Gierst, L. Vandenberghen, E. Nicholas, and A. Fraboni, *J. Electrochem. Soc.* **113**, 1025 (1966).
243. B. E. Conway and R. G. Barradas, *Electrochim. Acta* **5**, 319, 349 (1961).
244. B. E. Conway, R. G. Barradas, P. G. Hamilton, and J. Parry, *J. Electroanal. Chem. Interfacial Electrochem.* **10**, 485 (1965).
245. H. R. Hurwitz, *J. Electroanal. Chem. Interfacial Electrochem.* **10**, 35 (1965).
246. E. Dutkiewicz and R. Parsons, *J. Electroanal. Chem. Interfacial Electrochem.* **11**, 100 (1966).
247. B. Baron, P. Delahay, and D. J. Kelsh, *J. Electroanal. Chem. Interfacial Electrochem.* **18**, 184 (1968).
248. G. J. Hills and R. M. Reeves, *J. Electroanal. Chem. Interfacial Electrochem.* **42**, 355 (1973).
249. D. J. Schiffrin, *Trans. Faraday Soc.* **67**, 3318 (1971).
250. A. W. M. Verkroost, M. Sluyters-Rahbach, and J. H. Sluyters, *J. Electroanal. Chem. Interfacial Electrochem.* **24**, 1 (1970).
251. G. J. Hills and R. M. Reeves, *J. Electroanal. Chem. Interfacial Electrochem.* **31**, 269 (1971).
252. S. Lakshmanan and S. K. Rangarajan, *J. Electroanal. Chem. Interfacial Electrochem.* **27**, 127 (1970).
253. R. D. Lanier, *J. Phys. Chem.* **69**, 3992 (1965).
254. L. M. Baugh and R. Parsons, *J. Electroanal. Chem. Interfacial Electrochem.* **58**, 229 (1975).
255. S. Lindenbaum and G. E. Boyd, *J. Phys. Chem.* **68**, 911 (1964).
256. J. E. B. Randles and D. J. Schiffrin, *Trans. Faraday Soc.* **52**, 1509 (1956); *J. Electroanal. Chem. Interfacial Electrochem.* **10**, 480 (1965).
257. A. N. Frumkin, Z. A. Iofa, and M. A. Gerovich, *J. Phys. Chem. USSSR* **30**, 1445 (1956).
258. B. E. Conway and H. P. Dhar, *Croat. Chim. Acta* **45**, No. 1 (1973); *Electrochim. Acta* **19**, 445 (1974).
259. B. E. Conway, H. P. Dhar, and S. Gottesfeld, *J. Colloid Interface Science* (Kendall Award Symposium, 1972) **43**, 303 (1973).
260. S. Trasatti, *J. Electroanal. Chem. Interfacial Electrochem.* **33**, 351 (1971); **64**, 128 (1975).
261. B. B. Damaskin, O. A. Petrii, and V. V. Batrakov, in *Adsorption of Organic Compounds on Electrodes* (English transl.), R. Parsons, ed., Plenum Press, New York (1971), p. 86.

5

Potentials of Zero Charge

A. N. FRUMKIN, O. A. PETRII, and B. B. DAMASKIN

1. Introduction

The notion of the potential of zero charge (pzc) and the relevant term were introduced 50 years ago.[1] Later, the pzc was proved to be an important electrochemical characteristic of metal and to play a major role in electrocapillary and electrokinetic phenomena, electric double-layer structure, adsorption of ions and neutral organic molecules on the electrode, wetting phenomena, physicochemical mechanics of solids, photoemission of electrons from metal into solution, and in electrochemical kinetics. The introduction of the notion of pzc led to solution of the Volta problem and to rigorous interpretation of the attempts to measure or calculate the "absolute" electrode potential. All this testifies to the fundamental nature of the notion of pzc.

Many hundreds of papers have been devoted to the problem of pzc. The pzc of different metals were first compared by Frumkin.[2] In recent years some reviews have been published in which the pzc values are listed.[3–7] The theoretical validity of various methods of pzc determination and the reliability of experimental data are discussed in detail by Frumkin,[8] where a comprehensive history of the development of the notion of the electrode charge is given and different aspects of the problem of pzc are considered.

A. N. FRUMKIN (deceased), O. A. PETRII, and B. B. DAMASKIN • Institute of Electrochemistry, Academy of Sciences of the USSR, Moscow V-71, Leninsky Prospekt 31, USSR.

2. The Notion of the Electrode Charge

Before discussing the modern state of the problem of pzc, the notion of the charge of electrode surface will be considered briefly.

The conventional definition of the charge is based on the concept of the electric double layer at the metal/electrolyte interface, and the electrode charge is identified with the charge of the metal side of the double layer, i.e., with the deficiency or excess of electrons in the metal surface layer. This definition dates back to Helmholtz, who in the middle of the last century introduced the double-layer concept. It is evident that such an electrostatic definition postulates the dependence of the charge and hence, of the pzc, on the double-layer model used.

Another, thermodynamic approach to definition of the surface charge was suggested by Lippmann in his early papers.[9] Lippmann laid the foundations for the thermodynamic theory of electrocapillarity by deriving the famous equation

$$\partial\gamma/\partial E = -Q \tag{2.1}$$

where γ is the surface tension at the mercury/electrode-solution interface (for the physical sense of γ in the case of solid metals, see below), E is the electrode potential, and Q is a quantity which Lippmann called "the electric capacity of unit surface at constant potential difference." As follows from this definition, Q denotes the amount of electricity to be supplied to the electrode when its surface increases by unity in order that its potential should remain constant. Here, Lippmann did not use any concept of the electric double-layer structure. However, in his later papers, Lippmann, proceeding from Helmholtz's views, considered the quantity Q as the electrode surface charge, assuming it to be proportional to the potential difference between metal and solution.

The thermodynamic theory of electrocapillarity was developed further by Gibbs[10] and Planck.[11] Gibbs derived the adsorption equation, which was used by a number of authors as a basis in deriving Lippmann's equation.[12–18] According to Gibbs the right-hand side of Eq. (2.1) gives the surface density of adsorbed electrochemically active substance in electric units.†

Planck[11] derived Eq. (2.1) for a completely polarizable electrode ("vollkommen polarisierbare elektrode"), i.e., an electrode whose state is completely determined by the amount of electricity passed through it. He emphasized that this circumstance did not relate the quantity in question to the free charge on both sides of the electrode surface. Thus Planck's formulation clearly shows the difference between the two interpretations of the quantity Q, based on thermodynamics and electrostatics.

Frumkin[12,13] analyzed the electrocapillarity equation derived on the basis of Gibbs adsorption equation:

$$d\gamma = -Q\,dE - \sum_i \Gamma_i\,d\mu_i \tag{2.2}$$

† For detailed analysis of Gibb's concept on the physical sense of the right-hand side of Eq. (2.1), see Reference 19.

Here, Γ_i's are the Gibbs surface excesses, μ_i's are the chemical potentials of the system components with the exception of that of which the adsorption leads to charging of the surface, and E is the potential measured against a constant reference electrode. This analysis showed that, in a general case, the right-hand side of Eq. (2.1) cannot be equated with the free-charge density of the metal surface, σ. Two relations were obtained which, using the designations proposed by Frumkin *et al.*,[20] can be written as

$$\partial\gamma/\partial E = -\sigma - A_{Me^+} \tag{2.3}$$

$$\partial\gamma/\partial E = -\sigma + A_{Me} \tag{2.4}$$

Here, A_{Me^+} is the excess of metal in ionic form in the surface layer at constant metal phase composition, and A_{Me} is the excess of metal in atomic form dissolved in mercury due to formation of amalgam during polarization and at constant $[Me^+]$ value in the solution bulk. (A_{Me} and A_{Me^+} are expressed in electrical units.) It was shown, as exemplified by Zn amalgam in $ZnSO_4$ solution, that neglect of the second term in the right-hand side of Eq. (2.3) can lead to considerable errors. For a long time, Eqs. (2.3) and (2.4) found no practical use since chief attention of electrochemists was focused on the electric double-layer structure.

Beginning in 1934, in studies on the electrocapillarity theory and the electric double layer, wide use was made of the concept introduced by Koenig,[21] an ideally polarizable electrode, i.e., an electrode on the surface of which no transition of charged particles occurs between the two sides of the electric double layer. In the case of an ideally polarizable electrode, Q proves to be identical with the charge density of the metal side of the electric double layer σ, so that Eq. (2.2) can be rewritten as

$$d\gamma = -\sigma\, dE - \sum_i \Gamma_i\, d\mu_i \tag{2.5}$$

where the subscript i now refers to all system components.

Later, while numerous studies were devoted to electrocapillary phenomena at ideally polarizable electrodes, the electrodes at which charge transfer across the interface occurs and which, using a thermodynamic approach, should be considered as reversible, received relatively little attention. Thus Grahame and Whitney[15] derived an equation for a metal in the solution of its salt MeA (without supporting electrolyte), which in modern notation at $\Gamma_{H_2O} = 0$ is

$$d\sigma = -\Gamma_A\, d\mu_{MeA} \tag{2.6}$$

A completely similar equation was obtained earlier by Frumkin.[13] It is noteworthy that Grahame and Whitney in deriving this equation did not introduce the notion of charge at all.

Mohilner[18] gave a set of equations for reversible redox systems which

reduce to types of relations similar to Eqs. (2.3) and (2.4). Expressing the adsorption in electrical units, Mohilner's equations can be written as

$$(\partial\gamma/\partial E)_{\mu_R} = -(\sigma + \Gamma_O) \tag{2.7}$$

and

$$(\partial\gamma/\partial E)_{\mu_O} = -(\sigma - \Gamma_R) \tag{2.8}$$

These equations differ from Eqs. (2.3) and (2.4) in that in this case, Γ_O and Γ_R are Gibbs adsorptions of oxidant and reducer, respectively. Unlike the ideally polarizable electrode, Mohilner does not give a thermodynamic definition of the charge σ for a reversible electrode.

Further development of the problem of which quantity should be considered as the charge of the metal side of the electric double layer was influenced by the introduction by Lorenz[22] of the concept of a partial charge transfer. Assuming at first that one has to deal with an ideally polarizable electrode, it is of no importance that the side of the double layer, metal or ionic, to which the particle in the adsorbed state should belong is not known. It follows from the electroneutrality principle that

$$Q = \sum \Gamma_{A^-} - \sum \Gamma_{C^+} \tag{2.9}$$

where Γ_{A^-} is Gibbs adsorption of anion and Γ_{C^+} that of cation, expressed in electrical units (as is the case throughout the remainder of this text). According to Lorenz, in the case of the double layer at a mercury or liquid gallium surface, part of the charge of halogen and alkali metal (potassium, cesium) ions due to formation of a covalent bond, is transferred to the metal surface. Lorenz considers the interface between metal and solution from a microphysical point of view. The total charge on the metal side beyond this microphysical boundary is the true electrode charge, and the part of the charge transferred across the interface is expressed by the elementary (or microscopic, true) transfer coefficient λ. The methods of calculating the transfer coefficient λ proposed by Lorenz raise some objections.[23,24] However, in principle, the possibility of such transfer cannot be questioned since it is inevitable in the presence of a covalent bond between ions in the dense part of the double layer and the electrode metal.

The earlier studies of ion adsorption on platinum group metals,[25] and those of recent years, conducted with the use of combined radiochemical, electrochemical, and analytical methods,[26-33] led to the conclusion that in the case in question the adsorption of most ions involves charge transfer. The hydrogen atoms adsorbed on a platinum surface can be formally considered also as hydrogen ions for which the charge transfer coefficient is close to unity, though not equal to it.[20,33,34] Due to the partial charge transfer, the demarcation line between ideally polarizable and reversible electrodes is not clearly defined. However, as the magnitude of partial charge transfer is not known *a priori*, the free charge of an electrode surface, equal to the electron deficiency in the

surface layer of metal, cannot be identified with the quantity Q contained in the right-hand side of the Lippmann equation, and determined by Eq. (2.9).

An ambiguity in such a fundamental concept of electrochemistry as the electrode charge made it imperative that it should be analyzed in detail[20]; and it has been concluded that, both for an ideally polarizable electrode and for an electrode on which a reversible charge transfer is possible, a thermodynamically valid determination of the surface charge should be based on a refined Lippmann's concept. The electrode charge should be defined as the amount of electricity to be supplied to the electrode when its surface increases by unity with the concentration of the solution components remaining constant. The concentration of the solution components can be held constant by introducing them into solution in the amounts Γ_i (adsorbed amounts according to Gibbs).

A consistent thermodynamic treatment of the adsorption process of electrochemically active components can be based only on the definition of Gibbs adsorption as of the amount of substance to be introduced into the system in order to keep the composition of the bulk phases constant when the interface increases by unity. What happens to this addition subsequently is of no importance: adsorbed substance in an unchanged condition can form part of the equilibrium double layer or participate in the electrochemical reaction with escape or capture of electrons. Thus, e.g., in a hydrogen atmosphere, when the platinum electrode surface increases by unity in NaCl solution, a certain amount of hydrogen, Γ_H, disappears from the gas phase. This amount, however, is not equal to the amount of hydrogen adsorbed on unit surface, as would be the case in the absence of electrolyte solution. Indeed, part of the hydrogen which disappeared from the gas phase undergoes ionization, charging negatively the electrode surface; and the hydrogen ions formed are substituted in the surface layer by Na^+ ions and enter into the solution. When active carbon with a small amount of platinum is used as a hydrogen electrode in alkaline solution, this is what happens to the major part of hydrogen which disappeared from the gas phase.[35] In other words, the surface excess of hydrogen can be very small in spite of its significant Gibbs adsorption.

In the case of an ideally polarizable electrode when the electrode surface increases, the solution composition is kept constant by adding all its components except the solvent. But in the case of a reversible electrode whose potential is determined by the reaction

$$O + ne^- \rightleftarrows R \tag{2.10}$$

with increasing surface, the composition can be held constant by introducing into the system the O component in the amount Γ_O and the R component in the amount Γ_R without supplying electricity from outside. However, an alternative method is possible, viz., the substance participating in the redox process can be introduced in the amount $(\Gamma_R + \Gamma_O)$, adding it entirely as the O form or entirely as the R form. In the first version, in order to keep the solution composition constant, an additional amount of electricity $Q' = -\Gamma_R$ must be supplied to the

electrode. In the second version, the respective amount of electricity is $Q'' = \Gamma_O$. For the reversible electrode of type (2.10), two Lippmann's equations are valid:

$$(\partial\gamma/\partial E)_{\mu_O,\mu_i} = -Q' = \Gamma_R \tag{2.11}$$

and

$$(\partial\gamma/\partial E)_{\mu_R,\mu_i} = -Q'' = -\Gamma_O \tag{2.12}$$

where subscript μ_i indicates that the chemical potentials of the other system components not participating in the redox process are constant.

In accordance with Eqs. (2.11) and (2.12), Q' and Q'' should be considered as the charges of the reversible electrode corresponding to the two methods of changing its potential: at constant chemical potential of component O and at constant chemical potential of component R. If the chemical potential of one of the components of the redox system is held constant automatically, e.g., in the case of mercury in solution containing a mercury salt, only one of these two equations can be used (in this case, the second). On the basis of an experimental determination of the quantities Γ_R and Γ_O, or for a liquid electrode from a direct determination of the γ, E dependence at constant μ_O or μ_R, it is possible in the case of a reversible electrode to plot electrocapillary curves of two kinds.

The quantities Q' and Q'' can be called *total electrode charges* at constant chemical potential of oxidant or reducer, respectively.[20] This definition of the electrode charge is in keeping with the conventional concept of the charge, used in applied electrochemistry, as the amount of electricity to be obtained from the electrode upon its complete reduction (Q'') or (with opposite sign) upon its complete oxidation (Q'). In this case, however, the reduction and oxidation processes refer to unit surface and not to bulk phase.

The quantities Q' and Q'' by themselves give no indication of the free electricity density, σ, on the electrode surface. In order to relate Q' and Q'' to σ, it is necessary to go beyond the scope of thermodynamics and to use some model of the nature of the solution components in their adsorbed state. Let it be assumed, for example, that the charge transfer of the system components, except that expressed by Eq. (2.10), may be neglected, and the amount of oxidant per unit surface layer be denoted by A_O and the amount of reducer by A_R. (A_O and A_R are the surface excesses for a certain choice of the interface position.) Under these conditions

$$Q' = -\Gamma_R = \sigma - A_R \tag{2.13}$$

$$Q'' = \Gamma_O = \sigma + A_O \tag{2.14}$$

and hence

$$(\partial\gamma/\partial E)_{\mu_O} = -\sigma + A_R \tag{2.15}$$

$$(\partial\gamma/\partial E)_{\mu_R} = -\sigma - A_O \tag{2.16}$$

Equations (2.15), (2.16) generalize Eqs. (2.3), (2.4) and, at the same time, prove the erroneousness of Eqs. (2.7), (2.8). It follows from Eqs. (2.13) and (2.14) that

$$A_O + A_R = \Gamma_O + \Gamma_R = \Gamma_\Sigma \tag{2.17}$$

where Γ_Σ is the total extent of adsorption. For simplicity, in Eqs. (2.11), (2.12), (2.15), and (2.16) the potentials are given against a constant reference electrode.

In contrast to the total charge Q' and Q'', the quantity σ can be called the *free charge*. It should be remembered, however, that this name is somewhat conditional since in the derivation of Eqs. (2.15) and (2.16) the possibility of charge transfer, except in the process (2.10), was ignored.

In the case of an ideally polarizable electrode, $A_R = A_O = 0$, and the right-hand sides of Eqs. (2.14) and (2.16) give the free charge (assuming partial charge transfer to be absent).

The refinement of the notion of the electrode charge led to a consistent general phenomenological approach to the description of reversible chemisorption processes involving charge transfer.[34,36]

Thus, in discussing the problem of the pzc, account should be taken of the difference between the total (Q) and free (σ) charges of the electrode surface. Among the systems considered below, this applies directly to platinum group metals and activated carbon. In this case the following designations and terminology shall be used. For Q' the symbol Q shall be retained, and this quantity will be called the total surface charge, neglecting for brevity sometimes the condition $\mu_{H^+} = \text{const}$. Instead of Q'', the symbol Γ_{H^+} shall be used.

3. Methods of Determination of the Potentials of Zero Charge

3.1. Direct Determination of the Value or Sign of the Surface Charge

It follows from the definition of the total charge Q that it can be measured by the amount of electricity flowing in the external circuit, when the electrode surface increases by unity at $E = \text{const}$. In this case the possibility of charges arising on the electrode surface due to interaction with the oxidants or reducers present in solution must be ruled out, and the concentration of all the solution components being adsorbed must be held constant.

In the case of liquid metals, the pzc determination by this method is possible with the use of a dropping electrode, for which pzc corresponds to the zero value of the charging current. Semiquantitative measurements of the Q–E curves were made already in the last century; the first quantitative data obtained by this method are given by Frumkin.[12,14]

The sign of the charge of a liquid metal surface can be determined not only from the current to the growing drop, but also from the electric signal caused

by any surface deformation.[37,38] So far these methods have found use in determination of the pzc of mercury. An analog of the vibrating mercury surface method is a technique based on the application of the audio-electrochemical phenomena.[39]

Two versions of the determination of the pzc of solid metals were suggested which can be considered as analogs of those used for liquid metals and considered above.

In the elastic charging method developed by Gokhshtein,[40] it is the

Table 1

Recommended Potential of Zero Charge Values (against N.H.E.)

Metal	Solution	pzc	Reference
	Liquid metals		
Hg	NaF	−0.193	16
Ga	$HClO_4$ and HCl at $c \to 0$	−0.69 ± 0.01	61
Ga + In (16.7%)	0.001 *N* $HClO_4$	−0.68 ± 0.01	110
Tl amalgam (41.5%)	1 *N* Na_2SO_4	−0.65 ± 0.01	1
In amalgam (64.6%)	1 *N* Na_2SO_4	−0.64 ± 0.01	110
	Solid metals not adsorbing hydrogen		
Bi (polycrystalline)	0.002 *N* KF	−0.39	89
Bi(111)	0.01 *N* KF	−0.42	90
Cd	0.001 *N* NaF	−0.75	91
In	0.003 *N* NaF	−0.65	92
Pb	0.001 *N* NaF	−0.56	93
Sb	0.002 *N* $KClO_4$	−0.15	94
Sn	0.002 *N* K_2SO_4	−0.38	95
Tl	0.001 *N* NaF	−0.71	96
Ag(111)	0.001 *N* KF	−0.46	85, 86
Ag(100)	0.005 *N* NaF	−0.61	87
Ag(110)	0.005 *N* NaF	−0.77	85
Au(110)	0.005 *N* NaF	0.19	88

Metal	Solution	$E_{\sigma=0}$	$E_{Q=0}$
	Platinum metals[a] [31]		
Pt	0.3 *M* HF + 0.12 *M* KF (pH 2.4)	0.185	0.235
Pt	0.5 *M* Na_2SO_4 + 0.005 *M* H_2SO_4	0.16	0.20
Pt	0.5 *M* Na_2SO_4 + 0.01 *M* NaOH	—	−0.25
Pd	0.05 *M* Na_2SO_4 + 0.001 *M* H_2SO_4 (pH 3)	0.10	0.26
Rh	0.3 *M* HF + 0.12 *M* KF (pH 2.4)	−0.005	0.085
Rh	0.5 *M* Na_2SO_4 + 0.005 *M* H_2SO_4	−0.04	0.03
Ir	0.3 *M* HF + 0.12 *M* KF (pH 2.4)	−0.01	—
Ir	0.5 *M* Na_2SO_4 + 0.005 *M* H_2SO_4	−0.06	0.10

[a] The pzc of metals adsorbing hydrogen depends on solution pH. Here, the values for pH = 2–3 and pH = 12 only are given.

magnitude of the potential fluctuations arising upon periodic stretching of a metal tape immersed in solution which is measured. In this case the elongations are small enough to lie within the limits of elastic deformation. From the fluctuations of the tape potential, it is possible to determine the value of $Q + (\partial Q/\partial \ln s)_E$, where s is the electrode area. In the case of a solid metal, the value of $(\partial Q/\partial \ln s)_E$, generally speaking, is not zero, which limits the possibilities of determining the pzc by this method†

Jakuszewski and Kozlowski developed and widely used the immersion method[41] based on the determination of the potential at which the direction of the current between a stationary electrode and an electrode newly immersed in solution changes. In this case it is assumed that current is consumed only in charging the electric double layer arising upon immersion in the solution. The prerequisite of the fulfillment of this condition is a complete absence on the metal surface before its immersion of adsorbed oxygen or oxides as well as of adsorbed hydrogen. However, the fulfillment of these conditions in real systems presents considerable difficulties and cannot always be controlled. Therefore all attempts at refining the immersion method were directed to improvement of the surface preparation of solid electrodes.[42,43]

3.2. Development of Electrodes with Zero Charge

The methods of developing electrodes with zero charge are similar to those considered above.

In the case of liquid metals, use can be made of dropping or streaming electrodes, which was already pointed out by Helmholtz. In principle, surface increase allows a decrease of the charge density to negligible values and permits the direct determination of the pzc if the initial potential difference value is not restored due to interaction between metal and solution. The efficiency of a dropping electrode can be enhanced by increasing rapidly the surface (Paschen) and/or in a more modern version, by removing carefully the traces of depolarizers (oxygen, mercury salts) from solution and eliminating the possibility of its contamination by traces of difficulty-soluble mercury salts from the reference electrode or from the walls of vessels. The dropping (or streaming) electrode method was widely used for determination of the pzc of mercury by Grahame[44] and also for determination of the pzc of indium amalgams by Butler.[45] If the pzc lies in the potential range in which an amalgam electrode can be considered with good approximation to be an ideally polarizable one, the pzc values obtained by the streaming electrode method can be considered as being the values of the potential of zero free charge. If, however, equilibrium is established on the freshly formed amalgam surface between metal dissolved in mercury and

† Some primitive attempts to determine the surface charge from the direction of the current passing in solution from a stationary metal wire to a wire subjected to stretching were made in 1809 by Kroichkoll.

its ions, the pzc determined by means of the streaming electrode is the potential of zero total charge at constant reducer concentration, i.e., the metal concentration in amalgam.

While the problem of preparing an ideally polarizable electrode with a zero charge is solved by increasing the surface, the method of zero solutions, in which the vanishing of the charge density is ensured by changing the solution composition, is more suitable for a reversible electrode. The zero solutions method, the idea of which was suggested by Nernst at the beginning of this century, was developed by Palmaer, Smith, and Moss. Palmaer measured the current flowing between a streaming electrode and a stationary mercury surface in the same solution and varied the composition in such a manner that the strength of this current should be zero. He believed that thus the potential reached the "absolute zero." Frumkin and Cirves[46] used the zero solutions method for determination of the pzc of thallium and cadmium amalgams. The potential difference between amalgam and solution was varied by adding to solution the corresponding metal salt. An attempt was made to extend the zero solutions method to sodium amalgams,[47] but in that case the results seemed to be affected by chemical interaction of amalgam with solution.

The zero solutions method was used more than once in combination with the immersion method for determination of the pzc of solid metals.[48] However, the difficulties associated with the possibility of the double-layer formation due to ionization of adsorbed gases or discharge of solution ions upon immersion of a solid electrode were overcome only for degassed activated carbon,[49] which has a large surface. The absence of any changes in the solution composition in such cases showed that no electric double layer was formed at the immersed electrode.

By means of the zero solutions method, some authors obtained for a number of metals the pzc lying in the range 0.4–0.5 V (N.H.E.). This potential, independent of the metal nature, was called "the Billitzer (Billiter) zero potential." However, a critical analysis[4,8,50] of the data on Billitzer potentials shows that they are partly erroneous (for a mercury electrode) and partly applicable (for solid metals) to metals with oxidized surface.

Instead of introducing into solution an electrode with a clean surface from the outside, it is possible to obtain a clean surface of the solid electrode immediately in the solution by mechanical treatment. Andersen, Anderson, Perkins, and Eyring[51–53] measured the potential of an electrode the surface of which was renewed by scraping or cutting with the use of a rotating blade from a hard material (scrape potential). If one assumes that, in spite of continuous renewal, there has been time for equilibrium to be established between metal surface and solution, in the general case the scrape potential should correspond to the potential of zero total charge. In many cases the obtained pzc values are actually close to the optimum values of the zero total charge.[3,4,54]

The scraping method, however, is not free of some drawbacks. The surface arising during scraping or cutting has a higher chemical activity due to the appearance on it of a large number of dislocations,[55] which facilitate chemical

interaction between metal and solvent. Possibly, the characteristics of this surface differ somewhat from those of a "normal" surface. In the case of platinum group metals, whose pzc depends on solution pH, the adsorption phenomena attending the formation of an equilibrium surface layer can lead to a change in the pH value when the surface increases rapidly in nonbuffer solutions. This change could be responsible for the appearance of a plateau on the curves expressing the dependence of the pzc of platinum group metals, obtained by the scrape method, on pH in the range of medium pH values,[52] which was not observed in other studies. Finally, the crystallographic characteristics of the surface arising as the result of mechanical treatment are uncertain; however, as will be shown below, the dependence of the pzc on face index has been conclusively established for a number of cases.

Noninski and collaborators[56] determined the pzc of electrodes from the change of the sign of the current passing through a "self-cleaning" rotating electrode in an inert atmosphere. Basically, this method should yield the same results as the determination of the scrape potentials.

3.3. Electrocapillary Methods

Up to now the classic measurement of electrocapillary curves, i.e., the determination of the dependence of surface tension on potential, remains a widely used method for determination of the pzc of liquid metals. According to what has been said above, the position of the maximum of the electrocapillary curve gives the potential of the zero total charge of the electrode ($E_{Q=0}$). It is necessary, however, to elucidate the physical sense of surface tension. This term is usually understood to mean the work expended under reversible conditions in increasing the interface by unity, e.g., by 1 cm^2. This increase can be achieved in different ways, e.g., by stretching, or splitting in the case of a solid, which must be carried out reversibly. In the case of a liquid surface, the work expended in the two cases is the same. This is not so with a crystalline solid body. Thus, if one stretches reversibly a solid crystal face, the work dW expended in stretching by ds generally depends on the direction of stretching. Therefore, the quantity $\gamma^* = \partial W/\partial s$ is a vector, while the reversible work γ necessary for formation of the unit surface is a scalar. The physical sense of the difference between γ^* and γ, which was pointed out already by Gibbs,[10] is associated with the fact that the surface formed by stretching, in the case of a solid, is not identical with an unstretched surface. The thermodynamic equations, which are a particular case of the general Gibbs adsorption equation, e.g., the Lippmann equation, contain the quantity γ, which becomes identical with the surface tension γ^* in the case of liquids. Unfortunately, there is as yet no generally accepted term for γ in electrochemical literature. γ shall be called the reversible work of formation of the unit surface,[57] and the dependence of γ on E both for liquids and solids, the electrocapillary curve.

The electrocapillary curves of liquid metals are measured by a capillary

electrometer, which was suggested by Lippmann and improved by Gouy.[58] This capillary electrometer measures the pressure p necessary for forcing the liquid metal down to a certain point of a conical capillary wetted by electrolyte solution. Under the assumption that the capillary walls are completely wetted by electrolyte solution, $p = 2\gamma/r$, where r is the capillary radius at the meniscus level. Generally, the quantity r is not determined experimentally, and the capillary is calibrated by means of the solution for which the value of γ was determined by the sessile or hanging drop methods.

Grahame and collaborators[44] carried out precision determinations of the pzc by means of a capillary electrometer. A capillary electrometer was used also for the pzc determination for thallium[1] and indium[59] amalgams, gallium and its alloys[60,61] (Table 1). Figure 1 shows the electrocapillary curves of indium amalgams of different concentration, on which the influence of indium concentration on the pzc of amalgam is clearly evident. In view of the possibility of metal sticking to glass and partly for other reasons, attention of research workers is centered on the methods of determination of the γ, E curves from the sessile drop profile, the time of formation, weight, and volume of the detaching drop, and the maximum pressure when the drop grows at the tip of a turned-up capillary (for more detail see Reference 8). The latter method seems to be very promising. Drop methods can easily be made automatic.

The electrocapillary measurements give the potential values of the zero total charge, which, in the case of an ideally polarizable electrode, are identical with the potential of the zero free charge ($E_{\sigma=0}$) if Lorenz partial charge transfer is ignored. When the ideal polarizability condition is not fulfilled, the pzc can be assessed by determining the equilibrium γ, E dependences at constant chemical potentials of the oxidized and reduced forms, respectively, i.e., the electrocapillary curves of the first and second kind.[62]

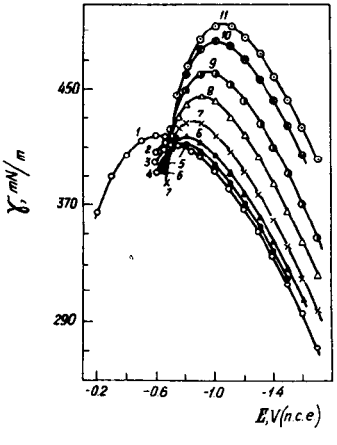


Figure 1. Electrocapillary curves of indium amalgam in 1 M KBr + 0.005 M H_2SO_4. Indium content in amalgam: 1, 0; 2, 0.19; 3, 0.85; 4, 1.97; 5, 3.50; 6, 7.80; 7, 16.70; 8, 30.40; 9, 43.10; 10, 62.20; 11, 70.30 wt %.[59]

Numerous attempts were made to extend the electrocapillary methods to solid electrodes. Gokhshtein[63,64] developed the method of determination of estance—the dependence of surface tension γ^* on electrode charge $\partial\gamma^*/\partial Q$. This quantity is related to the derivative of surface tension with respect to potential by the equation

$$\frac{\partial\gamma^*}{\partial Q} = \frac{\partial\gamma^*}{\partial E} \cdot \frac{\partial E}{\partial Q} = \frac{1}{C} \cdot \frac{\partial\gamma^*}{\partial E} \tag{3.1}$$

where C is the differential capacity of the electrode.

In Gokhshtein's device the electrode is in the form of an L-shaped plate, the bottom face of which is in contact with the electrolyte. Periodic changes of the electrode potential at a definite frequency lead to fluctuations of the surface tension force on this face. The resulting bending vibrations of the electrode are transferred to the piezoelectric cell connected to it, and thence, as an electric signal they come to the input of a selective amplifier. The oscillograms "surface tension amplitude $\Delta\gamma^*$–electrode potential" are taken at a fixed amplitude of the charge density of the electrode ΔQ, which allows consideration of these dependences when plotted as $|\partial\gamma^*/\partial Q| - E$. In the case of a solid body, it can be easily shown that

$$\partial\gamma^*/\partial E = -Q - (\partial Q/\partial \ln s)_E \tag{3.2}$$

It follows from (3.1) and (3.2) that the measurement of $\partial\gamma^*/\partial Q$ can be used as a method for the pzc determination if the second term in the right-hand side of Eq. (3.2) is small as compared to the first term. In the case of liquid metals, $(\partial Q/\partial \ln s)_E = 0$ since when the liquid surface is stretched, it remains identical with itself. For solid metals the quantity $(\partial Q/\partial \ln s)_E$ depends on the metal nature. The contribution of this term is comparatively small for Pb, Bi, Tl, and Cd. In these cases the estance measurements characterize correctly the influence of the anion on the pzc (Figure 2). However, for Pt the second term in Eq. (3.2) can be much larger than the first term. Due to the existence of the term $(\partial Q/\partial \ln s)_E$,

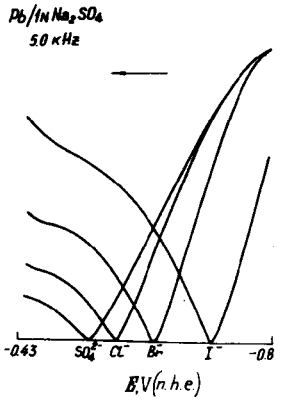


Figure 2. Influence of surface-active anions on the position of the estance zero on a lead electrode in 0.5 M H_2SO_4 with 0.15 M NaCl, NaBr, and NaI additions.[64]

the estance measurements by alternating current of different frequency give information on the properties of the double layer which cannot be obtained by any other methods.[64] However, for the pzc determinations in the case of solid electrodes, the estance measurements can be used only if there are reasons to suppose that $(\partial Q/\partial \ln s)_E \ll Q$.

Some other methods of determining the quantity $\partial\gamma^*/\partial E$ were proposed. Thus Beck observed the change in the length of a stretched metal tape with changing potential.[65] By means of a laser-optical system, Bockris and co-workers measured the dependence on potential of the bending of a thin glass strip metallized on one side and fastened from one end.[66,67] The pzc of carbon was determined by Soffer and Folman[68] from the relationship between surface tension and the linear dimensions of a rigid porous body.

The dependence of the value of γ on the solid metal potential can be assessed from the change of the contact angle θ at the electrode/gas/solution interface according to the equation

$$\gamma_{12} + \gamma_{23} \cos\theta = \gamma_{13} \tag{3.3}$$

where γ_{12}, γ_{13}, and γ_{23} are the values of γ for the interfaces metal/solution, metal/gas, and solution/gas, respectively. The dependence of θ on E was first measured by Möller in 1908. Reproducible data were obtained in 1932.[69]

A direct measurement of the contact angle can be substituted by measuring the liquid rise in a metal capillary,[70] or by measuring the rise of the solution meniscus at a vertical metal surface[71,72] or a wire. The determination of the θ–E curve in the case of mercury points to the dependence of γ_{13} on potential. Hence, at the metal/gas interface under equilibrium conditions there exists a thin wetting solution film.[69] The main obstacle in using this method is the difficulty of determing the equilibrium values of θ in the case of solid interfaces.

According to Rehbinder's theory, the quantity γ determines the work expended in brittle breakdown or plastic deformation of solids. This concept was used as a basis for developing some methods of the pzc determination from the potential dependence of hardness, inverse creep rate, and yield point.[73,74] These parameters characterizing the strength of a solid reach their maximum value at the pzc (Figure 3). In spite of the fact that the work expended in real

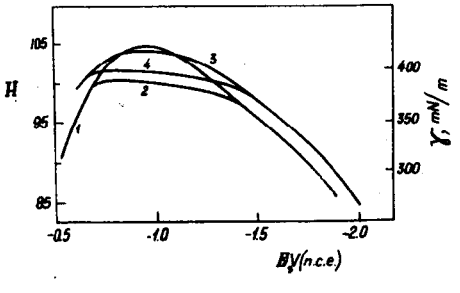


Figure 3. Dependence of the hardness (H) of thallium on the potential in the solutions 0.5 M Na_2SO_4 (1) and 0.5 M Na_2SO_4 + 0.185 M *iso*-$C_5H_{11}OH$ (2), and electrocapillary curves for 41.5% thallium amalgam in solutions of 0.5 M Na_2SO_4 (3) and 0.5 M Na_2SO_4 + 0.175 M *iso*-$C_5H_{11}OH$ (4).[73]

conditions differs from the reversible work γ, the methods developed by Rehbinder and his school lead to reasonable pzc values. The determination of the dependence on potential of the breakdown of a metal under the action of ultrasound and hydroabrasion gives also reasonable approximate values.[75]

Bockris and collaborators suggested a method for determining the pzc from the maximum on the curve of the dependence of external friction on potential.[76,77] The decrease of external friction observed when rubbing surfaces are charged is explained by repulsion between two diffuse double layers arising on base metal and on the sliding contact.[77] When investigating hardness by means of Herbert's pendulum, Rehbinder and collaborators[78] showed that when the pendulum exerts a heavy pressure on the bearing causing it to break, at the pzc the damping decrement of pendulum oscillations is minimal since the pzc corresponds to maximum hardness. When the pressure of the pendulum on the bearing decreases, external friction plays a dominant role in the damping of pendulum oscillations, and at the pzc the damping decrement becomes maximal since the pzc corresponds to maximum external friction. (For interpretation of the experiments with a pendulum, see also References 8 and 50.)

3.4. Adsorption Methods

If, during formation of the electric double layer, the Gibbs adsorption of a certain component Γ_i is not compensated by its supply from outside, its content in the electrolyte solution changes; and in the case when a conductor of the first class in equilibrium with the solution has a variable composition, its composition also changes. In the case of gas electrodes (hydrogen, oxygen), changes in composition also occur due to the double-layer formation. Therefore, basically, the determination of the changes in the composition of the solution or the gas phase can be used for investigation of the double-layer structure and for finding the pzc.

The adsorption effects associated with the electric double-layer formation were first observed at the beginning of this century by Palmaer and Billitzer. The importance of the adsorption methods became evident when they were applied to disperse platinum[25] and activated carbon.[79] It was assumed that the surface charge is caused by ionization of adsorbed hydrogen and oxygen to form H^+ and OH^- ions or by discharge of the latter, and is accompanied by a change in the solution acidity. In the case of electrodes with developed surfaces, the acidity change can be established by usual analytical methods, which make it possible to find Γ_{H^+} or Γ_{OH^-}. If the interface position is chosen so that $\Gamma_{H_2O} = 0$, $\Gamma_{H^+} = -\Gamma_{OH^-}$, and it will be sufficient to consider only Γ_{H^+}. As was shown earlier, this quantity characterizes the total charge of the second kind at $\mu_H = \text{const}$.

In experiments with platinum metals in determining Γ_{H^+}, the value of $\Delta\Gamma_{H^+}$ was found when passing from the reversible hydrogen potential to the given value of the potential E_H. (E_H is the electrode potential measured against

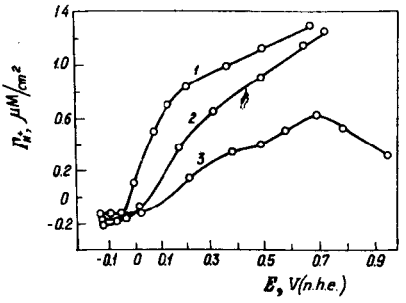


Figure 4. Dependence of Γ_{H^+} on potential on a Pt/Pt electrode in acidified solutions of salts. Initial composition of solutions: 1, 1 *M* NaBr + 0.01 *M* HBr; 2, 1 *M* NaCl + 0.01 *M* HCl; 3, 0.5 *M* Na_2SO_4 + 0.005 *M* H_2SO_4.[25]

a normal hydrogen electrode in the same solution.) Then, the value of Γ_{H^+} at $E_H = 0$ was determined in an experiment in which a dry electrode was introduced into the initial solution in a hydrogen atmosphere. After determination of Γ_{H^+} at $E_H = 0$, it was possible to plot the Γ_{H^+}–E_H curve.[25,28]

Figures 4 and 5 show the dependences of Γ_{H^+} on E_H at a Pt/Pt electrode in acidified and alkalized salt solutions.[25,80] These dependences allow one to find the potentials at which the condition $\Gamma_{H^+} = 0$ is valid, i.e., to determine the potentials of zero total charge (pztc) of the second kind. The measurement of the dependence of Γ_{H^+} on the alkali metal cations concentration showed that when these are present in sufficient excess, the H^+ ions are completely displaced from the ionic side of the electric double layer ($A_{H^+} = 0$), and the quantity Γ_{H^+} proves to be equal to the free surface charge σ[30] [see Eq. (2.4)]. For this reason pztc of the second kind was called the potential of zero free charge (pzfc).

Figures 4 and 5 clearly show the specific features of the σ, E_H curves, typical of platinum metals and responsible for the difference of their behavior from that of a mercury electrode, viz., slight dependence of σ on E_H at small E_H, decrease of σ with increasing E_H when adsorbed oxygen appears on the surface in acid solutions containing no halogen anions, and weak dependence of σ on E_H in alkaline solutions in the absence of surfactant anions. These specific features are associated with the adsorption of hydrogen and oxygen on platinum and with their influence on the adsorption of the solution ions.

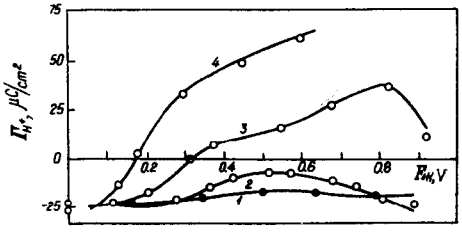


Figure 5. Dependences of Γ_{H^+} on potential on a Pt/Pt electrode in solutions: 1, 0.01 *M* KOH; 2, 0.01 *M* KOH + 1 *M* KCl; 3, 0.01 *M* KOH + 1 *M* KBr; 4, 0.01 *M* KOH + 1 *M* KI. The values of Γ_{H^+} are referred to true electrode surface.[33]

It follows from the definition of Γ_{H^+} and the electroneutrality condition that

$$\Gamma_{H^+} = \Gamma_{A^-} - \Gamma_{C^+} \tag{3.4}$$

Thus pztc's of the second kind can be defined also as the potential at which $\Gamma_{A^-} = \Gamma_{C^+}$. Such a method of determining the pzc with the use of tracers for finding Γ_{A^-} and Γ_{C^+} was proposed by Balashova.[26] The most accurate measurements of Γ_{A^-} and Γ_{C^+} were made by means of the technique proposed by Kazarinov.[81] Figure 6 illustrates the determination of pzfc by means of the tracer technique. Curve 1 gives the dependence of cation adsorption and curve 2 that of anion adsorption on potential. The abcissa of their point of intersection determines pzfc; at this point curve 3, giving the dependence of $\Gamma_{H^+} = \sigma$ on E_H, passes through zero.

The pztc's of the first kind at which $\Gamma_H = 0$ can be determined in principle by direct measurement of the potential assumed by the previously carefully degassed electrode when it is immersed into solution. This method was successfully used for activated carbon;[49] but so far it has not been possible to apply it to platinum metals, owing to the difficulty of preparing degassed electrodes with developed surfaces. For this reason, for determination of pztc of the first kind, a nonthermodynamic method is used, based on the equation $\Delta\Gamma_H = \Delta A_H - \Delta\Gamma_{H^+}$, where ΔA_H is the change in the amount of adsorbed hydrogen per cm^2 surface. The substance of the method is illustrated by Figure 7, in which curves 1 and 2 represent the dependences $\Delta\Gamma_H - E_H$ and $\Gamma_{H^+} - E_H$, respectively. The origin of the abcissa corresponds to the zero value of σ, so that the abcissa of each point of curve 2 gives the value of Γ_{H^+}. Curve 3 is the dependence of E_H on ΔA_H, which was found by subtracting Γ_{H^+} from $-\Delta\Gamma_H$. At $E_H > 0.4$ V, the ΔA_H, E_H curve rises vertically, i.e., A_H no longer depends on E_H. It is natural to suppose that here begins the double-layer region of the charging curve, which extends up to the point at which oxygen deposition starts. (The oxygen region is not shown in Figure 7.) The point of intersection of curves 1 and 3 corresponds to the potential of zero free charge. The tangent to curve 3 in its

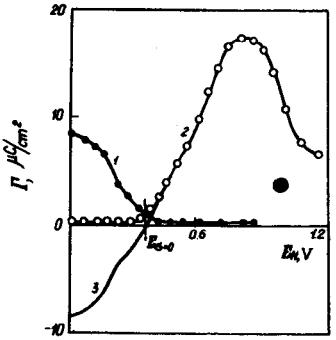


Figure 6. Dependences of the adsorption of Na^+ cations (1), SO_4^{2-} anions (2) and of the free surface charge (3) on the potential of a Pt/Pt electrode in solution: 5×10^{-4} *M* H_2SO_4 + 1.5×10^{-3} *M* Na_2SO_4.[111]

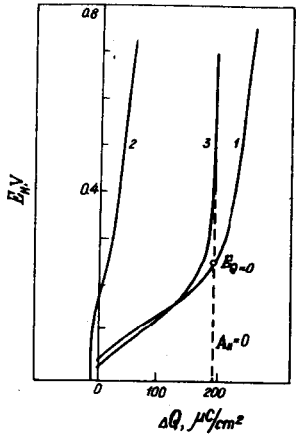


Figure 7. Dependences of the total (1) and free (2) surface charges and of the amount of adsorbed hydrogen (3) on potential on a Pt/Pt electrode in the solution 1 *M* KCl + 0.01 *M* HCl.[111]

vertical portion, as shown in the figure, intercepts on the abcissa a point corresponding to the zero value of A_H. The distance between any point of curve 3 and the straight line $A_H = 0$ is equal to A_H, and the horizontal distance between curves 1 and 3 is equal to σ. Therefore the length of the section of the straight line, parallel to the abscissa and drawn through the point of intersection of the straight line $A_H = 0$ and curve 1, between curves 1 and 3, determines simultaneously the values of A_H and σ on curve 1. Hence, at the point of intersection of curve 1 and the straight line $A_H = 0$, the quantity $\Gamma_H = A_H - \sigma$ vanishes. Thus the pztc of the first kind can be found.

The described method of determination of pztc of the first kind can be used only in the presence of an ideal double-layer region, which is the case only in solutions containing surface-active anions, e.g., in acidified solutions of chlorides or bromides or in alkalized solutions of iodides.[31] However, if the value of the total charge in a certain solution is known, then the dependence of Γ_H on the electrode potential can be obtained and, hence, pztc of the 1st kind determined for the same electrode in other solutions by measuring the shift of the electrode potential upon substitution of one solution by another at constant total charge value $Q = -\Gamma_H$. This condition is fulfilled if the potential shift is measured on an isolated electrode, and the possibility of molecular hydrogen and oxygen or some other oxidants or reducing agents, except H^+ and OH^- ions, getting into solution is ruled out.

The dependences of Γ_{H^+} on E_H can be calculated if one knows the values of the potential shifts with changing solution pH at constant total charge Q,[28] i.e., under the so-called isoelectric conditions. In fact, the Gibbs adsorption equation for a reversible system formed of the components H, CA, and HA at $\Gamma_{H_2O} = 0$ is as follows[29]:

$$d\gamma = -\Gamma_H \, d\mu_H - \Gamma_{HA} \, d\mu_{HA} - \Gamma_{CA} \, d\mu_{CA} \qquad (3.5)$$

where Γ_{HA} and Γ_{CA} are the Gibbs adsorptions, and μ_{HA} and μ_{CA} are the chemical potentials of acid and salt. If [CA] $\gg$ [HA], so that it can be assumed that μ_{CA} = const, taking into account the relations $\Gamma_{HA} = \Gamma_{H^+}$, $d\mu_H = -dE_H$ and $\Gamma_H = -Q$, from Eq. (3.5), the following is obtained:

$$(\partial\Gamma_{H^+}/\partial E_H)_{\mu_{HA},\mu_{CA}} = -(\partial E_H/\partial\mu_{HA})_{Q,\mu_{CA}}(\partial Q/\partial E_H)_{\mu_{HA},\mu_{CA}} \tag{3.6}$$

or

$$(\partial\Gamma_{H^+}/\partial E_H)_{\mu_{H^+},\mu_{CA}} = -(\partial E_H/\partial\mu_{H^+})_{Q,\mu_{CA}}(\partial Q/\partial E_H)_{\mu_{H^+},\mu_{CA}} \tag{3.7}$$

The derivative $(\partial E_H/\partial\mu_{H^+})_{Q,\mu_{CA}}$ gives the value of the potential shift for as small a change in the solution composition as possible under isoelectric conditions. The technique of measurement of this quantity was developed by Frumkin *et al.*[28] The second factor in the right-hand side of Eq. (3.7) represents the slope of the charging curve of the first kind in the HA + CA solution. Thus, from Eqs. (3.6) and (3.7), the value of $\partial\Gamma_{H^+}/\partial E_H$ for the solution of given composition can be found; and hence, one can determine the dependence of Γ_{H^+} on E_H from a single value of this coefficient found in the experiment. The calculated dependences of Γ_{H^+} on E_H were compared with those found experimentally for Pt, Rh, Ir, Pd, and Ru electrodes with developed surfaces in acidified and alkalized Na_2SO_4, KCl, and KBr solutions and in KI and KOH solutions.[28–33] The comparison proved the validity of Eqs. (3.6) and (3.7) and, hence, of Eq. (3.5) and allowed determination of the areas of its practical applicability. At the same time, this comparison of calculation and experiment revealed the reliability of the pzc determination by adsorption methods.

3.5. Methods Based on the Dependence of the Properties of the Diffuse Part of the Double Layer on the Surface Charge

Several methods of determination of the potential of zero free charge are based on the influence of the surface charge σ on the space distribution of potential within the diffuse part of the electric double layer.

3.5.1. Differential Capacity Minimum

The most important of the methods under consideration is the determination of the position of the minimum on the curve showing the dependence of the differential capacity C on the electrode potential, E. This method was proposed by Vorsina and Frumkin.[82]

It follows from the Gouy–Chapman theory that the diffuse layer thickness in the case of symmetrical electrolyte is maximal at $\sigma = 0$ and is inversely proportional to $c^{1/2}$, where c is the electrolyte concentration. The dependence of the diffuse layer thickness on concentration leads to a decrease of its capacity with dilution of the solution, which in sufficiently diluted solutions affects the total electrode capacity. As a result, a minimum appears on the C–E curves,

whose potential in diluted solutions of surface-inactive electrolytes approaches pzfc.

Grahame[16] proposed to model the electric double layer by means of two capacitors with the capacities C_1 and C_2 connected in series, which leads to the relation

$$\frac{1}{C} = \frac{1}{C_1} + \frac{1}{C_2} \tag{3.8}$$

where C_1 is the dense layer capacity and C_2 is the diffuse layer capacity. According to Grahame, in the absence of specific adsorption, the value of C_1 should not depend on the electrolyte concentration, which makes it possible to find, using the diffuse double-layer theory, the C–E dependence for an arbitrary concentration if the C_1–E dependence has been determined from experimental C values and calculated C_2 values for any one concentration. These conclusions were verified by Grahame for the case of aqueous NaF solution. It was shown that they extend to systems with weak specific adsorption.[83]

It follows from Eq. (3.8) that at constant C_1, a linear dependence of $1/C$ on $1/C_2$ with the slope equal to unity should be valid (Parsons–Zobel criterion).†

The differential capacity measurements afford reliable data on the pzc only if certain conditions are fulfilled. First of all, it is necessary that the electricity supplied to the electrode/electrolyte interface should be expended only in charging the double layer. A criterion of the fulfillment of this condition is the absence of the frequency dependence of the capacity component of impedance which is being measured. Another criterion is a good fit of the measured capacity values at different solution concentrations to Eq. (3.8).

The method of the pzc determination from the capacity minimum was used, apart from mercury, for other liquid metals: thallium and indium amalgams, gallium, gallium–indium, and gallium–thallium alloys. The capacity measurements of the electric double layer for determination of the pzc of solid electrodes were carried out for the first time by Borisova, Ershler, and Frumkin in 1948. However, considerable time was needed to improve sufficiently the technique of preparation of the solution and of the solid electrode surface, so that the C–E curves satisfying the conditions pointed out above could be obtained. A significant contribution to the development of these techniques was made by Leikis and co-workers, Bagotskaya, Grigoryev, and by Past and Palm in USSR. Quite satisfactory C–E curves with respect to their shape and the dependence on the electrolyte concentration were obtained at an early stage of development of these studies by Randles in England. A further step in the development of the technique of these measurements was the transition from polycrystalline surfaces to faces of single crystals (Budewski and co-workers).

† The deviation of the slope from unity in the case of solid electrodes can be associated with the difference between true and apparent electrode surface and also with crystallographic inhomogeneity of the solid electrode surface. Such deviation is observed also, however, for liquid gallium.[84] It was suggested by Frumkin *et al.*[84] that it may be indicative of a difference in the dielectric constant of water in the diffuse layer and in the solution bulk.

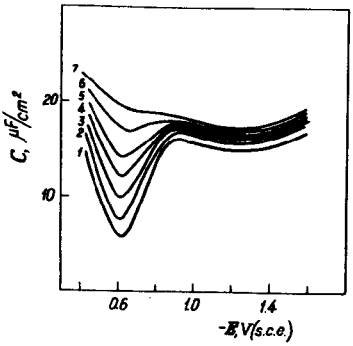


Figure 8. Differential capacity curves of a bismuth electrode in KF solutions: 1, 0.001 *M*; 2, 0.002 *M*; 3, 0.005 *M*; 4, 0.01 *M*; 5, 0.02 *M*; 6, 0.05 *M*; 7, 0.1 *M*.[89]

At present reliable data on the pzc have been obtained by the capacity minimum method for the following metals: Ag (111),[85,86] Ag (100),[87] Ag (110),[85] Au (110),[88] Bi (polycrystalline),[89] Bi (111),[90] Cd,[91] Ga,[60,61] In,[92] Pb,[93] Sb,[94] Sn,[95] Tl.[96] As an illustration of the determination of the pzfc from the capacity minimum, some data for a Bi electrode are given in Figure 8.

In the pzc determination solutions of alkali metal fluorides were used for most electrodes, due to the low adsorbability of the F^- ion. However, on tin the fluorine ion proves to be surface active, and optimum results are obtained with perchlorates. In unsymmetrical surface-inactive electrolytes, the minimum on the *C–E* curves shifts in the direction of more negative σ values in the case of a higher anion charge and in the positive direction in the case of a higher cation charge.

The *C–E* curves of polycrystalline and single-crystal silver electrodes have been compared, and an attempt was made to describe the *C–E* curve of a polycrystal as an additive sum of the *C–E* curves of individual faces of a single crystal[97]:

$$C = C_{(111)}\theta_{(111)} + C_{(100)}\theta_{(100)} + C_{(110)}\theta_{(110)} \tag{3.9}$$

where $C_{(111)}$, $C_{(100)}$, and $C_{(110)}$ are the capacities on individual faces of a single crystal and $\theta_{(111)}$, $\theta_{(100)}$, and $\theta_{(110)}$ are the fractions of these faces on the surface of a polycrystalline electrode. As can be seen from Figure 9, the calculated curve roughly corresponds to the experimental one. It appeared that, since the *C–E* curves of the single-crystal faces of silver, as with other electrodes, are unsymmetrical, when they are added in compliance with Eq. (3.9), the minimum on the total capacity curve lies closer to the minimum of the *C–E* curve of the face whose pzc has the most negative value. This means that the minimum on the *C–E* curve of polycrystalline silver does not correspond to its pzc, i.e., the potential at which

$$\sigma = \sigma_{(111)}\theta_{(111)} + \sigma_{(100)}\theta_{(100)} + \sigma_{(110)}\theta_{(110)} = 0 \tag{3.10}$$

but is located more negatively than this potential.

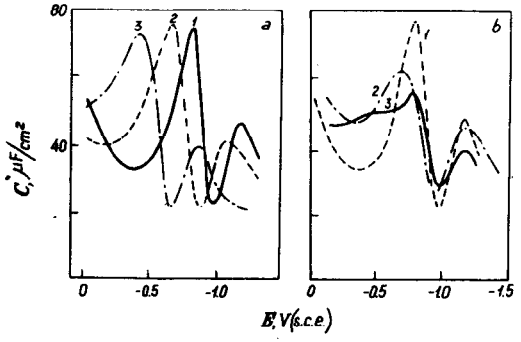


Figure 9. Differential capacity curves of a silver electrode in 0.01 M NaF: (a) for the faces {110} (1); {100} (2) and {111} (3) of Ag single crystal. (b) for the face {110} (1), for polycrystalline silver (2), and the curve calculated by means of Eq. (3.9) (3) at $\theta_{(110)} = 0.31$, $\theta_{(100)} = 0.23$, and $\theta_{(111)} = 0.46$.[97]

In principle, this complication caused by crystallographic inhomogeneity of the surface extends to all polycrystalline electrodes. A significant difference between the pzc and the potential of the minimum of the C–E curve of a polycrystalline electrode is to be expected only in the case when the pzc of individual faces differ by some tenths of a volt. In the case of Bi and, probably, Pb, Cd, In, Sn, Tl, and Sb, the potential of the minimum on the C–E curve of a polycrystal can be roughly equated with the pzc of the metal.

In the case of metals of the VIII group of the Periodic System, the interpretation of the C–E curves, apart from the difficulties associated with the crystallographic surface inhomogeneity, is further complicated by the fact that the double-layer capacity is superimposed by the pseudocapacity of the adsorbed hydrogen ionization and by ionization of the metal itself (in the case of the iron group metals). Nevertheless, repeated attempts to determine the pzc's of these metals are reported in the literature.[8,27] The data on the capacity minimum for platinum cannot be considered conclusive as yet. The C–E curves for an iron electrode satisfying the above criteria have been obtained.[98] But in order to draw definitive conclusions, it is necessary to perform measurements on individual faces of an iron single crystal.

The electrolyte concentration at which a minimum appears on the C–E curve, caused by the double-layer diffuseness at the pzc, depends on the ratio between the first and the second terms in the right-hand side of Eq. (3.8). It is the higher, the larger is C_1. (For example, for mercury the concentration is $\sim 10^{-2}$ M and for Ga $\sim 10^{-1}$ M.) The sensitivity of the signal being measured to a change in the differential capacity of the diffuse layer can be considerably increased by applying to an electrochemical cell two sinusoidal currents of the same amplitude and similar frequencies ω_1 and ω_2.[99] The voltage amplitude of the vibrations arising in the circuit is recorded as a function of the difference

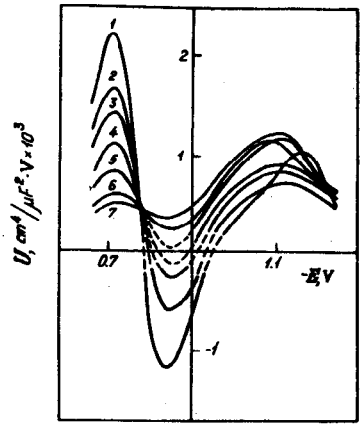


Figure 10. Dependence of U on potential on cadmium in NaF solutions: 1, 0.026 M; 2, 0.04 M; 3, 0.06 M; 4, 0.09 M; 5, 0.13 M; 6, 0.20 M; 7, 0.30 M.[100]

frequency ($\omega_1 - \omega_2$). The value of the amplitude of these vibrations U at the cell terminals is

$$U = \text{const}\,(1/C^3)(dC/dE) \tag{3.11}$$

Using Grahame's model it is possible to show that the U–E curves measured in electrolytes of different concentration must intersect at the pzc. This conclusion was confirmed by measurements on mercury and cadmium[100] (Figure 10).

3.5.2. *Electrokinetic Phenomena*

When a tangential electric field is applied to the interface between two phases at which an electric double layer exists, pondermotive forces arise at this interface which set into motion, depending on experimental conditions, the particle present in the liquid (electrophoresis) or the bulk of the liquid (electro-osmosis). On the other hand, any motion along the interface between two phases gives rise to potential differences, for example, when solid particles are falling in liquid (sedimentation potential) or when a liquid is forced through a diaphragm (streaming potential). These phenomena can be considered to be the reverse of electrophoresis and electro-osmosis. The velocity of electrokinetic motion of a particle of an arbitrary shape in liquid medium in a uniform electric field of the strength X is given by the equation[101]

$$v_E = \tfrac{1}{4}\varepsilon\zeta X/\pi\eta \tag{3.12}$$

where ε is the dielectric constant of the solution, η is its viscosity, ζ is a certain effective potential difference within the electric double layer, the so-called electrokinetic (or zeta) potential. Equation (3.12) is applicable to a particle from a hard metal, if the polarizability of the metal/solution interface is large enough.

Billitzer was the first to use the electrokinetic phenomena to find the pzc (which Billitzer thought was the absolute zero of potential) from the reversal of the zeta-potential sign. This was determined from the direction of the electrophoresis of metal suspensions, from the deviation of wires or of a small suspended metal sphere in the electric field and from the potentials arising when metal particles are falling in a vertical tube filled with electrolyte (silver, gold, platinum, iron). The experimental part of Billitzer's studies raised some objections, but the reversal of the sign of ζ at very positive potentials ($+0.4 - +0.5$ against N.H.E.) is undoubtedly a real fact. As was shown by Balashova and Frumkin,[102] under appropriate experimental conditions, the electrokinetic measurements in the case of platinized platinum lead to pzc values comparable to those obtained from the adsorption measurements. If follows from these experiments that, in the absence of surface oxidation and specific ion adsorption, the electrokinetic methods can afford information on the potential of zero free charge.

An electric field in electrolyte solution causes a liquid metal drop to move. This phenomenon, discovered by Christiansen in 1903, can be observed on a sessile or on a free-falling mercury drop. Its mechanism is essentially different from electrophoretic motion of solid particles. The electric field in solution sets up a potential difference and, hence, a difference in the surface tension between different points of the interface. As a result, the interface starts to perform tangential motion, which push the mercury drop away from the surrounding medium. According to the quantitative theory of these phenomena developed by Frumkin and Levich[103,104] and experimentally proven by Frumkin and Bagotskaya, the potential of the drop at which velocity of tangential motion of its surface vanishes, coincides with the potential of the electrocapillary curve maximum. The studies on electrocapillary phenomena do not provide new information on the pzc, but are of independent interest, especially in connection with the problem of polarographic maxima.

3.5.3. *Photoemission of Electrons from Metal into Solution*

Photoemission of electrons from a metal into the electrolyte solution is among relatively new phenomena in electrochemistry which could be used for pzfc determination. Photoemission of electrons occurs when a metal electrode is illuminated by light, the quantum energy of which exceeds the work function in the metal/solution system.[105] The emitted electrons are thermalized and solvated (at distances from the electrode of the order of 10–100 Å), and then enter into reaction with the electron acceptors specially added to the solution (e.g., H_3O^+, N_2O, NO_3^-, etc.). Cathodic polarization of the electrode decreases the work function and therefore increases the photoemission rate.

In the case of relatively diluted solutions, when the de Broglie wavelength of an emitted electron λ is less than the thickness of the diffuse part of the double

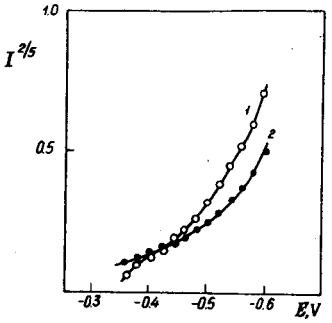


Figure 11. Dependences of $I^{2/5}$ on potential in 10^{-3} M HCl (1) and 10^{-3} M HCl + 9×10^{-3} M KCl (2) on a mercury electrode. Potentials are referred to SCE.[106]

layer, a theoretical analysis of the photoemission process[106] leads to the following relation for the photoemission current:

$$I = A[\hbar\omega - \hbar\omega_0 - e_0(E - \psi_1)]^{5/2} \tag{3.13}$$

where A is a constant, $\hbar\omega$ is the light quantum energy at the frequency ω, $\hbar\omega_0$ is the work function in the metal solution system at the potential $E = 0$, measured against some reference electrode, and ψ_1 is the potential at the point which is at the distance of the order of λ from the electrode. The correction for the ψ_1 potential is similar to that introduced into the equation of electrochemical kinetics to take account of the diffuseness of the electric double layer. At pzfc, $\psi_1 = 0$, and the photocurrent–potential curves for electrolyte solutions of different concentration should intersect (Figure 11).

The described method was used to determine the pzc of some metals (Pb, Bi, Cd, In, Hg), which proved to be in good agreement with the independent measurements from the differential capacity minimum.[106] A possible error in these determinations is about 0.02–0.03 V.

3.5.4. *Interaction of Two Double Layers*

The presence of the diffuse electric double layer leads to repulsion between two charged surfaces. As was shown by Deryaguin, Voropaeva, and Kabanov,[107] this effect can be utilized for finding the pzc. The quantity to be determined experimentally is the force barrier which is necessary to surmount in order that two threads crossed at an angle of 90° should come into contact. The force barrier was measured by means of a torsion balance with a vertical suspension; one of the threads acted as the weight lever. The second thread could be brought close to the first thread or drawn away from it. The contact between the threads, which was evidenced by the disappearance of ohmic resistance between them, arose when the suspension was twisted to an angle depending on the barrier height. At the pzc, the Coulomb portion of the force barrier disappears; at the distance from the pzc greater than 0.15–0.2 V, it reaches the limiting value in accordance with the theory of repulsion between diffuse layers.[107] Also, in

agreement with the theory, the Coulomb portion of the force barrier disappears with increasing electrolyte concentration. The method under consideration was used for Pt, Au, and Fe, the greatest attention being given to Pt.[108] However, the solution purification seemed to be insufficient (especially in the case of Pt) to ensure the cleanliness of the small surface in contact with a relatively large solution volume. Moreover, it is difficult to compare the data with the results obtained by other methods due to the absence of information on the pH of the test solution. It would be desirable if this method, which has a serious theoretical basis and elegant equipment at its disposal, should be verified under more carefully elaborated electrochemical conditions of the experiment.

It should be stressed that the results of all the methods based on the diffuse layer properties are affected by the crystallographic surface inhomogeneity. Therefore, with the use of these methods, it is possible to obtain reliable data on the pzc only for single-crystal electrodes.

4. Influence of Metal Nature, Solution Composition, and pH on the Potentials of Zero Charge

Numerous studies carried out with the use of the methods described above revealed the dependence of the pzc on a large number of factors: metal nature, solution composition, solvent nature, temperature, and, in the case of hydrogen- and oxygen-adsorbing metals, on the pH of the medium. It seems reasonable to attempt elucidation of the role of each of these factors separately.

The influence of the metal nature can be followed if one examines the behavior of different metals in the same solvent at constant temperature and considers only the electrolyte solutions in which the interaction of their ions with the electrode metal is determined by electrostatic forces alone. Such ions are assumed to be adsorbed nonspecifically. When nonspecifically adsorbable ions approach the electrode surface, they retain their hydration sheath. When this condition is not fulfilled, specific adsorption results. Specific adsorption can be the result of the interaction of ion with electrode metal, which is accompanied by partial loss of the hydration sheath (according to Lorenz, also by partial charge transfer) as well as loss of ion expulsion from the water bulk, especially in the case of large organic ions.

Practically all ions to a greater or lesser degree show specific adsorbability at the electrode/solution interface. However, in the presence of weak specific adsorption, the shift of the pzc often proves to be less than 0.1 mV, i.e., less than the present accuracy of determination of this quantity.[83] To weakly adsorbable ions belong the cations of alkali and alkali–earth metals; their adsorbability decreases with the crystallographic radius. Among the anions the specific adsorbability is the least pronounced for F^-, HF_2^-, BF_4^-, and PF_6^- ions and also for some doubly charged anions, such as SO_4^{2-} or CO_3^{2-}. The structure of the double layer near the pzc is the less distorted by specific ion adsorption, the lower is solution concentration; and the independence of the found pzc value of

the electrolyte concentration in a sufficiently wide concentration range indicates that the influence of specific adsorption has been eliminated. Thus, determining the pzc with sufficiently diluted electrolyte solutions whose ions do not show appreciable specific adsorbility, or extrapolating to infinite dilution, one obtains the pzc values depending only on the nature of the metal and the solvent. Presently, at ordinary temperatures a reliable set of pzc values is available, primarily for aqueous solutions. If the solution composition to which a particular pzc value refers is not specially indicated, it is understood that the pzc value of a metal was obtained in aqueous solutions at ordinary temperatures and, as far as possible, not distorted by specific adsorption. For this value Antropov suggests the term "zero point of metal" and recommends to differentiate between the notions "zero point" and "potential of uncharged surface."[129] However, in the absence of specific adsorption of ions or neutral surface-active substances as well, one must take into account the potential difference resulting from the orientation of solvent molecules,[7,12-14] which to a considerable extent eliminates the difference between the pzc in the presence or absence of specific adsorption.

From a short review of the methods proposed for the pzc determination, it follows that for liquid metals it is possible to use equally well the electrocapillary measurements, a dropping electrode, and the determination of the potential of the differential capacity minimum of the diffuse layer. In the case of solid metals, the most reliable results are obtained by adsorption measurements, and in the case of ideally polarizable electrodes, the determination of the position of the differential capacity minimum of the diffuse layer yields the most reliable results. In the latter case the obtained values are simultaneously the potentials both of zero free ($E_{\sigma=0}$) and zero total ($E_{Q=0}$) charges. However, in the case of hydrogen-adsorbing metals, the quantities $E_{Q=0}$ and $E_{\sigma=0}$ do not coincide. In Table 1 are given the data for various metals, which can be considered as recommended pzc values. These data relate to the temperature about 25°C, except gallium (32°C). They give an idea of the dependence of the pzc on the nature of the metal.

The influence of solution composition on the pzc was studied by many authors. Figure 12 shows the electrocapillary curves of mercury in equimolar NaF, NaCl, NaBr, and NaI solutions.[111] The specific anion adsorption shifts the pzc in the negative direction; the shift increases with rising surface activity of anions in the sequence $F^- < Cl^- < Br^- < I^-$. Specifically adsorbed cations, e.g., Tl^+ cations, shift the pzc in the positive direction.[112]

Esin and Markov,[113] and also Iofa, Ustinsky, and Eiman,[114] were the first to study quantitatively the influence of the surface-active anion concentration on the pzc of mercury. It was found that when the activity of an electrolyte containing surface-active anions changes by an order, the shift of the pzc in the negative direction is ~100–200 mV; whereas, from the double-layer theory, assuming the charge of specifically adsorbed anions to be uniformly diffuse, one-half of that would be expected. On Grahame's suggestion an abnormally

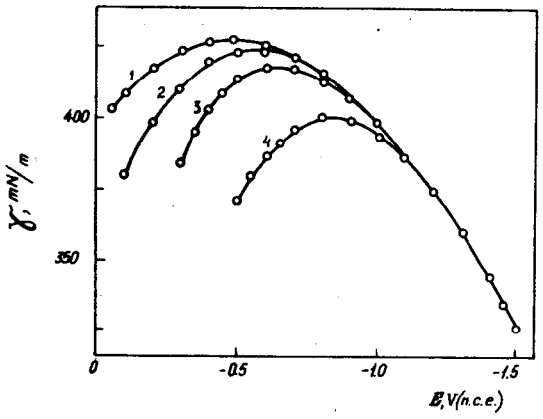


Figure 12. Electrocapillary curves of a mercury electrode in solutions: 1, 0.9 *M* NaF; 2, 0.9 *M* NaCl; 3, 0.9 *M* NaBr; 4, 0.9 *M* NaI.[111]

large pzc shift was called the Esin–Markov effect. To explain the shift of the pzc observed in the presence of surface-active anions, Frumkin's concept of the discrete nature of adsorbed ions was used. This concept formed the basis of the model theories of the Esin–Markov effect developed in numerous papers.[111,115]

From the basic electrocapillarity equation, in the case of an ideally polarizable electrode, Frumkin and Parsons[116,117] have shown that it is possible to obtain a thermodynamic relation for the dependence of the potential of constant free charge on electrolyte concentration, which in a particular case of 1,1-valent electrolyte is of the form

$$(\partial E/\partial \ln a_{\pm})_{\sigma} = -(RT/F)[\partial(\Gamma_{C^+} + \Gamma_{A^-})/\partial\sigma]_{a_{\pm}} \qquad (4.1)$$

At $\sigma = 0$ this relation describes the dependence of the pzc on $\ln a_{\pm}$. It is clear from Eq. (4.1) that the Esin–Markov effect should be observed in cases when the adsorption both of anions and cations increases with σ. Under this condition the Esin–Markov effect is observed not only at $\sigma = 0$, but also at any constant σ.

The studies carried out by the adsorption methods and by the isoelectric potential shifts method showed that on platinum metals pztc of the first and second kinds shift in the negative direction in the presence of specifically adsorbed anions and in the positive direction in the presence of specifically adsorbed cations.[31] By virtue of the presence of two total charges, Q and $\Gamma_{H^+} = \sigma$, for platinum metals it is necessary to introduce two Esin–Markov coefficients, $(\partial E/\partial \ln a_{\pm})_{Q,\mu_{H^+}}$ and $(\partial E/\partial \ln a_{\pm})_{\sigma,\mu_{H^+}}$. The following thermodynamic relations were obtained for these quantities[29,31]:

$$(\partial E/\partial \ln a_{\pm})_{Q,\mu_{H^+}} = -(RT/F)[\partial(\Gamma_{C^+} + \Gamma_{A^-})/\partial Q]_{a_{\pm},\mu_{H^+}} \qquad (4.2)$$

$$(\partial E/\partial \ln a_{\pm})_{\sigma,\mu_{H^+}} = -(RT/F)[\partial(\Gamma_{C^+} + \Gamma_{A^-})/\partial\sigma]_{a_{\pm},\mu_{H^+}} - 2\frac{(\partial A_H/\partial \ln a_{\pm})_{E,\mu_{H^+}}}{(\partial\sigma/\partial E)_{a_{\pm},\mu_{H^+}}} \quad (4.3)$$

These relations become identical with each other and with relation (4.1) for an ideally polarizable electrode when $A_H = 0$ and $Q = \sigma$. The direct determinations of Esin-Markov coefficients on a platinized platinum electrode in the double-layer region showed[29-33] that, unlike mercury, in the case of adsorption of Cl^- ion on a positively charged platinum surface, the discreteness is not evident: when the HCl concentration increases by an order, $E_{\sigma=\text{const}}$ shifts in the negative direction only by ~58 mV. The disappearance of discreteness points to the covalent nature of the bond between metal and specifically adsorbed anions, leading to transition of a major portion of the adsorbed anion charge to the metal surface.

The suggestion that the ions adsorbed on indifferent electrodes pass into adatomic state before the reversible potential is established in the relevant system was first made by Haissinsky in 1933. The comparison of the extent of adsorption of surface-active anions and cations on platinum metals with their contribution to the potential difference between metal and solution led to a convincing conclusion about the charge transfer and an essentially covalent nature of the bond in the case under consideration.[27] The measurements of the superequivalent cation adsorption on a positively charged platinum surface carried out in 0.003 *M* NaA + 0.001 *M* HA solutions, where *A* is SO_4^{2-}, Cl^-, Br^-, or I^-, clearly demonstrated the dependence of the degree of polarity of the bond on the anion nature[31] (Figure 13). The cation adsorption was determined by the tracer technique. In sulfate solutions of the above concentration, superequivalent cation adsorption is not observed due to small surface activity of the SO_4^{2-} ion. In chloride solutions there exists superequivalent adsorption of Na^+, even if small, still measurable, which is nearly independent of potential; this is responsible for the absence of the Esin–Markov effect. In bromide solutions superequivalent

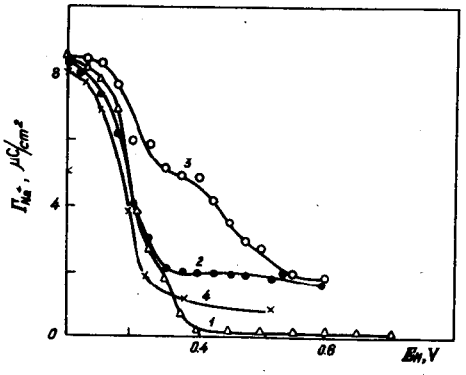


Figure 13. Dependences of the adsorption of Na^+ cations on the potential of a Pt/Pt electrode in solutions: 1, 5×10^{-4} *M* H_2SO_4 + 1.5×10^{-3} *M* Na_2SO_4; 2, 10^{-3} *M* HCl + 3×10^{-3} *M* NaCl; 3, 10^{-3} *M* HBr + 3×10^{-3} *M* NaBr; 4, 5×10^{-4} *M* H_2SO_4 + 3×10^{-3} *M* NaI.[111]

Na^+ adsorption reaches an appreciable value, but drops with increasing potential due to the strengthening of the anion bond with the surface when its positive charge increases. In iodide solutions, in spite of a high adsorbability of I^- ion, superequivalent adsorption is very small, which points to the transition of I^- ion into the atomic state in the case of adsorption on platinum.

These conclusions are supported by the comparison of the dependences of the adsorption of anions on their concentration c, which is given by the logarithmic isotherm

$$\theta = \text{const} + (1/f) \ln c \tag{4.4}$$

where θ is the coverage and the coefficient f is an empirical constant approximately summing the influence of surface inhomogeneity and the effect of the repulsive forces. According to Bagotzky *et al.*[118] the value of f for smooth platinum in the case of neutral molecules is 14–15 and for the HSO_4^- ion ~77, for Cl^-, Br^-, and I^- ions ~18, 15, 14, respectively. In other words, as the surface activity increases, the behavior of anions approaches that of uncharged particles. The covalent nature of the bond of specifically adsorbed anions on platinum metals is consistent with the slow establishment of equilibrium, and exchange can be followed by means of tracers.[26,27,33] The rate of exchange of the Br^- ion on platinum and palladium drops appreciably with increasing E_H, which testifies to an increase of covalence of the bond when passing to more positive potentials.

When the strength of the bond between specifically adsorbed ions and the platinum surface increases, the concept of the pzc itself becomes ambiguous. This is clearly illustrated by the data obtained by tracer techniques on electrodes previously covered with strongly adsorbed iodine or thallium atoms.[31] Thus an electrode was kept in KI or Tl_2SO_4 solution. After it had been removed from solution and washed several times with water to eliminate the weakly bound ions and to determine the amount of strongly bound ones, it was immersed in an acidified Na_2SO_4 solution to measure the adsorption of Na^+ and SO_4^{2-} ions. The results of these measurements are given in Figures 14 and 15. The conclusions about the value of the pzc depend on which part of the double layer one considers the charge of strongly adsorbed ions to belong. If one ascribes it to the metal charge, the position of the pzc is determined by the condition $\Gamma_{Na^+} = \Gamma_{SO_4^{2-}}$, which corresponds to the point of intersection of the curves 1–4, on the one hand, and of the curves 1′–4′, on the other, in Figures 14 and 15. Under this assumption, the adsorption of I^- shifts the pzc toward more positive (Figure 14) and the adsorption of Tl^+ toward more negative (Figure 14) potential values, i.e., the signs of the shift of the pzc prove to be opposite to those which are usually ascribed to these ions. If, however, the charge of chemisorbed ions is considered to belong to the ionic side, the pzc should be determined from the conditions $\Gamma_{Na^+} = \Gamma_{SO_4^{2-}} + \Gamma_{I^-}$ or $\Gamma_{Na^+} + \Gamma_{Tl^+} = \Gamma_{SO_4^{2-}}$, respectively. As can be seen from the position of curves 5 in Figures 14 and 15, with such approach, the adsorption of Tl^+ leads to the shift of the pzc to more positive

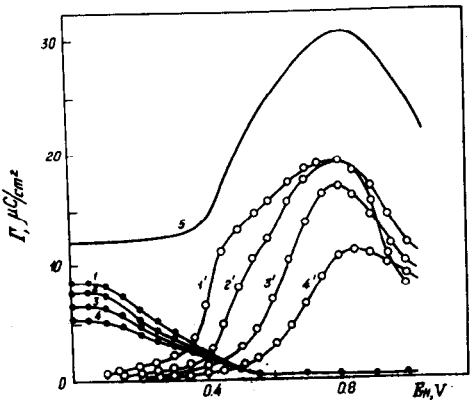


Figure 14. Dependences of the adsorption of Na^+ cations (1–4) and SO_4^{2-} anions (1′–4′) on the potential of a Pt/Pt electrode with iodine ions preadsorbed on its surface in the amounts: 1,1′—0; 2,2′—12; 3,3′—26; 4,4′—38 μC/cm². Curve 5—the dependence of $\Gamma_{I^-} + \Gamma_{SO_4^{2-}}$ on E_H at $\Gamma_{I^-} = 12$ μC/cm².[33]

values; and the adsorption of I^- should lead to a shift of the pzc to very negative values, which, however, is not realized experimentally. The first assumption, probably, approaches more closely the real picture, since under experimental conditions, the adsorption of iodine and thallium to a large extent occurs in the atomic form with formation of a dipole bond between the metal and adsorbed atoms. In the case of iodine, the negative dipole end and, in the case of thallium, the positive end, is turned toward the solution. The question as to whether the chemisorbed particle charge should be ascribed to solution or to the metal side of the double layer arose first when the influence of the oxidation of a Pt electrode on its adsorption properties was considered.[25]

The assumption that strongly chemisorbed anions shift the pzc of metal in the direction of more positive values was used in the interpretation of the action of corrosion inhibitors of iron.[119,120]

It follows from the above data that pzc of platinum metals depend on

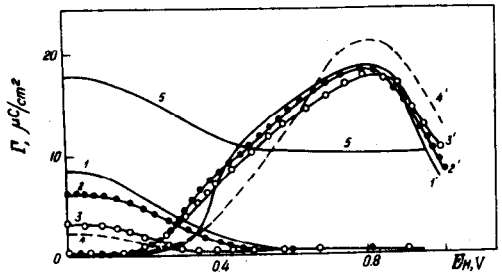


Figure 15. Dependences of the adsorption of Na^+ cations (1–4) and SO_4^{2-} anions (1′–4′) on the potential of a Pt/Pt electrode with thallium ions preadsorbed on its surface in the amounts: 1,1′—0; 2,2′—10; 3,3′—26; 4,4′—53 μC/cm². Curve 5—the dependence of $\Gamma_{Tl^+} + \Gamma_{Na^+}$ on E_H at $\Gamma_{Tl^+} = 10$ μC/cm².[33]

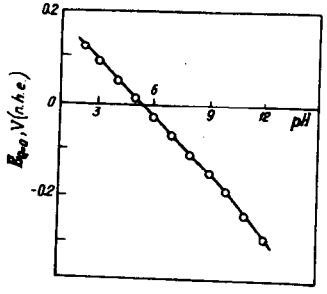


Figure 16. Dependence of the potentials of zero total charge on the solution pH for a Pt electrode in 0.1 *M* KCl.[123]

solution pH. This phenomenon was first detected by Šlygin *et al.*[25] In recent years the studies of Kheifets and Krasikov[121] have given impetus to the investigation of the pH dependence of the pzc. To obtain a complete picture of the dependence of the pzc on solution pH, a method of potentiometric titration at constant total surface charge Q was developed.[122] This titration is carried out with the use of an electrode with its developed surface in an inert-gas atmosphere at open circuit. Previously, the electrode is kept for a long time at a given E_H value so that after breaking the circuit, E_H of the electrode remains constant. The electrode potential must comply with the condition $E_H \geqslant 0.04$ V. The pH value is determined by means of a glass electrode. The composition of solutions is chosen so that the supporting electrolyte concentration should always be higher than that of the H^+ or OH^- ions and practically should not change during titration. Under these conditions; $\Gamma_{H^+} = \sigma$. The potentiometric titration under the conditions specified above gives the dependence of E on pH, corresponding to the value of Q preset at the initial pH. In particular, if $Q = 0$, the $E_{Q=0}$–pH dependence can be directly determined. Such dependence is shown in Figure 16 for a Pt/Pt electrode in 0.1 *N* KCl. Its slope is 40–45 mV per unit pH in the pH range 2–10 and ~55 mV in the pH range 10–12.[123]

It follows from Eqs. (2.13) and (3.5) that

$$(\partial E/\partial \mathrm{pH})_Q = -2.3(RT/F)[1 - (\partial\sigma/\partial A_H)_{pH}]^{-1} \qquad (4.5)$$

In acidified solutions in the pH range studied, the pztc of the first kind lies within the hydrogen region, in which $(\partial\sigma/\partial A_H)_{pH}$ has a small negative value; in alkaline solutions it is close to zero due to the slight dependence of σ on E_H, which leads to the observed dependence of $E_{Q=0}$ on pH. The physical sense of this conclusion is quite clear since the value of Q in the hydrogen region is determined primarily by the term $-A_H$, and the dependence of A_H on E_H varies comparatively little with the solution pH. As a result $Q = -\Gamma_H$ vanishes at the E_H values varying relatively little with the solution pH.

With the use of the titration method at constant Q, it is possible to obtain not only $E_{Q=0}$–pH dependence, but also that of $E_{\sigma=0}$ on pH. For this purpose the E, pH curves corresponding to different Q values are used. Figure 17 shows a set of such curves for a Pt/Pt electrode in 0.1 *N* KCl. The vertical sections on

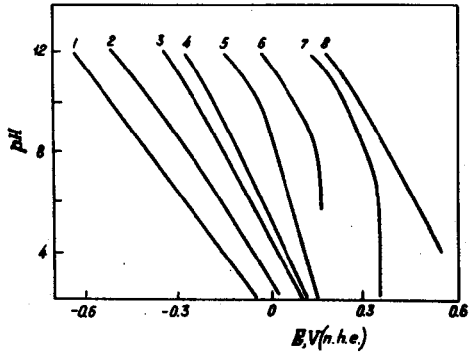


Figure 17. Dependences of the potential E of a Pt/Pt electrode on the solution pH in 0.1 M KCl under isoelectrical conditions at different Q: 1, −152; 2, −82.5; 3, −10; 4, 0; 5, 13; 6, 25; 7, 38; 8, 60 $\mu C/cm^2$.[123]

the curves correspond to the passage of the electrode through the double-layer region within which $E_{Q=const}$ does not depend on pH. By means of the E–pH dependences from the charging curves of the first kind (Q–E curves) measured in acidified (pH = 2.5) and alkalized (pH = 12) solutions, the charging curves of the first kind were plotted at intermediate pH. Then, by means of Eq. (3.7), from the slopes of the E–pH dependences and the Q–E curves, the derivatives $(\partial\sigma/\partial E_H)_{pH}$ were calculated. By integration of the $(\partial\sigma/\partial E_H)_{pH}$–$E_H$ curve, it is possible to find the σ, E_H dependence. The integration constant was determined from the values of $\Gamma_{H^+} = \sigma$ at $E_H = 0$, obtained by potentiometric titration at the atmospheric pressure of hydrogen.[31]

The results of the calculation of the σ–E_H curves are shown in Figure 18. The points of intersection of these curves with the abscissa give the pzfc values,

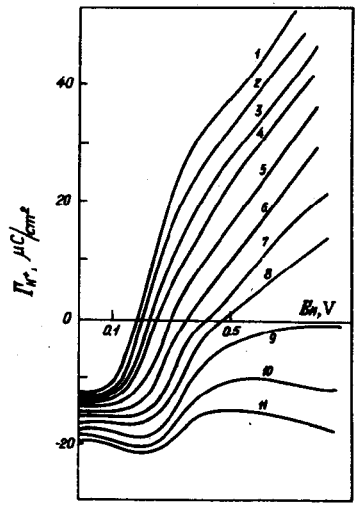


Figure 18. Dependences of the free surface charge of a Pt/Pt electrode on E_H in 0.1 M KCl at different pH: 1, 2.3; 2, 3; 3, 4; 4, 5; 5, 6; 7, 8; 8, 9; 9, 10; 10, 11; 11, 12.[123]

$(E_H)_{\sigma=0}$. It is clear from Figure 18 that as pH increases a transition occurs to the surface negatively charged in the measurable E_H range. To explain this phenomenon it is necessary to take into account a simultaneous action of two factors. First, when pH increases, the potential range in which the measurements are performed shifts in the negative direction relative to the constant reference electrode, which should lead to an increase of the negative charge at constant E_H and hence to an increase of the cation adsorption. Secondly, with increasing pH desorption of adsorbed hydrogen becomes difficult if the Pt–H dipole is turned with its negative end toward the solution and oxygen deposition is facilitated. The arising hydrated oxide groups are slightly acid. As a result, the adsorption of cations in the form, say, $PtOK^-$, becomes possible, which leads to desorption of anions from the platinum surface. Thus, in alkaline solutions a transition takes place from the adsorption of cations caused by ionization of adsorbed hydrogen atoms and decreasing with increasing E_H, to the adsorption of cations by the surface oxide groups, increasing in a certain E_H range. At pH = 10 in a relatively large E_H range, the conditions are established when the Pt surface practically does not carry a free charge.

Figure 19 gives the dependence of $E_{\sigma=0}$ on solution pH in 0.1 *N* KCl. In the pH range 2.3–5.0, the potential $E_{\sigma=0}$ shifts in the cathodic direction by 35 mV when pH increases by a unit. In the pH range 5–9, the shift of $E_{\sigma=0}$ proves to be small; at pH > 7, $E_{\sigma=0}$ begins to shift in the positive direction with increasing pH. A complex shape of the $E_{\sigma=0}$–pH curve is due to the circumstance that $E_{\sigma=0}$ shifts from the hydrogen region to the double-layer region and, then, to that of adsorbed oxygen deposition.

From Eqs. (2.14) and (3.5) by some simple transformations, it is possible to obtain the relation

$$(\partial E/\partial \mathrm{pH})_{\sigma,\mu_{Cl^-}} = -2.3(RT/F)(\partial A_H/\partial\sigma)_{E_H}[(\partial A_H/\partial\sigma)_{E_H} - 1]^{-1} \qquad (4.6)$$

At the potentials corresponding to $\sigma \doteq 0$, anion adsorption and hydrogen adsorption are mutually antagonistic. This is associated with the polarity of the $Pt–H_{ads}$ bond whose negative end is turned toward the solution. Therefore, the quantity $(\partial A_H/\partial\sigma)_{E_H}$ is negative, and in absolute value it increases with rising

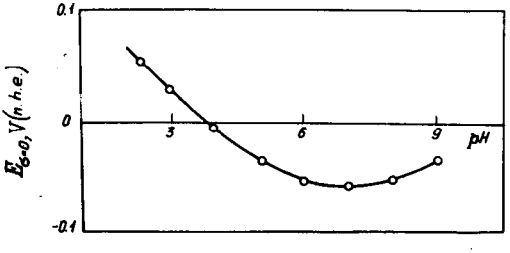


Figure 19. Dependence of the potential of zero free charge of a Pt/Pt electrode in 0.1 *M* KCl on the solution pH.[123]

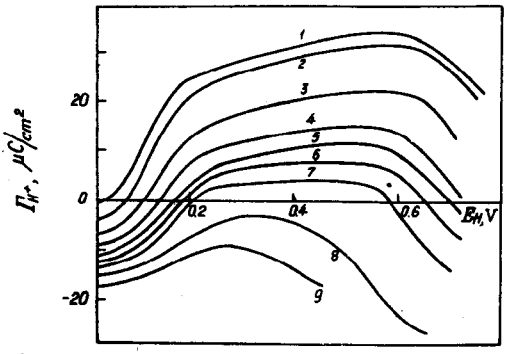


Figure 20. Dependences of the free surface charge of a Rh electrode on E_H in 0.1 M KCl at different pH: 1, 3; 2, 4; 3, 5; 4, 6; 5, 7; 6, 8; 7, 9; 8, 10; 9, 11.[124]

specific adsorbability of the anion. As a result, according to Eq. (4.6), $E_{\sigma=0}$ decreases with increasing pH with the slope which at small pH approaches 2.3 RT/F per unit pH when the adsorbability of the anion rises. These considerations apply to the hydrogen region. In the double-layer region, $A_H = 0$ and, hence, $(\partial E/\partial \mathrm{pH})_{\sigma=0} = 0$. At pH $\approx$ 7, $E_{Q=0} = E_{\sigma=0}$, which is natural since these values of E lie within the double layer of Pt in 0.1 N KCl, where $Q = \Gamma_{H^+} = \sigma$. It is possible, however, that the overlapping of hydrogen and oxygen regions is important here also since at more positive E_H, the derivative $(\partial A_H/\partial\sigma)_{E_H} < 1$ and $E_{\sigma=0}$ shifts into the positive direction with increasing pH.

Figure 20 gives a set of the σ–E_H curves for a rhodium electrode in 0.1 N KCl at different pH.[124] At $E_H \approx 0.6$ V, these curves show a decay associated with oxygen adsorption and similar to that on the σ–E_H curves of Pt in sulfate solutions (Figure 4). In the case of Pt in chloride solutions, such decay is absent (Figure 18). The curve for rhodium, owing to its great oxidizability, shows a decay in chloride medium as well. When pH rises, the beginning of the decay shifts in the direction of less positive potentials. In the pH range 6–9, the σ–E_H curves cut the abcissa twice, ie., there are two conditional pzfc lying in the hydrogen and oxygen regions, respectively. The distance between them is 0.4–0.6 V. At pH > 9, the rhodium surface carries a negative charge at all E_H values.

While in the hydrogen region the experimental values of $(\partial E/\partial \mathrm{pH})_{\sigma=0}$ vary within 0–50 mV depending on solution composition and nature of the metal, in the oxygen region the values of this derivative are much larger. For example, in the case of a rhodium electrode in 0.1 N KCl, the shift in the negative direction of the pztc lying in the oxygen region per unit pH is $\sim$180 mV. By substituting $-A_{OH}$ for A_H, Eq. (4.6) yields

$$(\partial E/\partial \mathrm{pH})_\sigma = 2.3(RT/F)(\partial A_{OH}/\partial \mu_{OH^-})_{E_H}(\partial\sigma/\partial\mu_{OH^-})_{E_H}{}^{-1} \times [(\partial A_{OH}/\partial\mu_{OH^-})_{E_H}(\partial\sigma/\partial\mu_{OH^-})_{E_H}{}^{-1} + 1]^{-1} \quad (4.7)$$

It is evident that $(\partial E/\partial \mathrm{pH})_\sigma$ can be less than $-2.3RT/F$ if $(\partial A_{\mathrm{OH}}/\partial \mu_{\mathrm{OH}^-})_{E_\mathrm{H}} > 0$, and $(\partial \sigma/\partial \mu_{\mathrm{OH}^-})_{E_\mathrm{H}} < 0$.

It follows from the above that, for evaluation of the quantity $(\partial E/\partial \mathrm{pH})_{\sigma=0}$, it is very important to know the effective polarity of the $\mathrm{Pt\text{–}H_{ads}}$ and $\mathrm{Pt\text{–}O_{ads}}$ bonds. One can get an idea of the polarity of the $\mathrm{Pt\text{–}H_{ads}}$ bond by comparing the quantities $X = (\partial E/\partial A_\mathrm{H})_\sigma$ and $Y = (\partial E/\partial \sigma)_{A_\mathrm{H}}$. The calculations of the values of X and Y have been performed and analyzed.[27,30]

Using Eqs. (2.11) and (2.12) for the redox system, H, H^+, when the H^+ and OH^- ion concentrations are small compared to those of other system components, the following relations are obtained:

$$(\partial \gamma/\partial E)_{\mu_{\mathrm{H}^+}} = \Gamma_\mathrm{H} = -Q \tag{4.8}$$

and

$$(\partial \gamma/\partial E)_{\mu_\mathrm{H}} = (\partial \gamma/\partial E)_{E_\mathrm{H}} = -\Gamma_{\mathrm{H}^+} = -\sigma \tag{4.9}$$

Integration of Eq. (4.8) gives the electrocapillary curve of the first kind of platinum accurate to the integration constant. The value of Q is found from the charging curves if the potential of zero total charge $E_{Q=0}$ is known. Since the absolute value of γ for platinum is not known, the result of integration can be most conveniently represented in the form of $\Delta\gamma, E$ curves, where $\Delta\gamma = \gamma - \gamma_0$, and γ_0 is the value of γ at the platinum/solution interface at the maximum of the electrocapillary curve of the first kind for any arbitrary solution. Frumkin and Petrii[31] used the solution 10^{-2} N H_2SO_4 + 1 N Na_2SO_4. With such a choice $\Delta\gamma \leqslant 0$ (except with fluoride solutions[125]). For integration of Eq. (4.9) leading to the $\Delta\gamma$–E curves of the second kind, the data on the dependence of σ on E at constant E_H is essential and can be determined by comparing the σ–E_H curves obtained at different pH.

Figure 21a gives the electrocapillary curves of platinized platinum of the first and second kind for platinized platinum borrowed from Frumkin and Petrii.[31] Curve 1 has been obtained from the charging curve for a

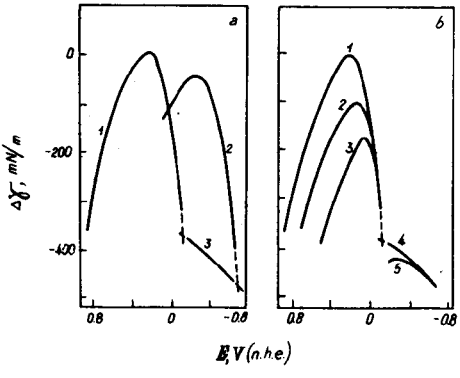


Figure 21. Electrocapillary curves of a Pt/Pt electrode: (a) curves of the first kind in 5 × 10^{-3} M H_2SO_4 + 0.5 M Na_2SO_4 (1), 10^{-2} M NaOH + 0.5 M Na_2SO_4 (2) and a curve of the second kind in 0.5 M Na_2SO_4 at E_H = 0 (3); (b) curves of the first kind in 5 ×. 10^{-3} M H_2SO_4 + 0.5 M Na_2SO_4 (1), 10^{-2} M HCl + 1 M KCl (2), 10^{-2} M HBr + 1 M KBr (3) and curves of the second kind at E_H = 0 in 0.5 M Na_2SO_4 (4), in 0.1 M KI (5).[31]

10^{-2} N H_2SO_4 + 1 N Na_2SO_4 solution and extrapolated to $E_H = 0$. From the value of $\Delta\gamma$ in this solution, it is possible to pass to its value in a 10^{-2} N NaOH + 1 N Na_2SO_4 solution at $E_H = 0$ by means of the electrocapillary curve of the second kind (curve 3, Figure 21a), which allows one to determine the position of the curve of the first kind of the second solution (curve 2). In Figure 21b, the electrocapillary curves of the first and second kind for platinum in solutions containing different anions are compared.[31] The position along the vertical line of the maxima of the electrocapillary curves of the first kind in acidified KCl and KBr solutions was chosen in such a way to ensure the coincidence of the $\Delta\gamma$–E dependences at such E_H values at which the anion nature no longer affects the values of Q and σ. The position of the $\Delta\gamma$, E curves of the first kind of acidified salt solutions with different anions resembles that for mercury. But the slope of both branches of the electrocapillary curves of platinum is greater than in the case of mercury since the quantities A_H and A_{OH} in their absolute values are significantly larger than σ. A distinctive characteristic of the behavior of the two metals is the dependence of the position of the electrocapillary curves of the first kind on solution pH. In Figure 21b, the maximum on the curves of the second kind, i.e., the potential of zero conditional free charge at $E_H = 0$, can be observed only in the NaI supporting electrolyte ($E_{\sigma=0} = -0.31$ V). In the case of SO_4^{2-}, Cl^-, and Br^- anions in the pH range accessible to investigation at $E_H = 0$, $\sigma < 0$.

A more complete picture of the dependence of γ on solution pH can be obtained from the electrocapillary curves of the first and second kind in Figure 22 (Pt in 0.1 N KCl), plotted with the use of the results of potentiometric

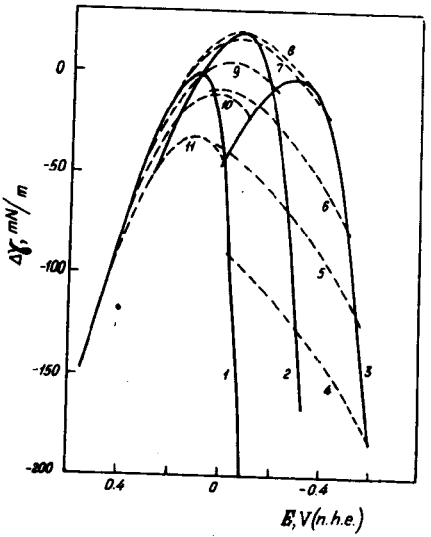


Figure 22. Electrocapillary curves of the first kind (1–3) and of the second kind (4–11) of a Pt/Pt electrode in 0.1 M KCl solution with pH 2.3 (1); 7 (2); 12 (3) and at E_H = 0.10 (4); 0.15 (5); 0.20 (6); 0.30 (7); 0.40 (8); 0.50 (9); 0.60 (10); and 0.70 (11) V.[33]

titration at constant charge. As can be seen from Figure 22, in acidified solutions the values of γ at the maximum of the electrocapillary curves of the first kind are higher than in alkaline solutions. This is due to the fact that, at $E_{Q=0}$ in acid solution, the surface coverage by ions and atoms is less than in the alkaline one. The decrease of Cl^- adsorption when passing from pH 2.3 to pH 7 leads to increase of γ at the maximum of the electrocapillary curve of the first kind. With further increase of pH, the hydrogen and oxygen adsorption regions begin to overlap, which decreases γ. The fact that curves 2 and 8 of Figure 22 practically coincide in a certain range of E is a consequence of the equality $Q = \sigma$, since these sections of the curves lie in the double-layer region.

The existence of two types of electrocapillary curves for platinum metals is accounted for by the fact that the reversible work of surface formation γ is a function of two variables μ_H and μ_{H^+}, and hence when plotted in the coordinates γ, μ_H and μ_{H^+}, it represents a certain surface. The section of this surface by the plane μ_{H^+} = const gives the electrocapillary curve of the first kind, and its section by the plane μ_H = const gives the electrocapillary curve of the second kind.

In the experiments described above, the values of $E_{Q=0}$ and $E_{\sigma=0}$ were obtained for electrolytic deposit of platinum metals under the conditions of maximum approach to equilibrium between solution and electrode. Bockris and coworkers[126] studied the pH dependence of the pzfc of smooth platinum free of adsorbed hydrogen. For this purpose a platinum electrode, reduced in hydrogen by heating for a short time to 400°C, was kept at 450°C in an argon atmosphere and, after cooling, was introduced into the solution at the potential $E_H > 0.4$ V to avoid hydrogen adsorption. Then, for the electrodes thus prepared, the C–E curves were plotted. In sufficiently diluted solutions these curves showed a minimum, which disappeared when the overall solution concentration increased. The C–E curves did not exhibit any marked frequency dependence, but their shape and position at different concentrations were other than those generally observed in the case of mercury or "mercurylike" metals. The dependence of the potential of the minimum E_{min} (N.H.E.) on pH was expressed by the relation

$$E_{min} = 0.56 - 2.3(RT/F)\text{pH} \qquad (4.10)$$

A short cathodic polarization of the electrode down to $E_H = 0.2$ V led to a shift of E_{min} in the direction of more negative potentials on the subsequently plotted C–E curve. Bockris and co-workers interpreted the obtained values of E_{min} as the pzc of platinum free of adsorbed hydrogen. They explained the dependence of pH by specific adsorption of the hydroxyl ion obeying a logarithmic isotherm.

The thermodynamic interpretation of these results, however, is not clear. The coefficient 59 mV in the $E_{\sigma=0}$–log C_{OH^-} dependence on the surface free of adsorbed gases should point to a practically complete transfer of the adsorbed anion charge to the metal, as was discussed earlier. In other words, it is the

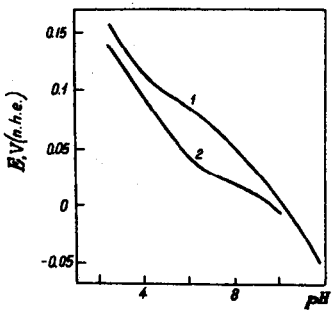


Figure 23. Dependences of pztc (1) and pzfc (2) on pH in 0.05 M K_2SO_4 for a carbon black electrode.[127]

chemisorption of the radical OH which would be in question, rather than the specific adsorption of the OH^- ion. Without the assumption of the presence of strong chemisorption, it also would be impossible to explain the adsorption of OH^- in acid solutions. Thus the interpretation of the above-mentioned authors leads to the conclusion that, if the differential capacity minima observed in their experiments really point to the zero free charge, it must be the zero charge of the oxidized surface. It should be noted that in the case of strong specific adsorption of OH^- ions, as with other ions, the capacity minimum method cannot give the pzc of the surface free from adsorbed material.

The dependences of $E_{Q=0}$ and $E_{\sigma=0}$ on pH have also been obtained for electrodes from activated sugar carbon and carbon black (containing 0.2% Pt/g) by potentiometric titration at constant total charge.[127] The values of σ for carbon adsorbents, as for Pt metals, at all E_H decreases with increasing pH. In Figure 23, the dependences of $E_{Q=0}$ and $E_{\sigma=0}$ on pH for a carbon black electrode are compared. In plotting the $E_{Q=0}$, pH curve, it was assumed that, at pH = 2.4 in acidified 0.1 N K_2SO_4 solution, $E_{Q=0} = +0.16$ V (N.H.E.). The mean shift of the pztc in the pH range 2.4–10 is ~20 mV per unit pH. The shift of $E_{\sigma=0}$ is ~30 mV per unit pH in the pH range 2.4–6, and in the neutral region (pH = 6–8), only ~10 mV per unit pH. For interpretation of these results, the relations (4.5) and (4.6) considered above were used.

5. Potentials of Zero Charge and the Adsorption of Organic Compounds on Electrodes

The discussion of this important problem shall begin with the consideration of the relation between the pzc and the potentials of the adsorption–desorption peaks on the differential capacity curves in the presence of organic compounds. So far the adsorption–desorption peaks have been obtained for different liquid and solid electrodes: Hg, Bi, Pb, Sb, Zn, Cd, Sn, In, Tl, Ag, liquid and solid Ga, and In + Ga and Ga + Tl alloys. (The relevant references are given in Chapter 8 of this volume.) With the exception of mercury, bismuth, and silver, only cathodic adsorption–desorption peaks could be observed for the metals listed

above since in other cases anodic peaks fall within the region of anodic dissolution of the metal. The similarity in the behavior of adsorption of organic compounds on these metals suggests that the position of the cathodic adsorption–desorption peak permits one to draw some quantitative conclusions about the pzc of the metal adsorbent. It can be shown, however, that in the general case this conclusion is erroneous, and the adsorption behavior of the metal is determined not only by its pzc value, but also by its hydrophilic properties.[7,8] Therefore, in principle, the difference between the pzc and the cathodic adsorption–desorption potential (E_d) at a certain concentration of organic substance and surface-inactive supporting electrolyte solution can be used as a criterion of the hydrophilic properties of metals: the stronger are the hydrophilic properties of a metal, the less is ($E_d - E_{\sigma=0}$). This criterion is, however, only a qualitative one since the position of E_d depends not only on the free energy gain upon substitution of water molecules by those of organic substance, but also on some other parameters characterizing the adsorbed layer.

In Table 2, the values of $E_d - E_{\sigma=0}$ and of the charges σ_d, corresponding to E_d in a supporting electrolyte solution and in the presence of an organic substance (0.1 M n-$C_5H_{11}OH$), are compared for different metals.[7] The data on the dependence of ($E_d - E_{\sigma=0}$) on the nature of the metal are also illustrated in Figure 24.

As can be seen from Table 2, in spite of large differences between the values of $|E_d - E_{\sigma=0}|$ for different metals, the values of $|\sigma_d|$, both in pure electrolyte solution and in the presence of an organic substance, depend little on the nature of the metal. (On the average in the supporting electrolyte solution, $|\sigma_d| \approx 13.1$ $\mu C/cm^2$; and in the solution with 0.1 M n-$C_5H_{11}OH$ addition, $|\sigma_d| \approx 9.1$ $\mu C/cm^2$.) This result permits approximate evaluation of the pzc on the basis of the C–E curves measured in 0.1 N solution of a surface-inactive electrolyte and in

Table 2

Maxima of Adsorption and Potentials of Zero Charge

Metal	$\lvert E_d - E_{\sigma=0}\rvert$ (V)	$\lvert\sigma_d\rvert$ ($\mu C/cm^2$)		Electrolyte
		Supporting electrolyte solution	Supporting electrolyte solution + n-$C_5H_{11}OH$	
Ga	0.32	13.0	8.0	0.1 M $NaClO_4$
In + Ga	0.45	12.4	9.4	0.05 M Na_2SO_4
In	0.51	13.2	9.2	0.05 M Na_2SO_4
Cd	0.55	14.3	9.5	0.1 M KF
Sn	0.63	13.2	9.3	0.05 M Na_2SO_4
Pb	0.67	12.8	9.4	0.05 M Na_2SO_4
Bi	0.71	12.5	9.0	0.05 M K_2SO_4
Hg	0.74	13.3	9.3	0.1 M NaF

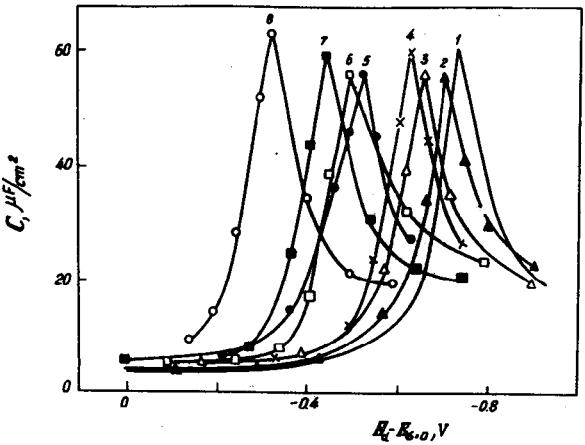


Figure 24. Cathodic sections of the differential capacity curves with an adsorption–desorption peak in 0.1 M n-$C_5H_{11}OH$ solution in the presence of 0.1 M NaF, KF, $NaClO_4$, and 0.5 M Na_2SO_4 supporting electrolytes on different metals: 1, Hg; 2, Bi; 3, Pb; 4, Sn; 5, Cd; 6, In; 7, In + Ga; 8, Ga.[7]

the same solution with n-amyl alcohol addition. Indeed, if the electrode charge at E_d is known, it is possible to obtain the value of $E_{\sigma=0}$ by reverse integration of the C–E curves. However, this estimate will be reliable only under the condition that, in the region of sufficiently large negative charges (within which σ_d falls), different metals have approximately the same compact layer density (C_1). Figure 25 shows the C_1–σ curves for electrodes from indium, cadmium, tin, lead, mercury, antimony, and bismuth and also the C–σ curve for a gallium electrode in 0.5 M Na_2SO_4 not corrected for the diffuse layer capacity.† As can be seen from this figure, at $\sigma = \sigma_d$ the capacities for different metals differ only slightly, i.e., at $E = E_d$ the differences in the hydrophilic properties smooth over to a considerable extent, which leads to identical conditions of organic substance desorption. If, however, the differences in the hydrophilic properties of a metal are retained in the region of large negative σ, the double-layer capacity will be affected, and the adsorption–desorption peak will not correspond to the constant value of σ_d. Neither will the constant value of σ_d be retained under conditions where an organic substance can interact specifically with the electrode surface.

The differences in the hydrophilic properties observed at the pzc depend on the surface charge values and, hence, to what extent water chemisorption begins to manifest itself. While at sufficiently negative potentials the capacities for different metals (except indium and its alloy with gallium) differ little, at the pzc,

† The difference of this curve from the C_1, σ dependence should not be large due to the high concentration of the supporting electrolyte solution.

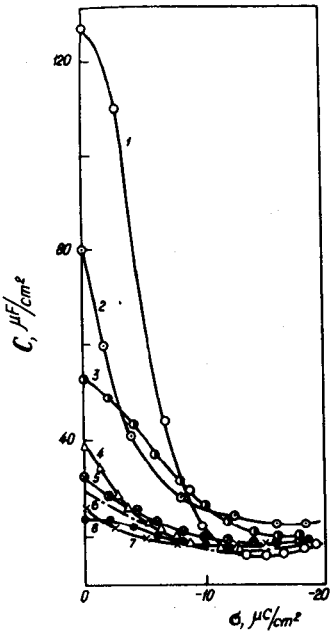


Figure 25. Dependences of the differential capacity of the Helmholtz layer on the surface charge on different metals: 2, In; 3, Cd; 4, Sn; 5, Pb; 6, Hg; 7, Bi; 8, Sb. Curve 1 for Ga is not corrected for the diffuse layer capacity.[7]

the capacity increases markedly in the sequence Bi, Sb < Hg < Pb < Sn < Cd < In < Ga. This sequence nearly coincides with that in which, according to Table 2, the value of $|E_d - E_{\sigma=0}|$ decreases. However, in the case of Bi and Sb, the low capacity values near the pzc can be due to the semiconducting nature of these metals, rather than to their low hydrophilic properties.

The absence of a simple connection between E_d and the pzc, even for mercurylike metals, shows that great care should be taken in extending the results on the adsorption of organic compounds, obtained by means of electrocapillary curves or by some other method for mercury, to solid metals as is done by Antropov[128,129] on the assumption that at equal values of $E - E_{\sigma=0}$ (according to Antropov at equal potential values in the reduced or ϕ scale), the adsorbability of organic compounds, to the first approximation, does not depend on the nature of the metal. This point of view, which is common in electrochemical and corrosion literature, takes an approximate account of the influence of the electric double layer on adsorption, but makes no allowance for the specific character of the interaction of an uncharged metal surface with molecules of water and the organic substance. As will be shown below, the situation becomes even more complicated for metals on whose surface hydrogen and oxygen are adsorbed.

Thus, from the value of E_d measured at a single supporting-electrolyte

concentration, it is impossible to deduce quantitatively the value of the pzc. Recently, Damaskin, Batrakov, and Ipatov[130,131] have shown that it is possible to obtain more detailed information from measurements of E_d by determining its dependence on the supporting-electrolyte concentration, c_{el}, over a wide range of its values. At sufficiently low c_{el}, an increase of the supporting electrolyte concentration, leads to an increase of the double-layer capacity and, hence, of its desorbing action, causing E_d to approach the pzc. The shift of the cathodic desorption peak in the direction of more positive potentials is limited, however, by another effect, viz., by the salting out of the organic substance by the supporting electrolyte at sufficiently high concentrations of the latter. This salting out leads to increased activity of the substance being adsorbed, which is equivalent to the increase of its concentration, and hinders desorption. As a result, the dependence of E_d on c_{el} (or on log c_{el}) passes through an inflection (Figure 26). As follows from the theory set forth by Damaskin *et al.*,[130,132] the electrode charge in the supporting-electrolyte solution at the potential E_{ex}, corresponding to the inflection on the E_d–log c_{el} curve, is equal to

$$|\sigma_0| = 2.3kF\Gamma_m\left\{(c_{ext})^{3/2}\left[\frac{4A}{2.3kF\Gamma_m} + (c_{ext})^{1/2}\right]\right\}^{1/2} \qquad (5.1)$$

where c_{ext} is the supporting-electrolyte concentration at the inflection of the E_d–log c_{el} curve, k is the salting out coefficient, Γ_m is the limiting adsorption of the organic substance, $A = (\varepsilon RT/2\pi)^{1/2}$, and ε is the dielectric constant of water.

As previously shown,[130] relation (5.1) is valid if the conditions given below are satisfied: the organic substance adsorption on the electrode surface is reversible and localized within one monolayer. The adsorption isotherm is congruent with E in the potential range ~ 100 mV in which E_d depends on c_{el}. At these potentials hydrogen or oxygen atoms are not adsorbed on the electrode surface. The desorption potential corresponds to a definite surface coverage (say, $\theta = 0.5$), and the surface layer properties at the maximum coverage by the organic substance do not depend on c_{el}.

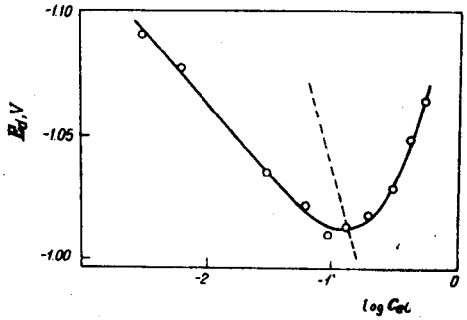


Figure 26. Dependence of the cathodic potential of camphor desorption from the mercury electrode surface on NaF concentration. Camphor concentration 3×10^{-4} *M*.[132]

When these conditions are satisfied (electrodes with a sufficiently high hydrogen overvoltage, an organic substance giving a condensed monolayer upon adsorption, a surface-inactive supporting electrolyte), formula (5.1) permits calculation of the electrode charge in the supporting-electrolyte solution, σ_0, at $E = E_d$.

If the charge value at a definite electrode potential is known, it is possible by means of the C–E dependence to find the pzc. In the case of metals considered at the beginning of this section, such determinations of the pzc are of no practical interest since the value of $E_{\sigma=0}$ can be determined more easily and more accurately from capacity measurements in diluted solutions. This is not the case, e.g., with zinc. The pzc of zinc lies at more positive potentials than the normal potential of a Zn/Zn^{+2} electrode, i.e., it lies in the region of active Zn dissolution. By means of the method described above, it is possible to determine the charge on the Zn surface at potentials at which the Zn electrode can be considered to be ideally polarizable, and, by means of the C–E curve, to continue the determination of σ_0 up to maximum admissable values. Naturally, further approach to $E_{\sigma=0}$ requires extrapolation. Such calculation was performed on the assumption that the values of Γ_m for camphor, which was chosen as a surfactant, are the same for mercury and zinc.[131] The extrapolation (Figure 27) leads to the values of $E_{\sigma=0} = -0.77$ V for the face (0001) and about -0.9 V for a prismatic face. The estimation of the accuracy of this method shows that the error in the determination of the pzc can be ~ 0.05 V.

The measurement of the dependence of adsorption of an organic substance Γ_{org} on E was used by Bockris and his school for the determination of the pzc by an indirect method.[126,133] The idea of this method is as follows. Since, in the absence of specific ion adsorption, the pzc does not depend on electrolyte concentration, the change of this concentration does not affect the state of the surface at the pzc and should not affect the value of Γ_{org} at the pzc. Thus, by determining the dependence of Γ_{org} on E at different inorganic electrolyte concentrations, it is possible to find the pzc ($E_{\sigma=0}$) from the point of intersection

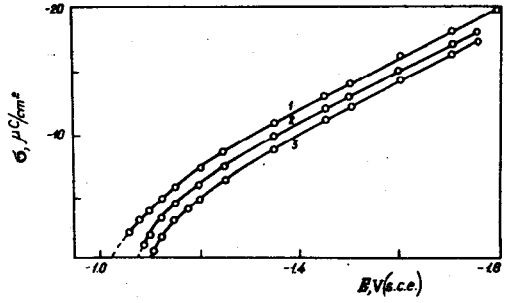


Figure 27. Dependences of the surface charge on potential in 0.1 M KCl (pH = 3.7) for different faces of zinc single crystal: 1, (0001); 2, (1010); 3, (1120).[131]

of the curves giving this dependence. The applicability of this method is based on the assumption that the introduction of the organic substance does not itself lead to a shift of the pzc. If this were so, the adsorption of the organic substance should be a maximum at the pzc, i.e., the common point of the Γ_{org}, E curves at different concentrations should also be the point of maximum adsorption. In a general case, this assumption is not valid (see Chapter 8 of this volume and Bockris and Reddy,[168] where a relation of the potential of maximum adsorption to the pzc is derived). The shift of $E_{\sigma=0}$ during adsorption of organic substances ($\Delta E_{\sigma=0}$) can reach 0.5 V and more; the character of the $E_{\sigma=0}$–θ dependence is determined by the adsorbate nature. In the case of adsorption of aliphatic compounds, the dependence of $E_{\sigma=0}$ on θ is usually monotonic and can be described by means of the two-parallel-capacitor model. In the case of adsorption of aromatic or heterocyclic compounds, the sign of $\Delta E_{\sigma=0}$ may change with an increase in θ, due to the change in the orientation of adsorbed molecules. Under these conditions the dependence of $E_{\sigma=0}$ on θ can be described by the three-parallel-capacitor model.

If $\Delta E_{\sigma=0} \neq 0$, the $\Delta\gamma$–E and the Γ_{org}–E curves measured at different c_{el} also have a common point at the potential of maximum adsorption $E_0 = E_m$[134] (Figure 28a). In the case, the common point of the Γ_{org}–E curves does not coincide with the pzc. However, this conclusion is valid only at sufficiently low electrolyte concentrations, when the salting-out effect can be neglected (e.g., in NaF solutions at $c_{el} \leqslant 0.05\ M$). In the presence of the salting-out effect, however, the $\Delta\gamma$–E and Γ_{org}–E curves intersect twice; the intersection points lie on both sides of E_m (Figure 28b). In this case one of the intersection points may coincide with the pzc. (It is not possible to predict at what electrolyte concentration this will occur.)

The adsorption of organic substances on iron and platinum group metals is accompanied by a strong chemical interaction with the electrode metal and, probably, by a partial dissociation of the molecules being adsorbed (Chapter 8 of this volume). The experimental determination of the dependence of Γ_{org}

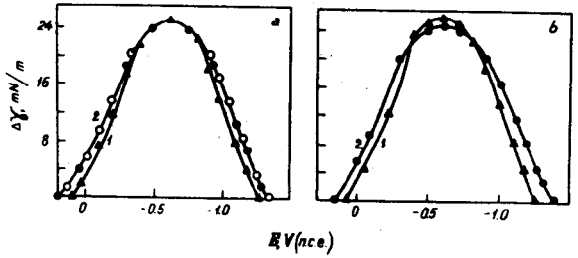


Figure 28. Dependence on potential of the surface tension decrease of mercury caused by ethyl acetate adsorption from its 0.1 M solution in the presence of different NaF concentrations. (a) NaF concentrations: 1, 0.05 M; 2, 0.07 M. Open circles on curve 2—theoretical calculation. (b) NaF concentrations: 1, 0.1 M; 2, 0.007 M.[134]

on E on platinum usually leads to a symmetrical bell-shaped curve, which Bockris and his school interpreted in the same terms as similar curves observed in the adsorption of neutral molecules on mercury.[126] With such an interpretation, E_m could be assumed to lie close to the pzc of platinum. (The degree of deviation is deduced by Bockris and Reddy.[168])

Frumkin[135] gave a different interpretation to the bell shape of the Γ_{org}–E curves on hydrogen- and oxygen-adsorbing metals, according to which the decrease of Γ_{org} with distance from the maximum of the bell-shaped curve is defined primarily by the appearance of adsorbed hydrogen and oxygen on the surface. From this point of view, which explains also the dependence of E_m on solution pH observed by Bockris and co-workers, the potential of the adsorption maximum should be associated with the potential of zero total charge $E_{Q=0}$, rather than with $E_{\sigma=0}$. Some attempts to substantiate the theory developed experimentally by Frumkin[135] failed since no organic substance was found whose adsorption on platinum at ordinary temperatures would be reversible and, thus, could be used to check the conclusions of the thermodynamic theory. The shape of the adsorption vs. potential curve proves to be defined not only by a decrease of adsorbability with distance from E_m, but also by desorption of the organic substance due to its oxidation or hydrogenation. Moreover, the adsorption of these organic substances leads to a deep disturbance of the electric double-layer structure at the platinum/solution interface, which would make it difficult to establish the relationship between the quantities $E_{\sigma=0}$ and E_m even for a reversible adsorption process.

It follows that, though the existence of qualitative relations between the increase of the total charge of a Pt electrode and the decrease of adsorbability of organic compounds is unquestionable,[135] the determination of $E_{\sigma=0}$ and $E_{Q=0}$ of platinum and, probably, of other platinum metals cannot generally be based on that of the dependence of Γ_{org} on potential.

The study of the adsorption of organic compounds on iron leads only to semiquantitative results regarding the position of the pzc of this metal.[8] Of significant interest is a marked change in the adsorption properties of an iron electrode when surface-active halogen anions or the SH^- ion is introduced into solution.[8,119,136] Thus, e.g., in the presence of I^- ions, iron acquires the ability to adsorb $N(C_4H_9)_4^+$ ions in the potential range in which the iron surface seems to be positively charged. Probably, chemisorbed I^- ions belong to the metal side of the double layer of iron and not to the ionic side, as in the case of platinum considered above. In the case under consideration, the pzc shifts in the direction of more positive values as compared to $E_{\sigma=0}$ of the uncovered surface, which leads, at a given E = const, to an increase of cation adsorption. Anion chemisorption, however, not only causes $E_{\sigma=0}$ to shift to more positive values, but also makes the iron surface hydrophobic. Therefore, in the presence of halogen ions, an increase is observed in the adsorption not only of cations, but also of neutral molecules, though this effect is less pronounced than in the case of positively charged particles.

6. Potentials of Zero Charge and the Nature of the Medium

Above, the experimental data on the pzc obtained with aqueous electrolyte solutions was considered. It is natural to compare these results with those obtained in different media. This discussion shall begin with the simplest case of the medium being a vacuum.

6.1. Metal/Vacuum Interface

When considering this interface, one encounters the question, which quantity measurable in a vacuum is to be compared with the difference of the pzc of two metals? As was shown[1] this is the Volta (contact) potential arising between the surfaces of two metals in a vacuum when a conducting contact is established between them by means of a conductor of the first kind or as a result of direct contact.

The formulation of the problem of the relationship between the Volta potential and the pzc was preceded by a dispute, which lasted for over a hundred years, as to the extent to which the contact potential arising upon contact of metals, in the absence of chemical interaction, determined the electromotive force of a galvanic cell in which the same metals are used as electrodes. This problem arose at the end of the 18th century and became known as the Volta problem.

As follows from thermodynamics, the Volta potential is equal to the difference of the work functions of metals Me_2 and Me_1 ($W_e^{Me_2}$ and $W_e^{Me_1}$). The Volta potential can also be determined as the potential difference, taken with the opposite sign, which is to be applied to the ends of the circuit (a) in Figure 29 to eliminate the potential drop in a vacuum. On the other hand, evidently, the Volta potential between metals Me_2 and Me_1 is equal to the difference of the surface potentials of these metals χ^{Me_2} and χ^{Me_1}, plus the Galvani potential at the Me_2/Me_1 interface ($\Delta_{Me_2}{}^{Me_1}\phi$):

$$-\Delta_{Me_2}{}^{Me_1}\psi = W_e^{Me_1} - W_e^{Me_2} = \chi^{Me_1} - \chi^{Me_2} - \Delta_{Me_2}{}^{Me_1}\phi \qquad (6.1)$$

Since it is more convenient to compare the potential differences at the ends of the galvani circuit (b), in Figure 29, with the potential difference at the ends of the circuit (a), the quantity $-\Delta_{Me_2}{}^{Me_1}\psi = \Delta_{Me_1}{}^{Me_2}\psi$, which figures in the left-hand side of Eq. (6.1), shall be used rather than the Volta potential value $\Delta_{Me_2}{}^{Me_1}\psi$.

The determination of the pzc gave a correct answer to the question about the relation between the potential difference at the ends of the galvanic circuit and the Volta potential. It is the difference between the pzc of two metals that defines the fraction of the total potential difference which can be compared with the Volta potential in a vacuum. To this fraction must be added the potential differences in the electric double layers at the metal/solution interface.

The analogy between the difference of the pzc of two metals in the absence

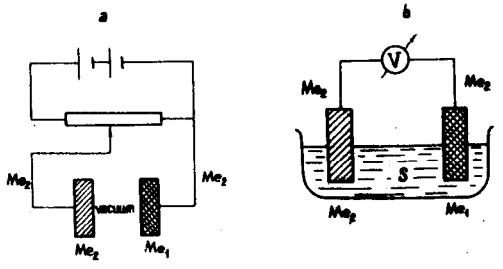


Figure 29. Circuits from two different uncharged metals Me_1 and Me_2, separated by vacuum (a) and solution (b).

of specific adsorption, $\Delta E_{\sigma=0}$, and the Volta potential in a vacuum, $\Delta_{Me_1}{}^{Me_2}\psi$, becomes apparent if circuit (a) in Figure 29 is compared with circuit (b) in which the vacuum is substituted by an electrolyte solution; but on both metals $\sigma = 0$. Thus the main difference between the circuit formed by metals in a vacuum and the usual galvanic circuit—the existence of ionic double layers at the metal/electrolyte interface—is not to be found here, but a metal surface in a vacuum is substituted by a metal surface in contact with an electrolyte solution. The determination of the pzc of a concentrated thallium amalgam[1] and of liquid gallium[137] showed that the contribution of the contact potentials to the potential difference at the ends of the galvanic circuit may be quite large.

Taking into account the possibility of a change of the dipole potential jump in the surface layer of water, which was discussed by Frumkin,[138] and also the possibility of a change of the value of χ^{Me} upon contact of an uncharged metal water,[139-141] the expression for $\Delta E_{\sigma=0}$ is obtained from Figure 29:

$$\begin{aligned}\Delta E_{\sigma=0} &= E_{\sigma=0}{}^{Me_1} - E_{\sigma=0}{}^{Me_2} \\ &= -\chi^{Me_2(s)} + \chi^{s(Me_2)} - \chi^{s(Me_1)} + \chi^{Me_1(s)} + \Delta_{Me_1}{}^{Me_2}\phi \\ &= \Delta_{Me_1}{}^{Me_2}\psi - [\chi^{s(Me_1)} - \chi^{s(Me_2)}] + [\delta\chi^{Me_1} - \delta\chi^{Me_2}] \\ &= \Delta W_e^{\circ} - \Delta\chi^{s(Me)} + \Delta(\delta\chi^{Me}) \end{aligned} \tag{6.2}$$

Here, $\chi^{s(Me)}$ is the potential jump caused by the orientation of the solvent (water) dipoles at the metal/solution interface at the pzc ($\chi^{s(Me)} > 0$, if the positive dipole end is turned toward the solution). $\delta\chi^{Me} = \chi^{Me(s)} - \chi^{Me}$; χ^{Me} is the surface potential of the metal, and $\chi^{Me(s)}$ the potential jump in the metal phase at the pzc; $\Delta W_e = W_e{}^{Me_1} - W_e{}^{Me_2}$. Equation (6.2) expresses in an analytical form the necessity of introducing corrections into the relation between the difference of the pzc and the Volta potential for the dependence on the metallic nature of the orientation of solvent molecules and for the disturbance of the electron density distribution in the metal as the result of its contact with solvent. This equation can be rewritten also as

$$\Delta E_{\sigma=0} = \Delta W_e + (\Delta_s{}^{Me_1}\psi)_{\sigma=0} - (\Delta_s{}^{Me_2}\psi)_{\sigma=0} \tag{6.3}$$

where $(\Delta_s{}^{Me}\psi)_{\sigma=0}$ is the Volta potential metal solution at $\sigma = 0$.

Thus for the difference in the pzc of two metals in any solvent to coincide quantitatively with the difference in work functions, it is necessary that the Volta potential between metal and solution at the pzc should not depend on the nature of the metal or should be zero. This is equivalent to equating the quantities $\Delta\chi^{s(Me)}$ and $\Delta(\delta\chi^{Me})$ to zero, or having them exactly compensate each other. The assumption that the Volta potential between a metal and aqueous solutions at the pzc is equal to zero was used by Jakuszewski and Antropov to prove the exact equality of the quantities ΔW_e and $\Delta E_{\sigma=0}$ (see References 4 and 142). However, neither the lack of dependence of the values of $(\Delta_s^{Me}\psi)_{\sigma=0}$ upon the metal nor their being identified to zero can be proved theoretically, though it is not impossible that in many cases the difference in $(\Delta_s^{Me}\psi)_{\sigma=0}$ in the right-hand side of Eq. (6.3) can be much less than ΔW_e. Were $(\Delta_s^{Me}\psi)_{\sigma=0}$ equal to zero, the Galvani potential at the metal/solution interface at the pzc would have to be the sum of the surface potentials of the metal and water with corresponding signs, an unlikely coincidence. The lack of dependence of this quantity upon the nature of the metal would point to the same deviations from this additivity with changing nature of the metal. The above assumption is proven to be invalid, in particular, by results which point to a change in the work function of xenon during adsorption on different metal surfaces.[143]

Finally, the quantity $(\Delta_s^{Me}\psi)_{\sigma=0}$ can be measured, and a direct measurement shows that it is not equal to zero. The Volta potential measurements performed by Klein and Lange[138] led to the value of $(\Delta_{H_2O}^{Hg}\psi)_{\sigma=0} = -0.33$ V. More accurate measurements of the Volta potential at the mercury/solution interface made by Randles,[144] in combination with Grahame's value of $E_{\sigma=0}^{Hg} = -0.193$ V, led to the value of $(\Delta_{H_2O}^{Hg}\psi)_{\sigma=0} = -0.26$ V.

If the value of $(\Delta_s^{Hg}\psi)_{\sigma=0}$ were zero, the difference $(\Delta_{s_1}^{Me}\psi)_{\sigma=0} - (\Delta_{s_1}^{Me}\psi)_{\sigma=0}$ for two different solvents should also be zero. Experimentally, however, this is not the case. Indeed, determining the differences of the potentials ΔE_I and ΔE_{II} at the ends of the circuits

NCE	aqueous solution	air	nonaqueous solution (s)	aqueous solution	NCE (I)

and

NCE	aqueous solution	Hg at $\sigma = 0$	nonaqueous solution (s)	aqueous solution	NCE (II)

one can obtain

$$\Delta E_I - \Delta E_{II} = (\Delta_s^{Hg}\psi)_{\sigma=0} - (\Delta_{H_2O}^{Hg}\psi)_{\sigma=0} \tag{6.4}$$

Table 3 summarizes the experimental data for some solvents.[145] The last column of this table gives the values of $(\Delta_s^{Hg}\psi)_{\sigma=0}$ calculated by means of Eq. (6.4) under the assumption that $(\Delta_{H_2O}^{Hg}\psi)_{\sigma=0} = -0.26$ V.

Table 3
Volta Potentials

Solvent	ΔE_{I} (V)	ΔE_{II} (V)	$(\Delta_s^{\mathrm{Hg}}\psi)_{\sigma=0}$ (V)
Water	0	0	−0.26
Methanol	−0.38	−0.13	−0.51
Ethanol	−0.37	−0.20	−0.44
Dimethylformamide	−0.65	−0.24	−0.67
Dimethylsulfoxide	−0.57	−0.15	−0.68
Acetone	−0.57	−0.22	−0.61

As can be seen from the table, the Volta potentials $(\Delta_s^{\mathrm{Hg}}\psi)_{\sigma=0}$ depend significantly on the nature of the solvent, which testifies once more to the fact that the values of the Volta potentials at $\sigma = 0$ are not zero.

Attempts to compare the experimental data on $\Delta E_{\sigma=0}$ and ΔW_e will be considered here. Novakovsky, Ukshe, and Levin[146] found that the data at their disposal fit best the relation

$$E_{\sigma=0} = 1.02W_e - 4.88 \tag{6.5}$$

which is close to the relation

$$E_{\sigma=0} = W_e - 4.78 \tag{6.6}$$

which they deduced assuming $(\Delta_s^{\mathrm{Me}}\psi)_{\sigma=0}$ to be constant.

Later, a similar equation with a somewhat modified constant in the right-hand side was compared more than once with the experimental data, e.g., by Frumkin,[3] where its semiquantitative nature was pointed out

$$E_{\sigma=0} = W_e - 4.72 \tag{6.7}$$

The value of the constant 4.72 was chosen in accordance with the data obtained for mercury.

Argade and Gileadi[147] considered Eq. (6.7) to be valid. A somewhat different relation was derived earlier from the experimental data by Vasenin.[148] According to Vasenin,

$$E_{\sigma=0} = 0.86W_e - 4.25 \tag{6.8}$$

Vasenin explains the difference of the coefficient before W_e from unity by the dependence of the orientation of adsorbed water molecules on the nature of the metal.

A far-reaching attempt to refine the relation between $E_{\sigma=0}$ and W_e was made by Trasatti.[6.149] Having considered the values of W_e which, in his opinion, are most reliable,[150] Trasatti draws the conclusion that the relation of W_e to $E_{\sigma=0}$ cannot be expressed by a linear relation which would cover all metals.[6.149,151] According to Trasatti, for *sp* metals, with the exception of Ga and Zn (Sb, Hg, Sn, Bi, In, Pb, Cd, Tl), an approximate relation is

$$E_{\sigma=0} = W_e - 4.69 \tag{6.9}$$

which is no different from Eq. (6.7); for the transition metals (Ti, Ta, Nb, Co, Ni, Fe, Pd), an approximate relation is

$$E_{\sigma=0} = W_e - 5.01 \tag{6.10}$$

In choosing the values of $E_{\sigma=0}$ in the case of metals not adsorbing hydrogen, Trasatti gives preference to those obtained from the position of the minimum on the C–E curve. For platinum metals Trasatti uses the pzc values found by the method suggested by Eyring and co-workers in neutral solutions, assuming that, unlike the pzc values obtained from adsorption measurements, the values thus found refer to metal surfaces free of adsorbed gases. However, the surface renewal without the supply of electricity from outside in the presence of water can at best (if all error sources are eliminated) lead to the disappearance of the total, but not the free, charge.

According to Trasatti, it is possible to derive a relation between $E_{\sigma=0}$ and W_e covering all metals if account is taken of the dependence of $\chi^{H_2O(Me)}$ on the nature of the metal, and the quantity $\delta\chi^{Me}$ is considered to be constant. This relation is

$$E_{\sigma=0} = W_e - 4.61 - 0.40\alpha \tag{6.11}$$

where α is the degree of orientation of water molecules, which, according to Trasatti, increases in the sequence Au, Cu < Hg, Ag, Sb, Bi < Pb < Cd < Ga. The enthalpy of the reaction $Me + \frac{1}{2}O_2 \rightarrow MeO$ also increases in this sequence, which allows one to associate the degree of orientation of adsorbed water molecules and, hence, the quantity $\chi^{H_2O(Me)}$, with the interaction between oxygen atoms and the metal surface.[152] The choice in the above sequence for Cu and Ag does not seem to be fully justified.

Trasatti relates α to the effective electronegativity of the metal surface α_{Me} by the following equation:

$$\alpha = (2.10 - \varkappa_{Me})/0.6 \tag{6.12}$$

The concept of electronegativity as a chemical property characterizing individual atoms was introduced by Pauling. Extending it to the surface of metals, Trasatti considered it necessary to define more accurately Pauling's values of $\varkappa_{Me}$ (Pauling calculates only to the first decimal place) and, in the case of gold, copper and transition metals, to correct them using the empirical relations between the work function and electronegativity. As a result, Trasatti obtains

$$\varkappa_{Me} = 0.50W_e - 0.29 \tag{6.13}$$

for *sp* metals except Ga, Zn, and Al, for which

$$\varkappa_{Me} = 0.50W_e - 0.55 \tag{6.14}$$

It follows from Eqs. (6.11) and (6.12) that

$$E_{\sigma=0} = W_e - 6.01 + 2/3\varkappa_{Me} \tag{6.15}$$

whence, using Eq. (6.13)

$$E_{\sigma=0} = 1.33W_e - 6.20 \tag{6.16}$$

for *sp* metals except Ga, Zn, and Al.

As in Vasenin's papers,[148] the deviation from unity of the slope of the $E_{\sigma=0}$–W_e dependence is associated with the allowance for the change of water orientation with the nature of the metal; but, here, the effect is ascribed an opposite sign. With zero orientation of water (Cu, Au), according to Eq. (6.11)

$$E_{\sigma=0} = W_e - 4.61 \tag{6.17}$$

and with maximum orientation (Al, transition metals, roughly Ga),

$$E_{\sigma=0} = W_e - 5.01 \tag{6.18}$$

The final results of the processing of the experimental data by Trasatti are given in Figure 30. Straight lines corresponding to Eqs. (6.17) and (6.18) bind the region of possible values of W_e as a function of $E_{\sigma=0}$. Straight lines lying within this region give the W_e, $E_{\sigma=0}$ dependence for certain groups of metals which are now combined, but not in the α constancy principle. However, the values of W_e used in plotting this graph in some cases (Tl, and also Cd, Pb) are (following Trasatti's terminology) *electrochemical* values. In other words, they do not represent the result of direct measurements of W_e in a vacuum, but were corrected to bring them into better conformity with the electrochemical behavior of a particular metal.

In spite of the fact that the quantitative calculations of Trasatti are open to objections, his study is noteworthy as an attempt to take into account systematically the influence of the value of $\delta\chi^{H_2O}$ on the relation of W_e to $E_{\sigma=0}$. Quite correct is the Trasatti statement that, at present, for many metals the values of $E_{\sigma=0}$ are much more reliable than those of W_e.

For metals for which there exist reliable pzc values and σ–E dependences, Frumkin and co-workers[7] attempted to compare the values of ΔW_e with

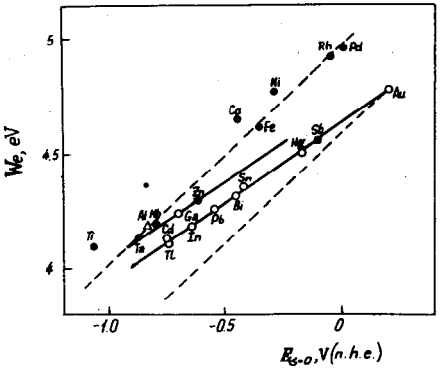


Figure 30. Dependence of the potential of zero charge of metals on the work function. Solid circles—physical work functions; open circle—electrochemical work functions; open triangle—the potential of zero charge value, unavailable experimentally.[149]

those of $\Delta E_{\sigma=q}$, where q has a negative value as large as possible. The comparison is based on the assumption that, at sufficiently negative surface charge, water molecules are oriented similarly and the quantities $\chi_{\sigma=q}{}^{H_2O(Me)}$ and $\delta\chi^{Me}$ can be considered to be independent of the nature of the metal. Such comparison, however, is valid only if the Helmholtz layer capacities are the same for the metals being compared. Otherwise, identical charges will not correspond to identical potential drops in the dense layer. As can be seen from Figure 24, at $\sigma = -18\ \mu C/cm^2$, this condition is satisfied for the whole group of metals under consideration except indium for which a correction is to be introduced based on the similarity of the surface properties of indium and an In + Ga alloy. The quantities $\Delta E_{\sigma=0}$, $\Delta E_{\sigma=q}$ (at $q = -18\ \mu C/cm^2$) and ΔW_e are compared in Table 4.

As can be seen from the table, the differences between the values of the quantities in the first and second columns are large for cadmium and gallium. In Figure 31, plotted from the data of Table 4, the dependences of ΔW_e on $\Delta E_{\sigma=0}$ and on $\Delta E_{\sigma=q}$ are shown. The values of W_e were taken from the first summary table by Trasatti.[6] An exception was made only for Ga, viz., $W_e^{Hg} - W_e^{Ga}$ was taken to be 0.2. As can be seen from Figure 31, the experimental values of ΔW_e fall somewhat better on the straight line with a slope of 45° if, instead of the values of $\Delta E_{\sigma=0}$, those of $\Delta E_{\sigma=q}$ are plotted on the abcissa, which confirms the necessity of taking account of the quantity $\chi^{H_2O(Me)}$ in considering the relations between the pzc and the work function.

In the light of the foregoing, it is of interest to measure the work functions of metals when water vapors are adsorbed on their surface. If one assumes that the water adsorption layers arising in this case on metal surfaces pretreated in a vacuum behave similarly to a water layer adsorbed from surface-inactive

Table 4

Differences of Potentials for $\sigma = 0$ and $\sigma = -18\ \mu C/cm^2$

Metal	$E_{\sigma=0}{}^{Hg} - E_{\sigma=0}{}^{Me}$ (V)	$E_{\sigma=-18}^{Hg} - E_{\sigma=-18}^{Me}$ (V)	$W_e^{Hg} - W_e^{Me}$ (eV)
Sb	−0.04	—	−0.06
Bi	0.20	0.17	0.21
Sn	0.19	0.10	0.15
Ga	0.50	0.17–0.18	0.20
In	0.46	0.34 (corr.)	0.42
In + Ga	0.43(CH_3CN)	0.33–0.34 (H_2O, corr.) 0.34–0.35 (CH_3CN)	—
Ga + Tl	0.51	0.40	—
Tl	0.52	—	0.48
Pb	0.37	0.36	0.32
Cd	0.56	0.35	0.38

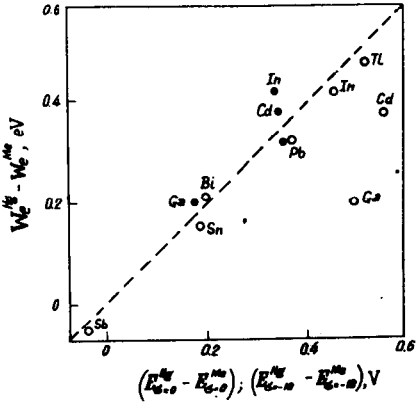


Figure 31. Dependence of $W_e^{Hg} - W_e^{Me}$ on $E_{\sigma=0}^{Hg} - E_{\sigma=0}^{Me}$ (open circles) or $E_{\sigma=-18}^{Hg} - E_{\sigma=-18}^{Me}$ (solid circles).[8]

electrolyte solutions, it is the difference in the work functions in the presence of water vapors $\Delta W_{e(H_2O)}$ which should be primarily compared with the difference of the pzc of respective metals. The most reliable data on the influence of water vapors on W_e[153] show that they practically (within ± 0.05 eV) do not affect the W_e of mercury, silver, and lead and cause a decrease of W_e for gallium, iron, and platinum. However, in the latter cases there remains a difference between $\Delta E_{\sigma=0}$ and $\Delta W_{e(H_2O)}$ of the order of 0.1–0.2 V. To find the reasons for these differences requires a more thorough analysis of the phenomena involved in the adsorption of water vapors on metals.

6.2. Metal/Nonaqueous Solution Interface

Gouy[58] and Frumkin[14] were the first to perform accurate measurements of the electrocapillary curves in nonaqueous solvents. Recently, a large number of electrocapillary and capacity measurements have been made in different nonaqueous solvents (alcohols, amides, acetonitrile, ethylene and propylene carbonates, dimethylsulfoxide, liquid ammonia, etc.), mainly at mercury and bismuth electrodes. It is difficult to use the obtained data to elucidate the physical sense of the pzc, since it is impossible to compare unambiguously the potentials measured in two different solvents. Such a comparison is equivalent to the evaluation of the potential difference at the interface between electrolyte solutions in two different solvents, which requires some hypothetical assumptions.[8] Therefore it is expedient to consider only studies in which the pzc has been determined in nonaqueous solvents for two different metals.

In measurements in nonaqueous media, aqueous reference electrodes are often used and give rise in the measuring circuit to an interface between the two solvents. Since this is a nonequilibrium interface, the value of the potential difference established across it depends on the method of the interface formation;

Table 5

The Differences of the Potentials of Zero Charge of Bismuth and Mercury in Different Media

Solvent	$E_{\sigma=0}^{Bi} - E_{\sigma=0}^{Hg}$ (V)
Water	−0.19
Methanol	−0.18
Ethanol	−0.19
Dimethylformamide	−0.18
Dimethylsulfoxide	−0.19
Acetonitrile	−0.13

and it is possible to compare the pzc of two metals in the cases when the construction of the interface remains constant in all experiments. The comparison is more correct if, after measuring the pzc of the metal being investigated in the same cell, the pzc of a streaming mercury electrode is measured.

A large number of pzc determinations were carried out by Jakuszewski and co-workers,[154] but they used the immersion method for this purpose, which makes it necessary to exercise caution in handling their data.

In recent years reliable data have been obtained on the pzc of bismuth in different solvents, from which it is possible to find the differences of the pzc of bismuth and mercury. The results of this comparison[8] are given in Table 5. As it follows from the table, the difference of the pzc of bismuth and mercury for a number of solvents remains practically constant. In acetonitrile this difference is less than in other media; the reason for this phenomenon is not clear. Possibly, it is connected with the different structure of the interface between

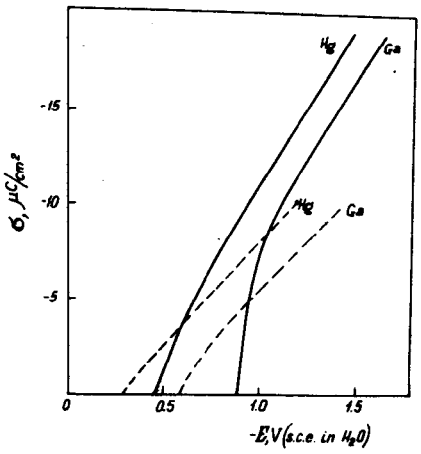


Figure 32. Dependences of the surface charge of mercury and gallium in 0.5 *M* Na_2SO_4 in water (solid curves) and in 0.1 *M* $LiClO_4$ in acetonitrile (dashed curves).[155]

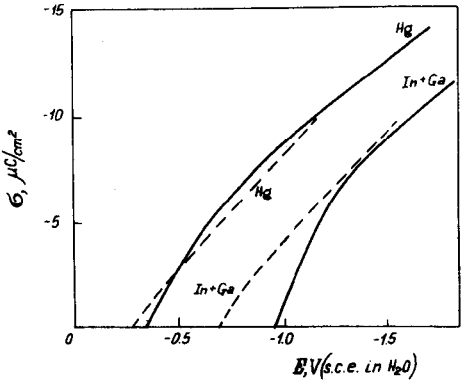


Figure 33. Dependences of the surface charge of mercury and an indium–gallium alloy in 0.1 *M* $LiClO_4$ in dimethylsulfoxide (solid curves) and in acetonitrile (dashed curves).[155]

nonaqueous and aqueous solutions in the reference electrode circuit in the pzc measurements of Bi and Hg. Similar circumstances could affect the values of $\Delta E_{\sigma=0}$ in the case of other solvents, and therefore, the data in the table need verification.

Frumkin and co-workers[155] compared the behavior of mercury, gallium, and eutectic indium–gallium alloy in water, acetonitrile, and dimethylsulfoxide. The pzc values vere found from the position of the differential capacity minimum in dilute solutions and with the use of a streaming electrode.

The differential capacity curves were used to calculate the dependences of the electrode surface charge on potential in different solvents (Figures 32 and 33) and to determine the values of $E_{\sigma=q}^{Me_2} - E_{\sigma=q}^{Me_1}$.

Table 6, in which the obtained results are summarized, shows that the values of $E_{\sigma=0}^{Ga} - E_{\sigma=0}^{Hg}$ and $E_{\sigma=0}^{In+Hg} - E_{\sigma=0}^{Hg}$ depend strongly on the nature of the solvent; the difference in the pzc increases in the sequence acetonitrile < water < dimethylsulfoxide in accordance with the increase in this sequence of the chemisorption interaction between the metal surface and the

Table 6

Differences of Potentials for $\sigma = 0$ and $\sigma = q$ in Various Solvents

$Me_1 - Me_2$	Solvent	$E_{\sigma=0}^{Me_2} - E_{\sigma=0}^{Me_1}$ (V)	$E_{\sigma=q}^{Me_2} - E_{\sigma=q}^{Me_1}$ (V)
Ga – Hg	Acetonitrile	0.29	0.23
	Water	0.50	0.17
	Dimethylsulfoxide	0.71	—
(In + Ga) – Hg	Acetonitrile	0.42	0.37
	Water	0.48	(0.34)[a]
	Dimethylsulfoxide	0.63	0.43

[a] In the case of aqueous solutions, the value of $E_{\sigma=q}^{Hg} - E_{\sigma=q}^{In+Ga}$ could be determined only approximately.

solvent molecules. At the same time the solvent affects less the difference of potentials of the same negative charge, which is determined by the difference of the work functions of the respective metals.

6.3. Metal/Electrolyte Melt Interface

For molten electrolytes the scope of the experimental data on the dependence of the pzc on the nature of the metal is larger than for nonaqueous solvents. Here, the main method of pzc determination is that of the measurement of electrocapillary curves. The first attempts at such measurements were made by Luggin, Hevesy, and Lorenz. Later, many systems were studied by Karpachev, Stromberg and co-workers, Kuznetsov and co-workers, and Smirnov and co-workers. In making electrocapillary measurements in molten electrolytes, it is necessary to keep in mind two possible error sources: the nonideal polarizability of metals in salt melts, and the wetting of glass capillary walls by liquid metals.

Along with electrocapillary measurements, the differential capacity measurements are of great importance for the investigation of the metal–melt interface. Randles and White[156] were the first to measure the capacity of mercury in mixtures of low-temperature molten electrolytes. Ukshe and co-workers carried out systematic studies of the electrode–melt interface by means of this method.[157] It was found that the C–E curves for liquid and solid electrodes show a well-defined minimum. Often, these curves are of an almost symmetrical and nearly parabolic form (Figure 34), but in the case of some systems, inflections or steps arise on the branches of the parabola. The appearance of steps is associated with adsorption processes, the nature of which, however, is not clear. The capacity measured in molten halides depends on the ac frequency, which is associated with faradaic processes. However, at a frequency of 20 kcps and

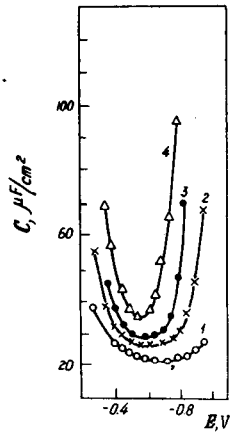


Figure 34. Differential capacity curves of a lead electrode in KCl + LiCl melt (1:1) at different temperatures: 1, 450°C; 2, 600°C; 3, 700°C; 4, 800°C. Reference electrode—Pb/KCl + LiCl (1:1), 2.5 mol % $PbCl_2$.[157]

higher, the difference of the capacity being measured from the double-layer capacity is no more than 10%–15%. The availability of the data on the double-layer capacity in electrolyte melts made it possible to compare the measured electrocapillary curves with the results of the double integration of the C–E curves.[157,158] The data thus obtained for Pb in chloride melts are given in Figure 35. In integrating, the value of $E_{\sigma=0}$ found from the electrocapillary measurements was used. It practically coincides with the potential of the minimum of the differential capacity curve. Good agreement between the calculated and experimental electrocapillary curves proves that capacity values obtained at high frequencies do represent the electric double-layer capacity, and the readings of the capillary electrometer do give correctly the dependence of interfacial tension on potential.

The minimum on the C–E curve of salt melts lies at potentials close to the potential of the maximum γ, though in some cases a scatter is observed, probably associated with the errors committed in comparing the potentials of the reference electrodes used in different studies. A fairly complete picture can be seen in Table 7.[8,157] All potentials are given against a reference electrode Pb/2.5 wt % $PbCl_2$, LiCl + KCl.

The data obtained in electrolyte melts cannot be explained in terms of the concepts of the double-layer structure generally used in interpretation of the phenomena in electrolyte solutions. A double-layer structure involving layers of ions of alternating sign is more probable, as first pointed out by Esin.[159] Such a picture was considered and theoretically substantiated by Dogonadze and Chizmadjev.[158,160]

The present state of the theory of electrolyte melts at the interface with metals does not permit one to draw definite enough conclusions regarding the coincidence of the pzc and E_{min}, especially for the general case in which the radii and polarizability of cations and anions are different. Therefore, generally speaking, unlike the situation with diluted electrolyte solutions, a similarity between the potential of the minimum on the C–E curve and the pzc in melts can be considered only as an empirically established fact.

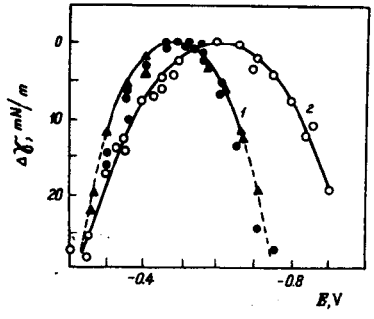


Figure 35. Electrocapillary curves of lead in NaCl (curve 1) and KCl (curve 2) melts at 820°C. The curves were obtained by integration of the capacity curves. Points—experimental data.[157]

Table 7

Potentials of Zero Charge for Metals in Contact with Molten Salts

Me	LiCl + KCl at 450°C		LiCl + KCl and NaCl + KCl at 700°C	
	Electrocapillary curves, $E_{\sigma=0}$ (V)	Capacity minimum, $E_{\sigma=0}$ (V)	Electrocapillary curves, $E_{\sigma=0}$ (V)	Capacity minimum, $E_{\sigma=0}$ (V)
Pb	0	0	0	0
Tl	−0.18 −0.10	−0.22[a]	−0.11	−0.32
Cd	−0.16 −0.09 −0.17	— — —	— — —	−0.25 — —
Ag	—	—	+0.08[b]	+0.06
In	−0.07 −0.04	−0.05 −0.22	−0.06 −0.17[d]	−0.23 —
Zn	−0.08 −0.05 −0.15	— — —	— — —	— — —
Ga	+0.07 +0.13[c]	+0.05 −0.10	+0.11 —	−0.06 —
Sn	+0.24 +0.26[a] +0.28	+0.19[a] — —	+0.30 — —	+0.15 +0.23 —
Bi	+0.17 +0.24[a] +0.28	+0.35 — —	+0.21 +0.25[d] —	+0.35 +0.23 —
Hg	+0.37	—	—	—
Sb	—	—	+0.61 +0.62	+0.38 +0.37

[a] 500°C.
[b] 1050°C.
[c] 400°C.
[d] NaCl, KCl, RbCl, CsCl, 700–900°C.

Unfortunately, so far the determination of the differential capacity minimum has been the only method suggested for determination of the pzc of solid metals in melts. Ukshe and co-workers carried out some determinations of E_{min} for solid electrodes (Ag, Pt, Mo, C).[157] Ukshe and Bukun consider the obtained values of E_{min} to be close to the pzc. Delimarsky determined the pzc from the value of E_{min} for a large number of solid electrodes.[161]

Almost from the beginning of the investigation of the electrocapillary phenomena in melts, particular attention was given to the problem of the relationship between the differences of the pzc in melts and in solutions. Its correct interpretation is complicated by the fact that in addition to the change in the nature of the solvent, there is also a significant change of temperature.

Denoting by index L the quantities pertaining to the metal–electrolyte melt interface and following Ukshe and Bukun,[157] one can write

$$(E_{\sigma=0}^{Me_1} - E_{\sigma=0}^{Me_2})_{H_2O} - (E_{\sigma=0}^{Me_1} - E_{\sigma=0}^{Me_2})_L = \Delta T \frac{\partial \Delta W_e}{\partial T} + (\Delta W_m^{Me_1} - \Delta W_m^{Me_2}) + [(\Delta_{Me_1}^{H_2O}\psi)_{\sigma=0} - (\Delta_{Me_2}^{H_2O}\psi)_{\sigma=0} + (\Delta_{Me_2}^{L}\psi)_{\sigma=0} - (\Delta_{Me_1}^{L}\psi)_{\sigma=0}] \quad (6.19)$$

Thus a distinction between the differences of $E_{\sigma=0}$ in aqueous medium and in a melt are the result of the difference in the temperature dependences of the work functions of the two metals, the change in the difference of the work functions due to melting of the metals $\Delta W_m^{Me_1} - \Delta W_m^{Me_2}$, if this occurs in the temperature range considered, and finally the change in the difference of Volta potentials at the uncharged metal–electrolyte interface when passing from water to the melt. The possibility of a change in the work function upon melting is defined by the difference in the work functions for different single-crystal faces. Therefore, it would be expedient to compare the data for aqueous solutions and melts without changing the state of aggregation of metals and, if this condition cannot be satisfied, to use for solid metals the data for polycrystalline specimens, for which the pzc values of individual faces are averaged, so that a minimum change would be expected upon melting.

The published data on the temperature coefficient of the work function are not reliable enough to make meaningful conclusions. Both the theoretical analysis and the experimental data show that this coefficient should be within 10^{-5}–10^{-4} eV/°K. Hence, it follows that when temperature changes by 400–700 K, the contribution of the temperature dependence of the work function to the shift of the pzc should exceed 0.05–0.10 V. Thus as a first approximation the temperature dependence of the difference of the pzc can be neglected, and the values of the differences of the pzc obtained in melts can be used for comparison with those obtained in aqueous solutions. In comparing the differences of the pzc in solutions and melts, the quantity in square brackets in Eq. (6.19) should be considered to be of greatest importance.

In Table 8, the values of $E_{\sigma=0}^{Me} - E_{\sigma=0}^{Pb}$ are compared in aqueous solutions and in molten media.[8] Wherever possible, the values of the shift of the pzc corrected for the water orientation, i.e., the values of $E_{\sigma=q}^{Me} - E_{\sigma=q}^{Pb}$ at negative $\sigma = q$, are given. The second and third columns list the values of $E_{\sigma=0}^{Me} - E_{\sigma=0}^{Pb}$ determined from the position of the maximum of the electrocapillary curve in halide melts. The last column gives the values of $\Delta W_e = W_e^{Me} - W_e^{Pb}$ taken from a table by Trasatti[150]; the value for Te is taken from Fomenko.[162]

On the whole the agreement between the values of $\Delta E_{\sigma=0}$ in aqueous solutions, of $\Delta E_{\sigma=0}$ in halide melts, and the values of ΔW_e can be considered

Table 8

Differences of Potentials of Zero Charge of Various Metals with Respect to That for Lead

Me	$\Delta E_{\sigma=0}$ (V) Aqueous solutions	$\Delta E_{\sigma=0}$ (V) LiCl + KCl 450°C	$\Delta E_{\sigma=0}$ (V) LiCl(NaCl + KCl) 700°C	$\bullet\Delta W$ (eV)
Te	1.16(?)	1.05	0.83	0.73
Hg	0.37(0.36)	0.44	—	0.49
Sb	0.41	—	0.56	0.55
Sn	0.18(0.26)	0.27	0.30	0.34
Bi	0.17(0.19)	0.27	0.30	0.28
Pb	0.00(0.00)	0.00	0.00	0.00
In	−0.09(0.02)	−0.05	−0.07	0.07
Ga	−0.13(0.18)	0.09	0.06	0.24
Tl	−0.15	−0.11	−0.11	−0.17
Cd	−0.19(0.01)	−0.15	—	0.04

satisfactory. After correction for the effect of the water dipoles orientation, for Ga the values of $\Delta E_{\sigma=0}$ in aqueous medium and in melts have the same sign.

At the present state of the measuring technique in melts, only the data obtained by one and the same investigator can be considered to be completely comparable. The most reliable results of the comparison of the values of $\Delta E_{\sigma=0}$ in chloride melts and ΔW_e were obtained by Kuznetsov and co-workers.[163] The value of ΔW_e was determined directly from the shift of the diode characteristic when passing from a streaming electrode from metal Me_1 to the alloy $Me_1 + Me_2$, and not from the difference of the work functions measured in independent experiments. To reduce the risk of contaminating one metal by the vapors of the other, a metal with a higher vapor tension was chosen as Me_1. The results of these measurements are listed in Table 9. The accuracy of the measurement of ΔW_e was estimated by the above authors to be ± 0.05 V.

In these experiments the greatest approach between the difference of the pzc in halide melts and the difference in the work functions was achieved (the

Table 9

Differences of Work Functions and Potentials of Zero Charge among Various Metals

Me_1	Me_2 (at %)	$\Delta E_{\sigma=0}$ (V)	ΔW_e (eV)
Sn	Sn + 0.15% Te	−0.18	−0.15
Sn	Sn + 23.8% Tl	0.24	0.17
Sn	Sn + 53% Cd	0.27	0.25
Bi	Bi + 3.6% Te	−0.25	−0.30
Bi	Bi + 9% Te	−0.33	−0.35
Tl	Tl + 50% Te	−0.67	−0.65

root-mean-square deviation only 0.04 V). It is not clear, however, whether these conclusions could be extended to a wider range of systems.

6.4. Metal/Solid Electrolyte Interface

Recently, a method has been developed for the determination of the pzc of molten metal at the interface with the solid electrolyte (ZrO_2) from the dependence of the contact angle on polarization.[164] The results of the pzc determination at this interface are not numerous as yet and do not warrant any theoretical generalization.

7. Potentials of Zero Charge and Electrochemical Kinetics

Electrochemical reactions occur within the limits of the electric double layer, and their rate depends on its structure. At a given electrode potential and ionic strength of solution, the structure of the electric double layer is determined primarily by the pzc value. Thus, the connection between the rate of electrochemical reactions and the pzc is established. In a general case the position of the pzc influences the kinetics of electrochemical processes through the ψ_1 correction and through the influence of the double-layer charge on the adsorption and orientation of solvent molecules and other solution components. Different aspects of the relationship between the pzc and the characteristics of electrode reactions have been considered in detail.[8] Here, the discussion shall be restricted to the possibility of determining the pzc from the kinetic data and the use of these data for confirmation of the correctness of the pzc determination by other methods.

Frumkin was the first to show that if the rate of the establishment of equilibrium between the surface layer and the solution bulk is large as compared to that of the electrode process, then, in the absence of concentration polarization, the current density i is

$$i = k_0 n F c_i^0 \exp\left\{\frac{F}{RT}[-\alpha n_a E + (\alpha n_a - z_i)\psi_1]\right\} \tag{7.1}$$

where k_0 is a constant, n is the total number of electrons participating in the electrochemical process, α is the transfer coefficient, n_a is the algebraic number of electrons transferred from the electrode to a reacting particle in an elementary act of the process, and z_i is the charge of the reacting particle.

It is easily found from Eq. (7.1) that the hydrogen overvoltage should decrease with a decrease in the absolute value of ψ_1, i.e., with decreasing diffuseness of the double layer if $\psi_1 > 0$, and should increase if $\psi_1 < 0$. In surface-inactive electrolyte solutions at the pzc, $\psi_1 = 0$, and therefore, in these solutions the reaction rate should not depend on the supporting electrolyte concentration. In principle this conclusion can be used as a basis in the pzc determination. A tendency of the η–log i curves of hydrogen evolution to draw closer as the pzc is

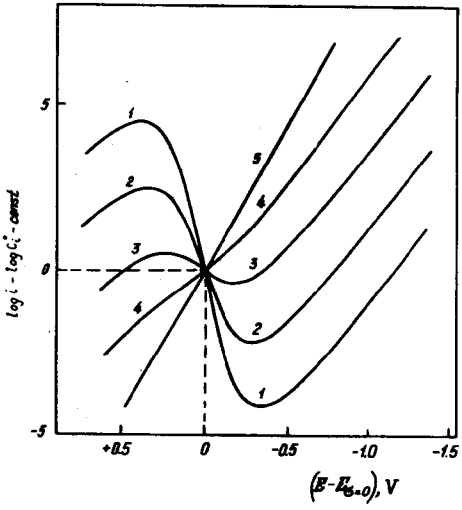


Figure 36. Polarization curves calculated by means of Eq. (7.1) at $z_1 = -2$, $\alpha = 0.5$ for the ψ_1 potentials corresponding to the potential of the outer Helmholtz plane of a mercury electrode in solutions: 1, 0.001 *M* NaF; 2, 0.01 *M* NaF; 3, 0.1 *M* NaF; 4, 0.9 *M* NaF; 5, $\psi_1 = 0$.[111]

approached in solutions of different concentrations was pointed out for bismuth by Palm and Tenno.[165]

The pronounced ψ_1 effects leading to a change in the shape of the i–E curves were studied in detail for anion electroreduction reactions. Figure 36 shows the polarization curves of a double-charged anion electroreduction in the presence of different concentrations of a specifically nonadsorbable 1,1-valent electrolyte, calculated by means of Eq. (7.1).[111] $E_{\sigma=0}$ is the abscissa of the common point of intersection of the curves at different supporting electrolyte concentrations. So far, such intersection was observed only in the case of $S_2O_8^{2-}$ anion reduction at a dropping mercury electrode from solutions in dimethylsulfoxide (Figure 37). It was stated that the intersection of the curves actually lies at the

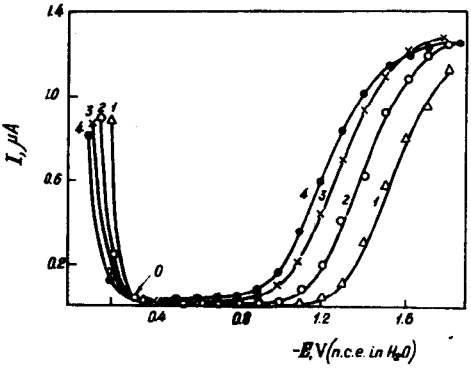


Figure 37. Polarograms of $S_2O_8^{2-}$ anion electroreduction on a dropping mercury electrode from the solutions 5×10^{-4} *M* $Na_2S_2O_8$ in dimethylsulfoxide in the presence of $NaClO_4$ in concentrations: 1, 10^{-2} *M*; 2, 2.5×10^{-2} *M*; 3, 5.0×10^{-2} *M*; 4, 1.0×10^{-1} *M*. 0—the intersection point of the curves roughly corresponding to $E_{\sigma=0}$.[166]

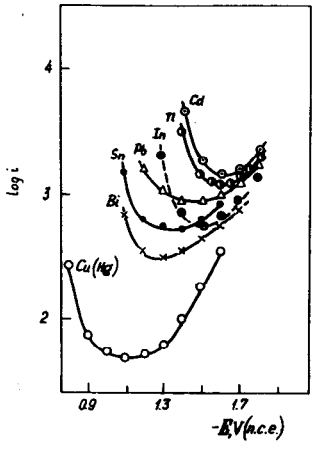


Figure 38. Dependence of the reduction rate of the $S_2O_8^{2-}$ anion in 5×10^{-4} *M* $Na_2S_2O_8 + 9 \times 10^{-3}$ *M* NaF on potential at rotating disk electrodes from Cu(Hg), Bi, Sn, Pb, In, Tl, Cd.[167]

pzc.[166] The intersection could be observed because of a low rate constant of electroreduction of $S_2O_8^{2-}$ from this solvent. The use of this method for the pzc determination in other systems is not easy since it involves elimination of the diffusion difficulties. For such systems it is possible to assess the correctness of the calculation of the ψ_1–E dependences, and hence the correctness of the choice of the pzc value for the cathode material by comparing the experimental i–E curves with Eq. (7.1). It is especially convenient to use for this purpose the dependence of $\log i + (z_1F/2.3RT)\psi_1$ on $-(E - \psi_1)$, which became known as the corrected Tafel plot[115] (CTP). As follows from Eq. (7.1), in the absence of specific adsorption of the reacting particle and the reaction product, the CTP should be be invariant under a change of the supporting electrolyte concentration.

Figures 38 and 39 give the results of the comparison of the polarization curves and CTP for different metals in the electroreduction reaction of S_2O_8.[167] Though the polarization curves differ strongly for different metals, the CTP show

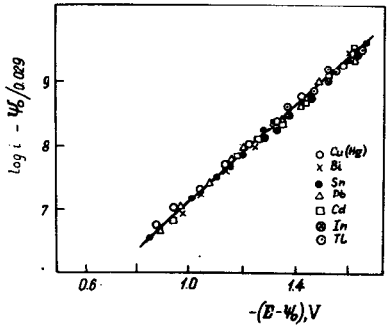


Figure 39. Corrected Tafel plots of the $S_2O_8^{2-}$ anion electroreduction in the same solutions and at the same metals as in Figure 38.[167]

fairly good coincidence. This coincidence confirms the correctness of the pzc values used in calculations. However, the solution of the inverse problem, viz., the finding of an accurate pzc value from the experimental log i–E curve, presents difficulties, since when the nature of the electrode changes, it is not only the pzc value which changes, but also the character of the σ–E dependence and hence the shape of the ψ_1–E curve; this is associated with the influence of water chemisorption on the capacity of the double layer.

The coincidence of the CTP proves conclusively that the work function into a vacuum does not figure directly in the equations of electrochemical kinetics.

8. Conclusion

Considerable progress has been made in the development of the methods of the pzc determination both for ideally polarizable and reversible electrodes. For some metals reliable pzc values have been obtained by these methods. Various factors influencing the pzc have been defined; and the relationship between the pzc and other characteristics of metals, as well as the role of the pzc in electrochemical kinetics, has been established.

At the same time there are many electrochemical systems for which reliable pzc values have not been obtained. In further studies the crystallographic inhomogeneity of polycrystalline electrodes can gravely complicate the conventional interpretation of experimental data. In particular the minimum on the differential capacity curve in dilute solutions of a symmetrical surface-inactive electrolyte may not coincide with the pzc. In this case it is necessary to change from polycrystalline to single-crystal electrodes, at any rate in investigating metals for which the pzc of individual faces differ by some tenths of a volt. Such a change is also necessary for better elucidation of the role of the pzc in the kinetics of electrode processes.

The increasing use of nonaqueous solvents in electrochemistry requires further systematic determinations of the pzc in nonaqueous media.

Finally, it might be well to point out the importance of obtaining more reliable data on the work functions, which will permit a more accurate determination of the quantitative relationship between the work function and the pzc.

References

1. A. Frumkin and A. Gorodetzkaja, *Z. Phys. Chem.* **136**, 451–472 (1928).
2. A. Frumkin, *Phys. Z. Sowjetunion* **4**, 239–261 (1933).
3. A. Frumkin, *Svensk Kem. Tidskrift* **77**, 300–322 (1965).
4. R. Perkins and T. Andersen, in *Modern Aspects of Electrochemistry*, J. O'M. Bockris and B. E. Conway, eds., Vol. 5, Plenum Press, New York (1969), pp. 203–290.
5. L. Campanella, *J. Electroanal. Chem.* **28**, 228–232 (1970).
6. S. Trasatti, *J. Electroanal. Chem.* **33**, 351–378 (1971).
7. A. Frumkin, B. Damaskin, N. Grigoryev, and I. Bagotskaya, *Electrochim. Acta* **19**, 69–74 (1974).
8. A. Frumkin, *Zero Charge Potentials*, Nauka, Moscow (1979).

9. G. Lippmann, *Pogg. Ann. Phys.* **149**, 546–561 (1873).
10. W. Gibbs, "Equilibrium of heterogeneous substances (1877–1878)," in *Collected Works*, Vol. 1, Longmans, Green, New York (1928).
11. M. Planck, *Ann. Phys.* **44**, 385–428 (1891).
12. A. Frumkin, *Electrocapillary Phenomena and Electrode Potentials*, Odessa (1919).
13. A. Frumkin, *Philos. Mag.* **40**, 363–385 (1920).
14. A. Frumkin, *Z. Phys. Chem.* **103**, 43–70 (1923).
15. D. Grahame and R. Whitney, *J. Am. Chem. Soc.* **64**, 1548–1552 (1942).
16. D. Grahame, *Chem. Rev.* **41**, 441–501 (1947).
17. R. Parsons and M. Devanathan, *Trans. Faraday Soc.* **49**, 404–409 (1953).
18. D. Mohilner, in *Electroanalytical Chemistry*, A. Bard, ed., Vol. 1, Marcel Dekker, New York (1966), pp. 241–409.
19. A. Frumkin, *J. Electroanal. Chem.* **64**, 247–251 (1975).
20. A. Frumkin, O. Petrii, and B. Damaskin, *J. Electroanal. Chem.* **27**, 81–100 (1970).
21. F. Koenig, *J. Phys. Chem.* **38**, 111–128 (1934).
22. W. Lorenz, *Z. Phys. Chem.* **218**, 272–276 (1961).
23. B. Damaskin, *Elektrokhimiya* **5**, 771–796 (1969).
24. R. Parsons, in *Advances in Electrochemistry and Electrochemical Engineering*, P. Delahay, ed., Vol. 7, Interscience, New York (1970), pp. 177–219.
25. A. Šlygin, A. Frumkin, and W. Medvedovsky, *Acta Physicochim. URSS* **4**, 911–928 (1936).
26. N. Balashova and V. Kazarinov, in *Electroanalytical Chemistry*, A. Bard, ed., Vol. 3, Marcel Dekker, New York (1969), pp. 135–197.
27. A. Frumkin, N. Balashova, and V. Kazarinov, *J. Electrochem. Soc.* **113**, 1011–1025 (1966).
28. A. Frumkin, O. Petrii, and R. Marvet, *J. Electroanal. Chem.* **12**, 504–515 (1966).
29. A. Frumkin, O. Petrii, A. Kossaya, V. Entina, and V. Topolev, *J. Electroanal. Chem.* **16**, 175–191 (1968).
30. A. Frumkin and O. Petrii, *Electrochim. Acta* **15**, 391–403 (1970).
31. A. Frumkin and O. Petrii, *Electrochim. Acta* **20**, 347–359 (1975).
32. B. Damaskin, O. Petrii, and V. Batrakov, *Adsorption of Organic Compounds on Electrodes*, Plenum Press, New York (1971), Chap. 9.
33. O. Petrii, *Itogi Nauki i Tekhn. Elektrokhim.* **12**, 56–98 (1977).
34. B. Grafov, E. Pekar, and O. Petrii, *J. Electroanal. Chem.* **40**, 179–186 (1972).
35. B. Bruns and A. Frumkin, *Z. Phys. Chem.* **147**, 125–146 (1930).
36. A. Frumkin, B. Damaskin, and O. Petrii, *Z. Phys Chem.* **256**, 728–736 (1975).
37. A. Watanabe, *J. Electrochem. Soc.* **110**, 72–79 (1963).
38. Yu. Gerasimenko, M. Gerasimenko, and L. Antropov, *J. Electroanal. Chem.* **63**, 275–282 (1975).
39. F. Kukoz and L. Kukoz, *Zh. Fiz. Khim.* **36**, 703–708 (1962).
40. A. Gokhshtein, *Dokl. Akad. Nauk SSSR* **187**, 601–604 (1969).
41. B. Jakuszewski and Z. Kozlowski, *Rocz. Chem.* **36**, 1873–1877 (1962).
42. V. Endrasic, *J. Electroanal. Chem.* **22**, 157–164 (1969).
43. S. Kim, *J. Phys. Chem.* **77**, 2787–2789 (1973).
44. D. Grahame, E. Coffin, J. Cummings, and M. Poth, *J. Am. Chem. Soc.* **74**, 1207–1211 (1952).
45. J. Butler, *J. Phys. Chem.* **70**, 2312–2318 (1966).
46. A. Frumkin and F. Cirves, *J. Phys. Chem.* **34**, 74–85 (1930).
47. V. Smirnov, L. Demchuk, D. Semchenko, and L. Antropov, *Tr. Novocherk. Politekh. Inst.* **134**, 65–74 (1962).
48. H. Göhr and M. König, *Z. Phys. Chem.* (*N.F.*) **74**, 115–138 (1971).
49. A. Frumkin, E. Ponomarenko, and R. Burshtein, *Izv. Akad. Nauk SSSR Ser. Khim.*, 1549–1555 (1963).

50. A. Frumkin, *Z. Elektrochem.* **59**, 807–822 (1955).
51. T. Andersen and R. Perkins, *J. Am. Chem. Soc.* **86**, 4496 (1964).
52. T. Andersen, J. Anderson, D. Bodé, and H. Eyring, *J. Res. Inst. Catal. Hokkaido Univ.* **16**, 449–476 (1968).
53. G. Clark, T. Andersen, R. Valentine, and H. Eyring, *J. Electrochem. Soc.* **121**, 618–622 (1974).
54. O. Petrii and Nguen van Tue, *Elektrokhimiya* **6**, 408–411 (1970).
55. N. Tomashov, N. Strukov, and L. Vershinina, *Elektrokhimiya* **5**, 26–31 (1969).
56. H. Noninski and E. Lazarova, *Elektrokhimiya* **11**, 1103–1106 (1975).
57. A. Frumkin, O. Petrii, and B. Damaskin, *J. Electroanal. Chem.* **35**, 439–440 (1972).
58. G. Gouy, *Ann. Phys. (Paris)* **6**, 3–36 (1916).
59. N. Polianovskaya and A. Frumkin, *Elektrokhimiya* **1**, 538–544 (1965).
60. A. Frumkin, N. Polianovskaya, and N. Grigoryev, *Dokl. Akad. Nauk SSSR* **157**, 1455–1458 (1964).
61. I. Bagotskaya, A. Morozov, and N. Grigoryev, *Electrochim. Acta* **13**, 873–879 (1968).
62. A. Frumkin, N. Polianovskaya, and B. Damaskin, *J. Electroanal. Chem.* **73**, 267–277 (1976).
63. A. Gokhshtein, *Elektrokhimiya* **2**, 1318–1326 (1966).
64. A. Gokhshtein, *Surface Tension of Solids and Adsorption*, Nauka, Moscow (1976).
65. T. Beck, *J. Phys. Chem.* **73**, 466–468 (1969).
66. R. Fredlein, A. Damyanovič, and J. O'M. Bockris, *Surface Sci.* **25**, 261–264 (1971).
67. R. Fredlein and J. O'M. Bockris, *Surface Sci.* **46**, 641–652 (1974).
68. A. Soffer and M. Folman, *J. Electroanal. Chem.* **38**, 25–43 (1972).
69. A. Frumkin, A. Gorodetzkaya, B. Kabanov, and N. Nekrassov, *Zh. Fiz. Khim.* **3**, 351–367 (1932).
70. M. Bonnemay, G. Bronoel, O. Jonville, and E. Levart, *C. R. Acad. Sci. Ser. C* **260**, 4262–5265 (1965).
71. I. Morcos and H. Fisher, *J. Electroanal. Chem.* **17**, 7–11 (1968).
72. I. Morcos, *J. Electrochem. Soc.* **121**, 1417–1421 (1974).
73. E. Venstrem and P. Rehbinder, *Dokl. Akad. Nauk SSSR* **68**, 329–332 (1949).
74. V. Likhtman, L. Kochanova, D. Leikis, and E. Shchukin, *Elektrokhimiya* **5**, 729–733 (1969).
75. F. Kukoz and S. Semenchenko, *Elektrokhimiya* **1**, 1454–1458 (1965).
76. J. O'M. Bockris and R. Parry-Jones, *Nature* **171**, 930–931 (1953).
77. J. O'M. Bockris and R. Sen, *Surface Sci.* **30**, 237–241 (1972).
78. E. Venstrem, V. Likhtman, and P. Rehbinder, *Dokl. Akad. Nauk SSSR* **107**, 105–107 (1956).
79. E. Kuchinsky, R. Burshtein, and A. Frumkin, *Acta Physicochim. URSS* **12**, 795–830 (1940).
80. O. Petrii, A. Frumkin, and Yu. Kotlov, *J. Res. Inst. Catal. Hokkaido Univ.* **16**, 367–375 (1968).
81. V. Kazarinov, *Elektrokhimiya* **2**, 1170–1175 (1966).
82. M. Vorsina and A. Frumkin, *C. R. (Dokl.) Acad. Sci. URSS* **24**, 918–921 (1939).
83. B. Damaskin, *J. Electroanal. Chem.* **65**, 799–814 (1975).
84. A. Frumkin and B. Grigoryev, *Elektrokhimiya* **8**, 412–413 (1972).
85. G. Valette, *C. R. Acad. Sci. Ser. C* **273**, 320–323 (1971).
86. E. Sevastyanov, T. Vitanov, and A. Popov, *Elektrokhimiya* **8**, 412–413 (1972).
87. T. Vitanov, A. Popov, and E. Sevastyanov, *Elektrokhimiya* **10**, 346–349 (1974).
88. A. Hamelin and J. Lecoueur, *Collect. Czech. Chem. Commun.* **36**, 714–721 (1971).
89. U. Palm and B. Damaskin, *Itogi Nauki i Tekh. Elektrokhim.* **12**, 99–143 (1977).
90. A. Frumkin, M. Pyarnoya, N. Grigoryev, and U. Palm, *Elektrokhimiya* **10**, 1130–1133 (1974).
91. D. Leikis, V. Panin, and K. Rybalka, *J. Electroanal. Chem.* **40**, 9–12 (1972).

92. N. Grigoryev, I. Gedvillo, and N. Bardina, *Elektrokhimiya* **8**, 409–412 (1972).
93. K. Rybalka and D. Leikis, *Elektrokhimiya* **3**, 383–386 (1967).
94. M. Khaga and V. Past, *Elektrokhimiya* **5**, 618–620 (1969).
95. T. Ehrlich, Yu. Kukk, and V. Past, *Uch. Zap. Tartu Gos. Univ.*, No. 289, 9–13 (1971).
96. I. Dagaeva, D. Leikis, and E. Sevastyanov, *Elektrokhimiya* **3**, 891–893 (1967).
97. G. Valette and A. Hamelin, *J. Electroanal. Chem.* **45**, 301–319 (1973).
98. L. Rybalka, D. Leikis, and A. Zelinsky, *Elektrokhimiya* **12**, 1340–1341 (1976).
99. V. Levich, B. Khaikin, and B. Grafov, *Dokl. Akad. Nauk SSSR* **153**, 1374–1377 (1963).
100. V. Mishuk, E. Solomatin, V. Elkin, and L. Knotz, *Elektrokhimiya* **11**, 1897–1898 (1975).
101. H. Kruyt, ed., *Colloid Science*, Vol. I Elsevier, Amsterdam (1952), p. 194.
102. N. Balashova and A. Frumkin, *C. R. (Dokl.) Acad. Sci. URSS* **20**, 449–452 (1938).
103. A. Frumkin, *Izv. Akad. Nauk SSR Otd. Khim. Nauk*, 223–232 (1945).
104. V. Levich, *Physicochemical Hydrodynamics*, Prentice-Hall, Englewood Cliffs, New Jersey (1962).
105. G. Barker, A. Gardner, and D. Sammon, *J. Electrochem. Soc.* **113**, 1182–1197 (1965).
106. A. Brodsky, Yu. Gurevich, Yu. Pleskov, and Z. Rotenberg, *Modern Photoelectrochemistry. Photoemission Phenomena*, Nauka, Moscow (1974).
107. T. Voropaeva, B. Deryagin, and B. Kabanov, *Dokl. Akad. Nauk SSSR* **128**, 981–984 (1959).
108. T. Voropaeva, B. Deryagin, and B. Kabanov, *Izv. Akad. Nauk SSSR Otd. Khim. Nauk*, 257–263 (1963).
109. L. Antropov, M. Gerasimenko, and Yu. Gerasimenko, *Elektrokhimiya* **9**, 731–736 (1973).
110. A. Frumkin, N. Polianovskaya, I. Bagotskaya, and N. Grigoryev, *J. Electroanal. Chem.* **33**, 319–328 (1971).
111. B. Damaskin and O. Petrii, *Introduction in Electrochemical Kinetics*, *Visshaya Shkola*, Moscow (1975).
112. A. Frumkin, in *Surface Phenomena in Chemistry and Biology*, Pergamon Press, London (1958), pp. 189–194.
113. O. Esin and B. Markov, *Acta Physicochim. URSS* **10**, 351–364 (1939).
114. Z. Iofa, B. Ustinsky, and F. Eiman, *Zh. Fiz. Khim.* **13**, 934–939 (1939).
115. P. Delahay, *Double Layer and Electrode Kinetics*, Interscience, New York/London (1965).
116. A. Frumkin, *Zh. Fiz. Khim.* **30**, 2066–2069 (1956).
117. R. Parsons, The Esin and Markov effect, in *Proceedings of the Second International Congress on Surface Activity*, *Electrical Phenomena*, Butterworths, London (1957), pp. 38–44.
118. V. Bagotzky, Yu. Vassilyev, J. Weber, and J. Pirtskhalava, *J. Electroanal. Chem.* **27**, 31–46 (1970).
119. Z. Iofa and G. Rozhdestvenskaya, *Dokl. Akad. Nauk SSSR* **91**, 1159–1162 (1953).
120. A. Frumkin, *Usp. Khim.* **24**, 933–950 (1955).
121. V. Kheifets and B. Krasikov, *Zh. Fiz. Khim.* **31**, 1992–1998 (1957).
122. A. Frumkin, O. Petrii, and T. Kolotyrkina, *Elektrokhimiya* **10**, 1741–1745 (1974).
123. A. Frumkin, O. Petrii, and T. Kolotyrkina-Safonova, *Dokl. Akad. Nauk SSSR* **222**, 1159–1162 (1975).
124. R. Notoya and O. Petrii, *Dokl. Akad. Nauk SSSR* **226**, 1117–1120 (1976).
125. B. Podlovchenko, N. Epshtein, and A. Frumkin, *J. Electroanal. Chem.* **53**, 95–104 (1974).
126. J. O'M. Bockris, S. Argade, and E. Gileadi, *Electrochim. Acta* **14**, 1259–1283 (1969).
127. A. Frumkin, A. Korobanov, V. Vilinskaya, and R. Burshtein, *Dokl. Akad. Nauk SSSR* **229**, 153–155 (1976).
128. L. Antropov, *Kinetics of Electrode Processes and Null Points of Metals*, SCIR, New Delhi (1960).
129. L. Antropov, *Privedennaya, Ii, ϕ-Shkala Potentialov i ee Ispolsovanie pri Isuchenii Kinetiki Elektrokhimicheskih Reakzii*, Znanie, Leningrad (1965).

130. B. Damaskin and V. Batrakov, *Elektrokhimiya* **10**, 140–143 (1974).
131. V. Batrakov, B. Damaskin, and Yu. Ipatov, *Elektrokhimiya* **10**, 144–147 (1974).
132. B. Damaskin, E. Stenina, V. Yusupova, and N. Fedorovich, *Elektrokhimiya* **8**, 1409–1414 (1972).
133. H. Dahms and M. Green, *J. Electrochem. Soc.* **110**, 466–467 (1963).
134. A. Frumkin, B. Damaskin, and S. Dyatkina, *Elektrokhimiya* **10**, 1402–1406 (1974).
135. A. Frumkin, *Dokl. Akad. Nauk SSSR* **154**, 1432–1433 (1964).
136. Z. Iofa, V. Batrakov, and Cho-Ngok Ba, *Electrochim. Acta* **9**, 1645–1653 (1964).
137. A. Frumkin and A. Gorodetzkaya, *Z. Phys. Chem.* **136**, 215–227 (1928).
138. A. Frumkin, *J. Chem. Phys.* **7**, 552–553 (1939).
139. B. Ershler, *Usp. Khim.* **21**, 237–249 (1952).
140. A. Frumkin, *Usp. Khim.* **15**, 385–402 (1946).
141. R. Parsons, in *Modern Aspects of Electrochemistry*, J. O'M. Bockris and B. Conway, eds., Vol. 1, Academic Press, New York (1954), pp. 103–179.
142. J. O'M. Bockris and A. K. Reddy, *Modern Electrochemistry*, Plenum Press, New York (1970), p. 707.
143. R. Ford and J. Pritchard, *Trans. Faraday Soc.* **67**, 216–221 (1971).
144. J. Randles, "Real hydration energies of ions," *Trans. Faraday Soc.* **52**, 1573–1581 (1956).
145. B. Damaskin and R. Kaganovich, *Elektrokhimiya* **13**, 293–296 (1977).
146. V. Novakovsky, E. Ukshe, and A. Levin, *Zh. Fiz. Khim.* **29**, 1847–1852 (1955).
147. S. Argade and E. Gileadi, "*The potential of zero charge*," in *Electrosorption*, E. Gileadi, ed., Plenum Press, New York (1967), pp. 87–115.
148. R. Vasenin, *Zh. Fiz. Khim.* **27**, 878–880 (1953); **28**, 1672–1675 (1954).
149. S. Trasatti, in *Advances in Electrochemistry and Electrochemical Engineering*, Vol. 10, H. Gerischer and C. W. Tobias, eds., Interscience, New York/London (1977), pp. 213–322.
150. S. Trasatti, *Chim. Ind. (Milan)* **53**, 559–564 (1971).
151. S. Trasatti, *J. Chem. Soc. Faraday Trans. I* **68**, 229–236 (1972).
152. S. Trasatti, *J. Electroanal. Chem.* **64**, 128–134 (1975).
153. R. Burshtein, N. Shurmovskaya, T. Kalish, and L. Larin, *Elektrokhimiya* **13**, 799–804 (1977).
154. B. Jakuszewski, M. Przasnyski, H. Scholl, and A. Siekowska, *Electrochim. Acta* **29**, 119–123 (1975).
155. A. Frumkin, I. Bagotskaya, and N. Grigoryev, *Z. Phys. Chem. (N.F.)* **98**, 3–7 (1975).
156. J. E. B. Randles and J. L. White, *Trans. Faraday Soc.* **51**, 185 (1955).
157. E. Ukshe and N. Bukun, *Itogi Nauki i Tekh. Rastvory. Rasplavy* **2**, 140–171 (1975).
158. E. Ukshe, N. Bukun, D. Leikis, and A. Frumkin, *Electrochim. Acta* **9**, 431–439 (1964).
159. O. Esin, *Zh. Fiz. Khim.* **30**, 3–19 (1956).
160. R. Dogonadze and Yu. Chizmadjev, *Dokl. Akad. Nauk SSSR* **157**, 944–947 (1964).
161. Yu. Delimarsky, *Issledovaniya v oblasti elektrokhimii ionnikh rasplavov*, Naukova Dumka, Kiev (1971).
162. V. Fomenko, *Emissionnie svoistva materialov*, Naukova Dumka, Kiev (1970).
163. V. Kuznetzov, L. Zagainova, N. Loginova, I. Lubimtseva, N. Onoprienko, and L. Tsimbal, *Dokl. Akad. Nauk SSSR* **138**, 156–158 (1961).
164. V. Salnikov, S. Karpachev, and A. Filyaev, *Elektrokhimiya* **10**, 1384–1386 (1974).
165. U. Palm and T. Tenno, *J. Electroanal. Chem.* **42**, 457–462 (1973).
166. N. Fedorovich, M. Levi, B. Damaskin, and A. Shlepakov, *Dokl. Akad. Nauk SSSR* **225**, 148–151 (1975).
167. A. Frumkin, N. Nikolaeva-Fedorovich, N. Berezina, and Kh. Keis, *J. Electroanal. Chem.* **58**, 189–201 (1975).
168. J. O'M. Bockris and A. K. Reddy, *Modern Electrochemistry*, Plenum Press, New York (1973), Chap. 9.

6

Electric Double Layer on Semiconductor Electrodes

YU. V. PLESKOV

1. Introduction

The properties of the semiconductor–electrolyte interface, as compared with the metal–electrolyte interface, are determined to a great extent by the electronic structure of the solid. Certainly, in the case of metal electrodes, variations in their electronic structure are manifested by peculiarities of the electrochemical behavior, but this effect is masked by what may be called the effect of the chemical nature of the electrode material. As regards semiconductors, doping with minute amounts of impurities, without affecting the chemical nature of a solid, has a profound effect on the physical properties and this is clearly exhibited in its electrochemical behavior.

So, in considering the semiconductor–electrolyte interface, the key factor is elucidation of a relationship between the electronic structure of a solid and its electrochemical properties. Therefore, although some electrodes of a nonmetallic nature (e.g., carbon) have already been considered, the origin of the electrochemistry of semiconductors should be attributed to Brattain and Garrett,[1] 1955. Using the theory of the space charge developed by them[2] for the semiconductor–gas interface they showed that the electrophysical properties of germanium played a decisive role in the specific features of its electrochemical behavior (photopotential, rectification of electric current, etc.).

YU. V. PLESKOV • Institute of Electrochemistry, Academy of Sciences of the USSR, Moscow V-71, Leninsky Prospekt 31, USSR.

Subsequently, the germanium electrode served as a model in the electrochemistry of semiconductors, as did mercury in the electrochemistry of metals. In 1957, Bohnenkampf and Engell,[3] using the method of differential capacity familiar to electrochemists, demonstrated the characteristic features of the double layer on semiconductors: penetration of an electric field deep into a solid and involvement of two types of mobile charges—electrons and holes—in the formation of the electrode charge. Some equations for the relation of current to potential at the semiconductor–solution interface were formulated for the first time by Green.[5] Later, on germanium too, fine features of the double layer due to adsorption and dipole surface groups were examined: the "solid-state side" of the interface was investigated by Brattain and Boddy and the "electrolyte" side, by Gerischer, Pleskov *et al.*

The extensive development of semiconductor electrode studies was stimulated, on the one hand, by the desire to go beyond the framework of metal electrodes in the examination of electrified interfaces and, on the other hand, by the technological requirements of a developing industry of semiconductor devices. Along with more comprehensive research into the principles of the electrochemistry of semiconductors, the range of semiconducting materials used as electrodes was extended. In 1960, Dewald[4] was the first to investigate the electrode behavior of a wide-band-gap semiconductor–zinc oxide. This material was followed by cadmium sulfide (Tyagai), gallium arsenide (Gerischer, Memming, Gatos), titanium dioxide (Veselovsky), and nickel oxide (Yeager). In connection with the study of germanium and silicon electrodes, one should also mention the names of Efimov and Erusalimchik, Harten, Gobrecht, Lazorenko-Manevich, Tomashov, and Paleolog.

If the papers devoted to semiconductor electrodes are classified for simplicity under two types, "double-layer" and "kinetic," in the first group a definite peak falls on 1965. Subsequently, the "center of gravity" of the investigations was transferred to the study of the electrode kinetics on semiconductors. In the seventies, however, interest was revived with respect to the specific features of the structure of the semiconductor–electrolyte interface. This is associated, on the one hand, with the fact that an ever-increasing number of new semiconducting materials is being brought into technological use, for instance, in connection with the problem of utilization of solar energy. On the other hand, it was discovered that semiconductors, being transparent to light (with the quantum energy not in excess of the band gap), were indispensable in making electrodes for modern optical methods in electrochemistry, such as multiple distorted total internal reflection, electroreflectance, etc. (see the relevant chapters of the present treatise).

Since many aspects of the double-layer structure on semiconductors are omitted from the present chapter due to its limited scope, it would be interesting for readers to acquaint themselves with the origin of the study of semiconductor electrochemistry in the excellent reviews by Green,[5] Dewald,[6] and Gerischer.[7] A systematic account of the electrochemistry of semiconductors can be found in

the book by Myamlin and Pleskov.[8] The principal notions and relations from semiconductor physics, which will be needed to understand the material presented, can be found in a brief but systematic account "for electrochemists" in the book by Bockris and Reddy,[9] and in more comprehensive monographs by Many *et al.*[10] and Frankl.[11]

2. The Theory of Double Layer on Semiconductor Electrodes

2.1. Charge and Potential Distribution

When a semiconductor comes into contact with an electrolytic solution, an electric double layer arises at the interface. Its features are determined first, by a low concentration of free electrons in the semiconductor and secondly, by the presence of two types of free charges, negative (conduction electrons) and positive (holes).

In the simple case—the absence, for example, of the specific adsorption of ions, dipole molecules, etc.—the charge of the "electrolytic" plate σ_{el} is compensated for by the charge of the "solid-state" plate σ_{sc} of the double layer:

$$\sigma_{sc} + \sigma_{el} = 0 \tag{2.1}$$

But the charge σ_{sc}, unlike that on the surface of a metal electrode, can no longer be regarded as concentrated on the electrode surface. In fact, because of the low conductivity of the semiconductor, the electric field penetrates deep into its bulk, and a space charge arises at the semiconductor surface in the same way (qualitatively), as there is a diffuse ionic charge in the dilute electrolyte at the electrode surface (Figure 1).

Hereafter, an interface at which no electrochemical reactions occur will be considered. In other words, the electrode is ideally polarizable, so that the interface can formally be represented as a leak-free capacitor. This condition is not too rigid, because on semiconductor electrodes, as opposed to metal ones, electrochemical reactions are strongly inhibited.[12–14]

For calculating the space charge value and distribution,[2] one should write Poisson's equation

$$\frac{d^2\phi(x)}{dx^2} = -\frac{4\pi}{\varepsilon_{sc}}\rho(x) \tag{2.2}$$

where $\phi(x)$ and $\rho(x)$ are the potential and charge density at point x (the x axis being directed from the surface, $x = 0$, into the semiconductor) and ε_{sc} is the semiconductor dielectric constant.

The charge density in the semiconductor is composed of mobile charges (electrons, holes) and immobile ones (ionized donors and acceptors):

$$\rho(x) = e[-n_e(x) + n_p(x) - N_D + N_A] \tag{2.3}$$

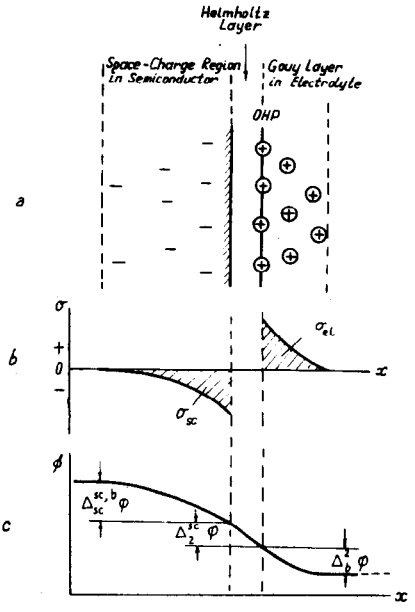


Figure 1. Structure of the double layer (a) and the distribution of charge (b) and potential (c) at the semiconductor-electrolyte interface.

where n_e, n_p, N_D, and N_A are, respectively, the concentrations of electrons, holes, charged donors, and acceptors and e is the electron charge. While ionized impurity atoms are usually distributed uniformly over the entire bulk of the semiconductor, i.e., N_D and N_A are independent of x, the concentrations of mobile charges $n_e(x)$ and $n_p(x)$ within the space charge region, where there is an electric field, differ from those in the electrically neutral bulk of the semiconductor, n_e^0 and n_p^0. Mobile charges obey the Boltzmann distribution:

$$n_e(x) = n_e^0 \exp\{e[\phi(x) - \phi_b^{sc}]/kT\} \tag{2.4a}$$

$$n_p(x) = n_p^0 \exp\{-e[\phi(x) - \phi_b^{sc}]/kT\} \tag{2.4b}$$

where ϕ_b^{sc} is the potential deep in the semiconductor (beyond the double layer).

Even from the form of Eqs. (2.2) and (2.3), one can see the profound analogy between the electron–hole space charge inside the semiconductor and the ionic diffuse double layer in the electrolyte. In both cases, the Poisson equation is written and solved in a similar manner and yields basically similar results.

The quantitative distinction of the cases in question arises from an important qualitative distinction between the semiconductor and the electrolyte. The electrolyte contains only two types of charges, cations and anions, both of which are mobile and occur in the 1:1 electrolyte bulk in equal concentrations. In the semiconductor, in addition to mobile charges (electrons and holes), there

are also immobile ionized impurity atoms. The concentration of the latter is arbitrarily variable by doping the semiconductor and thereby setting the electron and hole concentrations which are no longer equal (except for an intrinsic semiconductor which is quite analogous in this respect to the 1:1 electrolyte). This circumstance endows the semiconductor interfaces with an additional "degree of freedom," diversifying the prevailing situations as compared with the Gouy layer in the electrolyte.

Prior to presenting the general solution of the equations given above, it is useful to consider the qualitative picture taking the simplest special case as an example: a moderately doped semiconductor (one may consider an n type), in which $N_D \gg N_A$, $n_e^0 \gg n_p^0$, and $n_e^0 \simeq N_D$, and potential differences in the space region which are small compared with kT/e ($\equiv RT/F$). This enables one to expand the exponents in Eqs. (2.4), and within the first term of the expansion in ϕ as a result of various simplifications one gets the following expression for the charge density:

$$\rho(x) = -\frac{e^2 n_e^0}{kT}\phi(x) \tag{2.5}$$

Integrating Eq. (2.2), upon substitution of expression (2.5) into it, yields

$$\left(\frac{d\phi}{dx}\right)^2 = \frac{4\pi e^2 n_e^0}{\varepsilon_{sc} kT}\phi^2(x) \tag{2.6}$$

Hence, the electric field strength at the semiconductor surface is

$$\mathscr{E}_{sc} = -\frac{d\phi}{dx}\bigg|_{x=0} = \frac{\Delta_{sc}^{sc,b}\phi}{\kappa_{sc}^{-1}} \tag{2.7}$$

where $\Delta_{sc}^{sc,b}\phi = \phi^{sc,b} - \phi_{x=0}{}^{sc}$ is the potential drop in the space charge region in the semiconductor and the quantity

$$\kappa_{sc}^{-1} = (\varepsilon_{sc} kT/4\pi e^2 n_e^0)^{1/2} \tag{2.8}$$

which is known as the Debye length, characterizes, in full analogy to the situation in the ionic diffuse layer, the extension of the space charge deep into the semiconductor phase.

So, expression (2.7) can be interpreted as follows: a space charge layer existing inside the semiconductor is equivalent, together with the interface, to a plane capacitor with the distance between the plates κ_{sc}^{-1}, the electric field inside the capacitor being constant ($\mathscr{E}_{sc}$).

In a physical sense, the semiconductor–electrolyte interface should be regarded as a capacitor, both plates of which—the space charge in the semiconductor and the ionic Gouy layer in the solution—have a diffuse character. They are separated by a "dielectric intermediate layer"—the Helmholtz layer. Nevertheless, the equivalent electric circuit of the interface, as will be shown

below, can be represented for convenience as three series-connected capacitors corresponding to the three above-mentioned regions, i.e., each of them can formally be represented as a separate capacitor.

The thickness of these regions is quantitatively characterized by the Debye lengths for the semiconductor κ_{sc}^{-1} and for the electrolyte κ^{-1}. The Helmholtz layer has a thickness d_H of atomic size. The first two quantities, as follows from Eq. (2.8), and a similar expression for κ^{-1}, are inversely proportional to the square root of the charge concentration in a corresponding phase—the majority carrier concentration in the semiconductor (n_e^0) or the ion concentration in a solution. These concentrations usually differ by many orders of magnitude. For example, the carrier concentration in intrinsic germanium n_e^0 is 2×10^{13} per cm^3, which is about equal to the number of ions in purest water. In a 0.01 *M* electrolyte solution, the ion concentration is about 10^{19} per cm^3. Accordingly, in intrinsic germanium, the thickness of the space charge region κ_{sc}^{-1} is 10^{-4} cm; with allowance for the dielectric constant, it is 100 times larger than that of the diffuse layer in a centrinormal aqueous electrolyte solution ($\kappa^{-1} \simeq 10^{-6}$ cm). In more heavily doped semiconductors, the thickness of the space charge region decreases to 10^{-5} or even 10^{-6} cm, but still remains of a greater order of magnitude than the diffuse ionic layer in slightly dilute electrolytic solutions used in most electrochemical experiments.

Applying this approach to metal electrodes, one should put $n_e^0 \to \infty$ in Eq. (2.8) (in metals the free-electron concentration is about 10^{22} per cm^3). It follows that $\kappa_M^{-1} \to 0$, i.e., the charge becomes concentrated on the electrode surface, just as the whole of the charge of the ionic layer is concentrated within the outer Helmholtz plane, as soon as the solution concentration becomes sufficiently high.

The interphase (Galvani) potential drop $\Delta_{el}^{sc}\phi$ is distributed among the three above-mentioned regions. The potential drop in the space charge region, as follows from Eq. (2.7), is $\Delta_{sc}^{sc,b}\phi = \mathscr{E}_{sc}\kappa_{sc}^{-1}$. By analogy, the potential drop in the Gouy layer can be written as $\Delta_b^2\phi = \mathscr{E}_{el}\kappa^{-1}$ and in the Helmholtz layer, as $\Delta_2^{sc}\phi = \mathscr{E}_H d_H$, where $\mathscr{E}_{el}$ and $\mathscr{E}_H$ are the electric field strength values in the respective regions. Consequently:

$$\Delta_{el}^{sc}\phi = \Delta_{sc}^{sc,b}\phi + \Delta_2^{sc}\phi + \Delta_b^2\phi = \mathscr{E}_{sc}\kappa_{sc}^{-1} + \mathscr{E}_H d_H + \mathscr{E}_{el}\kappa^{-1} \qquad (2.9)$$

In the simplest case under consideration, when there are no fixed charges (adsorbed ions, surface states, etc.) at the boundary separating the three regions, the following electrostatic induction equalities hold, i.e.,

$$\varepsilon_{sc}\mathscr{E}_{sc} = \varepsilon_H\mathscr{E}_H = \varepsilon_{el}\mathscr{E}_{el} \qquad (2.10)$$

where ε_H and ε_{el} are the dielectric constants of the medium within the Helmholtz layer and in the diffuse ionic layer. From Eqs. (2.9) and (2.10), one can see that the potential drops in the regions making up the interface are proportional

(when the dielectric constant is of the same order of magnitude) to the thicknesses of these regions:

$$\frac{\Delta_{sc}^{sc,b}\phi}{\Delta_b^2\phi} = \frac{\kappa_{sc}^{-1}\varepsilon_{el}}{\kappa^{-1}\varepsilon_{sc}}, \qquad \frac{\Delta_{sc}^{sc,b}\phi}{\Delta_2^{sc}\phi} = \frac{\kappa_{sc}^{-1}\varepsilon_H}{d_H\varepsilon_{sc}} \tag{2.11}$$

Since, as has been demonstrated above, $\kappa_{sc}^{-1} \gg d_H$, $\kappa_{sc}^{-1} \gg \kappa^{-1}$ then $\Delta_{sc}^{sc,b}\phi \gg \Delta_2^{sc}\phi$, $\Delta_{sc}^{sc,b}\phi \gg \Delta_b^2\phi$, i.e., practically the whole of the interphasial Galvani potential is concentrated within the space charge region in the semiconductor.

In the following, unless otherwise stated, the interface between a semiconductor and a sufficiently concentrated electrolyte solution is considered, so that the potential drop in the Gouy layer $\Delta_b^2\phi$ can be neglected.

The above calculation was made for the simple special case. Solving Eqs. (2.2) and (2.3) for an arbitrary potential drop and an arbitrary degree of semiconductor doping yielded the following formulas for the electric field strength on the semiconductor surface[2]:

$$\mathscr{E}_{sc} = \pm(8\pi kTn_i/\varepsilon_{sc})^{1/2}F(Y, \lambda) \tag{2.12}$$

and for the space charge of a semiconductor:

$$\sigma_{sc} = -\frac{\varepsilon_{sc}\mathscr{E}_{sc}}{4\pi} = \mp\frac{\varepsilon_{sc}kT}{2(2)^{1/2}\pi e\kappa_{sc,i}^{-1}}F(Y, \lambda) \tag{2.13}$$

Here the following notation is used: $Y = e\Delta_{sc}^{sc,b}\phi/kT$ is the dimensionless potential drop in the space charge region; $\kappa_{sc,i}^{-1}$ is the Debye length for an intrinsic semiconductor with the free-electron concentration $n_{e,i}$; its value is obtained by substituting the value $n_{e,i}$ into Eq. (2.8) in place of n_e^0; $\lambda = (n_p^0/n_e^0)^{1/2} = n_p^0/n_{e,i} = n_{e,i}/n_e^0$ is the parameter characterizing the degree of semiconductor doping; and

$$F(Y, \lambda) = [\lambda(e^{-Y} - 1) + \lambda^{-1}(e^Y - 1) + (\lambda - \lambda^{-1})Y]^{1/2} \tag{2.14}$$

The function $F(Y, \lambda)$ was calculated by Kingston and Neustadter[15] and for high values of Y, by Seiwatz and Green.[16] It is given in the quoted papers as graphs and as tables[17] whence its values are taken for numerical calculations involving the space charge.

In Eq. (2.12) the plus sign is chosen when $Y > 0$ and the minus sign, when $Y < 0$. (It should be kept in mind that the sign of Y, as well as of $\Delta_{sc}^{sc,b}\phi$, is opposite to the sign of the potential $\Delta_b^2\phi$ customary for electrochemists since in calculating $\Delta_b^2\phi$, for zero one takes the potential deep inside the solution and in calculating $\Delta_{sc}^{sc,b}\phi$, the potential inside the semiconductor. Therefore, for example, the decrease in the positive value of $\Delta_{sc}^{sc,b}\phi$ and Y corresponds to the increase in the positive charge of the electrode σ_{sc}.)

The use of general formulas (2.12) and (2.13) does not affect the qualitative picture of the charge and potential distribution at the interface as compared with the simple picture outlined above, at least not at high values of $|Y|$. Only

with a large interphase potential drop and a great charge in the semiconductor does the potential drop in the Helmholtz layer $\Delta_2^{sc}\phi$ become comparable in magnitude with that in the space charge region $\Delta_{sc}^{sc,b}\phi$.

Thus, semiconductor electrodes have the following basic features:

(1) The interphase potential drop is usually concentrated mostly within the semiconductor phase, whereas the contribution from the Helmholtz layer is usually small or negligible. This circumstance is of decisive importance in describing the kinetics of electrochemical reactions on semiconductors.

(2) The charge of a semiconductor electrode is not localized on its surface but is diffuse in character. This leads to a characteristic dependence of the differential capacity of the semiconductor electrode on potential and gives rise to such phenomena as (electronic) surface conductivity and a strong photopotential, which do not occur on metal electrodes.

2.2. Surface Conductivity

Under the electric field effect, electron and hole concentrations at the semiconductor surface differ from those in the bulk [Eqs. (2.4)]. Naturally, the conductivity of the surface region (which is a function of free-carrier concentrations) differs from the bulk conductivity of a semiconductor. This difference is quantitatively characterized by a quantity referred to as surface conductivity:

$$K_s = e(\lambda_e\Gamma_e + \lambda_p\Gamma_p) \tag{2.15}$$

where λ_e and λ_p are electron and hole mobilities while Γ_e and Γ_p are their surface excesses defined (as are surface excesses of ions in the ionic diffuse layer) as the difference between the total number of free carriers of a given type (per unit surface of the electrode) at a given potential and the number which would occur if concentrations up to the surface maintained the same value as in the bulk phase. Quantitative relations for surface excesses as functions of potential were derived by Garrett and Brattain,[2] and here it suffices to consider the qualitative picture.

Figure 2 illustrates in qualitative form the distribution of electron and hole concentrations near the surface of the semiconductor electrode at different signs of its charge. The upper part of the figure (A) refers to an intrinsic semiconductor and its lower part (B), to an extrinsic one (*n* type).

In the intrinsic semiconductor the electron and hole concentrations are equal ($n_e^0 = n_p^0 = n_e^2$) and much higher than the concentration of ionized donors or acceptors ($n_e^2 \gg N_D, N_A$). In cathodic bias, the electrode is undergoing enrichment with electrons and depletion in holes [Figure 2A(a)], whereas at anodic bias, it is enriched with holes and depleted in electrons [Figure 2A(c)]. At equilibrium at any point $n_e n_p = \text{const} = (n_e^2)^2$. The shaded areas in Figure 2 represent surface excesses of electrons and holes. What takes place in the space charge region when the semiconductor electrode is charged can be expressed in

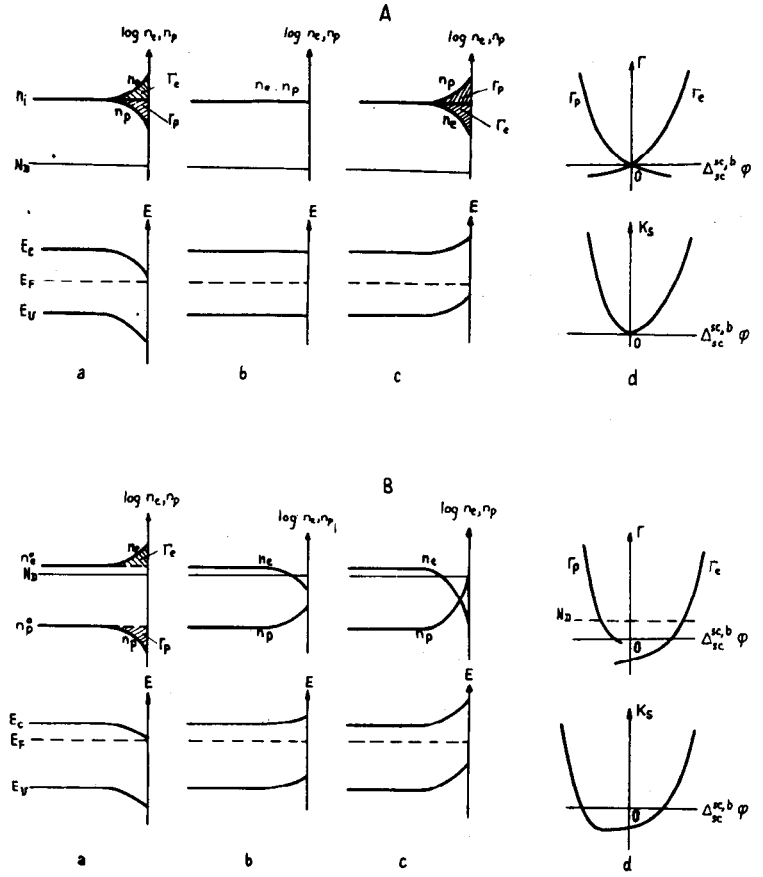


Figure 2. Distribution of free-carrier concentrations n_e, n_p and the band bending at the semiconductor surface (a–c); surface excessess Γ_e, Γ_p and surface conductivity K_s as functions of potential (d). (A) An intrinsic semiconductor: (a) the surface enriched with electrons; (b) the flat-band potential; (c) the surface enriched with holes. (B) An extrinsic semiconductor (n type): (a) the accumulation layer; (b) the depletion layer; (c) the inversion layer. In parts Aa and Ba the shaded areas correspond to surface excesses of electrons and holes.

terms of a semiconductor band diagram. Since the energy of an electron level in the electric field changes by the value $e\phi(x)$, where $\phi(x)$ is the electric potential at a point x, at the electrode surface the energy bands are bent, as shown in Figure 2: at cathodic bias downward and at anodic bias upward. If the electrode is uncharged, the electron and hole concentrations therein have a constant value up to the surface ($n_e = n_e^0$, $n_p = n_p^0$) and the bands are not bent ($\Delta_{sc}^{sc,b}\phi = 0$)

[Figure 2A(b)]. Therefore, the potential at which the semiconductor electrode is uncharged is called the *flat-band potential* (ϕ_{fb})—this is a semiconductor equivalent to the potential of the zero (free) charge of the metal electrode.

The right side of Figure 2 shows the dependence of the surface excesses of free carriers Γ_e and Γ_p and of the surface conductivity, K_s, on the potential drop in the semiconductor $\Delta_{sc}^{sc,b}\phi$. With increasing $|\Delta_{sc}^{sc,b}\phi|$, the surface excesses vary rapidly and from Eq. (2.15), one can readily understand why the dependence of the surface conductivity on the potential is represented by a curve with a minimum at the flat-band potential.

It is easy to see that the situations described above for electron–hole diffuse layer are analogous to those encountered for the ionic diffuse layer on a metal electrode in dilute electrolyte solutions. Ionic surface conductivity is an electrokinetic phenomenon. It should be kept in mind, however, that with the ionic and electronic charges equal in magnitude, the ionic surface conductivity is several orders of magnitude lower than the electronic one because of the difference in mobilities of ions and electrons (holes).

In an extrinsic semiconductor, electron and hole concentrations in the bulk may differ by many orders. (This is reflected in the notions "majority current carriers" and "minority current carriers," depending upon their contribution to the conductivity of the sample bulk.) As regards the space charge region, three cases can be distinguished.

(1) An accumulation layer: The surface region of the electrode is enriched with majority carriers [Figure 2B(a)].

(2) An inversion layer: The surface region is enriched with minority carriers so that their contribution to the space charge exceeds the contribution from the majority (in the bulk) carriers [Figure 2B(c)].

(3) A depletion layer: The space charge is composed of ionized impurity atoms (the so-called Mott–Schottky layer).

This case, intermediate between the two above-mentioned ones, is observed in extrinsic semiconductors at moderate values of $\Delta_{sc}^{sc,b}\phi$; so that in the surface region the majority carrier concentration has decreased, but the minority carrier concentration has not yet increased markedly. Hence, for example, for an *n*-type semiconductor [Figure 2B(b)] $n_e^s \ll N_D$, $n_p^s \ll N_D$ (n_e^s and n_p^s being concentrations at the surface). The depletion layer is more pronounced in semiconductors with a wide band gap, which, in practice, are always doped to obtain a sufficiently high conductivity. Such a situation, in contrast to those described earlier, can no longer be realized in the ionic double layer in an electrolyte, because it has no immobile charges similar to impurity ions in a semiconductor.

Since, in practice, there are no mobile charges in the depletion layer, the conductivity is lower than that in the electrically neutral bulk of a semiconductor. Consequently, the surface conductivity [which by definition—see Eq. (2.15)—is *excess* conductivity] is negative, as shown graphically in the right side of Figure 2B.

In calculating the surface conductivity, one should keep in mind that the mobilities of electrons and holes in the space charge region may be lower than in the semiconductor bulk[18] as a result of their scattering by the surface.

2.3. Differential Capacity

The differential capacity corresponding to the space charge in a semiconductor is defined as

$$C_{sc} = -\frac{d\sigma_{sc}}{d\Delta_{el}^{sc}\phi} \tag{2.16}$$

The formula for C_{sc} can be obtained by differentiating Eq. (2.13) for the charge:

$$C_{sc} = \frac{\varepsilon_{sc}}{4(2)^{1/2}\pi\kappa_{sc,i}^{-1}} \frac{|-\lambda e^{-Y} + \lambda^{-1}e^{Y} - \lambda - \lambda^{-1}|}{[\lambda(e^{-Y} - 1) + \lambda^{-1}(e^{Y} - 1) + (\lambda - \lambda^{-1})Y]^{1/2}} \tag{2.17}$$

In the case of an intrinsic semiconductor $\lambda = 1$, formula (2.17) transforms to the expression

$$C_{sc,i} = \frac{\varepsilon_{sc}}{2(2)^{1/2}\pi\kappa_{sc,i}^{-1}} \cosh \frac{e\,\Delta_{sc}^{sc,b}\phi}{2kT} \tag{2.18}$$

which becomes identical, after appropriate replacement of the notation, to the formula for the capacity of the ionic diffuse layer. The dependence of the capacity on potential is represented by a curve with a minimum (Figure 3A); the latter lies at the flat-band potential of the semiconductor electrode.

Formulas (2.17) and (2.18), as well as Eq. (2.13), have been obtained under the assumption that free electrons and holes in the semiconductor bands obey the Maxwell–Boltzmann statistics. This is true at moderate electrode charges when the Fermi level is located far enough ($\Delta E \geqslant 3kT$) from the boundaries of the band gap at the surface. When the charge of the semiconductor electrode is sufficiently high, the foregoing condition does not hold; and for describing the free-carrier distribution, the Thomas–Fermi statistics should be used. Here, the increase in charge and capacity with potential slows down as a result of restrictions imposed by the finite density of states in the bands.[16] This is schematically displayed in Figure 3. Finally, with further charging, when the thickness of the space charge layer is reduced to a size comparable to the wavelength of a thermal electron, in calculations of charge and capacity, one should take into account the quantum effects in the space charge region.

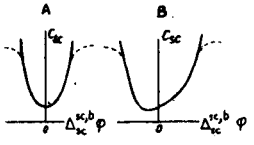


Figure 3. Qualitative dependence of the capacity of the semiconductor on potential. (A) an intrinsic semiconductor; (B) an extrinsic semiconductor. The dashed line shows the finite density of states limitations.

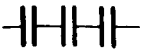


Figure 4. Equivalent electric circuit of an ideally polarizable semiconductor electrode.

The capacity–potential curve for an extrinsic semiconductor is asymmetric (Figure 3B); the potential of the minimum is no longer equal to the flat-band potential. A relatively flat portion of the curve corresponding to the depletion layer is noteworthy [cf. Figure 2B(d) for surface conductivity]. In this region, if the conditions $\lambda^{-1} \gg \lambda$ and $\lambda e^{-Y} \ll \lambda^{-1}$ are satisfied and allowing for $n_e^0 \simeq N_D$, formula (2.17) can be simplied and reduced to the form usually used in the treatment of experimental capacity curves obtained under the conditions of the depletion layer:

$$C_{sc}^{-2} = (8\pi/\varepsilon_{sc} e N_D)(|\Delta_{sc}^{sc,b}\phi| - kT/e) \tag{2.19}$$

As is evident from the formula, the plot C_{sc}^{-2}–$\Delta_{sc}^{sc,b}\phi$ (the Mott–Schottky plot) represents a straight line which intersects the potential axis at kT/e from the flat-band potential; and from the straight-line slope, it is possible to find the donor concentration in the semiconductor, N_D.

The simple equivalent circuit of an ideally polarizable semiconductor electrode comprises three series-connected leak-free capacitors which display capacities of the space charge region in the semiconductor C_{sc}, of the Helmholtz layer C_H, and of the Gouy layer in the electrolyte C_{el} (Figure 4). The quantitative distinction between the capacities C_{sc} and C_{el} is determined by the difference in free-carrier concentration between the corresponding phases. As can be seen from Eq. (2.18) and from a similar formula for the capacity of the Gouy layer, these capacities are inversely proportional to the corresponding Debye lengths κ_{sc}^{-1} and κ^{-1}. The capacity of the Helmholtz layer

$$C_H = \frac{\varepsilon_H}{4\pi d_H} \tag{2.20}$$

is also inversely proportional to its thickness d_H. Since (Section 2.1) d_H, $\kappa^{-1} \ll \kappa_{sc}^{-1}$, then C_H, $C_{el} \gg C_{sc}$. For example, the capacity of an intrinsic germanium electrode at a minimum is of the order of 10^{-2} μF/cm^2, while the capacity of the Helmholtz layer is about 10 μF/cm^2. The total capacity is determined by the capacitor with the *minimum* capacity. The semiconductor electrode capacity is thus usually determined by the semiconductor plate of the double layer. Only when the charge of the electrode is very high can the capacity, C_{sc}, become close in order of magnitude to C_H.

2.4. Surface States

2.4.1. Effect on Potential Distribution

Apart from a system of energy levels forming the bulk properties of a semiconductor, there exists an additional system of levels at its surface.[19,20]

Corresponding to these surface levels are quantum states in which an electron is localized at the surface and cannot go into the bulk without energy exchange with the surrounding medium ("surface states").

Surface levels arise from adsorption (the Shockley levels) and from the discontinuity of a crystal lattice (Tamm levels). Although the existing phenomenological theory of surface states adequately describes their formal electrical characteristics, the microscopic nature of surface levels and detailed relationship between their characteristic parameters (energy, relaxation time, electron and hole capture cross sections) and the physicochemical properties of surface atoms have yet to be carefully studied.

The surface levels are characterized primarily by energy E_{ss} and concentration N_{ss}. The occupation of a level by an electron is determined by the Fermi function:

$$f_F = \{1 + \exp[(E_{ss} - E_F)/kT]\}^{-1} \tag{2.21}$$

so that the total number of electrons at the surface levels is $n_{ss} = N_{ss} f_F$. In Eq. (2.21), E_F stands for the Fermi level.

The surface electric field affects the occupation of levels by electrons. The electron energy in the electric field varies; therefore the quantity E_{ss} should be represented as

$$E_{ss} = E_{ss}^{\circ} - e\Delta_{sc}^{sc,b}\phi \tag{2.22}$$

With respect to the donor surface levels (positively charged when free of electrons and neutral when occupied by electrons), one can write the total charge as

$$Q_{ss} = e(N_{ss} - n_{ss}) = eN_{ss}\{1 + \exp[(E_F - E_{ss}^{\circ} + e\Delta_{sc}^{sc,b}\phi)/kT]\}^{-1} \tag{2.23}$$

Surface states, if large in number, have a significant effect on the potential distribution in the double layer.

The electric field strength in the Helmholtz layer $\mathscr{E}_H$ is related to the field strength at the semiconductor surface $\mathscr{E}_{sc}$ and to the charge at the surface levels by the relation

$$\varepsilon_H \mathscr{E}_H = \varepsilon_{sc}\mathscr{E}_{sc} + 4\pi Q_{ss} \tag{2.24}$$

If Q_{ss} is sufficiently great, so that the first term on the right side of Eq. (2.24) can be neglected, then for the potential drop in the Helmholtz layer, one obtains

$$\Delta_2^{sc}\phi = \mathscr{E}_H d_H = 4\pi e N_{ss} d_H \varepsilon_H^{-1}\{1 + \exp[(E_F - E_{ss}^{\circ} + e\Delta_{sc}^{sc,b}\phi)/kT]\}^{-1} \tag{2.25}$$

The ratio of the potential drops in the Helmholtz layer and the space charge layer is now (with $e\Delta_{sc}^{sc,b}\phi/kT = Y$)

$$\frac{d\Delta_2^{sc}\phi}{d\Delta_{sc}^{sc,b}\phi} = \frac{4\pi e^2 N_{ss} d_H \exp[(E_F - E_{ss}^{\circ})/kT + Y]}{kT\varepsilon_H\{1 + \exp[(E_F - E_{ss}^{\circ})/kT + Y]\}^2} \tag{2.26}$$

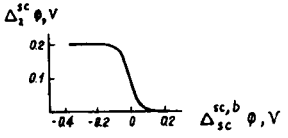


Figure 5. Dependence of the potential drop in the Helmholtz layer on the potential drop in the space charge layer at a high density of surface states.[8] The parameters chosen for calculation: n-type germanium, $\lambda = 0.1$, $N_{ss} = 10^{13}\,\mathrm{cm}^{-2}$, $E_{ss}^{\circ} = E_F$.

For weak ionization of the donor levels, one can neglect the 1 in the curly brackets in the denominator and simplify Eq. (2.26):

$$\frac{d\,\Delta_2^{sc}\phi}{d\,\Delta_{sc}^{sc,b}\phi} = \frac{4\pi e^2 N_{ss}\, d_H}{kT\varepsilon_H \exp\left[(E_F - E_{ss}^{\circ})/kT + Y\right]} = \frac{4\pi e\, d_H}{kT\varepsilon_H} Q_{ss} \qquad (2.27)$$

Thus the potential distribution within the double layer is related to the surface charge value. If $Q_{ss} \simeq kT\varepsilon_H/4\pi e\, d_H$, $\Delta_2^{sc}\phi \simeq \Delta_{sc}^{sc,b}\phi$, i.e., *the potential drop in the Helmholtz layer becomes comparable with that in the semiconductor.* Estimates show that this critical value of the number of surface states in order of magnitude is 10^{13} per cm^2 (i.e., approximately 1% of the number of surface atoms of a crystal).

It should be remembered that the filling of surface levels with electrons is a steep function of potential [Eqs. (2.21) and (2.22)]. Therefore, if the levels are monoenergetic (i.e., all have the same energy, E_{ss}°), with a change in the potential drop in the semiconductor $\Delta_{sc}^{sc,b}\phi$, the surface charge Q_{ss} as well as the potential drop in the Helmholtz layer $\Delta_2^{sc}\phi$, change rapidly from negligible values to some limiting values. This change occurs in the vicinity of the value $\Delta_{sc}^{sc,b}\phi$ at which $E_F = E_{ss}^{\circ} - e\Delta_{sc}^{sc,b}\phi$, the width of the corresponding curve being several kT/e units (Figure 5). If at the surface there is a set of levels characterized by different energies E_{ss}°, the potential drop in the Helmholtz layer varies smoothly in a wide potential range. At a sufficient number of surface states, the semiconductor electrode surface begins to lose its specific features: it becomes "metallized."

So, in the general case in the charge balance for the double layer, one should take into account not only the space electronic charge in the semiconductor σ_{sc} and the ionic charge in the electrolyte σ_{el}, but also the charge in surface states, Q_{ss}. Also, there is a charge of specifically adsorbed ions in the inner Helmholtz plane σ_{ad}, so that

$$\sigma_{sc} + \sigma_{el} + Q_{ss} + \sigma_{ad} = 0 \qquad (2.28)$$

This is illustrated by Figure 6. It should be kept in mind that the sign of the charge Q_{ss} is not directly related to that of the space charge, just as the sign of specifically adsorbed ions is not directly related to that of electrostatically adsorbed ions in the outer Helmholtz plane.

One more remark should be made concerning the interrelationship between adsorbed ions (atoms, molecules) and surface states. It has been mentioned that adsorption is a factor responsible for the occurrence of surface states.

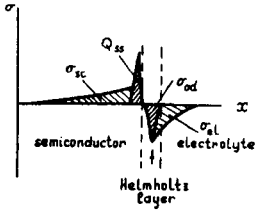


Figure 6. Schematic representation of the charge distribution in the double layer in the presence of surface states and specifically adsorbed ions.

One might think that the charges Q_{ss} and σ_{ad} should be identified in such a way that the ions in the inner Helmholtz plane are located so close to the semiconductor surface that they appear to be "built" into it. However, the deciding factor here is not the spatial arrangement of charges in the double layer but their nature and the character of their interaction with phases. Surface states exchange charge with the conduction band or valence band of the semiconductor and adsorbed particles with the solution.

Finally, dipoles are also involved in the formation of the double layer. They do not contribute to the charge balance [Eq. (2.28)], but some potential drop $\Delta_{dip}^{sc}\phi$ is associated with them. The question concerns the oriented adsorption of solvent molecules, the polar bonds of semiconductor surface atoms with adatoms, e.g., chemisorbed oxygen, and, in the general case, the "surface dipole" inherent in the semiconductor surface. This dipole potential drop changes only to a small extent with a change in the electrode potential; however, it is rather sensitive to the character of pretreatment of the surface and to the composition of the surrounding medium.

2.4.2. *Effect on Differential Capacity*

Since the charge on the surface states is a function of potential, a certain capacity is due to this charge. The formula for the differential capacity of surface states is obtained by differentiating relation (2.23) for the surface charge:

$$C_{ss} = \frac{e^2}{kT}\frac{N_{ss}\exp\left[(E_F - E_{ss}^{\circ})/kT + Y\right]}{\{1 + \exp\left[(E_F - E_{ss}^{\circ})/kT + Y\right]\}^2} \tag{2.29}$$

The dependence of C_{ss} on the potential drop in a semiconductor is represented by a curve with a maximum (Figure 7). At large positive or negative values of

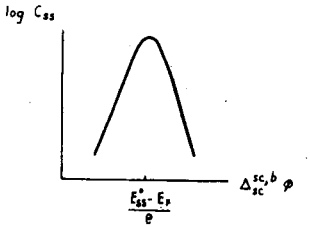


Figure 7. Schematic representation of the dependence of the capacity of surface states on potential.

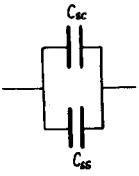


Figure 8. Equivalent electric circuit of a semiconductor electrode in the presence of surface states (the capacities of the Helmholtz layer and Gouy layer being omitted).

$\Delta_{sc}^{sc.b}\phi$ such that $|(E_F - E_{ss}^{\circ})/kT| \ll |Y|$, the capacity of surface states falls off exponentially with the potential:

$$C_{ss} \simeq \frac{e^2}{kT} N_{ss} \exp(-|Y|) \tag{2.30}$$

At a potential $Y = (E_F - E_{ss}^{\circ})/kT$, the capacity of surface states is maximal and equal to $C_{ss}^{max} = e^2 N_{ss}/kT$. At a high concentration of surface levels, e.g., at $N_{ss} = 10^{14}$ cm^{-2}, this capacity is around 100 μF/cm^{-2}, i.e., comparable in magnitude to the capacity of the Helmholtz layer.

Since the total charge on the semiconductor plate of the double layer is equal to the sum of σ_{sc} and Q_{ss}, the capacity of this plate is also equal to the sum of C_{sc} and C_{ss}. In the equivalent electric circuit of the interface, the capacity of space charge and that of surface states are connected in a parallel manner (Figure 8).

Returning to the potential distribution between the semiconductor and the Helmholtz layer, the condition (2.26) can now be expressed in terms of differential capacities. Comparing formulas (2.26) with (2.29) and taking into account formula (2.20) for the capacity of the Helmholtz layer, it is easy to obtain $d\Delta_2{}^{sc}\phi/d\Delta_{sc}^{sc.b}\phi = C_{ss}/C_H$; in a general form $d\Delta_2{}^{sc}\phi/d\Delta_{sc}^{sc.b}\phi = (C_{ss} + C_{sc})/C_H$.

3. The Semiconductor-Electrolyte Interface at Quasiequilibrium

3.1. Relaxation Characteristics of Space Charge and Surface States

The relations for space charge and capacity derived above do not involve time as a parameter. In obtaining them it was assumed that in any action on the semiconductor–electrolyte system, sufficient time is left for this system to attain equilibrium. In practice, however, this condition is often violated, accidentally or intentionally, and relaxation processes arise in a semiconductor electrode which are connected either with the final rate of transport of charges or with the final rate of their capture to the surface levels and release from the levels.

Suppose the electrode potential varies with time. According to Eq. (2.13) a change in potential corresponds with a definite change in the space charge.

In a metal electrode with its large bulk electron concentration, charging of the surface involves no difficulties; but in a semiconductor the rate of this process is often limited because of a low concentration of free charges.

If the rate of electron and hole recombination–generation processes in a semiconductor is low (as is the case, for example, in germanium), its influence on charge transport in a thin space charge region can be neglected, and then the only possible way of changing the space charge is by charge exchange with the neutral semiconductor bulk. Beyond the double layer the excess or lack of free carriers compared with their equilibrium concentrations is compensated for in the course of generation–recombination. This process occurs at a distance from the surface which is approximately equal to the diffusion length of minority carriers, L_p. The latter is $L_p = (D_p\tau)^{1/2}$, where D_p and τ are the diffusion constant and lifetime of minority carriers, respectively. In germanium and silicon, usually, $L_p \gg \kappa_{sc}^{-1}$.

In the neutral semiconductor bulk, the motion of majority carriers results from migration under the effect of a potential gradient. (Their transport number is equal to 1.) Minority carriers are transported by diffusion under the effect of a concentration gradient. (Their transport number is close to 0.) The first process occurs instantaneously; the second, at a low concentration of minority carriers in the bulk, may become the slow step in electrode charging. Thus it appears that slow relaxation of the space charge will occur if it is composed of minority carriers, i.e., it represents the inversion layer.

The relaxation characteristics of the space charge were calculated (assuming $L_p \gg \kappa_{sc}^{-1}$) for two major cases: (1) a small harmonic perturbation signal (compared with $kT/e \equiv RT/F$) and (2) a stepwise superposition of a much larger signal. The first case[21,22] corresponds to impedance measurement and the second[23] to taking galvanostatic charging curves. The corresponding calculations are cumbersome. It is convenient to consider qualitatively measurement of the inversion layer differential capacity.

The space charge of the inversion layer is made up of the charge on minority carriers (holes in an n-type semiconductor) and the charge on the immobile ionized donors: $\sigma_{sc} = \sigma_p + \sigma_D$. Variation in each of these components with potential provides a contribution to the total capacity: $C_{sc} = C_p + C_D$. (The donor charge varies as a result of variation in the thickness of the space charge region with potential.) At a sufficiently high value of $\Delta_{sc}^{sc,b}\phi$, the equilibrium "hole' capacity is higher than the "donor" one, as schematically shown in Figure 9.

With periodic oscillations of the potential, the charge variation is accompanied by motion of holes from the double layer to the neutral bulk of the semiconductor and conversely; so that beyond the double layer, the hole concentration undergoes periodic oscillations. This perturbation extends into the semiconductor for a distance which depends on the ac frequency:

$$L_\omega = \mathrm{Re}[D_p\tau/(1 + i\omega\tau)]^{1/2}$$

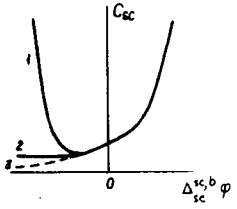


Figure 9. Differential capacity at various frequencies. An extrinsic semiconductor; (1) $\omega \to 0$ (static capacity); (2) $\omega \to \infty$; (3) the calculated "donor" capacity of the depletion layer C_D.

where ω is the ac frequency and $i = (-1)^{1/2}$. Physically, the picture observed is somewhat similar to that encountered when an alternating current is superimposed on a metal electrode in the reversible redox system: the diffusion front periodically propagates from its surface into the solution bulk. At low frequencies the layer thickness L_ω is equal to the diffusion length L_p. Here, an alternating perturbation signal does not upset equilibrium in the double layer and the capacity measured is equal to the "static" capacity C_{sc} (corresponding to $\omega \to 0$) [Eq. (2.17)].

With increasing frequency ω, the thickness of the "diffusion layer" L_ω, from which holes move into the space charge region, decreases; accordingly, variations in the charge on the holes of the double layer σ_p with periodic variations in the potential $\Delta_{sc}^{sc,b}\phi$ become limited. In the limit in which $\omega \to \infty$, the thickness $L_\omega \to 0$, i.e., the double layer becomes as if isolated from the neutral bulk of the semiconductor in terms of the exchange of minority carriers with it. The corresponding capacitative component C_p decreases to a small value (determined by the redistribution of the available holes within the double layer with variations in $\Delta_{sc}^{sc,b}\phi$), and the total high-frequency capacity turns out to be close to the capacity determined by donors C_D (Figure 9). In accordance with the foregoing, this decrease in capacity with frequency manifests itself in the potential range corresponding to the inversion layer, the accumulation layer capacity being independent of frequency.

A similar effect of capacity decrease could be observed in the ionic diffuse layer in dilute electrolyte solutions on metal electrodes. In practice, however, as mentioned, in an electrolyte it is not possible to realize a situation analogous to an extrinsic semiconductor. Therefore in a dilute electrolyte (equivalent to an intrinsic semiconductor), the trivial effect of resistance of the solution bulk comes to the forefront.

The occupation of surface levels by electrons with the superimposition of an alternating potential varies as $n_{ss} = N_{ss} f_F$, where f_F is the function of $\Delta_{sc}^{sc,b}\phi$ (Section 2.4.1). The law of charge conservation at the levels takes the form

$$\frac{\partial Q_{ss}}{\partial t} = -e\frac{\partial n_{ss}}{\partial t} = e(R_e - R_p)$$

where R_e and R_p are fluxes of electrons from the conduction band and of holes from the valence band to the levels, respectively. It is easy to write the kinetic

equations for these quantities:

$$R_e = \vec{k}_e(N_{ss} - n_{ss})n_e^s - \overleftarrow{k}_e n_{ss} \tag{3.1a}$$

$$R_p = \vec{k}_p(N_{ss} - n_{ss}) - \overleftarrow{k}_p N_{ss} n_p^s \tag{3.1b}$$

where n_e^s and n_p^s are the electron and hole concentrations at the surface, which are functions of the potential $\Delta_{sc}^{sc,b}\phi$ [Eqs. (2.4)], and k are the rate constants for the corresponding processes involving capture of carriers by the levels and their release. The relaxation time τ_{ss} is the known combination of these rate constants.[21,22] The frequency dispersion of the capacity of the surface states is given by

$$C_{ss}(\omega) = C_{ss}(\omega = 0)\frac{1 - i\omega\tau_{ss}}{1 + \omega^2\tau_{ss}^2} \tag{3.2}$$

where $C_{ss}(\omega = 0)$ is the static capacity of surface states determined by Eq. (2.29)

It is evident in expression (3.2) that at high frequencies, $\omega \gg \tau_{ss}^{-1}$, the capacity decreases with increasing frequency and $C_{ss} \sim \omega^{-2}$. It is appropriate to mention that the adsorption capacity of a metal electrode also has quantitatively identical frequency characteristics.[24] This is not surprising, because the adsorption–desorption processes are described by kinetic equations which formally check with Eqs. (3.1). The relaxation time, along with energy and concentration, is a characteristic of surface levels. As to the relaxation time, the levels are divided into fast and slow. The fast levels have a relaxation time between 10^{-6} and 10^{-3} sec and the slow ones, of the order of seconds, or even more. The concentration of slow levels is usually much higher than the fast ones. Therefore, the slow levels have a decisive influence on the potential distribution in the double layer, while the fast ones influence the frequency characteristics of a semiconductor electrode. Both the space charge capacity and the capacity of surface states decrease with increasing ac frequency. Evaluations show that for a semiconductor which is not heavily doped (or for potentials at which the surface is not highly enriched with minority carriers) the space charge relaxes more rapidly than the surface levels. Therefore, by increasing the frequency, one can eliminate the surface levels. At sufficiently high frequencies, only the first of the two parallel capacities, C_{sc} and C_{ss} (Figure 7), is measured.

3.2. Photopotential

When a semiconductor is illuminated with light whose quantum energy exceeds the band gap, generation of electron–hole pairs occurs. The depth of light penetration into the semiconductor (and, respectively, the thickness of the layer in which carriers are produced) is $1/\alpha$, where α is the light adsorption coefficient. With increasing light quantum energy, α increases near the fundamental absorption edge of the semiconductor and reaches a value of 10^4–10^6, whereafter it remains unchanged. Thus for strongly absorbed light, $1/\alpha \leqslant \kappa_{sc}^{-1}$.

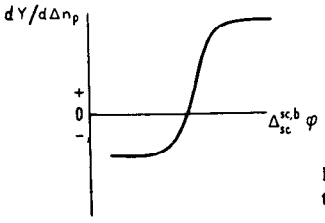


Figure 10. Schematic dependence of the photopotential on the potential drop in a semiconductor.

Nonequilibrium electrons and holes, produced within the space charge region, diffuse into the semiconductor bulk and recombine at a distance of the order of the diffusion length L_p. Electron and hole concentrations at the boundary between the space charge region and the neutral semiconductor bulk increase as against equilibrium ones: $n_p^* = n_p^0 + \Delta n_p$, $n_e^* = n_e^0 + \Delta n_e$ (for reasons of electrical neutrality $\Delta n_p = \Delta n_e$). The quantity $\lambda^* = (n_p^*/n_e^*)^{1/2}$ also varies with respect to the equilibrium value $\lambda = (n_p^0/n_e^0)^{1/2}$.

The electrons and holes generated by light move in the electric field of the space charge in opposite directions. This separation of photocarriers results in an electric field, which partially compensates that existing before illumination. Therefore the potential drop in the space charge region decreases. This change $(\Delta_{sc}^{sc,b}\phi)^* - (\Delta_{sc}^{sc,b}\phi)$ (or $Y^* - Y$) is called the photopotential.

Calculation of the photopotential[2] yields for low illumination intensity values (Δn_p and Δn_e are small compared with the equilibrium concentration of minority carriers) the following simple relation:

$$\frac{dY}{d\,\Delta n_p} \sim \frac{1 - e^Y}{1 + \lambda^{-2} e^Y} \tag{3.3}$$

illustrated in Figure 10.

One can see—as follows from qualitative considerations—that at an uncharged electrode ($\sigma_{sc} = 0$, $\Delta_{sc}^{sc,b}\phi = 0$), the photopotential is absent and $dY/d\,\Delta n_p = 0$. *A photopotential measurement can thus serve as a convenient tool for determining the flat-band potential.*

So, illumination of the semiconductor leads to an "unbending" of the energy bands at the surface (Figure 11). With increasing illumination intensity (and,

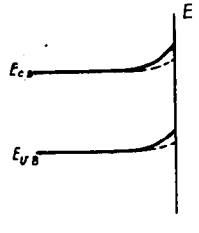


Figure 11. "Unbending of the bands" on illumination of the semiconductor surface. Solid line: the band boundaries in the dark; dashed line: under illumination.

hence, Δn_p and Δn_e), the band bending at the surface $|Y|$ progressively decreases and becomes zero. The limiting photopotential value (at high light intensity) is therefore equal to the initial "dark" value of the band bending, Y.

The characteristic feature of the behavior of semiconductor electrodes at quasiequilibrium is reflected in electron and hole recombination processes at the surface. Their investigation, combined with capacity and conductivity measurements, enables one to determine the kinetic characteristics of surface states $\vec{k}$ and $\overleftarrow{k}$ [see Eqs. (3.1)]. This point is discussed in detail by Myamlin and Pleskov.[8]

4. Distinctive Features of the Experimental Study of Semiconductor Electrodes

4.1. Basic Methods

The methods employed in the electrochemistry of semiconductors can be divided into groups. The first group includes methods that have been borrowed from semiconductor physics and the second, normal electrochemical methods.

Among the methods of the first group, that of surface conductivity was the first to be put into practice. This is not surprising because it is an analog of the so-called "field effect" used in the study of the "dry" semiconductor surface. Within the realm of its applicability, it gives reliable values of the potential drop in a semiconductor $\Delta_{sc}^{sc,b}\phi$, for it is insensitive to the influence of surface states.

For measuring surface conductivity, a current is passed along the electrode in the form of a thin wafer with the aid of an additional pair of contacts. It is surprising that one can measure the conductivity of a specimen in a highly conducting solution, and that this solution does not shunt the specimen. In reality, the critical parameter is the impedance of the semiconductor–electrolyte interface, not the resistivity of the solution bulk. Since the electrode is polarizable, i.e., faradaic processes are absent, a direct current passed along its surface is confined within the electrode irrespective of the conductivity of the medium The use of an alternating current to measure the surface conductivity does involve difficulties due to *capacitive* shunting of the specimen by the electrolyte.

This disadvantage of the surface conductivity method contributes to the fact that in recent years it has been replaced by the differential capacity method. The capacity measurement at various frequencies makes it possible to extract information on the spectrum of surface states and on nonequilibrium processes in the double layer. At a frequency of 10^5 Hz, it becomes possible to eliminate the contribution of surface states to the capacity and to measure the space charge characteristics.

The photopotential method is used for quick and direct measurement of the flat-band potential. The necessary requisite for ideal polarizability of an electrode is ensured here by the fact that the electrode is illuminated by the

intermittent flashing light rather than by using light of constant intensity. If the flash duration is less than RC, where R and C are the resistance and capacity of the semiconductor–electrolyte interface, during each flash the interface remains impermeable to current; and therefore the constancy of the space charge is not upset. On the other hand, as noted previously, it is easy to realize the condition of ideal polarizability, since the rate of electrochemical reactions on semiconductor electrodes is lower than the corresponding rate on metal ones. It is necessary to point out the low sensitivity of the differential capacity and photopotential methods to low faradaic currents at the interface; fast surface states cause more interference.

In recent years spectroscopic and optical methods have found many applications in the electrochemistry of semiconductors.[25,26] Potentiodynamic i–E curves and charging curves are widely used for investigation of semiconductor electrodes.

4.2. Some Details of Experimental Techniques

The properties of both bulk and surface semiconductors are sensitive to the degree of perfection in its crystalline structure and to the presence of impurities. Therefore, as a rule, in the electrochemistry of semiconductors, single-crystal electrodes are used with the surface oriented in a definite manner about the principal crystallographic axes. Special requirements are imposed on the preparation of the electrode surface prior to measurements.

After machining (cutting, polishing), the surface layer of a crystal contains many lattice defects (the "damaged layer"). In order to expose the inner region of a crystal having a perfect structure, the specimen is subjected to chemical or electrochemical etching. Particular care is taken to purify the reagents used.

A high resistance in the semiconductors accounts for marked ohmic potential drops. This circumstance causes one to choose optimum geometry in the electrode. Higher requirements are placed on the quality of electric contacts: they must be ohmic (i.e., nonrectifying) with a low junction resistance.

5. Structure of the Double Layer on Semiconductor Electrodes

5.1. Space Charge

To determine the structure of the double layer at a semiconductor electrode, it is necessary to find the distribution of the potential drop between the Helmholtz layer and the diffuse charge regions in the semiconductor and in the electrolyte: $\Delta_{el}{}^{sc}\phi = \Delta_{sc}^{sc,b}\phi + \Delta_2{}^{sc}\phi + \Delta_b{}^2\phi$. But the potential drop in the Helmholtz layer separating the two phases $\Delta_2{}^{sc}\phi$ cannot be determined experimentally for well-known reasons. The other two Galvani potential components $\Delta_{sc}^{sc,b}\phi$ and $\Delta_b{}^2\phi$, each of which is localized wholly within the corresponding

phase, are, in principle, accessible for experimental determination. However, there are no reasonably convenient and reliable methods for their *direct* measurement, and these quantities are generally calculated from other quantities measured experimentally. For example, the potential drop in a semiconductor $\Delta_{sc}^{sc,b}\phi$ can be calculated from the differential capacity, surface conductivity or photopotential using the space charge theory outlined above. (In the same way, it is possible to find the space charge as well as the electric field strength at the surface, which is important in the discussion of kinetic data.) In fitting the theoretical curve C_{sc}–$\Delta_{sc}^{sc,b}\phi$ or K_s–$\Delta_{sc}^{sc,b}\phi$ to an experimental curve, where the same values are plotted against the electrode potential, E, one makes use of characteristic points such as the potential of the capacity minimum or flat-band potential (for an intrinsic semiconductor, they are equal). Thereupon, it is easy to find an empirical relationship between the scales of the electrode potentials, E, and the potential drops in the semiconductor, $\Delta_{sc}^{sc,b}\phi$. One should take into consideration the following relation:

$$\Delta E = \Delta\Delta_2{}^{sc}\phi + \Delta\Delta_{sc}^{sc,b}\phi \qquad (5.1)$$

(For simplicity, a sufficiently concentrated solution is considered, so that $\Delta_b{}^2\phi = 0$.) Thus, while the absolute value of $\Delta_2{}^{sc}\phi$ remains unknown, it is possible to find its change due to variation in the state of the semiconductor surface, degree of polarization, adsorption, etc.

The above is illustrated by Figure 12, which displays dependence of the surface conductivity of a germanium electrode on its potential in methyl formamide. (The choice of this solvent is motivated by the fact that the range of ideal polarizability in it is wide and includes the minimum of surface conductivity, not always realizable in aqueous solutions.) The same figure also gives the theoretical curve K_s–$\Delta_{sc}^{sc,b}\phi$ calculated from Eq. (2.15). Here, the scales E and $\Delta_{sc}^{sc,b}\phi$ were chosen equal. Comparing these curves, one can see that the experimental curve is wider than the theoretical one. This signifies that the change in the electrode potential, ΔE, corresponding to some change in the surface conductivity, is greater than the change in the potential drop in the semiconductor, $\Delta\Delta_{sc}^{sc,b}\phi$. In other words, the electrode polarization changes not

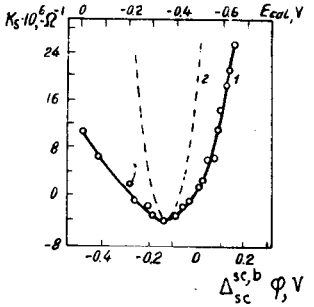


Figure 12. Experimental dependence of the surface conductivity of a germanium electrode on potential (1) and the calculated dependence of the surface conductivity on the potential drop in a semiconductor (2); *n*-type germanium, 30 Ω cm, the methyl formamide solution of KBr.[27]

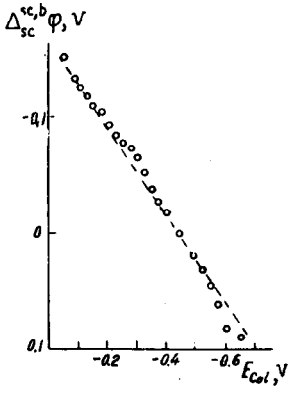


Figure 13. Dependence of the potential drop in a semiconductor on the electrode potential (calculated from Figure 12).[27]

only the potential drop in the semiconductor but also the potential drop in the Helmholtz layer, *the latter being by no means small.* Figure 13 presents the dependence of $\Delta_{sc}^{sc,b}\phi$ on E, calculated from Figure 12, which shows [see Eq. (5.1)] that $d\,\Delta_2{}^{sc}\phi/d\,\Delta_{sc}^{sc,b}\phi \simeq 1$. In accordance with Section 2.4.1, it thus appears that on a germanium electrode the density of surface states is high; and *it is these states which define the potential distribution in the double layer.*

The distinctive feature of these levels is a long relaxation time (on germanium, it is 1–10 sec). If the electrode potential (and, along with it, the space charge) varies with time at a higher rate, the levels do not have time to relax and the charge Q_{ss} on them remains constant. As a result the potential drop in the Helmholtz layer $\Delta_2{}^{sc}\phi$ preserves a value which may not be small but is constant. Therefore, using fast potential sweep, one can dispose of the influence of the Helmholtz potential drop, that is, realize the case $\Delta E = \Delta\Delta_{sc}^{sc,b}\phi$, and obtain a "narrow" capacity or surface conductivity curve which resembles the theoretical one (Figure 14).

On a silicon electrode the surface is coated with fairly thick oxide layer,

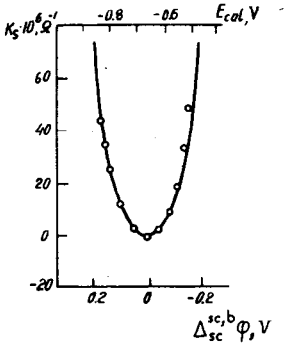


Figure 14. Dependence of the surface conductivity of germanium on the electrode potential at a fast potential sweep.[28] Circles: experimental values; solid line: calculation of the dependence of K_s on the potential drop in a semiconductor.

which interferes with measurements of the surface properties. In such a situation Harten[29] obtained a curve, K_s–E, which resembles the theoretical one, K_s–$\Delta_{sc}^{sc,b}\phi$; that is, he realized the case $\Delta_2{}^{sc}\phi = \text{const}$.

Most of the data on the structure of the double layer on semiconductor electrodes have been obtained to date by the differential capacity method. It is possible to use capacity measurements for calculating $\Delta_{sc}^{sc,b}\phi$ in cases where one manages to dispose of the influence of fast surface states and to isolate the space charge capacity C_{sc} alone (cf. Figure 8). For this condition it is necessary (not always sufficient) to take the following steps: (1) to free the electrode surface and the electrolyte solution of traces of impurities that may give rise to fast surface states; (2) to make the measuring frequency high enough for relaxation of persisting surface states to be eliminated (but not high enough so that slow relaxation of the space charge is observed).

Brattain and Boddy[30] were the first to solve this problem for a germanium electrode. The electrode surface was cleaned by mild anodic etching directly in the working solution. The solution was first freed of traces of ions of heavy metals (responsible for fast states on the germanium surface; see Section 5.3) by conditioning the solution over germanium powder; the metals are deposited on germanium by use of an exchange reaction. The capacity was measured using the pulse method with a pulse length of 10 μsec. Under these conditions, Brattain and Boddy obtained the C–E curve illustrated in Figure 15. With a correction for roughness of the electrode surface the capacity at a minimum agrees with that calculated by Eq. (2.17). Consequently, surface states do not contribute to the measured capacity, at least in the vicinity of the minimum of the C–E curve.

As in measurements of surface conductivity (see above), slow relaxation in the Helmholtz layer is observed. Slow variations in the electrode potential are accompanied by variations in the potential drops both in the space charge layer in germanium and in the Helmholtz layer, and the experimental C–E curve turns out to be wider than the theoretical C_{sc}–$\Delta_{sc}^{sc,b}\phi$ curve. With a fast potential sweep, the Helmholtz potential drop remains unchanged, $\Delta\Delta_2{}^{sc}\phi = 0$, and the C–E curve closely resembles the theoretical one.

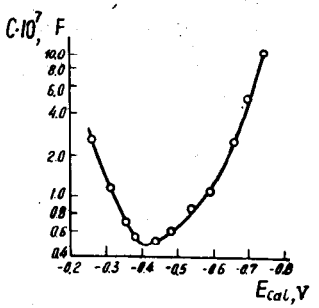


Figure 15. Differential capacity of a germanium electrode.[30] n-type germanium, 42 Ω cm; 0.1 N K_2SO_4 solution (pH 7.4). (Reprinted by permission of the publisher, The Electrochemical Society, Inc.)

On a silicon electrode, the usual measured capacity is higher than the calculated value of C_{sc}. The "natural" oxide, formed on silicon making contact with the aqueous solution, seems to be a source of fast surface states. Only in some cases, e.g., in concentrated hydrofluoric acid solutions, is the electrode capacity close to C_{sc}, and the potential change due to electrode polarization concentrated within the space charge region in a semiconductor.[31]

When intrinsic semiconductors with a band gap more than 1 eV wide are insulators, electrochemical measurements become more difficult (see Chapter 8). As electrode materials, they are employed only when doped with donor or acceptor impurities, and the parameter λ is always either much greater or much smaller than 1. Owing to this circumstance (see Section 2.2), there appear to be conditions for the formation of a depletion layer when in the space charge region there are no free carriers and the charge is formed by ionized donors or acceptors. In the vicinity of the flat-band potential, the depletion layer is converted to an accumulation one. As far as the inversion layer is concerned, attempts to observe it on semiconductors with a wide band gap failed either due to its slow relaxation (see Section 3.1) or, more probably, to the fact that the potential of transformation of the depletion layer to the inversion layer lies beyond the range of the ideal polarizability of the electrode.

The capacity curves of wide-band-gap semiconductor electrodes are given by Eq. (2.19). In the coordinate system C^{-2}–E, a straight line is obtained (the Mott–Schottky plot), by the slope of which one can, in principle, calculate the donor (or acceptor) concentration in a semiconductor and by the point of intersection with the potential axis, the flat-band potential, ϕ_{fb}.

An example of such a line obtained by Dewald[4] is displayed in Figure 16 for a zinc oxide electrode (the band gap being 3.2 eV; doped with indium, it represents an n-type semiconductor). The capacity is practically independent of the measuring frequency in a broad frequency range (50 Hz to 100 kHz). This is a rare case; the capacity of semiconductor electrodes varies to a greater or

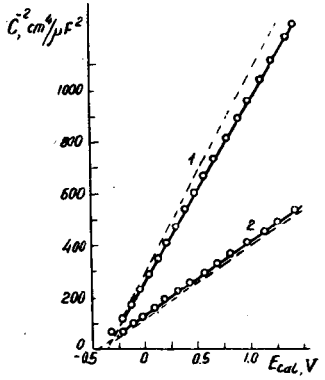


Figure 16. Capacity of the depletion layer in a zinc oxide electrode.[4] ZnO conductivity: (1) 0.59 Ω^{-1} cm^{-1}; (2) 1.79 Ω^{-1} cm^{-1}. 1 N KCl solution (pH 8.5). Dashed line: calculation by Eq. (2.19). (Reprinted with permission from *The Bell System Technical Journal*, Copyright 1960, The American Telephone and Telegraph Company.)

lesser extent with frequency (see below). The dashed line represents the theoretical curves in the calculation of which use was made of the donor concentration values, N_D, derived from Hall measurements. The discrepancy between the experimental and calculated capacity values is not greater than 2%. On this basis, Dewald drew two conclusions: (1) on a zinc oxide electrode the density of fast surface states with a relaxation time of 10^{-2}–10^{-5} sec is low, not exceeding 10^9 cm^{-2}; (2) even at a slow electrode potential sweep (and the curves of Figure 16 were taken thusly), only the potential drop in the space charge layer is variable, while the Helmholtz potential drop, being quite large, remains constant.

Qualitatively, the same capacity characteristics as zinc oxide are demonstrated, with some variations, by other semiconductors with a wide band gap: cadmium sulfide,[32] potassium tantalate,[33] silicon carbide,[34] stannic oxide,[35] and titanium dioxide.[36] In some cases complications arise. Thus the C^{-2}–E straight lines of gallium arsenide have a kink which is likely to result from ionization at some critical potential of donors whose levels lie deep in the band gap.[37] On nickel oxide, the C–E curves reflect a high density of fast surface states.[38] In heavily doped specimens (with a majority carrier concentration of 10^{18}–10^{20} cm^{-3}), a substantial contribution to the capacity measured comes from the capacity of the Helmholtz layer, and the point of intersection of the C^{-2}–E straight line with the potential axis no longer coincides with the flat-band potential.[39] Sometimes, an undefined feature of the pretreatment of the electrode surface accounts for distortion of the C–E curve and for a strong frequency dependence of the capacity.

Photopotential measurements offer the simplest way of determining the flat-band potential. Figure 17 gives photopotential curves for a variety of n- and p-type germanium electrodes having different resistivity. They resemble the theoretical curve of Figure 10. The point of intersection with the potential

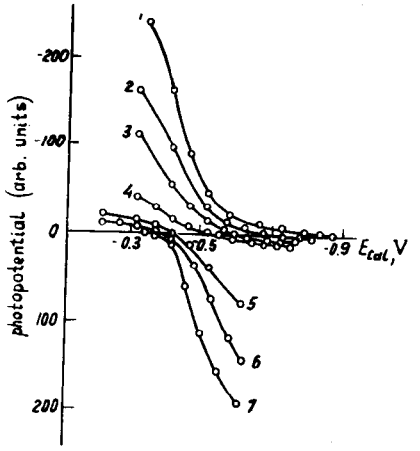


Figure 17. Photopotential of a germanium electrode.[53] (1) n type, 0.004 Ω cm; (2) n type, 3 Ω cm; (3) n type, 20 Ω cm; (4) n type, 40 Ω cm; (5) p type, 10 Ω cm; (6) p type, 3 Ω cm; (7) p type, 0.5 Ω cm. 1 N NaOH solution.

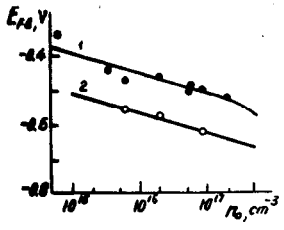


Figure 18. Dependence of the flat-band potential of zinc oxide on the bulk concentration of free electrons.[41] 1 *N* KCl solution (pH 8.5). Pretreatment: (1) etching in 85% H_3PO_4; (2) etching in 2 *N* KOH. (Reprinted with permission from *The Bell System Technical Journal*, Copyright 1960, The American Telephone and Telegraph Company.)

axis—the flat-band potential—shifts towards negative potentials when going from *p*-type specimens to *n*-type ones, i.e., with increasing bulk concentration of free electrons. This shift is shown in Figure 18 for zinc oxide electrodes. It reflects the thesis, known in the electrochemistry of metals, that the zero charge potentials of various electrodes differ by the same value as their work functions do.[40] But it is only with semiconductor electrodes that one can observe this effect alone, without complications due to distinctions in the chemical nature of the metals compared.

It is interesting to consider the degree of doping of a semiconductor on its flat-band potential, using a properly open electrochemical circuit (Figure 19) at the flat-band potential. Since change in the impurity concentration determining the majority carrier concentration does not affect the chemical behavior of the semiconductor, in particular, the surface dipole structure, neither does it affect the Galvani potential at the semiconductor–solution interface (where, consequently, $\Delta_2^{sc}\phi = \text{const}$, and $\Delta_{sc}^{sc,b}\phi = 0$ at $E = \phi_{rb}$). (On the contrary, for metal electrodes, the Helmholtz potential drop at the zero charge potential of an electrode is different on different metals owing to their varying interaction with the solution, e.g., owing to different adsorption of a solvent. This circumstance leads to uncertainty in the qualitative correlation of the work function and zero charge potential.) The potential difference in the circuit and, hence, the flat-band potential, depends on the potential drop at the interface between the semiconductor and the electric contact metal (A). This drop, as well as the work function of the semiconductor, is determined by the chemical potential of electrons in the semiconductor and changes by $2.3kT/e$ with a tenfold change in the free electron concentration. As can be seen from Figure 18, the flat-band

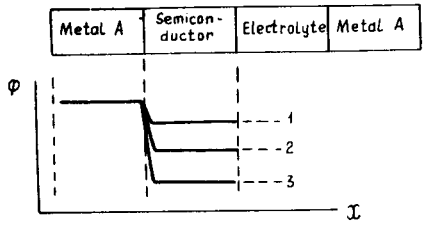


Figure 19. The profile of the potential at the flat-band potential of a semiconductor electrode 1, 2, and 3: Specimens with different electron concentration.

potential shifts by 59 mV when the free-electron concentration has increased by one order of magnitude.

Finally, the relaxation characteristics in semiconductor electrodes shall be discussed.

Although in some instances, like that of the above-mentioned zinc oxide in a neutral solution, the capacity is independent of frequency, this is an exception. As a rule, one can observe a frequency dependence of the capacity, which is dissimilar in different potential ranges. Under the conditions of accumulation, it should be associated with relaxation of fast surface states. With increasing frequency, the observed capacity decreases. The simple dependence $C \sim \omega^{-2}$ [Eq. (3.2)] which should arise from a single energy level has never been observed; usually, $C \sim \omega^{-1/2}$ or $C^{-1} \sim \log \omega$. However, individual energy levels would contribute to the total electrode capacity only in a narrow potential range in which the Fermi function f_F [Eq. (2.21)] is different from zero or one. In practice however, the frequency dependence of the capacity exists over a wide potential range. This leads to the use of more complex models, e.g., a set of surface states, whose density N_{ss} is a function of the energy E_{ss}°[41] of the surface states, or dispersion of the dielectric constant of a thin hypothetical semiconductor surface layer.[42] This problem has undergone little exploration.

For the inversion layer, capacity dispersion is higher and rises with increasing degree of doping. Evidently, the influence of fast surface states is complemented by slow diffusion in the neutral semiconductor bulk adjacent to the space charge layer (Section 3.1).

Qualitatively, the same regularities which apply to the differential capacity (measured with a potential change which is small compared with kT/e) are observed on "fast" charging curves, i.e., under the conditions of a great potential change.[43]

5.2. The Helmholtz Layer

The flat-band potential of semiconductor electrodes ϕ_{fb} is not a constant characterizing the semiconducting material alone. It is dependent (apart from the type of conductivity; see Section 5.1) upon the solution composition, the state of the electrode surface, its crystallographic orientation, adsorption, etc. Since at $E = \phi_{fb}$ there is no potential drop in the space charge region, $\Delta_{sc}^{sc,b}\phi = 0$, these variations in ϕ_{fb} reflect nothing more than variations, as functions of the listed factors, in the potential drop in the Helmholtz layer. Measurements of the flat-band potential have become one of the chief methods of investigation of the Helmholtz layer on semiconductor electrodes, since many conventional methods developed in the electrochemistry of metals are of limited usefulness here by virtue of masking by the space charge in a semiconductor.

On germanium electrodes, the flat-band potential is dependent on the solution pH, shifting toward negative values by 59 mV with pH changing by 1 (Figure 20). The same character of the ϕ_{fb}–pH dependence was observed on

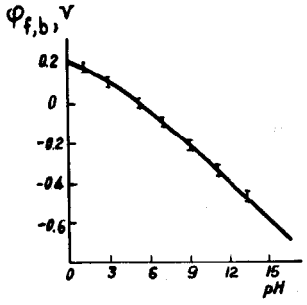


Figure 20. Dependence of the flat-band potential of germanium on the solution pH.[44] Intrinsic germanium; potentials vs. normal hydrogen electrode.

zinc oxide,[45] titanium dioxide,[36] stannic oxide,[35] and gallium arsenide.[46] (On cadmium sulfide and some other materials, the flat-band potential is independent of pH.[36])

The cause of the dependence of ϕ_{fb} on the solution pH becomes clear if one takes into consideration the important effect of the oxidation state of the electrode surface on ϕ_{fb}. At a stationary potential of a germanium electrode in electrolyte solutions in which germanium oxides are soluble (e.g., in hydrofluoric acid), there are no phase oxides, but there is chemisorbed oxygen. The coverage of the surface with oxygen is ca. 1 layer. During strong cathodic polarization oxygen is reduced and the surface is covered with adsorbed hydrogen (or germanium hydride). The transition from the "oxide"- to "hydride"-type surface is accompanied by the shift of the flat-band potential by 0.6 V toward negative values.[47] Qualitatively, the same shift in oxidation and reduction of the surface is observed on electrodes of other semiconductors, although the chemical nature of surface reactions involved is not always clear.[48]

The dependence of the flat-band potential on the oxidation state and on pH can be explained on the assumption[44] that surface –OH groups dissociate:

$$\diagdown\!\!\diagup\!\!\text{Ge—OH} + H_2O \rightleftarrows \diagdown\!\!\diagup\!\!\text{Ge—O}^- + H_3O^+ \qquad (5.2)$$

This equilibrium depends on pH and (since it occurs within the Helmholtz layer) on the potential drop in this layer, $\Delta_2{}^{sc}\phi$. On the basis of thermodynamic consideration of equilibrium, (5.2), Hoffmann-Perez and Gerischer[44] obtained for the Helmholtz potential drop the following expression:

$$\Delta_2{}^{sc}\phi = \text{const} - \frac{2.3RT}{F}\,\text{pH} \qquad (5.3)$$

which, as is evident, for example, from Figure 20, well describes the experimental data.

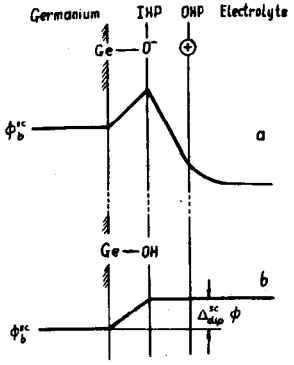


Figure 21. Potential distribution in the double layer on a germanium electrode at the flat-band potential. (a) With partial dissociation of the surface oxide; (b) at the isoelectric point of the surface oxide.

On the other hand, the Ge–O bond is polar and a dipole potential drop is associated with chemisorbed oxygen. This drop scarcely depends on pH but varies with the coverage of the surface with oxygen.

At the pzc of germanium, the electronic charge in a semiconductor σ_{sc} is absent but the ionic charge in the double layer σ_{el} does not disappear; neither does the contribution to the Helmholtz potential drop associated with it. The structure of the double layer and the potential distribution in it are shown in Figure 21a. It resembles the case of a metal electrode at the pzc in a solution of specifically adsorbing ions. The charge of surface GeO^- groups σ_{ad} is neutralized by the cation charge σ_{el} in the outer Helmholtz plane (and in a dilute electrolyte, in the diffuse Gouy layer as well) [see Eq. (2.28)]; the charge of surface states to a first approximation can be disregarded.

An increase in the solution acidity shifts equilibrium (5.2) to the left. At some value of pH, the dissocation of the surface oxide groups is suppressed (isoelectric point). This pH value can be determined, for example, by measuring the ζ potential of germanium in dilute solutions, approximately equal to the potential drop in the diffuse ionic layer $\Delta_b{}^2\phi$. According to Sparnaay,[49] $\zeta \simeq 0$ at pH 2.5. (This is close to the isoelectric point of GeO_2.) In the "isoelectric" solution at the flat-band potential of germanium, there remains in the Helmholtz layer only the dipole potential drop (Figure 21b) $\Delta_{dip}{}^{sc}\phi$ owing to the polarity of the Ge–O bonds, the inherent surface dipole of crystal, and oriented adsorption of solvent molecules.[50]

The I^- ions, adsorbing on the germanium surface, seem to replace the –OH groups, thereby changing the properties of the surface dipole. Connected with this is the shift of ϕ_{fb} in iodide solutions.[51] Anions $SO_4{}^{2-}$, $ClO_4{}^-$, $NO_3{}^-$, cations of alkali metals and many organic substances do not change ϕ_{fb} on germanium.

The structure of the Helmholtz layer described for germanium applies, with modifications, to other semiconductors. The common feature is thus, an unexpectedly low value of the Helmholtz layer capacity (3–6 $\mu F/cm^2$)

Table 1

Flat-Band Potentials of Semiconductor Electrodes

Semiconductor	Type of conductivity	Solution composition, pH	E (V) (vs. saturated calomel electrode)	Reference
Ge	*i*	pH 7	−0.4	44, 53
ZnO	*n*	1 *N* KCl, borate buffer (pH 8.8)	−0.42	54
CdS	*n*	1 *N* KCl	−0.9	55
CdSe	*n*	1 *N* KCl	−0.66	55
ZnSe	*n*	1 *N* KCl	−0.82	55
ZnTe	*p*	1 *N* KCl	−0.8	55
CdTe	*p*	1 *N* KCl	−0.95	55
CdTe	*n*	1 *N* KCl	−0.33	55
TiO_2	*n*	pH 7	−0.65	56
SnO_2	*n*	pH 6, 8	0	35
GaAs	*n*	1 *N* KOH	−1.35	37
SiC	*n*	0.05 *M* H_2SO_4	−1.6	34
GaP	*n*	1 *N* H_2SO_4	−1.15	57
GaP	*p*	1 *N* H_2SO_4	+0.95	57
Si	*n*	1 *N* KCl	0[a]	58

[a] Obtained by extrapolation to the zero thickness of the oxide layer.

estimated by various methods on germanium,[52] zinc oxide,[4] and potassium tantalate.[33]

Table I sums up published data on flat-band potentials. From the foregoing discussion it follows that for most (if not all) semiconductor electrodes, this quantity is a function of the oxidation state; and it is possible to distinguish two more or less definite states of the surface: "extremely oxidized" and "extremely reduced" (cf. "oxide" and "hydride" germanium surfaces). Although the surface state has not been accurately defined in all studies, the results of which are given in Table I, taking into account the dependence of the flat-band potential on the type of conductivity (see Figure 17), *p*-type specimens concern a highly oxidized surface, and for *n*-type specimens, the surface is highly reduced.

From a knowledge of the flat-band potential, one can calculate the position of the Fermi level, E_F, and of the boundaries of the semiconductor energy bands E_C and E_V on the electrode potential scale.[34,35] Here, the following relations[8,11] must be used:

$$E_C - E_F = kT \ln (N_{CB}/n_e^0)$$
$$E_F - E_V = kT \ln (N_{VB}/n_p^0) \qquad (5.4)$$

where N_C and N_V are the densities of states in the conduction and valence band. The position of the band boundaries for various semiconductors is

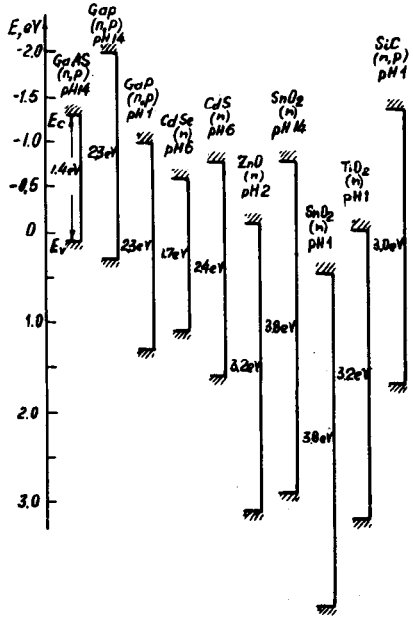


Figure 22. Position of the boundaries of the conduction and valence band of various semiconductors in aqueous solutions vs. normal hydrogen electrode.[34]

illustrated in Figure 22. These data are important, especially for discussions of electrochemical kinetics: depending upon which band is closest to the potential of the redox system selected, the solution and semiconductor exchange either free electrons or holes (rather, valence band electrons).[7,13]

5.3. Fast Surface States

The differential capacity method in combination with measurements of the surface conductivity and surface recombination velocity is still the basic method of the investigation of fast surface states. Boddy and Brattain[59] found that introduction of ions of heavy metals (gold, silver, or copper) into solution in concentrations of only 10^{-7}–10^{-5} mol/liter appreciably increases the differential capacity of a germanium electrode (Figure 23). In accordance with the equivalent circuit of the interface (Figure 8), the measured capacity can be divided into the capacity of the space charge region C_{sc} (solid line in Figure 23) and the capacity of surface states C_{ss}. The latter is represented in Figure 24 as a function of the potential drop in the space charge region $\Delta_{sc}^{sc,b}\phi$. (The quantity $\Delta_{sc}^{sc,b}\phi$ was determined using the surface conductivity method which is useful in the case considered as it is not affected by surface states.) The C_{ss}–$\Delta_{sc}^{sc,b}\phi$ curve (dashed line) can be represented as the sum of two curves marked in Figure 24 by solid lines and corresponding to two surface levels (cf. Figure 7). Using Eq. (2.29),

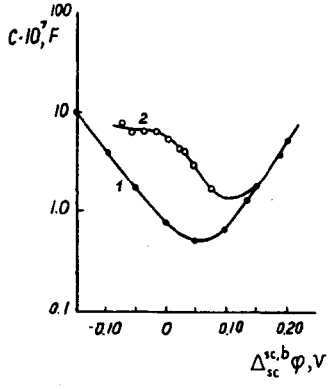


Figure 23. Increase in the differential capacity of a germanium electrode with deposition of copper on its surface.[69] 0.1 N K_2SO_4 solution, pH 7.4, the copper concentration: (1) 0; (2) 5×10^{-7} mol/liter. (Reprinted by permission of the publisher, The Electrochemical Society, Inc.)

the level concentration N_{ss} was calculated from the maximum capacity value and the energy E°_{ss}, from the position of the maximum in the potential scale. One of these levels was found to be the recombination center. Measurements of the surface recombination velocity have made it possible to determine the electron and hole capture cross sections σ_e and σ_p equal to the quotient of the rate constants k_e and k_p (see Section 3.1) by the thermal velocity of an electron in a semiconductor (10^7 cm/sec). Table 2 presents results for three metals deposited on the germanium surface. The level energy values are referred to the energy of the midgap E_i. (It should be noted[8,11] that $E_F - E_i = -kT \ln \lambda$ where $\lambda = (n_p^0/n_e^0)^{1/2}$.)

The work of Boddy and Brattain[59] is the classical example of the simultaneous employment of various methods for the determination of a whole set of the formal characteristics of surface states. Even in this more widely explored case, the physicochemical nature is still poorly understood. Further, it is not yet clear whether states arise from the interaction proper between metals and

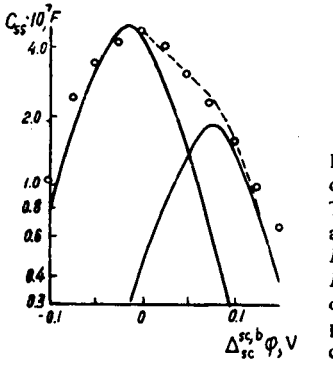


Figure 24. Capacity of surface states due to deposition of copper on the surface of a germanium electrode.[69] The solid lines represent curves calculated by Eq. (2.29) at the following parameters: (1) $(E^{\circ}_{ss} - E_i)/kT = 2.2$, $N_{ss} = 1.26 \times 10^{11}$ cm^{-2}; (2) $(E^{\circ}_{ss} - E_i)/kT = -1.3$, $N_{ss} = 0.44 \times 10^{11}$ cm^{-2}. Dashed line: the sum of two calculated curves; Circles: experimental values. (Reprinted by permission of the publisher, The Electrochemical Society, Inc.)

Table 2

Characteristics of Surface Levels on Germanium due to Deposition of Metals[59]

Parameter	Cu	Ag	Au
Level 1			
$(E^{\circ}_{ss} - E_i)/kT$	−1.9	−4.1	−0.9
N_{ss} (cm^{-2})	10^{11}	1.9×10^{11}	1.8×10^{11}
Level 2			
$(E^{\circ}_{ss} - E_i)/kT$	1.2	−0.55	2.5
N_{ss} (cm^{-2})	1.9×10^{10}	10^{11}	4.5×10^{10}
σ_p (cm^2)	6.0×10^{-14}	2×10^{-14}	4.1×10^{-15}
σ_e (cm^2)	1.5×10^{-16}	0.74×10^{-16}	1.4×10^{-16}

germanium or from variations in the structure of a surface oxide due to deposition of metals, or whether this deposition activates lattice defects of an electrode emerging to its surface. Noble metals, while being deposited on the germanium surface by the substitution mechanism, do not coat it uniformly but form separate clumps of metal. The concentration of these clumps on the surface is equal in order of magnitude to that of surface states N_{ss}.

Apart from deposition of metals, another source of surface states is cathodic polarization of germanium electrodes. In the case of moderate polarization, the capacity, as well as the surface recombination velocity, markedly increases.[60] It is assumed[61,62] that here surface states are associated with a structure of a radical type, which is an intermediate stage in the transformation (see Section 5.2) of the "oxide" germanium surface to a "hydride" one:

$$\text{—Ge—OH} \xrightarrow[+H^+]{+e^-} \text{—Ge}\cdot \xrightarrow[+H^+]{-p} \text{—Ge—H} \qquad (5.5)$$

where p stands for a hole. Difficulties involved in the quantitative investigation of surface states of this type come from the fact that, demonstrated previously, reduction of chemisorbed oxygen changes the potential distribution at the interface.

In strong cathodic polarization accompanied by evolution of hydrogen, hydrogen atoms penetrate deep into the germanium lattice and, acting as the recombination center, reduce the lifetime of carriers.[6,63] Germanium thus hydrogenated behaves more as metal than as semiconductor. In particular, its capacity rises to approximately 10 μF/cm^2.[64]

6. Conclusions

The significance of the electrochemistry of semiconductors is not confined to the creation of a general picture of the surface properties of electrodes made

of single-crystal semiconducting materials. Thus it has given impetus to investigation of nonconventional interphasial boundaries such as insulator–electrolyte[65] and the solid-electrolyte–metal boundary. The principal notions and mathematical formalism of the electrochemistry of semiconductors are thereby used to advantage.

Furthermore, interest in the study of semiconductor electrodes has been encouraged by the fact that objects with semiconducting properties often occur in the electrochemistry of metals. Such objects include oxide and other films, multilayers of adsorbed organic substances on the surface of metal electrodes, and the like. Oftentimes, some anomalies of their electrochemical behavior are qualitatively explained by their semiconductor nature. Attempts to apply to them the quantitative theory developed for single-crystal semiconductors have been only partially successful. As regards the theory of noncrystalline solids including amorphous semiconductors, development has been rather limited.

Another complication involved in investigation of oxide layers on metals stems from the fact that they often have, apart from electron conductivity, an ionic conductivity, which affects their electrochemical behavior.[66] As a result, there exists a gap between the electrochemistry of single-crystal semiconductors and the electrochemistry of oxide films on metals, notably valve metals, that has not yet been bridged.

Finally, in questions concerning thin films (for example, those between the layer of a new phase and the adsorbed layer), semiconductor physics, in particular the band theory, remains doubtful.

In recent years a trend has appeared toward development, on the one hand, of new methods of investigation of the semiconductor–electrolyte interface and, on the other hand, of various applications of this interface for measuring the bulk characteristics of a semiconductor. For example, research into electroreflectance has made it possible to extract information about the structure of energy bands and the nature of interband transitions in a wide variety of materials.[25] Measurement of a surface photopotential offers a way of determining the diffusion length of minority carriers.[67] In these and other methods, the electrolyte is used as a convenient blocking (i.e., impermeable to a faradaic current) contact for a semiconductor, which is transparent to light, possesses a low resistance and allows the surface potential to be readily modulated.

Among the immediate objectives in the investigation of semiconductor interfaces are the following:

(1) Elucidation of the nature of surface states (with the use of the data of the electrochemical kinetics on semiconductor electrodes).

(2) Examination of the behavior of thin semiconductor films (including those thinner than the Debye length of semiconductor) as well as dielectric films on the semiconductor surfaces.

(3) Elucidation of the role of quantum effects in the space charge region, which seem to be important in electro-optical phenomena.

(4) Investigation of the electrochemistry of polycrystal and amorphous semiconductors, as well as heavily doped semiconducting materials and semimetals.

References

1. W. H. Brattain and C. G. B. Garrett, *Bell Syst. Tech. J.* **34**, 129–170 (1955).
2. C. G. B. Garrett and W. H. Brattain, *Phys. Rev.* **99**, 376–396 (1955).
3. K. Bohnenkampf and H.-J. Engell, *Z. Elektrochem.* **61**, 1184–1196 (1957).
4. J. F. Dewald, *Bell Syst. Tech. J.* **39**, 615–639 (1960).
5. M. Green, "Electrochemistry of the Semiconductor-Electrolyte Interface," in *Modern Aspects of Electrochemistry*, J. O'M. Bockris, ed., Vol. 2 Butterworths, London (1959), pp. 343–407.
6. J. F. Dewald, "Semiconductor Electrodes," in *Semiconductors*, N. B. Hannay, ed., Reinhold, New York (1959).
7. H. Gerischer, in *Physical Chemistry. An Advanced Treatise*, H. Eyring, ed., Vol. 9, Academic Press, New York, (1970), pp. 463–542.
8. V. A. Myamlin and Yu. V. Pleskov, *Electrochemistry of Semiconductors*, Plenum Press, New York (1967).
9. J. O'M. Bockris and A. K. N. Reddy, *Modern Electrochemistry*, Plenum Press, New York (1970).
10. A. Many, Y. Goldstein, and N. B. Grover, *Semiconductor Surfaces*, North-Holland, Amsterdam (1965).
11. D. R. Frankl, *Electrical Properties of Semiconductor Surfaces* (Pergamon Press, Oxford, 1967).
12. H. Gerischer, *Z. Phys. Chem.* (*N.F.*) **27**, 48–79 (1961).
13. H. Gerischer, in *Advances in Electrochemistry and Electrochemical Engineering*, P. Delahay, ed., Vol. I, Interscience, New York, (1961), pp. 139–232.
14. R. R. Dogonadze and Yu. A. Chizmadzhev, *Dokl. Akad. Nauk SSSR* **150**, 333–336 (1963).
15. R. H. Kingston and S. F. Neustadter, *J. Appl. Phys.* **26**, 718–730 (1955).
16. R. Seiwatz and M. Green, *J. Appl. Phys.* **29**, 1034–1040 (1958).
17. G. E. Picus, ed., *Physics of Semiconductor Surface*, Izdatel'stvo Inostrannoi Literatury, Moscow (1959), pp. 359–421.
18. J. R. Schrieffer, *Phys. Rev.* **97**, 641–652 (1955).
19. Ig. Tamm, *Phyz. Z. Sowjetunion* **1**, 733–746 (1932).
20. J. Bardeen, *Phys. Rev.* **71**, 717–727 (1947).
21. F. Berz, *J. Phys. Chem. Solids* **23**, 1795–1805 (1962).
22. Yu. Ya. Gurevich and V. A. Myamlin, *Izv. Akad. Nauk SSSR Ser. Khim.*, 1776–1784 (1964).
23. V. A. Tyagai and Yu. Ya. Gurevich, *Fiz. Tverd. Tela* **7**, 12–22 (1965).
24. A. N. Frumkin and V. I. Melik-Gaikazyan, *Dokl. Akad. Nauk SSSR* **77**, 855–858 (1971).
25. M. Cardona, *Modulation Spectroscopy* (Academic Press, New York, 1969).
26. E. Yeager and J. Kuta, in *Physical Chemistry. An Advanced Treatise*, H. Eyring, ed., Vol. 9, Academic Press, New York (1970), pp. 346–462.
27. M. D. Krotova and Yu. V. Pleskov, *Phys. Status Solidi* **3**, 2119–2126 (1963).
28. H.-U. Harten and R. Memming, *Phys. Lett.* **3**, 95–96 (1962).
29. H.-U. Harten, *Z. Naturforsch.* **16a**, 1401–1406 (1961).
30. W. H. Brattain and P. J. Boddy, *J. Electrochem. Soc.* **109**, 574–582 (1962).

31. R. Memming and G. Schwandt, *Surface Sci.* **5**, 97–110 (1966).
32. V. A. Tyagai, *Izv. Akad. Nauk SSSR Ser. Khim.*, 34–39 (1964).
33. P. J. Boddy, D. Kahng, and Y. S. Chen, *Electrochim. Acta* **13**, 1311–1328 (1968).
34. M. Gleria and R. Memming, *J. Electroanal. Chem.* **65**, 163–175 (1975).
35. F. Möllers and R. Memming, *Ber. Bunsenges. Phys. Chem.* **76**, 469–475 (1972).
36. T. Watanabe, A. Fujishima, and K. Honda, *Chem. Lett. (Japan)*, 887–900 (1974).
37. T. P. Birintseva and Yu. V. Pleskov, Izv. Akad. Nauk SSSR Ser. Khim., 251–257 (1965).
38. D. Yohe, A. Riga, and E. Yeager, *Electrochim. Acta* **13**, 1351–1358 (1968).
39. K. Degryse, W. P. Gomes, F. Cardon, and J. Vennik, *J. Electrochem. Soc.* **122**, 711–712 (1975).
40. A. Frumkin and A. Gorodetzkaja, *Z. Phys. Chem.* **136**, 451–472 (1928).
41. M. D. Krotova, V. A. Myamlin, and Yu. V. Pleskov, *Elektrokhimiya* **4**, 579–580 (1968).
42. E. C. Dutoit, R. L. van Meirhaeghe, F. Cardon, and W. P. Gomes, *Ber. Bunsenges Phys. Chem.* **29**, 1206–1213 (1975).
43. H. A. Roolaid, M. D. Krotova, and Yu. V. Pleskov, *Surface Sci.* **12**, 261–268 (1968).
44. M. Hoffman-Perez and H. Gerischer, *Z. Elektrochem.* **65**, 771–775 (1961).
45. F. Lohmann, *Ber. Bunsenges. Phys. Chem.* **70**, 428–434 (1966).
46. W. H. Laflere, F. Cardon, and W. P. Gomes, *Surface Sci.* **44**, 541–552 (1974).
47. Yu. V. Pleskov, *Elektrokhimiya* **1**, 4–11 (1965).
48. V. A. Tyagai, G. Ya. Kolbasov, V. N. Bondarenko, and O. V. Snitko, *Fiz. Tech. Poluprovodn.* **6**, 2325–2338 (1972).
49. M. J. Sparnaay, *Rec. Trav. Chim. Pays-Bas* **79**, 950–956 (1960).
50. P. J. Boddy and W. H. Brattain, *J. Electrochem. Soc.* **110**, 570–576 (1963).
51. W. H. Brattain and P. J. Boddy, *Surface Sci.* **4**, 18–32 (1966).
52. Yu. V. Pleskov, *Elektrokhimiya* **3**, 513–516 (1967).
53. Yu. V. Pleskov and V. A. Tyagai, *Dokl. Akad. Nauk SSSR* **141**, 1135–1138 (1961).
54. T. Freund and S. R. Morrison, *Surface Sci.* **9**, 119–132 (1968).
55. V. A. Tyagai and G. Ya. Kolbasov, *Elektrokhimiya* **11**, 1514–1521 (1975).
56. Z. A. Rotenberg, T. V. Dzhavrishvili, Yu. V. Pleskov, and A. L. Asatiani, *Elektrokhimiya*, **13**, 1803–1806 (1977).
57. R. Memming, *J. Electrochem. Soc.* **116**, 785–790 (1969).
58. V. A. Tyagai, A. M. Evstigneev, V. N. Bondarenko, and O. V. Snitko, *Elektrokhimiya* **8**, 1773–1780 (1972).
59. P. J. Boddy and W. H. Brattain, *J. Electrochem. Soc.* **109**, 812–818 (1962).
60. M. D. Krotova and Yu. V. Pleskov, *Elektrokhimiya* **2**, 222–228 (1966).
61. H. Gerischer, A. Mauerer, and W. Mindt, *Surface Sci.* **4**, 431–439 (1966).
62. R. Memming and G. Neumann, *Surface Sci.* **10**, 1–90 (1968).
63. Yu. V. Pleskov, *Dokl. Akad. Nauk SSSR* **126**, 111–114 (1959).
64. E. A. Efimov and I. G. Erusalimchik, *Zh. Fiz. Khim.* **33**, 441–446 (1959).
65. W. Mehl and J. Hale, in *Advances in Electrochemistry and Electrochemical Engineering*, P. Delahay, ed., Vol. 6, Interscience, New York (1967), pp. 399–458.
66. J. W. Diggle, ed., *Oxides and Oxide Films* Vols. 1 and 2, Marcel Dekker, New York (1973).
67. V. V. Eletsky and Yu. V. Pleskov, *Elektrokhimiya* **2**, 817 (1966).

7

Insulator/Electolyte Interface

L. I. BOGUSLAVSKY

1. Introduction

As little as 15 years ago the term "an electrochemistry of insulators" would have made no sense. The insulator was thought to be a nonconductive material. The pioneering work of Kallman and Pope[1-3] disproved this view. By investigating monocrystals of aromatic hydrocarbons they used electrolytic instead of metallic contacts for the supply of electric current. They showed that dark conduction and photoconductivity of insulators can be increased by many orders of magnitude with the help of a suitably chosen redox system in the electrolyte. The same authors performed simple energy estimations, which indicated that a redox reaction which proceeds on contact is the reason for the high efficiency of electrolytic contacts, in contrast to metallic ones.

Another important step was taken by Mehl,[4-6] who investigated limiting currents at insulating electrodes. Gerischer[7,8] performed an extensive study of the processes of sensitization of oxidation–reduction transformations in semiconductors and insulating electrodes. Concepts involving the dependence of the charge transfer on the energy of solvent reorganization[11,12] were applied by Mehl, Hale, and Lohman,[5] and by Gerischer and Memming,[9,10] to the study of injection currents and photoelectrochemical processes of insulating electrodes. Below, we shall often refer to a comprehensive review of Mehl and Hale,[13] which is the only one available on the subject. A discussion of the

L. I. BOGUSLAVSKY • Institute of Electrochemistry, Academy of Sciences of the USSR, USSR, Moscow V-71, Leninsky Prospekt 31, USSR.

photosensitization processes is based on the review paper by Gerischer and Willig.[14] We have considered the investigation of specific adsorption at insulating electrodes.[15,16]

2. Concerning Differences between Insulating and Metal Electrodes

Investigations of the insulator/electrolyte interface are related to one of the well-known fields of electrochemistry, i.e., the electrochemistry of semiconductors.[17] The difference between a semiconductor and an insulator is rather conditional. Apart from the large forbidden band gap, the insulator is characterized by a small conductivity in comparison with semiconductors of the Ge and Si type. Substances such as TiO_2 and ZnO may be called insulators. But our concept of an insulator shall include those materials the conductivity of which cannot be increased by the introduction of impurities, as it can in the case of TiO_2 and ZnO. Monocrystals of anthracene and other polycyclic aromatic hydrocarbons form a typical example of insulating electrodes. One can also look upon polymeric films, e.g., terylene and Teflon, as *insulator electrodes.*

An insulating electrode differs significantly from a metallic one by having an extremely small concentration of carriers. Such a quantitative difference between metals and insulators, the concentration of mobile charges, results, as first shown by Green,[18] in a qualitative difference of the potential distribution at the interface, and hence, in the mechanism of the influence of the electric field on the velocity of the electrochemical reaction. At an interface between a metal electrode and the solution, the entire electric field is situated in the double-layer space of the electrolyte. The field intensity in the Helmholtz layer may reach 10^7–10^8 V/cm. Such high values of field intensity change the energy barrier for particles undergoing changes on the electrode. This leads to a variation of the electrochemical reaction rate constant. The applied field plays a role in the energy factor. The situation changes drastically at the insulator/electrolyte interface. A drop of the potential ϕ at the insulator/electrolyte interface takes place in three regions: (1) in the region confined by the space charge in anthracene ϕ_s, (2) in a dense part of the double layer containing no free charges (Helmholtz layer), ϕ_H, and (3) in a diffuse part of the double layer in the electrolyte, ϕ_d.

On the basis of these assumptions one can develop a model of the double layer shown in Figure 1a, b, c.

By using an external power supply, one can change the value of the space charge in the insulator. One can achieve a value of the applied voltage such that the energy of electrons inside the solid and at the surface would be identical. This situation may be depicted by flat bands up to the interface boundary. A polarization of the insulating electrode makes a positive space charge appear, which heightens the electron energy in the surface layer, and then the bands

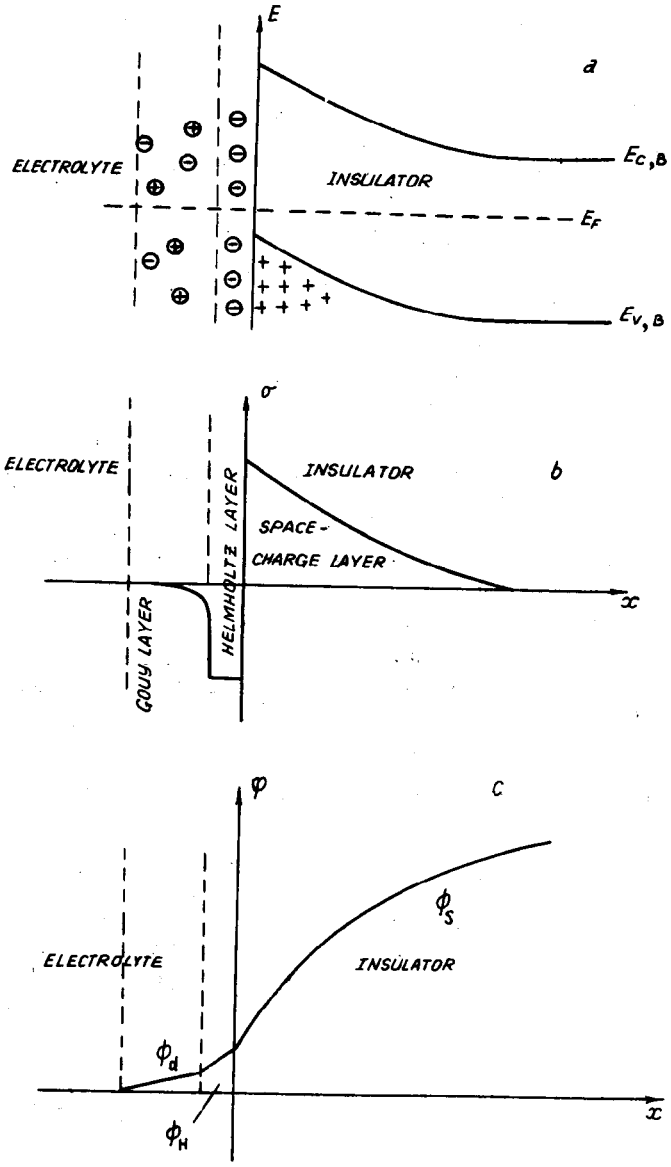


Figure 1. The band bending (a), distribution of the charge (b), and potential (c) at the insulator/electrolyte interface.

should curve upward. At negative polarization, on the contrary, the space charge layer has an excess of negative charges, and the bands curve downward. When the insulator interacts with the electrolyte, a drop of external voltage occurs in the dielectric. The potential drop in the double layer in the aqueous phase may be significantly too small to shift the energy barrier of the reaction. The electric field in the insulator regulates the concentration of charges (electrons or holes) at the interface. The concentration of electrons or holes affects the rate of the reaction by means of a preexponential or an entropy factor. Electrons in the conduction band and holes in the valence band participate differently in the interface reactions. When the insulating electrode is introduced into the redox system, the oxidation–reduction potential, measured relative to the reference electrode, will not depend on the material of the electrode. This assertion, important but not evident, may be illustrated in the following way.

3. Thermodynamic Approach to the Insulator/Electrolyte Interface

Let an aqueous solution between the insulator and electrolyte be at equilibrium, which is achieved by means of the electron-exchange reaction proceeding at the interface:

$$A \rightleftarrows A^- + p \tag{3.1}$$

In a state of equilibrium, the sum of the electrochemical potentials of both phases are equal, so that

$${}^{w}\bar{\mu}_{A^+} = {}^{w}\bar{\mu}_{A^-} + {}^{D}\bar{\mu}_{p} \tag{3.2}$$

The indices w and p denote a phase, to which a particle is assigned. By assuming that in the depth of the solution the electrostatic potential is equal to zero, one can express Eq. (3.2) through a sum of chemical and electrochemical potentials:

$${}^{w}\mu^{\circ}_{A} + RT \ln {}^{w}c_{A} = {}^{w}\mu^{\circ}_{A^-} + RT \ln {}^{w}c_{A^-} + {}^{D}\mu^{\circ}_{p} + RT \ln c_{p} + ({}^{w}\phi + {}^{D}\phi) \tag{3.3}$$

Value $({}^{w}\phi + {}^{1}\phi)$ denotes a Galvani potential $\Delta\phi$ at the insulator/electrolyte interface.

$$\Delta\phi = ({}^{w}\phi + {}^{D}\phi) = \frac{1}{F}[({}^{w}\mu^{\circ}_{A} - {}^{w}\mu^{\circ}_{A^-}) - {}^{D}\mu^{\circ}_{p} - RT \ln {}^{w}c_{p}] + \frac{RT}{F} \ln \frac{{}^{w}c_{A}}{{}^{w}c_{A^-}} \tag{3.4}$$

As follows from this equality, $\Delta\phi$ depends not only on the properties of the redox system, but on the chemical potential of holes in the dielectric as well.

A single Galvani potential cannot be measured experimentally. In practice, one measures the electrode potential by assembling an electrochemical cell involving an insulator electrode:

1	2	3	4	1
Me	insulator	electrolyte redox system	reference electrode	Me (I)
	$\Delta\varphi_{12}$	$\Delta\varphi_{23}$	$\Delta\varphi_{34}$	$\Delta\varphi_{41}$

The electrode potential measured in the cell (I) consists of the sum of the potential drops at the interface:

$$E = \Delta\varphi_{12} + \Delta\varphi_{23} + \Delta\varphi_{34} + \Delta\varphi_{41} \tag{3.5}$$

In the state of insulator–metal equilibrium it should be assumed that electrochemical potentials of electrons in both phases are equal:

$$^{M}\bar{\mu}_e = {}^{D}\bar{\mu}_p \tag{3.6}$$

In this case, with $\Delta\varphi_{12} + \Delta\varphi_{23}$ and Eq. (6.4), one can get

$$\Delta\varphi_{12} + \frac{1}{F}({}^{w}\mu^{\circ}_{A} - {}^{w}\mu^{\circ}_{A^-} - {}^{M}\mu_e) + \frac{RT}{F}\ln\frac{{}^{w}c_A}{{}^{w}c_{A^-}} \tag{3.7}$$

Since $\Delta\varphi_{34}$ and $\Delta\varphi_{41}$ do not depend on the dielectric–electrolyte boundary state, then

$$E = \text{const} + \frac{RT}{F}\ln\frac{{}^{w}c_A}{{}^{w}c_{A^-}} \tag{3.8}$$

From this equation it follows that in the cell (I), the potential drop at the insulator/electrolyte interface, measured relative to any reference electrode, is determined by a redox potential of the system contained in the electrolyte, but does not depend on the chemical potential of carriers in the insulator.

If there is not one, but several redox systems† in the electrolyte solution, then the electrode takes the potential of the redox system whose exchange current is higher.

Mehl[4,5] measured the exchange currents of various redox reactions at anthracine and showed that some of them have an exchange current comparable with that observed on the platinum electrode. Therefore it is of interest to clarify whether it is possible to observe oxidation–reduction potentials of various redox systems, as was possible for metallic electrodes. Thus a study was made of the anthracene electrode potential in the redox system of 0.1 *M* ferro/ferricyanide solution, 0.1 *M* Ce^{+3}/Ce^{4} at different pH's of the solution.[20]

Figure 2 illustrates a dependence of the redox potential of anthracene and platinum electrodes on the ferro/ferricyanide solution with pH of the buffer equal to 6.99. As seen, the potential of the anthracene electrode does not depend on the relation of the oxidizer and reductant in solution, and forms a straight line parallel to that obtained for a glass electrode. Hence the reaction

$$Fe(CN)_6^{3-} + e \rightleftarrows Fe(CN)_6^{4-} \tag{3.9}$$

is not potential determining, and there evidently proceeds some other reaction, the current density of which is greater than that of reaction (3.9). Some information on the reaction at a high exchange current may be obtained if we take into account the fact that the anthracene can be easily oxidized, particularly in the

† We do not consider here a possible homogeneous interaction in the volume of a solution.

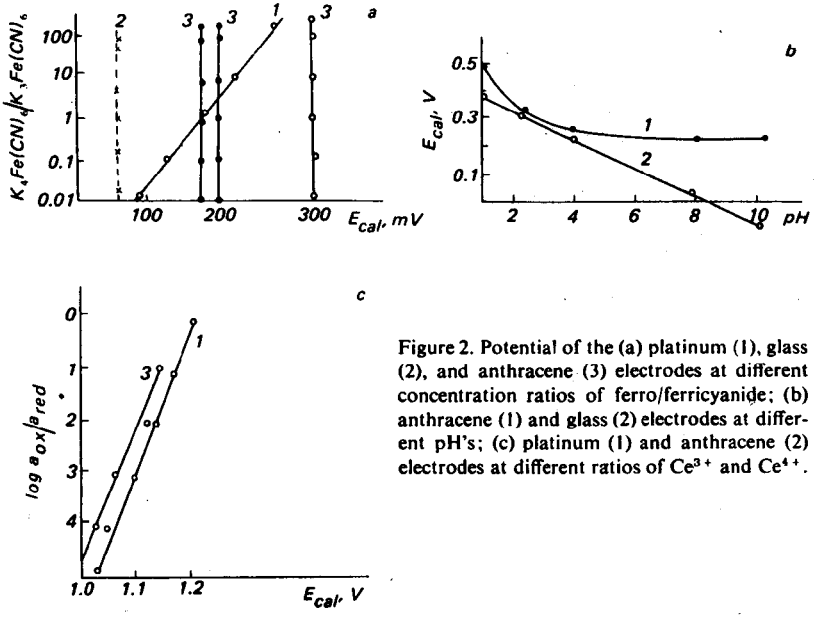


Figure 2. Potential of the (a) platinum (1), glass (2), and anthracene (3) electrodes at different concentration ratios of ferro/ferricyanide; (b) anthracene (1) and glass (2) electrodes at different pH's; (c) platinum (1) and anthracene (2) electrodes at different ratios of Ce^{3+} and Ce^{4+}.

presence of water molecules.[20,21] An absorption peak registers at 3430 cm^{-1} and may be assigned to the OH group. The existence of mobile protons in the systems concerned has been earlier supposed.[21,23] Using this as a base, one can assume that anthraquinone may participate in a reaction similar to that proceeding in the quinone–hydroquinone system. Then, in acid solutions, the following rea ion takes p' ce:

$$R + 2H^+ + 2e \rightleftarrows RH_2 \tag{3.10}$$

This reaction is also an oxidation–reduction reaction, but, in the acid region, its potential depends on pH. In Eq. (3.10), anthraquinone is denoted as R, and the quinone as RH_2. One obtains

$$E = E^\circ + \frac{RT}{2F} \ln \frac{c_R}{c_{RH_2}} - 0.059\,\text{pH} \tag{3.11}$$

In an alkaline solution, one should allow for dissociation proceeding in accordance with

$$\begin{aligned} RH_2 &\rightleftarrows RH^- + H^+ \\ RH^- &\rightleftarrows R^{2-} + H^+ \end{aligned} \tag{3.12}$$

From the analysis of the quinone–hydroquinone-type systems it follows that in an alkaline solution such a dissociation is essential and affects the redox

potential of the system.[19] The dependence of the anthracene electrode potential (Figure 2b) on the pH of the solution follows from the above.

Thus molecules existing at the anthracene surface can exchange protons with the solution, which results in the appearance of an electrode potential at the boundary with the electrolyte in those cases when the exchange current of reactions (3.10) and (3.12) is higher than that of the redox reaction (3.9). A high exchange current in system (3.10) may be due to the fact that one of the reaction components is situated at the electrode surface, thus facilitating an electron exchange with anthracene.

When an anthracene electrode is located in the solution with a high redox potential (e.g., a system containing 0.1 N Ce^{3+}/Ce^{4+} + 1 N H_2SO_4), its potential is only 25–30 mV more negative than the potential of a platinum electrode in the same solutions (Figure 2c). Thus, if the anthracene is situated in the Ce^{3+}/Ce^{4+} system, the electrode potential is determined by the redox system.

4. Determination of the Potential due to Adsorbed Iodine at the Anthracene Electrode

A feature of the insulating electrode is the deep electric field penetration into the electrode. By solving a Poisson equation for the insulator/electrolyte interface, one can determine the potential distribution in the insulator over a layer thickness d, where the potential Ψ ceases to vary due to the screening of the surface charge field. The thickness of the layer after which the surface charge is screened is determined by

$$d_D = \left(\frac{\varepsilon RT}{4\pi e^2 n}\right)^{1/2} \tag{4.1}$$

where n is the number of electrons in the insulator and d_D is the Debye length.

By using Eq. (4.1) for the determination of value d_D, one can see that in the insulator with a very small carrier concentration, e.g., $n = 10^5$–10^6 cm^{-3}, the Debye length may reach several centimeters. But, in practice, traps in the insulator greatly reduce the depth of penetration of the field. An essential distinction of the insulating electrode from the semiconductor is the fact that the thickness of the insulating electrode may be less than the Debye length in it. It is then possible to obtain a mutual influence of the potential distribution at opposite sides of the insulating membrane. One can thus obtain information on the structure of the electric double layer at the interface.

Let us consider an insulator/electrolyte interface. At one of the boundaries, let us assume a reaction of the type

$$A^- \rightleftarrows A + e \tag{4.2}$$

If an external field is applied to the system, then in order to determine the current through the interface it is necessary to solve a system of equations

$$I = en_{e,p}uE + ukT\frac{dn}{dx} = \text{const}(x)$$
$$\frac{dE}{dx} = \frac{4\pi}{\varepsilon}\rho \tag{4.3}$$

where i is the current density, u the mobility of carriers, and ρ, E, and n the density of the space charge, electric field intensity, and the current carrier concentration, respectively. If the current density through the interface is small in comparison with the exchange current density, then reaction (4.2) does not violate equilibrium, and the boundary conditions may be written as

$$n_{\text{I}} = N_c \exp\left[-(E_c - E_F)_{\text{I}}/kT\right]$$
$$n_{\text{II}} = N_c \exp\left[-(E_c - E_F)_{\text{II}}/kT\right] \tag{4.4}$$

where n_{I} and n_{II} are the current carrier concentration at the front and rear surfaces of the dielectric, respectively, and N_c the density of electron states in the conduction band. Expressions $(E_c - E_F)_{\text{I}}$ and $(E_c - E_F)_{\text{II}}$ denote the distance from a Fermi level to the conduction band bottom at the front and rear insulator surfaces.

For reasons to be discussed below, electrolyte contacts are used in place of the expected metal ones. The potential distributions for systems with electrolytic and metallic contacts coincide. Electrolytic contacts are more advantageous because by varying the composition of the solution, one can smoothly change the work function of the contacts. This can be readily demonstrated by replacing one contact with another. For the metallic contacts the solution of Eq. (4.3) with boundary conditions (4.4) is known[24]; it represents the current confined by a space charge:

$$I = \frac{9\varepsilon u}{32\pi d^3}\Delta\Psi^2 \tag{4.5}$$

Here, ε and u are the dielectric permittivity and mobility of current carriers in the insulator, respectively, and d is the sample thickness. When the contacts are metals with the same work function, then, when a potential difference V_{12} is applied to the sample, if the contacts are metallic, a Volta potential, $\Delta_d{}^0\Psi$, appears between 0 and d in the dielectric. It is algebraically added to the potential difference V_{12} applied to the sample:

$$\Delta\Psi = \Delta_d{}^0\Psi \pm V_{12} \tag{4.6}$$

(the sign before V_{12} depends on the direction of applied voltage).

A principal difference between the electrolytic and metallic contact systems is the fact that a part of the mutual potential jump $\Delta\varphi_{\text{I-II}}$ between the phases I and II occurs in the electrolyte. Equilibrium distribution of the potential is shown schematically in Figure 3. A total equilibrium potential jump $\Delta\varphi_{\text{I-II}}$ is

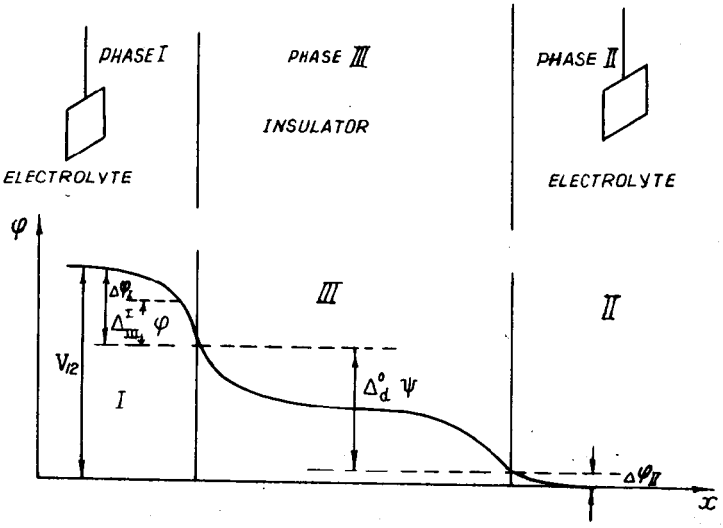


Figure 3. Potential distribution in the electrolyte (I)/insulator (III)/electrolyte (II) system. $\Delta\varphi_I - \Delta\varphi_{II}$, equilibrium difference of Galvani potentials between phases I and II; $\Delta\varphi_I$, $\Delta\varphi_{II}$, the potential jumps in double electric layer in the phases I and II; $\Delta_{III}{}^I\varphi$, the potential jump caused by a specific adsorption, and $\Delta_d{}^o\psi$, the potential defined in the text.

comprised of the potential jumps $\Delta\varphi_I$ and $\Delta\varphi_{II}$ in the electric double layers in the I and II phases; of the potential jump $\Delta\varphi_a$ connected with a specific adsorption of particles at the interface I–III, and of the potential drop $\Delta_d{}^o\Psi$ in the insulator. The value $\Delta_d{}^o\Psi$ may be identified with the Volta potential at a specific thickness d of the anthracene. The thickness of phase III should be sufficiently small in comparison with the Debye length in the anthracene (d_i) in the presence of equilibrium carriers. Under these conditions the plates of the double electric layer on both sides of the insulating membrane are not independent. Region III in this case behaves similarly to the vacuum diode and the value $\Delta_d{}^o\Psi$ at these conditions may be identified with the Volta potential.

If the potential, $\Delta_d{}^o\Psi$, is expressed through the chemical potentials of ions participating in the reactions at the interface of phases I–III and II–III and through the equilibrium jumps of potentials in phases I and II (using the condition of equilibrium in the system at the absence of the current), then, by undergoing a conventional closed thermodynamic cycle, including electron transfer from the phase I through the vacuum to phase II, and then phase I, it is easy to show that

$$\Delta_d{}^o\Psi = \frac{kT}{e} \ln \frac{c_{red}}{c_{ox}^{I}} - \Delta\varphi_a + B \qquad (4.7)$$

where B is the constant depending on the choice of the solution.

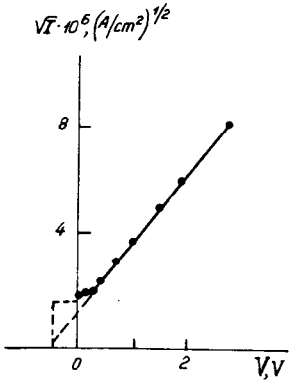


Figure 4. The current vs. applied voltage in an aqueous solution of 1 *M* KI + 2 × 10^{-2} *M* I_2, anthracene, and 1 *M* NaCl.

Figure 4 shows a typical initial part of the potential–current characteristics in the coordinate system (V, $I^{1/2}$). At a voltage up to 1 V, the voltage–current characteristic corresponds to the linear dependence of current on the voltage. In this voltage range, a diffusion mechanism of charge transfer predominates. The Henry–Mott law is valid, and the square-law variation of current on the voltage is observed. In the assumed coordinate system, this part of the dependence is represented by a straight line. If the obtained line is extrapolated up to the intersection with the voltage axis (dashed line), then the interaction point with this axis, in accordance with Eq. (4.6), represents the potential, $\Delta_d{}^0\Psi$, described by Eq. (4.7).

To estimate the effect of iodine concentration variation at the front electrode (Figure 4) on the value $\Delta_d{}^0\Psi$, the redox potentials of the solutions used have been measured relative to the saturated calomel electrode. The term $(kT/e) \ln c_{red}/c_{ox}{}^1$ of Eq. (4.7) contributes little to the value of $\Delta_d{}^0\Psi$, i.e., the measured value is caused largely by a variation of the potential jump due to the specific adsorption of the iodine.

By using data on the quantity of iodine adsorbed on the anthracene electrode,[15] one can obtain a change of the potential $\Delta_d{}^0\Psi$ depending on the quantity of adsorbed iodine, shown in Figure 5, indicating the number of adsorbed layers. Various curves can be obtained by variation of the left-side solution of Figure 3. Addition of sodium thiosulfate to the left solution leads to a change in the potential difference in phase II. With increase of the sodium thiosulphate concentration, the curve drops (Figure 5, curves 2 and 3), but the value of $\Delta_d{}^0\Psi$ in the region $n_L > 1$ remains constant. Curve 1a (Figure 5) illustrates in more detail an initial part of the studied curve.

From Eq. (4.7) one can determine the value $\Delta\varphi_a(n_L)$. With the surface covered with the iodine, value $\Delta\varphi_a$ increases rapidly up to 2 V, and with a further increase of n_L it changes weakly. The largest changes of $\Delta\varphi_a$ occur during

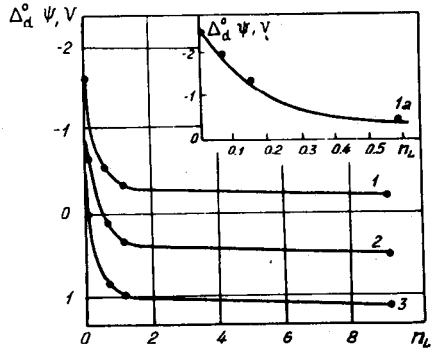


Figure 5. The change of potential during adsorption from the aqueous solution 1 *M* KI on the anthracene cathode depending on number of I^0 layers for different solutions in the left compartment: 1 and 1a, 1 *M* NaCl; 2, 1 *M* NaCl + 10^{-2} *M* $Na_2S_2O_3$; 3, 1 *M* NaCl + 5×10^{-2} *M* $Na_2S_2O_3$.

the formation of the first monolayer. Further monolayers of the iodine do not significantly change the value of $\Delta\varphi_a$.

5. Electrochemical Injection and the Exchange Currents Occurring on the Insulating Electrodes

The main distinction between insulating and metallic electrodes in respect to redox reactions is that for the electron-exchange reaction at the insulator surface it is necessary that the electron transfers take place in the vicinity of the conduction band bottom or the top of the valence band.[7] The Franck–Condon principle is applicable to that process because the electron transition is more rapid than the variation of atomic coordinates in the dielectric continuum of the solvent, where the redox system is available, and in the insulator, where the injected charges go.[11]

Owing to thermal fluctuations, when a molecule interacts with the ambient medium, the level of an electron in a molecule fluctuates to the regions of the most probable energy states E_{red} or E_{ox}. Such fluctuations of the energy level may be described by a Gaussian distribution (see Figures 10 and 11). For example, for a donor level, the distribution function W_{red} with allowance for the normalized term A_{red} is

$$A_{red} = \left(\frac{1}{4\pi kT\lambda_i}\right)^{1/2} \tag{5.1}$$

$$W_{red}(E) = A_{red} \exp\left[-\frac{(E - E_{red}^\circ)^2}{4kT_i\lambda_i}\right]. \tag{5.2}$$

The velocity of electron transfer from a donor to an electrode may be expressed through that of the electron exchange between two isoenergetic levels, both on the electrode and in the solution, one of them being populated and the other

free. Electron transfer from a donor to an electrode is equivalent to the anode current

$$I = B_{red} c_{red} \int_{-\infty}^{\infty} \kappa_{red}(E) W_{red}(E) D(E)\, dE \tag{5.3}$$

Here B_{red} is the constant in which all the values are included independent of the instantaneous energy states, as well as the number of collisions, the steric factor, and the normalized term A_{red}; $\kappa(E)$, the transition probability for an electron at the condition of energy conservation ($E_{in} = E_{fin}$). Finally, the function $D(E)$ denotes the density of the populated states on the electrode.

Since the rate of the redox reaction at the insulating electrode surface is restricted by a concentration of the current carriers at the interface,[5.26] then the exchange current of the redox reaction at the interface should depend on a typical redox potention of the solution, E_{redox}, and be proportional to the reagent concentration c_{red} or c_{ox}:

$$I_n^0 = A^* c_{red} \exp\left[-\frac{n^2\lambda_i - E_n + e(E_{redox} - \Psi fB)}{4\lambda n^2 kT}\right]$$
$$I_p^0 = A^* c_{ox} \exp\left[-\frac{n^2\lambda_i + E_p + e(E_{redox} - \Psi fB)}{4\lambda n^2 kT}\right] \tag{5.4}$$

In these equations, I_n^0 and I_p^0 are the exchange currents of any redox reaction at the electrode, A^* is the constant velocity of the reaction, c_{ox} and c_{red} the concentrations of the oxidant and the reductant, respectively, at an external plane of the Helmholtz double layer at the equilibrium potential, and n the number of electrons participating in the reaction. The parameter λ_i characterizes the energy change in ionic solvation, when, as a result of redox reactions, the ion gains and loses an electron. As seen from Eq. (5.4) the maximum current I^0 should depend on the concentration of the reductant or the oxidant $I^0 \sim c_{ox}(c_{red})$.

The limiting current, being determined by the exchange current, is characterized by a situation where all the injected charges are discharged in the electrode depth under the field action, so the charge concentration at the surface is near to zero. Since the external potential drop occurs very largely in the insulator, the potential drop in the double layer is negligible so that the potential distribution in the electrolyte solution is at equilibrium.

Exchange currents at anthracene single crystals were observed for the first time by Mehl,[6] who showed that at a certain value of applied field, the current does not change with an increase in voltage:

$$I_n = I_n^0 \left(\frac{n_n}{n_n^0} - 1\right)$$
$$I_p = I_p^0 \left(1 - \frac{n_p}{n_p^0}\right) \tag{5.5}$$

where I_n and I_p are the electron and hole currents, and n_n and n_p the concentrations of electrons and holes in anv part of voltage–current curves. It should be

noted that not all limiting currents can be identified with the exchange currents.[27] For instance, a limiting cathode current on the anthracene electrode in $Fe(CN)_6^{3-}/Fe(CN)_6^{4-}$ system cannot be identified as the exchange current of the redox reaction because the electrode potential in that system does not correspond to the given redox system concerned.

One can observe and investigate charge injection by means of other aromatic hydrocarbons,[13,14] as well as by using terylene and Teflon films, 5–40 μm thick.[28] The redox systems Ce^{4+}/Ce^{3+} and Mn^{7+}/Mn^{4+} in H_2SO_4 solutions of pH = 2 were used, as well as the I^0/I^- system, as the injecting solutions. The insulating electrode, which contacts the injecting solution, is the cathode. On the other side of the film, a solution of 1 *M* NaCl was used as the contact.

Figure 6a shows the dependence of applied voltage on current on a logarithmic scale for anthracene and Teflon electrodes in a different redox system. As seen from Figure 6a, the current density increases greatly, in some cases up to 150–200 V, after which the current becomes almost independent of applied field.

For the anthracene cathode, a limiting current does not depend on the crystal thickness because it is determined by the rate of the Ce^{4+} ion reduction (Figure 6b). Using a Teflon film, the value of the limiting current decreases with the growth of the film thickness (Figure 6c). According to Figures 5 and 6 for the anthracene electrode, Eq. (5.4) predicts a linear dependence on the oxidant concentration, and is quite valid. A feature of the Mn^{7+}/Mn^{4+} system is a participation of hydrogen ions in the reaction; the limiting current, therefore, should depend on the proton concentration in the solutions, as this is experimentally observed (Figure 7a, curves 1, 2)

$$MnO_4^- + 8H^+ + 5p \rightarrow 4H_2O + Mn^{2+} \qquad (5.6)$$

For polymer film limiting currents, the dependence ranges from 0.5 to 0.75. The specific adsorption of iodine on the anthracene (Figure 7b, curve 3) results in a sharp dependence of the limiting current on the acceptor concentration. A steeper dependence than that which follows from Eq. (5.4), and the dependence on the film thickness, indicate that the limiting currents observed with the polymer films certainly cannot be identified with the exchange currents on polymer electrodes.

A particular feature of injection currents on terylene and Teflon films is their much smaller value compared with those on athracene (Figure 7a, b). The low limiting injection current is due to the fact that the reaction seems to proceed not on the total surface but only on the film defects. Also, a part of the injected carrier is captured by traps in the surface layer of the film.[29]

Specific adsorption is probably characterized by a partial transfer of charge from an adsorbed particle to the electrode. Therefore an electrostatic charge in the insulator should lead to a change in the effective dipole moment of the specifically adsorbed particle. This will lead, in turn, to a change of limiting current in the presence of electrochemical injection with the participation of

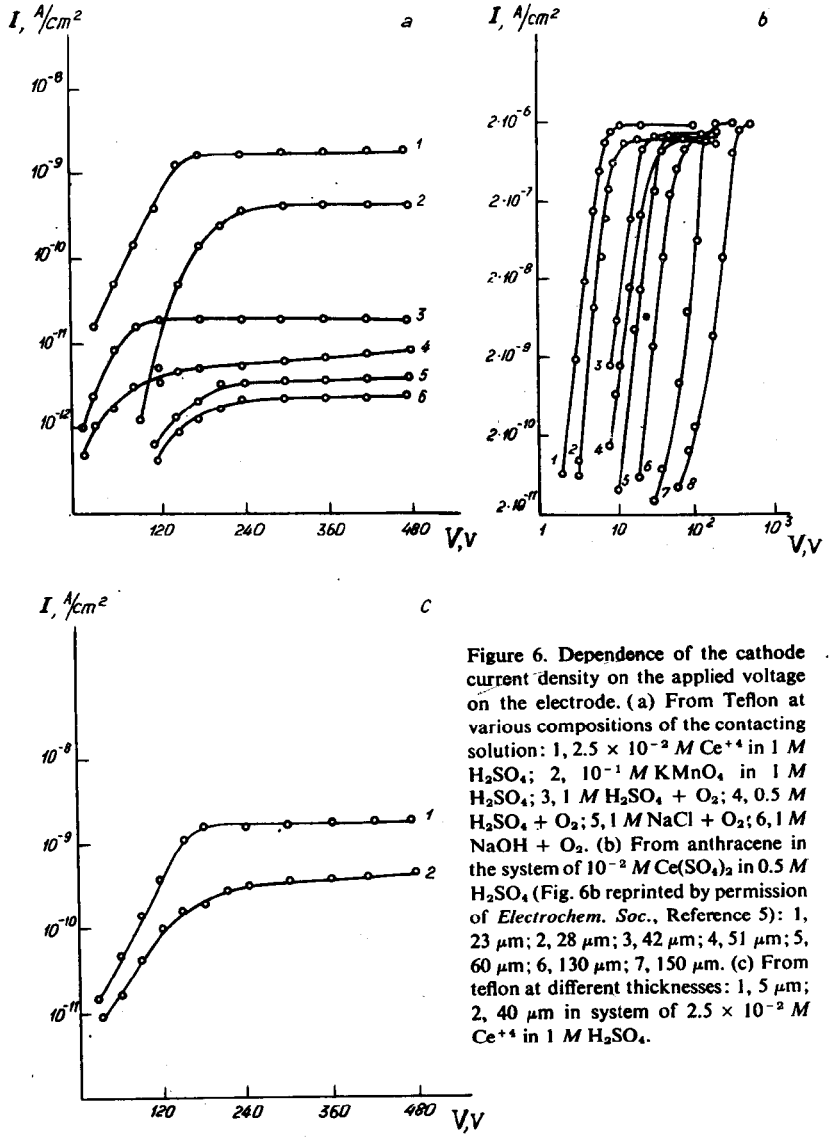


Figure 6. Dependence of the cathode current density on the applied voltage on the electrode. (a) From Teflon at various compositions of the contacting solution: 1, 2.5×10^{-2} *M* Ce^{+4} in 1 *M* H_2SO_4; 2, 10^{-1} *M* $KMnO_4$ in 1 *M* H_2SO_4; 3, 1 *M* $H_2SO_4 + O_2$; 4, 0.5 *M* $H_2SO_4 + O_2$; 5, 1 *M* NaCl + O_2; 6, 1 *M* NaOH + O_2. (b) From anthracene in the system of 10^{-2} *M* $Ce(SO_4)_2$ in 0.5 *M* H_2SO_4 (Fig. 6b reprinted by permission of *Electrochem. Soc.*, Reference 5): 1, 23 μm; 2, 28 μm; 3, 42 μm; 4, 51 μm; 5, 60 μm; 6, 130 μm; 7, 150 μm. (c) From teflon at different thicknesses: 1, 5 μm; 2, 40 μm in system of 2.5×10^{-2} *M* Ce^{+4} in 1 *M* H_2SO_4.

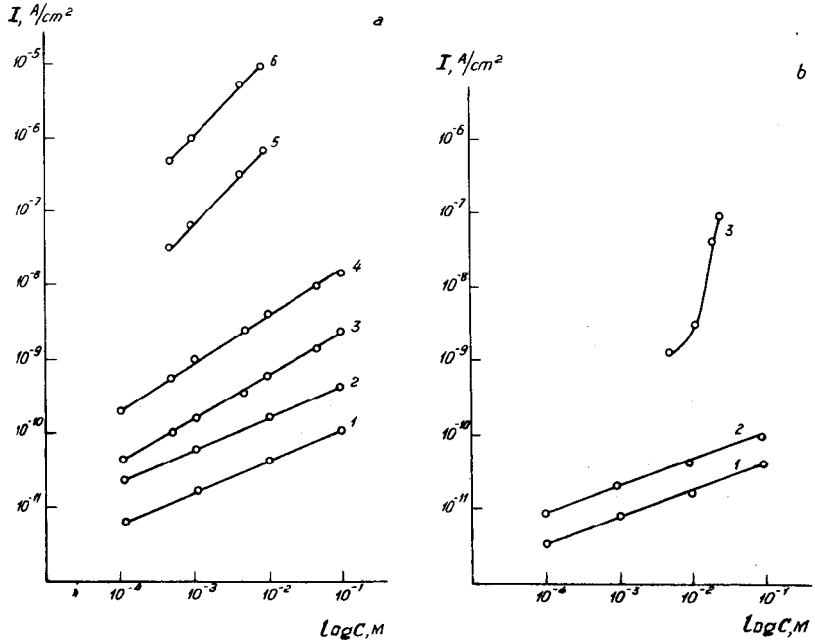


Figure 7. Density of limiting cathode current (a) versus $KMnO_4$ concentration on the Teflon electrode in the neutral solution (1) in 1 *M* H_2SO_4: on the anthracene (6) on concentration of Ce^{4+} in 1 *M* H_2SO_4 on Teflon (3) and terylene (4) electrodes, on the anthracene as well (5). (b) limiting current density versus concentration I_2 in 1 *M* KI on the Teflon (1) and terylene (2) electrodes, as well as on anthracene (3).

adsorbed particles. An effect of the sign of electric charge has been observed when investigating limiting cathode currents through the dielectric polymer films 5, 10, and 20 μm thick in the iodine/iodide system. Figure 8a, b shows a comparison of the cathode injection currents obtained by means of the film cathodes in the Ce^{4+}/Ce^{3+}. I^0/I^- redox system. The electrolyte contact at the opposite side was a 1 *M* solution of KCl. The iodine seems to be specifically adsorbed by defects in the polymer film. The charge transfer to the iodine adsorbed by the film increases when the positive electret charge is positive, and this interacts with the surface, where hole injection proceeds:

$$I^0 + R \rightarrow (I^{-\delta} \cdots R^{+\delta}) \rightarrow I^- + R^+ \qquad (5.7)$$

Figure 8b shows that the positive charge stimulates an increase in the limiting injection current of the system I^0/I^-, but does not affect the limiting current of injection in the Ce^{4+}/Ce^{3+} system (Figure 8a).

The reduction of Ce^{4+} occurs without participation of the adsorbed state

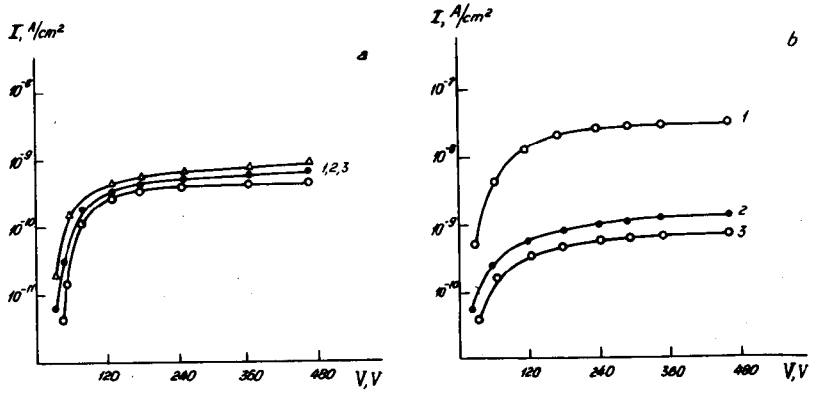


Figure 8. Cathode voltage–current curves for a terylene electrode in the iodine/iodide system (film thickness of 10 μm). (a) The film surface contacting with the Ce^{3+}/Ce^{4+} system is charged: 1, positively; 2, nonpolarized; 3, negatively; (b) the same in the I^0/I^- system.

upon charge transfer. Hence the limiting current of Ce^{4+} reduction is not affected by a sign of the electret charge. The effect of the electret state on the injection current is indicative of the fact that the field in the polarized film changes nonlinearly with distance from the surface—the greatest potential jump occurs in the surface layer.

By using two different injecting contacts, one can simultaneously observe the injection of holes and electrons occurring on opposite sides of an isolating membrane. Mehl and Büchner[5,25] observed that phenomenon as a result of an anthracene membrane interaction with a solution of anthracene and $AlCl_3$ in nitromethane, which injects the holes, and of a lithium solution in ethylenediamine, which injects the electrons. The recombination of holes and electrons results in the appearance of light quanta. Figure 9 shows a dependence of radiation intensity on the current density. The radiation spectrum coincides

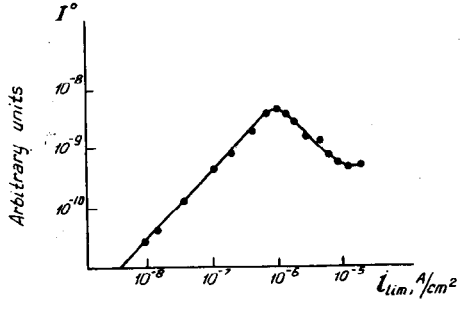


Figure 9. Intensity of luminescence as a function of the double injection current in the anthracene monocrystal (reprinted by permission of *J. Electrochem. Soc.*, Reference 5).

with that of anthracene fluorescence, which is excited by hole and electron recombination leading to the appearance of the first excited singlet state of anthracene.

6. Photoelectrochemical Processes on the Insulating Electrodes

For insultating electrodes one can distinguish three regions of quantum energy where photoelectrochemical processes are observed. In the short-wave region where interband transitions are possible, light absorption gives a hole–electron pair (Figure 10a). Such processes have been investigated by broad forbidden bandwidth semiconductors, e.g., TiO_2, and were likely to have been observed on the anthracene electrode with the iodine/iodide system.[26,27] A reverse process is also possible (Figure 10b). The charges produced by a double injection at opposite sides of the anthracene membrane combine with the

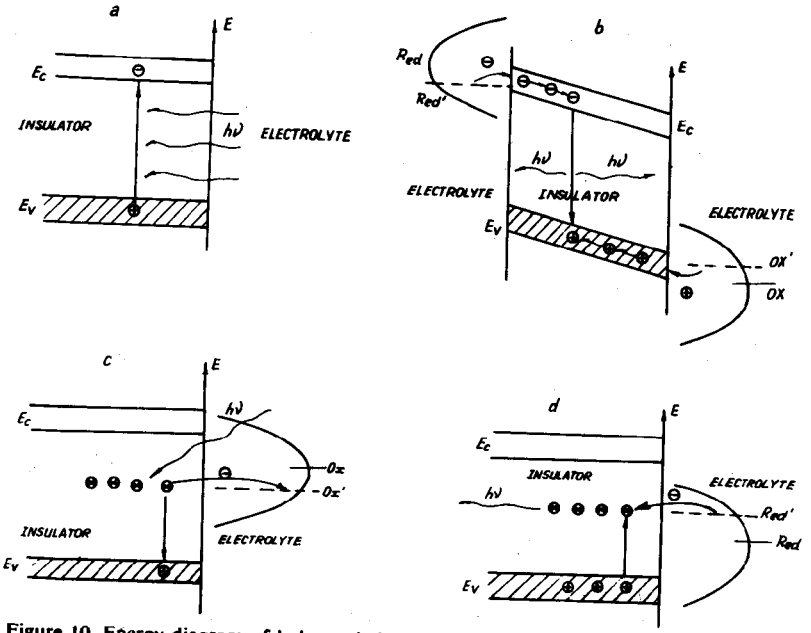


Figure 10. Energy diagram of holes and electrons in the insulator: (a) under illumination with energy higher than the forbidden bandwidth; (b) reverse process, i.e., the electron recombination in the conduction band and holes in the valence band, resulting in the emission of light quanta; (c) illumination with light with energy sufficient for the appearance of excitons in the insulator reacting with the oxidant in the solution; (d) a reverse process, i.e., a reaction of holes with the reductant in the solution leading to the appearance of excitons.

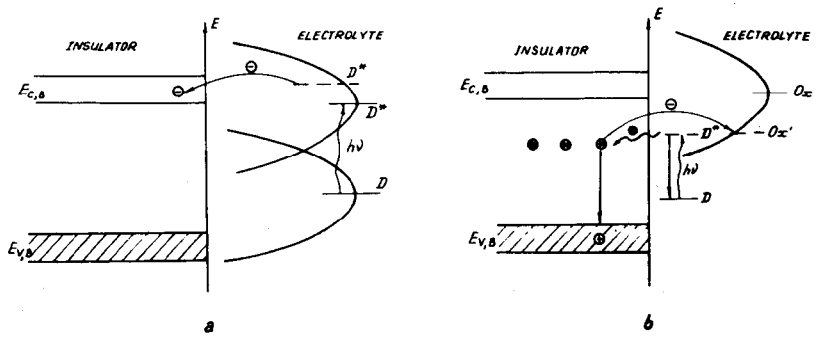


Figure 11. Energy diagram of current carriers in the insulator. Illumination by light with energy sufficient for the excitation of a sensitizer molecule, which is oxidized and delivers an electron to the conduction band (a) and transmits excitation to the insulating electrode (b).

radiation of light quanta, whose energy is equal to that of the forbidden band in an anthracene crystal (Figure 9).[25] At lower quantum energies, where interband transitions are impossible, the photocurrent arises due to the appearance of excitons as a result of the action of light, and their further decay into current carriers as a result of interaction with the redox system in the electrolyte (Figure 10c).[7,33]

In a reverse process, excitons are generated during the redox reaction (Figure 10d). Finally, at the lowest quantum energies, where the insulator electrode does not absorb, one can observe an appearance of the photocurrent, sensitized by a component, which is excited by light in that wavelength region. Here, two alternative processes are possible: first, an excited molecule captures an electron on the electrode (Figure 11a); second, from the molecule the excitation goes to the electrode with a further dissociation into the charge carriers (Figure 11b).

The above-mentioned three spectral regions corresponding to various photoelectrochemical processes on the insulating electrodes are shown by Figure 12. It shows a dependence (arbitrary units) of the effective quantum yield β on the anthracene cathode when it interacts with the iodine/iodide system in the case when the injecting contact is on the left and the degree of the surface coverage by the iodine is equal to 1.[16]

At photon energies ranging from 5.12 to 3.8 eV, commensurate with the anthracene forbidden bandwidth, the value is minimal and corresponds to the photocurrent caused by the interband transitions. The second region of Figure 12 corresponds to the photon energies from 3.8 to 3.1 eV, which coincides with the region of a strong singlet absorption of the anthracene. The excitons participate in the region of a strong single absorption $h\nu \sim 3.4$ eV during electrochemical charge separation.

Finally, the process of photosensitization by adsorbed iodine occurs on the

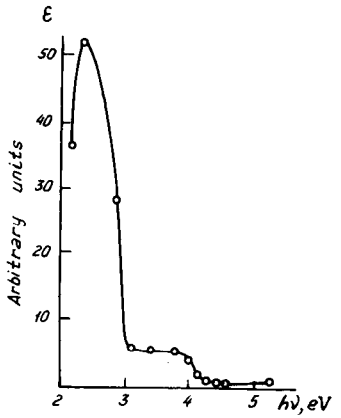


Figure 12. Dependence of the efficient quantum yield on the exciting photon energy at constant coverage $n_L = 1$ in the aqueous solution iodine–iodide, $E = 10^5$ V/cm.

anthracene cathode at quantum energies 3–2.3 eV. In this spectral range, the spectrum of photoconductivity overlaps with that of the iodine absorption, and the maximum on the curve corresponds to an iodine absorption maximum.

7. Reactions of Excitons at the Insulator/Electrolyte Interface

Electrochemical reactions occurring at band transitions of electrons have been investigated in detail by using conventional semiconductor electrodes.[17] However, electrochemical reactions with the participation of excitons represent a new type of electrode process. In crystals of aromatic hydrocarbons, movable singlet and triplet Frenkel excitons appear during illumination. When the excitons reach a surface, one of the following processes is possible: (1) an exciton reflects from the interface boundary; (2) it is captured into the energy level at the surface positioned lower than inside the crystal; (3) an exciton is quenched due to its energy being scattered in the lattice transitions; (4) the excitation may be transferred to the solution components, e.g., adsorbed at the surface. Under certain conditions, the energy released as a result of decay may be used for a formation of a current carrier pair. In this case, the photocurrent produces information about the exciton interaction with the insulator surface.[32] When investigating a photoexcitation of molecular crystals it should be remembered that, due to the van der Waals interaction between molecules in a crystal, an overlapping between molecular orbitals of neighbor molecules is insignificant. In particular, for anthracene, due to[26] the energy of two interacting molecules, it is within the limits of $5–30 \times 10^{-16}$ erg. Therefore, an interaction of a singlet exciton with an acceptor in the solution may be described as an interaction of separate anthracene molecules (R) with an A molecule in the solution:

$$R^* + A \underset{k_2^*}{\overset{k_1^*}{\rightleftarrows}} R^{\pm} + A^{\mp} \qquad (7.1)$$

Since the coefficient of light absorption in anthracene is of 3.2×10^4 for 390-nm wavelength, then at the crystal thickness of 20–30 μm the light is totally absorbed in the crystal. Hence, to estimate the exciton concentration at the crystal surface, one can neglect the processes occurring on the unilluminated side, and a semi-infinite crystal can be considered.

A diffusion equation for singlet excitons,

$$D^* \frac{d^2c^*}{dx^2} - \frac{c^*}{\tau^*} + KI_0 \exp(-Kx) = 0 \tag{7.2}$$

has been solved by Eremenko and Medvedev[30]:

$$c^* = \tau^* KI_0\{a \exp[x(D^*\tau^*)^{-1/2}] + \beta \exp[x(D^*\tau^*)^{-1/2}] + \exp(-Kx)(1 - K^2D^*\tau^*)^{-1}\} \tag{7.3}$$

Here D^*, c^*, and τ^* are the diffusion coefficient, concentration, and lifetime of singlet exciton, respectively, I_0 and K the light intensity and coefficient of light absorption in the crystal, and α and β the constants. For a semi-infinite crystal $c_x = 0$ at $x \to \infty$, hence $\beta = 0$. From Eq. (7.3), at the conditions that the total flux of excitons at the surface is to the rate of exciton decay due to injection, we get

$$D^* \frac{dc^*}{dx} = k_1^* c^* c_{A^\pm} - k_2^* c_{n,p} \cdot c_A \tag{7.4}$$

By solving Eq. (7.3) at condition (7.4) one can determine the exciton concentration at the surface of $c^*(0)$:

$$c^*(0) = \frac{I_0/k_1^* c_{A^\pm}}{1 + [k_1^* c_{A^\pm}(D^*c^*)^{1/2}]^{-1}} \left\{[1 + K^{-1}(D^*\tau^*)^{-1/2}] + \frac{k_2^* c_A c_{n,p}(0)}{I_0}\right\} \tag{7.5}$$

The current flowing through the insulator consists of dark and photocomponents:

$$I = q[k_1^* c^*(0) c_{A^\pm} - k_2^* c_{n,p}(0) c_A + k_1^* c_{A^\pm} - k_2^* c_{n,p}(0) c_A] \tag{7.6}$$

where q is the molar density of states in the conduction band. From equations (7.3) and (7.6) one can determine the surface concentration of current carriers $c_{n,p}$ for $I = 0$ and $I = I^0$. As shown by Hale and Mehl,[26,34] in the case of the illumination of the interface, the limitng current I_{lim} is connected with the exchange current I^0 of the dark injection and the light intensity by the equation

$$\frac{I_{lim} - I^0}{qFI_0} = f_1 f_2 \tag{7.7}$$

Here

$$f_1 = \frac{1}{1 + (1/K)(D^*\tau^*)^{-1/2}}$$

and

$$f_2 = \frac{1}{1 + (1/k_1^*)c_{A^\pm}(\tau^*/D^*)}$$

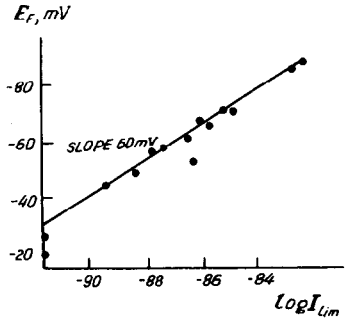


Figure 13. Photoelectromotive force vs. current. Photoinjection at the tetracene/water interface (reprinted by permission of *Electrochem. Acta* , Reference 26).

the probabilities of appearance of the excition at the surface and its disappearance due to the reaction of charge separation due to Eq. (7.1). From the same system of equations one can obtain a value of the photopotential in the crystal with a thickness d depending on the ratio of the exchange current to the maximum photocurrent:

$$\Delta E_F = \frac{RT}{qF} \ln \frac{I_{lim}}{I^0} \tag{7.8}$$

Figure 13 illustrates value ΔE_F obtained in (7.8) as a function I_{lim} in tetracene in the presence of oxygen. The obtained slope of 60 mV is indicative of the validity of the above-developed model for the carrier generation by light in the region of the exciton absorption of the insulator. The calculations do not allow for the interaction of an oxidant or a reductant with the anthracene surface. This simplification is valid when no adsorption is observed of the electrochemically active component from the solution at the insulator surface, or in the case when the adsorption is caused by van der Waals forces. In the presence of specific adsorption an interaction of the electrochemically active component with the insulator molecules greatly changes the rate of the process.

8. Photosensitized Reactions with Participation of Excited Molecules in the Electrolyte

If the quantum energy does not cause the appearance of excited states in the insulating electrode, then a photocurrent can arise due to the light absorption in a given wavelength region by molecules at the contact. Then, the electron-excited molecules react with an insulating electrode with formation of current carriers. On the electrodes, where the process of excitation quenching is insignificant, one can distinguish two conditions necessary for the occurrence of this process. Firstly, energy levels of a donor and an acceptor at both sides of the interface should be approximately equal. Secondly, a steric correspondence

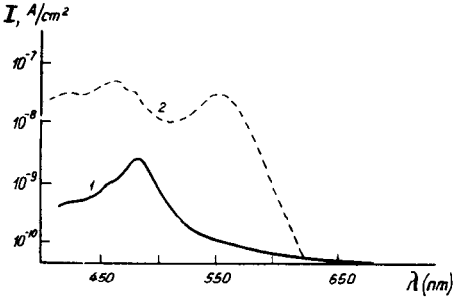


Figure 14. Spectral dependence of the photocurrent (1) and sensitizer current (2) in the presence of the 10^{-5} *M* rhodamine B on the perylene electrode (reprinted by permission of *Electrochem. Acta*, Reference 31).

between an adsorbed molecule and a crystal molecule is important.[14] Figure 14 shows an influence of rhodamine B adsorbed on the surface, on the photocurrent of a perylene monocrystal.

In the absence of illumination when the dye is adsorbed on the surface of a crystal consisting of a molecule R, the molecules of the adsorbate and adsorbent are mainly in the ground state ($^1D_0 \cdots {}^1R_0$). During illumination and absorption by the dye, there occurs an excitation of the dye molecules $^1D_0$:

$$(^1D_0 \cdots {}^1R_0) + h\nu \rightarrow (^1D_* \cdots {}^1R_0) \tag{8.1}$$

which may lead to a generation of holes:

$$(^1D_* \cdots {}^1R_0) \rightarrow (D^- \cdots {}^1R_0) + p \tag{8.2}$$

or the triplet excitons in a crystal:

$$(^1D_* \cdots {}^1R_0) \rightarrow (^1D_0 \cdots {}^3R_*) \tag{8.3}$$

whose recombination gives rise to a decelerated fluorescence:

$$2^3R_* \rightarrow {}^1R_* + {}^1R_0 \rightarrow 2{}^1R_0 + h\nu \tag{8.4}$$

To obtain an effective occurrence of the process (7.7), it is necessary that the field draw off the holes from the surface. The storage of D^- is prevented by means of a space reaction with the oxidant Ox:

$$D^- + Ox \rightarrow D + Red \tag{8.5}$$

In fact, the above consideration represents a simplified description of the process. No account is taken of the interaction of the sensitizer adsorbed molecules with each other and with the crystal surface. If there exists an attractional interaction of the adsorbed molecules of rhodamine B, it would lead to the appearance of dimeric and polymeric forms at the surface. As a result, a spectrum of the photosensitized photocurrent would not coincide with the absorption spectrum of the individual molecules of rhodamine B.[9,14,31]

7.3.97 B 16

9. Conclusion

Electron-exchange reactions and electrochemical transformations with exciton participation are known to proceed both in insulators and semiconductor electrodes. But the particular features of these processes are seen most vividly with the help of insulating electrodes. An understanding of these processes seems to be important for electrochemical interpretation in biology. One can assert with assurance that the electron-exchange properties of biological membranes are not rare in living nature but are the basis of such fundamental processes are respiration in animals or the utilization of light energy by plants.

From the physicochemical standpoint, a membrane, through which an electron is transmitted, may be easily represented as an insulating layer separating two phases with oxidation–reduction systems which interact with different sides of the membrane. Thus to understand the processes of electron transfer through biomembranes, it is necessary to investigate and to understand the processes occurring at the insulator/electrolyte interface.

An electrochemical interpretation of the photosynthesis process assumes that the light absorbed by the photosynthetic pigments in the membranes of chloroplasts is used effectively in redox reactions with resulting oxidation of water accompanied by oxygen evolution and reduction of pyridinnucleotides.

A study of photoeffects from metallic electrodes in solution showed that a transformation of quantum energy into chemical energy proceeds with rather low efficiency. A much higher efficiency of the process can be achieved by illuminating semiconductor electrodes of the type TiO_2.[7,8,14] But such semiconductors produce electron–hole pairs due to a direct excitation of electrons. Mean while, a study of the electrophysical properties of insulating films of chlorophyll indicates that these films are close to molecular organic insulators, such as phthalocyanines or aromatic hydrocarbons, e.g., anthracene.

References

1. H. Kallman and M. Pope, *Nature* **188**, 935–936 (1960).
2. H. Kallman and M. Pope, *J. Chem. Phys.* **32**, 300–301 (1960).
3. H. Kallman and M. Pope, *Rev. Sci. Instrum.* **29**, 993–994 (1958).
4. M. Mehl and F. Lohman, *Electrochem. Acta* **13**, 1459–1467 (1968).
5. W. Mehl, J. M. Hale, and F. Lohman, *J. Electrochem. Soc.* **113**, 1166–1174 (1966).
6. W. Mehl, *Ber. Buns. Ges. Phys. Chem.* **69**, 583–589 (1965).
7. H. Gerischer, *Ber. Buns. Ges. Phys. Chem.* **77**, 772–782 (1973).
8. H. Gerischer, "Semiconductor electrochemistry," in *Physical Chemistry—An Advanced Treatise*, Vol. 9a, H. Eyring, D. Henderson, and W. Jost, eds., Academic Press, New York (1970) pp. 463–542.
9. H. Gerischer, "Photochemistry of adsorbed species," *Faraday Discuss Chem. Soc.* **58**, 219–236 (1974).
10. R. Memming and F. Möllers, *Ber. Buns. Ges. Phys. Chem.* **76**, 475–481 (1972).
11. R. R. Dogonadze, A. M. Kuznezov, and Ju. A. Chizmadgev, *Zh. Phizi Ch. Chimyia* **38**, 1195–1202 (1964).

12. V. G. Levich, in *Advances in Electrochemistry and Electrochemical Engineering*, Vol. 6, P. Delahay, ed., Interscience, New York (1967), pp. 249–371.
13. W. Mehl and J. M. Hale, "Insulator Electrode Reaction," in *Advances in Electrochemistry and Electrochemical Engineering*, Vol. 6, P. Delahay and C. W. Tobias, eds., Interscience, New York (1967), pp. 399–458.
14. H. Gerischer and F. Willig, "Reaction of excited dye molecules at electrodes," in *Topics in Current Chemistry*, Vol. 61, Springer-Verlag, Berlin (1976), pp. 31–84.
15. L. I. Boguslavsky and B. T. Lozhkin, *Electrochem. Acta* **17**, 1007–1026 (1972).
16. L. I. Boguslavsky and B. T. Lozhkin, *Surface Sci.* **38**, 413–432 (1973); **38**, 413–432 (1973).
17. V. A. Mjamlin and Yu. V. Pleskov, *Elektrokhimiya Poluprovodnikov*, Nauka, Moskow (1965) (in Russian).
18. M. Green, "Electrochemistry of the semiconductor electrolyte interface," in *Modern Aspects of Electrochemistry*, Vol. 2, J. O'M. Bockris, ed., Butterworths, London (1959), pp. 373–707.
19. S. Glesston, *Vvedenie v Elektrokhimiyu*, Inostran. Literature, Moskow (1951) (in Russian).
20. L. I. Boguslavsky, *Elektrokhimiya* **3**, 894–900 (1968) (in Russian).
21. K. Kawasaki, K. Kanou, and M. Ilizuki, *Surface Sci.* **5**, 263–266 (1966).
22. R. C. Jarnagin, J. Gilliland, Jr., and J. S. Kim, *J. Chem. Phys.* **39**, 573–579 (1963).
23. R. Matejec, *Ber. Buns. Ges. Phys. Chem.* **68**, 964–972 (1964).
24. A. Rose, *Concepts in Photoconductivity and Applied Problems*, Interscience, New York (1963).
25. W. Mehl and W. Büchner, *Kristallen Z. Phys. Chem.* **47**, 76–88 (1965).
26. W. Mehl, "Reaction at organic semiconductors," in *Reactions of Molecules at Electrodes*, N. S. Hush, ed., Interscience, New York (1971).
27. W. Mehl, J. M. Hale, and J. S. Drary, *Ber. Buns. Ger. Phys. Chem.* **73**, (1969) 855–859.
28. A. A. Khatiashvili and L. I. Boguslavsky, *Elektrokhimiya* **11**, (1975) 1635–1639 (in Russian).
29. V. M. Fridkin and I. S. Zholudev, *Fotoelektrety in Elektrofotograficheskiy protsess*, Izd AN SSSR, Moskow (1960) (in Russian).
30. V. V. Eremenko and V. S. Medvedev. *Fiz. Tverd. Tela* **2**, 1572–1576 (1960).
31. H. Gerischer, M. E. Michel-Beyerle, F. Rebentrost, and H. Tributsch, *Electrochem. Acta* **13**, 1509–1515 (1968).
32. W. Mehl and J. M. Hale, "Charge Transfer Processes with Electronically Excited Anthracene Molecules," *Discuss Faraday Soc.* N45, 52–66 (1968).
33. J. W. Steketee and J. de Jonge, Photoconductance and spectral absorption of anthracene, *Philips Res. Report* **17**, 363–381 (1962).
34. J. M. Hale and W. Mehl, *Electrochem. Acta* **13**, 1483–1495 (1968).

8

The Adsorption of Organic Molecules

B. B. DAMASKIN and V. E. KAZARINOV

1. Introduction

The term "adsorption" usually refers to a phenomenon associated with a change in the concentration of the substance undergoing adsorption (adsorbate) near the interface, as compared with the concentration of this substance in the bulk of the phase. If the adsorbate concentration increases with decreasing distance to the interface, the adsorption is termed positive (curve 1 in Figure 1). Conversely, negative adsorption refers to a decrease in the concentration near the interface (curve 2 in Figure 1). Constant concentration up to the interface (line 3 in Figure 1) points to the absence of adsorption.

The adsorption from the gas phase is caused by interaction forces between the adsorbate molecules and the adsorbent surface. Adsorption from solution is a more complex case. It should be treated as a reaction of substitution of the solvent molecules. Finally, in the case of adsorption at the electrode/solution interface (electrosorption), an account should be taken also of the interaction of the solvent molecules and adsorbate particles present on the metal surface with the electric field in the double layer. Thus, in the latter case, adsorption is determined by three types of interactions: electrode–adsorbate, electrode–solvent, and adsorbate–solvent; the first two types depend strongly on the charge of the electrode surface.

B. B. DAMASKIN and V. E. KAZARINOV • Institute of Electrochemistry, Academy of Sciences of the USSR, Moscow V-71, Leninsky Prospekt 31, USSR.

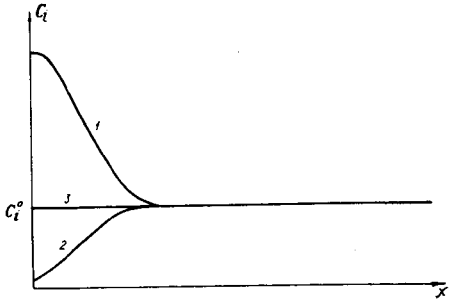


Figure 1. Schematic dependence of the ith component concentration on the distance to the interface: 1, at positive adsorption; 2, at negative adsorption; 3, in the absence of adsorption.

Often, in the case of adsorption of organic compounds on electrodes, adsorbate molecules retain their chemical individuality and exchange readily with the same molecules from the solution bulk. This adsorption is reversible and the thermodynamic laws of the surface phenomena are valid in its case.[1] On the other hand, in the case of very strong specific interaction of organic molecules with the electrode, surface compounds can be formed and adsorbed molecules can break down. Under such conditions, the equilibrium between the organic molecules in solution and the chemisorbed particles on the electrode surface is distrubed.[2-5] The methods of investigation and the phenomenology of this irreversible adsorption of organic compounds on electrodes differ significantly from those of reversible adsorption.[6]

2. Reversible Adsorption of Organic Substances

2.1. Qualitative Relationships of Reversible Adsorption of Organic Substances on Ideally Polarizable Electrodes

If the current supplied to the electrode surface is consumed only in charging the electric field in the double layer, the electrodes are ideally polarizable. As a rule, the adsorption of organic substances on ideally polarizable electrodes is studied by measuring the electrocapillary and differential capacity curves; the electrocapillary method is applicable only to liquid electrodes. The first systematic measurements of electrocapillary curves in the presence of additions of various organic compounds were carried out by Gouy.[7]

Typical forms of electrocapillary curves in solutions of organic substances are given in Figure 2. The adsorption of organic substance decreases the surface tension γ; its maximum decrease is observed near the potential of zero charge ($E_{\sigma=0}$) in the supporting electrolyte solution (Figure 2a). As the electrode charge (σ) increases, the electric field in the double layer starts to draw in more polar water molecules, which eventually leads to desorption of organic molecules and to the coincidence of the γ, E curves for a pure supporting electrolyte solution and for a solution with an addition. If the adsorbed organic molecules contain

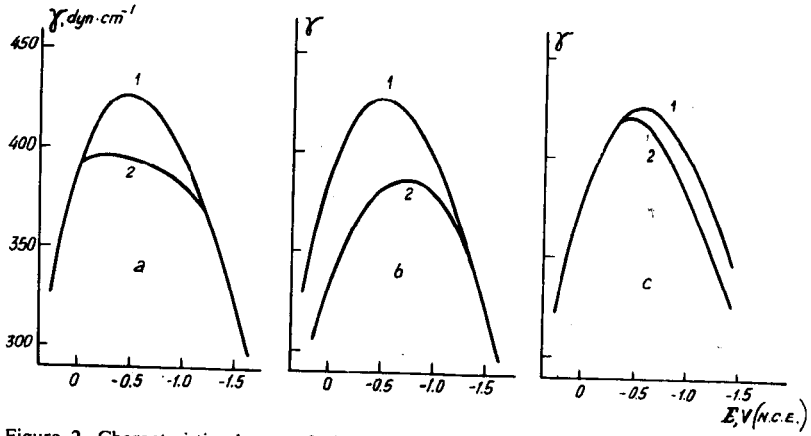


Figure 2. Characteristic shapes of electrocapillary curves: a, for adsorption of neutral aliphatic compounds; b, for the adsorption of aromatic and sulfur-containing compounds and also organic anions; c, for adsorption of organic cations (1, curves in supporting electrolyte solution 1 N Na_2SO_4; 2, curves with organic additions—*a*, 0.1 M n-$C_5H_{11}OH$; *b*, 1 M pyrogallol; c, 0.1 N $[(C_2H_5)_4N]OH$). (From Gouy.[7])

a system of π-electron bonds or a sulfur atom with an unshared electron pair, these electrons interact with the positive charges of the electrode surface at $\sigma > 0$, and the desorption of organic molecules is hindered (Figure 2b). Organic anions behave in the same manner. On the other hand, electrostatic attraction of the organic cations to the negatively charged electrode surface hinders their desorption at $\sigma < 0$ (Figure 2c). The shift of the electrocapillary maximum with respect to $E_{\sigma=0}$ in the supporting electrolyte solution is an indication of the orientation of the adsorbed dipoles of organic substance (or of ion pairs in the supporting electrolyte) on the uncharged electrode surface.

Beginning with the studies of Gouy,[7] measurements of electrocapillary curves have been widely used for investigation of the adsorption of numerous organic compounds on mercury. The experimental data published before 1971 have been summarized and systematized in a table by E. Horn, and this table takes up a quarter of the book by Jhering.[8] More recently, electrocapillary measurements have been carried out in connection with the investigation of the adsorption on a mercury electrode of esters, various amino acids, pyridine derivatives and some of its structural analogs, furan derivatives, cresol and cresolate anions, amides, some halogenated alcohols, nitriles and their halogen derivatives, aniline and its derivatives, coumarin, various organic sulfides and thiophene, camphor, borneol, and adamentanol, as well as different organic cations and anions.† A completely automatic, computer-controlled instrument

† From studies reported in 1971–1976 in the *Journal of Electroanalytical Chemistry*, *Electrochimica Acta*, and *Elektrokhimiya*.

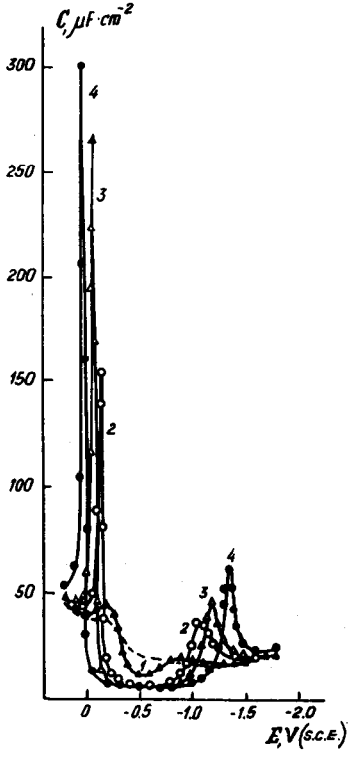


Figure 3. Differential capacity curves of a mercury electrode in 0.1 N Na_2SO_4 solution (dashed curve) and with 2-butanol additions in concentrations: 1, 0.05 M; 2, 0.2 M; 3, 0.4 M; 4, 1.4 M.

has been used for measuring the electrocapillary curves in the studies of 2-butanol adsorption on mercury.[9] Electrocapillary measurements on other liquid metals in the presence of organic substances has been very limited.[10–13] When passing from mercury to indium and thallium amalgams, and also to gallium, the shape of the γ–E curves hardly changes, but generally, the adsorbability of the organic substance decreases somewhat.

The typical shape of the differential capacity curves (C–E curves) in the presence of an organic substance (2-butanol) is shown in Figure 3. As was pointed out earlier, the organic substance is adsorbed near $E_{\sigma=0}$. Its adsorption is accompanied by a decrease of the dielectric constant of the double-layer ε and by an increase of the distance between the plates, δ. This results in a decrease of the integral capacity $K = \varepsilon/4\pi\delta$. At a sufficient distance from $\sigma = 0$, the organic substance is desorbed and K rises accordingly. The differential capacity being measured correlates with the integral capacity by the equation

$$C = K + (E - E_{\sigma=0})\frac{dK}{dE} \tag{2.1}$$

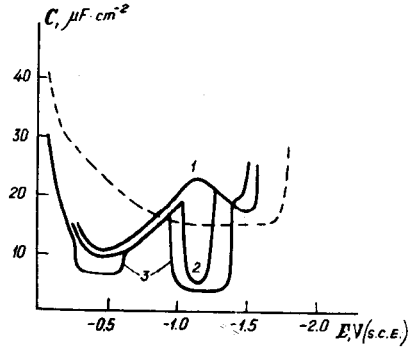


Figure 4. Differential capacity curves of a mercury electrode in 0.5 *M* NaF solution + 0.1 *M* phosphate buffer pH = 7 (dashed curve) and also with adenosine additions in concentrations: 1, 1.1×10^{-3} *M*; 2, 3.3×10^{-3} *M*; 3, 1.1×10^{-2} *M*. (From Vetter.[15])

The second term in this equation is greater than zero, which leads to the appearance of typical adsorption–desorption peaks on the *C–E* curves (Figure 3). The *C–E* curve of this shape in the presence of *n*-octyl alcohol was first obtained by Proskurnin and Frumkin.[14] It should be noted that the higher the adsorption–desorption peaks are, the larger is the value of dK/dE, i.e., the more drastically the organic substance is desorbed.

If the potential change involves a rearrangement of the double layer associated, for instance, with the reorientation of adsorbed organic molecules with formation or disruption of condensed films, etc., the corresponding changes of *K* in compliance with Eq. (1.1) lead to a more complex shape of the *C–E* curves. Under conditions, additional peaks or characteristic "pits" appear on the *C–E* curves[15] (Figure 4). Since the changes in the surface layer structure affect the shape of the γ–*E* curves to a lesser degree, differential capacity measurements prove to be more suitable for investigation of such structural effects.

Jehring's[8] table summarizes the differential capacity measurements carried out on a mercury electrode during the period from 1935 to 1970, using hundreds of organic substances. In more recent studies the differential capacity measurements often complemented electrocapillary studies of the adsorption of organic substances on mercury and were used for investigation of the adsorption on mercury of ketones, esters, adipic acid, coumarin, various organic cations, some high-molecular-weight compounds, and biologically active substances (DNA, nucleosides, steroids, cyclodextrins). Measurements of the *C–E* curves were also used for investigation of the coadsorption of two organic substances and for investigation of the influence of the supporting electrolyte on the adsorption of organic molecules and cations.†

Differential capacity measurements were also used for investigation of the adsorption of organic substances on other liquid and solid electrodes. The first measurements of this kind were performed by Borisova, Ershler, and Frumkin.[16]

† From studies reported in 1971–1976 in the *Journal of Electroanalytical Chemistry*, *Electrochimica Acta*, *Electrokhimiya*, and *Collection of Czechoslovak Chemical Communications*.

However, only when more perfect methods of purification of metals and preparation of smooth surfaces were developed did it become possible to study systematically the adsorption of organic substances on electrodes other than mercury. First, U. Palm and co-workers[17,18] investigated the adsorption on bismuth of a wide variety of aliphatic, aromatic, and heterocyclic compounds. In recent years, the C–E curves in solutions of different organic substances, primarily of aliphatic alcohols, were obtained for lead,[19,20] cadmium,[21,22] zinc,[23,24] tin,[25,26] thallium,[27] antimony,[28] indium,[29] silver,[30,31] and also for liquid electrodes from gallium,[11] thallium amalgam,[32] eutectic alloy In + Ga,[29,33] and alloy Ga + Tl.

As follows from a comparison of Figures 3 and 5, to a first approximation the C–E curves on solid electrodes in the presence of organic substances are similar to those on mercury. However, on most of the metals studied, it is possible to observe only cathodic adsorption–desorption peaks, since anodic peaks lie in the region of electrochemical dissolution of the electrode. On polycrystalline electrodes, the adsorption peaks on the C–E curves are lower and broader than those on single-crystal electrodes as the result of the energetics of the inhomogeneity surface.[23] In some cases of capacity measurements on polycrystalline electrodes, splitting of the adsorption–desorption peaks can be observed.[18,23] Figure 6 illustrates this phenomenon by the adsorption of propyl acetate on the surface of a polycrystalline bismuth electrode. The extreme right-hand cathodic peak practically coincides with the adsorption–desorption peak of propyl acetate on the (111) face of a Bi electrode. Thus the splitting of the adsorption peaks on the C–E curves points to the appearance on the electrode

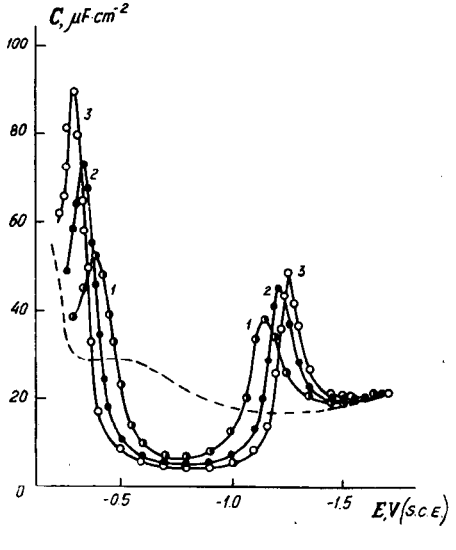


Figure 5. Differential capacity curves of a bismuth electrode in 1 N solution of the mixture K_2SO_4 + H_2SO_4 (dashed curve) and also with n-C_4H_9COOH additions in concentrations: 1, 0.04 M; 2, 0.06 M; 3, 0.08 M. (From Palm and Damaskin.[18])

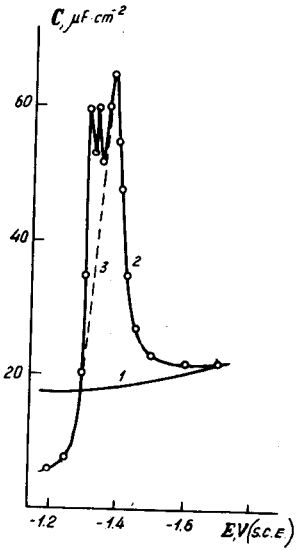


Figure 6. Cathodic sections of the differential capacity curves of a bismuth electrode in 1 N Na_2SO_4 solution (1) and with 0.06 M propyl acetate addition: 2, for polycrystalline bismuth; 3, for face (111) of bismuth single crystal. (From Palm and Damaskin.[18])

surface of crystallites with different orientations on their crystal faces. The fact that the splitting of the peaks on the C–E curves is observed for very few organic substances studied indicates that there must be a definite structural correspondence between the polycrystalline electrode surface and the organic molecule.

With a silver electrode, the heterogeneity of the polycrystalline surface is responsible for slow establishment of the adsorption equilibrium and possibly for partial irreversibility of the adsorption of organic substances.[30] At the same time, on the dislocation-free faces (100) and (111) of Ag single crystals, the adsorption behavior of aliphatic alcohols is similar to the data for the mercury electrode.[31] However, if growth steps appear on the surface of a single-crystal Ag electrode, in Na_2SO_4 solutions with aliphatic alcohol additions, the capacity increases in the region of maximum adsorption of organic substance and the peaks on the C–E curves move apart (Figure 7).[31] With increasing length of the growth steps, this effect is enhanced (Figure 7), but it disappears when NaF is used as a supporting electrolyte instead of Na_2SO_4.[31]

A comparison was made between the C–E curves on liquid and solid gallium in the presence of n-hexyl and n-amyl alcohols.[34,35] The results obtained depend strongly on the degree of purification both of metal and solution. The surface of very pure gallium, particularly in the solid state, seems to possess a higher chemical activity, which leads to significant differences in the shape of the C–E curves on liquid and solid electrodes.[35] On the other hand, measurements on a Ga electrode prepared from slightly impure metal showed that the

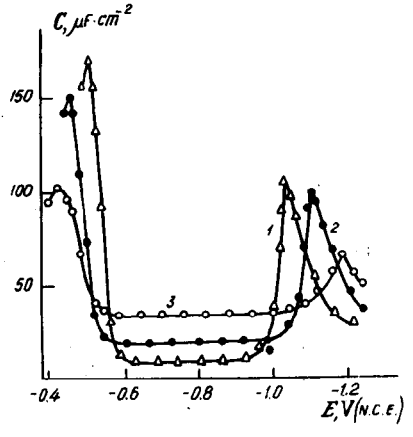


Figure 7. Differential capacity curves of a single-crystal silver electrode [face (100)] in 0.1 N Na_2SO_4 + 0.3 M n-$C_5H_{11}OH$ solution with different density of growth steps: 1, $L = 1.5 \times 10^4$ cm^{-1}; 2, $L = 5.9 \times 10^4$ cm^{-1}; 3, $L = 3 \times 10^5$ cm^{-1}. (From Vitanov and Popov.[31])

C–E curves in solutions with additions of n-$C_6H_{13}OH$ are not dependent on the aggregation state of the electrode.[34] Apparently, this is associated with the inactivation of the Ga electrode surface caused by the adsorption of surface-active impurities from the bulk of the metal phase.

2.2. Thermodynamics of Surface Phenomena in the Case of Adsorption of Organic Substances on an Ideally Polarizable Electrode

A thermodynamic treatment of an ideally polarizable electrode leads to an equation, given below, which relates the reversible surface work (in the case of liquid interfaces, the surface tension) at constant pressure and temperature to the electrode charge σ, the potential E, the surface excesses Γ_i, and the chemical potentials μ_i of different solution components[36]:

$$d\gamma = -\sigma\, dE - \frac{\sigma}{z_j F} d\mu_j - \sum_i \Gamma_i\, d\mu_i \tag{2.2}$$

Here, the subscript j stands for the solution component (ion) with respect to which the reference electrode is reversible and z_j is the charge of this ion (with its sign); F is the faraday. If the aqueous solution contains organic substances and 1,1-valent supporting electrolyte CA and the reference electrode is reversible with respect to the anion A^-, Eq. (2.2) takes the form

$$d\gamma = -\sigma\, dE_- - \Gamma_+\, d\mu_{CA} - \Gamma_{org}\, d\mu_{org} - \Gamma_{H_2O}\, d\mu_{H_2O} \tag{2.3}$$

When the conditions $E_- = \text{const}$ and $\mu_{CA} = \text{const}$ are valid, we have

$$-\left(\frac{\partial\gamma}{\partial\mu_{org}}\right)_{E_-,\mu_{CA}} = \Gamma_{org} + \Gamma_{H_2O}\left(\frac{\partial\mu_{H_2O}}{\partial\mu_{org}}\right)_{E_-,\mu_{CA}}$$

$$= \Gamma_{org} - \Gamma_{H_2O}\frac{N_{org}}{N_{H_2O}} = \Gamma_{org}^{(H_2O)} \tag{2.4}$$

where N_{org} and N_{H_2O} are the mole fractions of organic substance and water. The experimentally determinable quantity, $\Gamma_{org}^{(H_2O)}$, is called the relative surface excess. The absolute surface excesses, Γ_{org} and Γ_{H_2O}, cannot be determined without additional model assumptions.[37]

The relative surface excess differs from the surface concentration, i.e., from the number of the adsorbate molecules directly bound on the unit electrode surface, though both these quantities have the same dimensions (e.g., mol/cm^2). The most significant differences arise at high adsorbate concentrations when the dividing Gibbs plane, corresponding to the condition $\Gamma_{H_2O} = 0$, shifts significantly from the interface.[37,38] In the case of positive adsorption, this shift is in the direction of the solution,[37] and the physical sense of $\Gamma_{org}^{(H_2O)}$ can be expressed by the area of the shaded figure on the diagram in Figure 8a. With decreasing organic substance concentration, the Gibbs plane approaches the electrode surface, and the value of $\Gamma_{org}^{(H_2O)}$ is determined by the area of the shaded figure in Figure 8b. Only when the whole excess of organic substance is localized within one monolayer and $N_{org} \ll N_{H_2O}$, is the value of $\Gamma_{org}^{(H_2O)}$ nearly equal to the surface concentration of the organic substance (Figure 8c). These conditions, however, are not always satisfied, and thus the curves of the dependence of $\Gamma_{org}^{(H_2O)}$ on c_{org} can show maxima and minima[38] in spite of the fact that the dependence of surface concentration upon c_{org} is characterized by a typical curve tending to the limit corresponding to complete surface coverage with adsorbate.

To maintain the condition $\mu_{CA} = \text{const}$, required by Eq. (2.4), it is possible to use either CA solutions saturated with respect to salt,[38] or to control the constancy of μ_{CA} by measuring the potential of a cell with electrodes reversible with respect to C^+ and A^-.[39,40] Simultaneously for strictly thermodynamic calculations of $\Gamma_{org}^{(H_2O)}$ it is necessary to measure independently the activity a_{org} in the solutions studied. Owing to the difficulties involved in simultaneous determinations of the activity of the salt and of the organic substance in solution, the strictly thermodynamic studies of the adsorption of organic substances which have been carried out so far are few in number. Such studies have been made for the adsorption on a mercury electrode of ethyl alcohol with NaCl and NH_4Cl as supporting electrolytes,[38] acetone with HCl as the supporting electrolyte,[39] and also of secondary and tertiary butyl alcohols with Na_2SO_4 as the supporting electrolyte.[9,40] Such strictly thermodynamic calculations can be performed only for liquid electrodes, for which direct measurements of surface tension are possible.

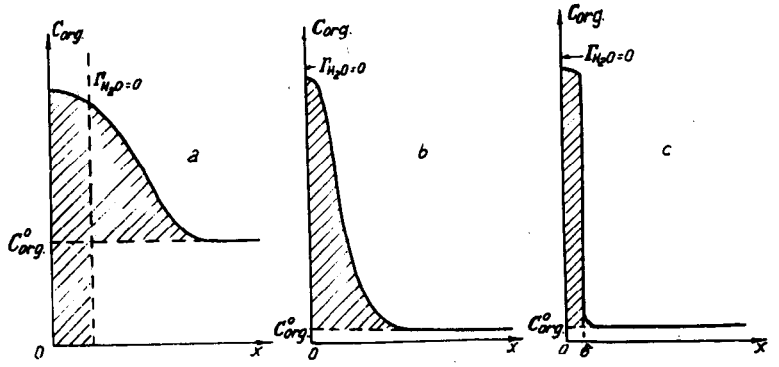


Figure 8. Possible types of the dependence of organic substance concentration on distance to the interface, explaining the physical sense of the relative surface excess (hatched areas) under different conditions: a, large volume concentration of organic substance; b, small volume concentration organic substance; c, small volume concentration of organic substance with its excess localized within the monolayer of thickness δ.

In most studies of the adsorption of organic substances on electrodes in which the Gibbs equation is used, measurements have been carried out in solutions with constant electrolyte concentration, c_{el} = const, differentiation of γ has been performed with respect to ln c_{org}, and the potential has been measured against a constant reference/electrode connected with the experimental solution by an electrolytic bridge of saturated KCl solution.[6,8,41,42] This method of processing experimental data is approximate and the quantity being determined is

$$\Gamma^*_{org} = -\frac{1}{RT}\left(\frac{\partial\gamma}{\partial \ln c_{org}}\right)_{E,c_{el}} \tag{2.5}$$

It differs from the relative adsorption $\Gamma^{(H_2O)}_{org}$.

On the basis of Eqs. (2.2)–(2.5), it is possible to obtain a formula relating Γ^*_{org} to $\Gamma^{(H_2O)}_{org}$ in the presence of a 1,1-valent supporting electrolyte:

$$\Gamma^*_{org} = (\Gamma_- - \Gamma_+)\left(\frac{\partial \ln f_-}{\partial \ln c_{org}}\right)_{c_{el}} + 2\Gamma_+\left(\frac{\partial \ln f_\pm}{\partial \ln c_{org}}\right)_{c_{el}} + \Gamma^{(H_2O)}_{org}\left[1 + \left(\frac{\partial \ln f_{org}}{\partial \ln c_{org}}\right)_{c_{el}}\right]$$

$$\approx \Gamma^{(H_2O)}_{org} + \Gamma^{(H_2O)}_{org}\left(\frac{\partial \ln f_{org}}{\partial c_{org}}\right)_{c_{el}} c_{org} + (\Gamma_+ + \Gamma_-)\left(\frac{\partial \ln f_\pm}{\partial \ln c_{org}}\right)_{c_{el}} \tag{2.6}$$

where f_i are the activity coefficients.

The second approximate equation in Eq. (2.6) assumes $f_- \approx f_\pm$. Thus the relative error in the substitution of $\Gamma^{(H_2O)}_{org}$ by Γ^*_{org} is

$$\frac{\Gamma^*_{org} - \Gamma^{(H_2O)}_{org}}{\Gamma^{(H_2O)}_{org}} = \left(\frac{\partial \ln f_{org}}{\partial c_{org}}\right)_{c_{el}} c_{org} + \frac{\Gamma_+ + \Gamma_-}{\Gamma^{(H_2O)}_{org}}\left(\frac{\partial \ln f_\pm}{\partial c_{org}}\right)_{c_{el}} c_{org} \tag{2.7}$$

The error due to the second term on the right side of Eq. (2.7) at the experimentally used concentrations is small and can be neglected to the first approximation.[43,44] More important is the error due to the term $(\partial \ln f_{org}/\partial c_{org})_{c_{el}c_{org}}$.[40] Since $(\partial \ln f_{org}/\partial c_{org})_{c_{el}} < 0$, at large organic substance concentrations, the value of Γ^{*}_{org} may prove to be much less than that of $\Gamma^{(H_2O)}_{org}$.[40]† However, in the region of high c_{org}, in which these effects arise, the physical sense of $\Gamma^{(H_2O)}_{org}$ usually does not coincide with the notion of surface concentration (Figure 8a), which complicates the interpretation of the $\Gamma^{(H_2O)}_{org} - a_{org}$ isotherms. For example, such isotherms for secondary butyl alcohol are given in Figure 9. It would seem that the rise on these curves at large a_{org} should point either to formation of a second adsorbate layer, or, as Nakadomari et al.[9] believe, to a change in the orientation of adsorbed molecules which would be accompanied by increase of their surface concentration due to increase of the monolayer thickness. In both cases, a decrease in the double-layer capacity would be expected in the region of increasing $\Gamma^{(H_2O)}_{org}$, which, however, is not the case, as follows from Figure 3. Thus a suggested conclusion is that the observed increase of $\Gamma^{(H_2O)}_{org}$ does not correspond to the increase of the surface concentration of secondary butyl-alcohol.‡

The measurements carried out at c_{el} = const allow the extension of the approximate thermodynamic method of investigation of the adsorption of organic molecules to solid electrodes. In fact, when constant supporting electrolyte concentrations are used in the region of sufficiently large negative E, in which organic molecules are desorbed under the action of the electric field, differential capacity curves (the C, E curves) measured in the presence of organic substance additions, coincide with the C–E curve in a pure supporting electrolyte

† Consideration was given to the error $(\partial \ln f_{org}/\partial c_{org})_{a_\pm c_{org}}$, associated with the substitution of a_{org} by c_{org} not at c_{el} = const, but $a_\pm$ = const.[40] Since

$$\left(\frac{\partial \ln f_{org}}{\partial c_{org}}\right)_{c_{el}} = \left(\frac{\partial \ln f_{org}}{\partial c_{org}}\right)_{a_\pm} - \left(\frac{\partial \ln f_{org}}{\partial c_{el}}\right)_{c_{org}} \left(\frac{\partial c_{el}}{\partial c_{org}}\right)_{a_\pm} \tag{2.8}$$

and $(\partial \ln f_{org}/\partial c_{el})_{c_{org}} > 0$, $(\partial c_{el}/\partial c_{org})_{a_\pm} < 0$, the derivative $(\partial \ln f_{org}/\partial c_{org})_{c_{el}}$ has a less negative value than the derivative $(\partial \ln f_{org}/\partial c_{org})_{a_\pm}$. In other words, the error in the value of Γ_{org} being determined, which is due to the substitution of a_{org} by c_{org} at c_{el} = const, is less than at $a_\pm$ = const.

‡ Nakadomari *et al.*[9] consider that in all cases the true surface concentration of the organic substance can be calculated if Eq. (2.4) is complemented by the relation

$$s_{org}\Gamma_{org} + s_{H_2O}\Gamma_{H_2O}/L = 1 \tag{2.9}$$

where s_{org} and s_{H_2O} are the areas per mole of adsorbed organic molecules and water, respectively, and L is the number of aqueous monolayers corresponding to a monolayer of organic substance. However, as follows from Figure 8, this conclusion is valid only under the condition that the whole surface excess of organic substance is localized within one monolayer. Apparently, at high 2-butanol concentrations (as at high ethanol concentration)[38] this condition is not fulfilled and the physical sense of Γ_{org}, found by solving the set of Eqs. (2.4) and (2.9), does not correspond to the surface concentration of the organic substance.

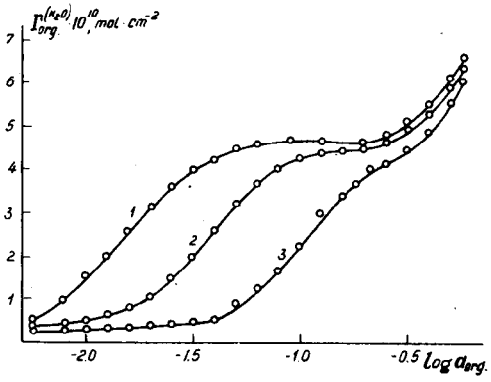


Figure 9. Adsorption isotherms of 2-butanol on a mercury electrode from constant activity Na_2SO_4 solutions ($a_\pm = 0.07$): 1, at the potential of maximum adsorption ($E = E_m$); 2, at $E = E_m - 0.35$ V; 3, at $E = E_m - 0.55$ V. (From Nakadomari *et al.*[9])

solution (Figures 3 and 5).† Thus, by using the reverse integration method (from the potential of the merging of the C–E curves), it is possible to obtain a series of the σ–E curves, and then a series of electrocapillary curves in the presence of different organic substance additions (accurate to a common constant). Figures 5, 10 and 11 illustrate this by the adsorption of *n*-valeric acid on a Bi electrode.

According to the described method, the electrocapillary curves are obtained with an accuracy of a common constant (e.g., γ_0^{max}), $d(\gamma - \gamma_0^{max}) = d\gamma$; and hence, by means of Eq. (2.5), it is possible to calculate the adsorption isotherm $\Gamma^*_{org} - c_{org}$ for a solid electrode. However, another method has found wider use, namely, the plotting of a two-dimensional isotherm, $\Delta\gamma - \log c_{org}$, where $\Delta\gamma$ is the decrease of the reversible surface work at a given E or at $\sigma = 0$, caused by adsorption of the organic substance. This method does not require graphic differentiation, eliminates errors associated with the dependence of f_{org} on c_{org}, and at the same time allows comparison of the surface activity of organic substances at different interfaces. As shown for the first time by Frumkin,[46,47] the comparison of two-dimensional pressure isotherms at the metal/solution (at $\sigma = 0$) and solution/air interfaces reveals the specific features of the interaction of adsorbed molecules with the electrode surface. Additional information on this interaction can be obtained also by comparing the adsorption potential ΔE at the relevant interfaces. At the electrode/solution interface, the quantity ΔE_{Me} represents the shift of the potential of zero charge caused by the organic substance adsorption: $\Delta E_{Me} = E_{\sigma=0}^{(\Gamma)} - E_{\sigma=0}^{(\Gamma=0)}$; at the solution/air interface $\Delta E = \chi^{(\Gamma=0)} - \chi^{(\Gamma)}$, where χ is the surface potential of the solution.

The relative positions of two-dimensional pressure isotherms characterize the change in the adsorption energy $\Delta(\Delta G_a)$ when passing from one system to another; the adsorption energy is larger in the system in which the same value

† In the case of measurements at $a_\pm = \text{const}$, different organic substance concentrations correspond to different c_{el}, and therefore in the region of organic substance desorption the C–E curves (and also the σ–E and γ–E curves) do not coincide.[9,40,45]

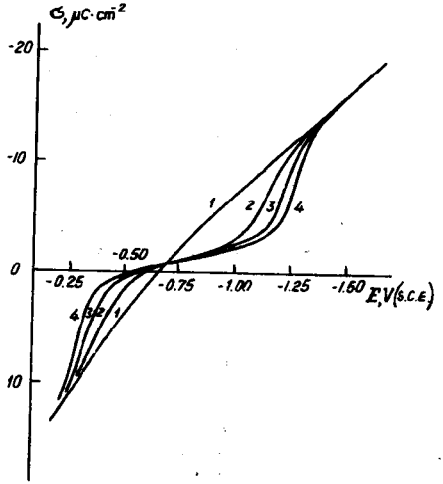


Figure 10. Charging curves of a bismuth electrode (obtained by inverse integration of the C–E curves) in the solution of 1 N mixture of K_2SO_4 + H_2SO_4 (1) and also with n-C_4H_9COOH additions in concentrations: 2, 0.04 M; 3, 0.06 M; 4, 0.08 M. (From Palm and Damaskin.[16])

of $\Delta\gamma$ is reached at a lesser organic substance concentration. To a first approximation at given $\Delta\gamma$ = const,

$$\Delta(\Delta G_a) = RT \ln (c'_{org}/c''_{org}) \qquad (2.10)$$

At the solution/air interface, the adsorption energy of the organic substance ΔG_a is defined by a "squeezing out" effect, i.e., the energy gain due to the restoration of the bonds between the solvent molecules (in aqueous solutions

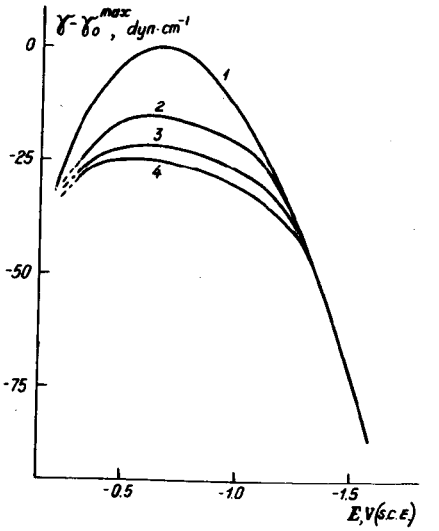


Figure 11. Electrocapillary curves of a bismuth electrode (obtained by inverse integration of the σ–E curves) in the solution of 1 N mixture of K_2SO_4 + H_2SO_4 (1) and also with n-C_4H_9COOH additions in concentrations: 2, 0.04 M; 3, 0.06 M; 4, 0.08 M. (From Palm and Damaskin.[16])

primarily the hydrogen bonds) upon transition of an organic molecule from solution bulk to the surface. At the solution/metal interface, the organic substance adsorption is accompanied also by displacement of adsorbed solvent molecules. Therefore, here the value of ΔG_a, aside from the "squeezing out" effect, is determined also by the difference in the energies of interaction of adsorbate and solvent molecules with the metal surface. With neutral organic molecules, this difference is characterized by the value of $\Delta(\Delta G_a)$, calculated by means of Eq. (2.10), in which the quantities c'_{org} and c''_{org} refer to the solution/metal and solution/air interfaces, respectively.

For aliphatic alcohols, acids and amines with one functional group, the decreases of γ at the solution/mercury and solution/air interfaces are the same to the first approximation[48] (curves 1 and 1′ in Figure 12). This means that the energy of interaction of uncharged mercury with these compounds is compensated for by the energy of interaction of mercury with water: $\Delta G_{Hg-org} \approx \Delta G_{Hg-H_2O}$. However, perfluorinated aliphatic compounds in the same concentration prove to be less active at the solution/mercury interface[48] (curves 2 and 2′ in Figure 12). Thus the interaction of these compounds with the mercury surface is weaker and cannot compensate for that of mercury with water molecules. On the other hand, when passing to chlorine- and bromine-substituted compounds $|\Delta G_{Hg-org}| > |\Delta G_{Hg-H_2O}|$ and the surface activity of these compounds at the interface with mercury is significantly higher than on the free solution surface.[46,47] A similar result is observed for thiocompounds and for aliphatic compounds with several functional groups.[46,47,49]

In comparing the adsorption behavior of aromatic and hydroaromatic compounds at the solution/mercury and solution/air interfaces, Gerovich[50,51] was the first to establish the existence of π-electron interaction between organic molecules containing π bonds and the mercury surface. At the mercury/solution

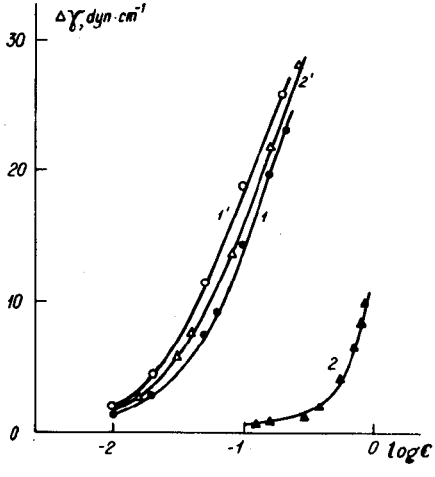


Figure 12. Two-dimensional isotherms for adsorption of butyric acid (1 and 1′) and perfluorinated butyric acid (2 and 2′) on free solution surface (1′ and 2′) and on uncharged mercury surface (1 and 2). Supporting electrolyte: 1 N Na_2SO_4. (From Frumkin and Damaskin.[48])

interface, the surface activity of these compounds is also higher than at the interface with air. This is explained by the flat orientation of organic molecules in which case π electrons cause an increase in the adsorption energy due to the donor–acceptor interaction. Here, a certain role is played by the interaction of the polar group with the electrode. Curves 1 and 1′ in Figure 13 illustrate the two-dimensional pressure isotherms at the solution/mercury and solution/air interfaces in the presence of phenol. When passing from phenol to perfluorophenol, π electrons are drawn away by fluorine atoms and the π-electron interaction decreases.[52]

In the case of organic ions, the difference in the adsorption behavior at the solution/metal and solution/air interfaces, in addition to the reasons mentioned earlier, is due to the effect of image forces. If the solution is considered to be a continuum with dielectric constant ε_1, in accordance with the laws of electrostatics, the force F, acting on the ion with the charge $z_i e_0$ at the distance x from the interface with the other phase which has the dielectric constant ε_2, can be calculated from the equation

$$F = \frac{z_i^2 e_0^2}{4x^2} \frac{\varepsilon_1 - \varepsilon_2}{\varepsilon_1(\varepsilon_1 + \varepsilon_2)} \tag{2.11}$$

At the interface with air, $\varepsilon_2 = 1$ and hence $F > 0$, i.e., image forces hinder the adsorption of ions at this interface. On the other hand, at the metal/solution interface $\varepsilon_2 \to \infty$, $F < 0$, and the image forces favor positive ion adsorption. Thus the difference in the surface activity of organic ions at the solution/air and solution/metal interfaces can be due to a large degree to the effect of the image

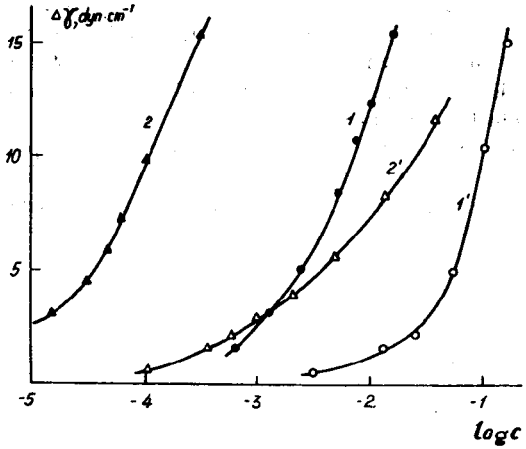


Figure 13. Two-dimensional pressure isotherms for adsorption of phenol (1 and 1′) and tetrabutylammonium cations (2 and 2′) on free solution surface (1′ and 2′) and on uncharged mercury surface (1 and 2). Supporting electrolyte: 1 N Na_2SO_4. (From Frumkin and Damaskin[48]; Damaskin *et al.*[53])

Table 1
Change in the Adsorption Energy of Some Organic Compounds When Passing from the Solution/Air Interface to the Solution/Bismuth and Solution/Mercury Interfaces ($\Delta\gamma \leqslant 5$ dyne/cm)

Compound	$-\Delta(\Delta G_a)$ (kcal/mole)	
	Bi	Hg
Benzene	0.0	0.5
Toluene	0.4	0.7
Phenol	1.0	1.8
Aniline	1.2	2.5
o-Toluidine	1.5	2.2
p-Toluidine	1.3	2.0
Benzoic acid	1.3	1.7
Pyrocatechol	1.8	2.7
Resorcin	2.4	2.9
Hydroquinone	2.8	3.7
Pyridine	0.6	0.9

forces. The experimental data[53] confirm this conclusion (curves 2 and 2′ in Figure 13).

The two-dimensional pressure isotherms for a number of aromatic compounds at the solution/bismuth and solution/air interfaces are compared.[17,18] Table 1 lists some of the values of $\Delta(\Delta G_a)$ at $\Delta\gamma \leqslant 5$ dyne/cm calculated by means of Eq. (2.10) for the transition from the interface with air to the solution/Bi or solution/Hg interfaces. As seen from the table, the values of $|\Delta(\Delta G_a)|$ for mercury are 0.3–1.3 kcal/mol higher than for bismuth. One of the reasons for a lower surface activity of organic compounds on bismuth is a stronger adsorption of water molecules on bismuth than on mercury.† Account should be also taken of the semiconductor nature of the Bi electrode, which is responsible for decreased π-electron interaction of molecules of aromatic compounds with the bismuth surface.[17,18] When passing to a Cd electrode, which has even stronger hydrophilic properties, the surface activity of organic compounds becomes lower than for bismuth.[21,22] This is clearly illustrated in Figure 14 by the two-dimensional pressure isotherms for aniline.

As the comparison of two-dimensional pressure isotherms characterizes the difference in the adsorption energies of the organic compounds investigated at different interfaces, the structure of the surface layer and primarily the orientation of adsorbed molecules can be assessed from the values of the adsorption potential, ΔE. Thus, for instance, the positive values of ΔE are usually associated with the orientation of organic molecules in which the

† As follows from the comparison of the data on the adsorption on mercury and bismuth of simple aliphatic compounds (alcohols, acids, ketones), the interaction energy of bismuth with water is 0.3–0.4 kcal/mol greater than that of mercury with water.[17,18]

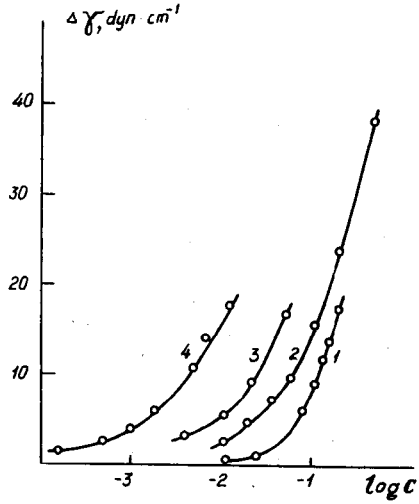


Figure 14. Two-dimensional pressure isotherms for adsorption of aniline on free solution surface (1) and also on uncharged cadmium (2), bismuth (3), and mercury (4) surface. Supporting electrolyte: 0.1 *N* surface-inactive electrolyte solution. (From Rybalka *et al.*[22])

negative dipole end is directed toward the solution.[6,46–48,54,55] A certain contribution to the positive side of ΔE can also be made by the displacement from the surface layer of the water dipoles oriented with their positive end toward the solution. However, it does not seem possible to ascribe only to this effect the experimentally observed values of $\Delta E > 0$.[54,55] The negative values of ΔE point either to the orientation of the adsorbed dipoles of organic molecules with their positive ends toward the solution, or to the shift of π electrons in the direction of metal in the case of flat orientation of the molecules of aromatic or heterocyclic compounds. Since the π electron interaction is absent at the solution/air interface, the positive value of ΔE (at $\Delta\gamma$ = const or at Γ = const), as a rule, changes sign or decreases sharply at transition to the solution/metal interface. A more detailed consideration of the dependences of ΔE on Γ (or on $\Delta\gamma$) at the solution/air and solution/metal interfaces requires, however, some model assumptions about the structure of the adsorption layer.

2.3. Phenomenological Description with the Use of Macromodels of the Reversible Adsorption of Organic Substances on Electrodes

In developing macromodels of the surface layer, it is assumed that under the conditions of constant supporting electrolyte concentration (c_{el} = const), the electrode potential,† its charge and also the bulk and surface concentrations of organic substance‡ are related by two equations

$$f_1(\phi, \sigma, \theta) = 0 \tag{2.12}$$

† The electrode potential can be conveniently referred to the potential of zero charge in the supporting electrolyte solution $\phi = E - E_{\sigma=0}^{(\gamma=0)}$, so that $d\phi = dE$.

‡ In what follows these shall be denoted by c and $\Gamma = \Gamma'_m\theta$, where θ is the relative surface concentration of the organic substance and Γ'_m is the value of Γ at $\theta = 1$.

and

$$f_2(\theta, c) = 0 \tag{2.13}$$

at ϕ = const or at σ = const.

Equation (2.13) is usually called the adsorption isotherm and Eq. (2.12) the surface layer model proper. For example, according to the two-parallel-capacitor model suggested by Frumkin[56] at ϕ = const

$$\sigma = \sigma_0(1 - \theta) + \sigma'\theta \tag{2.14}$$

where σ_0 is the electrode charge in the supporting electrolyte solution ($\theta = 0$), and σ' is the value of σ at $\theta = 1$. In accordance with Eq. (2.14), the electric double layer can be visualized as two capacitors connected in parallel, with only water molecules being present between the sides of one of these capacitors and only molecules of organic substance between the sides of the other. The electrostatic energies of the unit surface of a two-layer capacitor at given θ and at $\theta = 0$ are equal to $\int_{\sigma_{\phi=0}}^{\sigma} \phi\, d\sigma$ and $\int_{\sigma}^{\sigma_0} \phi\, d\sigma_0$, respectively. Since at ϕ = const, it is necessary during the adsorption process to remove from the unit surface of the capacitor sides the charge $(\sigma_0 - \sigma)$, which requires the work $(\sigma_0 - \sigma)\phi$, the electrostatic energy of adsorption per unit surface is

$$\int_{\sigma_{\phi=0}}^{\sigma} \phi\, d\sigma - \int_0^{\sigma_0} \phi\, d\sigma_0 + (\sigma_0 - \sigma)\phi$$

$$= \sigma\phi - \int_0^{\phi} \sigma\, d\phi - \sigma_0\phi + \int_0^{\phi} \sigma_0\, d\phi + (\sigma_0 - \sigma)\phi = \int_0^{\phi} (\sigma_0 - \sigma)\, d\phi$$

One mole of organic substance occupies the surface $1/\Gamma = 1/\Gamma_m\theta$, and thus the electrostatic energy of adsorption per 1 mole at a potential ϕ is

$$W_a = \frac{1}{\Gamma_m\theta} \int_0^{\phi} (\sigma_0 - \sigma)\, d\phi \tag{2.15}$$

In conjunction with Eq. (2.14), this gives

$$W_a = \frac{1}{\Gamma_m} \int_0^{\phi} (\sigma_0 - \sigma')\, d\phi \tag{2.16}$$

In other words, within the framework of the two parallel capacitors model, adsorption energy does not depend on Γ (or on θ), so that taking into account the Boltzmann equation, the adsorption isotherm can be written as

$$B(\phi)c = f(\theta) \tag{2.17}$$

where the adsorption equilibrium constant is

$$B(\phi) = B_0 \exp\left(-\frac{W_a}{RT}\right) = B_0 \exp\left[-\frac{1}{RT\Gamma_m} \int_0^{\phi} (\sigma_0 - \sigma')\, d\phi\right] \tag{2.18}$$

Adsorption isotherms obeying Eq. (2.17) are often considered congruent with the potential. Thus the two-parallel-capacitor model is equivalent to the assumption of the congruence of the adsorption isotherms with the electrode potential.

Another method of obtaining Eqs. (2.17) and (2.18) on the basis of the two-parallel-capacitor model is to combine Eq. (2.14) with the approximate form of the basic electrocapillarity equation:

$$d\gamma = -\sigma\, dE - RT\Gamma\, d\ln c \qquad (\text{at } c_{el} = \text{const}) \tag{2.19}$$

where Γ is assumed to be the surface concentration of the organic substance and not its surface excess (e.g., References 6 and 41). Since both methods lead to the same result, the following conclusion may be drawn: with respect to the model approach, the quantity Γ, calculated with the use of the approximate equation (2.19) [i.e., by means of Eq. (2.5)], is nearer physically to the surface concentration than to the strictly thermodynamic surface excess $\Gamma_{org}^{(H_2O)}$, determined by Eq. (2.4).

The second equation of Frumkin's model theory[56] [Eq. (2.13)] actually defines concretely the form of the function $f(\theta)$ in Eq. (2.17):

$$Bc = \frac{\theta}{1-\theta}\exp(-2a\theta) \qquad (\text{at } \phi = \text{const}) \tag{2.20}$$

This equation, which is known as Frumkin's isotherm, was first deduced[57] by introducing a correction into Langmuir's isotherm to take account of the intermolecular interaction of adsorbed particles. Thus, if the attraction constant $a > 0$, the attractive forces between adsorbate particles predominate; at $a < 0$ it is the repelling forces which predominate; and at $a = 0$ the attractive and repelling forces are mutually compensated. The applicability of the isotherm (2.20) for description of nonlocalized adsorption, which has sometimes been questioned,[58] has been maintained by Frumkin.[59]

Frumkin's theory, based on the combination of Eqs. (2.14) and (2.20) was used to describe the adsorption on a mercury electrode of *tert*-amyl alcohol from 1 N NaCl + x M *tert*-$C_5H_{11}OH$ solution.[56] It was assumed that

$$\sigma' = \int_{\phi_N}^{\phi} C'\, d\phi \approx C'(\phi - \phi_N) \tag{2.21}$$

where C' is the double-layer capacity at $\theta = 1$ and ϕ_N is the shift of the potential of zero charge when passing from $\theta = 0$ to $\theta = 1$. Then, the expressions for σ and $B(\phi)$ take the form

$$\sigma = \sigma_0(1-\theta) + C'(\phi - \phi_N)\theta \tag{2.22}$$

and

$$B(\phi) = B_0 \exp\left[-\frac{\Delta\gamma_0 + C'\phi(\phi_N - \phi/2)}{RT\Gamma_m^{\infty}}\right] \tag{2.23}$$

where $\Delta\gamma_0 = \int_0^{\phi} \sigma_0\, d\phi$.

Under conditions when the capacity C' is much less than the capacity in the supporting electrolyte solution C_0, the assumption $C' \approx$ const, which was contained in Eqs. (2.21)–(2.23), hardly affects the conclusion of the theory. Figure 15 illustrates good agreement between the calculated and experimental

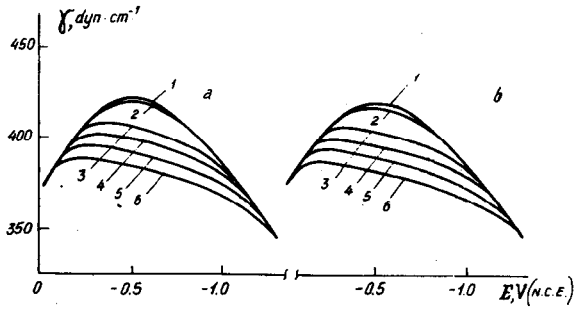


Figure 15. Electrocapillary curves, experimental (a) and calculated with the use of the two parallel capacitors model (b) of a mercury electrode in 1 *N* NaCl + *x M tert*-$C_5H_{11}OH$ solutions: 1, $x = 0$; 2, $x = 0.01$; 3, $x = 0.05$; 4, $x = 0.1$; 5, $x = 0.2$; 6, $x = 0.4$. (From Frumkin.[56])

γ–E curves in the system under consideration.[56] However, a similar comparison of the differential capacity curves, which are more sensitive to the changes in the surface layer structure, reveals considerable discrepancies between theory and experiment[6] (Figure 16).

In the Frumkin–Damaskin theory,[6,41,42] to take account of the deviations from the two-parallel-capacitor model, it was assumed that the quantity a in the isotherm (2.20) is not a constant but a certain function of ϕ: $a(\phi)$. Then, as can be readily shown,[6] instead of Eqs. (2.22) and (2.23), the following equations are obtained:

$$\sigma = \sigma_0(1 - \theta) + C'(\phi - \phi_N)\theta - RT\Gamma_m\theta(1 - \theta)\frac{da}{d\phi} \qquad (2.24)$$

$$B(\phi) = B_0 \exp\left[-\frac{\Delta\gamma_0 + C'\phi(\phi_N - \phi/2)}{RT\Gamma_m}\right] \exp(a_0 - a) \qquad (2.25)$$

where a_0 is the value of a at $\phi = 0$. Under the assumption of the dependence of a on ϕ, effectively complete agreement between the calculated and experimental C–E curves was obtained for the adsorption of simple aliphatic compounds (alcohols, acids, amines, ketones, esters) on electrodes from mercury, bismuth, lead, cadmium, tin, In + Ga, and Ga + Tl alloys and also on zinc single crystals.[6,18,19,21,23–25,33] Figure 17 shows the agreement between calculation and experiment for the case of adsorption of *n*-butyl alcohol on the face (0001) of a single-crystal Zn electrode.[24] Simultaneously, in these calculations the adsorption parameters (a_0, C', ϕ_N, Γ_m, B_0) are determined, which characterize the surface layer structure during adsorption of the organic compound being studied. On this basis it is possible to compare quantitatively the adsorption properties of different electrodes, in particular, the free adsorption energy ΔG_a at $\phi = 0$, related to B_0 by the expression $-\Delta G_a = RT \ln(55.5B_0)$.

In Table 2 the above-mentioned parameters are given for the adsorption of *n*-butyl alcohol on different electrodes. As follows from Table 2, according to

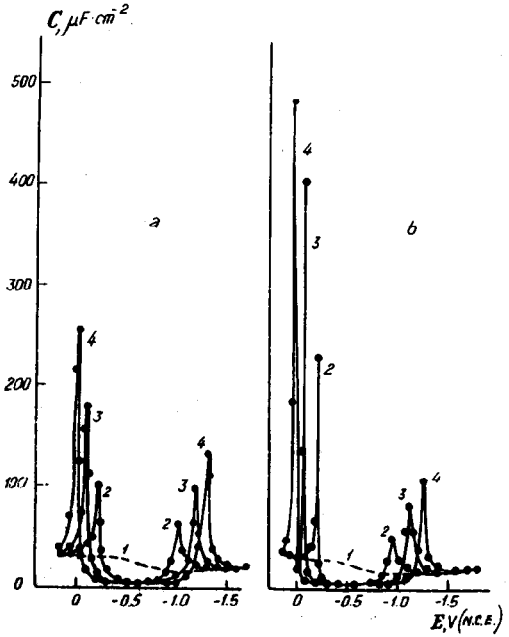


Figure 16. Differential capacity curves, calculated with the use of the two-parallel-capacitor model (a) and experimental (b), of a mercury electrode in 0.9 *N* NaF + *x M tert*-$C_5H_{11}OH$ solutions: 1, $x = 0$; 2, $x = 0.03$; 3, $x = 0.1$; 4, $x = 0.3$. (From Damaskin *et al.*[6])

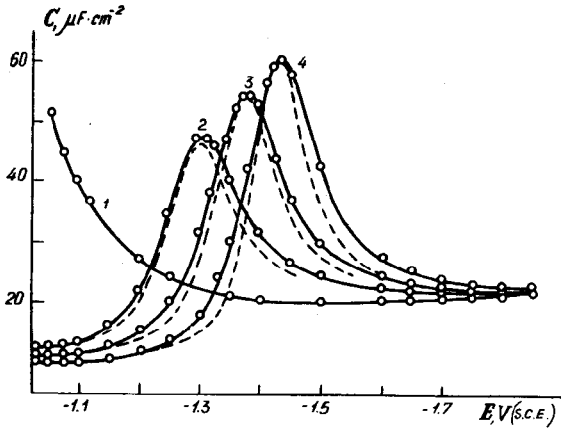


Figure 17. Differential capacity curves of a single-crystal zinc electrode [face (0001)] in acidfied (pH 3.7) 0.1 *N* KCl solution (curve 1) and also with *n*-C_4H_9OH additions in concentrations: 2, 0.3 *M*; 3, 0.5 *M*; 4, 0.7 *M*. Solid lines, experimental data; dashed lines, calculated with the use of the two-parallel-capacitor model. (From Ipatov *et al.*[24])

Table 2
Parameters Characterizing the Adsorption of n-Butyl Alcohols on Different Electrodes

Metal	a_0	C' (μF/cm^2)	ϕ_N (V)	$\Gamma_m \times 10^{10}$ (mol/cm^2)	B_0 (liter/mol)
Hg	1.28	4.8	0.24	5.18	11.2
Bi	1.18	4.8	0.27	5.25	7.2
Pb	1.20	4.9	0.24	4.80	10.0
Cd	1.32	7.2	0.15	5.75	3.1
Sn	1.20	5.1	0.25	5.07	8.2
In + Ga	1.25	5.4	0.25	4.95	5.8
Ga + Tl	1.30	3.9	0.29	4.86	4.9
Face(0001) Zn	1.50	9.4	0.10	6.17	2.9

the decrease in the adsorption energy of *n*-butanol (i.e., the value of B_0), the metals studied form the series Hg > Pb > Sn > Bi > In + Ga > Ga + Tl > Cd > Zn (0001), which parallels an increase in the hydrophilic properties of the metal surface.[60,61] For most of the electrodes studied, the parameters a_0, C', ϕ_N, and Γ_m depend little on the nature of the metal. Only in the case of the most hydrophilic metals (Cd and Zn) is there a marked increase of C' and Γ_m and a decrease of ϕ_N, which seems to be due to interaction of the metal with the OH group.[21]

The accuracy of the calculation of a_0, C', ϕ_N, Γ_m, and B_0 from the γ–E and C–E curves was statistically assessed.[62] Greater accuracy can be reached if these parameters are determined from differential capacity curves. On the other hand, in strictly thermodynamic calculations, electrocapillary measurements prove to be more convenient.[45]

If molecules of the organic substance can be adsorbed on the electrode surface in two positions (e.g., vertical, which predominates at $\sigma < 0$, and flat, which is due to the π-electron interaction predominant at $\sigma > 0$), the properties of the surface layer can be described by means of the three-parallel-capacitor model.[63] According to this model,

$$\sigma = \sigma_0(1 - \theta_1 - \theta_2) + C_1\theta_1(\phi - \phi_{N_1}) + C_2\theta_2(\phi - \phi_{N_2}) \qquad (2.26)$$

where θ_1 and θ_2 are the surface fractions covered by organic substance molecules in positions 1 and 2, respectively; C_i are the double-layer capacities at $\theta_i = 1$ (it is assumed that $C_1 = \text{const}$ and $C_2 = \text{const}$); and ϕ_{N_i} are the shifts of the potential of zero charge when passing from the supporting electrolyte solution to $\theta_i = 1$. It can be shown[63] that Eq. (2.26) agrees with Eq. (2.19) under the conditions when the adsorption of organic substance is described by the system of isotherms:

$$B_1(\phi)c = \frac{\theta_1}{n_1(1 - \theta_1 - \theta_2)^{n_1}} \exp(-2n_1a_{11}\theta_1 - 2n_1a_{12}\theta_2)$$
$$B_2(\phi)c = \frac{\theta_2}{n_2(1 - \theta_1 - \theta_2)^{n_2}} \exp(-2n_2a_{22}\theta_2 - 2n_2a_{12}\theta_1) \qquad (2.27)$$

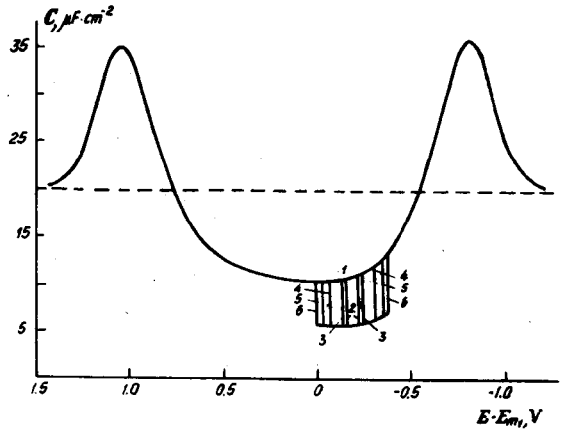


Figure 18. Differential capacity curves calculated with the use of the three-parallel-capacitor model at $a_{11} = 2$; $a_{12} = a_{22} = 0$; $n_1 = 1$; $n_2 = 2$; $C_0 = 20\ \mu F\ cm^{-2}$; $C_1 = 5\ \mu F\ cm^{-2}$; $C_2 = 10\ \mu F\ cm^{-2}$; $\Gamma_m = 6 \times 10^{-10}$ mol cm^{-2} and at relative concentrations ($B_{m1}c_{org}$): 1, 1.035; 2, 1.040; 3, 1.047; 4, 1.096; 5, 1.148; 6, 1.202. (From Damaskin.[64])

where

$$B_i(\phi) = B_{0i} \exp\left[-\frac{\Delta\gamma_0 + C_i\phi(\phi_{Ni} - \phi/2)}{RT\Gamma_{mi}}\right], \quad (i = 1, 2) \qquad (2.28)$$

Here, a_{11}, a_{12}, and a_{22} characterize the intermolecular interaction of particles in the positions 1–1, 1–2, and 2–2, respectively, and n_1 and n_2 stand for the number of solvent molecules (or their clusters) which are displaced by an adsorbate molecule in position 1 and position 2, respectively.

The three-parallel-capacitor model was used for qualitative interpretation of the adsorption behavior of a number of aromatic and heterocyclic compounds on mercury[63] and also on bismuth.[18] In the presence of strong attractive interaction between vertically oriented molecules (large $a_{11} > 0$), this model allows one to describe the phenomenon of two-dimensional condensation, observed when the orientation of adsorbed molecules changes from flat to vertical.[64] Figure 18 shows the C–E curves typical for this case which have "pits," the sides of which correspond to the processes of formation and breakdown of the condensed film during the reorientation of adsorbed molecules. As indicated earlier, such C–E curves were observed experimentally in the case of adsorption on mercury of various nucleosides.[8,15] Originally, the three-parallel-capacitor model was suggested for description of the coadsorption of two organic substances.[65]

If in Eqs. (2.27) $\theta_1 = 0$ or $\theta_2 = 0$, for description of the adsorption of organic molecules in one position the following isotherm results:

$$Bc = \frac{\theta}{n(1-\theta)^n} \exp(-2na\theta) \qquad (2.29)$$

from which Frumkin's isotherm (2.20) follows as a particular case at $n = 1$. It follows from the comparison of the experimental data with Eq. (2.29) that for most of the systems studied $n \approx 1$.[6,66-68] This result was explained[66,67] by association of adsorbed molecules into small clusters containing 3–4 water molecules. One should keep in mind, however, that with the existing accuracy of the experimental data, n may vary within 0.5–1.5.[68]

Batrakov and Damaskin[23] showed that the n-parallel-capacitor model can be used for quantiative description of the adsorption of organic substances on polycrystalline electrodes, the surface of which is characterized by the presence of a considerable number of sites with different adsorption energies and different values of $E_{\sigma=0}$, but with the same difference of capacities $(C_0 - C')_n$. In this case, it is assumed that in calculating the total surface coverage with adsorbate, the adsorption of the organic substance on each site obeys Frumkin's isotherm (2.20) with the same value of a, but with different values of B, typical of a uniformly inhomogeneous surface.

An alternative approach to the development of macromodels for description of the adsorption of organic substances on electrodes was suggested by Parsons.[58,69] At a given σ = const, the potential differences at surface sites covered by solvent and organic substance molecules add up

$$\phi = \phi_0(1 - \theta) + \phi'\theta \tag{2.30}$$

where

$$\phi_0 = \int_0^\sigma \frac{1}{C} d\sigma \quad \text{and} \quad \phi' = \phi_N + \int_0^\sigma \frac{1}{C'} d\sigma \approx \phi_N + \frac{\sigma}{C'} \tag{2.31}$$

If, however, the organic substance is adsorbed in two positions, instead of Eq. (2.30), we should write

$$\phi = \phi_0(1 - \theta_1 - \theta_2) + \left(\phi_{N_1} + \frac{\sigma}{C_1}\right)\theta_1 + \left(\phi_{N_2} + \frac{\sigma}{C_2}\right)\theta_2 \tag{2.32}$$

Combination of Eqs. (2.19) and (2.30) yields the isotherm

$$B(\sigma)c = f(\theta) \tag{2.33}$$

and combination of Eqs. (2.19) and (2.32) gives the system of isotherms

$$\begin{aligned} B_1(\sigma)c &= f_1(\theta_1, \theta_2) \\ B_2(\sigma)c &= f_2(\theta_1, \theta_2) \end{aligned} \tag{2.34}$$

The isotherms (2.33) as well as $B_1(\sigma)c = f_1(\theta_1; \theta_2 = 0)$ and $B_2(\sigma)c = f_2(\theta_1 = 0; \theta_2)$ are congruent with the electrode charge.

The quantitative calculations of θ–E, γ–E, and C–E curves by means of Parsons' model are not acceptable due to the fact that this model is more sensitive to errors in the value of C' and to the necessary assumption $C' \approx$ const† than the two-parallel-capacitor model. In fact, at medium values of θ in Eq. (2.14), the first term is of decisive importance, so that the error in the value of C' (i.e., in σ') hardly affects the total change σ. On the other hand, under the

† The true dependence of C' on potential cannot be determined experimentally. The possibility of discarding the assumption C' = const was discussed.[21]

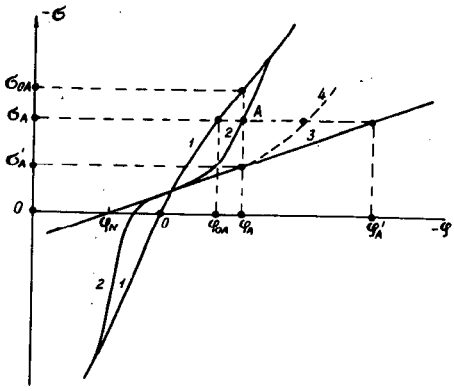


Figure 19. Schematic dependence of the electrode charge on its potential: 1, in pure supporting electrolyte solution; 2, in the presence of aliphatic organic substance (c_{org} = const); 3, with complete surface coverage by organic substance ($\theta = 1$) at C' = const; 4, at $\theta = 1$ but with capacity C' increasing with cathodic polarization.

same conditions in Eq. (2.30) the term $\phi'\theta$, which is very sensitive to the capacity C' and to the assumption $C' \approx$ const, is larger in absolute value. What has been said can be explained by means of the charging curves in Figure 19. This figure shows that, to describe the adsorption of the organic substance at point A with the coordinates (ϕ_A, σ_A) by means of the two-parallel-capacitor model, it is sufficient to assume that the condition C' = const is valid in the potential range from ϕ_N to ϕ_A. However, to describe adsorption at the same point A by means of Parsons' model, it is necessary to assume that the condition C' = const is valid in a wider potential range: from ϕ_N to ϕ_A'. If the true dependence of σ on ϕ at $\theta = 1$ lies as shown by line 4 in Figure 19, the error in the value of θ calculated for point A by means of Eq. (2.14) at C' = const, is negligible since the use of Eq. (2.30) at C' = const can lead to the values of θ at this point which are 2–3 times lower than they should be.

Hansen[70] also proposed a model, according to which

$$\sigma = [K_0(1 - \theta) + C'\theta](\phi - \phi_N\theta) \tag{2.35}$$

where K_0 is the integral capacity in the supporting electrolyte solution, i.e., $K_0 = (1/\phi)\int_0^\phi C_0\, d\phi$. In a physical sense Hansen's model corresponds to two parallel layers from molecules of the organic substance and water located between an ideal conductor and dielectric.[71] This model, however, has not been widely used, although it represents correctly the linear dependence of the adsorption potential on θ at the solution/air interface in solutions of different aliphatic compounds.[46–49]

It can be shown that the equations of the three macromodels, Frumkin's, Parsons', and Hansen's, can be obtained as particular cases of the following relation[72]:

$$\sigma = \frac{\sigma_0(1 - \theta) + nC'\theta[\phi - \phi_N(k - k\theta + \theta)]}{1 + n\theta - \theta} \tag{2.36}$$

Thus at $n = k = 1$ one has Eq. (2.14) of the two-parallel-capacitor model; at $n = K_0/C'$, $k = 1$, Eq. (2.30) of Parsons' model; and at $n = 1$, $k = K_0/C'$,

Eq. (2.35) of Hansen's model. In a physical sense the parameters n and k characterize the dependence on θ of the relations ε/δ and μ/δ, where ε is the dielectric constant of the adsorption layer, δ is its mean thickness, and μ is the component of the dipole moment of an adsorbed organic substance molecule normal to the surface. Thus, e.g.,

$$\left(\frac{\mu}{\delta}\right)_\theta : \left(\frac{\mu}{\delta}\right)_{\theta=1} = \frac{nk - n(k-1)\theta}{1 + n\theta - \theta} \tag{2.37}$$

For the two-parallel-capacitor model, the relation μ/δ is constant, which may be the result of the compensation of the change of μ and δ with increasing θ. Thus, e.g., in the case of simple aliphatic compounds with one functional group, increase of θ can be expected to be attended by an increase of μ due to the change in the dipole orientation (from flat to vertical) and an increase of δ due to the moving apart of the electric double-layer sides. If, however, a change of μ is not compensated for by a corresponding change of δ, there should be some deviations from the two-parallel-capacitor model. To the first approximation, these deviations can be described by a formal introduction of the dependence of the attraction constant a on potential ϕ.[72]

Equation (2.36) was used to describe the adsorption of a number of organic compounds on mercury and bismuth electrodes. In all the systems studied, the parameters n and k differed slightly from unity. This result supports the conclusion that at $C' = \text{const}$, Frumkin's model[56] describes these systems better than those of Parsons[58] or Hansen.[70] At $n \approx 1$, it is also possible to combine Eq. (2.36) with the isotherm (2.20), which in the general case is not correct since Eq. (2.36) corresponds strictly to the isotherm of the form[73]

$$B(\phi)c = \frac{\theta}{1-\theta} \exp\left[-a(\phi)\frac{\theta(2 + n\theta - \theta)}{(1 - n\theta + \theta)^2}\right] \tag{2.38}$$

where

$$B(\phi) = B_0 \exp\left[-\frac{\Delta\gamma_0 + C'\phi(k\phi_N - \phi/2)}{RT\Gamma_m/n}\right] \tag{2.39}$$

and

$$a(\phi) = a_0 + (n/RT\Gamma_m)[(n-1)(\Delta\gamma_0 - C'\phi^2/2) + (kn-1)C'\phi_N\phi] \tag{2.40}$$

It can be readily seen that Eq. (2.38) at $n = 1$ gives the isotherm (2.20) and relations (2.39) and (2.40) at $n = k = 1$ lead to formula (2.23) and $a = \text{const}$. In the general case, at $n \neq 1$ and $k \neq 1$, the rigorous order of calculations with the use of the generalized surface layer model is described by Damaskin and Kuriakov.[74]

2.4. The Molecular Theory of Adsorption of Organic Compounds on Electrodes

For a proper knowledge of the surface layer structure, its dependence on the adsorbate concentration and the electrical variable (potential or electrode

charge), it is necessary to develop a quantitative molecular theory of adsorption of organic substances on electrodes. However, in spite of some attempts to develop such molecular theories,[75-79] the problem remains a complex one. The reason for this is the complex nature of the electrode/solution interface in the presence of adsorbed organic molecules. In fact, when the adsorption isotherm is written in the form

$$\exp\left(-\frac{\Delta G_A^\circ + \mu X}{kT}\right)c = f(\Gamma) \tag{2.41}$$

it is necessary to preset the orientation of an adsorbed molecule on the electrode surface to determine the normal component of the dipole moment; it is necessary to assess a possible change in the dipole moment of the organic molecule as compared with its value in the gas phase, which is caused by the interaction with the metal surface and the solvent molecules; it is necessary to calculate the electric field strength X at the site on which the adsorbate molecule is located, taking into consideration both the electrode charge and the field set up by the remaining dipoles of the solvent and organic substance. Also, the adsorption energy ΔG_A° at $X = 0$ must be calculated, and this is determined by the difference in the energies of interaction with the electrode surface of adsorbate and solvent molecules, as well as by the algebraic sum of the interaction energies adsorbate–solvent, adsorbate–adsorbate, and solvent–solvent. Finally, one must determine the statistical distribution function of adsorbate and solvent molecules between the surface and the solution bulk, taking into account their geometric form and size, to be able to write more concretely the form of the function $f(\Gamma)$.

In the first molecular theory advanced by Butler,[75] it was assumed that the field X is proportional to the potential ϕ. With this assumption, Eq. (2.41) goes over into relation (2.17), and Butler's model becomes equivalent to a two-parallel-capacitor model: in it the capacities C_0 and C' were interpreted in terms of the polarizability of water molecules and those of the organic substance and the quantity ϕ_N in terms of the dipole moment of an organic molecule. In Butler's theory, the quantity ΔG_A° was determined experimentally, and an assumption was made that the function $f(\Gamma)$ represented a Henry isotherm. This assumption was not fulfilled, and this confined the application of Butler's theory to a region of low surface coverages with the organic substance.

A similar approach to that of Butler for the development of the molecular theory of adsorption was suggested much later by Damaskin and Frumkin.[42] Its central idea is as follows. Since the two-parallel-capacitor model in combination with the isotherm (2.20) forms a good basis for a quantitative interpretation of the γ–E and C–E curves in the presence of organic substances, the object of the molecular theory should be a theoretical calculation of the dependence of C_0 on E, values C', Γ_m, ϕ_N, and B_0 as well as the molecular-statistical substantiation of the isotherm (2.20), including the evaluation of the quantity a contained in it. This approach was further developed by Damaskin *et al.*[78,79]

Earlier, Bockris and collaborators[76,77] assumed the field X to be propor-

tional to the electrode charge σ. With this assumption, Eq. (2.41) goes over into relation (2.33), and Bockris's theory could be seen as the molecular basis for Parsons' macromodel. The equation resulting from this model is

$$B(\sigma) = B_{\sigma=0} \exp\left[-(1/RT\Gamma_m)\int_0^\sigma (\phi' - \phi_0)\, d\sigma\right] \tag{2.42}$$

where the quantities ϕ' and ϕ_0 are determined from formulas (2.31). However, in Bockris' theory the total change in the adsorption energy with changing electrode charge was associated as a first approximation only with the work of displacement from the surface of polar water molecules (the solute dipoles being taken to be situated outside the Helmholtz layer), so that

$$B(\sigma) = B_m \exp\left[-(1/RT\Gamma_m)\int_{\sigma_m}^\sigma \Delta\chi\, d\sigma\right] \tag{2.43}$$

Here, B_m is the maximum value of $B(\sigma)$ corresponding to the charge $\sigma = \sigma_m$, at which the potential drop $\Delta\chi$, caused by water dipoles in the double layer, is zero (due to the number of water dipoles with opposite orientation being the same: $N_\downarrow = N\uparrow$). The molecular model aspect of the theory consists of the calculation of the dependence of $\Delta\chi$ on σ, while the chemical component of the adsorption energy (at $\Delta\chi = 0$) was determined from the experimental data.

If a plot of $\Delta\chi$ vs. σ shown in Figure 17 of Reference 76 is used, the integral $\int \Delta\chi\, d\sigma$ between the limits $\sigma = \sigma_m$ and $\sigma = \sigma_m - 6$ gives the energy 0.15 μJ/cm^2. A smaller result is obtained with the $\Delta\chi$–σ curve calculated with a more recent refined model.[80]† Using the older model, assuming $\Gamma_m = 5 \times 10^{-10}$ mol/cm^2 (the result characteristic for adsorption of many organic compounds), in accordance with formula (2.43), one finds that at $T = 298$ K

$$\frac{B(\sigma_m - 6)}{B_m} = \exp\left(-\frac{0.15 \times 10^{-6}}{8.315 \times 298 \times 5 \times 10^{-10}}\right) \approx 0.89$$

Experiment shows that when passing from the charge of maximum adsorption to $\sigma = \sigma_m - 6$, the adsorption equilibrium constant decreases some ten times, i.e., $B(\sigma_m - 6)/B_m \approx 0.1$.[81] If the dependence of $\Delta\chi$ on σ is chosen in accordance with the experimental data on the adsorption of organic substances,[81] one can obtain an unusual value of the double-layer capacity in a pure supporting electrolyte solution.[82] This fact gave rise to criticism of the original Bockris model.[82,83]

Thus it can be concluded that only the early steps have so far been taken in the development of the molecular theory of adsorption of organic compounds on electrodes.

† In the original theory,[76] it was assumed that all the water molecules present on the surface contribute to the setting up of the potential drop, but in the Helmholtz equation the coefficient 2π was used instead of the coefficient 4π. In the more recent model,[80] the coefficient 4π was used, but the model involved dimer formation on the electrode to the extent of 0.5 mole fraction dimer which later does not contribute to $\Delta\chi$. In Reference 80, the change in $\Delta\chi$ from 0 to 15 μC/cm^2 is 0.15 V. In the model used in the result given,[76] the change Δf over the same range was 0.12 V.

3. Irreversible Adsorption of Organic Substances

The main features of the irreversible adsorption of organic substances were established in the past two decades for catalytically active platinum metals. Intensive studies in this direction were carried out in different countries, their primary object being to elucidate the mechanism of the processes occurring in fuel cells and during electrosynthesis of organic compounds.

Advances in the study of the adsorption of organic substances on catalytically active electrodes are associated with the development and refinement of new experimental methods of investigation. For electrodes from smooth metals, these are pulse potentiostatic and galvanostatic methods,[84-87] and for electrodes from metals with a developed surface, basically the methods of electro-oxidation and electroreduction in the adsorbed layer.[88-90] The application of tracers method in conjunction with electrochemical measurements[4,91-95] was found to be particularly valuable.

3.1. General Regularities of the Adsorption of Organic Substances on Catalytically Active Electrodes

The first Γ–E dependences were obtained in the studies of methanol adsorption on smooth platinum by the complex potentiostatic pulses method[87] and in the investigation of naphthalene adsorption on platinized platinum by the tracers method.[96] These studies showed that the Γ–E dependence is in the form of a bell-shaped curve with a maximum at the potentials 0.4–0.5 V referred to a reversible hydrogen electrode in the same solution. In the case of methanol, the data were explained in terms of the thermodynamics of reversible processes, with allowance for hydrogen and oxygen adsorption on the platinum electrode, and by analogy with the mercury electrode in the case of naphthalene, by competing adsorption of solvent and organic substance molecules in a varying electric field.

A. N. Frumkin considered the thermodynamics of reversible adsorption of organic substances which is not accompanied by dissociation of molecules, taking into account the adsorption of gases on the electrode surface.[97] He showed that in reversible systems on hydrogen- and oxygen-adsorbing metals, the potential range in which the adsorption of these gases occurs is that at which the adsorption of the organic substance is at a minimum. Indeed, the basic thermodynamic equation which allows one to determine the influence of hydrogen adsorption on that of the organic substance is

$$-\left(\frac{\partial\Gamma_{org}}{bE}\right)_{\mu_{org}} = F\left(\frac{\partial\Gamma_H}{\partial\mu_{org}}\right)_E = F\left(\frac{\partial A_H}{\partial\mu_{org}}\right)_E - \left(\frac{\partial\sigma}{\partial\mu_{org}}\right)_E \qquad (3.1)$$

where A_H is the amount of hydrogen adsorbed on the unit electrode surface.

It follows from Eq. (2.44) that the change of the standard free energy of adsorption of the organic substance (ΔG_a) in the presence of hydrogen adsorption is determined by the relation

$$\left(\frac{\partial \Delta G_a}{\partial E}\right)_{\Gamma_{org}} = -\left(\frac{\partial \sigma}{\partial \Gamma_{org}}\right)_E + F\left(\frac{\partial A_H}{\partial \Gamma_{org}}\right)_E \tag{3.2}$$

A similar relation in the presence of adsorbed oxygen is of the form

$$\left(\frac{\partial \Delta G_a}{\partial E}\right)_{\Gamma_{org}} = \left(\frac{\partial \sigma}{\partial \Gamma_{org}}\right)_E + 2F\left(\frac{\partial A_O}{\partial \Gamma_{org}}\right)_E \tag{3.3}$$

where A_O is the surface concentration of adsorbed oxygen. These relations show that in the case of platinum electrode, the reversible adsorption of organic substances must be influenced by adsorbed hydrogen and oxygen, rather than by the free surface charge.

More recent studies on the adsorption of a large number of organic substances, including methanol, benzene, and naphthalene, proved, however, that the adsorption of organic substances on platinum metals is irreversible. This is evidenced primarily by the absence of exchange between organic molecules adsorbed on the electrode and identical molecules in solution. Moreover, it was established by different methods that upon contact with the electrode, organic substances undergo chemical transformations including dehydrogenation, self-hydrogenation, oxidation, and dissociation of molecules with rupture of the bonds between carbon atoms. It is the products of these transformations which are absorbed on the electrodes. Therefore, the term "adsorbed organic substance" (methanol, ethanol, etc.) in the case of electrodes from catalytically active metals refers to the sum of products of variable composition, depending on the conditions under which adsorption occurs, in particular, on the electrode potential.

The amount of physically adsorbed organic substance forms only a small fraction ($< 1\%$) of the total amount present on the electrode. The investigation of the behavior of physically adsorbed organic substances in the presence of an excess of chemisorbed products presents difficulties owing to the insufficient accuracy of the methods used.[87,95,98,99] Due to the irreversible nature of the adsorption of organic substances, the literature data on the dependence of the extent of adsorption on the concentration in solution cannot be considered as *true* equilibrium adsorption isotherms.

Thus in the adsorption of organic substances on platinum metals, the chief role is played by factors associated with the chemical interaction of adsorbate with the surface of a catalytically active electrode, while the physical factors, which determine the adsorption of organic substances on mercurylike metals, are of lesser importance. The structural features and composition of the adsorbed layer on platinum metals are also defined by the specific nature of the absorbate –adsorbent interaction, which is responsible for the difficulty of investigating

such systems. In each particular case, it is necessary to determine the composition, structure of adsorbed particles, and the nature of the bonds with the adsorbent surface as a function of various factors (electrode potential, solution pH, etc.).

As pointed out earlier, the most effective method of studying adsorption on electrodes from platinum metals with developed surface is the radioactive tracer technique,[81] used in conjunction with electrochemical methods. The data on a series of consecutive experiments, shown schematically in Figure 20, testify to the informative value of this approach to the study of the adsorption of organic substances. The measurements usually begin with the investigation of the adsorption kinetics and of the shifts of the electrode potential upon introduction of the organic substance into solution. The organic substance is introduced into an electrochemical cell filled with the supporting electrolyte solution in which the electrode is immersed. The electrode is maintained at a given potential. At open circuit the electrode potential changes; but if the potential is kept constant (closed polarization circuit), the current flows through the external circuit (Figure 20a, b, curves 1). As the potential or current changes, the particles containing a tracer atom accumulate on the electrode surface (Figure 20a, b, curves 2). These measurements permit one to draw conclusions about the adsorption kinetics of the organic substance and afford some preliminary information on the adsorption mechanism. As a rule, the shift of the electrode potential in the cathodic direction is caused by dehydrogenation of the organic substance and the potential shift in the anodic direction by its hydrogenation. If, however, at the adsorption potential, the steady oxidation current of organic substance is zero, and no organic products of other than initial composition are present in solution, the whole amount of electricity observed to flow upon adsorption can be assumed to have been expended in ionization of adsorbed hydrogen.

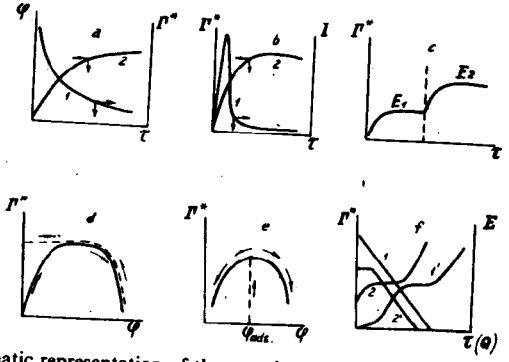


Figure 20. Schematic representation of the experimental data obtained in the investigation of the adsorption of organic substances by the tracer method and the electrochemical methods used in conjunction.

The stoichiometric composition of an adsorbed particle can be assessed by comparing the amount of adsorbed carbon-containing particles, calculated from the tracer measurements, with the amount of hydrogen formed during adsorption, determined by integration of the current–time curves for adsorption under potentiostatic conditions, or from the charging curve in the case of adsorption at open circuit.

By studying consecutively the adsorption kinetics of the organic substance at different potentials, it is possible to obtain the dependence of the extent of adsorption (or the surface coverage by the organic substance) on the electrode potential (Figure 20c, d). Since adsorption of organic substance on platinum is irreversible, the shape of the Γ–E curve depends on the direction of the electrode potential change (Figure 20d). The reasons for the decrease of Γ_{org}, when the electrode potential shifts in the cathodic or anodic direction from the potentials of maximum adsorption, can be established by determining the composition and amount of products formed as the result of desorption and the amount of electricity consumed in this process (Figure 20e). Generally, the reason for desorption is electro-oxidation or electroreduction of the adsorbed products.

For determination of the composition of the adsorption products of organic substances containing one carbon atom, it is necessary to know either the amount of adsorbed carbon-containing particles and the consumption of electricity in their electro-oxidation to a known product (e.g., carbon dioxide),[100,101] or the amount of the desorption product formed, its composition and the total electricity consumed in its oxidation.[98,102] To determine the product composition of more complex organic substances, it is necessary to have at one's disposal the experimental data on the adsorption of these substances containing a labeled atom in different positions.

Simultaneously, with measurement of the electro-oxidation of the adsorbed product of the organic substance in the adsorbed layer, the decrease in the amount of organic substance retained on the electrode is recorded (by measuring its radioactivity).† The reciprocal of the slope of the curves of the amount of oxidized adsorbate versus the amount of the electricity passed gives the mean number of electrons expended for electro-oxidation of one carbon-containing chemisorbed particle (Figure 20f).

The number of surface sites of adsorbent per adsorbed particle can be determined by studying the influence of organic substance adsorption on the amount of adsorbed hydrogen. For this purpose, with the amount of chemisorbed substance known (determined by the tracer method), the amount of adsorbed hydrogen is measured by the potentiostatic or galvanostatic methods. Then, by comparing the number of adsorbed sites per a chemisorbed particle with its stoichiometric composition, one can obtain some idea of the structure of this particle.[87]

† The electricity passed is assumed to be totally expended in electro-oxidation of the adsorbed product.

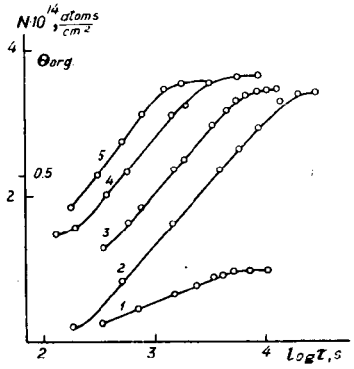


Figure 21. Change with time of the extent of adsorption of methanol on platinized platinum from the solution of the composition 0.1 *M* CH_3OH + 0.5 *M* H_2SO_4 at different potentials: 1, 0.1; 2, 0.2; 3, 0.3; 4, 0.4; 5, 0.5 V. (From Kazarinov *et al.*[95])

3.2. Adsorption of Methanol on Platinum

The investigation of adsorption of organic substances on platinum received the greatest attention, the most detailed studies having been made on the adsorption of methanol on platinum (more than 100 papers).

Investigation of the adsorption kinetics of methanol on smooth and platinized platinum in the potential range 0.0–1.0 V showed that the adsorption rate is described by the equation

$$V_{ads} = Kc \exp(-\alpha f\theta_{org} - \alpha f\theta_H - \alpha f\theta_O) \tag{3.4}$$

where K is a constant for the adsorption rate, c is the adsorbate concentration in solution, f is a "surface inhomogeneity factor," α is the transfer coefficient, θ_{org} is the surface coverage by the organic substance, θ_H is the surface coverage by hydrogen, and θ_O is the surface coverage by oxygen (Figures 21 and 22).

Earlier, this equation was widely used to describe adsorption processes from the gas phase and has become known as the Roginskii–Zel'dovich equation.

Figures 21 and 22 show that the adsorption rate of methanol decreases in the range of hydrogen and oxygen adsorption potentials and changes insignificantly at $E = 0.3$–0.5 V, where the surface coverage by adsorbed gases is small. It is also clear from these data that the linear dependence of Γ_{org} on log τ is observed both on smooth and platinized platinum, though in the two cases the adsorption rate constants per unit true surface differ by a factor of 20–30.

The investigation of the adsorption kinetics of methanol in the range of high anodic potentials 1.0–2.5 referred to a reversible hydrogen electrode shows that this process can be described both by the Roginskii–Zel'dovich equation and by Benchem–Bart's equation, according to which

$$\Gamma = K\tau^{1/n} \tag{3.5}$$

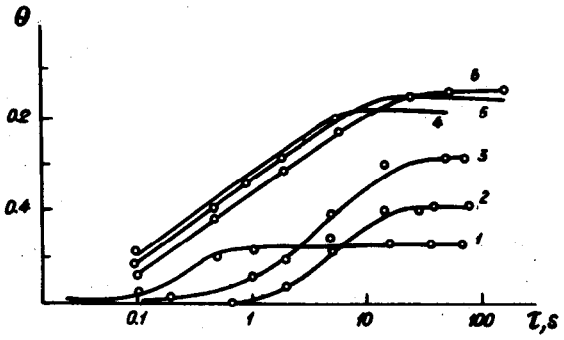


Figure 22. Change with time of the extent of adsorption of methanol on smooth platinum from the solution of the composition 0.5 *M* CH_3OH + 0.5 *M* H_2SO_4 at different potentials: 1, 0.2; 2, 0.3; 3, 0.4; 4, 0.5; 5, 0.6; 6, 0.7 V. (From Vasilyev *et al.*[87])

where K and $n \geqslant 2$ are constants and τ is the time. For a final solution of the problem of adsorption kinetics in this potential range, further studies are necessary.

Methanol, as well as other organic compounds, in the range of high anodic potentials, undergoes chemisorption. The shief methods for its investigation are the pulse methods and the radioactive tracer techniques. In the latter case, the radioactivity of adsorbed substance may be measured after the electrode has been removed from solution and washed in the supporting electrolyte, although it may also be measured *in situ*.

Due to the irreversible nature of methanol adsorption, the dependence of its extent of adsorption on the electrode potential is determined by the experimental conditions. Thus, for instance, the Γ–E curve is bell shaped with a maximum at the potentials 0.3–0.55 V if the potential is changed jumpwise from 1.0 V to the chosen adsorption potential in the range 0.0–0.6 V. If, however, methanol is at first adsorbed at the potentials of maximum adsorption (0.3–0.55 V), and the electrode potential is shifted into the cathodic direction, no decrease of methanol adsorption is observed.[87,103,104] The decrease of the extent of adsorption at $E > 0.55$ V is associated with methanol oxidation, since in this potential range the rates of its adsorption and electro-oxidation become commensurable. The decrease of Γ under the conditions where methanol adsorption is carried out at the potentials less than 0.3 V is connected with the presence on platinum of adsorbed hydrogen, which hinders the adsorption of the organic substance.[87,95,98,105] The available data on the dependence of the extent of methanol adsorption on electrode potential, obtained by the tracers technique and by electrochemical methods, show good agreement (Figure 23).[95] The value of Γ during a certain time of contact of the electrode with solution increases linearly with the logarithm of the initial methanol concentration in solution and remains constant if later c_{CH_3OH} is decreased. The maximum surface coverage by the adsorption product is $\sim 3 \times 10^{14}$ particles per 1 cm^2 of true surface.

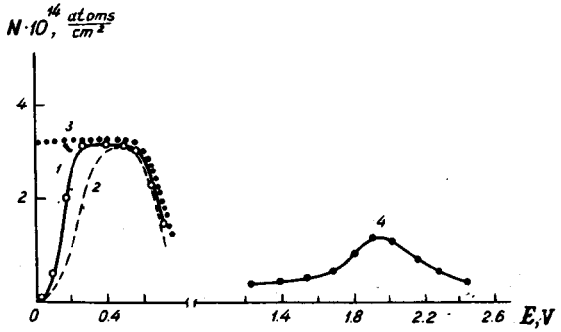


Figure 23. Dependence of the extent of adsorption of methanol on the potential of a platinum electrode in the solution of the composition: 0.1 *M* CH_3OH + 0.5 *M* H_2SO_4 obtained by different methods: 1, measured by the tracer method on a Pt/Pt electrode by shifting *E* from 0.0 to 0.6 V in the adsorbate solution after the steady-state value of the extent of adsorption has been reached at each *E*; 2, plotted from the steady-state values of the extent of adsorption reached at each given potential value. The measurements were made on smooth platinum by the pulse method; 3, obtained by shifting *E* from 0.7 to 0.0 V. The measurements were made on platinized platinum by electro-oxidation in the adsorbed layer; 4, the measurements were made by the tracer method on smooth platinum. (From References 87, 95, 98, 103–105.)

The nature of the methanol adsorption product was determined by comparing the amount of hydrogen formed during methanol adsorption at open circuit with the amount of electricity consumed in the electro-oxidation of the adsorption product. The ratio of these amounts proved to be close to unity. Since the electro-oxidation product of adsorbed methanol is CO_2 alone, its stoichiometric composition was identified as a particle of the composition COH,[106] formed during methanol adsorption according to the scheme

$$CH_3OH \rightarrow COH + 3H_a$$

The direct determinations of the amount of CO_2 formed during electro-oxidation, and of the amount of the methanol adsorption product on platinum, carried out by the tracer technique showed the number of electrons per carbon-containing particle to be 2.5 ± 0.3.[98] This means that, along with the particle of the composition COH, other particles seem to be adsorbed, which for their oxidation require a lesser number of electrons, e.g., particles of the composition COOH or CO. Apparently, depending on the experimental conditions, the ratio between particles of composition COH, CO, and COOH can vary, which accounts for differences in the experimental data of some authors. The mean number of electrons necessary for the electro-oxidation of the adsorption product to CO_2 can be determined more accurately with allowance for the data on the change of the electric double-layer charge and from the change in the

values of A_H and A_O during oxidation of an adsorbed organic particle. The identity of the composition of the methanol chemisorption product in the experiments of different authors is proved by its identical electrochemical behavior, in particular, by the coincidence of the data on electro-oxidation in the adsorbed state.

The platinum–particle bond of composition COH has a dipole moment, which causes a positive shift of potential. This conclusion was drawn from the data on the shift of the potential of zero charge $E_{\sigma=0}$ in the positive direction. At maximum coverage of the platinum surface by particles of composition COH, this potential shift is ~220 mV (Figure 24). The influence of the surface coverage by COH particles on the shift of $E_{\sigma=0}$ can be described by the two-parallel-capacitor model.[107]

On the one hand, the adsorption kinetics of methanol obey laws characteristic of the processes described by the uniformly inhomogeneous surface model. On the other hand, it follows from the data on methanol desorption at anodic potentials that this process obeys laws characteristic of homogeneous surfaces.[95] This is evidenced also by the results obtained by the differential isotopic methods in the system platinum–methanol. Apparently, such behavior of methanol is associated with specific features of the desorption process of organic substances which involves the interaction of two particles: a carbon-containing particle and an oxygen-containing one.

3.3. Adsorption on Platinum of Other Organic Compounds

The regularities of formaldehyde adsorption on platinum investigated by the tracer technique and electrochemical methods[87,108,109] prove to be similar to those for methanol.

The main adsorption product of formic acid is also COH particles, formed as the result of the reduction of formic acid molecules.[2,3,87,110–112] Along with these particles, particles of the composition COOH can be detected, which are

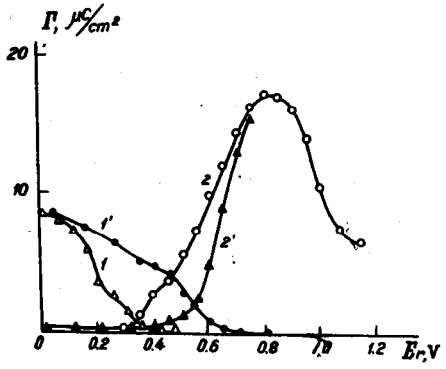


Figure 24. Dependence of the extents of adsorption of sodium cations (curves 1, 1') and sulfuric acid anions (curves 2, 2') on the potential of a Pt/Pt electrode in 10^{-3} N H_2SO_4 + 3 × 10^{-3} N Na_2SO_4 solution obtained in the absence (curves 1, 2) and in the presence of chemisorbed methanol (curves 1', 2'). (From Stenin *et al.*[107])

less stable in the adsorbed state. The ratio between the amounts of these two kinds of particles on the surface depends on the electrode potential and solution pH.

Such simple substances as CO and CO_2 interact with the platinum electrode surface to form an adsorption product whose behavior is similar in all respects to that of the strong chemisorption products of methanol, formaldehyde, and formic acid.[84,113–115]

The data of most authors on the adsorption of methanol, formaldehyde, and CO_2 on platinum are in good agreement.[87] The difference in the experimental data is greatest for the adsorption of CO and formic acid.[2–4,98,111,112,115] Apparently, this can be explained by the fact that the reactions of catalytic reduction of CO and formic acid (with an intermediate reduction product of CO) to particles of composition COH are highly sensitive to the presence of different impurities and to the conditions of the preparation of the electrode surface. It should be kept in mind that the adsorption processes of organic compounds, even if they contain only one carbon atom, include several consecutive oxidation or reduction reactions, and their limiting step can vary depending on the experimental conditions.

Thus, in the case of CH_3OH, CH_2O, HCOOH, CO, and CO_2, the main adsorption product is a particle of composition COH bound with three platinum atoms. No satisfactory explanation of the stability of the COH particle in the adsorbed state is available at present.

The interaction with the platinum electrode surface of organic compounds containing more than one carbon atom proves to be more complicated. This is associated with the possibility of dissociation of organic molecules involving rupture of the C–C bond during adsorption and with the possibility of adsorption of their carbon-containing fragments. The large experimental difficulties arising in the investigation of these processes can be exemplified by ethanol.[87,116,117] In the case of ethanol adsorption, two kinds of adsorbed particles could be found on the surface: particles whose adsorption behavior is identical to that considered above for the adsorption product of methanol, and particles removed by cathodic polarization. The composition of the former was identified as COH and that of the latter as an incompletely dehydrogenated ethanol molecule. The ratio of the amounts of these particles on the surface is defined by the solution pH and the adsorption potential. Like methanol, ethanol is adsorbed on platinum in the range of high anodic potentials as well.

Considerable attention was given to the investigation of the adsorption of acetic acid.[118–120] In dilute solutions, its adsorption product behaves as a weakly surface-active anion (Figure 25); in concentrated solutions, a CH_3COOH molecule can break along the C–C bond, which complicates the investigation of this process. In the range of high anodic potentials, the adsorption behavior of acetic acid is characterized by the presence of several adsorption maxima on the Γ–E curve (Figure 25), the adsorption of acetate ions being directly related to the kinetics of Kolbe electrosynthesis.

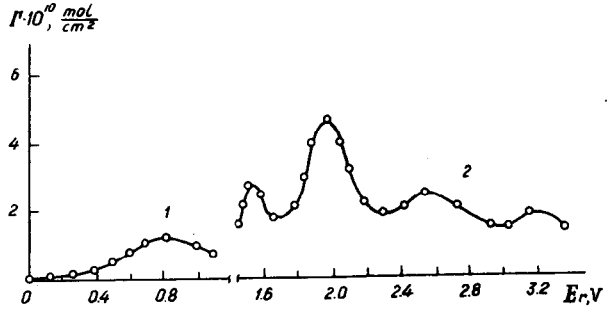


Figure 25. Dependence of the extent of adsorption of acetic acid on the potential of a platinum electrode in 10^{-3} *M* CH_3COONa + 10^{-3} *M* CH_3COOH solution (curve 1) and in 0.5 *M* CH_3COONa + 0.5 *M* CH_3COOH (curve 2). (The measurements were performed by the tracer method.) (From Kazarinov and Girina[119] and Yakovleva *et al.*[121])

Upon contact of a platinum electrode with chloro- or bromoacetic acids, the molecule undergoes dehalogenation followed by adsorption of chlorine ions and carbon-containing fragments.[121]

The investigation of the adsorption on platinum of aliphatic organic compounds containing three or more carbon atoms showed that with increasing carbon chain length, the degree of breakdown of the molecule during adsorption decreases.

In connection with work on the development of fuel cells, great interest was shown in the investigation of the adsorption of saturated and unsaturated hydrocarbons.[116,118,122] The basic regularities of their adsorption on platinum have much in common with those established in the investigation of the adsorption on platinum of alcohols, aldehydes and organic acids. In particular, this is associated with the fact that the position of the adsorption maximum on the Γ–E curve depends on the ratio between the adsorption and electro-oxidation (electroreduction) rates of organic substances, which in its turn depends on the nature of the substance. The adsorption of hydrocarbons on platinum also involves dehydrogenation and breaking of the C–C bonds.

The presence of an aromatic ring in the molecule does not affect the main regularities of the adsorption of organic compounds described (Figure 26) above (adsorption kinetics, shape of the Γ–E and Γ–log c dependences, irreversible nature of adsorption). The desorption of aromatic compounds in the range $E > 0.7$ V is caused by their oxidation to CO_2. At high anodic potentials these compounds also can be adsorbed. During adsorption on platinum, aromatic organic compounds exhibit some specific features; in particular, at the adsorbate concentrations in solution close to saturation, they form polylayers on the surface. The stoichiometric composition of the adsorption products of aromatic compounds has not been established.[5,118]

The investigation of the adsorption of organic compounds afforded some

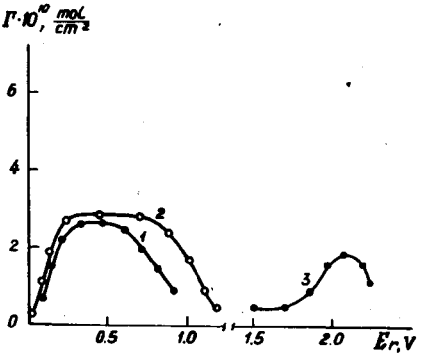


Figure 26. Dependences of the extents of adsorption of benzene on the potential of a platinum electrode in 2×10^{-2} M C_6H_6 + 0.5 M H_2SO_4 solution plotted from the steady state values of the extent of adsorption reached at each given potential (curves 1, 3) and from the data obtained with E changing from 0.0 to 1.0 V. (The measurements were made by the radioactive tracer method.) (From Kazarinov *et al.*[5])

information on their electro-oxidation mechanism on platinum. It was found, in particular, that the oxidation of adsorbed organic particles occurs with participation of the OH radical. Under steady-state conditions of the oxidation of organic substances, they simultaneously undergo adsorption, which, as pointed out above, for most organic substances includes several steps. For this reason, a product in any stage of adsorption can undergo oxidation. In other words, oxidation can proceed by several parallel reactions and lead to formation of different products. From which of the parallel reactions the oxidation of organic substance will mainly proceed depends on the experimental conditions (solution pH, electrode potential, adsorbate concentration in solution). With such an oxidation mechanism, accumulation of chemisorbed particles can be observed on the electrode surface, which practically do not participate in the oxidation process, and can even hinder it. In the case of oxidation of organic compounds containing more than one carbon atom, the oxidation mechanism is more complex since the number of possible reaction patns for the oxidation process increases. At present, the oxidation processes of alcohols, aliphatic acids, and hydrocarbons have received the most study.[87,116,118]

The investigation of the behavior of organic compounds on other platinum metals showed that the adsorption of these compounds on Ir, Rh, Pd is similar to that on Pt. The metal nature affects the degree of decomposition of organic compounds, the rate constant of adsorption, and a degree of oxidation.[123]

For more detailed information on the history of the development of the concepts of the organic compounds adsorption on platinum metals, the reader should consult reviews published in recent years.[4,6,87,98,111,116,118,124,125]

References

1. W. Gibbs, Equilibrium of heterogeneous substances, in *Collected Works*, Vol. 1, Longmans, Green, New York–London–Toronto (1931).
2. O. A. Petry, B. I. Podlovchenko, A. N. Frumkin, and Hira Lal, *J. Electroanal. Chem.* **10**, 253–269 (1965).

3. B. I. Podlovchenko, O. A. Petry, A. N. Frumkin, and Hira Lal, *J. Electroanal. Chem.* **11**, 12–25 (1966).
4. G. Horanyi, *J. Electroanal. Chem.* **51**, 163–178 (1974).
5. V. E. Kazarinov, A. N. Frumkin, E. A. Ponomarenko, and V. N. Andreev, *Elektrokhimiya* **11**, 860–866 (1975).
6. B. B. Damaskin, O. A. Petrii, and V. V. Batrakov, *Adsorption of Organic Compounds on Electrodes*, Plenum Press, New York (1971).
7. G. Gouy, "Sur la fonction électrocapillaire," *Ann. Chim. Phys.* **8**, 291–363 (1906); **9**, 75–139 (1906).
8. H. Jehring, *Elektrosorptionsanalyse mit der Wechselstrompolarographie*, Akademie, Berlin (1974).
9. H. Nakadomari, D. M. Mohilner, and P. R. Mohilner, *J. Phys. Chem.* **80**, 1761–1772 (1976).
10. N. S. Polianovskaya and A. N. Frumkin, *Elektrokhimiya* **1**, 538–545 (1965).
11. A. Frumkin, N. Polianovskaya, N. Grigoryev, and I. Bagotskaya, *Electrochim. Acta* **10**, 793–802 (1965).
12. M. M. Andrusev, N. H. Aiupova, and B. B. Damaskin, *Elektrokhimiya* **2**, 1480–1482 (1966).
13. A. Frumkin, N. Polianovskaya, B. Damaskin, and O. Os'kina, *J. Electroanal. Chem.* **49**, 7–15 (1973).
14. M. Proskurnin and A. Frumkin, *Trans. Faraday Soc.* **31**, 110–115 (1935).
15. V. Vetterl, *J. Electroanal. Chem.* **19**, 169–173 (1968).
16. T. I. Borisova, B. V. Ershler, A. N. Frumkin, *Zh. Fiz. Khim.* **22**, 925–929 (1948).
17. U. V. Palm and V. E. Past, *Usp. Khim.* **44**, 2035–2047 (1975).
18. U. V. Palm and B. B. Damaskin, Itogi nauki i tekhniki, *Elektrokhimiya* **12**, 99–143 (1977).
19. N. B. Grigoryev and D. N. Machavariani, *Elektrokhimiya* **5**, 87–90 (1969).
20. N. B. Grigoryev and D. N. Machavariani, *Elektrokhimiya* **8**, 406–409 (1972).
21. L. E. Rybalka, D. I. Leikis, and B. B. Damaskin, *Elektrokhimiya* **9**, 62–65 (1973); **9**, 414–417 (1973); **11**, 9–14 (1975).
22. L. E. Rybalka, B. B. Damaskin, and D. I. Leikis, *Elektrokhimiya* **10**, 1367–1371 (1974).
23. V. V. Batrakov and B. B. Damaskin, *J. Electroanal. Chem.* **65**, 361–372 (1975).
24. Yu. P. Ipatov, V. V. Batrakov, and V. V. Shalaginov, *Elektrokhimiya* **12**, 286–290 (1976).
25. N. B. Grigoryev, V. P. Kuprin, and Yu. M. Loshkarev, *Elektrokhimiya* **9**, 1842–1845 (1973).
26. N. B. Grigoryev, V. P. Kuprin, Yu. M. Loshkarev, and R. V. Malaya, *Elektrokhimiya* **11**, 1400–1403 (1975).
27. N. B. Grigoryev, V. A. Bulavka, and Yu. M. Loshkarev, *Elektrokhimiya* **11**, 1404–1406 (1975).
28. E. S. Sevastyanov and D. I. Leikis, *Izv. Akad. Nauk SSSR Ser. Khim.* 450–453 (1964).
29. N. B. Grigoryev, S. A. Fateev, and I. A. Bagotskaya, *Electrokhimiya* **8**, 1525–1528 (1972).
30. M. M. Andrusev, A. B. Ershler, and G. A. Tedoradze, *Elektrokhimiya* **6**, 1159–1162 (1970).
31. T. Vitanov and A. Popov, *Trans. Soc. Adv. Electrochem. Sci. Technol.* **10**, 5–27 (1975).
32. A. N. Frumkin, O. A. Petry, and N. V. Nikolaeva-Fedorovich, *Dokl. Akad. Nauk SSSR* **147**, 878–881 (1962).
33. N. B. Grigoryev and A. M. Kalyuzhnaya, *Elektrokhimiya* **10**, 1287–1288 (1974).
34. D. I. Leikis and E. S. Sevastyanov, *Dokl. Akad. Nauk SSSR* **144**, 1320–1323 (1962).
35. N. B. Grigoryev, S. A. Fateev, and I. A. Bagotskaya, *Elektrokhimiya* **8**, 583–586 (1972).
36. J. O'M. Bockris and A. K. N. Reddy, *Modern Electrochemistry*, Plenum Press, New York (1970).

37. E. A. Guggenheim and N. K. Adam, *Proc. R. Soc. London Ser. A* **139**, 218–236 (1933).
38. R. S. Maizlish, I. P. Tverdovsky, and A. N. Frumkin, *Zh. Fiz. Khim.* **28**, 87–101 (1954).
39. Z. Borkowska, *J. Electroanal. Chem.* **63**, 379–392 (1975).
40. D. M. Mohilner and H. Nakadomari, *J. Electroanal. Chem.* **65**, 843–862 (1975).
41. A. N. Frumkin and B. B. Damaskin, *Modern Aspects of Electrochemistry*, J. Bockris and B. Conway, eds., Vol. 3, Butterworths, London (1964), pp. 149–223.
42. B. B. Damaskin and A. N. Frumkin, *Reactions of Molecules at Electrodes*, N. Hush, ed., Wiley Interscience, London (1971), pp. 1–44.
43. A. de Battisti and S. Trasatti, *J. Electroanal. Chem.* **54**, 1–17 (1974).
44. A. Abd-El-Nabey, A. de Battisti, and S. Trasatti, *J. Electroanal. Chem.* **56**, 101–115 (1974).
45. D. M. Mohilner, J. C. Kreuser, H. Nakadomari, and P. R. Mohilner, *J. Electrochem. Soc.* **123**, 359–366 (1976).
46. A. Frumkin, *Ergeb. Exakten Naturwiss.* **7**, 235–275 (1928).
47. A. Frumkin, *Colloid Symp. Ann.* **7**, 89–104 (1930).
48. A. Frumkin and B. Damaskin, *Pure Appl. Chem.* **15**, 263–281 (1967).
49. R. I. Kaganovich, B. B. Damaskin, and I. M. Ganzhina, *Elektrokhimiya* **4**, 867–871 (1968).
50. M. A. Gerovich, *Dokl. Akad. Nauk SSSR* **96**, 543–546 (1954).
51. M. A. Gerovich and G. F. Rybalchenko, *Zh. Fiz. Khim.* **32**, 109–115 (1958).
52. B. B. Damaskin, M. M. Andrusev, V. M. Gerovich, and R. I. Kaganovich, *Elektrokhimiya* **3**, 667–671 (1967).
53. B. B. Damaskin, R. I. Kaganovich, V. M. Gerovich, and S. L. Diatkina, *Elektrokhimiya* **5**, 507–511 (1969).
54. A. N. Frumkin, Z. A. Iofa, and M. A. Gerovich, *Zh. Fiz. Khim.* **30**, 1455–1468 (1956).
55. B. B. Damaskin and A. N. Frumkin, *J. Electroanal. Chem.* **34**, 191–199 (1972).
56. A. Frumkin, *Z. Phys.* **35**, 792–802 (1926).
57. A. Frumkin. *Z. Phys. Chem.* **116**, 466–484 (1925).
58. R. Parsons. *J. Electroanal. Chem.* **7**, 136–152 (1964).
59. A. Frumkin, *J. Electroanal. Chem.* **7**, 152–155 (1964).
60. A. Frumkin, B. Damaskin, N. Grigoryev, and I. Bagotskaya, *Electrochim. Acta* **19**, 69–74 (1974).
61. S. Trasatti, *J. Chim. Phys.* **72**, 561–574 (1975).
62. D. E. Broadhead, K. G. Baikerikar, and R. S. Hansen, *J. Phys. Chem.* **80**, 370–375 (1976).
63. B. B. Damaskin, *J. Electroanal. Chem.* **21**, 149–156 (1969).
64. B. B. Damaskin, *Elektrokhimiya* **13**, 816–820 (1977).
65. G. A. Tedoradze, R. A. Arakelyan, and E. D. Belokolos, *Elektrokhimiya* **2**, 563–571 (1966).
66. R. Parsons, *J. Electroanal. Chem.* **8**, 93–98 (1964).
67. B. B. Damaskin, *Elektrokhimiya* **1**, 63–67 (1965).
68. K. G. Baikerikar and R. S. Hansen, *Surface Sci.* **50**, 527–540 (1975).
69. J. M. Parry and R. Parsons, *J. Electrochem. Soc.* **113**, 992–999 (1966).
70. R. S. Hansen, D. J. Kelsh, and D. H. Grantham, *J. Phys. Chem.* **67**, 2316–2326 (1963).
71. B. B. Damaskin, *Elektrokhimiya* **1**, 1123–1126 (1965).
72. B. Damaskin, A. Frumkin, and A. Chizhov, *J. Electroanal. Chem.* **28**, 93–104 (1970).
73. B. N. Afanasyev, B. B. Damaskin, G. I. Avilova, and N. A. Borisova, *Elektrokhimiya* **11**, 593–596 (1975).
74. B. B. Damaskin and Yu. N. Kuriakov, *Elektrokhimiya* **13**, 98–102 (1977).
75. J. A. V. Butler, *Proc. R. Soc. London Ser. A* **122**, 399–416 (1929).
76. J. O'M. Bockris, M. A. V. Devanathan, and K. Müller, *Proc. R. Soc. London Ser. A* **274** 55–79 (1963).
77. J. O'M. Bockris, E. Gileadi, and K. Müller, *Electrochim. Acta* **12**, 1301–1321 (1967).

78. V. A. Kiryanov, V. S. Krylov, and B. B. Damaskin, *Elektrokhimiya* **6**, 533–541 (1970).
79. V. A. Kiryanov, V. S. Krylov, B. B. Damaskin, and A. V. Chizhov, *Elektrokhimiya* **6**, 1020–1023 (1970); **6**, 1518–1522 (1970).
80. J. O'M. Bockris and M. A. Habib, *Electrochim. Acta* **22**, 41–46 (1977).
81. R. G. Barradas and J. M. Sedlak, *Electrochim. Acta* **17**, 1901–1905 (1972).
82. B. Damaskin and A. Frumkin, *Electrochim. Acta* **18**, 925–926 (1973).
83. B. B. Damaskin, *J. Electroanal. Chem.* **23**, 431–440 (1969).
84. S. Gilman, *J. Phys. Chem.* **66**, 2657–2661 (1962).
85. M. W. Breiter, *Electrochim. Acta* **8**, 447–457 (1963).
86. T. C. Franklin and R. D. Sothern, *J. Phys. Chem.* **58**, 951–960 (1954).
87. Yu. B. Vasilyev and V. S. Bagotzky, Intermediate chemisorbed particles in electrocatalysis, in *Problems of Kinetics and Catalysis, 16. Surface Compounds in Heterogeneous Catalysis*, Nauka, Moscow (1975), pp. 260–290.
88. A. I. Slygin, in *Proceedings of the III Conference on Electrochemistry*, M. Izd. Akad. Nauk SSSR, (1953), p. 322.
89. T. O. Pavela, *Ann. Acad. Sci. Fenn. Ser. A2* **59**, (1954).
90. A. N. Frumkin and B. I. Podlovchenko, *Dokl. Akad. Nauk SSSR* **150**, 349–351 (1963).
91. E. A. Blomgren and J. O'M. Bockris, *Nature* **186**, No. 4721, 305–307 (1960).
92. E. Gileadi, *J. Electroanal. Chem.* **11**, 137–149 (1966).
93. G. Horanyi, J.-Solt, and F. Nagy, *J. Electroanal. Chem.* **31**, 87–94 (1971).
94. V. E. Kazarinov, *Elektrokhimiya* **2**, 1170–1174 (1966).
95. V. E. Kazarinov, G. Ya. Tysyachnaya, and V. N. Andreev, *J. Electroanal. Chem.* **65**, 391–401 (1975).
96. J. O'M. Bockris, M. Green, D. A. J. Swinkels, *J. Electrochem. Soc.* **111**, 743–745 (1964).
97. A. N. Frumkin, *Dokl. Akad. Nauk SSSR* **154**, 1432–1436 (1964).
98. M. W. Breiter, Adsorption of organic species on platinum metal electrodes, in *Modern Aspects of Electrochemistry*, No. 10, ed. B. E. Conway and J. O'M. Bockris, eds., Plenum Press, New York (1975), pp. 161–209.
99. G. Horanyi, D. Hegedüs, and E. M. Rizmayer, *J. Electroanal. Chem.* **40**, 393–397 (1972).
100. V. E. Kazarinov and G. Ya. Tysyachnaya, *Elektrokhimiya* **6**, 892 (1970).
101. J. Sobkowski and A. Wieskowski, *J. Electroanal. Chem.* **34**, 185–190 (1972).
102. V. F. Stenin, V. E. Kazarinov, and B. I. Podlovchenko, *Elektrokhimiya* **5**, 442–446 (1969).
103. M. W. Breiter, *J. Electroanal. Chem.* **15**, 221–230 (1967).
104. V. S. Entina and O. A. Petrii, *Elektrokhimiya* **3**, 1237–1242 (1967).
105. T. Biegler, *Austral. J. Chem.* **22**, 1583–1588 (1969).
106. B. I. Podlovchenko and E. P. Gorgonova, *Dokl. Akad. Nauk SSSR* **156**, 673–676 (1964).
107. V. F. Stenin, G. Ya. Tysyachnaya, B. I. Podlovchenko, and V. E. Kazarinov, *Elektrokhimiya* **7**, 1384–1388 (1971).
108. V. E. Kazarinov and G. Ya. Tysyachnaya, *Elektrokhimiya* **8**, 592–595 (1972).
109. T. Loucka and J. Weber, *J. Electroanal. Chem.* **21**, 329–338 (1969).
110. S. B. Brammer, *Elektrokhimiya* **4**, 243–247 (1968).
111. A. Capon and R. Parsons, *J. Electroanal. Chem.* **44**, 1–7 (1973).
112. V. E. Kazarinov, G. Ya. Tysyachnaya, and V. N. Andreev, *Elektrokhimiya* **8**, 396–399 (1972).
113. I. Giner, *Electrochim. Acta* **8**, 857–863 (1963).
114. A. B. Fasman, G. B. Padiukova, and D. V. Sokol'ski, *Dokl. Akad. Nauk SSSR* **150**, 856–861 (1963).
115. V. E. Kazarinov, V. N. Andereev, and G. Ya. Tysyachnaya, *Elektrokhimiya* **8**, 927–930 (1972).

116. D. V. Sokol'sky and G. D. Zakumbaeva, *Adsorption and Catalysis at the VIII Group Metals in Solution*, Nauka, Kaz. SSR, Alma-Ata, (1973).
117. V. E. Kazarinov and S. V. Dolidze, *Elektrokhimiya* **8**, 284–293 (1972).
118. L. A. Mirkind, *Usp. Chim.* **44**, 2088–2119 (1975).
119. V. E. Kazarinov and G. P. Girina, *Elektrokhimiya* **3**, 107–109 (1967).
120. G. A. Arkharova, G. A. Bogdanovsky, G. D. Vovchenko, and Yu. B. Vasilyev, *Vestn. Mosk. Univ. Ser. Khim.* **4**, 114–117 (1976).
121. A. A. Yakovleva, S. N. Kaidalova, Ya. B. Skuratnik, and V. I. Veselovsky, *Elektrokhimiya* **8**, 1799–1803 (1972).
122. A. G. Pshenichnikov, A. M. Bograchev, and R. H. Burshtein, *Elektrokhimiya* **5**, 1054–1057 (1969).
123. V. S. Bagotzky, Yu. B. Vassiliev, O. A. Khazova, and S. S. Sedova. *Electrochim. Acta* **16**, 913–938 (1971).
124. B. Piersma and E. Gileadi, in *Modern Aspects of Electrochemistry*, No. 4, J. O'M. Bockris, ed., Plenum Press, New York (1966), pp. 47–175.
125. B. Piersma, "Organic Adsorption at Electrodes," in *Electrosorption*, E. Gileadi, ed., Plenum Press, New York (1967), pp. 19–52.

9

The Double Layer in Colloidal Systems

ROBERT JOHN HUNTER

1. Charge and Potential Distribution at Interfaces

1.1. Potential Distribution in the Double Layer

The classical statistical mechanical description of the double layer was proposed by Gouy and Chapman, and modified by the later work of Stern[1] and, particularly, Grahame,[2] from his studies of adsorption at the dropping mercury electrode. That theory is discussed in detail elsewhere in this volume (Chapter 3) so only a very brief resume will be needed here.

In colloid systems the electrostatic potentials over much of the double layer are such that $|ze\psi| \gg kT$ and so the complete, nonlinear form of the Poisson–Boltzmann (PB) equation must be solved. Despite the theoretical limitations on that equation,[3] the alternative approaches (e.g., Reference 4) have not had much impact on colloid science, partly because problems like surface roughness, or modified surface structure, make it much more difficult to pin down the limitations of the P.B. equation. The analytical simplicity of its solution [Eq. (1.4) below] is also very useful when we come to consider the problem of double-layer interaction, which introduces its own quite considerable complexities.

ROBERT JOHN HUNTER • Department of Physical Chemistry, University of Sydney, Sydney, New South Wales 2006, Australia.

1.1.1. The Flat Double Layer

The Poisson–Boltzmann equation in this case may be written, for a symmetric electrolyte,

$$\frac{d^2\psi}{dx^2} = \frac{2n^0ze}{\varepsilon} \sinh \frac{ze\psi}{kT} \tag{1.1}$$

where $\varepsilon = \varepsilon_0\theta$ is the permittivity of the dispersion medium, ε_0 is the permittivity of free space ($= 8.85 \times 10^{-12}$ F m^{-1}), θ is the dielectric constant, and n^0 is the number of ions per unit volume in the bulk solution. In colloidal systems it is usually possible to apply the treatment for symmetrical electrolytes even to unsymmetric cases because the behavior is overwhelmingly determined by the valency of the counterion and the valency of the co-ion can, to all intents and purposes, be ignored.[5]

A first integration of equation (1.1) with the appropriate boundary conditions gives

$$\frac{d\psi}{dx} = \frac{-2\kappa kT}{ze} \sinh \frac{ze\psi}{2kT} \tag{1.2}$$

where κ is the Debye–Hückel parameter:

$$\kappa = \left(\frac{e^2 \sum n_i^0 z_i^2}{\varepsilon kT}\right)^{1/2} = \left(\frac{2e^2 n^0 z^2}{\varepsilon kT}\right)^{1/2} \tag{1.3}$$

The second integration gives for the potential $\psi(x)$

$$\tanh [z\tilde{\psi}(x)/4] = [\tanh (z\tilde{\psi}_0/4)]\, e^{-\kappa x} \tag{1.4}$$

where $\tilde{\psi}(x) = e\psi(x)/kT$ is the reduced potential. Plots of this function for various values of ψ_0 show an approximately exponential falloff in electrostatic potential† to about 1% of its value at the surface in a distance of order $x = (4 \text{ or } 5)/\kappa$. Thus, although $1/\kappa$ is taken as the "thickness of the double layer," it should be noted that double-layer interaction effects can occur between colloidal particles which are separated by distances of order $10/\kappa$.

The surface density of charge, σ_0, is given by

$$\sigma_0 = -\varepsilon\left(\frac{d\psi}{dx}\right)_{x=0} = \frac{4n^0ze}{\kappa} \sinh \frac{z\tilde{\psi}_0}{2} \tag{1.5}$$

and hence the differential capacitance of the double layer is

$$C = d\sigma_0/d\psi_0 = \varepsilon\kappa \cosh (z\tilde{\psi}_0/2) \tag{1.6}$$

The applicability of these equations to the electrode/solution interface is at present accented by electrochemists: it is important to note that the flat-plate approximation is valid for many colloid chemical systems. In a 10^{-2} M solution

† The potential used here is that due to free charge at the interface. It is related to the Galvani potential (φ) as follows: $\psi_0 = {}^{M}\Delta_2 - \chi_{\text{dipole}}$, where the last term is usually ignored.

the value of $1/\kappa$ is about 3 nm so that κa will exceed 100 for colloidal particles whose radius a exceeds about 300 nm, which is well within the colloidal range.

The major limitation to this treatment is the assumption that the Gouy–Chapman model, composed of infinitesimally small ions immersed in a uniform dielectric, can be expected to reasonably represent the double layer right up to the plane where ψ_0 is measured. We will take this point up in Section 1.1.3 below.

1.1.2. The Double Layer around a Sphere

The complete Poisson–Boltzmann equation can no longer be solved in closed form for the case of spherical symmetry. The linearized equation and its solution

$$\psi(r) = \psi_0 a \exp\left[-\kappa(r - a)/r\right] \tag{1.7}$$

so familiar from the Debye–Hückel theory of strong electrolytes, is of some use in the description of colloidal systems of fairly low surface potential and as a comparison standard for more exact solutions.

A few numerical solutions of the complete equation were calculated as early as 1928[6] and more extensive tabulations[7,8] have since appeared, as adjuncts to the solution of the electrophoresis problem (see Section 2.4 below). An analytical representation of these tabulated data has been supplied by Stigter,[9] and a few analytical approximation formulas[10,11] are available to suit different situations, though one of these[12] has been critized by Semenikhin and Sigal.[13] These refinements are important for exact calculations on the theory but the principal findings of colloid science can be more readily grasped by concentrating initially on the more elementary linear solution [Eq. (1.7)] for most purposes if one is forced to treat the particles as spheres (i.e., $\kappa a \simeq 1$). One useful outcome of the approximate solutions is an accurate expression for the surface density of charge, which was proposed empirically by Loeb, Wiersema, and Overbeek,[8] and later given an analytical justification.[14,15]. The expression is[13]

$$\sigma_0 = \frac{2n^0 ze}{\kappa}\left(2\sinh\frac{z\tilde{\psi}_0}{2} + \frac{4\tanh z\tilde{\psi}_0/4}{\kappa a}\right) \tag{1.8}$$

which reduces to Eq. (1.5) for large κa; for small values of $\tilde{\psi}_0$ it yields the approximate expression derived from Debye–Hückel theory:

$$\sigma_0 = \frac{\varepsilon(1 + \kappa a)}{a}\psi_0 \tag{1.9}$$

1.1.3. The Stern Model: Compact and Diffuse Double Layers

This too is a subject which is dealt with at length elsewhere[15a] and will only be touched on here. Stern's modification[1] to the Gouy–Chapman theory was designed to overcome the objection, cited above, that the ions in the double layer are regarded as infinitesimally small and able to approach arbitrarily close to the surface. Stern introduced a single molecular layer in which the finite

ionic dimensions were taken into account.[16] Since then this model has been refined by Grahame[2] and many others† to take more explicit account of not only the ionic sizes in the layers near the phase boundary, but also the orientation of solvent dipoles around the ions and at the actual interface.

Much of our detailed knowledge of this region of the double layer has come from studies at the metal electrode/solution interface (notably the dropping mercury electrode). Although the compact layer in colloidal systems is very similar to that at the Hg/solution interface there are notable differences, especially in oxide systems, which will be discussed below (Section 1.2).

The introduction of the Stern or compact layer allows the Gouy–Chapman theory to be applied to the diffuse part of the double layer so that in Eqs. (1.4)–(1.9), ψ_0 and σ_0 are replaced by ψ_d and σ_d, the parameters characterizing the outer Helmholtz plane (OHP). There is a considerable body of evidence[18] that the PB equation is much more satisfactory when used in that role, especially in colloidal systems where the diffuse double-layer potential seldom rises much above 100 mV, and then only in extremely dilute solution.

It should also be noted that detailed models of the compact layer, to the extent that they take explicit account of dipole orientations in that region, go some way towards estimating the value of $\Delta\chi_{\text{dipole}}$. If they are extended to include the influence of the Stern layer charge on the permittivity of the inner region they can to some extent eliminate the rather arbitrary assumption made in equating ψ_0 to ${}^{M}\Delta_{2}\varphi$ (see footnote on page 398).

1.1.4. The Double Diffuse Double Layer

In some situations the space charge at the interface is thought to be distributed in a diffuse layer in both phases. This would certainly be expected in oil/water emulsion systems, but has also been suggested in relation to the AgI surface and that of some (porous) oxides.

The oil/water interface was treated by Verwey and Niessen[19] and their treatment is discussed by Verwey and Overbeek[20] and by Sparnaay.[21] If the diffuse layer is assumed to obey the PB equation in both phases then the overall phase difference potential due to the charges, ψ_o, is the sum of the potential drops in the two phases: $\psi_o = \psi_o^{\alpha} + \psi_o^{\beta}$. Integrating the Poisson equation establishes the equality of the dielectric displacement at the junction between the two phases:

$$\varepsilon_{\alpha}\left(\frac{d\psi^{\alpha}}{dx}\right)_{x=0} = \varepsilon_{\beta}\left(\frac{d\psi^{\beta}}{dx}\right)_{x=0} \tag{1.10}$$

and substituting Eq. (1.2) we obtain

$$(n_0^{\alpha}\varepsilon_{\alpha})^{1/2} \sinh (z\tilde{\psi}_0^{\alpha}/2) = (n_0^{\beta}\varepsilon_{\beta})^{1/2} \sinh (z\tilde{\psi}_0^{\beta}/2) \tag{1.11}$$

† See, for example, Reference 17.

which introduces the Boltzmann equation. The potential distribution in the two phases is evidently determined by the ratio

$$\alpha = \left(\frac{n_0^{\alpha}\varepsilon_{\alpha}}{n_0^{\beta}\varepsilon_{\beta}}\right)^{1/2} \tag{1.12}$$

and Figure 1 shows the relation between α and the potentials ψ_0^{α} and ψ_0^{β} for two particular values of ψ_0 ($z\tilde{\psi}_0 = 4$ and $z\tilde{\psi}_0 = 8$).

Low values of ε tend to be associated with low values of n_0 and so α may differ markedly from unity. In the oil/water system most of the potential drop thus occurs in the oil phase. The extent of the double layer can also be much larger in the oil than the water. Although it is determined by the ratio

$$\frac{\kappa_{\beta}}{\kappa_{\alpha}} = \left(\frac{n_0^{\alpha}\varepsilon_{\alpha}}{n_0^{\beta}\varepsilon_{\beta}}\right)^{1/2} \tag{1.13}$$

so that n_0 and ε offset one another to some extent, the double layer thickness in the oil can be of order 1 cm.

More elaborate approaches along these lines have been applied to the AgI/solution interface[21] and to the porous oxide surface, e.g., on SiO_2.[22]

1.2. Simultaneous Charge and Potential Measurements on the Double Layer

At the completely polarizable Hg/solution interface an arbitrary potential difference can be established by the imposition of an external emf. Although the absolute value of the potential difference between the interior of the mercury and the bulk electrolyte is uncertain, one can be much more confident about changes in that potential as the external emf is changed. Since the area of the

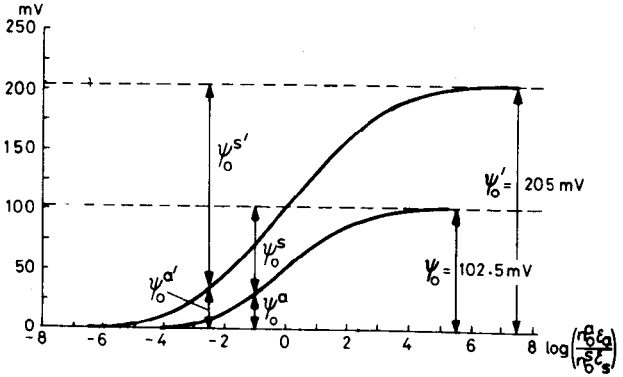


Figure 1. Distribution of a total potential drop ψ_0 of 102.5 and 205 mV, respectively, over two phases as a function of log α (see text). (From Reference 113 with permission.)

mercury drop is also unequivocally determinable, it is a relatively simple matter to determine the differential capacitance, per unit area, of the interface and to compare it with Eq. (1.6).

In colloidal systems the situation is somewhat different. In the AgI/solution system, for example, the corresponding electrode is reversible to Ag^+ or I^- ions and its potential is determined by the concentration of these ions in the solution. Because the electrode is solid its absolute area is difficult to determine directly and contamination problems would normally preclude one from attempting a direct measurement of the electrode capacitance. There is also the problem of suppressing the Faradaic current[23] when an imposed measuring potential is applied to the electrode system. Nevertheless some direct measurements of the capacitance of AgI electrodes have recently been made[24] and they are encouraging.

A much more straightforward technique, which takes advantage of the special properties of colloidal systems, is to measure directly the uptake of potential-determining ions onto the AgI surface as a function of its potential. This can be done by immersing an Ag/AgI electrode into a colloidal suspension of silver iodide particles, whose surface can be assumed to be identical with that of the electrode. The large surface area of AgI so generated makes possible a direct measurement of the absolute surface charge. A known quantity of Ag^+ or I^- ions is added to the system and the resulting potential of the Ag/AgI electrode enables an estimate to be made of the amount of Ag^+ or I^- remaining in solution. The difference is then assumed to be adsorbed onto the surface.

Using this technique Lyklema and Overbeek[25] obtained plots of σ_0 against ψ_0 which were very similar to those obtained at the Hg/solution interface.[23] The differential capacity of the AgI/solution interface in the presence of KF is shown in Figure 2. As one would expect, the total capacitance at low electrolyte concentrations and low potentials is very close to that given by double-layer

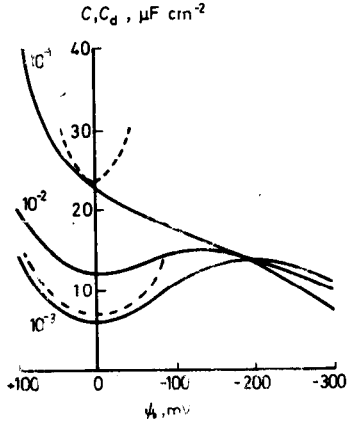


Figure 2. Differential capacitance, C, of the double layer on AgI in 10^{-3} M, 10^{-2} M, and 10^{-1} M KF solutions as function of the potential, ψ_0. Dotted lines: capacity C_d according to the diffuse double-layer theory. (From Lyklema and Overbeek[25] by courtesy of Academic Press.)

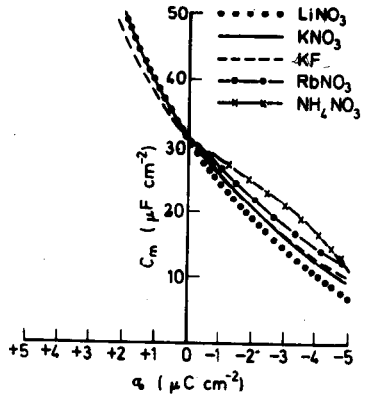


Figure 3. Inner-layer capacitance, C_m, on the AgI surface in solutions of some monovalent electrolytes. (From Lyklema and Overbeek[25] by courtesy of Academic Press.)

theory [Eq. (1.6)]. The behavior at higher concentrations and potentials is characteristic of the AgI surface since it is dominated by the behavior of the inner-layer capacitance, C_m. Figure 3 suggests that for AgI this capacitance is given approximately by

$$C_m \simeq 31 + 5\sigma_0 \qquad (1.14)$$

where C_m is in $\mu F\ cm^{-2}$ and σ_0 is in $\mu C\ cm^{-2}$.

Other solid/solution interfaces have been studied in the same way. For oxide systems the potential-determining ions are H^+ and OH^-. By adding acid or alkali and following the solution pH with a glass electrode, similar plots can be drawn, but in this case the value of ψ_0 is somewhat uncertain because of the inadequacy of the simple Nernst equation (see Refs. 27–33). Nevertheless, it is abundantly clear that these systems have an enormous apparent capacitance. Figure 4 shows a typical comparison drawn up by Lyklema[23] between the oxide and AgI surfaces using as abscissa the quantity (pH − pH°) or (pAg − pAg°).

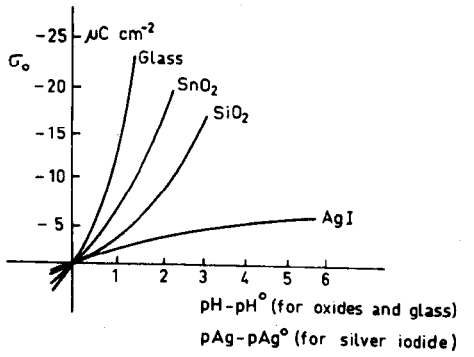


Figure 4. Comparison of the surface charge (due to OH^-) on several oxides with that on silver iodide (due to I^-). Ionic strength $I = 10^{-1}$ M KCl or KNO_3 (From Lyklema[23] by courtesy of Theorex.)

This quantity is directly proportional to ψ_0 for the silver system but overestimates ψ_0 for the oxide systems.[26] The disparity in capacitance is therefore even more marked than the figure indicates.

In the oxide systems the capacitance is obviously influenced greatly by the solid phase and several models have been proposed to account for the large values obtained. Some modify the Nernst equation for ψ_0,[27-29] while alternate explanations have been offered by Bérubé and de Bruyn[30] for the TiO_2/water system and by Yates *et al.*[31] for the general oxide/solution interface. This latter is a "site-binding" model which is similar to the Stern model but assumes that the counterions can form closely associated ion pairs with the surface charge. The resulting dipole must be assumed to lie almost parallel to the solid surface in order to account for the charge–potential curves.

The main obstacle to refinement of the models is the uncertainty surrounding the exact nature of the interface. Even if it is not actually porous, and many systems show little evidence of porosity, it is still significantly disordered and the concept of an idealized plane at which a surface potential can be identified is undoubtedly an oversimplification. Perhaps a unified description of all oxides will always prove elusive and a detailed description of individual systems will only become possible when the whole arsenal of spectroscopic and surface chemical techniques has been brought to bear on each well-characterized and reproducible system in turn.

There exists another experimentally measurable double-layer parameter in colloidal systems and that is the electrokinetic or zeta (ζ) potential. This is the potential in the "plane of shear" between a moving colloidal particle and the surrounding medium (see Section 2 below). Interpretation of ζ-potential measurements is a little uncertain because of the uncertainty in the exact location of the plane of shear within the double layer. Nevertheless, it has become common practice in recent years to test models of the solid–solution interface by attempting to reconcile simultaneously the experimental data on surface charge with the corresponding measured ζ potential as a function of the concentration of both potential determining and indifferent electrolyte ions. The work already alluded to[27-33] especially on oxide surfaces, is all developed on this basis so we must now turn to a consideration of the electrokinetic potential, and particularly, the limitations of that concept.

2. Electrokinetic Phenomena

2.1. The Electrokinetic (ζ) Potential

Electrokinetic phenomena occur when one (electrically charged) phase moves with respect to an adjoining phase. When a liquid moves through the pores of a solid or particles move through a surrounding liquid, the interaction between the mechanical and electrical forces can be used to acquire some knowledge of the electrical potential in the interphase region. The principal

electrokinetic effects are (i) *electro-osmosis*, in which a liquid moves past a solid (e.g., through pores) under the influence of an external electric field, (ii) *electrophoresis*, in which particles move through a liquid under the influence of an external electric field, (iii) *streaming potential*, where a liquid is forced past a solid surface and the resulting potential is measured, and (iv) *sedimentation potential*, in which the electrostatic potential generated by the settling of particles is measured.

The mathematical analysis of this relative movement is in all cases carried out with the aid of certain simplifications and idealizations, of which the most important, *especially when one phase is a solid*, is the *surface of shear*. This is an imaginary surface which lies close to the solid surface and within which the fluid remains stationary. In the case of fluid flowing through a capillary, the surface of shear would be expected to be a cylinder of radius slightly smaller than that of the capillary and coaxial with it. The potential in this plane of shear, relative to the bulk fluid, is called the zeta (ζ) potential. It is obviously the potential at some point in the double layer but its exact location is a matter of debate (see Section 2.5 below).

There is also the question of whether it is appropriate to regard the shear (or slipping) plane as infinitesimally thin, with all liquid outside it being assumed to possess the bulk properties. The question is examined in some detail by Davies and Rideal[34] and by Haydon[35] and their conclusions are that significant departures from bulk properties occur outside the shear plane. Nevertheless, we will use the concept for the preliminary analysis and return to a consideration of the reliability of the results in Section 2.5.

2.2. Electro-osmosis

2.2.1. In Single Capillaries

The theory of the process was first given in its present form by von Smoluchowski,[36] who considered the movement of liquid past a flat solid wall under the influence of an applied field. If the surface is negatively charged, an element of volume in the adjoining liquid will carry a positive space charge. As these positive ions move under the influence of the electric field they draw the liquid along with them. The surface of shear is in this case some small distance, δ, from the solid wall (Figure 5). The velocity of the liquid will be expected to rise from a value of zero in the plane of shear to some limiting value, v_{EO}, at "infinite" distance from the wall. "Infinite" in this context means the point at which the concentrations of positive and negative charges are indistinguishable (say, about $5/\kappa$). The velocity v_{EO} is the electro-osmotic velocity, and in a wide capillary ($\kappa r \gg 1$) most of the liquid will be traveling with this velocity.

The forces on an element of volume of the liquid in the absence of an externally applied pressure are shown in Figure 6 and it is apparent that

$$\mathscr{E}Q = \mathscr{E}\rho A\, dx = \eta A\left(\frac{dv_z}{dx}\right)_x - \eta A\left(\frac{dv_z}{dx}\right)_{x+dx}$$

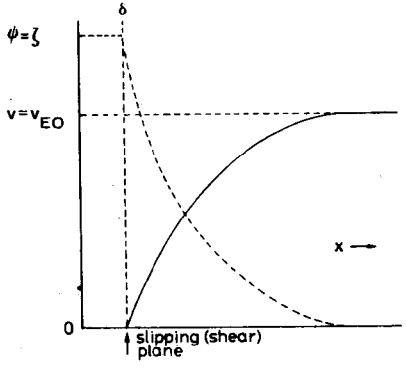


Figure 5. The variation of fluid velocity (solid line) and potential (dashed line) with distance from surface.

or

$$\mathscr{E}\rho\, dx = -\eta\left(\frac{d^2v_z}{dx^2}\right) dx \tag{2.1}$$

Substituting for ρ, the volume density of charge from Poisson's equation gives

$$\mathscr{E}\varepsilon \frac{d^2\psi}{dx^2}\, dx = \eta \frac{d^2v_z}{dx^2}\, dx \tag{2.2}$$

This equation can be integrated from a point in the bulk liquid ($dv_z/dx = 0$, $d\psi/dx = 0$) to a point in the double layer. A second integration this time to the shear plane gives

$$\frac{1}{\mathscr{E}}\int_{v_{EO}}^{0} dv_z = \int_0^{\zeta} \frac{\varepsilon}{\eta}\, d\psi \tag{2.3}$$

Making the usual assumption that ε and η assume their bulk values (ε_a, η_a) up to the shear plane, the electro-osmotic mobility v, is given by

$$v = \frac{v_{EO}}{\mathscr{E}} = -\int_0^{\zeta} \frac{\varepsilon}{\eta}\, d\psi = -\frac{\varepsilon_a \zeta}{\eta_a} \tag{2.4}$$

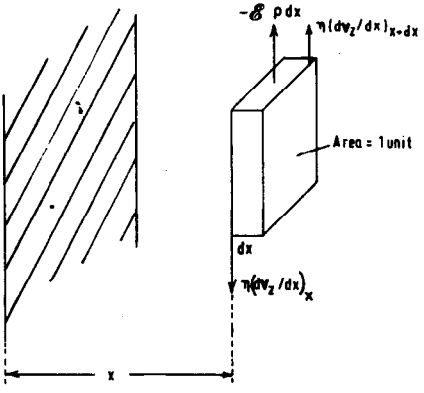


Figure 6. The forces on a slab of liquid in the neighborhood of a charged interface when subjected to a tangential electric field.

Note that, in deriving this equation, no special assumptions are made about the structure of the double layer, except that it obeys Poisson's equation. The inherent assumption is, however, that no charge or liquid movement occurs in the region $0 \leqslant x \leqslant \delta$.

Direct measurement of the electro-osmotic velocity is possible using suspended particles to follow the movement of the liquid, but it is more usual to measure the total volume of liquid displaced through the capillary in unit time

$$V = \pi r^2 v_{EO} = -\pi r^2 \frac{\varepsilon\zeta}{\eta} \mathscr{E} \tag{2.5}$$

The cross-sectional area of the capillary can be eliminated by measuring the current flow, i.

$$\frac{i}{\mathscr{E}} = \pi r^2 \lambda_0 \tag{2.6}$$

where λ_0 is the electrical conductivity of the liquid. Substituting (2.6) in (2.5) then gives

$$\frac{V}{i} = -\frac{\varepsilon\zeta}{\eta\lambda_0} \tag{2.7}$$

Equation (2.6) is valid only if all of the current flow occurs through the bulk liquid. In narrow capillaries and especially at low concentrations a disproportionate fraction of the current flows along the capillary surface and this *surface conduction* effect requires that Eq. (2.6) and (2.7) be modified to read

$$\frac{i}{\mathscr{E}} = \pi r^2 \lambda_0 + 2\pi r \lambda_s \tag{2.8}$$

and

$$\frac{V}{i} = -\frac{\varepsilon\zeta}{\eta(\lambda_0 + 2\lambda_s/r)} \tag{2.9}$$

where λ_s is the surface conductivity. For water in glass capillaries $\lambda_s \simeq 10^{-8}$–$10^{-9}\ \Omega^{-1}$ and, for $r \simeq 0.1$ cm, significant effects of surface conduction can be expected at concentrations below about $10^{-3.5}\ M$.

2.2.2. *Electro-osmotic Counter Pressure*

Instead of determining the volume of liquid transported under zero pressure difference it is possible to measure the electro-osmotic effect by applying a counterpressure which is just sufficient to prevent any net liquid flow. The back flow is given by Poiseuille's equation and so

$$V = \frac{\pi p r^4}{8\eta l} = \pi r^2 \varepsilon \frac{\zeta}{\eta} \mathscr{E} = \frac{\varepsilon i \zeta}{\eta \lambda_0}$$

i.e.,

$$P = 8\frac{\varepsilon\zeta}{r^2}\mathscr{E} = 8\frac{\varepsilon i\zeta}{\pi r^4 \lambda_0}.$$

where $P(=p/l)$ is the pressure gradient across the capillary. The final expression must, of course, be corrected in the usual way for surface conduction effects.

2.2.3. Electro-osmosis in Porous Plugs

Porous plugs may be composed of (i) uniform spherical granules, (ii) fibers, (iii) plates packed more or less regularly, (iv) bundles of capillaries, or (v) irregularly shaped particles more or less regularly packed. Provided that (i) the local radius of curvature of the particles is always large compared to $1/\kappa$, (ii) the pore size is large compared to $1/\kappa$, and (iii) the effects of surface conduction are negligible, it can be shown† that Eq. (2.4) remains valid.

For fine capillaries ($\kappa r \leqslant 10$) the double layer cannot develop completely in the capillary and a more detailed analysis of the potential distribution must be carried out. A brief description of the necessary modifications has been given by Hunter.[38] The resulting equations are of little use in the measurement of ζ potentials but are necessary for an understanding of water flow in microporous systems (such as desalination membranes).

The effect of surface conduction is discussed in Section 2.3.2 below since electro-osmosis and streaming potential are similarly affected.

2.2.4. Measurement of Electro-osmotic Flow

The electro-osmotic velocity of the liquid can be measured directly in single capillaries by observing the motion of colloidal particles suspended in the liquid. In effect, one observes simultaneously the electrophoretic motion of the particles and the electro-osmosis of the liquid under the same applied electric field. If the capillary is closed at both ends, the electro-osmotic flow in one direction sets up a pressure gradient which drives the liquid back down the center of the tube. The liquid velocity profile is parabolic with the (constant) particle velocity superimposed on it. The observed particle velocity in a cylindrical capillary can be shown to be[39]

$$v = v_E + v_{EO}(2y^2/r^2 - 1) \tag{2.10}$$

where y is the distance from the axis, v_E is the electrophoretic velocity, and v_{EO} is the electro-osmotic velocity. The observed particle velocity at the wall ($y = r$) is

$$v = v_E + v_{EO}$$

and at the axis where $y = 0$, $v = v_E - v_{EO}$. The electrophoretic velocity v_E can be obtained at the "stationary level," i.e., where the liquid velocity is zero and Eq. (2.10) shows that this occurs when $y = r/2^{1/2} = 0.707r$. v_{EO} can then be obtained from the velocity on the tube axis.

The main problem with this method is that the particles may adsorb on the capillary walls and modify the surface properties. In any case it is obviously not applicable for porous plugs and the total electro-osmotic volume flow per unit

† See Reference 37; actually proved for the streaming potential but equally valid for the electro-osmotic flow.

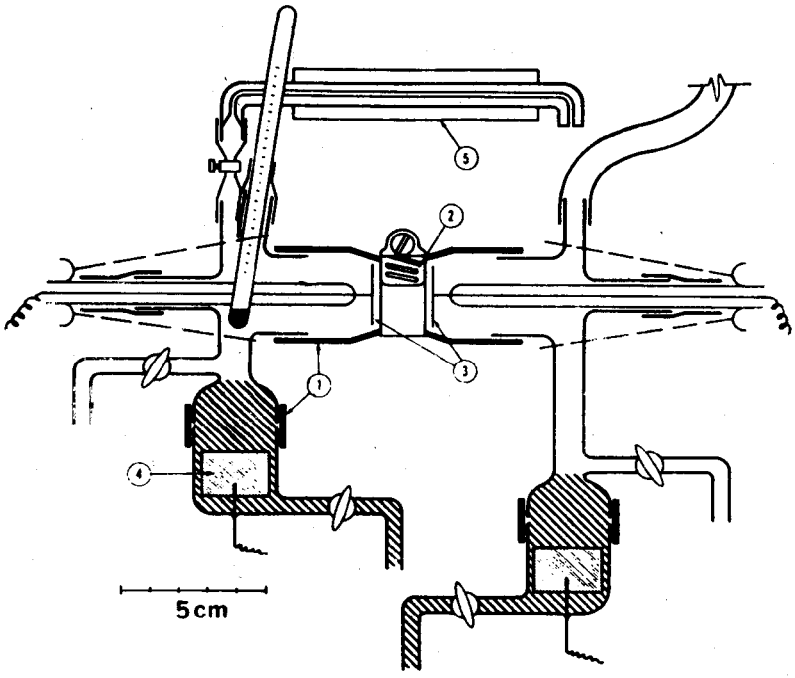


Figure 7. Cell for measuring conductance, permeability, and electro-osmosis of fiber plugs. (1) Tygon sleeves; (2) tubing clamp around fiber filing; (3) Pt gauze electrodes for measuring conductivity; (4) reversible Ag/AgCl electrodes for application of electric field; (5) 2 mm capillary tube for measurement of electro-osmotic volume. (From Stigter[41] by courtesy of Academic Press.)

time must then be measured. This is normally done by following the motion of a bubble in an auxiliary tube which is connected in parallel with the capillary or plug to be measured. The auxiliary tube may be either closed[40] or open, as is the case with Stigter's apparatus[41] shown in Figure 7. The problems associated with these measurements have been examined by Biefer and Mason,[42] and a review of the present understanding of the subject has been given recently by Dukhin and Deryaguin.[43]

2.3. Streaming Potential

2.3.1. In Single Capillaries

When an electrolyte solution is forced through a capillary, the charges in the mobile part of the double layer are carried towards one end. This constitutes

a streaming current, I_s, and the accumulation of ions of one sign at one end of the capillary generates a potential difference between the capillary ends. The resulting back flow of current, I_c, in the steady state, will be equal to I_s and a steady potential difference, the streaming potential, E_s, will be established across the capillary. This potential can be measured with a high impedance electrometer. Its relation to the ζ potential is derived as follows.

The velocity of the liquid at a distance y from the axis of the capillary is given by Poiseuille's equation

$$v(y) = p\frac{r^2 - y^2}{4\eta l} \doteq \frac{prx}{2\eta l} \tag{2.11}$$

where $x = r - y$. The approximation holds only near the wall of the capillary but this is where the streaming current is generated. The streaming current is, by definition,

$$I_s = \int_0^r 2\pi y v(y)\rho(y)\, dy \tag{2.12}$$

and substituting Eq. (2.11) for v and the Poisson equation for ρ gives

$$I_s = \frac{\pi r^2 p}{l}\int_r^0 \frac{\varepsilon}{\eta} x\frac{d^2\psi}{dx^2}\, dx = -\pi r^2\frac{\varepsilon_s p}{\eta_s l}\zeta \tag{2.13}$$

where again it is assumed that ε and η have their bulk values up to the shear plane where $\psi = \zeta$ and the fluid velocity is zero. This current can be measured directly using a low impedance ammeter. (In practice the current is about 10^{-9} A and can be measured[44] with a dc microvoltmeter across a resistance of about 1 kΩ. So long as the voltage generated is much less than the expected streaming potential the impedance can be considered to be "low.")

The streaming potential, E_s, generated by this current causes a conduction current, I_c, given by

$$I_c = \frac{\pi r^2 E_s \lambda_0}{l} + \frac{2\pi r E_s \lambda_s}{l} \tag{2.14}$$

and under steady state conditions ($I_s + I_c = 0$). We have

$$\frac{E_s}{p} = \frac{\mathscr{E}}{P} = \frac{\varepsilon\zeta}{\eta(\lambda_0 + 2\lambda_s/r)} \tag{2.15}$$

where P is the pressure gradient ($= p/l$). The equality of the ratio E_s/p and V/i [see Eq. (2.9)] is quite general and can be established using the principles of irreversible thermodynamics.[45]

It should be noted that measurement of streaming current in single capillaries obviates the difficulties caused by surface conduction, which is significant only in its influence on the streaming potential.

2.3.2. Potential and Current Measurements in Porous Plugs

The streaming potential exhibited by a porous plug is affected by geometry and surface conduction in the same way as the electro-osmotic flow. The detailed treatment of geometrical effects, especially in fine capillaries, would, however, take us far beyond the scope of the current work. Some discussion of the problem is given by Dukhin and Deryaguin[46] and a fuller review is currently in preparation.[47]

The effect of surface conduction must be discussed briefly because it is significant in all capillary porous systems at low salt concentrations. It becomes obvious when a plot of apparent ζ potential, ζ', is made against electrolyte concentration. If no correction is made for surface conduction such plots show a maximum at about 10^{-3} M electrolyte. At lower concentrations the absolute value of the streaming potential developed is diminished because of the large contribution made to the conduction current, I_c, by the surface conductivity.

The first attempt to correct for the effect was made by Briggs,[48] who suggested that it was sufficient to measure the conductivity of the liquid *in the plug* in order to determine the quantity $(\lambda_0 + 2\lambda_s/r)$ in Eq. (2.15). This is done by determining the resistance, R^0, of the plug when filled with a liquid of high salt concentration ($\geqslant 0.1$ M) when the surface conduction can be assumed to be negligible. The effective conductivity, λ_p, at other concentrations is given by

$$\lambda_p = (\lambda_0 + 2\lambda_s/r) = \lambda^0 R^0/R_{exp} \tag{2.16}$$

where λ^0 is the conductivity of the concentrated salt solution and R_{exp} is the measured resistance.

Although this procedure has been criticized[49,50] as being inexact for a system of capillaries of different radii connected in series and parallel, it has been shown to be a useful approximation.[51] It seems that provided the capillaries are conical in shape so that there are no rapid changes in radius the error in using Eq. (2.16) is not serious.[52] An elaborate procedure has been developed by Ghosh *et al.*[53,54] where plugs can be constructed using identical material with uniform but differing values of the radius.

For streaming current measurements, the surface conduction does not enter the problem directly but does have some influence on the determination of the effective cross-sectional area for current flow [the πr^2 term in equation (2.13)]. Neale[55] replaces Eq. (2.13) by

$$I_s = -\frac{\varepsilon\zeta}{\eta} P(1 - F)A\tau \tag{2.17}$$

where F is the volume of the solids per unit volume of the plug, A is its cross sectional area, and τ is a pore orientation factor, related to the tortuosity of the electrical path through the plug. According to Mason *et al.*[56,57] it is not possible to evaluate ζ from Eq. (2.17) but only a quantity which is proportional to ζ. Ghosh and Pal,[58] however, have developed an analysis which does seem

to give consistent ζ values for the types of system studied by Mason *et al.* (i.e., plugs of fibers). They replace the term $(1 - F)\tau$ in Eq. (2.17) by $\{x[1 + mF/(1 - F)]\}^{-1}$, where x and m are constants and obtain a linear plot of $\varepsilon P/\eta I_s$ against $F/(1 - F)$ from which ζ may be evaluated.

2.4. Electrophoresis

2.4.1. Theory of Electrophoretic Mobility

The analysis of the electro-osmotic effect given in Section 2.2 above can equally well be applied to the electrophoretic motion of a particle, provided that the radius is large compared to the double-layer thickness ($\kappa a \gg 1$). If the particle behaves as an insulator, and essentially all of them do,[59] the lines of force of the imposed electric field mostly run parallel to the particle surface. Fixing the coordinate system in the liquid then gives, for the mobility of the solid,

$$\mu = \frac{\varepsilon_a \zeta}{\eta_a} \tag{2.18}$$

An alternate analysis given by Hückel[60] suggested the relationship

$$\mu = \frac{2\varepsilon_a \zeta}{3\eta_a} \tag{2.19}$$

and Henry[61] subsequently established that these two formulations resulted from the different ways in which the influence of the particles on the electric field lines had been introduced. Equation (2.19) assumes that the particle does not influence the field lines significantly and this is true only when the particle conductivity is the same as the liquid or when $\kappa a \ll 1$.

In the general case,

$$\mu = \frac{\varepsilon_a \zeta}{\eta_a} X_1(\kappa a) \tag{2.20}$$

where $X_1(\kappa a)$ varies from 2/3(as $\kappa a \to 0$) to unity (as $\kappa a \to \infty$). Unfortunately this equation is valid only for very small values of the zeta potential ($\zeta \ll 25$ mV) and for larger values of ζ the effects of electrophoretic retardation and relaxation must also be included, just as in the theory of electrolyte conduction. The early approximate analytical solutions of this problem by Overbeek[62] and Booth[63] have been supplanted by a numerical solution first provided by Wiersema, Loeb, and Overbeek.[64] An excellent review of the early literature is provided by Overbeek and Wiersema[65] and a brief outline is given by Hunter.[38] Essentially, the problem involves solving simultaneously:

(*i*) ***The Poisson equation***

$$\text{div grad } \Lambda = -\rho/\varepsilon \tag{2.21}$$

where Λ is the total electrostatic potential

(*ii*) *A Nernst–Planck expression*

$$\operatorname{div}\left(\mp\frac{n_\pm z_\pm e}{f_\pm}\operatorname{grad}\Lambda - \frac{kT}{f_\pm}\operatorname{grad} n_\pm + n_\pm \mathbf{v}\right) = 0 \qquad (2.22)$$

where the $f_\pm$ are frictional coefficients and $\mathbf{v}$ is the velocity of the liquid with respect to the particle.

(*iii*) *The continuity equation*

$$\operatorname{div}\mathbf{v} = 0 \qquad (2.23)$$

and (iv) the steady state Navier–Stokes equation with inertial terms neglected:

$$-\eta \operatorname{div}\operatorname{grad}\mathbf{v} + \operatorname{grad} p + \rho \operatorname{grad}\Lambda = 0 \qquad (2.24)$$

with appropriate boundary conditions.

Wiersema *et al.*[64] provided a solution for the case of a solvent with two ionic species and their tabulated results are commonly used for calculating ζ from mobility measurements. The calculation is, however, not easy to do because one must interpolate from various tables and graphs. The scheme cannot be used with an arbitrary collection of ions of varying mobilities; there are convergence problems for high values of ζ ($|\zeta| > \sim 150$ mV for a 1:1 electrolyte and $> \sim 25$ mV for a 2:2 electrolyte) and the results at high κa have also been challenged by Dukhin and Deryaguin.[43]

O'Brien and White[66] have provided a numerical solution which does not suffer from these drawbacks. They show that the problem can be broken into two simpler problems: the calculation of (i) the force required to move a particle at a velocity $\mathbf{v}$ without an applied field and (ii) the force required to hold the particle fixed in the presence of an applied field $\mathscr{E}$.

The total force acting on the particle in the mobility problem is the sum of these two forces, and the requirement that the net force be zero leads to an expression for the mobility in terms of the asymptotic forms obtained for the electrolyte velocity far from the particle in each of these problems. They show that the mobility is independent of the dielectric constant of the particle and of the electrostatic boundary conditions on the particle surface. The mobility is then expressible as the ratio of two constants obtainable from the asymptotic solutions of the separate problems cited above. The simplifications in the computer program are considerable and the result is a program which can be economically applied to any experimental data; any number of arbitrary ionic mobilities can be introduced and no limitations are anticipated in the particle mobilities which can be handled. The general results of their analysis are summarized in Figures 8 and 9. Note in particular the maximum in the value of reduced mobility which occurs at $|\zeta| \approx 120$–160 mV for values of κa larger than 3.

2.4.2. Measurement of Electrophoretic Mobility

The mobility of colloidal particles in a known electric field can be measured by direct observation of their movement in an ultramicroscopic (or dark field

microscope) arrangement. The particles are placed in a cylindrical or rectangular capillary and the field is applied via a pair of electrodes immersed in the suspension medium. An outline of the expected behavior is given in Section 2.2.4 above. This is called the *microelectrophoretic* procedure and it permits direct measurement of mobility at low particle concentrations; coagulation effects are minimized and mobilities of mixed systems can be separately evaluated in favorable cases. One of the drawbacks of the method is that when measuring the particle velocity at the stationary level (see Section 2.2.4 above), the velocity gradient is so large that small errors in focusing (due to the depth of field of the microscope objective) can cause serious errors in the mobility. This problem is eliminated in the two-tube cell[67,68] in which observations are made on the tube axis where the velocity gradient is zero.

With laser illumination, particles significantly smaller than 0.1 μm can be observed in the microelectrophoresis process, but for still smaller systems other methods must be used. The moving boundary method can be used down to 100 Å or less with a suitable optical system for detecting the boundary. The theory of this method has been reviewed by Longsworth[69] and a recent formulation given by Tokiwa.[70]

Another procedure for small particles, particularly the micelles of colloidal electrolytes (i.e., soaps and detergents), is the tracer method first used by Brady[71] and developed by Mysels *et al.*[72,73] In principle, it can be used for

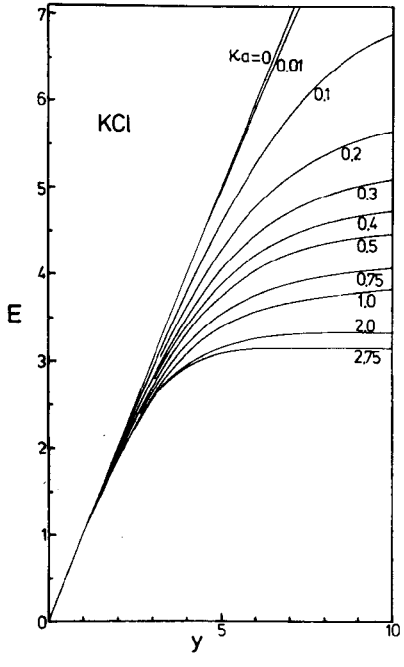


Figure 8. Plot of E, the dimensionless mobility [$E = 3\eta_u e\mu/2\epsilon kT$; cf. Eq. (2.19)] against the dimensionless ζ potential, $y(=e\zeta/kT)$ for low values of κa. In this region the mobility increases monotonically with ζ.

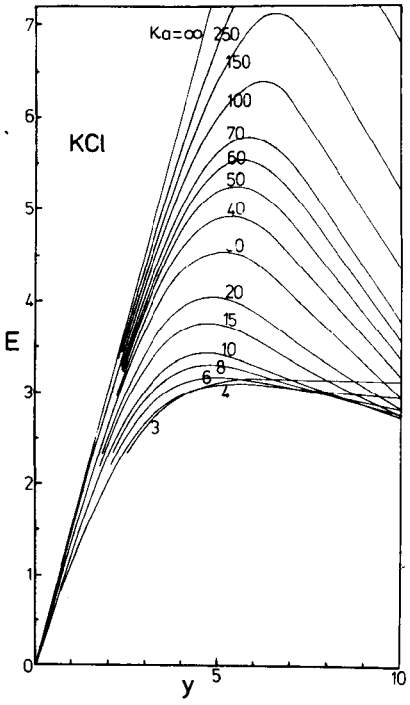


Figure 9. Variation of reduced mobility, E with reduced ζ potential, y, for larger values of κa.

any system into which a readily detectable tracer can be incorporated irreversibly. Radioactive tracers and water insoluble dyes have been used for the purpose.

The mass transport method has been used for some 50 years[74] but has recently been revived by the design of a special cell[75] which is claimed to give satisfactory mobility values even on quite concentrated suspensions.[76]

Finally, the most recent and sophisticated development is the method of electrophoretic light scattering which can be applied to colloid particles of any size. In effect, a laser light scattering measurement is conducted in the presence of an electric field. The Doppler broadening of the frequency of the scattered light can be used to calculate the diffusion coefficient of the particles, and the shift in the center frequency of the light, caused by the imposition of an electric field, can be used to calculate the electrophoretic mobility. The shift is very small (~ 100 Hz for an incident frequency of 6×10^{14} Hz) but with a laser light source it can be detected by heterodyning† the scattered light with the input beam and detecting the output of the difference frequency. The method is very fully reviewed by Ware.[76a]

† Mixing to produce a beat frequency.

2.5. Position of the Plane of Shear

2.5.1. Modified Viscosity and Permittivity in the Double Layer

If, in the derivation of Smoluchowski's equation, it is assumed that ε and η may be influenced by the electric field in the double layer, one can show that Eq. (2.4) in the form

$$\mu = -\int_0^{\zeta} \frac{\varepsilon}{\eta}\, d\psi$$

is still valid.[77] Davies and Rideal[78] made some attempt to estimate how ε and η might be affected by the double-layer electric field and concluded that the ratio ε/η would begin to fall if the field strength exceeded about 10^5 V cm^{-1} and would be reduced to zero for fields greater than 10^6 V cm^{-1}. Such fields are possible in the neighborhood of a colloidal particle.

Lyklema and Overbeek[79] tackled the problem analytically assuming that ε was constant and that η varied in accordance with

$$\eta = \eta_a[1 + f(d\psi/dx)^2] \tag{2.25}$$

Using estimates of the viscoelectric coefficient, f, suggested by work on organic liquids,[80] they concluded that corrections to the Smoluchowski equation would be significant (e.g., a 20% correction in 0.01 M solution for $\zeta = 75$ mV). Their value of f (10.2×10^{-16} V^{-2} m^2) was considered by Stigter[81] and by Hunter[82] to be too high by a factor of 10–50 for the oil–water interface in the presence of surfactants, but more recently Hunter and Leyendekkers[83] have obtained a value of $\sim 10^{-15}$ V^{-2} m^2 for water near a clay mineral surface. The Lyklema and Overbeek conclusions should, therefore, be relevant to that surface.

2.5.2. Position of the Plane of Shear

Stigter[81] showed that a nonzero value of f could be related to an apparent shift in the plane of shear by a distance, Δ, where

$$\Delta = A\kappa^{-1}[\arctan(A \cosh \tilde{\zeta}/2) - \arctan A] \tag{2.26}$$

and

$$A = [2fC/(1 - 2fC)]^{1/2}$$

Here C is a function of electrolyte concentration ($C = 14.28 \times 10^{15} mi$ V^2 m^{-2} if m is the electrolyte concentration in mol l^{-1}). The experimental data on micelles suggest that Δ is less than 1 Å, corresponding to a value of about 10^{-16} V^{-2} m^2 for the constant f. Carroll's[83a] analysis of Haydon's earlier data[83b] also suggests that in these micellar systems the shear plane is close to the plane of the stabilizing head groups. A similar conclusion was reached by Smith[84] for the silver iodide surface in the neighborhood of the p.z.c., and more recently Lyklema[85] has extended this conclusion to higher values of the surface potential of AgI.

Finally, it may be noted that direct measurements of both viscosity[88] and dielectric constant[87] in the neighborhood of the interface suggest that effects are small outside the first few molecular layers from the surface.[88]

In general, it may be concluded that the shear plane is close to but possibly not coincident with the outer Helmholtz plane though it should be noted that a shift of 1–2 Å can make ζ differ significantly from ψ_d, especially in moderately concentrated solutions.

2.6. Electroviscous Effects

The presence of an electrical double layer around a colloidal particle modifies the flow behavior of a suspension of such particles; this is called the electroviscous effect. In their review of the phenomenon, Conway and Dobry-Duclaux[89] distinguish between a primary, secondary, and tertiary effect. The primary effect is caused by the ionic atmosphere lagging behind the particle in a shear field so that additional viscous energy must be expended to keep the suspension flowing. The secondary effect is caused by double-layer interactions between approaching particles, while the tertiary effect refers to changes in the conformation of polyelectrolytes due to changes in intramolecular double-layer forces.

A brief review of these effects has been given by Napper and Hunter,[90] and a more extensive treatment is given by Goodwin.[91]

In order to determine the magnitude of these effects we must first separate out the hydrodynamic processes which would occur even in the absence of double-layer effects. This is not easy to do since particles with no diffuse double layer at all would exhibit attractive (van der Waals) interaction forces and would consequently coagulate. It is, therefore, necessary to reach some compromise between minimizing double-layer effects and providing a stable colloidal sol.[92] When this is done the relative viscosity (η/η_s, where η_s is the viscosity of the suspension medium) can be represented by a power series:

$$\eta/\eta_s = \eta_r = \sum_{i=0} k_i \phi^i \tag{2.27}$$

where ϕ is the volume fraction of colloid particles and $k_0 = 1$ and $k_1 = 2.5$, as suggested by Einstein. Evaluation of the higher coefficients has proved to be a very difficult problem[91] and a more heuristic approach, first suggested by Mooney[93] has been used by Dougherty and Krieger (see Reference 92) to arrive at the relation

$$\eta_r = (1 - k\phi)^{-[\eta]/k} \tag{2.28}$$

where $[\eta]$ is the intrinsic viscosity, which is taken to be an empirical constant whose value should approach the Einstein coefficient, 2.5, in the absence of double-layer effects. This equation gives a very good description of the effect of particle concentration up to values of $\phi = \sim 0.62$, which is almost close packing.[94]

The primary electroviscous effect concerns the behavior of individual particles and consequently causes a modification of k_1 in Eq. (2.27) or $[\eta]$ in Eq. (2.28). The secondary effect, being due to two-body interactions, modifies the value of k_2 in Eq. (2.27) and the parameter k in Eq. (2.28).

2.6.1. The Primary Electroviscous Effect

This problem was first examined by Smoluchowski,[95] who published without proof an equation which would require that

$$k_1 = 2.5\left[1 + \frac{1}{\lambda_0 \eta_s a^2}\left(\frac{\zeta e}{2\pi}\right)^2\right] \tag{2.29}$$

where a is the particle radius. This equation was expected to be satisfactory for large κa, where the effect is in any case very small. A derivation was subsequently published by Krasny-Ergen[96] but with a factor of 3/2 multiplying the second term in the parentheses.

A more complete treatment has since been given by Booth[97] for all values of κa, provided ϕ is not too large and neither is ζ. Booth's solution was expressed in the form

$$\eta_r = 1 + 2.5\phi\left(1 + \sum_{n=1}^{\infty} a_n \zeta^n\right) \tag{2.30}$$

and since $a_1 = 0$ and only the first two terms were evaluated, we can write

$$k_1 = 2.5[1 + q^* \tilde{\zeta}^2 Z(\kappa a)(1 + \kappa a)^2] \tag{2.31}$$

where

$$q^* = \frac{\varepsilon kT \sum_{i=1}^{s} n_i z_i^2 w_i^{-1}}{\eta_s e^2 \sum_{i=1}^{s} n_i z_i^2} \tag{2.32}$$

and $Z(\kappa a)$ is given as a power series in κa. w_i is the velocity per unit force of an ion of type i and the summation is carried out over all of the ions in the system. If all ions are assumed to have the same mobility, Eq. (2.31) reduces to the Krasny-Ergen relation for large values of κa. Eq. (2.31) has been tested experimentally by Stone-Masui and Watillon[98] and found to be satisfactory over the range $1 < \kappa a < 10$ for the conditions under which it was derived (low ϕ values).

2.6.2. The Secondary Electroviscous Effect

Since the secondary electroviscous effect involves double-layer interactions between approaching particles it causes a modification to the value of k_2 in Eq. (2.27). Fortunately, the effect is so large that it can be studied at low volume fractions ($\phi < 0.03$) where the effects of particle self-crowding are negligible so the uncertainty in the value of k_2 for uncharged spheres is unimportant. Stone-Masui and Watillon[98] use plots of $(\eta_r - 1)/\phi$ to obtain values of k_1 and k_2 to compare with theoretical estimates.

A theoretical treatment of the secondary effect was given by Chan, Blachford, and Goring[99] based on the notion that as two particles approach, the repulsion between them alters their trajectories; the two particles form a temporary doublet whose center-to-center distance is larger than that for the corresponding uncharged system and the energy dissipation is consequently larger. The separation distance was calculated by balancing the hydrodynamic force with that due to the electrical double layer (since the van der Waals forces are negligible at these distances). Their result was

$$k_2 = 1.125(1 + \delta_c/a)^5 \tag{2.33}$$

where $2\delta_c$ is the distance of closest approach.

Although this expression gives doublet separations of the right order of magnitude, the experimental results[98] differ from the theoretical predictions by as much as 800% in some cases. The dependence on δ_c^5 obviously makes the result extremely sensitive to the calculated separation distance.

A more elaborate analysis for the behavior at low rates of shear has recently been given by Russel,[100] who shows that

$$k_2 = \beta(\kappa a)^{-5} \tag{2.34}$$

where β is a dimensionless parameter which is found to vary approximately as $[\ln(\alpha/\ln\alpha)]^{4.5}$, where α is the ratio of electrostatic to Brownian forces. Russel argues that the spatial distribution of particles in a stationary suspension is determined by the balance between electrostatic and Brownian (thermal diffusion) forces, since the van der Waals forces are negligible at modest volume fractions. Any imposed flow disturbs this distribution and generates a net hydrodynamic force on each particle. The resulting translations dissipate energy, which is observed as an increase in viscosity.

When compared with the experiments of Stone-Masui and Watillon,[98] Russel's analysis is a significant improvement on the earlier model,[99] especially at low values of ϕ. At higher volume fractions, multiple-particle interactions become important and the agreement becomes less satisfactory.

The double-layer interactions become increasingly important at low electrolyte concentrations, and multiparticle effects can then become dominant even at quite modest volume fractions.[92] Such systems can form ordered arrays where they behave as liquid crystals stabilized by double-layer forces and separated by distances of the order of the wavelength of light.[101,102]

2.6.3. The Tertiary Electroviscous Effect

A detailed treatment of this effect is beyond the scope of the present work and the reader is referred to other treatments.[103,104]

2.6.4. Systems Involving Strong Electrical Interactions

Many systems of technological interest consist of particles between which there are quite strong attractive forces. They may be electrostatic or, say, van

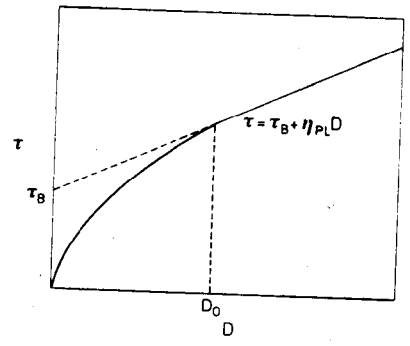


Figure 10. Characteristic flow diagram [shear stress (τ) vs. shear rate (D)] for a coagulated colloidal sol showing plastic–pseudoplastic behavior.

der Waals forces but even in the latter case they are modified by an overlying electrostatic (double-layer) repulsion. Such systems usually exhibit plastic or pseudoplastic behavior (i.e., a reduction in viscosity with increasing shear rate and, possibly, some elastic behavior). Goodeve[105] treated such systems by separating out the viscous energy dissipation from that caused by interparticle interaction. This work was extended by Gillepsie,[106] who showed that the extra energy dissipation due to particle interactions was given by

$$E_s = (\pi^2 a^3/3\phi^2)\tau_B \tag{2.35}$$

where τ_B is the Bingham yield value (see Figure 10). Michaels and Bolger[107] attempted to interpret this energy in terms of van der Waals attractions, and in a series of papers Hunter *et al.*[108,109] extended this analysis by incorporating the repulsive (double-layer) forces. In this latter work the system is assumed to be composed of flocs of particles which maintain a separate identity above the critical shear rate (D_0 in Figure 10). Below D_0 the flocs are able to form aggregates which increase in size as the shear rate is lowered. An analysis of this model allows one to establish verifiable relationships between the rheological parameters (τ_B, D_0, and η_{PL}) and the colloidal characteristics[110,111] (particle radius, a, ϕ, and ζ) and even to predict the elastic properties of such systems.[112] Comparisons with experiment have so far confirmed the predicted relationships.

3. The Double Layer in Colloid Stability

3.1. Coagulation Behavior of Electrostatically Stabilized Sols

Colloidal systems are traditionally divided into two types: *lyophilic* and *lyophobic*—literally, "solvent loving" and "solvent hating." Proteins and other polyelectrolytes fall into the first category and most of the systems discussed above fall into the second. Crystals of a lyophilic colloid, when placed in a suitable solvent, will imbibe the solvent, swell, and may form a homogeneous dispersion without the need for mechanical agitation. For such sols the disperse state is more thermodynamically stable than the crystal in contact with solvent.

Lyophobic sols, on the other hand, do not spontaneously disperse when placed in contact with the dispersion medium. Much mechanical work must be put into such systems to break the particles down to colloidal size and distribute them through the solvent or dispersion medium. Furthermore, the resulting dispersion is thermodynamically unstable with respect to the original solid in contact with dispersion medium. The Gibbs free energy of the system is at a minimum when the colloidal particles have been reaggregated to form a single crystal. A "stable" lyophobic colloid is, therefore, only relatively stable; it is stabilized kinetically by the presence of a repulsive energy barrier which prevents most of the particle–particle collisions from resulting in actual contact. A pair of particles which manages to surmount this barrier and make contact will remain in contact. To prepare reasonably stable sols it is necessary to develop potential barriers which result in less than 1 in 10^6 collisions (1 in 10^9 for more concentrated sols) being effective.

One of the most important ways to establish such a stabilizing barrier is by the adsorption of an electric charge onto the particles. A repulsion then occurs as soon as the double layers on two approaching particles being to overlap. That repulsion must be large enough to dominate over the van der Waals attraction, which occurs between all particles as a result of the dispersion forces which occur between their atoms. In colloidal systems these dispersion forces are of quite long range (up to 100 nm) compared to the attractive forces between single atoms, which span only about 1 nm.

Because the sign and magnitude of the surface potential is so easily controlled by addition of specific adsorbates, and the extent of the double layer is so easily modified by electrolyte concentration, the magnitude of the repulsive interaction can be varied over a very wide range. The stability of the sol, and everything which depends on that stability (e.g., optical and rheological properties) can therefore readily be controlled by proper management of double-layer characteristics.

The broad features of stability behavior have been known for almost a century since the pioneering work of Schulze, Hardy, and Freundlich (briefly reviewed in Reference 113, pp. 81, 82). One of the most characteristic features of a sol is the critical coagulation concentration (c.c.c.), which is the electrolyte concentration at which coagulation first begins to occur rapidly. This corresponds to the point at which the repulsive barrier has been reduced to such a level as to be ineffective so that all, or almost all, collisions between particles result in coagulation; the rate of coagulation is then determined by the rate of diffusion of particles towards one another.

The critical coagulation concentration (c.c.c.) depends on the type of electrolyte being used and, in particular, on the valency of the counterion. Divalent ions are about 60 times as effective as monovalent ions and trivalent ions are several hundred times as effective as monovalent ions in bringing about coagulation. This very strong valence dependence, for *indifferent* electrolyte ions, is referred to as the Schulze–Hardy rule. Some typical c.c.c. values are

Table 1

Some Critical Coagulation Concentration (c.c.c.) Values[a,b]

Valency of counterions	Sol of As_2S_3 (negatively charged)		Sol of Au (negatively charged)		Sol of $Fe(OH)_3$ (positively charged)	
Monovalent	LiCl	58			$\frac{1}{2}BaCl_2$	9.65
	NaCl	51	NaCl	24	NaCl	9.25
	KNO_3	50	KNO_3	23	KNO_3	12.00
Divalent	$MgCl_2$	0.72	$CaCl_2$	0.41	K_2SO_4	0.205
	$MgSO_4$	0.81	$BaCl_2$	0.35	$MgSO_4$	0.22
	$ZnCl_2$	0.69			$K_2Cr_2O_7$	0.195
Trivalent	$AlCl_3$	0.093				
	$\frac{1}{2}Al_2(SO_4)_3$	0.096	$\frac{1}{2}Al_2(SO_4)_3$	0.009		
	$Ce(NO_3)_3$	0.080	$Ce(NO_3)_3$	0.003		

[a] Reproduced from Reference 113, p. 82, with permission.
[b] Values given in millimoles per liter.

given in Table 1, which clearly shows the importance of the valence of the cation for negatively charged sols and the anion for positively charged sols. In these cases the ions are acting by compressing the double layer, while the surface potential can be assumed to remain constant (provided that thermodynamic equilibrium is maintained for the potential-determining ions as the particles approach one another) (see Section 3.3.2 below).

Ions which are specifically adsorbed (e.g., surfactants), or which react with the potential-determining ions, will have a different behavior pattern. A sol which is stabilized by H^+ ions (e.g., an oxide) will be positively charged. As the pH is raised the potential-determining ions are gradually neutralized until, in the neighborhood of the p.z.c. the sol begins to coagulate. Further addition of OH^- ions will reverse the charge on the sol and may make it stable until the ionic strength is increased to a point where double-layer compression becomes apparent (pH > 11); a second coagulation region will then be experienced.

3.2. Total Potential Energy of Interaction between Particles

It will be shown below (Section 3.3) that when two particles approach sufficiently closely so that their double layers overlap, they experience a repulsive interaction, the magnitude of which can be calculated from the reduction which occurs in the Gibbs free energy. The repulsive energy (V_R) rises exponentially as the particles approach and reaches a finite value when they are in contact (Figure 11). At the same time the particles experience a van der Waals (dispersion) attraction energy (V_A) which varies approximately as the inverse square of the separation and increases in magnitude without limit as the particles approach. The functional form of these two energies is such that the attraction always dominates over the repulsion at both large and small separations. A stable sol is one for which the repulsion dominates over the attraction at some

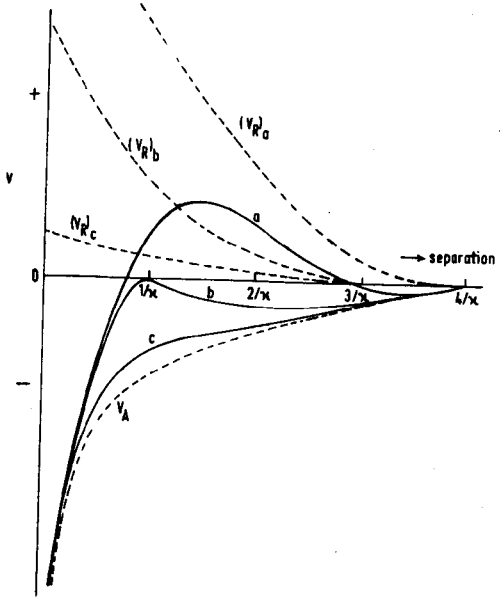


Figure 11. Total potential energy of repulsion for (a) stable, (b) marginal, and (c) unstable sol $|\zeta|_a > |\zeta|_b > |\zeta|_c$.

intermediate separation (see Figure 11). The width and, more importantly, the height of this potential barrier determine the stability of the colloidal sol.

These concepts were developed in the 1930s and 1940s, first by the Soviet colloid scientist Deryaguin and physicist Landau and subsequently, and independently, by Verwey and Overbeek[5] in the Netherlands, and are now referred to as the DLVO theory of colloid stability.

3.3. The Potential Energy of Repulsion

3.3.1. Under Constant Potential Conditions

3.3.1.1. Repulsion Between Flat Plates

The Gibbs free energy of a double layer, or system of double layers, can be calculated by using imaginary charging procedures rather like those used in the Debye–Hückel theory of strong electrolytes. Since the double layer forms spontaneously when the colloid particle is placed in the solvent, the free energy of formation is necessarily negative. It is made up of a chemical part ($-\sigma_0\psi_0$ per unit area) and an electrical part similar to that for a charged condenser. The total free energy is

$$\Delta G = -\sigma_0\psi_0 + \int_0^{\sigma_0} \psi' \, d\sigma_0' = -\int_0^{|\psi_0|} \sigma_0' \, d\psi_0' \tag{3.1}$$

where the primes denote surface properties at various stages in the charging process. For a single double layer, substituting (1.5) in (3.1) and integrating gives

$$\Delta G(\infty) = -\frac{8n^0kT}{\kappa}\left(\cosh\frac{ze\psi_0}{2kT} - 1\right) \tag{3.2}$$

where the symbol ∞ implies that the double layer is infinitely separated from all other double layers.

When two double layers begin to interact the potential profile between them is somewhat modified (Figure 12). The slope of the potential at the particle surface is decreased in absolute magnitude and, hence, according to Eq. (1.5), so too is the surface charge density. It is this discharge of the double layer which leads to the increase in free energy as the particles approach. The repulsion potential energy is given by

$$V_R = 2[\Delta G(d) - \Delta G(\infty)] \tag{3.3}$$

where d is the separation distance.

Unfortunately, the calculation of $\Delta G(d)$ is not as simple as the calculation of $\Delta G(\infty)$. The potential profile between two flat plates is, in the general case, given as an implicit function of the distance in terms of elliptic integrals of the first kind. Equation (3.1) turns out to be of limited use for interacting double layers because an explicit relation cannot be written for the dependence of σ_0 on ψ_0 at various particle separations. An alternative, but equivalent expression to Eq. (3.1),

$$\Delta G(d) = \int_0^1 \frac{d\lambda}{\lambda}\int \psi'\rho'\,dV \tag{3.4}$$

proves to be more useful; here λ is a charging parameter and the primes refer to the properties of the electrolyte between the plates as the charging occurs. The free energy can then be expressed as a function of the separation ($2d$), the surface potential, and the potential midway between the plates (ψ_m). If the origin is placed midway between the plates then

$$\Delta G(d) = -2\varepsilon(kT/ze)^2\kappa k^{-1/2}\{2(\cot\varphi)(1 - k^2\sin^2\varphi)^{1/2} - 4[E(k, \tfrac{1}{2}\pi) - E(k, \varphi)] + \tfrac{1}{2}\kappa\,dk^{-1/2}(3 - 2k - k^2)\} \tag{3.5}$$

where $k = \exp(-ze\psi_m/kT)$; $\sin\varphi = k^{-1/2}\exp[-ze\psi_0/2kT]$ and $E(k, \varphi) = \int_0^\varphi (1 - k^2\sin^2\theta)^{1/2}\,d\theta$ is the elliptic integral of the second kind.

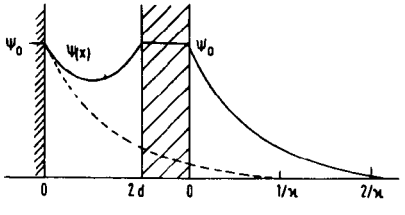


Figure 12. Schematic representation of the electrical potential between two plates, in comparison with that for a single double layer (after Overbeek[113]).

Values of V_R calculated from Eqs. (3.2), (3.1), and (3.5) are given by Verwey and Overbeek[5] and by Overbeek[113] for various values of surface potential and of κd, and these are very useful for calculating the exact (DLVO) repulsion between large flat plates with thin double layers. There are, however, many situations in which approximate relations are of sufficient accuracy and vastly more convenient to use, especially if one wishes to incorporate the repulsion energy or force as an element in a more elaborate model. We will therefore now examine some of the more important approximate expressions.

The repulsive *force* P between two approaching double layers was shown by Langmuir[114] to be given by

$$P = 2n^0kT(\cosh ze\psi_m/kT - 1) \tag{3.6}$$

and since

$$V_R = -2\int_{\infty}^{d} P\,dd \tag{3.7}$$

all that is required is an explicit relation between ψ_m and the separation, $2d$. For small degrees of interaction the potential in the midplane is approximately equal to the sum of the potentials from the two separate plates [$\psi_m \simeq 2\psi(d)$], and under these conditions

$$V_R = \frac{64n^0kT}{\kappa}\gamma^2 e^{-2\kappa d} \tag{3.8}$$

where $\gamma = \tanh(ze\psi_0/4kT)$. A better approximation for weak interactions is given by Verwey and Overbeek[115]:

$$V_R = \frac{32n^0kT}{\kappa}\gamma^2(1 - \tanh \kappa d) \tag{3.9}$$

3.3.1.2. *Repulsion between Spherical Particles*

If the radius of the spheres is large compared to the double-layer thickness $\kappa a \gg 1$, an ingenious procedure suggested by Deryaguin[116] enables V_R to be calculated from the corresponding flat-plate interaction. For the "exact" calculation, Verwey and Overbeek[117] supply a tabulation of the V_R function for various values of ψ_0 and κH_0, where H_0 is the distance of closest approach of the spheres.

If the approximate equation (3.9) is used in the Deryaguin method the repulsion between spheres is given by[118]

$$V_R = 2\pi\varepsilon a\psi_0^2 \ln[1 + \exp(-\kappa H_0)] \tag{3.10}$$

and this is the most commonly used approximation for such systems. It is most suitable when κa is large and is least accurate for values of H_0/a in the range 0.3–0.9 (see Figure 13). A more accurate procedure has since been developed by Levine *et al.*[119,120]

For smaller particles ($\kappa a \simeq 1$) the Deryaguin procedure breaks down and solutions are available only for small potentials (using the Debye–Hückel

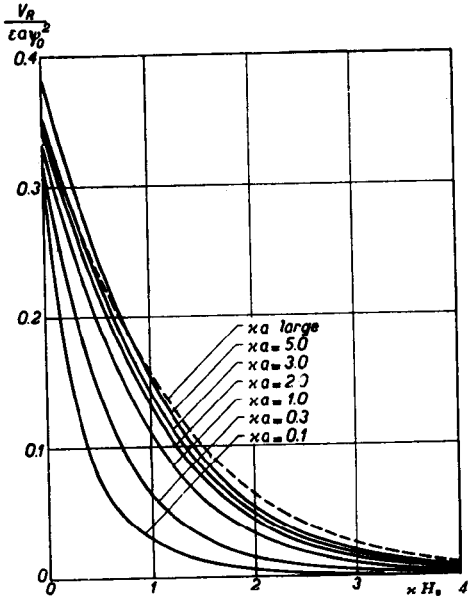


Figure 13. Potential energy of repulsion between two spherical particles for different values of κa. (From Overbeek[113] with permission.)

linearization (Section 1.1.2)). The potential must be expanded in spherical harmonics and the resulting expressions for V_R are far from elegant. An estimate of the repulsion can, however, be obtained from the expression[121]

$$V_R = \frac{4\pi\varepsilon\psi_0^2 a \exp(-\kappa H_0)}{2 + H_0/a} \tag{3.11}$$

though this equation overestimates V_R for small values of H_0 by up to 40% in the worst possible case for small values of κa (< 0.1).

3.3.2. *Under Constant Charge Conditions*

Throughout Section 3.3.1 it was assumed that as the particles approached one another their surface potentials remained constant. This corresponds to maintaining thermodynamic equilibrium between the potential-determining ions on the particle surface and in the bulk solution. This will be the case in most equilibrium measurements of particle interaction (see Section 3.5.4 below) but it may not hold during a normal collision, and almost certainly will break down for collisions under rapid shearing conditions. A more appropriate theoretical condition might then be that the surface charge remain constant during a collision, as suggested by Frens.[122] Using this condition, Wiese and Healy[123] derive the following approximate expression:

$$V_R^{\sigma} = V_R^{\psi} - \frac{2\pi\varepsilon a_1 a_2(\psi_1^2 + \psi_2^2)}{a_1 + a_2} \ln[1 - \exp(-2\kappa H_0)] \tag{3.12}$$

for a pair of particles of different radius and surface potential. The superscript on V_R refers to the quantity being held constant. This expression holds only for relatively small potentials ($\psi_{1,2} < 50$ mV, say) and has been extended by Honig and Mul.[124] The corresponding analysis for flat plates is given by Jones and Levine.[125]

The repulsion is always greater at constant charge since the surface potential rises without limit as the particles approach. In practice, the true V_R must lie somewhere between V_R^{ψ} and V_R^{σ}.

3.3.3. Repulsion between Dissimilar Surfaces

Equation (3.12) introduces for the first time in this analysis the possibility of the approaching surfaces being different. This is an important consideration in the coagulation of mixtures, in flotation (where a mineral particle interacts with an air bubble), and in many other technological situations. Such systems were first investigated by Deryaguin,[126] whose original calculations have been extended by Devereux and de Bruyn[127] in a collection of tables for flat-plate interactions. Extensive reviews of the area have been prepared[128,129] and a simple explanation of the main features of the behavior has been given by Hunter.[130] The analysis is conducted using "isodynamic curves"[126] which permit the V_R values for heterogeneous systems to be calculated from the corresponding values for homogeneous systems. The potential profile between two particles A and B of different potential (ψ_1 and ψ_2) can be constructed by introducing a third (imaginary) plate called the control which is placed at such a distance from the first plate A, that it generates a potential ψ_2 at the position of plate B (see Figure 14). Since the repulsion energy depends only on the potential and volume charge density between the plates [Eq. (3.4)] it is easy to see that

$$V_R(AB) = \tfrac{1}{2}V_R(AC) + \tfrac{1}{2}V_R(DB) \tag{3.13}$$

No new problem is involved in calculating the repulsion energy for the heterogeneous system, though, of course, the actual coagulation behavior can be quite complicated in such systems. It might be noted in passing that the interaction can be attractive at some separations, even if the particles have the

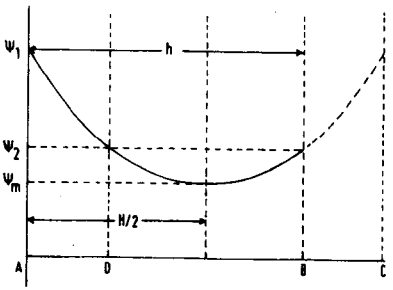


Figure 14. Construction of an isodynamic curve. Note that the repulsion between plates A and B is given by $V_{AB} = \frac{1}{2}V_{AC} + \frac{1}{2}V_{DB}$.

same sign of potential, though not if they have the same sign of charge. Also, attraction does not necessarily occur between particles with an unlike sign of charge.

3.4. The Potential Energy of Attraction

3.4.1. The Microscopic Approach

When the DLVO theory was first introduced, the potential energy of attraction, V_A, was calculated by assuming that the interaction of every pair of atoms in the two approaching particles was additive. The London dispersion interaction, v_A, between atoms can be written

$$v_A = -\lambda/r^6 \tag{3.14}$$

where λ depends on the polarizability of the atoms. Replacing the summations by integrations over both particles leads, for flat plates, to the expression[131]

$$V_A = -\frac{A}{48\pi}\left[\frac{1}{d^2} + \frac{1}{(d+\delta)^2} - \frac{2}{(d+\delta/2)^2}\right] \tag{3.15}$$

where $A = \pi^2 q^2 \lambda$ is commonly called the Hamaker constant and q is the number of atoms per unit volume. In most cases the thickness of the plates, δ, is much greater than their separation, $2d$, and Eq. (3.15) then reduces to

$$V_A = -A/48\pi d^2 \tag{3.16}$$

Note that the rate of decay of this interaction is slower than is the case for atoms, which is why it is referred to as the *long-range* van der Waals force. The value of A depends on the nature of the particles and the medium in which they are immersed and is of the order 5×10^{-21}–5×10^{-20} J (i.e., 1–10 kT).

For spherical particles the corresponding expression is[132]

$$V_A = -\frac{A}{6}\left(\frac{2}{s^2-4} + \frac{2}{s^2} + \ln\frac{s^2-4}{s^2}\right) \tag{3.17}$$

where $s = R/a$, R being the center-to-center distance. Putting $R = 2a + H_0$ and assuming that $H_0 \ll a$, we obtain, corresponding to Eq. (3.16)

$$V_A = -\frac{Aa}{12H_0} \tag{3.18}$$

indicating an even slower rate of decay in this case.

3.4.2. Electromagnetic Retardation

The temporary dipole-induced dipole interaction which is assumed to give rise to the attraction depends on a correlation between the dipole on one atom and that on another atom some distance away. As the distance between the particles increases, this correlation becomes poorer and poorer. In classical

terms one would say that the field generated by the first dipole is propagated with the speed of light and induces a dipole in the second atom. If the time taken to do that becomes comparable with the relaxation time of the first dipole then obviously the interaction will be much diminished. This manifests itself as a more rapid decrease in the attraction at larger distances. The energy V_A for flat plates then falls off as the inverse cube rather than the inverse square, a phenomenon referred to as *electromagnetic retardation.*

3.4.3. The "Macroscopic" Approach

The major limitation of the approach outlined in Section 3.4.1 is that it assumes pairwise additivity of the interactions between atoms. An alternative approach was suggested by Lifshitz[133] and a formal solution to the basic problem (two semi-infinite media of dielectric susceptibility ε_1 separated by a planar slab of material of susceptibility ε_2) was derived by Dzyaloshinskii, Lifshitz, and Pitaevskii.[134] This procedure depends on the notion that the attractive interaction is caused by the correlation of the natural fluctuations in electric charge density in different parts of a condensed medium. The fluctuations give rise to electromagnetic fields which are propagated through the medium and influence the development of fluctuations elsewhere so that all fluctuations are brought into some degree of correlation. An exact analysis requires the application of quantum field theory, which was the method used by Dzyaloshinskii *et al.*[134] Their result can be integrated to yield for the free energy of attraction[135]

$$G(d, T) = \frac{kT}{8\pi d^2} \sum_{n=0}^{\infty}{}' \int_{r_n}^{\infty} x \ln [(1 - \bar{\Delta}^2 e^{-x})(1 - \Delta^2 e^{-x})]\, dx \qquad (3.19)$$

where

$$\bar{\Delta} \equiv (s\varepsilon_2 - p\varepsilon_1)/(s\varepsilon_2 + p\varepsilon_1), \qquad \Delta \equiv (s - p)/(s + p) \qquad (3.20)$$

$$s \equiv (p^2 - 1 + \varepsilon_2/\varepsilon_1)^{1/2}, \qquad \varepsilon = \varepsilon(i\,\xi_n), \qquad \xi_n = (2\pi kT/\hbar)n \qquad (3.21)$$

and

$$p = (c/2\xi_n d\varepsilon_2^{1/2})x \qquad \text{for } n = 0, 1, 2, \ldots \qquad (3.22)$$

The symbols $\hbar$, k, and T have their usual significance and c is the velocity of light. The prime on the summation sign indicates that the first term ($n = 0$) is multiplied by $\frac{1}{2}$. The lower limit of the integral is given by

$$r_n \equiv 2\xi_n d\varepsilon_2^{1/2}/c \qquad (= x/p) \qquad (3.23)$$

which is the ratio of the travel time across the gap (of width d) and back, to the characteristic fluctuation time, $1/\xi_n$. Equation (3.19) appears to indicate an inverse square dependence of the attraction on distance [cf. Eq. (3.16)] but the van der Waals "constant" now becomes a function, not only of the properties of the materials, but also of distance (through the parameter p).

Application of the exact approach to more complicated geometries would be prohibitively difficult but a heuristic approach, first suggested by van Kampen,

has been applied successfully to a wide variety of problems, especially by Ninham and Parsegian.[135,136] An elementary description of the way in which an equation like (3.19) arises has been given by Hunter,[130] who also describes the early reviews in this area.

It should be noted that Eq. (3.19) introduces the temperature dependence of the attraction force and also the retardation effect, though in this more general formulation each different fluctuation frequency is, of course, affected to a different degree. It would appear at first that a prohibitive amount of information is required to calculate the attraction between two bodies (dielectric susceptibilities over the entire range of frequencies). It turns out, however, that quite accurate estimates can be made using the available spectroscopic data.[136] Each absorption band from the microwave through to the vacuum ultraviolet region of the spectrum makes a contribution to the attraction but the short wavelengths are rapidly retarded for large d values. The zero-frequency term is, of course, not retarded at all and can be dominant in aqueous systems,[137] though its significance is reduced in the presence of electrolytes.[138]

3.5. Experimental Tests of the DLVO Theory

3.5.1. The Kinetics of Coagulation

The rate at which a colloidal sol coagulates is determined by the magnitude of the potential energy barrier which separates the two particles (see Section 3.2 and Figure 11). It is not possible, however, to apply the simple criterion used in the elementary theory of chemical reaction rate. One cannot ask, "How many particles have sufficient energy to surmount the barrier," because it can easily be shown that any such particle would lose its energy by viscous dissipation in the surrounding liquid, before it penetrated the barrier (Reference 5, p. 164). Rather, one must solve the differential equation for the diffusion of particles towards a central particle in the presence of a field of force, as was done by Fuchs.[139]

The number of particles which pass through every (concentric) sphere surrounding a central particle and ultimately collide with it is given by[5]

$$Z = 4\pi R^2\left(D\frac{\partial N}{\partial R} + \frac{N}{f}\frac{\partial V}{\partial R}\right) \tag{3.24}$$

where R is the distance from the center of the central particle (considered fixed), D is the diffusion coefficient, N is the number of particles per unit volume, f is the frictional coefficient, and $V = V_A + V_R$ is the total energy of interaction. The appropriate boundary conditions are $N = 0$ at $R = 2a$ and $N = N_0$ at $R = \infty$ and the solution is then

$$Z = Z_0/W \tag{3.25}$$

where

$$W = 2a\int_{2a}^{\infty} e^{V/kT}\frac{dR}{R^2} = 2\int_{2}^{\infty} e^{V/kT}\frac{ds}{s^2} \tag{3.26}$$

Z_0 is the number of collisions which occur in the absence of a potential barrier and W is the stability ratio, which ranges from 1 for an unstable sol to 10^5 for a marginally stable one to 10^9 for a stable sol.

It turns out that W is determined entirely by the height of the potential barrier (V_{max}) and for $W = 10^5$ and 10^9 one requires that $V_{max} \doteqdot 15$ and 25 kT, respectively.

3.5.2. The Schulze–Hardy Rule

One of the earliest successes of the DLVO theory was a theoretical justification of the Schulze–Hardy Rule (Section 3.1, Table 1). The critical coagulation concentration (c.c.c.) should occur when the potential energy maximum disappears below the axis (Fig. 11, curve b). This will occur when $V_R + V_A = 0$ and $d(V_R + V_A)\,dd = 0$ simultaneously. Using Eq. (3.8) for V_R and (3.16) for V_A it is easy to show that this occurs when $\kappa d = 1$ (Figure 11, curve b). Substituting in (3.8) and (3.16) gives

$$\frac{64n^0kT}{\kappa}\gamma^2 e^{-2} - \frac{\kappa^2 A}{48\pi} = 0 \tag{3.27}$$

which can be rearranged, using the definition of κ, to

$$n^0 = \frac{18432\pi^2 e^{-4}\gamma^4\varepsilon^3 k^5 T^5}{z^6 e^6 A^2} \tag{3.28}$$

and at 25°C in water

$$\text{c.c.c.} = 8.65 \times 10^{-39}/z^6A^2 \tag{3.29}$$

in mol liter^{-1}, if A is in joules and the double-layer potential difference is large so that $\gamma \doteqdot 1$. The inverse sixth-power dependence of the c.c.c. on the valency is close to that observed in Table 1 though this approximate formula overestimates the value of A. (For a 1:1 electrolyte a c.c.c. of 50 mmol/liter corresponds to $A = 4.2 \times 10^{-19}$ J.)

3.5.3. Experiments on the Kinetics of Slow Coagulation

The critical coagulation concentration, by its nature, tells us little about the size of the potential energy barrier. Study of the rate of slow coagulation as a function of electrolyte concentration, surface potential, etc. could in principle afford a more stringent test of DLVO theory. In practice most experiments are interpreted by assuming the validity of DLVO theory and calculating the value of the Hamaker constant. The early work in this area was reviewed by Overbeek (Reference 113, p. 295 ff) and subsequently by Lyklema,[140] Gregory,[141] and Matijevic *et al.*[142,143] Reviews by Napper and Hunter[147,90] give a detailed account of the degree of success so far achieved in reconciling theory and experiment. The results are in accord with the theory though there remain peculiarities which are the subject of active current investigation (e.g., dependence of the Hamaker constant on electrolyte concentration[144]).

At best these kinetic measurements can only provide a limited test of the theory since they examine, in effect, only the height of the potential energy maximum. A more stringent test of the theory is provided by the equilibrium methods which examine the height of the barrier as a function of separation between particles.

3.5.4. Equilibrium Studies of the Force of Interaction

The first attempts to examine the force–distance relation experimentally were made by Norrish[145] using ordered layers of the clay mineral montmorillonite. This, and the subsequent work using lithium vermiculite,[146] showed that when an external force is applied to press the plates together the experimental relation between applied pressure and plate separation is close to the theoretical. When the external pressure is removed, however, the equilibrium spacing is smaller than is predicted by the theory. Much of the problem here can be traced to failure of the system to satisfy the conditions of the theoretical model. Presence of improperly aligned particles, surface asperities, and a heterogeneous charge distribution over the surface may contribute to the discrepancy.

A system which more exactly conforms to the model of flat plates is the thinning of a soap film. The initial experiments of Deryaguin, of Scheludko, and of Sonntag using this method are reviewed in the work of Lyklema and Mysels,[86] and again the agreement is impressive when an external (suction) pressure is being applied to the thinning film so that the repulsion forces dominate over the attractions.[147] Once again, however, there remains a discrepancy when the film is allowed to reach its own equilibrium thickness with no externally applied pressure. It is thinner than expected at low salt content and thicker than expected at high salt content. This discrepancy does not appear to be completely explicable in terms of the dependence of the Hamaker function [Eq. (3.19)] on electrolyte concentration.[147]

Undoubtedly, the most exciting development in this field at the moment is the direct measurement of the force–distance relation between atomically smooth surfaces of exfoliated mica in an electrolyte solution. These measurements (by Israelachvili and Adams[87]) provide, for the first time, a complete test of the theory, at least for this particular surface, and the results are very striking indeed. The apparatus used enables the separation between the surfaces to be varied from infinity down to a few angstrom units and the force can be measured with high accuracy and reproducibility. The agreement with the theory for 1:1 electrolytes is quite remarkable even up to 10^{-1} *M* electrolyte where one might expect the Poisson–Boltzmann equation to be unreliable (Figure 15). If the surfaces are pressed very close together (< 2 nm apart) one begins to see effects which are not adequately described by the "physical" forces of diffuse layer overlap. It is hardly surprising that at that point the detailed (chemical) nature of the interface (its adsorbed ions and the water structure) begins to become apparent. Discrepancies are noticeable for asymmetric electrolytes, where the

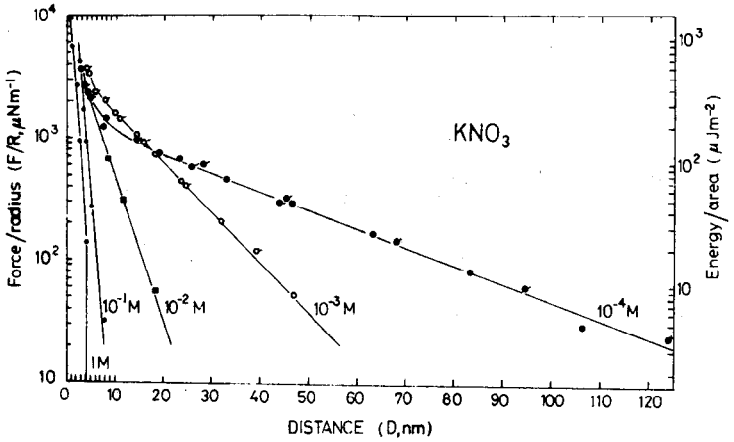


Figure 15. Experimental study of the force or energy of interaction between two macroscopic sheets of atomically smooth mica as a function of separation. The lines are calculated theoretically. (From Israelachvili and Adams.[98])

PB equation is less satisfactory. Much more data will be forthcoming from this apparatus in the near future as different salt systems and adsorbates are examined.

Another recent development is the study of order–disorder transitions in more concentrated colloidal sols. Monodisperse latex suspensions exhibit a spectacular iridescence effect which is attributable to an ordering of the particles on a lattice with a spacing comparable to the wavelength of visible light. The transition from order to disorder is determined by particle concentration and electrolyte concentration and it seems that only a proper statistical mechanical treatment involving many-body interactions can give a satisfactory description of the process.[90] Simple two-body interactions would even predict the wrong direction for the influence of electrolyte concentration on the ordering process, which appears to be akin to a phase transition.

4. Concluding Remarks

The above account outlines the current understanding of the significance of the double layer in colloid science. In addition to the reviews referred to above, there appear reviews of various aspects of the field in the journal *Advances in Colloid and Interface Science*[88] and in the series *Surface and Colloid Science*,[43] *Progress in Surface and Membrane Science*,[129] and *Recent Progress in Surface Science*.[35] A series of advanced monographs to cover the whole of colloid science is currently in preparation for publication by Academic Press under the editorship of R. H. Ottewill and R. L. Rowell.[47]

References

1. O. Stern, Z. *Elektrochem.* **30**, 508 (1924).
2. D. C. Grahame, *Chem. Rev.* **41**, 441 (1948).
3. J. G. Kirkwood, *J. Chem. Phys.* **2**, 767 (1934).
4. F. P. Buff and F. H. Stillinger, Jr., *J. Chem. Phys.* **39**, 1911 (1963).
5. E. J. W. Verwey and J. Th. G. Overbeek, *Theory of Stability of Lyophobic Colloids*, Elsevier, Amsterdam (1948), p. 24.
6. H. Müller, *Kolloidchem. Beih.* **26**, 257 (1928).
7. N. E. Hoskin, *Trans. Faraday Soc.* **49**, 1471 (1953).
8. A. L. Loeb, P. H. Wiersema, and J. Th. G. Overbeek, *The Electrical Double Layer Around a Spherical Colloidal Particle*, MIT Press, Cambridge, Massachusetts (1961).
9. D. Stigter, *J. Electroanal. Chem.* **37**, 61 (1972).
10. J.-Y. Parlange, *J. Chem. Phys.* **57**, 376 (1972).
11. S. L. Brenner and R. E. Roberts, *J. Phys. Chem.* **77**, 2367 (1973).
12. B. Abraham-Shrauner, *J. Colloid Interface Sci.* **44**, 79 (1973).
13. N. M. Semenikhin and V. L. Sigal, *J. Colloid Interface Sci.* **51**, 215 (1975).
14. S. S. Dukhin, N. M. Semenikhin, and L. M. Shapinskaj, *Dokl. Akad. Nauk. SSSR* **193**, 385 (1970).
15. V. L. Segal and V. E. Shamanskij, *Dokl. Akad. Nauk. Ukrainien SSR* **B4**, 346 (1970).

15a. J. O'M. Bockris and A. K. N. Reddy, *Modern Electrochemistry*, Vol. 2, Plenum Press, New York (1973), Chap. 7.

16. J. Th. G. Overbeek, in *Colloid Science*, H. R. Kruyt, ed., Vol. 1, Elsevier, Amsterdam (1952), p. 133.
17. J. O'M. Bockris, M. A. V. Devanathan, and K. Müller, *Proc. R. Soc. London Ser. A* **274**, 55 (1963).
18. D. A. Haydon, in *Recent Progress in Surface Science* J. F. Danielli, K. G. A. Pankhurst, and A. C. Riddiford, eds., Vol. 1, Academic Press, New York (1964), pp. 94–158.
19. E. J. W. Verwey and K. F. Niessen, *Philos. Mag.* **28**, 435 (1939).
20. E. J. W. Verwey and J. Th. G. Overbeek, *Theory of Stability of Lyophobic Colloids*, Elsevier, Amsterdam (1948), pp. 34–37.
21. M. J. Sparnaay, The electrical double layer, in *International Encyclopaedia of Physical Chemistry and Chemical Physics*, D. H. Everett, ed., Pergamon, Oxford (1972).
22. J. W. Perram, R. J. Hunter, and H. J. L. Wright, *Aust. J. Chem.* **27**, 461 (1974).
23. J. Lyklema, in *Physical Chemistry: Enriching Topics from Colloid and Surface Science*, H. van Olphen and K. J. Mysels, eds., IUPAC Commission 1.6, Theorex, La Jolla, California (1975), p. 288.
24. J. H. A. Pieper and D. A. de Vooys, *J. Electroanal. Chem.* **53**, 243–252 (1974).
25. J. Lyklema and J. Th. G. Overbeek, *J. Colloid Sci.* **16**, 595 (1961).
26. R. J. Hunter and H. J. L. Wright *J. Colloid Interface Sci.* **37**, 564 (1971).
27. J. Lyklema, *J. Electroanal. Chem.* **18**, 341 (1968).
28. J. Perram, R. J. Hunter, and H. J. L. Wright, *Chem. Phys. Lett.* **23**, 265 (1973); *Aust. J. Chem.* **27**, 461 (1974).
29. S. Levine, A. L. Smith, and A. C. Brett, Seventh International Congress on Surface Activity, Zurich, 1972.
30. Y. G. Bérubé and P. L. de Bruyn, *J. Colloid Interface Sci.* **28**, 92 (1968).
31. D. E. Yates, S. Levine, and T. W. Healy, *J. Chem. Soc. Faraday Trans. I* **70**, 1807 (1974).
32. H. J. L. Wright and R. J. Hunter, *Aust. J. Chem.* **26**, 1183, 1191 (1973).
33. S. Levine and A. L. Smith, *Discuss Faraday Soc.* **52**, 290 (1971).
34. J. T. Davies and E. K. Rideal, *Interfacial Phenomena*, Academic Press, New York (1963), pp. 140–144.

35. D. A. Haydon, in *Recent Progress in Surface Science*, J. F. Danielli, K. G. A. Pankhurst, and A. C. Riddiford, eds., Academic Press, London (1964), pp. 140 ff.
36. M. von Smoluchowski, *Bull. Intern. Acad. Sci. Cracovie*, p. 184 (1903).
37. J. Th. G. Overbeek, in *Colloid Science*, H. R. Kruyt, ed., Vol. I, Elsevier, Amsterdam (1952), p. 204.
38. R. J. Hunter, Electrochemical aspects of colloid chemistry, in *Modern Aspects of Electrochemistry*, No. 11, B. E. Conway and J. O'M. Bockris, eds., Plenum Press, New York (1975), Chap. 2.
39. A. E. Alexander and P. Johnson, *Colloid Science*, Oxford University Press, Oxford (1949), p. 310.
40. A. J. Ham and W. Hodgson, *Trans. Faraday Soc.* **38**, 217 (1942).
41. D. Stigter, *J. Colloid Sci.* **19**, 252 (1964).
42. G. J. Biefer and S. G. Mason, *J. Colloid Sci.* **9**, 20 (1954).
43. S. S. Dukhin and B. V. Deryaguin, Electrokinetic phenomena, in *Surface and Colloid Science*, Vol. 7, E. Matijevic, ed., J. Wiley, New York (1974), pp. 160–163.
44. R. M. Hurd and N. Hackerman, *Electrochem. Soc. J.* **102**, 594 (1955).
45. P. Mazur and J. Th. G. Overbeek, *Rec. Trav. Chim. (Pays-bas)* **70**, 83 (1951).
46. S. S. Dukhin and B. V. Deryaguin, Electrokinetic phenomena, in *Surface and Colloid Science*, Vol. 7, E. Matijevic, ed., J. Wiley, New York (1974), pp. 113–130.
47. R. J. Hunter, Electrokinetic effects—The theory and interpretation of zeta potential, in the series *Colloid Science*, R. H. Ottewill and R. L. Rowell, eds., Academic Press, New York (1981).
48. D. K. Briggs, *J. Phys. Chem.* **32**, 641 (1928).
49. J. Th. G. Overbeek and P. W. O. Wijga, *Rec. Trav. Chim.* **65**, 556 (1946).
50. A. J. Rutgers and R. Janssen, *Trans. Faraday Soc.* **51**, 830 (1955).
51. P. N. Zhukov and D. A. Fridrikhsberg, *Kolloidn. Zh.* **12**, 25 (1950).
52. S. S. Dukhin and B. V. Deryaguin, Electrokinetic Phenomena, in *Surface and Colloid Science*, E. Matijevic, ed., Vol. 7, J. Wiley, New York (1974), p. 150.
53. B. N. Ghosh, *Naturwiss.* **42**, 121 (1955).
54. B. N. Ghosh, S. C. Rakshit, and D. K. Chattoraj, *J. Indian Chem. Soc.* **30**, 601–606 (1953).
55. S. M. Neale, *Trans. Faraday Soc.* **42**, 473 (1946).
56. D. A. I. Goring, and S. G. Mason, *Can. J. Res.* **B28**, 307, 323 (1950).
57. G. J. Biefer and S. G. Mason, *Trans. Faraday Soc.* **55**, 1239–1245 (1959).
58. B. N. Ghosh and P. K. Pal, *Trans. Faraday Soc.* **56**, 116–122 (1960).
59. J. Th. G. Overbeek, in *Colloid Science*, H. R. Kruyt, ed., Vol. I, Elsevier, Amsterdam, (1952), p. 209.
60. E. Hückel, *Phys. Z.* **25**, 204 (1924).
61. D. C. Henry, *Proc. R. Soc. London Ser. A* **133**, 106 (1931).
62. J. Th. G. Overbeek, *Kolloid-Beih.* **54**, 287 (1943).
63. F. Booth, *Proc. R. Soc. London Ser. A* **203**, 514 (1950).
64. P. H. Wiersema, A. L. Loeb, and J. Th. G. Overbeek, *J. Colloid Interface Sci.* **22**, 78 (1966).
65. J. Th. G. Overbeek and P. H. Wiersema, in *Electrophoresis*, Vol. II, M. Bier, ed., Academic Press, New York (1967), Chap. I.
66. R. W. O'Brien and L. R. White, *J. Chem. Soc. Faraday Trans. II* **74**, 1607 (1978).
67. M. E. Smith and M. W. Lisse *J. Phys. Chem.* **40**, 399 (1936).
68. J. D. Hamilton and T. J. Stevens, *J. Colloid Interface Sci.* **25**, 519 (1967).
69. L. G. Longsworth, in *Electrophoresis*, Milan Bier, ed., Academic Press, New York (1959), Chaps. 3 and 4.
70. F. Tokiwa, *Adv. Colloid Interface Sci.* **3**, 389 (1972).
71. A. P. Brady, *J. Am. Chem. Soc.* **70**, 91; (1948).
72. H. W. Hoyer, K. J. Mysels, and D. Stigter, *J. Phys. Chem.* **58**, 385 (1954).

73. D. Stigter and K. J. Mysels, *J. Phys. Chem.* **59**, 45 (1955).
74. H. H. Paine, *Trans. Faraday Soc.* **24**, 412 (1928).
75. J. P. Olivier and P. Sennett, 3rd Annual Conference of the Clay Minerals Society, Pittsburgh, Pennsylvania, October 1966.
76. R. P. Long and S. Ross, *J. Colloid Sci.* **22**, 438 (1965).
76a. B. R. Ware, *Adv. Colloid Interface Sci.* **4**, 1–44 (1974).
77. J. Th. G. Overbeek, in *Colloid Science*, Vol. I, H. R. Kruyt, ed., Elsevier, Amsterdam (1952), p. 199.
78. J. T. Davies and E. K. Rideal, *Interfacial Phenomena*, 2nd Ed. Academic Press, New York (1963), pp. 140–144.
79. J. Lyklema and J. Th. G. Overbeek, *J. Colloid Sci.* **16**, 501 (1961).
80. E. N. da C. Andrade and C. Dodd, *Proc. R. Soc. London Ser. A* **204**, 449 (1951).
81. D. Stigter, *J. Phys. Chem.* **68**, 3600–3602 (1964).
82. R. J. Hunter, *J. Colloid Interface Sci.* **22**, 231 (1966).
83. R. J. Hunter and J. V. Leyendekkers, *J. Chem. Soc. Faraday I* **74**, 450 (1978).
83a. B. J. Carroll, *Ph.D. thesis*, University of Cambridge, 1970.
83b. D. A. Haydon, *Proc. R. Soc. London* **258A**, 319 (1960).
84. A. L. Smith, in *Dispersions of Powders in Liquids*, G. D. Parfitt, ed., Applied Science Press, London (1973), p. 113.
85. J. Lyklema, *J. Colloid Interface Sci.* **58**, 242 (1977).
86. J. Lyklema, P. C. Scholten, and K. J. Mysels, *J. Phys. Chem.* **69**, 116 (1965).
87. J. Israelachvili and G. Adams, *J. Chem. Soc. Faraday Trans. 1* **74**, 975 (1978).
88. B. E. Conway, "The State of Water and hydrated ions at interfaces," *Adv. Colloid Interface Sci.* **8**, 91 (1977).
89. B. E. Conway and A. Dobry-Duclaux, in *Rheology: Theory and Applications, Vol. 3*, F. R. Eirich, ed., Academic Press, New York (1960), p. 83.
90. D. H. Napper and R. J. Hunter, in *MTP International Review of Science—Physical Chemistry*, Ser. 2, M. Kerker, ed., Vol. 7, Butterworths, London (1974), pp. 161–213.
91. J. W. Goodwin, in *Colloid Science*, Vol. 2, Specialist Periodical Reports, Chemical Society, London (1975), pp. 246–293.
92. I. M. Krieger, *Adv. Colloid Sci.* **3**, 111 (1972).
93. M. Mooney, *J. Colloid Sci.* **6**, 162 (1951).
94. M. E. Woods and I. M. Krieger, *J. Colloid Interface Sci.* **34**, 91 (1970).
95. M. von Smoluchowski, *Kolloidzeit* **18**, 190 (1916).
96. W. Krasny-Ergen, *Kolloid-Z.* **74**, 172 (1936).
97. F. Booth, *Proc. R. Soc. London* **203A**, 533 (1950).
98. J. Stone-Masui and A. Watillon, *J. Colloid Interface Sci.* **28**, 187 (1968); **34**, 327 (1970).
98. J. Stone-Masui and A. Watillon, *J. Colloid Interface Sci.* **28**, 187 (1968); **34**, 327 (1970).
99. F. S. Chan, J. Blachford, and D. A. I. Goring, *J. Colloid Interface Sci.* **22**, 378 (1966).
100. W. B. Russel, *J. Colloid Interface Sci.* **55**, 590 (1976).
101. J. G. Brodnyan and E. L. Kelley, *J. Colloid Interface Sci.* **20**, 7 (1965).
102. I. M. Krieger and M. Eguiluz, *Trans. Soc. Rheology* **20**, 29–45 (1976).
103. F. O'osawa, *Polyelectrolytes*, Marcel Dekker, New York (1971).
104. J. Th. G. Overbeek, 'Polyelectrolytes, past, present and future', *Pure Appl. Chem.* **46**, 91–101 (1976).
105. C. F. Goodeve, *Trans. Faraday Soc.* **35**, 342 (1939).
106. T. Gillespie, *J. Colloid Sci.* **15**, 219 (1960).
107. A. S. Michaels and J. C. Bolger, *Ind. Eng. Chem. (Fundamentals)* **1**, 153 (1962).
108. R. J. Hunter and S. K. Nicol, *J. Colloid Sci.* **28**, 250 (1968).
109. J. P. Friend and R. J. Hunter, *J. Colloid Interface Sci.* **37**, 548 (1971).
110. B. A. Firth and R. J. Hunter, *J. Colloid Interface Sci.* **57**, 266 (1976).

111. T. G. M. van de Ven and R. J. Hunter, *Rheologica Acta* **16**, 534 (1977).
112. T. G. M. van de Ven and R. J. Hunter, *J. Colloid Interface Sci.* **68**, 135 (1979).
113. J. Th. G. Overbeek, in *Colloid Science*, H. R. Kruyt, ed., Vol. 1 Elsevier, Amsterdam (1952), pp. 115–127.
114. I. Langmuir, *J. Chem. Phys.* **6**, 893 (1938).
115. E. J. W. Verwey and J. Th. G. Overbeek, *Theory of Stability of Lyophobic Colloids*, Elsevier, Amsterdam (1948), p. 97.
116. B. V. Deryaguin, *Trans. Faraday Soc.* **36**, 203 (1940).
117. E. J. W. Verwey and J. Th. G. Overbeek, *Theory of Stability of Lyophobic Colloids*, Elsevier, Amsterdam (1948), p. 141.
118. E. J. W. Verwey and J. Th. G. Overbeek, *Theory of Stability of Lyophobic Colloids*, Elsevier Amsterdam (1948), p. 139.
119. L. N. McCartney and S. Levine, *J. Colloid Interface Sci.* **30**, 345 (1969).
120. G. M. Bell, S. Levine, and L. N. McCartney, *J. Colloid Interface Sci.* **33**, 335 (1970).
121. E. J. W. Verwey and J. Th. G. Overbeek, *Theory of Stability of Lyophobic Colloids*, Elsevier, Amsterdam (1948), p. 152.
122. G. Frens, *Ph.D. thesis*, University of Utrecht, 1968.
123. G. R. Wiese and T. W. Healy, *Trans. Faraday Soc.* **66**, 490 (1970).
124. E. P. Honig and P. M. Mul, *J. Colloid Interface Sci.* **36**, 258 (1971).
125. J. Jones and S. Levine, *J. Colloid Interface Sci.* **30**, 241 (1969).
126. B. V. Deryaguin, *Discuss. Faraday Soc.* **18**, 85 (1954).
127. O. F. Devereux and P. L. de Bruyn, *Interaction of Plane Parallel Double Layers*, MIT Press, Cambridge, Mass. (1963).
128. G. M. Bell and G. C. Peterson, *J. Colloid Interface Sci.* **41**, 542 (1972).
129. S. Usui, in *Progress in Surface and Membrane Science* Vol. 5, J. F. Danielli, M. D. Rosenberg, and D. A. Cadenhead, eds., Academic Press, New York (1972), p. 223.
130. R. J. Hunter, in *Modern Aspects of Electrochemistry*, No. 11, B. E. Conway and J. O'M. Bockris, eds., Plenum Press, New York (1975), pp. 56 ff.
131. J. H. de Boer, *Trans. Faraday Soc.* **32**, 21 (1936).
132. H. C. Hamaker, *Physica* **4**, 1058 (1937).
133. E. M. Lifshitz, *Sov. Phys.- JETP* **2**, 73 (1956).
134. I. E. Dzyaloshinskii, E. M. Lifshitz, and L. P. Pitaevskii, *Zh. Eksp. Teor. Fiz.* **37**, 229 (1959); *Sov. Phys.- JETP* **10**, 161 (1960).
135. B. W. Ninham and V. A. Parsegian, *Biophys. J.* **10**, 646 (1970).
136. B. W. Ninham and V. A. Parsegian, *J. Chem. Phys.* **52**, 4578 (1970); **53**, 3398 (1970).
137. D. G. Gingell and V. A. Parsegian, *J. Colloid Interface Sci.* **44**, 456 (1973).
138. D. J. Mitchell and P. Richmond, *J. Colloid Interface Sci.* **46**, 118 (1974).
139. N., Fuchs, *Z. Phys.* **89**, 736 (1934).
140. J. Lyklema, *Pontif. Acad. Scient. Scripta Varia* **31**, Contribution 7 (1967).
141. J. Gregory, *Adv. Colloid Interface Sci.* **2**, 396 (1969).
142. C. G. Force, E. Matijevic, and J. P. Kratohvil, *Kolloid Z. Z. Polym.* **223**, 31 (1968).
143. C. G. Force and E. Matijevic, *Kolloid Z. Z. Polym.* **224**, 51 (1968).
144. A. Lips and E. Willis, *J. Chem. Soc. Faraday Trans. 1* **69**, 1226 (1973).
145. K. Norrish, *Discuss. Faraday Soc.* **18**, 120 (1954).
146. K. Norrish and J. A. Rausell-Colom, *Clays Clay Miner.* **10**, 123 (1963).
147. D. H. Napper and R. J. Hunter, Hydrosols, in *MTP International Review of Science—Physical Chemistry*, Series I, Vol. 7, M. Kerker, ed., Butterworths, London (1972), pp. 241–306.

Annotated Author Index

Anderson, H., Statistical mechanical methods in the double layer, 179
Anderson, Anderson, and Eyring, and partial charge transfer, 186
Anderson and Bockris
  breakdown of contributions to specific adsorption, 187
  and partial charge transfer, 186
  and specific absorption of halide ions, 180
  and the theory of specific adsorption, 140
Annianson, and the radiotracer method, 155
Antropov, and his treatment of adsorption or organic compound, 262
Argade and Gileadi, their deduction of the relation of pzc to the cell potential, 270

Balashova, and radiotracer work, 140
Baron, Delahay, and Kelsh, simultaneous approach to specific adsorption, 209
Baugh and Parsons, absorption of guanidium ion from solution, 212
BDM (Bockris–Devanathan–Muller), their model of the double layer, 127
Beck, and the ribbon extension method, 161
Bickerman, and corrections of diffuse layer theory, 118
Biefer and Mason, their apparatus, 409
Billiter potential, abnormal, 230
Blomgren and Bockris
  and their isotherms, 191
  and the radiotracer method, 140, 155, 156
Bockris
  and contact adsorption, 138
  and the dependence of the potential of maximum on pH for organic adsorption, 266
  and the determination of pzc by the use of organic compound desorption, 264
  and the interpretation of the bell-shaped curve for adsorption, with organic molecules, 265
  and mechanism of AEC effects, 166
  second model involving bimers, and organic adsorption, 380
  and specific adsorption, 138
Bockris, Devanathan, and Muller
  their isotherm, 191
  and partial charge transfer, 186
Bockris and Habib
  development of isotherm, 191
  and the dimer model for water in the double layer, 129
  an interpretation of entropy maximum, 129
  treatment of multiple-imaging isotherm, 191
Bockris model, as basis for Parsons' macromodel, 377
Bockris and Reddy
  deduction of relationships between pzc and maximum of adsorption, 265
  and the lack of identity of maximum adsorption with the pzc, 265
  and semiconductor electrochemistry, 293
Boddy and Brattain, introduction to heavy metal ions, 323

Bode
and application of Anderson–Bockris theory, 187
his calculations of specific adsorption, 188
and partial charge transfer, 186
Bolt, and corrections to the diffuse double layer, 120
Booth
and electrophoretic mobility, 412
and electroviscous effects, 418
Bordowsky and Strehlow, diffuse double layer corrections, 120
Brattain and Boddy, and germanium electrodes, 315
Brattain and Garrett, the first paper on semiconductor electrochemistry, 291
Butler, and the pzc of india mamalgoms, 229

Carroll, and plane of shear, 416
Chapman, and the diffuse layer theory, 105
Chiu and Genshaw
explanation of discrepancies in ellipsometric method, 174
and the radiotracer method, 157
their work on specific adsorption, 173
Clausius–Clapeyron equation, in the double layer, 18
Conway
and associated solvent system effects in the double layer, 132
counterions in the Helmholtz layer, and their influence, 130
Conway and Barradas, and adsorption of organic compounds, 140
Conway and Bockris, the first suggestion of partial charge transfer, 180
Conway and Dobry-Duclaux, and various effects around colloidal particles, 417
Couchman and Davidson, and the Gibbs equation, and electrostrictional effects, 21
Curie, F. Jolliot, and the electrodeposition of radioelements, 155

Damaskin and Frumkin
and clusters of water in double layer, 128
inner layer water, diagramed, 129
and the pzc, maximum of adsorption relationship, 265
Davies and Rideal, and electrophoresis, 416
Debye length, 113
Defay, and the definition of surface tension, 20
Delahay, his approach to simultaneous adsorption, 206
Deryaguin
and interaction between double layers, 423
and measurement of interaction between the thin plates, 432
and repulsion, 425
Devanathan, and his data on the double layer, 164
Devanathan and Peries capacitance in electrocapillary methods are the same, 164
Deryaguin–Landau–Verwey–Overbeek (DLVO) theory
and colloidal stability, 423
tests of, 428
Devereaux and de Bruyn, and colliodal interactions, 427
Dogonadze and Chizmadjev, and double layer structure in nonaqueous solution, 278
Dukhin and Deryaguin, and the measurement of electrokinetic potentials, 409
Dupre equation, 102
Dutkiewiez and Parsons, thermodynamic approach to specific adsorption, 209
Dewald, and the flatband potential, 317

Esin–Markov plot, 94
Euler, and the investigation of absorption, 140
Everett, his contribution to the thermodynamic potentials, 13
Eyring, and work on the pzc, 271

Fawcett, and treatment of clusters in double layer, 129
Fermi level
and calculation of flatband potential, 322
and electrode potential, 49
Flory–Huggins, isotherm, 191
Flory–Huggins statistics
and adsorption isotherms, 195
in double layer, 129
Fomenko, and work function for tellurium, 280

Fredlein, Damjanovic, and Bockris, and the measurements of surface tension, on solids, 161
Frens, and repulsion during rapid shearing, 426
Friedel, and electron density calculations, 51
Frumkin
and comparison of potentials of charge of different metals, 222
and the concentration-polarization theory, 153
and double layer effects in electrode kinetics, 282
and double layer effects in kinetics, 117
and early electrocapillary curves in nonaqueous solution, 274
and electrocapillary curves, 223
and electrocapillary equations, 222
and "formal charge transfer coefficient," 43
his interpretation of the bell-shaped curve for organic adsorption, 266
and isoelectric change, 40
and the pzc, 270
the relation of cell between work function and potential of zero charge, 272
and specific adsorption, 138
and surface on the solid metals, 160
and the thermodynamics of irreversible adsorption, 381
and the thermodynamics of platinum metals, 39
and two-dimensional isotherms, 364
his work on the thermodynamics of platinum electrodes, 4
Frumkin's equation, for organic adsorption, 370
Frumkin's model, for organic adsorption, 370
Frumkin, Evanova, and Damaskin, Graham's method becomes inapplicable, 163
Fuchs, and repulsion theory in colloids, 430

Galvani, and potential difference, at interface, 64
Garrett and Brattain, and surface excess with semiconductors, 298
Gauss' theorem, and diffuse double-layer theory, 108
Gerischer
and dependence of flatband potential on the pH, 320
Gerischer (*cont.*)
sensitization of redox transformations, 329
Gerischer and Willig, and photosensitization, 330
Gerovich, and π-electron interactions, 366
Gibbs
his adsorption equation, 14, 16
and the concentration-polarization theory, 153
free energy in the double layer, 6
the original paper, 2
Gibbs surface excess, 146
definition, 137
exemplified, 23
Gileadi, and the radiotracer method, 156
Gillespie, and viscous energy dissipation, 420
Gokhstein
and specific surface work, 22
and surface stress, and the piezoelectric method, 21
Goodeve, and viscous energy dissipation, 420
Gouy, G., and the diffuse layer theory, 139
early work on organic adsorption, 354
and electrocapillary curves, 355
and the first electrocapillary curves, 274
Gouy, P.M., and definition of specific adsorption, 139
Gouy-Chapman-Stern, a model, 109
Gouy theory
limitations, summarized, 117
at semiconductors, 295
Grahame
and his basic idea, 140
his choice for specific adsorption, 152
his data for sodium fluoride, 176
his development of Stone's theory, 140
and the distance of closeness approach, 140
and his Essin-Markov plot, 94
his extension of Malsch's theory, 118
and an integrated capacitance relationship, 25
and ions bound to surface, 186
and the streaming electrode, for the pzc, 229
his test for diffuse double layer theory, 177
Grahame's capacitance method, for specific adsorption, 149

Grahame and Parsons, and the evaluation of γ, 185
Grahame and Soderberg
their determination of specific adsorption, 149
and their method for obtaining Gibbs surface excess, 95
and the zero charge potential, 150
Grahame and Whitney, and electrocapillary thermodynamics, 153
Green
and the first paper on semiconductor electrochemistry, 292
and the qualitative difference in potential dissolution at the interface between semiconductors and insulators, 330
Gregory, and coagulation, 431
Grahame and Whitney, and electrocapillary thermodynamics, 223

Hale and Mehl, and anthracene crystals, 347
Hamaker constant, 431
Hansen, and organic adsorption, 377
Hasted, innovation of dielectric constant to concentration, 119
Haydon, and shear planes, 405
Haydon and Taylor, and corrections of the diffuse double layer theory, 118
Heavens, and ellipsometry, 157
Helmholtz layer
at semiconductor-solution interface, 319
in solution, in semiconductor-solution interface, 303
Henry, his isotherm, 189
Honig and Mul, repulsion when zeta potential is small, 427
Hückel, and electrophoretic mobility, 412
Hunter
description of repulsion theories, 430
and the literature, 412
Hurwitz
calculation of simultaneous adsorption, 209
thermodynamic approach to simultaneous adsorption, 209

Israelachvili and Adams, measurement of exfoliated mica of repulsion, in exfoliated mica systems, 432

Jakuszewski and Kozlowski, and the immersion method, 229
Jhering
and the book with electrocapillary curves, 355
his table on differential capacity measurements, 357
Joshi, and double layer theory tests, 115
Joshi and Parsons, their examination of the diffuse double layer, 177

Kafalos and Gatos, and the radiotracer method, 155, 156
Kallman and Pope, pioneering work on insulator-electrode surfaces, 329
Kazarinov, and the radiotracer method, 156
Kingston and Neustadter, and charge in semiconductor, 297
Klein and Lange, and the dipole potential at the interface, 269
Koenig
and electrocapillary thermodynamics, 153
his work on thermodynamics, 3
Kovac
her results for the thiocyanate on mercury, 158
her work on specific adsorption, 173
Krasny-Ergen, and the primary viscous effect, 418
Kroichkoll, and the stretching of wires in 1809, 229

Landau, and interaction between double layers, 423
Langmuir, and repulsive forces, 425
Lawrance, his work on specific adsorption, 173
Lawrance and Mohilner, and surface tension vs. capacity as a method of obtaining data in the double layer, 169
Lawrance, Parsons, and Payne
and the double layer effects, 169
a finite contact angle?, 164
Levine
attempt to overcome sharp boundary difficulty, 203
and corrections to the double layer theory, 120
and diffuse double layer corrections, 122
his isotherm, 202

Levine, Bell, and Calvert, and multiple imaging, 201
Levine, Bell, and Smith, dipoles in the double layer, 128
Linford, and specific surface work, 20
Lippmann
and electrode charge, 222
his original work, 2
Lippman equation, 16, 85
Loeb, and self-atmosphere effects, 120
Lohman, Gerischer, and Memming, the solvent reorganization, 329
Longsworth, and theory of electrophoresis, 414
Lorentz–Lorenz equation, and specific adsorption, 158
Lorenz
bonding to mercury surface, 180
and determination of partial charge, 182
and partial charge transfer, 43, 181, 224
Lorenz's method, determination of partial charge, 182
Lyklema
and pH near interfaces, involving silver iodide, 403
and surface potential for silver iodide, 416
Lyklema and Overbeek
and analysis of electrophoretic mobility, 416
and charge–potential plots, 402

MacDonald, and qualitative theory of inner layer, 126
MacDonald and Barlow, and multiple energies, 201
Malsch, and dielectric constant depending upon fuel strength, 118
Many, and semiconductor electrochemistry, 293
Matijevic, and coagulation, 431
McCrakin, ellipsometry in homogeneous film, 159
McCrakin and Colson, and ellipsometry, 157
Mehl
exchange currents of redox reactions on anthracene, 333
limiting currents at insulating electrodes, 329
Mehl and Buchner, and anthracene electrodes, 343
Mehl, Hale, and Lohman, charge transfer and the solvent reorganization, 329
Mohilner
and electrocapillary thermodynamics for redox electrodes, 223
and expansion of equations in the double layer, 179
Mott-Schottky
their layer, 300
their plot, and the flatband potential, 316
Myamlin and Pleskov, and semiconductor electrochemistry, 293

Novakovsky, Ukshe, and Levin, and relation between pzc and cell potential, 270
Nernst, his equation, 3
Nernst–Planck, their equation, 413
Ninham and Parsegian, and repulsion theory for colloids, 430
Norrish, and the force–distance relationship, 432

O'Brien and White, and numerical solutions, 413
Ottewill and Rowell, monographs on colloidal systems, 433
Overbeek
and coagulation, 431
and electrophoretic mobility, 412

Paik, Genshaw, and Bockris, and the ellipsometric method for specific adsorption, 158
Palm, and adsorption on bismuth, 358
Palm and Tenno, and pzc effects on electrode kinetics, 283
Parsons
calculation of simultaneous adsorption, 209
and claimed invalidity of his model, 377
and tests of diffuse double layer theory, 115
Parsons' method, for specific adsorption, 149
Parsons and Davanathan, and electrocapillary thermodynamics, 153
Parsons and Trasatti, their examination of the diffuse double layer, 177
Parsons and Zolbel, interfacial tension measurements lower than those obtained from capacitance data, 164
Pauli principle, and Fermi level, 48

Payne, and his work on capacitance–surface-tension effects, 168
Planck, and the completely polarizable electrode, 222
Pleskov, and early equations for semiconductor electrochemistry, 291
Poirier, and extension of the diffuse layer theory, 122
Proskurnin and Frumkin
and the effect of octyl alcohol on the capacitance–potential curve, 357
and silver surfaces, 140

Randles, and the dipole potential at the interface, 269
Randles and White, their work on capacitance in nonaqueous solution, 277
Russel, analysis of electroviscosity effects, 419

Schulze–Hardy rule, and explanation of colloid theory in electrochemical terms, 431
Seiwatz and Green, and the charge in semiconductor, 297
Smith, and his work on silver iodide, 416
Sparnaay and Hurwitz, energy in the double layer, 120
Stern, his model, 109
Stern's isotherm, 187
Stigter
his apparatus, 409
and plane of shear, 416
Stillinger and Kirkwood, and double layer corrections, 122
Stone-Masui and Watillon, and the electroviscous effect, 418
Swinkels, Green, and Bockris, and the radiotracer method, 156

Tamm states, 303
Trasatti
his approach to water orientation, 131
and cell-potential relations, 270
and dipole potential difference, 273
and double-layer theory tests, 115
and the pzc related to the work function, 271
Trasatti (*cont.*)
relation to electronegativity, 271
and the relation of specific adsorption to water desorption, 189
and sticking on the glass capillary, 171
Tverdovskii and Frumkin, adsorption on solid metals, 161

Ukshe, capacitance in nonaqueous solution, 277
Ukshe and Bukun, potentials of zero charge, 279

Vasenin
and relations in cells, 268
and relationship to the dipole potential, 272
Vetter and Schulze, and partial charge transfer, 43, 183
Verwey and Niessen, entry into oil–water interface, 400
Verwey and Overbeek
and interaction between double layers, 423
and oil–water interfaces, 400
and repulsive forces, 425
Vijh, and demetallization of the surface, 205
Volta potential
and cell potential, 267
and potential of zero charge
Volta potentials, tabulated, 270
Vulca potential difference, 65

Watts-Tobin, and water dipoles in the double layer, 126
Wieckowski, and the radiotracer method, 156
Wiersema, Loeb, and Overbeek, electrophoretic mobility, 412
Wiese and Healy, and repulsion under constant charge conditions, 426
Williams, and self-atmosphere effects, 120
Wroblowa and Green, and the radiotracer method, 155

Yakushevsky and Antropov, and relations deduced for cells, 269

Subject Index

For some named effects, equations, etc. (e.g., Nernst equation), see the Annotated Author Index.

Absolute electrode potential, 72
Absolute potential, some values, 76
Absorption
  in anthracene crystals, 347
  of methanol on platinum, 86
ac effects
  and double layer, mechanism of, 166
  in double layer, suggested mechanism, 165
Activity coefficient, and specific adsorption, 213
Adsorbed oxygen, and organic adsorption, 382
Adsorption energy, of organic compounds, at bismuth-solution interface, 367
Adsorption isotherms, tabulated, 189
Adsorption
  isothermics with 2-butanol, 364
  of methanol, as a function of potential, 387
  on methanol, 383
  of organic compounds, and molecular model, 377
  of organic compounds, on ideally polarizable electrodes, 354
  of organic compounds, reversible, 354
  of organic compounds, thermodynamics, 360
  of organic molecules, 353
  of organic molecules, the potential dependence, 266
  on platinum, of organic compounds, 388
Alloys, in contact with two electrolytes, their thermodynamics, 35
Ambiguity, and fundamental concept in electrochemistry, 225
Amyl alcohol, adsorption of, 359
Anthracene
  and the adsorption of iodine, 335
  and exchange current density, 333
Approach, microscopic, to colloidal stability, 428

Bands, unbending of, 310
BDM (Bockris–Devanathan–Muller) model, of the double layer, 127
Billiter potential, abnormal, 230
Binary alloy, and electrocapillary thermodynamics, 33
Bockris model, as basis for Parson's macromodel, 377
Boundaries of conduction and valence band for various semiconductors, 323
Butyl alcohol, adsorption on different electrodes, 374

Camphor, desorption, from mercury electrodes and the pzc, 262
Capacitance
  of inner layer, diagramed, 125
  and surface tension, 24

Capacitance–concentration–potential plots, various, for organic compound adsorption, 361
Capacitance curves
associated with organic adsorption, 356
as a function of potential, 356, 359
and wide-gap semiconductors, 316
Capacitance hump
and disappearance with rise in temperature, 201
theory, 201
Capacitance humps, predicted, 199
Capacitance minima, tabulated, 198
Capacitance–surface-tension method in the double layer, concluding discussion, 172
Capacity, from the diffuse double layer theory, 109
Carrier concentration, and the surface states, 325
Cathodic current densities from Teflon to solution, 341
Cations, their surface excess, 90
Cell, diagramed, for electro-osmosis, 409
Cell potential
and electronegativity, 271
Volta potential and dipole potential, 268
Cell potentials, related to the pzc and work function, 270
Cells consisting of insulators and semiconductors, 336
Charge and potential measurements, for colloids, 401
Charge, as the variable, eliminates differences between capacitance and surface-tension measurements in double layer, 165
Charge carriers, and injection, 339
Charge dissolution, and surface states, 305
Charge distribution, at interface, 10
Charge due to specifically adsorbed hexafluorophosphate as a function of charge, 99
Charge injection, at anthracene cathodes, 341
Charge on semiconductor–solution interface, 297
Charge–potential curves, diagramed, 88
Charge–potential relationships, diagramed, 92
Charge related to the integral of capacity, 26
Charge related to specific surface excess, 93
Charge transfer, and thermodynamics, 9
Charging curves of bismuth electrodes, with organic compounds, 364
Chloride adsorption on platinum, various techniques, 174
Clausius–Clapeyron equation, in the double layer, 18
Clusters, in the double layer, 128
Coagulation
kinetics of, 430
tabulated, 422
theory of, 420
Colloidal stability, and double layers, 420
Colloidal systems, 397
Components of electrode potential, 47
Constant charge, and colloidal repulsion, 426
Contact, metal–metal, 56
Continuity equation, 413
Corrected Tafel plot (CTP), 284
Corrections due to neglect of absorption of water, 180
Crystal orientation, 52
Crystalline surfaces, and work function, 53
Current–potential and nonaqueous systems, 338

Debye length, 113
Definitions used in double layer, 89
Determination of partial charge, Lorenz's method, 182
Dielectric discontinuity, in double layer, 193
Dielectric slabs, energy across, 195
Difference of surface tension between capacitance and electrocapillary methods, as a function of concentration, 171
Differential capacitance
on bismuth electrodes, 358
for colloids, 402
as a function of potential, 176
of germanium electrode, with the deposition of copper, 323
of germanium electrodes, 315
in nonaqueous solution, as a function of potential, 277
Differential capacities of mercury, calculated and observed, 113
Differential capacity, 373
and Frumkin's theory, 375
of Helmholtz layer for various solid metals, 262

Differential capacity (*cont.*)
for KPF_6 in nonaqueous solution, diagramed, 104
and potential, 305
at semiconductor-solution interface, 301
with sodium fluoride, diagramed, 98
Diffuse double layer, various tests, 177
Diffuse double layer theory
and calculation of specific surface excess, 98
extensions, 114
limitations, 114
and surface excesses, 179
proofs, 114
validity, 175
Diffuse layer, for colloids, 400
Diffuse layer theory
presented, 107
validity, 105
Diffusion equations associated with anthracene crystals, 347
Dimensionless mobility, in electrophoresis, 414
Dimer model, in the double layer, 129
Dipole interactions, in the double layer, 126
Dipole model of the double layer, 127
Dipole potential
at the interface, and cell potential, 272
at the interface, determined 269
Dipole potential difference, 64
Direct determination of surface charge, 227
Discrepancies between capacitance and surface-tension measurements in double layer, 165
Dispersion energy, and adsorption isotherms, 196
Distinction of capacitance, and surface tension, 164
Distribution of concentration of electrons, in holes, at semiconductor-solution interface, 299
Distribution of potential charge in charge at insulator-solution interfaces, 331
DLVO (Deryaguin-Landau-Verwey-Overbeek) theory, and colloidal stability, 423
Double layer
around a sphere, 399
capacity, in amide solvents, tabulated, 104
flat, 398
Gibbs work, 2
on semiconductor electrodes, 291
Double layer (*cont.*)
at the semiconductor-solution interface, 294
depth of, 296
and theory, 293
some applications of simple theory, 110
structure, 312
thermodynamics methods, 1
thermodynamics and temperature, 27
without specific adsorption, 83
Double layer theory, and associated solvent systems, 132
Double layers, and colloidal stability, 420
Dupre equation, 102

Effect of potential distribution, at semiconductors, 302
Effect of specific adsorption, and concentration, 143
Electrical work function, as a function of temperature, diagramed, 53
Electrocapillary and capacitance methods, different or the same?, 162
Electrocapillary curves, 171
exemplified, 87
first determined by Gouy, 274
and Frumkin-Damaskin theory, 370
in nonaqueous solution, 278
shapes characteristic of organic compounds, 355
Electrocapillary equations, 5
deduction, 144
Electrocapillary method, for specific adsorption, 144
Electrocapillary thermodynamics
and binary alloys, 33
discussion, 152
and the double layer theory, 140
of partial dissociation, 42
Electrochemical kinetics, and potential of zero charge, 281
Electrochemical systems, interfacial regions, 2
Electrode, surface species in equilibrium with, but not present in, a bolt phase, 41
Electrode bending, a method for adsorption measurements in solid, 161
Electrode kinetic phenomena, 404
Electrode potential, 45
and the crystal orientation, 52
and Galvani potential difference, 71

Electrode potential (*cont.*)
of numerous situations, and absolute values, 75
origin, 60
relative, 70
and the work function, 47
Electrode potentials, in practical situations, 74
Electrode reactions, and potential, 77
Electromagnetic retardation, 428
Electron density
and diffuse layer theory, 108
and potential energy at metal–metal interfaces, tabulated, 58
and potential energy profiles, tabulated, 59
Electron levels, at surface of semiconductors, occupation, 308
Electron overlap potential, 51
Electron work function
as function of centering, tabulated, 54
of liquids, 54
of metals in polar liquids, 65
Electronically nonpolarizable interfaces, 72
Electro-osmosis, 405
in porous plug, 408
Electrophoresis, 412
Electrophoretic mobility
measurement of, 413
theory of, 412
Electrosorption valency, 185
Electrosorption valency methods, evaluation, 185
Electrostatic interaction during adsorption process, 197
Electroviscosity, 417
secondary, 418
theory of, 419
tertiary, 419
Electroviscous effects, 417
primary, 418
Ellipsometry, and roughness, 160
Ellipsometry and electrocapillary methods on mercury, compared, 173
Ellipsometry method, for specific adsorption, 157
Energies, in specific adsorption, 187
Energy
across five dielectric slabs, 195
across four dielectric slabs, 194
across smoothly varying dielectric slabs, 195
across three dielectric slabs, 193
Energy (*cont.*)
across two dielectric slabs, 192
diagramed, for electrons and polar liquids, and work function, 61
Energy diagrams, involving photoactivation, 346
Enthalpy, of oxide formation and water in the double layer, 131
Enthalpy and energy, temperature dependence in the double layer, 17
Equations, for thermodynamics in interfaces, basic, 12
Equilibrium, between two metals in contact, 57
Equilibrium concentration, at mercury–solution interface, tabulated, 3
Equivalent circuit, involving polarizable semiconductors, 302
Errors, due to neglect of activity coefficients, 363
Esin–Markov plot, 94
Evaluation of specific adsorption, 148
Excitons, and the insulator–solution interface, 347
Experimental techniques, for semiconductor–solution interface, 312
Expressions for double layer, compared, 130
Extensions, of diffuse double layer theory, 114

Fermi level
and calculation of flatband potential, 322
and electrode potential, 49
Flatband potential
and calculation of Fermi level, 321
and concentration of electrons, 318
and dependence on pH, mechanism, 320
and diffusion layer, 316
and germanium electrodes, 319
Mott–Schottky, 300
and pH, 320
and semiconductor–solution and semiconductor electrodes, 321
Flat plates
and repulsion, 427
repulsion between, theorized, 423
Flory–Huggins statistics
and adsorptions isotherms, 195
in double layer, 129
Fluid velocity, and distance from surface, 406

Forces, in specific adsorption, 186
Forces of interaction, between colloids, 432
Free charge, defined, 227
Free energies of adsorption, tabulated, 188
Frumkin, and two-dimensional isotherms, 364
Frumkin's equation, for organic adsorption, 370
Frumkin's model, for organic adsorption, 370

Gallium, adsorption on, 359
Gauss' theorem, and diffuse double-layer theory, 108
Gerischer, sensitization of redox transformations, 329
Germanium electrodes
  and the capacitance–potential plot, 315
  and flatband potential, 319
Gibbs adsorption equation, its applications, 16
Gibbs–Duhem equation
  for bulk phases, 15
  for separate phases, 8
Gibbs equation, and organic compound adsorption, 361
Gibbs surface excess, 146
  definition, 137
  exemplified, 23
Gouy theory
  limitations, summarized, 117
  at semiconductors, 295
Grahame's capacitance method, for specific adsorption, 149
Green, and the qualitative difference in potential dissolution at the interface between semiconductors and insulators, 330

Hale and Mehl, and anthracene crystals, 347
Hamaker constant, 431
Helmholtz layer
  at semiconductor–solution interface, 319
  in solution, in semiconductor–solution interface, 303
Hexyl alcohol, adsorption of, 359
Hump, predicted from capacitance–charge curve, 202

Ideal nonpolarizable interface, and its thermodynamics, 28, 32
Ideally polarizable electrode, 225
Ion–solvent interaction energy, for various anions, 143
Ionic adsorption, isotherms for, 189
Inflection, on coverage–charge curve with multiple imaging, 201
Inflection points
  and capacitance hump, 201
  in coverage–charge curves, 197
    calculated, 200
Injections, and exchange currents on insulator electrodes, 339
Inner layer
  capacity in the presence of ethylene carbonate, 130
  involving silver iodide, and the interface, 403
  structure, 124
Insulator–electrode interface, 329
Insulator electrodes, and injection of charge carriers, 339
Insulator–electrolyte thermodynamics, 332
Interface
  blocked, 2
  for metal–nonaqueous solution, 274
Interfaces, actual, 67
Interfacial tension
  as a function of concentration, diagramed, 163
  at a gold electrode, 162
  in mercury, 137
  several other names proposed for it, 20
Intrinsic semiconductor, capacity as a function of potential, 301
Invalidity, of diffuse double layer theory, 175
Inversion layer, and space charge, 307
Iodide, adsorbed on anthracene electrodes, 335
Ion exchange, and electrocapillary thermodynamics, 38
Ionic crystals, with interphases, their thermodynamics, 38
Isodynamic curves, diagramed, 428
Isoelectric change, 40
Isotherm
  deduction of, 195
  properties due to Blomgren and Bockris, 191
Isotherms
  multiple-energy, 201
  two-dimensional, 366

Jellium, 50

Kinetics, of slow coagulation, 431

Latex suspensions, theory for, 433
Laser illumination, in electrophoresis, 414
Limitations, of diffuse double layer theory 114
Limiting currents, at Teflon electrodes, 343
Linear sweep voltammogram, and electrocapillary thermodynamics, 40
Lippmann equation, 16, 85
Liquids, and polar surfaces, 55
Literature, for colloids, 433
Logarithmic isotherms, 142
Lorentz–Lorenz equation, and specific adsorption, 158
Luminescence, electrochemical, 344

Measured potentials, their meaning, 69
Measurement, of electro-osmosis, 408
Metal, in contact with solution of a single salt, thermodynamics, 22
Metal-electrolyte–melt interface, 277
Metal–nonaqueous solution interface, 274
Metal overlayers, a special case of metal–metal contacts, 60
Metal–polar-liquid contact, its thermodynamics, 61
Metallization of semiconductor–solution interface, 304
Methanol, adsorbed on platinum, 383
Methanol adsorption, irreversible, 386
Methods, for specific adsorption, 151
Microelectrophoresis, 414
Microscopic approach, to colloidal stability, 428
Microscopic sheets, interaction between, measured, 433
Mobility, reduced, and the theory of electrophoresis, 414
Model, of series capacitor, 112
Models, of double layer, 100
Molecular model for adsorption, first presented by Butler, 377
Multiple-energy isotherms, 201
Multiple-imaging isotherm, 191

Observed and calculated values for dC_+/dE, 97
Oil–water interface at colloids, 400
Operative electrode potential, 71
Organic adsorption, and hydrogen–oxygen adsorption, 383
Organic compounds, adsorption of, in Frumkin's theory, 372
Organic isotherm, a generalization, 377
Organic molecules, their adsorption, as interpreted by Bockris, 265
Organic substances, irreversible adsorption, 381
Origin of electode potentials, 60
Oxide systems, their capacitance, 404

Parsons' method, for specific adsorption, 149
Partial charge transfer
  and electrocapillary thermodynamics, 42
  enunciated by Lorenz, 1961, 4
  and Lorenz, 43, 181, 224
  a summary of viewpoint, 186
  and Vetter and Schultze, 183
Pauli principle, and Fermi level, 48
pH and flatband potential, 320
Phenol, adsorbed on mercury, 367
Photoelectrochemical measurements, and electrode potential, 74
Photoelectrochemical processes, 345
Photoelectromotive force, and current density, 347
Photoinjection, and current density, 347
Photopotential, 309
  and flatband potential, 310
  in semiconductors, 318
Photopotentials, and semiconductor–solution interface, 311
Photosensitized reactions, and excited molecules, 349
Pits, and condensed films, 375
Platinum, and methanol adsorption, 383
Platinum group metals, and specific adsorption, 224
Polarizable electrode, completely defined by Planck, 222
Polarizable interface, 67
Polarization curves, as a function of double layer structure, 283
Polishing, of semiconductors, 312
Polycrystalline surfaces, and work function, 53
Polymer films, and electrodes, 341

Potential
between plane of closest approach and bulk of solution, 110
and electrode reactions, 77
at interface, effective metal ions, 68
penetration into the semiconductor, 294
Potential differences, involved in semiconductor-solution interface, 296
Potential dissolution in double layer, pH dependence, 320
Potential distribution
in double layer, at semiconductors, 314
at flatband potential, 319
at the semiconductor–solution interface, 293
Potential drop
in Helmholtz layer, diagramed, 303
of semiconductor-solution interface, calculated, 314
Potential energy
of attraction, between colloidal particles, 428
as a function of separation, 423
of interaction between particles, 422
and repulsion, in colloid systems, 426
Potential energy profile, for metal-polar-liquid–vacuum system, diagramed, 65
Potentials
how one measures them, 69
at the pzc, tabulated, 272
Potential of zero charge (pzc), 137, 221
and electrochemical kinetics, 281
as a function of the solvent, 275
methods of determination, 227
in molten salts, 279
and nature of medium, 267
in nonaqueous solution, 280
recommended, tabulated, 228
related to work function, 101
tabulated, 76
and the work function, 272
Practical situations, and electrode potential, 74
Pressure, and double layer relations, 26
Pressure, electro-osmotic, theory of, 407
Proofs, of diffuse double layer theory, 114
Pure metal
in contact with nonelectrolyte in the solvent, thermodynamics, 32
and two salts in a solvent, thermodynamics, 28
Pzc, related to cell potential, 270
Pzc's
and relations in cells, 269
in various solvents, 276

Quasithermodynamic methods, for specific adsorption, 144
Quantum efficiency, as a function of wavelength, 347

Radiotracer measurements, and double layer work, 140
Radiotracer method, 156
and specific adsorption, 154, 155, 156
Real potential
of iron and water, tabulated, 56
and work function, 61
Reciprocal capacitance, versus reciprocal diffuse layer capacitance, diagramed, 96
Redox reactions
at insulator electrodes, equations for, 340
and insulators, 334
Relation of cell potential to electronegativity, 271
Relative electrode potential, 70
Relaxation, in space charge with semiconductors, 306
Relaxation time, at semiconductor–solution interface, 309
Repulsion
between dissimilar surfaces, 427
between flat plates, 423
between spherical particles, 425
Retardation, electromagnetic, 428
Ribbon extension method, for differential surface tensions, 161
Roughness, and specific adsorption, 160

Schulze–Hardy rule, and explanation of colloid theory in electrochemical terms, 431
Seal capillaries, and electro-osmosis, 405
Semiconducting phases, and electrocapillary thermodynamics, 36
Semiconductor electrochemistry, and reviews, 292
Semiconductor electrodes, and industrial application, 326
Semiconductor–electrolyte interface, 306

Semiconductor–solution interface, 312
experimental study, 311
and Helmholtz layer, 304
and metallization, 304
Semiconductors
and the boundaries of valency and induction vacuum, 323
polishing of, 312 and insulators, cells of, 337
Series capacity model, 112
Series model, for the inner double layer, 126
Shear plane, its position, 416
Shear stress, and surfaces, 21
Silicon electrodes, in coating of oxide, 314
Silver iodide, and surface potential, 416
Simultaneous adsorption, 213
of cations and anions, Delahay's approach, 206
methods compared and discussed, 211
results compared, 210
Single-electrode potential, 71
Single-imaging isotherm, 191
Space charge
and inversion layer, 307
and relaxation time, 309
at semiconductor–solution interface, 312
Sparnaay, and oil–water interfaces, 400
Specific adsorbability, and ionic radius, 142
Specific adsorption
detection, 100
determination, 144
equations for, 147
evaluation, 148
as a function of charge, diagramed, 140
on the gold electrode, 160
history, 139
method based on adsorbated concentration in solution, 154
of nitrate ions, 208
in presence of thallous ions, 208
and partial charge transfer, 180, 341
and radiotracer method, 154
and results obtained by electrocapillary, ellipsometry, and radiotracer methods, compared, 172
simultaneous, 207
of cations and anions, 205
and solvation sheath, 203
and temperature, 143
Specific surface excess, in terms of diffuse layer theory, 111
Spectroscopic and optical methods, for semiconductors, 312
Spreading effect, 51
Solid phases, their interfacial thermodynamics, 19
Solvation sheath, and specific adsorption, 203
"Squeezing out" effects, 365
Standard chemical potential, of iron and water, tabulated, 56
Standard model, for colloids, 400
Standard potentials, tabulated, 76
Standard state
and adsorption isotherms, 189
for electrons, in electrochemical calculations, 49
Stern's isotherm, 187
Streaming potential, 409
Supercequivalent adsorption, its definition, 138
Surface charge
on different faces of single crystals, 264
of nonaqueous solution, 275
Surface concentration, of magnesium, diagramed, 115
Surface conductivity, and semiconductor–solution interface, 293, 313
Surface coverage, from ellipsometry and capacitance, compared, 173
Surface dipole potential difference, 101
Surface excess
of anions, 90
as a function of charge density, 148
as a function of potential, 145
of organic compounds, 361
in simple solutions, 91
Surface of metals, described, 50
Surface potential, and silver iodide, 416
Surface states, 302
and cathodic polarization, 325
and deposition of metals, 325
elucidation of their nature, 326
and hole lifetime, 325
at semiconductors, 303
Shockley levels, 303
theory, 303
Surface tension
and capacitance, 24
decreased by sodium acetate, 265
on solid metals, 160
Surfaces, with shear stresses, 21

Tamm states, 303

Technique for measurement with colloidal interfaces, 402
Techniques, and double-layer investigations, 84
Temperature, and double-layer relationships, 26, 27
Temperature dependence, of specific adsorption, diagramed, 143
Terylene electrodes, and the iodine–iodide system, 343
Test, of capacitance–surface-tension difference in double-layer determinations, 164
Tests, of DLVO theory, 428
Tetraalkylammonium halides, and adsorption at mercury surfaces, 266
Tetracene–water surface, 347
Thermodynamic potentials, in the double layer, 14
Thermodynamic treatment consistent of absorption processes, 225
Thermodynamics
of adsorption of organic compounds, 360
for charged interfaces, 7
of insulator–solution interface, 332
for interfacial region, 15
of ion exchange membranes, 38
of ionic crystals, in the interphasial region, 37
of a metal in contact with a solution containing a single associating salt, 22
of a pure metal, in contact with a solution of an electrolyte and nonelectrolyte in a solvent, 32
of pure metal, in contact with two salts, 28
of single bulk phase, 4
of three-phase electrodes, with gaseous component in equilibrium with solution, 38
Thomas–Fermi statistics, and semiconductor–solution interfaces, 301
Three-part model, for double layer, 130
Three-phase electrode, its electrocapillary thermodynamics, 38
Two-capacitor model, 370
Two-position model, for double-layer water, 128

Validity of diffuse double-layer theory, 175
Velocity, and streaming potential, 410
Viscosity, and double layer, 416
Volta potential
and cell potential, 267
and potential of zero charge, 267
Volta potentials, tabulated, 270
Vulca potential difference, 65

Water, surface excess, and its neglect, 179
Water orientation, Trasatti's approach, 131
Ways of obtaining surface excess, 89
Wide-gap semiconductors, 292
Work function
and centering, 53
and crystal orientation, 52
and crystal phase, 53
and metal equilibrium, diagramed, 67
of metal in solution, diagramed, 67
of metals made for solutions, tabulated, 76
and potential of zero charge (pzc), 271, 272
and real potential, 61
and temperature coefficient, 280
Work function difference, and cell potential, 273
Work functions
differences among various metals, 281
tabulated, 50
Work of adhesion, tabulated, 103